BioMed Research International

Molecular Markers in the Diagnosis and Treatment of Cancer

Guest Editors: Murat Gokden, Aurelio Ariza, and Konstantinos Arnaoutakis

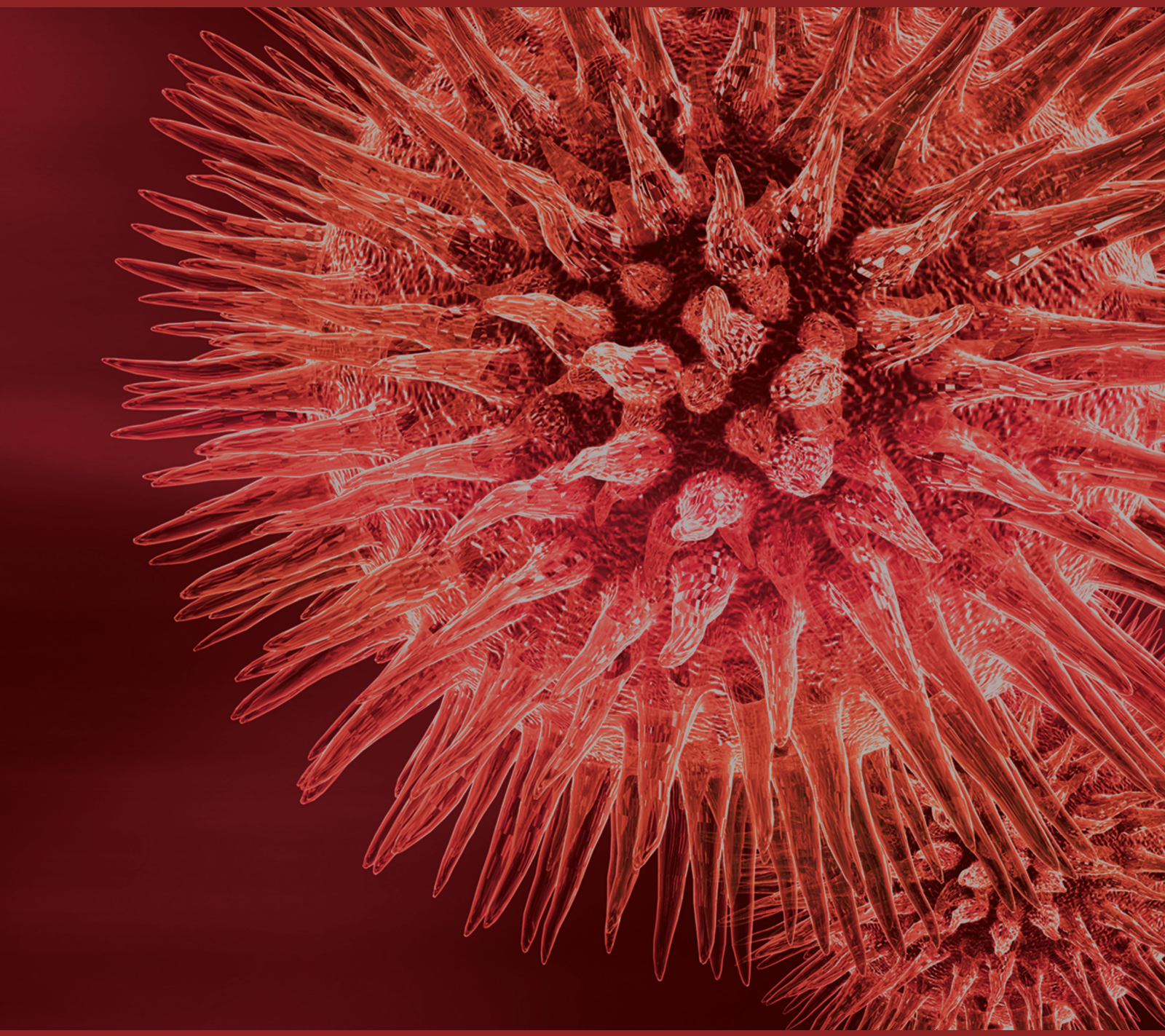

Molecular Markers in the Diagnosis and Treatment of Cancer

BioMed Research International

Molecular Markers in the Diagnosis and Treatment of Cancer

Guest Editors: Murat Gokden, Aurelio Ariza,
and Konstantinos Arnaoutakis

Contents

Hindawi Publishing Corporation
BioMed Research International
Volume 2015, Article ID 105217, 2 pages
http://dx.doi.org/10.1155/2015/105217

Editorial

Molecular Markers in the Diagnosis and Treatment of Cancer

Murat Gokden,[1] Aurelio Ariza,[2] and Konstantinos Arnaoutakis[3]

[1]*Department of Pathology, University of Arkansas for Medical Sciences, Little Rock, AR 72205, USA*
[2]*Department of Pathology, Autonomous University of Barcelona, 08916 Barcelona, Spain*
[3]*Hematology-Oncology Division, Department of Internal Medicine, University of Arkansas for Medical Sciences, Little Rock, AR 72205, USA*

Correspondence should be addressed to Murat Gokden; mgokden@uams.edu

Received 25 June 2015; Accepted 2 July 2015

Our understanding of cancer as a disease process has evolved tremendously over the centuries, culminating in the late 20th century with the discovery of oncogenes and tumor suppressor genes and subsequent understanding of carcinogenesis as it is depicted in the classic hallmarks of cancer paper by Hanahan and Weinberg [1]. Genetic and epigenetic alterations have been increasingly identified in many diseases, including a wide variety of neoplasms. As more of these alterations are being discovered, their significance in some diseases remains still obscure, while they have become diagnostic, prognostic, and predictive genetic signatures for others.

It is becoming clear that a given genetic alteration and associated molecular changes involving particular pathways in the neoplastic cell may not necessarily be specific for that particular type of cancer. Rather, such a genetic alteration represents a more general abnormality involved in the neoplastic transformation of a variety of cancers in different organs. For instance, mutations in *BRAF* can be seen in unrelated cancers such as melanoma, colorectal and lung carcinomas [2, 3], brain tumors [4], and hematolymphoid malignancies [5]. This paves the way to potentially identifying which of these alterations a cancer has, rather than the classical diagnostic approach of which organ it originates from or what the histologic type is, essentially redesigning the cancer taxonomy. This disease or organ-agnostic type of approach is also the mainstay of a "personalized" approach to cancer treatment.

Some of these alterations are also used as diagnostic aids in differential diagnostic settings, such as IDH-1 R132H identification by immunohistochemistry or the identification of other *IDH-1* or *IDH-2* mutations in diffuse gliomas, in contrast to well-circumscribed gliomas or reactive gliosis [6].

An increasingly growing number of these alterations are now the subject of targeted therapies especially in the form of small molecule kinase inhibitors. They can also provide significant prognostic (such as FLT-3 mutation in acute myelogenous leukemia) and predictive information, further blurring the boundaries between diagnosis and treatment, as well as between basic and clinical sciences. It is not enough anymore for pathologists to provide only diagnosis but also an array of molecular markers that facilitate the discussion about prognosis for given cancer and potential therapeutic options.

Of paramount importance are the explosion of knowledge in molecular biology and its clinical application in the form of molecular diagnostics, involving high-technology testing. Altogether, we have a better understanding of how such alterations operate in the process of oncogenesis, which in turn helps us better diagnose and treat neoplasms based on these alterations.

These discoveries have also influenced the pharmaceutical and biotechnological fields, resulting in development of additional treatment options for cancer patients: O^6-methylguanine DNA methyltransferase (*MGMT*) gene methylation status in glioblastoma and response to alkylating agents [7], *KIT* mutations in gastrointestinal stromal tumor (GIST) and response to imatinib [8], *ALK* gene rearrangements in *ALK*-positive nonsmall cell lung carcinoma and response to crizotinib [9], and EGFR mutations in nonsmall cell lung carcinoma and response to gefitinib [10] are a few

examples of how genetic alterations, identified by molecular diagnostic testing, can impact treatment decisions.

Despite this enormous success over the last 50 years since the discovery of DNA double helix and the discovery of the first human oncogene, there are still a lot of questions in regard to the optimal way of molecular testing, distinguishing between passenger and driver mutations in a tumor, dealing with the vast intra- and intertumor heterogeneity, and introducing other nongenetic molecular markers such as proteins (proteomics) and metabolites (metabolomics).

In this *special issue,* we present a variety of manuscripts that report technical, basic, and clinical research, molecular biology, and diagnostic and therapeutic aspects of neoplasia, as well as reviews of these subjects. The topics are not limited to a particular organ, system, or type of neoplasia. The manuscripts emphasize the importance of molecular markers in various aspects of neoplasia in an attempt to provide the reader with an up-to-date source of current research on molecular markers in cancer.

Acknowledgment

We thank all the authors, editors, and reviewers, whose expertise and contributions made this special issue possible.

Murat Gokden
Aurelio Ariza
Konstantinos Arnaoutakis

References

[1] D. Hanahan and R. A. Weinberg, "Hallmarks of cancer: the next generation," *Cell*, vol. 144, no. 5, pp. 646–674, 2011.

[2] G. S. Falchook, G. V. Long, R. Kurzrock et al., "Dabrafenib in patients with melanoma, untreated brain metastases, and other solid tumours: a phase 1 dose-escalation trial," *The Lancet*, vol. 379, no. 9829, pp. 1893–1901, 2012.

[3] S. Peters, O. Michielin, and S. Zimmermann, "Dramatic response induced by vemurafenib in a BRAF V600E-mutated lung adenocarcinoma," *Journal of Clinical Oncology*, vol. 31, no. 20, pp. e341–e344, 2013.

[4] C. Horbinski, "To *BRAF* or not to *BRAF*: is that even a question anymore?" *Journal of Neuropathology and Experimental Neurology*, vol. 72, no. 1, pp. 2–7, 2013.

[5] S. Dietrich, H. Glimm, M. Andrulis, C. von Kalle, A. D. Ho, and T. Zenz, "BRAF inhibition in refractory hairy-cell leukemia," *The New England Journal of Medicine*, vol. 366, no. 21, pp. 2038–2040, 2012.

[6] C. Horbinski, "What do we know about IDH1/2 mutations so far, and how do we use it?" *Acta Neuropathologica*, vol. 125, no. 5, pp. 621–636, 2013.

[7] M. E. Hegi, A.-C. Diserens, T. Gorlia et al., "MGMT gene silencing and benefit from temozolomide in glioblastoma," *The New England Journal of Medicine*, vol. 352, no. 10, pp. 997–1003, 2005.

[8] M. V. C. Silva and R. Reid, "Gastrointestinal stromal tumors (GIST): c-kit mutations, CD117 expression, differential diagnosis and targeted cancer therapy with imatinib," *Pathology and Oncology Research*, vol. 9, no. 1, pp. 13–19, 2003.

[9] B. J. Solomon, T. Mok, D.-W. Kim et al., "First-line crizotinib versus chemotherapy in ALK-positive lung cancer," *The New England Journal of Medicine*, vol. 371, no. 23, pp. 2167–2177, 2014.

[10] C. Gridelli, F. de Marinis, F. Cappuzzo et al., "Treatment of advanced non-small-cell lung cancer with epidermal growth factor receptor (EGFR) mutation or ALK gene rearrangement: results of an International expert panel meeting of the Italian association of thoracic oncology," *Clinical Lung Cancer*, vol. 15, no. 3, pp. 173–181, 2014.

Hindawi Publishing Corporation
BioMed Research International
Volume 2015, Article ID 528304, 6 pages
http://dx.doi.org/10.1155/2015/528304

Research Article

Clinical Impact of the KL-6 Concentration of Pancreatic Juice for Diagnosing Pancreatic Masses

Kazuya Matsumoto,[1] Yohei Takeda,[1] Kenichi Harada,[1] Takumi Onoyama,[1] Soichiro Kawata,[1] Yasushi Horie,[2] Teruhisa Sakamoto,[3] Masaru Ueki,[4] Norimasa Miura,[5] and Yoshikazu Murawaki[1]

[1]*Department of Gastroenterology, Tottori University Hospital, 36-1 Nishi-cho, Yonago 683-8504, Japan*
[2]*Department of Pathology, Tottori University Hospital, Yonago 683-8504, Japan*
[3]*Department of Surgery, Tottori University Hospital, Yonago 683-8504, Japan*
[4]*Center for Promoting Next-Generation Highly Advanced Medicine, Tottori University Hospital, Yonago 683-8504, Japan*
[5]*Department of Pharmacotherapeutics, Tottori University Hospital, Yonago 683-8504, Japan*

Correspondence should be addressed to Kazuya Matsumoto; ayano0620@hotmail.co.jp

Received 26 August 2014; Accepted 25 November 2014

Academic Editor: Aurelio Ariza

Background and Aim. Pancreatic juice cytology (PJC) is considered optimal for differentially diagnosing pancreatic masses, but the accuracy of PJC ranges from 46.7% to 93.0%. The aim of this study was to evaluate the clinical impact of measuring the KL-6 concentration of pancreatic juice for diagnosing pancreatic masses. *Methods*. PJC and the KL-6 concentration measurements of pancreatic juice were performed for 70 consecutive patients with pancreatic masses (39 malignancies and 31 benign). *Results*. The average KL-6 concentration of pancreatic juice was significantly higher for pancreatic ductal adenocarcinomas (PDACs) (167.7 ± 396.1 U/mL) and intraductal papillary mucinous carcinomas (IPMCs) (86.9 ± 21.1 U/mL) than for pancreatic inflammatory lesions (17.5 ± 15.7 U/mL, $P = 0.034$) and intraductal papillary mucinous neoplasms (14.4 ± 2.0 U/mL, $P = 0.026$), respectively. When the cut-off level of the KL-6 concentration of pancreatic juice was 16 U/mL, the sensitivity, specificity, and accuracy of the KL-6 concentration of pancreatic juice alone were 79.5%, 64.5%, and 72.9%, respectively. Adding the KL-6 concentration of pancreatic juice to PJC when making a diagnosis caused the values of sensitivity and accuracy of PJC to increase by 15.3% ($P = 0.025$) and 8.5% ($P = 0.048$), respectively. *Conclusions*. The KL-6 concentration of pancreatic juice may be as useful as PJC for diagnosing PDACs.

1. Introduction

Pancreatic cancer is the fifth leading cause of cancer death and has the lowest patient survival rate of any solid cancer. The 5-year survival rate for all patients with pancreatic ductal adenocarcinoma (PDAC) is less than 3.5% [1, 2]. On the other hand, the prognosis of pancreatic inflammatory lesions such as chronic pancreatitis (CP), autoimmune pancreatitis (AIP), and other rare tumors is much better. To differentiate PDAC from these inflammatory conditions is critical, because treatment strategies and prognoses differ. Endoscopic retrograde pancreatography (ERP) is the most commonly used examination for diagnosis and cytology, evaluating the pancreatic juice obtained through a cannula for pancreatography. Pancreatic juice cytology (PJC) is thought to be the most exact diagnostic modality for intraductal papillary mucinous carcinoma (IPMC). However, the accuracy of PJC for PDAC and IPMC has not been satisfactory [3–6], and other modalities are required to improve the accuracy for diagnosing malignancy.

MUC1, membrane-associated mucin, has various types based on different glycoforms in its extracellular domain and is widely expressed in gastrointestinal tissues. Many investigations have shown that aberrant expression of MUC1 in gastrointestinal cancer tissue has clinicopathological and biological importance in cancer disease [7–9]. KL-6 mucin, one kind of MUC1, has also been investigated, and it appears to have a significant relationship with malignant tumor

Table 1: Patients' characteristics.

	Pancreatic inflammatory lesion	IPMN	IPMC	PDAC
Number of patients (M/F)	12 (8/4)	19 (15/4)	5 (1/4)	34 (18/16)
Mean age, y (range)	65.6 (36–80)	71.7 (55–82)	79.6 (77–83)	69.9 (45–83)
Mean size of mass, mm (range)	—	30.0 (4–60)	28.2 (20–50)	31.6 (6–56)
Tumor marker (serum, SD)				
CEA	2.8 ± 2.3	3.6 ± 2.8	2.1 ± 2.0	21.4 ± 70.5
CA19-9	10.4 ± 9.0	9.3 ± 30.9	17.9 ± 17.3	1534.0 ± 3729.2[a]
Span-1	7.1 ± 5.9	12.5 ± 10.1	38.8 ± 41.6	935.0 ± 4163.4
DUPAN2	33.4 ± 30.8	59.1 ± 80.6	53.6 ± 55.0	2404.7 ± 10451.1
KL-6	249.2 ± 121.9	294.6 ± 210.3	280.4 ± 262.7	453.6 ± 503.7[b]

[*] Materials of which final diagnosis was obtained by operation or clinical follow-up.
[a] $P = 0.017$ compared with pancreatic inflammatory lesion.
[b] $P = 0.027$ compared with pancreatic inflammatory lesion.

behavior, especially cancer cell invasion and metastasis in various gastrointestinal cancers [7, 8, 10–12].

Inagaki et al. have demonstrated that MUC1 can be used effectively to diagnose intraductal papillary mucinous neoplasms (IPMN) with IPMC; all PDAC specimens were positive on immunohistochemical analysis for KL-6 mucin (unpublished data [13]). Shimamoto et al. reported the usefulness of the quantitative reverse transcription-polymerase chain reaction for MUC1 in pure pancreatic juice for the detection of IPMC [14].

This study extends previous findings by prospectively investigating the clinical benefits of measuring the KL-6 concentration of pancreatic juice from a large number of consecutive patients.

2. Patients and Methods

2.1. Patients. The Tottori University Hospital Institutional Review Board approved this study involving 70 consecutive patients who underwent PJC for pathological examination of pancreatic masses between October 2011 and December 2012 at the Tottori University Hospital. This study was performed according to the guidelines described in the Helsinki Declaration for biomedical research involving human subjects. All patients provided their written, informed consent for all procedures associated with the study.

The 70 patients with pancreatic disease included 42 men and 28 women, with ages ranging from 36 to 83 years and a mean age of 70.2 years (Table 1). A malignant lesion was present in 39 patients, including 19 men and 20 women, with ages ranging from 45 to 83 years and a mean age of 70.9 years. A benign lesion was present in 31 patients, including 23 men and 8 women, with ages ranging from 36 to 82 years and a mean age of 69.4 years.

2.2. Methods. The patients were referred for PJC based on the need to evaluate them for malignancies. Cytodiagnosis of the specimen was performed by Papanicolaou's method.

Pancreatic juice was collected in an inpatient endoscopy suite as previously described [15], using a lateral-viewing endoscope (JF260V; Olympus Optical Co., Ltd, Tokyo, Japan), a cannula (M00535700; Boston Scientific Corporation, Natick, MA, USA), and a 0.035-inch hydrophilic guidewire (M00556051; Boston Scientific Corporation). Over the guidewire, the cannula was advanced into the main pancreatic duct. The guidewire was then withdrawn, and pancreatic juice was collected using a syringe with the tip of the cannula in the MPD. The aspirated material was then evaluated by a cytopathologist (YH).

2.3. KL-6 Concentration Measurement. Pancreatic juice was obtained from a pancreatic duct. After pancreatic juice was centrifuged at 1000 rpm for 5 minutes, the cell pellet was subjected to cytological examination. The supernatant (10 μL) was used for measuring the KL-6 concentration. Human KL-6 levels were determined in duplicate with a PICOLUMI KL-6 kit (EIDIA, Tokyo, Japan), an electrochemiluminescence immunoassay (ECLIA) specific for human KL-6.

The immunohistochemical procedures were performed as reported previously [16]. The appropriate dilutions of KL-6 were decided using the pancreatic tissue in the cases of PDAC and IPMC. Pancreatic tissues were obtained by surgery, and, after being treated with 10% buffered formalin, the sliced tissues were embedded in paraffin in the standard manner. Sections, 4 μm thick, were dewaxed and then stained using the following method. Each case was first checked with a hematoxylin and eosin (H&E) stain, and appropriate sections were selected for further immunohistochemical stains. They were incubated with Histofine, Heat Processor Solution pH6 (Nichirei Biosciences Inc., Tokyo, Japan), for 40 min at 100°C and incubated with the monoclonal antibody anti-KL-6 (EIDIA, Tokyo, Japan) at a dilution of 1 : 20,000.

2.4. Final Diagnosis. The final diagnosis was determined based on the PJC results, clinical follow-up, and surgical pathology, if available. Patients without a malignant disease, excluding CP, AIP, and IPMN, were followed up by imaging examinations.

All patients were observed closely for immediate or delayed complications. The severity of post-ERCP pancreatitis was determined based on the criteria of Cotton et al. [17].

2.5. Data Analysis. Information about all patients undergoing PJC has been prospectively entered into a database since October 2011. The data recorded includes the location, type,

Table 2: Diagnostic ability of PJC and/or KL-6 measurement of pancreatic juice for differentiating pancreatic malignancy from pancreatic inflammatory lesion and IPMN.

	PDAC or IPMC (n = 39) and IPMN or pancreatic inflammatory lesion (n = 31)				
	Sensitivity, %	Specificity, %	PPV, %	NPV, %	Accuracy, %
KL-6 measurement	79.5 (31/39)	64.5 (20/31)	73.8 (31/42)	71.4 (20/28)	72.9 (51/70)
PJC	82.1 (32/39)	96.8 (30/31)	97.0 (32/33)	81.1 (30/37)	88.6 (62/70)
PJC and KL-6 measurement combined	97.4[a] (38/39)	96.8 (30/31)	97.4 (38/39)	96.8 (30/31)	97.1[b] (68/70)

*Materials of which final diagnosis was obtained by operation or clinical follow-up.
[a]P = 0.025 compared with cytopathology alone.
[b]P = 0.048 compared with cytopathology alone.

size, and endoscopic features of the lesion sampled, sample adequacy, cytology results, final diagnosis, and procedure-related complications.

Diagnostic power between subgroups was compared with the χ^2 test and the t-test. A P value less than 0.05 was considered significant. Statistical analysis was performed using IBM SPSS Statistics 21 (IBM JAPAN, Tokyo, Japan).

3. Results

Table 1 shows the subjects' characteristics. The malignant group included 34 PDACs and 5 IPMCs, while the benign group included 19 IPMNs and 12 pancreatic inflammatory lesions and benign strictures of the MPD. Both patients with IPMNs and benign pancreatic ductal strictures were followed up by EUS or CT for a mean of 18.7 months (range 13–27 months) but none were found to have a malignant disease.

Figure 1 shows the average KL-6 concentration of pancreatic juice in various pancreatic diseases. The average KL-6 concentration of pancreatic juice was significantly higher for PDAC (167.7 ± 396.1 U/mL) than for pancreatic inflammatory lesions and benign strictures of the MPD (17.5 ± 15.7 U/mL, P = 0.034). Furthermore, the KL-6 concentration was significantly higher in IPMC (86.9 ± 21.1 U/mL) than in IPMN (14.4 ± 2.0 U/mL, P = 0.026).

Immunohistochemical analysis showed KL-6 positivity in the cytoplasm of PDAC cells (Figure 2(a)) and IPMC cells (Figure 2(b)).

Figure 3 shows the receiver-operating characteristic (ROC) curve of pancreatic malignancy, which included PDAC and IPMC. The cut-off level of KL-6 was determined to be 16 U/mL for the differentiation of pancreatic malignancy from pancreatic inflammatory lesions and IPMN by the ROC curve. The AUC of the KL-6 analysis was 0.752. When comparing the KL-6 concentration in IPMC with that in IPMN, the ROC curve showed that the optimal cut-off value was from 32.7 to 39.4 U/mL. The AUC of KL-6 analysis was 1.000, an excellent test (data not shown).

Table 2 summarizes the diagnostic ability of PJC and/or KL-6 analysis to differentiate malignant disease (PDAC and IPMC) from benign disease (IPMN and pancreatic inflammatory lesion). The sensitivity, specificity, positive predictive value, negative predictive value, and accuracy of

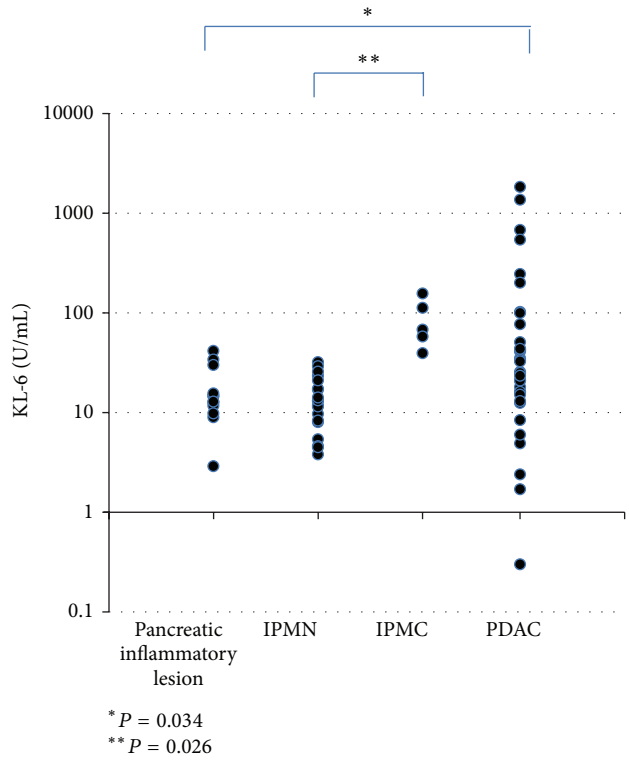

Figure 1: The KL-6 concentrations of pancreatic juice in various pancreatic diseases.

KL-6 concentration of pancreatic juice alone were 79.5%, 64.5%, 73.8%, 71.4%, and 72.9%, respectively, whereas those of pancreatic juice cytology alone were 82.1%, 96.8%, 97.0%, 81.1%, and 88.6%, respectively. Of the remaining 7 patients who remained undiagnosed by cytological assessment, the KL-6 concentration of pancreatic juice was measured in 6 (85.7%). Adding the KL-6 concentration of pancreatic juice to standard cytological assessment increased the sensitivity and accuracy of PJC by 15.3% (P = 0.025) and 8.5% (P = 0.048), respectively.

Table 3 shows the diagnostic ability of PJC and/or KL-6 analysis for differentiating IPMC from IPMN. The sensitivity, specificity, positive predictive value, negative predictive value, and accuracy of KL-6 concentration alone, and with PJC,

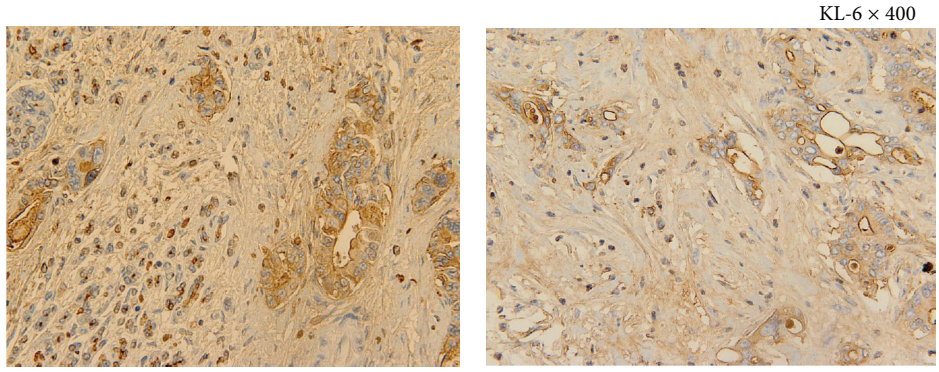

Figure 2: (a) Immunohistochemical staining of KL-6 (KL-6 × 400). KL-6 positivity is observed in the cytoplasm of PDAC cells. (b) Immunohistochemical staining of KL-6 (KL-6 × 400). KL-6 positivity is observed in the cytoplasm of IPMC cells.

Table 3: Diagnostic ability of PJC and/or KL-6 measurement of pancreatic juice for differentiating IPMC from IPMN.

	IPMC (n = 5) and IPMN (n = 19)				
	Sensitivity, %	Specificity, %	PPV, %	NPV, %	Accuracy, %
KL-6 measurement	100 (5/5)	100 (19/19)	100 (5/5)	100 (19/19)	100 (24/24)
PJC	100 (5/5)	100 (19/19)	100 (5/5)	100 (19/19)	100 (24/24)
PJC and KL-6 measurement combined	100 (5/5)	100 (19/19)	100 (5/5)	100 (19/19)	100 (24/24)

* Materials of which final diagnosis was obtained by operation or clinical follow-up.

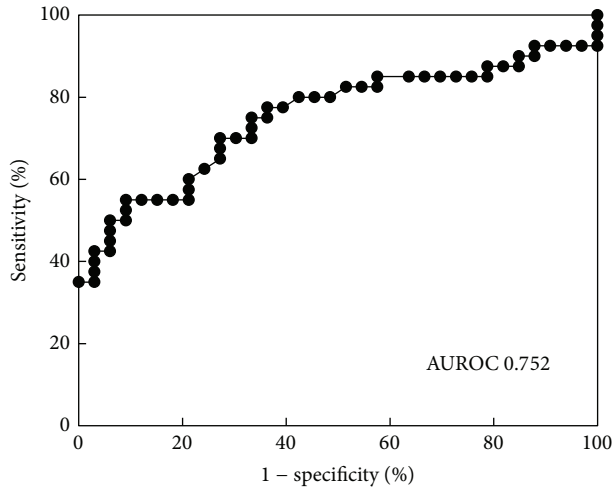

Figure 3: ROC curve of the KL-6 concentration of pancreatic juice for pancreatic malignancy. The cut-off level of KL-6 determined from the receiver-operating characteristic curve for differentiating pancreatic malignancy from benign stricture of the main pancreatic duct and IPMN is 16 U/mL. The AUC of the KL-6 analysis is 0.752.

were all 100% when the cut-off level of KL-6 concentration was from 32.7 to 39.4 U/mL for differentiating IPMC from IPMN.

Ten patients (14.3%) in this study developed complications following PJC, all of which were mild pancreatitis. All patients were cured with conservative treatment.

4. Discussion

Various tumor markers, such as CEA, CA19-9, Span-1, and DUPAN-2, have been widely used for detecting PDAC and IPMC [18]. Several authors have reported that the serum KL-6 concentration was measured in 44% of pancreatic cancer patients [19] and that the KL-6 (MUC1) concentration of PJC specimens can be measured [13, 14, 20]. However, published reports have included relatively small numbers of patients with PDAC and IPMC.

In the present study, a high KL-6 concentration was seen in 79.5% of patients with PDAC and IPMC. The sensitivity and accuracy of pancreatic juice cytology for the diagnosis of PDAC and IPMC were significantly improved by adding the KL-6 concentration. Among 7 cases whose PJC results were inconclusive or negative, 6 had elevated KL-6 concentrations in pancreatic juice and were finally diagnosed as having PDAC and IPMC. These findings indicate that the KL-6 concentration of pancreatic juice is clinically useful when PJC specimens are inadequate, making differentiation between malignant and benign conditions difficult. In addition, the KL-6 concentration is useful for discriminating IPMC from

IPMN, because the AUC of the KL-6 concentration of pancreatic juice was 1.000. Thus, when IPMN is suspected based on the clinical course or imaging findings, the KL-6 concentration of pancreatic juice may be helpful to exclude IPMN.

The measurement of KL-6 concentration did not affect the diagnostic power of PJC because the KL-6 concentration was checked using the pancreatic juice from which the cell pellet was removed for cytological examination.

Previous reports have shown that PJC has yielded sensitivities for pancreatic cancer that ranged from 33.3% to 67%, with specificity of 100%, PPV of 100%, NPV of 27.3% to 98%, and accuracy of 46.7% to 94% [4, 15, 21, 22]. A recent study showed the usefulness of PJC for pancreatic-ductal strictures, with sensitivity of 71.4% to 93%, specificity of 100%, PPV of 100%, NPV of 75% to 84.4%, and an accuracy of 88.8% to 94% [15, 22]. In the present prospective study, PJC showed excellent diagnostic ability for malignant pancreatic tumors [15].

The major complication of procedures associated with PJC is pancreatitis. In the present series, 10 patients (14.3%) developed mild pancreatitis after PJC; thus, we must restrict PJC to when we cannot acquire the evidence by endoscopic ultrasound-guided fine needle aspiration biopsy.

In conclusion, the KL-6 concentration of pancreatic juice strengthened the diagnostic ability of PJC for pancreatic tumors.

Conflict of Interests

The authors declare that there is no conflict of interests regarding the publication of this paper.

References

[1] B. Gudjonsson, "Cancer of the pancreas. 50 years of surgery," *Cancer*, vol. 60, no. 9, pp. 2284–2303, 1987.

[2] A. L. Warsaw and C. Fernandez del Castillo, "Pancreatic carcinoma," *The New England Journal of Medicine*, vol. 326, pp. 455–465, 1992.

[3] N. Uchida, H. Kamada, K. Tsutsui et al., "Utility of pancreatic duct brushing for diagnosis of pancreatic carcinoma," *Journal of Gastroenterology*, vol. 42, no. 8, pp. 657–662, 2007.

[4] T. Wakatsuki, A. Irisawa, M. S. Bhutani et al., "Comparative study of diagnostic value of cytologic sampling by endoscopic ultrasonography-guided fine-needle aspiration and that by endoscopic retrograde pancreatography for the management of pancreatic mass without biliary stricture," *Journal of Gastroenterology and Hepatology*, vol. 20, no. 11, pp. 1707–1711, 2005.

[5] M. Kawai, K. Uchiyama, M. Tani et al., "Clinicopathological features of malignant intraductal mucinous tumors of the pancreas: the differential diagnosis from benign entities," *Archives of Surgery*, vol. 139, no. 2, pp. 188–192, 2004.

[6] K. Ohuchida, K. Mizumoto, D. Yamada et al., "Quantitative analysis of human telomerase reverse transcriptase in pancreatic cancer," *Clinical Cancer Research*, vol. 12, no. 7 I, pp. 2066–2069, 2006.

[7] S. Nakamori, D. M. Ota, K. R. Cleary, K. Shirotani, and T. Irimura, "MUC1 mucin expression as a marker of progression and metastasis of human colorectal carcinoma," *Gastroenterology*, vol. 106, no. 2, pp. 353–361, 1994.

[8] Y. Hiraga, S. Tanaka, K. Haruma et al., "Immunoreactive MUC1 expression at the deepest invasive portion correlates with prognosis of colorectal cancer," *Oncology*, vol. 55, no. 4, pp. 307–319, 1998.

[9] S. Yonezawa, M. Horinouchi, M. Osako et al., "Gene expression of gastric type mucin (MUC5AC) in pancreatic tumors: its relationship with the biological behavior of the tumor," *Pathology International*, vol. 49, no. 1, pp. 45–54, 1999.

[10] H. Kashiwagi, H. Kijima, S. Dowaki et al., "DF3 expression in human gallbladder carcinoma: significance for lymphatic invasion," *International Journal of Oncology*, vol. 16, no. 3, pp. 455–459, 2000.

[11] J. Lüttges, B. Feyerabend, T. Buchelt, M. Pacena, and G. Klöppel, "The mucin profile of noninvasive and invasive mucinous cystic neoplasms of the pancreas," *The American Journal of Surgical Pathology*, vol. 26, no. 4, pp. 466–471, 2002.

[12] H.-K. Zhang, Q.-M. Zhang, T.-H. Zhao, Y.-Y. Li, and Y.-F. Yi, "Expression of mucins and E-cadherin in gastric carcinoma and their clinical significance," *World Journal of Gastroenterology*, vol. 10, no. 20, pp. 3044–3047, 2004.

[13] Y. Inagaki, H. Xu, M. Nakata et al., "Clinicopathology of sialomucin: MUC1, particularly KL-6 mucin, in gastrointestinal, hepatic and pancreatic cancers," *BioScience Trends*, vol. 3, no. 6, pp. 220–232, 2009.

[14] T. Shimamoto, M. Tani, M. Kawai et al., "MUC1 is a useful molecular marker for malignant intraductal papillary mucinous neoplasms in pancreatic juice obtained from endoscopic retrograde pancreatography," *Pancreas*, vol. 39, no. 6, pp. 879–883, 2010.

[15] K. Matsumoto, Y. Takeda, K. Harada, Y. Horie, K. Yashima, and Y. Murawaki, "Effect of pancreatic juice cytology and/or endoscopic ultrasound-guided fine-needle aspiration biopsy for pancreatic tumor," *Journal of Gastroenterology and Hepatology*, vol. 29, no. 1, pp. 223–227, 2014.

[16] Y. Ohtsuki, N. Nakanishi, J. Fujita et al., "Immunohistochemical distribution of SP-D, compared with that of SP-A and KL-6, in interstitial pneumonias," *Medical Molecular Morphology*, vol. 40, pp. 163–167, 2007.

[17] P. B. Cotton, G. Lehman, J. Vennes et al., "Endoscopic sphincterotomy complications and their management: an attempt at consensus," *Gastrointestinal Endoscopy*, vol. 37, no. 3, pp. 383–393, 1991.

[18] K. Watanabe, T. Oochiai, S. Kikuchi et al., "Dermokine expression in intraductal papillary-mucinous neoplasm and invasive pancreatic carcinoma," *Anticancer Research*, vol. 32, no. 10, pp. 4405–4412, 2012.

[19] N. Kohno, M. Akiyama, S. Kyoizumi, M. Hakoda, K. Kobuke, and M. Yamakido, "Detection of soluble tumor-associated antigens in sera and effusions using novel monoclonal antibodies, KL-3 and KL-6, against lung adenocarcinoma," *Japanese Journal of Clinical Oncology*, vol. 18, no. 3, pp. 203–216, 1988.

[20] H. Ito, T. Endo, T. Oka et al., "Mucin expression profile is related to biological and clinical characteristics of intraductal papillary-mucinous tumors of the pancreas," *Pancreas.*, vol. 30, no. 4, pp. e96–e102, 2005.

[21] A. Nakaizumi, M. Tatsuta, H. Uehara et al., "Usefulness of simple endoscopic aspiration cytology of pancreatic juice for diagnosis of early pancreatic neoplasm: a prospective study,"

Digestive Diseases and Sciences, vol. 42, no. 8, pp. 1796–1803, 1997.

[22] H. Uehara, K. Tatsumi, E. Masuda et al., "Scraping cytology with a guidewire for pancreatic-ductal strictures," *Gastrointestinal Endoscopy*, vol. 70, no. 1, pp. 52–59, 2009.

Hindawi Publishing Corporation
BioMed Research International
Volume 2015, Article ID 131685, 13 pages
http://dx.doi.org/10.1155/2015/131685

Research Article

Ki-67 Expression in CRC Lymph Node Metastasis Does Not Predict Survival

Sandra F. Martins,[1,2,3] Ricardo Amorim,[1,2] Sílvia Coelho Mota,[1] Luís Costa,[1] Fernando Pardal,[4] Mesquita Rodrigues,[5] and Adhemar Longatto-Filho[1,2,6,7]

[1] *Life and Health Sciences Research Institute (ICVS), School of Health Sciences, University of Minho, Campus of Gualtar, 4710-057 Braga, Portugal*
[2] *ICVS/3B's-PT Government Associate Laboratory, Braga/Guimarães, Campus of Gualtar, 4710-057 Braga, Portugal*
[3] *Surgery Department, Hospitalar Center Trás-os-Montes e Alto Douro, Unidade Hospitalar de Chaves, Avenida Dr. Francisco Sá Carneiro, 5400-279 Chaves, Portugal*
[4] *Pathology Department, Braga Hospital, Sete Fontes, São Victor, 4710-243 Braga, Portugal*
[5] *Coloproctology Unit, Braga Hospital, Sete Fontes, São Victor, 4710-243 Braga, Portugal*
[6] *Laboratory of Medical Investigation (LIM) 14, Faculty of Medicine, University of Sao Paulo, 01246-903 São Paulo, SP, Brazil*
[7] *Molecular Oncology Research Centre, 14784-400 Barretos, SP, Brazil*

Correspondence should be addressed to Adhemar Longatto-Filho; longatto@ecsaude.uminho.pt

Received 4 December 2014; Accepted 2 February 2015

Academic Editor: Konstantinos Arnaoutakis

Colorectal cancer is one of the most common malignancies and a leading cause of cancer death worldwide. Molecular markers may improve clinicopathologic staging and provide a basis to guide novel therapeutic strategies which target specific tumour-associated molecules according to individual tumour biology; however, so far, no ideal molecular marker has been found to predict disease progression. We tested Ki-67 proliferation marker in primary and lymph node metastasis of CRC. We observed a statistical significant difference between the positive rates of neoplastic cells positively stained by Ki-67 in both sites, with remarkable increased number of Ki-67 positive cells in primary tumor cells compared to cancer cells that invaded lymph nodes. We can speculate that the metastatic CRC in lymph node can be more resistant to the drugs that target cellular division.

1. Introduction

Colorectal cancer (CRC) is one of the most common malignancies and a leading cause of cancer death worldwide [1–5]. European countries rank the highest in the global statistics, in terms of both CRC incidence and mortality [4, 6], although in recent years, a decline in CRC mortality rates has been observed, mostly due to improvement in earlier diagnosis and treatment [4, 7].

In Portugal, official data revealed that CRC is the second most common type of cancer, in both men and women, and in 2008 it was responsible for 18.7% and 15.1%, respectively, of all cancer in Portugal [8]. Regarding mortality, unlike European data [9], there was an average increase of 3% from 2000 to 2005 [10] and in 2012 incidence and mortality rates are higher than European rates [11].

For CRC, the pathologic clinical stage is currently the single most important prognostic factor [1–4, 12, 13], correlating with long-term survival [4, 14–17], although it does not fully predict individual clinical outcome [4, 17–19]. This is particularly true for those tumours with intermediate stage disease (T3-T4N0M0) [19], where one-third of patients with tumour-free lymph nodes have recurrences, and therefore adjuvant chemotherapy may be beneficial [20]. In this group, carcinoma cells are not detected in lymph nodes by conventional staging methods in 24% of patients. So, lymphatic staging is essential to improve treatment of these patients, indeed one-third of the patients submitted to curative intent

surgery die of local and/or distant tumour recurrence [4, 15]. Abdominal lymph nodes (38%) are the second most frequent site of metastasis (38%), just after liver, that is, the organ most frequently involved (38–60% of cases) and followed by lung (38%) and peritoneum (28%) [4, 13].

A common feature of all cancers is the imbalance that exists between the proliferative activity and cell death; therefore, the evaluation of cell proliferation rate may be interesting in the study and characterization of tumours [21]. Some molecules, such as the Ki-67 protein, permit this assessment and are used as markers of proliferation because Ki67 expression is dependent of cell division rate; thus, overexpression of these markers may suggest a disruption in the proliferation mechanism leading to the appearance of tumours [21].

Ki-67 protein, when used to evaluate the percentage of dividing cells, allows us to determine neoplastic growth [21] and has been documented to correlate with neoplastic progression [22] showing different levels of expression between normal mucosa, adenoma, and adenocarcinoma [23], verifying a progressive increasing of positive Ki-67 expression from the first (normal mucosa) to the last part of the tissue (adenocarcinoma) [22, 24, 25].

Other studies correlate Ki-67 with the degree of malignancy, tumour invasiveness [25, 26], metastatic potential [21], patient survival, and the risk of relapse [27, 28]. Thus, a high Ki-67 expression in tumour cells is assumed to correlate with a poor tumour differentiation [24, 26] and an increased infiltration of the bowel wall (pT) [26]. Micev et al. [29] demonstrated that there is an association between Ki-67 expression and a less effective response in patients undergoing chemotherapy.

Other correlations with clinical and pathological data were also investigated and a correlation was detected between a high expression of this protein and the following variables: patient's age [25], tumour size [30], tumour localization [28], dysplasia degree [30], the presence of lymph node metastasis [22, 25, 28], and TNM [25] and Dukes [28] classification. Thus, the younger is the patient, the greater is the cellular proliferation and the lower is the degree of differentiation; with increasing malignancy a increased frequency of invasion and metastasis are observed and thus poorer prognosis [25].

In CRC, the analysis of colon adenomas has shown a different pattern for Ki-67 expression between normal tissue, adenomas, and adenocarcinomas, being limited to the crypts in normal tissue and expressed both in the crypts and in the surface epithelium in adenomatous polyps (tubular, villous) [31] and distributed homogeneously in adenocarcinoma [32]. Nussrat et al. [30] also observed an increase in Ki-67 rates being associated with the growth and rise of dysplasia in adenomas.

Studies on CRC indicated Ki-67 as a prognostic marker as the survival rate for patients with high expression of Ki-67 is significantly lower compared to those with low expression [25, 33–35] and a predictor of CRC recurrence [36]. Also significant associations were found between higher index of Ki-67 and increased tumour penetration [35, 37], the presence of lymph node [22, 35] and distant [35] metastasis, advanced TNM stage [32, 35], highest degree of differentiation, and subtypes of adenocarcinoma other than mucinous [38].

However, not all studies are in agreement, and no correlations were observed with patient age, gender, tumour location [22, 30, 33, 39], and the type of adenoma [30] for some of them. Allegra et al. [40] described inverse associations, with a lower rate of Ki-67 to be associated with greater recurrence and worse overall survival and Jansson and Sun [39] did not find any associations between index Ki-67 and clinicopathological data or prognosis.

Regarding the use of Ki-67 in CRC lymph node metastasis, no information is available, and the only similar study found compares Ki-67 index in primary tumour with peritoneal metastasis and had observed a lower proliferative index in metastasis compared with the primary tumour [41]. However, in other types of cancer, in particular breast cancer, a higher Ki-67 index was found in lymph node metastasis than in primary tumours [42–44], suggesting greater aggressiveness of these [42] and that the use of Ki-67 in lymph node metastasis may be important in selecting the appropriate treatment for certain subgroups of patients [45].

Therefore, given the limited information concerning Ki-67 index in CRC lymph nodes metastasis and primary tumour, this study becomes relevant to determine Ki-67 index in the primary tumour and, respectively, lymph nodes metastasis whilst trying to establish correlations with this and clinicopathological data and the patient's prognosis.

2. Materials and Methods

2.1. CRC Tumour Series. Tissue samples and data from 672 patients treated in Hospital de Braga, Portugal, between January 1, 2005, and January 1, 2010, with CRC diagnosis were collected prospectively. Tumour localization was recorded and classified as colon and rectum (between anal verge and 15 cm at rigid rectoscopy).

The histological type of CRC was classified by two experienced pathologists and tumour staging was graded according to the TNM classification, sixth edition [46]. Tissue microarrays (TMAs) were constructed with the CRC series of formalin-fixed, paraffin-embedded tissues and analyzed by immunohistochemistry. Prior to tumour construction, hematoxylin and eosin sections were reviewed to select representative areas of the tumour and normal-adjacent tissue. Each case was represented in the TMA by at least two cores of 0.6 mm.

2.2. Lymph Node Metastasis Series. From the same series of colorectal cancer, patients with the diagnosis of CRC lymph node metastasis were selected and a series of 210 patients were also collected.

Additionally, 35 patients, with the diagnosis of CRC but without lymph node metastasis, were also selected for control of protein lymph node expression (stages T1 and T2/N0).

TMAs were constructed with the lymph node metastasis series of formalin-fixed, paraffin-embedded tissues and analyzed by immunohistochemistry. Each case was represented in the TMA by at least two cores of 0.6 mm.

The study protocol was approved by the Ethics Committee of Hospital de Braga and ICVS.

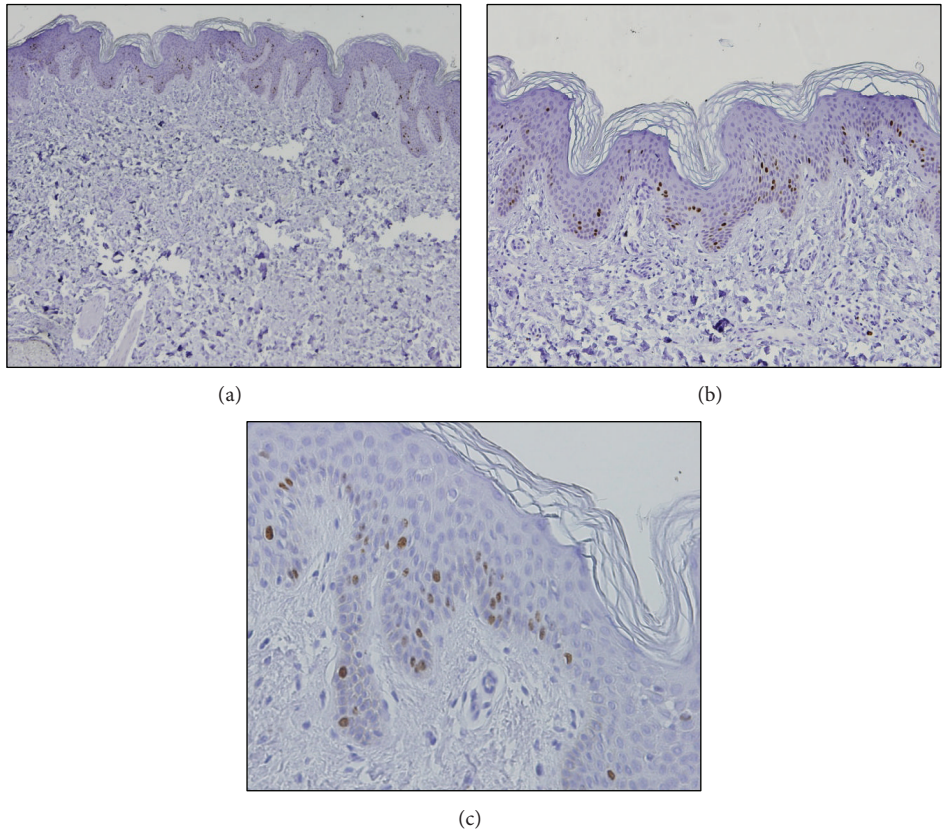

(a) (b) (c)

Figure 1: Immunohistochemical expression of Ki-67 in samples of skin: (a) original magnification ×40; (b) original magnification ×100; (c) original magnification ×200.

Table 1: Detailed aspects of the immunohistochemical procedure used to visualise the Ki-67.

Protein marker	Antigen retrieval	Peroxidase inactivation	Detection system	Antibody		
				Company	Dilution	Incubation period
Ki-67	Citrate Buffer 0.01 M pH = 6.0	3% H_2O_2 in methanol, 10 min.	RTU Vectastain ABC elite Reagent	GenNova	1 : 200	Overnight

2.3. Immunohistochemistry. CRC and lymph nodes TMAs protein expression was evaluated by immunohistochemistry. Detailed information is given in Table 1. After the immunohistochemical procedure, the slides were evaluated and then photographed under a microscope.

For positive control of the expression of Ki-67 a sample of the skin was used (Figure 1).

2.4. Immunohistochemical Evaluation. The percentage of immunoreactive cells was determined (which was named the Ki-67 index), counting a total of 100 cells per section at ×20 magnification, and each one was assigned a score from 0 to 3, as previously described by Pinheiro et al. [47].

Immunoreaction final score was defined as the sum of both parameters and grouped as negative (0-1) and positive (≥2). Evaluation of protein expression was performed by blind analysis by two observers and discordant cases were discussed in a double-head microscope in order to determine a final score.

2.5. Statistical Analysis. All data were analyzed using the Statistical Package for the Social Sciences, version 19.0 (SPSS Inc., Chicago, IL, USA). All comparisons were examined for statistical significance using Pearson's chi-square (χ^2) test and Fisher's exact test (when $n < 5$), with the threshold for significance $P < 0.05$. Survival curves were determined for overall survival by the Kaplan-Meier method and log-rank test.

Expression differences between lymph node metastasis and primary CRC were tested with McNemar test, with the threshold for significance $P < 0.05$.

3. Results

3.1. Ki-67 Expressions in CRC Samples. A total of 672 samples were organized into TMAs, including tumour and normal adjacent epithelium (NA^E). Sections were evaluated for immunoexpression and the obtained results are given in Table 2, which summarizes the frequency of Ki-67 expression in tumour cells and NA^E.

Table 2: Pattern of protein staining in tumour versus normal adjacent epithelium.

Protein marker		Immunoreaction	
Ki-67	*n*	Positive *n* (%)	*P*
CCR			
NA^E	140	34 (24.3)	**<0.001**
Tumour	506	345 (68.2)	
Lymph node			
Normal	2	2 (100.0)	0.502*
Metastasis	109	60 (55.0)	

NA^E: normal adjacent epithelium; *n*: total number of cases with and without expression of Ki-67; positive *n* (%): total number of cases with expression of Ki-67 and respective percentage.
*Comparisons were examined for statistical significance using Fisher's exact test (when $n < 5$).

We observed that 68.2% ($n = 345$) of the samples of tumour tissue were positive for Ki-67, as compared to 24.3% ($n = 34$) of samples of the samples of NA^E. Thus, it was concluded that the Ki-67 expression is significantly higher in tumour tissue ($P < 0.05$), such as is shown in Table 2.

Figure 2 shows representative cases of positive staining for Ki-67 in tumour cells and in NA^E.

3.2. Associations between Ki-67 Expressions in CRC Tissues and Clinicopathological Data. The associations observed between the expression of Ki-67 in CRC and the clinicopathological data are described in Tables 3 and 4.

Analyzing the results in these tables, we found an association between the expression of Ki-67 and "tumour penetration" ($P = 0.013$) and "tumour differentiation" ($P = 0.049$).

For "tumour penetration," we observed a decreasing expression of Ki-67 from the pT1 (79.3%) to pT3 (68.1%) tumours and then a rise in expression for adenocarcinoma with invasion of other organs or structures (pT4) (73.1%).

Regarding "tumour differentiation," we observed an increasing expression of Ki-67 from the well-differentiated to the undifferentiated tumours, namely, well differentiated (64.6%), moderately differentiated (70.2%), and poorly differentiated (85.1%). Conversely, undifferentiated tumours showed lower expression of Ki-67 compared to the degree of differentiation mentioned above.

We did not find any statistically significant relationship between clinicopathological data and Ki-67 index in CRC for the remaining assessed data.

3.3. Overall Survival Curves according to Ki-67 Expressions in CRC Tissues. No statistically significant association was observed for Ki-67 expression in CRC tissues ($P = 0.321$ for CRC, and $P = 0.213$ and $P = 0.874$ for colon cancer and rectal cancer evaluated separately, resp.), as observed in Figure 4.

Relatively to CRC, survival of patients that are negative for Ki-67 is 65.6% with a medium of survival of 65.0 ± 2.8 months after diagnosis, while Ki-67 positive patients present a survival of 62.3% with a medium of survival of 62.1 ± 2.1 months after diagnosis, such as is shown in Table 5.

3.4. Ki-67 Expressions in Lymph Node Metastasis Samples. A total of 210 samples were organized into TMAs. Additionally 35 patients, with the diagnosis of CRC but without lymph node metastasis, were also selected for control of protein lymph node expression (stages T1 and T2 N0). Sections were evaluated for immunoexpression and the obtained results are given in Table 2, which summarizes the frequency of Ki-67 expression in "normal" lymph nodes and lymph node metastasis.

We observed that 55.5% ($n = 60$) of the samples of lymph node metastasis were positive for Ki-67, compared to 100% ($n = 2$) of samples of the samples of "normal" lymph nodes. No significant correlation was observed ($P = 0.502$), such as is shown in Table 2 and Figure 3.

3.5. Associations between Ki-67 Expressions in Lymph Node Metastasis and Clinicopathological Data. The associations observed between the expression of Ki-67 in lymph node metastasis of CRC and the clinicopathological data are described in Tables 3 and 4. Analyzing these tables, we did not find any statistically significant relationship between clinicopathological data and Ki-67 index in lymph node metastasis.

3.6. Overall Survival Curves according to Ki-67 Expressions in Lymph Node Metastasis. Relatively to overall survival, patients with negative Ki-67 index present a survival of 65.3% with a medium of survival of 63.4±5.2 months after diagnosis, while Ki-67 index positive patients present a survival of 51.6% with a medium of survival of 50.0±4.6 months after diagnosis, such as is shown in Table 5.

No statistically significant association was observed for Ki-67 expression in CRC lymph node metastasis tissues ($P = 0.131$ for CRC, $P = 0.127$ and $P = 0.809$ for colon cancer and rectal cancer evaluated separately, resp.); however, a tendency for the relationship between a positive Ki-67 index and a lower overall survival was observed, such as is shown in Figure 5.

3.7. Comparing Ki-67 Index Expressions in Lymph Node Metastasis and Primary Tumour. Table 6 represents a comparison between Ki-67 index in the primary tumour and the respective lymph node metastasis. Analyzing this table, it appears that 12 of the cases with negative Ki-67 index in the primary tumour have positive index in lymph node metastasis and that 29 of those with positive index in the primary tumour have a negative index in lymph node metastasis, for a total of 41 discordant cases. This means that there is a significant difference ($P = 0.012$) between the index of Ki-67 in primary tumour and the respective lymph node metastasis. A smaller number of cases of positive Ki-67 index were also observed in lymph node metastasis ($n = 61$; 57.5%) than in the primary tumour ($n = 78$; 73.6%) as is schematized in Figure 6.

4. Discussion

The mechanisms that culminate in CRC development, growth, and metastization are still not fully understood.

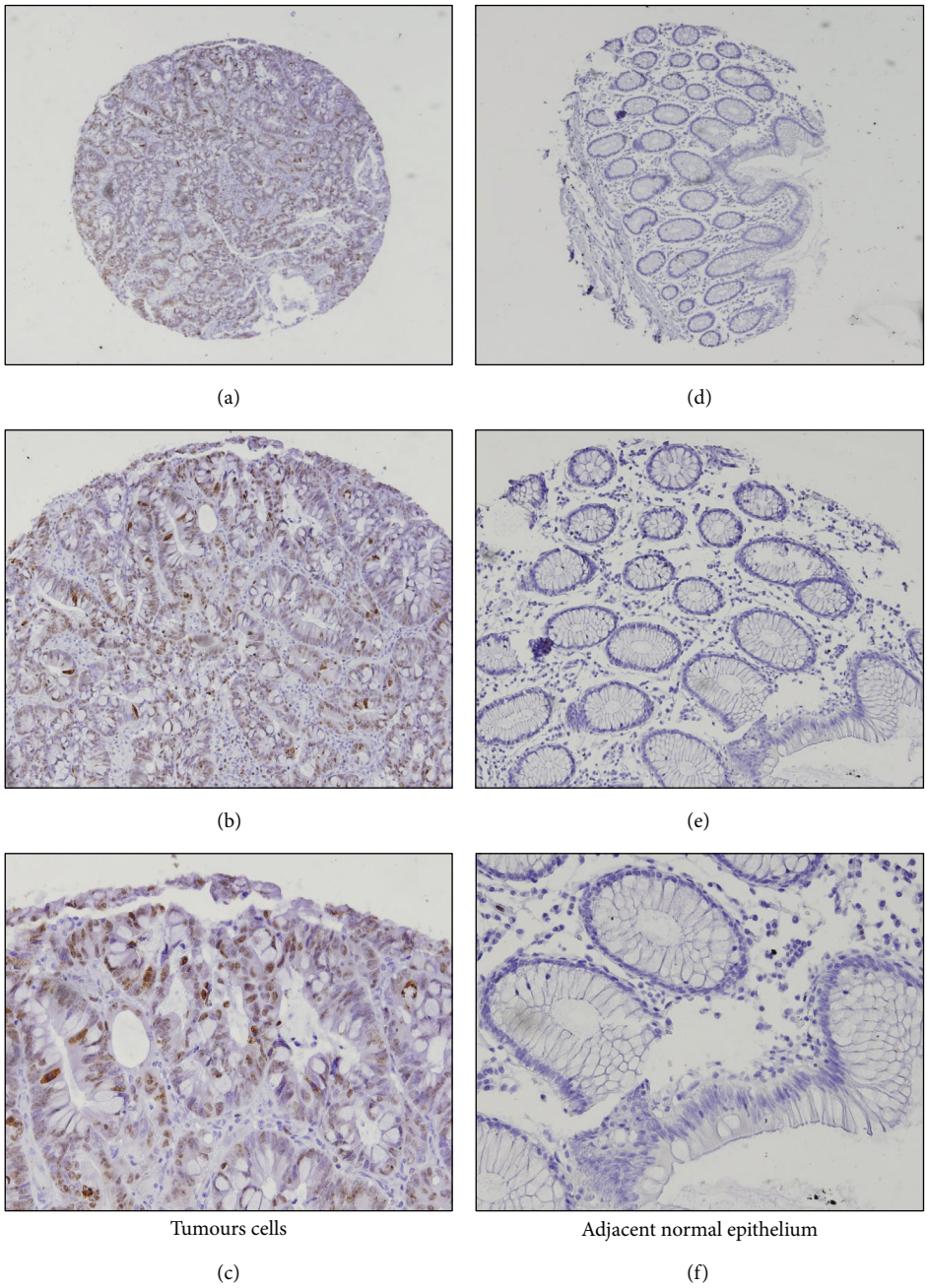

Figure 2: Immunohistochemical expression of Ki-67 in colorectal cancer samples: ((a) and (d)) original magnification ×40; ((b) and (e)) original magnification ×100; ((c) and (f)) original magnification ×200.

However, common to all cancers are the loss of cellular differentiation and the imbalance between proliferation and cell death; these processes, involved in carcinogenesis, due to its significance, are increasingly being targeted for study.

Ki-67 protein has been widely used as a marker of tumour proliferation [21, 48, 49], and several studies compare Ki-67 index with clinicopathological data and follow-up in CCR [22, 32, 35–40]. With regard to Ki-67 index in lymph node metastasis, as far as we know, this is the first study realized in CRC and, the more similar that we found in literature is the study of Yamauchi et al. [41], which compares Ki-67 index in primary CRC tumours with the respective nodules of peritoneal metastization.

In this study, we determine immunohistochemical expression of Ki-67 protein in CRC samples and respective lymph node metastasis and intended to evaluate possible associations between these expressions and several clinicopathological parameters and patient survival. Further comparison was performed between Ki-67 index in CRC and respective lymph nodes metastasis.

Regarding Ki-67 expression in CRC samples and NA^E we observed a significant expression of Ki-67 in the first over

Table 3: Assessment of correlation between Ki-67 expression and clinical data.

	Ki-67 in CRC			Ki-67 in lymph node metastasis		
	n	Positive *n* (%)	*P*	*n*	Positive *n* (%)	*P*
Gender						
Male	307	212 (69.1)	0.675	71	41 (57.7)	0.438
Female	180	121 (67.2)		38	19 (50.0)	
Age						
≤45	23	14 (60.9)	0.491	7	4 (57.1)	1.000*
>45	464	319 (68.8)		102	56 (54.9)	
Presentation						
Asymptomatic	88	63 (71.6)	0.474	19	8 (42.1)	0.212
Symptomatic	399	270 (67.7)		90	52 (57.8)	
Localization						
Colon	353	240 (68.0)	0.764	90	50 (55.5)	0.841
Rectum	134	93 (69.4)		19	10 (52.6)	
Macroscopic cancer type						
Polypoid	253	171 (67.6)	0.178	45	20 (44.4)	0.373
Ulcerative	111	76 (68.5)		31	20 (64.5)	
Infiltrative	38	22 (57.9)		11	6 (54.5)	
Exophytic	39	32 (82.1)		12	7 (58.3)	
Vilosous	2	2 (100.0)		1	0 (0)	
CEA (ng/mL)						
≤10	337	229 (68.0)	0.750	67	34 (50.7)	0.757
>10	73	51 (69.1)		22	12 (54.5)	

*Comparisons were examined for statistical significance using Fisher's exact test (when $n < 5$).

the second ($P < 0.001$). These results were expected, since due to its role as a marker of cellular proliferation, a higher expression was expected in tumour tissue than in normal epithelium. These results were also demonstrated by Lin et al. [25].

The same analysis was made for lymph nodes metastasis and "normal" lymph nodes, but no significant correlation was observed ($P = 0.502$). Possible explanations are the fact that "normal" lymph nodes are not truly normal, but of patients with CRC without lymph nodes metastasis (T1 and T2/N0) so this is a bias to be considered since they may already be under the influence of the tumour environment. Another fact that may influence this result is the small size sample of the "normal" lymph node, so further studies need to be realized with bigger samples and normal lymph nodes for control.

When analyzing the correlation of Ki-67 expression in CRC with pathological data, we found an association between the expression of Ki-67 and "tumour penetration" ($P = 0.013$) and "tumour differentiation" ($P = 0.049$).

For "tumour penetration," we observed a decreasing expression of Ki-67 from the pT1 (79.3%) to pT3 (68.1%) tumours and then a rise in expression for adenocarcinoma with invasion of other organs or structures (pT4) (73.1%).

The decreased expression of Ki-67 with the increasing tumour penetration is conflicting since we would expect an increase in expression with increasing tumour wall penetration, as is observed for pT4. But as the Ki-67 is only a marker of cellular proliferation, other factors may influence this outcome.

Regarding "tumour differentiation," we observed an increasing expression of Ki-67 from the well-differentiated to the undifferentiated tumours; conversely, undifferentiated tumours showed lower expression of Ki-67 compared to the degree of differentiation mentioned above.

As was observed by some authors [38, 50], the more undifferentiated is the tumour, the higher is the rate of cell proliferation and therefore Ki-67 index. This is not consistent with our findings; however, since the lower expression in undifferentiated tumours may be explained by the small size of this sample, further studies with larger series of undifferentiated tumours are necessary.

When analyzing the correlation of Ki-67 expression in lymph node metastasis with pathological data, any statistically significant relationship was observed. In the literature, no other studies realized in lymph node metastasis of CRC were found, and similar results were observed by Jansson and Sun [39] on the primary tumour but contradict the other studies analyzed [22, 25, 28–30, 32, 35–40].

In our series, we have not observed association between Ki-67 expression and patient's survival, for CRC ($P = 0.321$) and for lymph node metastasis ($P = 0.131$), series and the same was true when we considered separately colon cancer and rectal cancer. This was corroborated by the observations of Jansson and Sun [39]; however, these findings contradict, in part, the report of Valera et al. [35] that studied primary CRC tumours, and also contradict studies made with lymph node metastasis from breast cancer [43–45] and prostate

Table 4: Assessment of correlation between Ki-67 expression and pathological data.

		Ki-67 in CRC			Ki-67 in lymph node metastasis	
	n	Positive *n* (%)	*P*	*n*	Positive *n* (%)	*P*
Tumor size						
≤4.5 cm	279	190 (68.1)	0.519	65	39 (60.0)	0.211
>4.5 cm	179	127 (70.9)		40	19 (47.5)	
Histological type						
Adenocarcinoma	409	281 (68.7)		88	46 (52.3)	
Mucinous adenocarcinoma	50	32 (64.0)	0.665	13	8 (61.5)	0.483
Invasive adenocarcinoma	24	18 (75.0)		6	4 (66.7)	
Signet ring and mucinous	4	2 (50.0)		2	2 (100.0)	
Differentiation						
Well differentiated	209	135 (64.6)		38	19 (50.0)	
Moderately differentiated	208	146 (70.2)	**0.049**	46	26 (56.5)	0.670
Poorly differentiated	47	40 (85.1)		23	14 (60.9)	
Undifferentiated	4	3 (75.0)		1	1 (100.0)	
Tumour penetration						
pT1	34	23 (79.3)		2	2 (100.0)	
pT2	57	39 (68.4)	**0.013**	4	2 (50.0)	0.553
pT3	370	252 (68.1)		96	53 (55.2)	
pT4	26	19 (73.1)		7	3 (42.9)	
Spread to lymph nodes						
Absent	275	188 (68.4)	0.940	9	5 (55.6)	1.000*
Present	198	136 (68.7)		89	50 (56.2)	
Venous vessel invasion						
Absent	264	179 (67.8)	0.511	29	13 (44.8)	0.110
Present	201	142 (70.4)		74	46 (62.2)	
TNM						
Stage I	75	54 (72.0)				
Stage II	181	121 (66.9)	0.425			
Stage III	152	108 (71.1)		78	43 (55.1)	0.978
Stage IV	70	45 (64.3)		31	17 (54.8)	

*Comparisons were examined for statistical significance using Fisher's exact test (when $n \leq 5$).

Table 5: Survival analysis: frequency and relative frequency for overall survival and medium of time to death.

Ki-67	Tissue	*n*	Deaths *n* (%)	Median for survival time [95% confidence interval]	Log-rank test *P*
Negative	CRC	154	53 (65.6)	65.00 [59.49–70.52]	0.321
Positive		332	125 (62.3)	62.09 [58.06–66.12]	
Negative	Lymph node	49	17 (65.3)	63.48 [53.18–73.79]	0.131
Positive		62	30 (51.6)	50.07 [41.06–59.08]	

Table 6: Comparison between Ki-67 index in primary tumor and respective lymph node metastasis.

Ki-67 index in CRC	Ki-67 index in lymph node		
	Negative	Positive	Total *n* (%)
Negative	16	12	28 (26.4)
Positive	29	49	78 (73.6)
Total *n* (%)	45 (42.5)	51 (57.5)	106 (100)

Comparisons were examined for statistical significance using McNemar test.

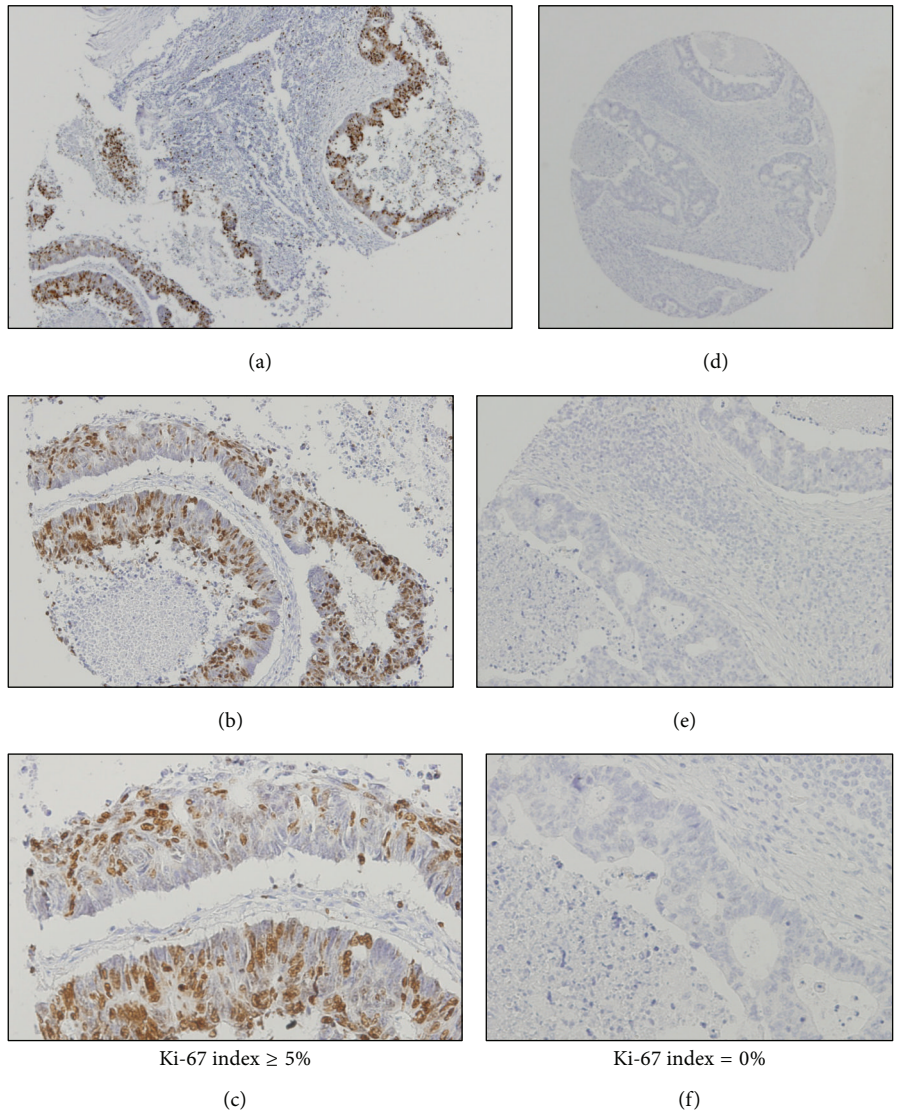

Figure 3: Immunohistochemical expression of Ki-67 in CRC lymph node metastasis samples: ((a) and (d)) original magnification ×40; ((b) and (e)) original magnification ×100; ((c) and (f)) original magnification ×200.

cancer [51], where a higher ki-67 index was associated with a worse patient survival.

Finally, we found association ($P = 0.012$) between Ki-67 index in primary tumour and the respective lymph node metastasis and also observed that Ki-67 index was more often positive in the primary tumour than in the respective lymph node metastasis. This result is consistent with the study carried out by Yamauchi et al. [41] to compare Ki-67 index in CRC primary tumour and respective nodules of peritoneal dissemination, which, as in the present study, present a greater proportion of proliferating cells in the primary tumour than in the nodules of peritoneal dissemination, not advancing; however, there is no explanation for this finding. Distinct results were observed for similar studies realized in breast cancer [42–44], where lymph node metastasis presents higher ki-67 index than primary tumour, but also no explanation was mentioned. Recently, Jo and colleagues have found a significant difference of higher Ki-67 proliferation in nodal metastasis and primary gastric cancer [52]. Most of the criticism of Ki-67 evaluation is related to the differences of antibodies, slide background, retrieval protocols applied in preparing the immunoreaction, and the scores used to evaluate the significance of Ki-67 proliferation rates. This concern is pertinent and most of the works that evaluate this premise did not reach a consensus. Interesting, automated evaluation of the Ki-67 labelled preparation has been adjudicated as superior than manual analyses. Moreover, subdividing the cases in low and high proliferative rate improve the *kappa* correlation. Besides these advisements, the lack of standard protocols among the laboratories limits the clinical relevance of the works [53].

This difference between Ki-67 index in primary CRC tumour and respective lymph node metastasis may explain the absence of correlation with clinicopathological data

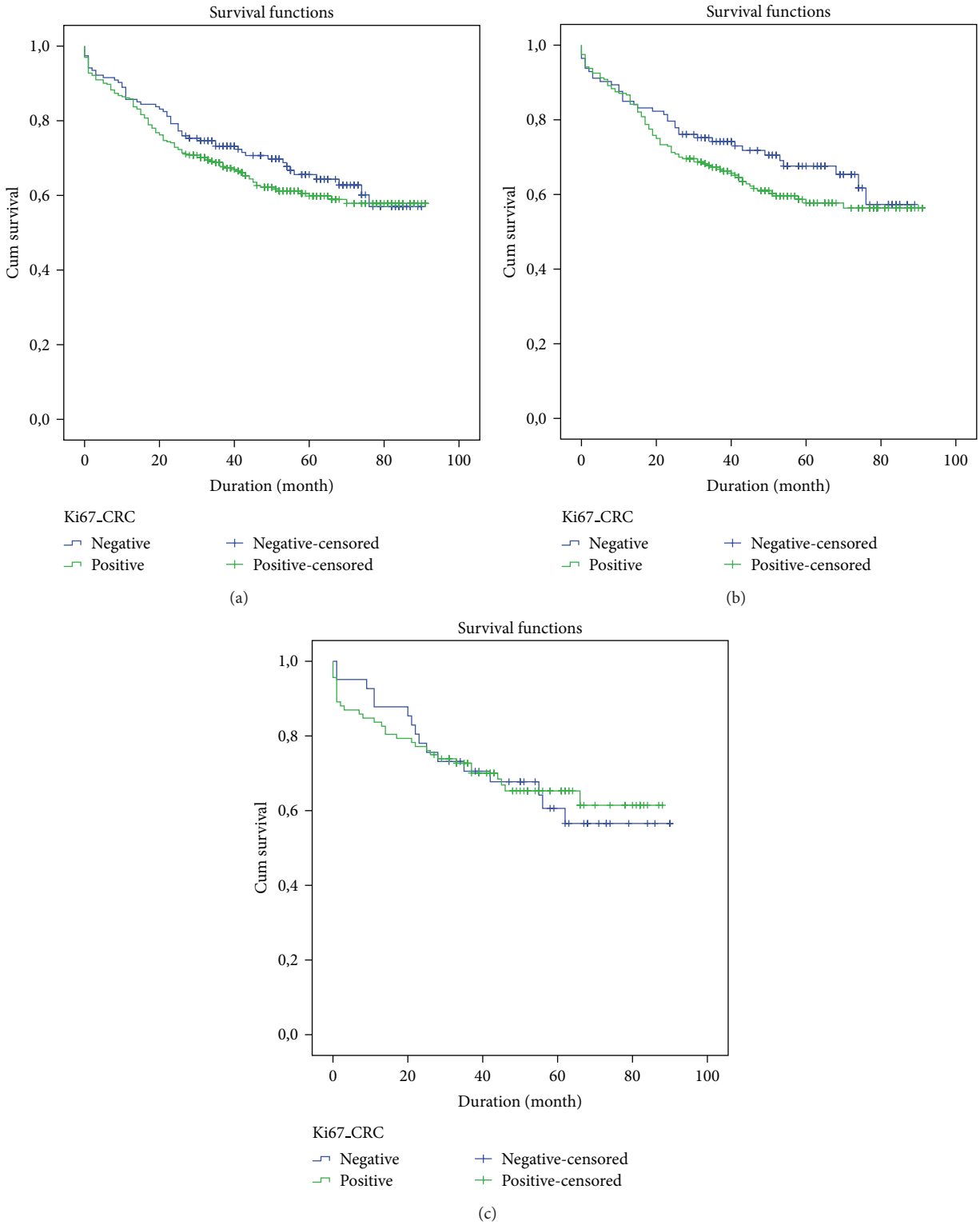

Figure 4: Survival curve of patients with CRC according to Ki-67, assessed by the log-rank test: (a) colorectal cancer: $P = 0.321$; (b) colon cancer: $P = 0.213$; (c) rectal cancer: $P = 0.874$.

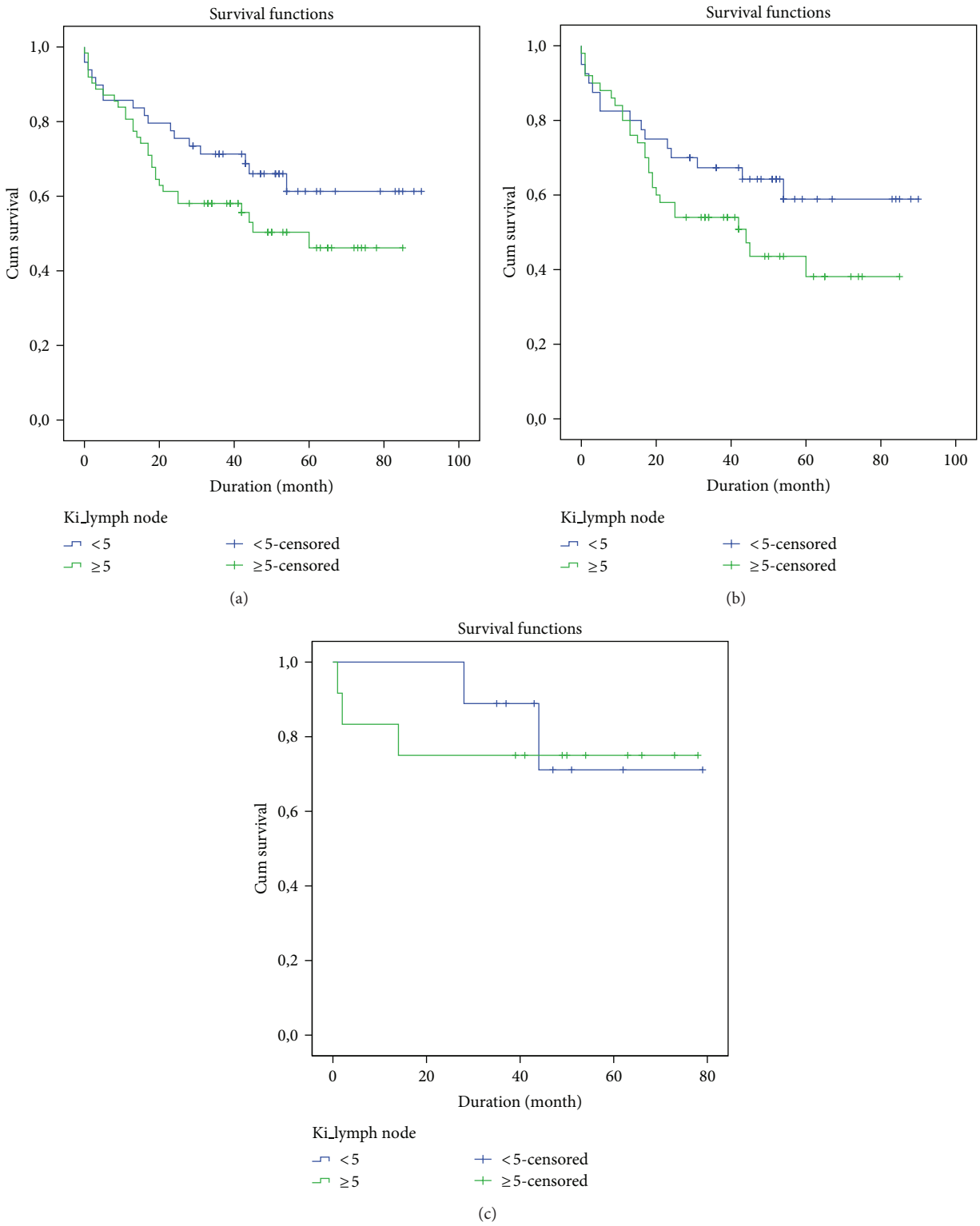

Figure 5: Survival curve of patients with CRC lymph node metastasis according to Ki-67, assessed by the log-rank test: (a) colorectal cancer: $P = 0.131$; (b) colon cancer: $P = 0.127$; (c) rectal cancer: $P = 0.809$.

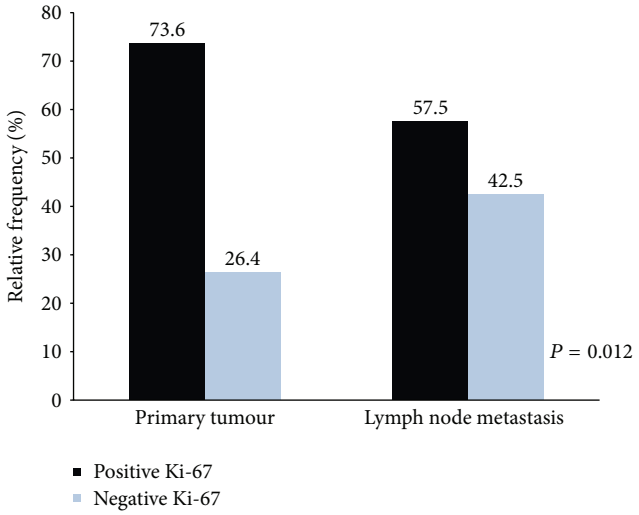

Figure 6: Graphic representation of Ki-67 index in primary CRC tumour and respective lymph node metastasis.

and survival observed in this study as it shows that the proliferative profile of the primary CRC tumour is different from that of its metastasis. One possible explanation for the low proliferative index of lymph node metastasis as compared to primary tumour is that lymph node cannot represent an optimal proliferative environment, since it is known that nutrient and oxygen deprivation induces cell cycle arrest, leading to a decreased proliferation rate [54]. Another possible explanation may be due to of Ki-67 own usage as a marker of cell proliferation, since Ki-67 expression seems to be influenced by nutrient intake of the cell [48].

The smaller number of patients with a positive Ki-67 index in lymph node metastasis can also contribute to the poor prognosis attributed to the presence of lymph node metastasis [32, 50, 55, 56] in CCR, since most antineoplastic agents target proliferating cells, cells with a low proliferation rate are more resistant to such treatment [53], and this hypothesis was also stated by Cabibi et al. [44], relatively to the subgroup of patients with breast cancer and lower ki-67 index in lymph node metastasis than in primary tumour.

5. Conclusions

In this study, we evaluated the immunohistochemical expression of Ki-67 in CRC and respective lymph node metastasis and simultaneously try to determine its correlation with clinicopathological data and patient survival. From the results obtained, it was found that this protein has higher expression in tumour tissue, supporting the hypothesis of involvement of Ki-67 in CRC and its role as a proliferative marker. Furthermore, in CRC samples, the association between the expression of this protein and the degree of tumour differentiation and penetration was found which enables Ki-67 to be used as a potential prognostic factor in CRC.

Although we have not obtained statistical significant results for lymph node metastasis series we observed a statistically significant difference between the Ki-67 index of the primary tumour and the respective lymph node metastasis, which is more often positive in the primary tumour. These results show that lymph node metastasis is composed of proliferating cells slower than that present in the primary tumour and it is hypothesized that the lymph node might not constitute an optimal environment for tumour cells proliferation or that Ki-67 might not be the more suitable proliferative marker for use in lymph node metastasis. This result also raises the possibility that tumour cells in lymph nodes can be more resistant to chemotherapy treatments, thus contributing to the poor prognosis of these patients.

Conflict of Interests

The authors declare that they have no conflict of interests.

References

[1] S. Svagzdys, V. Lesauskaite, D. Pavalkis, I. Nedzelskiene, D. Pranys, and A. Tamelis, "Microvessel density as new prognostic marker after radiotherapy in rectal cancer," *BMC Cancer*, vol. 9, article 95, 2009.

[2] G. Des Guetz, B. Uzzan, P. Nicolas et al., "Microvessel density and VEGF expression are prognostic factors in colorectal cancer. Meta-analysis of the literature," *British Journal of Cancer*, vol. 94, no. 12, pp. 1823–1832, 2006.

[3] H. Brenner, M. Hoffmeister, and U. Haug, "Should colorectal cancer screening start at the same age in European countries? Contributions from descriptive epidemiology," *British Journal of Cancer*, vol. 99, no. 3, pp. 532–535, 2008.

[4] S. F. Martins, R. M. Reis, A. M. Rodrigues, F. Baltazar, and A. Filho, "Role of endoglin and VEGF family expression in colorectal cancer prognosis and anti-angiogenic therapies," *World Journal of Clinical Oncology*, vol. 2, no. 6, pp. 272–280, 2011.

[5] S. F. Martins, E. A. Garcia, M. A. M. Luz, F. Pardal, M. Rodrigues, and A. L. Filho, "Clinicopathological correlation and prognostic significance of VEGF-A, VEGF-C, VEGFR-2 and VEGFR-3 expression in colorectal cancer," *Cancer Genomics & Proteomics*, vol. 10, no. 2, pp. 55–67, 2013.

[6] M. Zavoral, S. Suchanek, F. Zavada et al., "Colorectal cancer screening in Europe," *World Journal of Gastroenterology*, vol. 15, no. 47, pp. 5907–5915, 2009.

[7] C. Bosetti, F. Levi, V. Rosato et al., "Recent trends in colorectal cancer mortality in Europe," *International Journal of Cancer*, vol. 129, no. 1, pp. 180–191, 2011.

[8] Roreno, Corpo Humano—Roreno—Registo Oncológico Regional do Norte, http://www.roreno.com.pt/p.

[9] M. Malvezzi, P. Bertuccio, F. Levi, C. La Vecchia, and E. Negri, "European cancer mortality predictions for the year 2013," *Annals of Oncology*, vol. 24, no. 3, pp. 792–800, 2013.

[10] C. G. Pinto, A. T. Paquete, and I. Pissarra, "Colorectal cancer in Portugal," *European Journal of Health Economics*, vol. 10, no. 1, pp. S65–S73, 2010.

[11] J. Ferlay, E. Steliarova-Foucher, J. Lortet-Tieulent et al., "Cancer incidence and mortality patterns in Europe: estimates for 40 countries in 2012," *European Journal of Cancer*, vol. 49, no. 6, pp. 1374–1403, 2013.

[12] S. Gurzu, J. Jung, L. Azamfirei, T. Mezei, A. M. Cîmpean, and Z. Szentirmay, "The angiogenesis in colorectal carcinomas with and without lymph node metastases," *Romanian Journal of Morphology and Embryology*, vol. 49, no. 2, pp. 149–152, 2008.

[13] S. Cascinu, V. Georgoulias, D. Kerr, T. Maughan, R. Labianca, and M. Ychou, "Colorectal cancer in the adjuvant setting: perspectives on treatment and the role of prognostic factors," *Annals of Oncology*, vol. 14, no. 2, pp. 25–29, 2003.

[14] D. D. Alexander, J. Waterbor, T. Hughes, E. Funkhouser, W. Grizzle, and U. Manne, "African-American and Caucasian disparities in colorectal cancer mortality and survival by data source: an epidemiologic review," *Cancer Biomarkers*, vol. 3, no. 6, pp. 301–313, 2007.

[15] H. J. Calvo, G. D. Ortega, R. J. M. Pardo, M. A. J. López, and T. Cubo, "Biologia molecular del processo metastásico del cancer colorectal," *Cirugia Española*, vol. 68, pp. 577–587, 2000.

[16] S. Y. Zafar, A. P. Abernethy, D. H. Abbott et al., "Comorbidity, age, race and stage at diagnosis in colorectal cancer: a retrospective, parallel analysis of two health systems," *BMC Cancer*, vol. 8, article 345, 2008.

[17] L. A. G. Ries, P. A. Wingo, D. S. Miller et al., "The annual report to the nation on the status of cancer, 1973–1997, with a special section on colorectal cancer," *Cancer*, vol. 88, no. 10, pp. 2398–2424, 2000.

[18] R. S. Saad, Y. L. Liu, G. Nathan, J. Celebrezze, D. Medich, and J. F. Silverman, "Endoglin (CD105) and vascular endothelial growth factor as prognostic markers in colorectal cancer," *Modern Pathology*, vol. 17, no. 2, pp. 197–203, 2004.

[19] C. Barozzi, M. Ravaioli, A. D'Errico et al., "Relevance of biologic markers in colorectal carcinoma: a comparative study of a broad panel," *Cancer*, vol. 94, no. 3, pp. 647–657, 2002.

[20] A. J. Bilchik, M. DiNome, S. Saha et al., "Prospective multicenter trial of staging adequacy in colon cancer: preliminary results," *Archives of Surgery*, vol. 141, no. 6, pp. 527–533, 2006.

[21] T. Scholzen and J. Gerdes, "The Ki-67 protein: from the known and the unknown," *Journal of Cellular Physiology*, vol. 182, no. 3, pp. 311–322, 2000.

[22] K. Guzinska-Ustymowicz, E. Stepien, and A. Kemona, "MCM-2, Ki-67 and PCNA protein expressions in pT3G2 colorectal cancer indicated lymph node involvement," *Anticancer Research*, vol. 28, no. 1, pp. 451–457, 2008.

[23] D. Freitas, M. H. Goulão, E. Camacho et al., "Clinical relevance of proliferation biomarkers and p53 expression in rectal mucosa and sporadic colonic adenomas: a prospective study," *Hepato-Gastroenterology*, vol. 49, no. 47, pp. 1269–1274, 2002.

[24] H. A. Saleh, H. Jackson, G. Khatib, and M. Banerjee, "Correlation of bcl-2 oncoprotein immunohistochemical expression with proliferation index and histopathologic parameters in colorectal neoplasia," *Pathology & Oncology Research*, vol. 5, no. 4, pp. 273–279, 1999.

[25] M. X. Lin, Z.-F. Wen, Z.-Y. Feng, and D. He, "Expression and significance of Bmi-1 and Ki67 in colorectal carcinoma tissues," *Ai Zheng*, vol. 27, no. 12, pp. 1321–1326, 2008.

[26] P. Dziegiel, J. Forgacz, E. Suder, P. Surowiak, J. Kornafel, and M. Zabel, "Prognostic significance of metallothionein expression in correlation with Ki-67 expression in adenocarcinomas of large intestine," *Histology and Histopathology*, vol. 18, no. 2, pp. 401–407, 2003.

[27] X. Z. Bai, J. R. W. Masters, N. O'Donoghue et al., "Prognostic markers in clinically localised prostate cancer," *International Journal of Oncology*, vol. 14, no. 4, pp. 785–791, 1999.

[28] W. X. Gao, J. G. Feng, Y. F. Yang et al., "PCNA in colorectal carcinoma and the prognosis," *Xian Dai Yu Fang Yi Xue*, vol. 2, no. 34, pp. 225–229, 2007.

[29] M. Micev, M. Micev-Cosić, V. Todorović et al., "Histopathology of residual rectal carcinoma following preoperative radiochemotherapy," *Acta Chirurgica Iugoslavica*, vol. 51, no. 2, pp. 99–108, 2004.

[30] F. L. Nussrat, H. H. Ali, H. G. Hussein, and R. J. Al-Ukashi, "Immunohistochemical expression of ki-67 and p53 in colorectal adenomas: a clinicopathological study," *Oman Medical Journal*, vol. 26, no. 4, pp. 229–234, 2011.

[31] S. Toru and B. Bilezikçi, "Early changes in carcinogenesis of colorectal adenomas," *West Indian Medical Journal*, vol. 61, no. 1, pp. 10–16, 2012.

[32] Y. Hashimoto, M. Skacel, I. C. Lavery, A. L. Mukherjee, G. Casey, and J. C. Adams, "Prognostic significance of fascin expression in advanced colorectal cancer: an immunohistochemical study of colorectal adenomas and adenocarcinomas," *BMC Cancer*, vol. 6, article 241, 2006.

[33] C. T. F. Oshima, K. Iriya, and N. M. Forones, "Ki-67 as a prognostic marker in colorectal cancer but not in gastric cancer," *Neoplasma*, vol. 52, no. 5, pp. 420–424, 2005.

[34] C. Evans, I. Morrison, A. G. Heriot et al., "The correlation between colorectal cancer rates of proliferation and apoptosis and systemic levels plus their influence upon survival," *British Journal of Cancer*, vol. 94, no. 10, pp. 1412–1419, 2006.

[35] V. Valera, N. Yokoyama, B. Walter, H. Okamoto, T. Suda, and K. Hatakeyama, "Clinical significance of Ki-67 proliferation index in disease progression and prognosis of patients with resected colorectal carcinoma," *British Journal of Surgery*, vol. 92, no. 8, pp. 1002–1007, 2005.

[36] H. L. De Menezes, M. J. Jucá, E. G. D. A. Gomes, B. L. B. B. P. Nunes, H. O. Costa, and D. Matos, "Analysis of the immunohistochemical expressions of p53, bcl-2 and Ki-67 in colorectal adenocarcinoma and their correlations with the prognostic factors," *Arquivos de Gastroenterologia*, vol. 47, no. 2, pp. 141–147, 2010.

[37] C. Ghiţă, I. D. Vîlcea, M. Dumitrescu et al., "The prognostic value of the immunohistochemical aspects of tumor suppressor genes p53, bcl-2, PTEN and nuclear proliferative antigen Ki-67 in resected colorectal carcinoma," *Romanian Journal of Morphology and Embryology*, vol. 53, no. 3, pp. 549–556, 2012.

[38] U. Nabi, A. H. Nagi, and W. Sami, "Ki-67 proliferating index and histological grade, type and stage of colorectal carcinoma," *Journal of Ayub Medical College, Abbottabad*, vol. 20, no. 4, pp. 44–48, 2008.

[39] A. Jansson and X.-F. Sun, "Ki-67 expression in relation to clinicopathological variables and prognosis in colorectal adenocarcinomas," *APMIS*, vol. 105, no. 9, pp. 730–734, 1997.

[40] C. J. Allegra, S. Paik, L. H. Colangelo et al., "Prognostic value of thymidylate synthase, Ki-67, and p53 in patients with Dukes' B and C colon cancer: a National Cancer Institute-National Surgical Adjuvant Breast and Bowel Project collaborative study," *Journal of Clinical Oncology*, vol. 21, no. 2, pp. 241–250, 2003.

[41] H. Yamauchi, T. Suto, W. Kigure et al., "The progression potential of peritoneal dissemination nodules from gastrointestinal tumors," *International Surgery*, vol. 96, no. 4, pp. 352–357, 2011.

[42] F. Buxant, V. Anaf, P. Simon, I. Fayt, and J. C. Noël, "Ki-67 immunostaining activity is higher in positive axillary lymph nodes than in the primary breast tumor," *Breast Cancer Research and Treatment*, vol. 75, no. 1, pp. 1–3, 2002.

[43] D. Park, R. Kåresen, T. Noren, and T. Sauer, "Ki-67 expression in primary breast carcinomas and their axillary lymph node metastases: clinical implications," *Virchows Archiv*, vol. 451, no. 1, pp. 11–18, 2007.

[44] D. Cabibi, V. Mustacchio, A. Martorana et al., "Lymph node metastases displaying lower Ki-67 immunostaining activity than the primary breast cancer," *Anticancer Research*, vol. 26, no. 6B, pp. 4357–4360, 2006.

[45] K. Tawfik, B. F. Kimler, M. K. Davis, F. Fan, and O. Tawfik, "Ki-67 expression in axillary lymph node metastases in breast cancer is prognostically significant," *Human Pathology*, vol. 44, no. 1, pp. 39–46, 2013.

[46] F. L. Greene, D. L. Page, I. D. Fleming et al., Eds., *AJCC Cancer Staging Manual*, Springer, New York, NY, USA, 6th edition, 2002.

[47] C. Pinheiro, A. Longatto-Filho, C. Scapulatempo et al., "Increased expression of monocarboxylate transporters 1, 2, and 4 in colorectal carcinomas," *Virchows Archiv*, vol. 452, no. 2, pp. 139–146, 2008.

[48] D. C. Brown and K. C. Gatter, "Monoclonal antibody Ki-67: its use in histopathology," *Histopathology*, vol. 17, no. 6, pp. 489–503, 1990.

[49] J. Gerdes, U. Schwab, H. Lemke, and H. Stein, "Production of a mouse monoclonal antibody reactive with a human nuclear antigen associated with cell proliferation," *International Journal of Cancer*, vol. 31, no. 1, pp. 13–20, 1983.

[50] Y. Kubota, R. E. Petras, K. A. Easley, T. W. Bauer, R. R. Tubbs, and V. W. Fazio, "Ki-67-determined growth fraction versus standard staging and grading parameters in colorectal carcinoma: a multivariate analysis," *Cancer*, vol. 70, no. 11, pp. 2602–2609, 1992.

[51] M. Hosaka, Y. Takano, M. Iki, and et al, "Prognostic significance of Ki-67, p53, and Bcl-2 expression in prostate cancer patients with lymph node metastases: a retrospective immunohistochemical analysis," *Pathology International*, vol. 48, no. 1, pp. 41–46, 1998.

[52] M. J. Jo, J. Y. Park, J. S. Song et al., "Biopathologic features and clinical significance of micrometatasis in the lymph node of early gastric cancer," *World Journal of Gastroenterology*, vol. 21, no. 2, pp. 667–674, 2015.

[53] J. Harvey, C. Thomas, B. Wood et al., "Practical issues concerning the implementation of Ki-67 proliferative index measurement in breast cancer reporting," *Pathology*, vol. 47, no. 1, pp. 13–20, 2015.

[54] O. Trédan, C. M. Galmarini, K. Patel, and I. F. Tannock, "Drug resistance and the solid tumor microenvironment," *Journal of the National Cancer Institute*, vol. 99, no. 19, pp. 1441–1454, 2007.

[55] D. L. Longo, A. S. Fauci, D. L. Kasper, S. L. Hauser, J. L. Jameson, and J. Loscalzo, Eds., *Harrison's Principles of Internal Medicine*, McGraw-Hill, New York, NY, USA, 18th edition, 2012.

[56] T. E. Le Voyer, E. R. Sigurdson, A. L. Hanlon et al., "Colon cancer survival is associated with increasing number of lymph nodes analyzed: a secondary survey of intergroup trial INT-0089," *Journal of Clinical Oncology*, vol. 21, no. 15, pp. 2912–2919, 2003.

Hindawi Publishing Corporation
BioMed Research International
Volume 2015, Article ID 614845, 7 pages
http://dx.doi.org/10.1155/2015/614845

Research Article

Metastatic Salivary Gland Tumors: A Single-Center Study Demonstrating the Feasibility and Potential Clinical Benefit of Molecular-Profiling-Guided Therapy

Aron Popovtzer,[1,2] Michal Sarfaty,[1] Dror Limon,[1] Gideon Marshack,[1,2] Eli Perlow,[3] Addie Dvir,[4] Lior Soussan-Gutman,[4] and Salomon M. Stemmer[1,2]

[1] *Institute of Oncology, Davidoff Center, Rabin Medical Center, 39 Jabotinsky Street, 49100 Petah Tikva, Israel*
[2] *Sackler Faculty of Medicine, Tel Aviv University, Ramat Aviv, 69978 Tel Aviv, Israel*
[3] *Radiology Department, Rabin Medical Center, 39 Jabotinsky Street, 49100 Petah Tikva, Israel*
[4] *Oncotest-Teva Pharmaceutical Industries, Ltd., Hatee'na 1, 60850 Shoham, Israel*

Correspondence should be addressed to Aron Popovtzer; aronp@clalit.org.il

Received 22 January 2015; Accepted 5 May 2015

Academic Editor: Murat Gokden

We evaluated the use of molecular profiling (MP) for metastatic salivary gland adenoid cystic carcinoma (SACC), for which there is no standard treatment. MP (Caris Molecular Intelligence) was performed on biopsy samples from all metastatic SACC patients attending a tertiary medical center between 2010 and 2013 ($n = 14$). Treatment was selected according to the biomarkers identified. Findings were compared with all similarly diagnosed patients treated in the same center between 1996 and 2009 ($n = 9$). For each patient, MP identified 1–13 biomarkers associated with clinical benefit for specific therapies (most commonly low/negative TS, low ERCC1). Eleven patients (79%) received MP-guided treatment (2 died prior to treatment initiation, 1 opted not to be treated), with complete response in 1, partial response (PR) in 3, and stable disease in 4. In the historical controls, 2 patients (22%) were treated (1 had PR). Median (range) progression-free survival in the first line after MP was 8.2 months (1.4–49.5+). Median (range) overall survival from diagnosis of metastatic disease was 31.3 (1.4–71.1+) versus 14.0 (1.5–116) months in the historical controls. In conclusion, MP expands treatment options and may improve clinical outcomes for metastatic SACC. In orphan diseases where randomized trials cannot be performed, MP could become a standard clinical tool.

1. Introduction

Salivary gland adenoid cystic carcinoma (SACC) is characterized by slow progression, although recurrences after short disease-free intervals are relatively common. Once the disease metastasizes, one-third of patients die within 2 years [1]. Owing to the rarity of SACC, clinical trials investigating systemic therapies are scarce and sample sizes are limited. In the last decade, several small phase II trials of chemotherapeutics/targeted therapies for locally recurrent/metastatic SACC have yielded modest success, with objective response rates of 0–20%, stable disease (SD) rates of 20–87%, and median overall survival of 6–27 months [2–14]. Based on these findings, Laurie et al. in a systematic review of studies of advanced SACC suggested that the preferred treatment option is clinical trial participation [15]. This is also the first of two options recommended by the National Comprehensive Cancer Network (NCCN) guidelines. The second is standard therapy, which includes chemotherapy for patients with a performance status (PS) of 0–2 and watchful waiting for slow-growing disease [16].

Molecular profiling (MP) of tumors may be used to identify potential targets for which there are available therapies. It involves the application of immunohistochemistry (IHC), fluorescent/chromogenic in situ hybridization (FISH/CISH), microarray analyses, sequencing, and reverse transcription polymerase chain reaction (RT-PCR). Treatment based on MP findings has proved successful in a pilot study of a variety of refractory cancers and a separate study of metastatic breast cancer [17, 18].

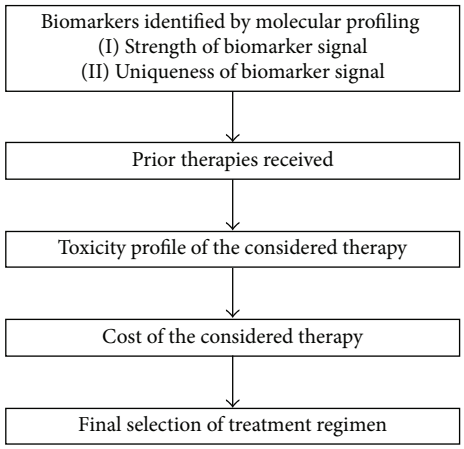

Figure 1: Considerations in choosing a treatment regimen after molecular profiling.

The objective of the present study was to evaluate a new MP-guided treatment paradigm in metastatic SACC in terms of feasibility and clinical outcomes.

2. Materials and Methods

2.1. Study Design. This single-center prospective cohort study included all patients with metastatic SACC who underwent MP at the Davidoff Center, Rabin Medical Center, from March 2010 to March 2013. The study was approved by the Institutional Review Board of Rabin Medical Center and all patients signed an informed consent. Therapy was selected on the basis of biomarkers identified by MP after considering multiple factors (Figure 1), including the strength and uniqueness of the biomarker signal, prior therapies received by the patient, the toxicity profile of the considered therapy, and the cost of the considered therapy. The regimens administered and the clinical outcomes were monitored prospectively; patients were followed until July 2014. Patient baseline characteristics and medical history were collected from the individual medical files.

The historical control cohort included all patients with metastatic SACC treated at the Davidoff Center from 1996 to 2009. Since the Davidoff Center has only recently become a referral center for head and neck malignancies, the historical cohort was considerably smaller than the study cohort. Patient data were collected from the medical files.

2.2. Molecular Profiling. MP was conducted on paraffin-embedded tissue taken from biopsy samples from the primary tumor or a metastatic lesion. Analyses were performed with the Caris Molecular Intelligence (CMI) tumor profiling service (Caris Life Sciences, Irving, TX) at the Caris Life Sciences Laboratories (Phoenix, AZ). They included IHC (for up to 18 targets), FISH/CISH to identify amplification in select genes, namely, *cMET* (the gene coding for the hepatocyte growth factor receptor protein; HGFR), epidermal growth factor receptor (*EGFR*), human epidermal growth factor receptor 2 (*HER2*), and topoisomerase II alpha (*TOP2A*). FISH was also used to identify rearrangement in the anaplastic lymphoma kinase (*ALK*) gene. Additionally, microarray analysis of over 80 targets and mutational analysis of *BRAF* (the gene coding for the serine/threonine-protein kinase B-raf protein), *KIT* (the gene coding for the mast/stem cell growth factor receptor Kit), *EGFR*, *KRAS* (the gene coding for the GTPase KRas protein), and *PIK3CA* (the gene coding for phosphatidylinositol 4,5-bisphosphate 3-kinase catalytic subunit alpha) were performed. In one patient, RT-PCR was used to determine gene expression.

IHC analysis was performed on formalin-fixed, paraffin-embedded tumor samples using commercially available detection kits, automated staining techniques (Benchmark XT, Ventana, Tusco, AZ, and AutostainerLink 48, Dako, Glostrup, Denmark), and commercially available antibodies-androgen receptor (AR), topoisomerases I and IIα (TOPO1, TOPOα) (Leica Biosystems, Buffalo Grove, IL); estrogen receptor (ER), progesterone receptor (PgR); c-Met; HER2 (Ventana); tyrosine protein c-Kit receptor kinase (c-Kit), EGFR, and phosphatase and tensin homolog (PTEN) (Dako); O(6)-methylguanine-methyltransferase (MGMT); P-glycoprotein (PGP); thymidylate synthase (TS) (Invitrogen, Grand Island, NY); transducing-like enhancer of split 3 (TLE3) (Santa Cruz, Santa Cruz, CA); ribonucleotide reductase M1 (RRM1) (Protein Tech, Chicago, IL); Serum protein acidic and rich in cysteine (SPARC) (monoclonal, R&D Systems, Minneapolis, MN; polyclonal, Exalpha, Shirley, MA); and tubulin beta-3 chain (TUBB3) (Covance, Madison, WI). Results were categorized by defined cutoffs based on published evidence. Scoring system and cutoffs for all antibodies are provided in Supplementary Table 1, available online at http://dx.doi.org/10.1155/2015/614845.

FISH was used for evaluation of the *HER2* (*HER2/CEP17* (chromosome 17 centromere) probe), *EGFR* (*EGFR/CEP7* probe), *TOPO2A* (*TOP2/CEP17* probe), and *cMET* (*c-MET/CEP7* probe; Abbott Molecular/Vysis, Abbott Park, IL). *HER2/CEP17* ratio >2.2 was considered amplified (based on guidelines from the College of American Pathology (CAP)/American Society of Clinical Oncology (ASCO) 2007). *EGFR* amplification was defined as *EGFR/CEP7* ratio ≥2 or ≥15 *EGFR* copies per cell in ≥10% of analyzed cells. *TOPO2A* amplification was defined as *TOPO2A/CEP17* ratio ≥2.0 and *cMET* was considered amplified if ≥5 *cMET* copies were detected on average.

Total RNA was extracted from tumor tissue and converted to cDNA. This cDNA sample was then subjected to a whole genome (24K) microarray analysis using Illumina cDNA-mediated annealing, selection, extension, and ligation process. The expression of a subset of 88 genes was then compared to a tissue-specific normal control and the relative expression ratios of these 88 target genes were determined as well as the statistical significance of the differential expression.

The types of analyses done and the specific targets assessed were determined by the amount of tissue sample available. If the amount was insufficient to perform all tests, the analyses were prioritized by the treating physician (based on various factors including prior therapies received, the likelihood of getting an actionable result for the particular

marker, having access to the therapy that may be recommended as a result of testing, etc.). Another determining factor was the timeframe in which the MP was performed. CMI profiling evolved over the period of the study, with advances in methodologies and the introduction of published data about the relationship between certain biomarkers and response/resistance to therapy. An actionable target was defined as a target associated with clinical benefit from the matching therapies.

2.3. Clinical Outcomes. Response to treatment was based on Response Evaluation Criteria in Solid Tumors (RECIST 1.1). Disease control rate was defined as the proportion of patients with complete response (CR), partial response (PR), or SD. Response rate was defined as the proportion of patients with CR or PR. Disease control rate was defined as the proportion of patients with CR, PR, or SD. We also evaluated clinical benefit by monitoring PS, as defined by the Eastern Cooperative Oncology Group (ECOG) criteria [19], over time.

2.4. Statistical Analysis. Fisher's exact test was used to assess differences in treatment rates between the study cohort and the historical control cohort. Log-rank test was used to compare survival between the cohorts.

3. Results

3.1. Patient Characteristics. Fourteen patients with metastatic SACC who were treated at the Davidoff Center between 2010 and 2013 and underwent MP were included in the study cohort. There were 9 male (64%) and 5 female (36%) patients of median age 57.5 years (range, 30–75) at diagnosis. Four patients (29%) had metastatic disease at diagnosis and 10 (71%) had localized disease at diagnosis which progressed to metastatic disease within a median of 25.3 months (range, 5.0–119.6) (Table 1). Three patients received treatment for metastatic disease prior to MP: paclitaxel, epirubicin, or cisplatin plus fluorouracil (5-FU) (1 each); none responded. At the time of progression to metastatic disease, 5 patients presented with a single metastatic site (lung, 4; brain, 1) and 9 with multiple metastatic sites (e.g., lung/liver, lung/spleen). At the time of MP, PS was 0 in 2 patients, 1 in 6 patients, and 2 in 6 patients.

The historical control cohort included 9 patients with metastatic SACC, of whom 4 (44%) were male. Median age was 58.0 years (range, 18–76). All were diagnosed with localized disease and underwent surgical resection. Progression to metastatic disease occurred within a median of 12.6 months (range, 3.0–71.0) from initial diagnosis. At the time of progression, 6 patients presented with a single metastatic site (all lung) and 3 with multiple metastatic sites (lung/liver, lung/bone, and lung/liver/bone) (Table 1).

3.2. Molecular Profiling Findings. The samples used for MP were derived from the primary tumor in 8 patients and metastasis in 6. IHC yielded reportable results for all samples. Microarray analysis was performed on 9 samples (successful in 6), FISH on 8 samples (successful in 5), and CISH on 2 samples (successful in 1). Molecular sequencing was performed on 4 samples and RT-PCR on one. Key MP findings for each patient in our study cohort are presented in Supplementary Table 2.

Table 1: Patient and tumor characteristics.

Characteristic	Study cohort $N = 14$	Control cohort $N = 9$
Gender, *n* (%)		
Male	9 (64.3)	4 (44.4)
Female	5 (35.7)	5 (55.6)
Age at diagnosis, years		
Median (range)	57.5 (30–75)	58 (18–76)
Stage at diagnosis		
Localized	10 (71.4)	9 (100)
Metastasized	4 (28.6)	0 (0)
Prior surgery		
Yes	9 (64.3)	9 (100)
No	5 (35.7)	0 (0)
Prior radiation		
Yes	9 (64.3)	8 (88.9)
No	5 (35.7)	1 (11.1)
Time to progression to metastatic disease, months		
Median (range)	25.3 (5.0–119.6)*	12.6 (3.0–71.0)
At progression to metastatic disease†		
Patients with a single metastatic site, *n* (%)	5 (35.7)	6 (66.7)
Patients with multiple metastatic sites, *n* (%)	9 (64.3)	3 (33.3)
Chemotherapy for metastatic disease		
Yes	3 (21.4)‡	2 (22.2)
No	11 (78.6)	7 (77.8)

*For patients presenting with localized disease.
†At presentation of metastatic disease.
‡Prior to molecular profiling.

Overall, at least one (median, 5.5; range, 1–13) actionable target was identified for each patient (median, 5.5; range, 1–13). IHC identified a median of 3 actionable targets per patient (range, 1–7), with the most common being negative/low TS (9 of 12 evaluable patients), negative/low ERCC1 (6 of 12 evaluable patients), and high TOPO1 (6 of 13 evaluable patients) (Table 2). It should be noted that the usefulness of ERCC1 as a biomarker has recently been questioned [20], and, consequently, ERCC1 testing is now available only upon request. None of the patients was HER2-positive by IHC, FISH, or CISH. Targets associated with an endocrine-therapy benefit included positive AR and positive ER/PgR (2 of 14 evaluable patients each) (Table 2). No *EGFR* gene amplification (4 evaluable patients) or *ALK* rearrangement (3 evaluable patients) was observed by FISH. Microarray analysis identified at least 2 actionable targets per patient (median, 8; range, 2–10) in 6 evaluable patients, including

Table 2: Actionable targets identified by molecular profiling in the study cohort.

Target	Number of patients out of total evaluable patients (n/N)	Frequency, %
Identified by IHC		
Negative/low TS	9/12	75
Negative/low ERCC1	6/12	50
High TOPO1	6/13	46
High SPARC*	4/11	36
Low MGMT	3/14	21
High TOP2A	2/11	18
Positive AR	2/14	14
Positive ER/PgR	2/14	14
Positive HER2	0/14	0
Identified by microarray analysis		
KIT overexpression	4/6	67
TOP2B overexpression	4/6	67
PDGFRA overexpression	3/6	50
PDGFRB overexpression	3/6	50
TOP2A overexpression	3/6	50
TYMS overexpression	2/6	33
VDR overexpression	2/6	33
ESR1 overexpression	2/6	33
SPARC overexpression	2/6	33
MGMT underexpression	2/6	33

*SPARC was considered high if either of the SPARC assays (using monoclonal or polyclonal anti-SPARC antibodies) was positive.
AR: androgen receptor; ER: estrogen receptor; ERCC1: excision repair cross-complementation 1; ESR1: estrogen receptor 1; HER2: human epidermal growth factor receptor 2; IHC: immunohistochemistry; MGMT: O-6-methylguanine-DNA methyltransferase; PDGFRA/B: platelet-derived growth factor receptor alpha/beta; PgR: progesterone receptor; SPARC: secreted protein acidic and rich in cysteine; TOPO1: topoisomerase I; TOP2A/B: topoisomerase IIA/B; TS/TYMS: thymidylate synthase; VDR: vitamin D receptor.

KIT overexpression and topoisomerase II beta (*TOP2B*) overexpression in 4 patients, each. RT-PCR identified 8 actionable targets in 1 evaluable patient, and sequencing analyses, conducted in 4 patients, revealed wild-type phenotypes for all evaluated genes.

3.3. Treatments and Clinical Outcomes. The treatments associated with the identified targets included agents that are routinely used in the metastatic SACC setting (i.e., cisplatin, 5-FU) and therapies that are rarely used in this setting (i.e., temozolomide, endocrine therapies) (Figure 2).

Of the 14 patients in the study cohort, 2 died before initiation of treatment and 1 opted not to be treated. Overall, 11 of 14 patients (79%) received MP-guided therapy. These included 1 patient whose sample underwent 2 panels of tests, CMI and sequencing, and whose therapy was selected based on the sequencing-identified mutation. In total, 18 MP-guided regimens were administered: 6 patients received 1 line of treatment each, 4 received 2 lines, and 1 received 4 lines.

Median duration of follow-up from initiation of MP-guided therapy was 11.8 months. In the first line of treatment, 1 of the 11 patients (9.1%) achieved CR which continued for >4 years, 3 (27.3%) achieved PR, and 4 (36.9%) had SD, for a response rate of 36% and a disease control rate of 73%. Median progression-free survival for first-line MP-guided therapy was 8.2 months; 1 patient had a progression-free survival of 49.5+ months (Figure 2). Median overall survival with metastatic disease was 31.3 months (range 1.4–71.1+) (Figure 3). In the 4 patients with CR/PR, the PS improved by 1 or 2 categories to 0. In 3 of the 5 patients with SD, PS improved by 1 category.

Of the historical control patients who attended our center before MP was available, only 2 (22%) were treated in the metastatic setting, as opposed to 11 (79%) in the study cohort ($P = 0.013$; Fisher's exact test). One of them received cisplatin/doxorubicin/cyclophosphamide for lung metastases and achieved a PR for 24 months, followed by disease progression. This patient also underwent radiation therapy and participated in 2 clinical trials, with no response. She died approximately 9 years after diagnosis of the metastatic disease. The second patient received cisplatin/doxorubicin/5-FU for liver and bone metastases with no response and died 47 days after progression to metastatic disease. The other 7 patients were not treated. Median overall survival with metastatic disease was 14.0 months (range, 1.5–116). It was shorter than for the study cohort (31.3 months), but the difference was not statistically significant, probably because of the small sample size ($P = 0.45$, log-rank test; Figure 3).

4. Discussion

Herein, we report a single-institution experience in implementing a targeted comprehensive MP testing in 14 patients with advanced SACC over a period of 4.5 years. MP findings were feasible, and the majority of patients (79%) were treated based on the molecular profile of their tumor, with some gaining substantial clinical benefit.

IHC analysis was successful in all samples, unlike microarray and FISH analyses which were not possible for all samples due to technical failure of the testing. In samples where microarray/FISH testing failed, high quality expression data could not be obtained despite multiple attempts. The ability to detect expression changes is directly proportional to the amount of tumor nuclei present in the patient sample. In comparison to microarray/FISH analyses, IHC may be performed on much smaller samples, needing a minimum of 100 tumor cells to be present; therefore, it could be more readily performed in samples with low tumor yield.

To study the efficacy of this approach, clinical outcomes were compared to historical control patients treated in the same institution. The results demonstrate that MP-guided therapy is feasible in this setting and leads to good clinical outcomes in patients who might otherwise not have further treatment options. The significantly greater number of patients in the study cohort who received therapy compared

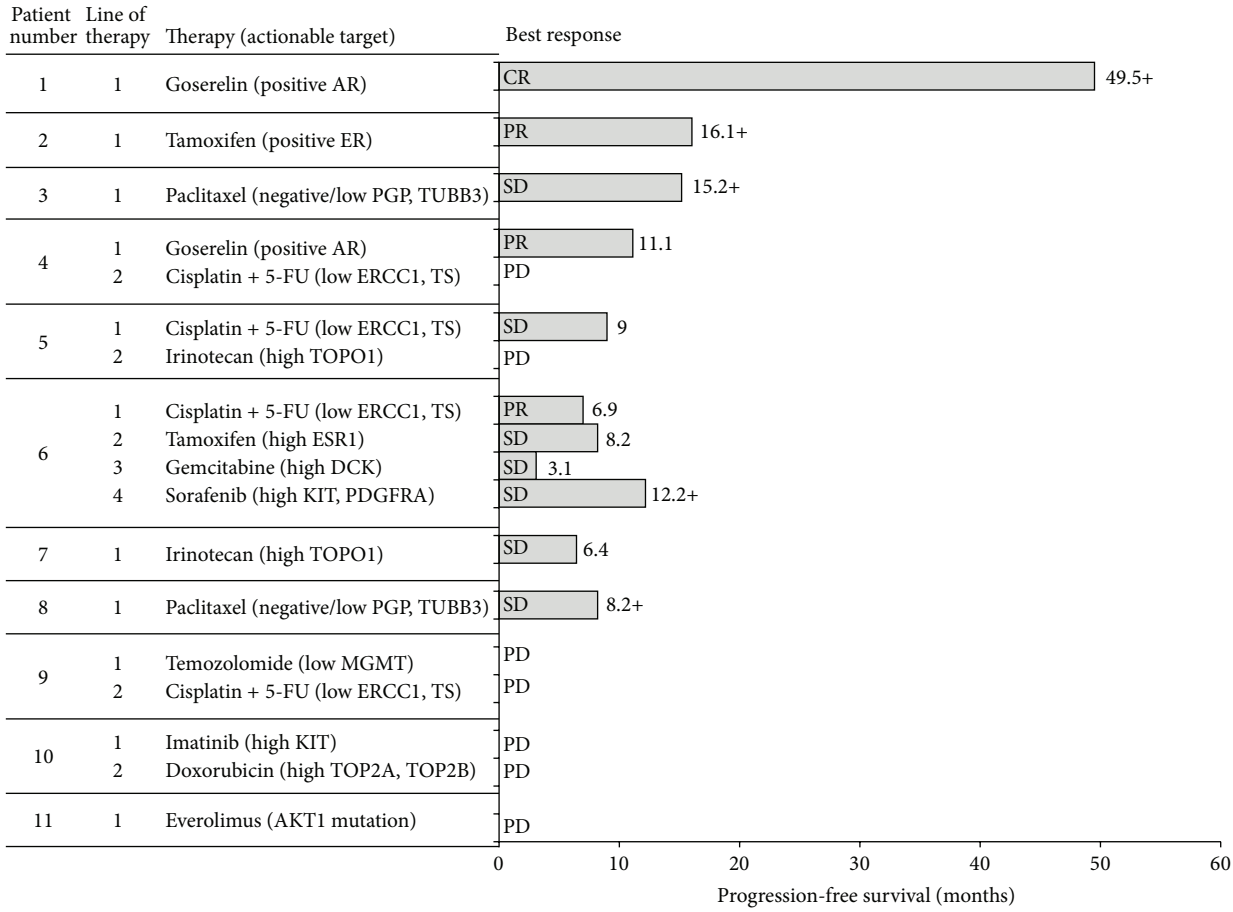

Figure 2: Treatment and progression-free survival in study cohort patients treated with MP-guided therapy ($n = 11$). 5-FU: fluorouracil; AR: androgen receptor; CR: complete response; DCK: deoxycytidine kinase; ESR1: estrogen receptor 1; ER: estrogen receptor; ERCC1: excision repair cross-complementation 1; MGMT: O-6-methylguanine-DNA methyltransferase; PDGFRA: platelet-derived growth factor receptor alpha; PGP: P-glycoprotein; PR: partial response; SD: stable disease; TOP2A/B: topoisomerase IIA/B; TOPO1: topoisomerase I; TS: thymidylate synthase; TUBB3: tubulin, beta 3 class III.

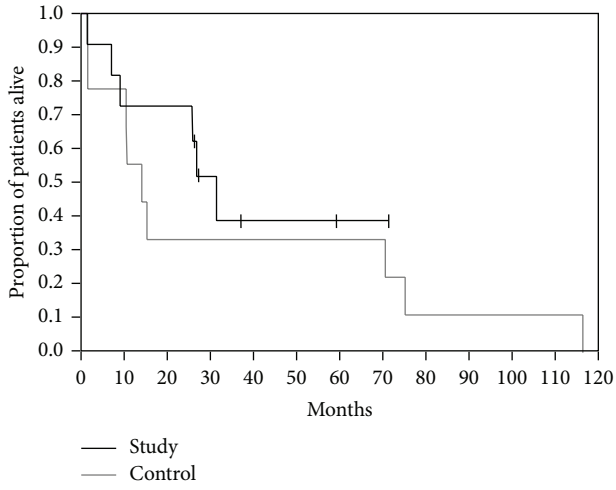

Figure 3: Kaplan-Meier survival curves (from diagnosis of metastatic disease) for study patients who received MP-guided therapy ($n = 11$) and historical control patients ($n = 9$). Tick marks indicate censored observations.

to the historical control cohort suggests that this approach broadens the armamentarium of available treatments for metastatic SACC and provides clinicians with the opportunity to offer additional therapy when sought by patients with disease progression or poor tolerability. We found that MP-guided therapy was associated with a disease control rate of 73% (CR 9.1%, PR 27.3%, and SD 36.4%) and an overall improvement in PS in patients with CR/PR/SD. The small number of patients restricts our ability to draw definitive conclusions. Nevertheless, the similar disease control rate and better response rate in the present study compared to phase II studies of advanced SACC published in the last decade [2–14] together suggest that MP-guided therapy may improve clinical outcomes. Notably, in this hard-to-treat patient population, SD is a desirable objective, as it may lead to improvements in disease-related symptoms, quality-of-life, and survival [21]. Furthermore, the overall survival of the study cohort was longer than that of the historical controls (albeit not significantly owing to the small sample sizes).

Treatment based on MP could be particularly beneficial for cancers with molecular heterogeneity and for low-prevalence cancers, which are hardly studied in clinical trials. Moreover, given that MP takes up to two weeks, this approach may be more suitable for relatively slowly progressing diseases such as SACC, and, even in these cases, it should be reserved for patients whose condition is relatively stable.

Previous studies have demonstrated the feasibility and potential clinical benefit of the MP-guided approach in a variety of refractory cancers and in metastatic breast cancer where it resulted in a ≥30% longer progression-free survival than for the last (pre-MP) regimen on which the patients progressed in 27% and 52% of cases, respectively [17, 18]. Although the progression-free survival ratio endpoint was inappropriate for our study, as most of the patients did not receive pre-MP chemotherapy for metastatic disease, our findings are compatible with these earlier studies and support the need for further investigations of MP-guided therapy.

MP-guided therapy is inherently limited by its ability to assess only tumor-based parameters (molecular characteristics of tumor cells and adjacent cells), without consideration of effects related to systemic drug distribution and some immunological aspects of cancer therapy [22, 23].

The study is limited by its nonrandomized design and inclusion of only 14 patients, although a sample this size may be adequate for such a rare disease. Furthermore, the Davidoff Center specializes in head and neck malignancies and, recently, patients from all over Israel have begun to be referred there. Consequently, our study cohort may have included a higher proportion of hard-to-treat patients compared to the general patient population.

In conclusion, our study suggests that MP-guided therapy is feasible for metastatic SACC and leads to substantial clinical benefit in some patients. This approach could be crucial for improving clinical outcomes as it facilitates personalized treatment. This study constitutes a proof of concept for the feasibility of this approach in other malignancies characterized by lack of standardized treatment, rarity of the tumor, and relatively slow disease progression.

Conflict of Interests

Addie Dvir and Lior Soussan-Gutman are employees of Oncotest-Teva Pharmaceutical Industries. The remaining authors declare no conflict of interests.

Acknowledgment

Medical writing assistance was provided by Caris Life Sciences.

References

[1] R. H. Spiro, "Distant metastasis in adenoid cystic carcinoma of salivary origin," *American Journal of Surgery*, vol. 174, no. 5, pp. 495–496, 1997.

[2] N. G. Chau, S. J. Hotte, E. X. Chen et al., "A phase II study of sunitinib in recurrent and/or metastatic adenoid cystic carcinoma (ACC) of the salivary glands: current progress and challenges in evaluating molecularly targeted agents in ACC," *Annals of Oncology*, vol. 23, no. 6, pp. 1562–1570, 2012.

[3] B. S. Glisson, G. Blumenschein, M. Francisco, J. Erasmus, R. Zinner, and M. Kies, "Phase II trial of gefitinib in patients with incurable salivary gland cancer," *Journal of Clinical Oncology*, vol. 23, abstract 5532, 2005, Proceedings of the American Society of Clinical Oncology.

[4] A. Argiris, M. A. Goldwasser, B. Burtness et al., "A phase II trial of PS-341 (bortezomib) followed by the addition of doxorubicin at progression in incurable adenoid cystic carcinoma of the head and neck: an eastern cooperative oncology group study," *Proceedings of the American Society of Clinical Oncology*, vol. 24, abstract 5573, 2006.

[5] M. Agulnik, E. W. E. Cohen, R. B. Cohen et al., "Phase II study of lapatinib in recurrent or metastatic epidermal growth factor receptor and/or erbB2 expressing adenoid cystic carcinoma and non-adenoid cystic carcinoma malignant tumors of the salivary glands," *Journal of Clinical Oncology*, vol. 25, no. 25, pp. 3978–3984, 2007.

[6] L. D. Locati, P. Bossi, F. Perrone et al., "Cetuximab in recurrent and/or metastatic salivary gland carcinomas: a phase II study," *Oral Oncology*, vol. 45, no. 7, pp. 574–578, 2009.

[7] J. M. Guigay, F. Bidault, S. Temam et al., "Antitumor activity of imatinib in progressive, highly expressing KIT adenoid cystic carcinoma of the salivary glands: a phase II study," *Journal of Clinical Oncology—ASCO Annual Meeting Proceedings*, vol. 25, no. 18, supplement, abstract 6086, 2007.

[8] C. H. Lin, R. F. Yen, Y. M. Jeng, C. Y. Tzen, C. Hsu, and R. L. Hong, "Unexpected rapid progression of metastatic adenoid cystic carcinoma during treatment with imatinib mesylate," *Head and Neck*, vol. 27, no. 12, pp. 1022–1027, 2005.

[9] M. R. Pfeffer, Y. Talmi, R. Catane, Z. Symon, A. Yosepovitch, and M. Levitt, "A phase II study of Imatinib for advanced adenoid cystic carcinoma of head and neck salivary glands," *Oral Oncology*, vol. 43, no. 1, pp. 33–36, 2007.

[10] S. J. Hotte, E. W. Winquist, E. Lamont et al., "Imatinib mesylate in patients with adenoid cystic cancers of the salivary glands expressing c-kit: a Princess Margaret Hospital Phase II Consortium Study," *Journal of Clinical Oncology*, vol. 23, no. 3, pp. 585–590, 2005.

[11] S. A. Laurie, L. L. Siu, E. Winquist et al., "A phase 2 study of platinum and gemcitabine in patients with advanced salivary gland cancer: a trial of the NCIC clinical trials group," *Cancer*, vol. 116, no. 2, pp. 362–368, 2010.

[12] P. J. Ross, E. M. Teoh, R. P. A'Hern et al., "Epirubicin, cisplatin and protracted venous infusion 5-Fluorouracil chemotherapy for advanced salivary adenoid cystic carcinoma," *Clinical Oncology*, vol. 21, no. 4, pp. 311–314, 2009.

[13] J. Gilbert, Y. Li, H. A. Pinto et al., "Phase II trial of taxol in salivary gland malignancies (E1394): a trial of the Eastern Cooperative Oncology Group," *Head and Neck*, vol. 28, no. 3, pp. 197–204, 2006.

[14] C. M. L. van Herpen, L. D. Locati, J. Buter et al., "Phase II study on gemcitabine in recurrent and/or metastatic adenoid cystic carcinoma of the head and neck (EORTC 24982)," *European Journal of Cancer*, vol. 44, no. 17, pp. 2542–2545, 2008.

[15] S. A. Laurie, A. L. Ho, M. G. Fury, E. Sherman, and D. G. Pfister, "Systemic therapy in the management of metastatic or locally recurrent adenoid cystic carcinoma of the salivary glands: a systematic review," *The Lancet Oncology*, vol. 12, no. 8, pp. 815–824, 2011.

[16] NCCN clinical practice guidelines in oncology, Head and Neck Cancers, Version 2, 2013, http://www.nccn.org/professionals/physician_gls/pdf/head-and-neck.pdf.

[17] D. D. Von Hoff, J. J. Stephenson Jr., P. Rosen et al., "Pilot study using molecular profiling of patients' tumors to find potential targets and select treatments for their refractory cancers," *Journal of Clinical Oncology*, vol. 28, no. 33, pp. 4877–4883, 2010.

[18] G. S. Jameson, E. Petricoin, J. C. Sachdev et al., "A pilot study utilizing molecular profiling to find potential targets and select individualized treatments for patients with metastatic breast cancer," *Journal of Clinical Oncology*, vol. 31, abstract TPS11123, 2013.

[19] M. M. Oken, R. H. Creech, D. C. Tormey et al., "Toxicity and response criteria of the Eastern Cooperative Oncology Group," *American Journal of Clinical Oncology*, vol. 5, no. 6, pp. 649–655, 1982.

[20] L. Friboulet, K. A. Olaussen, J.-P. Pignon et al., "ERCC1 isoform expression and DNA repair in non-small-cell lung cancer," *The New England Journal of Medicine*, vol. 368, no. 12, pp. 1101–1110, 2013.

[21] K. Kelly, "The benefits of achieving stable disease in advanced lung cancer," *Oncology*, vol. 17, no. 7, pp. 957–970, 2003.

[22] S.-F. Zhou, Y. M. Di, E. Chan et al., "Clinical pharmacogenetics and potential application in personalized medicine," *Current Drug Metabolism*, vol. 9, no. 8, pp. 738–784, 2008.

[23] L. Zitvogel, L. Apetoh, F. Ghiringhelli, and G. Kroemer, "Immunological aspects of cancer chemotherapy," *Nature Reviews Immunology*, vol. 8, no. 1, pp. 59–73, 2008.

Hindawi Publishing Corporation
BioMed Research International
Volume 2015, Article ID 192406, 7 pages
http://dx.doi.org/10.1155/2015/192406

Research Article

MET Expression in Primary and Metastatic Clear Cell Renal Cell Carcinoma: Implications of Correlative Biomarker Assessment to MET Pathway Inhibitors

Brian Shuch,[1] Ryan Falbo,[2] Fabio Parisi,[3] Adebowale Adeniran,[3] Yuval Kluger,[3] Harriet M. Kluger,[2] and Lucia B. Jilaveanu[2]

[1]*Department of Urology, Yale School of Medicine, New Haven, CT 06520-8058, USA*
[2]*Yale Cancer Center, Yale University School of Medicine, New Haven, CT 06520-8028, USA*
[3]*Department of Pathology, Yale University School of Medicine, New Haven, CT 06520-8023, USA*

Correspondence should be addressed to Lucia B. Jilaveanu; lucia.jilaveanu@yale.edu

Received 16 January 2015; Accepted 8 April 2015

Academic Editor: Aurelio Ariza

Aims. Inhibitors of the MET pathway hold promise in the treatment for metastatic kidney cancer. Assessment of predictive biomarkers may be necessary for appropriate patient selection. Understanding MET expression in metastases and the correlation to the primary site is important, as distant tissue is not always available. *Methods and Results*. MET immunofluorescence was performed using automated quantitative analysis and a tissue microarray containing matched nephrectomy and distant metastatic sites from 34 patients with clear cell renal cell carcinoma. Correlations between MET expressions in matched primary and metastatic sites and the extent of heterogeneity were calculated. The mean expression of MET was not significantly different between primary tumors when compared to metastases ($P = 0.1$). MET expression weakly correlated between primary and matched metastatic sites ($R = 0.5$) and a number of cases exhibited very high levels of discordance between these tumors. Heterogeneity within nephrectomy specimens compared to the paired metastatic tissues was not significantly different ($P = 0.39$). *Conclusions*. We found that MET expression is not significantly different in primary tumors than metastatic sites and only weakly correlates between matched sites. Moderate concordance of MET expression and significant expression heterogeneity may be a barrier to the development of predictive biomarkers using MET targeting agents.

1. Introduction

Small molecule tyrosine kinase inhibitors of the vascular endothelial growth factor receptors have been widely used as a standard of care for metastatic renal cell carcinoma (RCC) since FDA approval of the multiprotein kinase inhibitors, sunitinib, and sorafenib in early 2006 [1–3]. Since then, multiple new agents targeting this pathway have been developed and are in clinical use. While these agents may provide clinical benefit to patients, complete responses are exceedingly rare and are not durable and thus more effective agents are immediately needed [4, 5].

The MET pathway is constitutively phosphorylated/activated with loss of the VHL protein [6], a feature present in over 80% of cases of clear cell RCC (ccRCC) [7, 8]. *In vitro* studies have demonstrated that with VHL loss, activation of the MET pathway drives a more invasive phenotype [9]. Moreover, preclinical models of resistance to VEGFR-directed therapy are believed mediated by the Hepatocyte Growth Factor Receptor (MET) pathway [10]. MET might therefore be an important therapeutic target in ccRCC.

Limited data exists on the relationship of MET expression and prognosis in ccRCC. Clear cell renal tumors can have wide variability in MET expression. However, those with increased protein and mRNA levels have more aggressive pathologic characteristics and worse prognosis [11–13]. *In vitro* targeted inhibition of MET in ccRCC cell lines, in which its expression is upregulated, decreases proliferation

and colony formation [11], providing rationale to block this pathway either alone or in conjunction with the VEGFR pathway.

Multiple therapeutic strategies have been developed to block the MET pathway including several small molecule inhibitors and antibodies [14]. MET pathway inhibitors have been studied in kidney cancer. AMG102, a monoclonal antibody to the ligand of MET, Hepatocyte Growth Factor (HGF) was studied in a phase II trial but had limited efficacy with progression-free survival (PFS) of less than 4 months [15]. A tyrosine kinase inhibitor to VEGFR2 and MET, cabozantinib (XL184), was studied in a small phase I trial for RCC and later gained FDA approval for medullary thyroid cancer. Despite enrolling a heavily pretreated RCC population, there was significant antitumor activity with a 28% response rate and a 12.9-month PFS [16]. Further phase III studies with this FDA approved agent are currently ongoing in the first and second line metastatic setting.

In the era of targeted therapy, response may be dictated on whether the actual therapeutic target is present in the cancer cell. Therefore, the presence of an upregulated, overexpressed, or mutated pathway may serve as a useful predictive biomarker. Adaptive biomarker trials have become more common in recent years as clinicians have tried to match patients with an appropriate therapy. Previous studies have shown that MET expression in clear cell RCC can be variable [11], something that may influence therapeutic response. These studies, however, focused on expression in primary RCC specimens, while expression in corresponding metastatic tumors has not yet been characterized. In this study, we investigate the expression and correlation of MET in matched metastatic and primary clear cell renal tumors in order to aid future efforts to predict clinical response based on tissue expression.

2. Materials and Methods

2.1. Tissue Microarray (TMA) Construction. With Institutional Review Board approval (HIC #9505008219/2014), we reviewed charts of patients treated at Yale University between 1972 and 2011. A TMA was created from a cohort of thirty-four patients and all patients had matched nephrectomy and metastasectomy specimens. Patient and tumor characteristics and other clinical information have been described previously [17, 18]. Briefly, all patients had clear cell histology; however three (9%) had regions of sarcomatoid transformation. Four punches from each specimen and cell pellet controls were placed on separate blocks as previously detailed [17, 18].

2.2. Immunofluorescence and Automated Quantitative Analysis (AQUA). TMA slides were deparaffinized and processed for antigen-retrieval. Endogenous peroxidase activity was blocked before overnight incubation with MET4, a mouse anti-c-Met antibody (1 : 7500 dilution; kindly provided by Dr. George Vande Woude, Grand Rapids, MI). This antibody was validated and utilized in a previous study [11]. Anti-mouse secondary antibody (Envision, Dako North America, Inc., Carpinteria, CA) was used along with cyanine-5-tyramide (Cy5; Perkin Elmer, Inc., Waltham, MA) for signal amplification. A tumor mask was created by incubation with rabbit anti-cytokeratin (1 : 100 dilution; Cat. Number M5315, Dako) for 2 hours at room temperature. A goat anti-rabbit HRP-decorated polymer backbone (Envision, Dako) was used as a secondary reagent. Incubation with cyanine 2-tyramide (Cy2, Perkin Elmer, Inc., Waltham, MA) was used to visualize tumor mask. A nuclear mask was created by incubating with 4, 6-diamidine-2-phenylindole (DAPI) (Invitrogen, Carlsbad, CA, dilution 1 : 500). Coverslips were mounted with ProLong Gold antifade medium (Invitrogen/Life Technologies TM, Grand Island, NY).

2.3. Automated Image Acquisition and Analysis. High-resolution (1024 × 1024 pixels) images were obtained of each histospot as previously described [19]. In brief, monochromatic grayscale images were acquired with a 10x objective of an Olympus AX-51 epifluorescence microscope (Olympus) operating via an automated microscope stage. Digital image acquisition is driven by a custom program and macrobased interfaces with IPLabs software (Scanalytics, Inc.). For the tumor mask, we used the Cy2 signal while DAPI was used to identify the nuclei. The tumor mask is a binary image created from the cytokeratin image (Cy2 signal) of each histospot. DAPI images were used to create the nuclear compartment within each histospot. The membrane compartment within the tumor mask was defined by the perimembranous coalescence of cytokeratin signal with specific exclusion of the nuclear compartment. MET signal was visualized by Cy5, compartmentalized, and expressed as the average signal intensity within the assayed component (AQUA score), with scores on a scale of 0–255.

2.4. Data Analysis. JMP 5.0 software was used for analysis (SAS Institute, Cary, NC). Associations between continuous AQUA scores and clinical/pathological parameters were assessed by analysis of variance. Correlations between the AQUA scores of matched primary and metastatic histospots were calculated paired sample t and chi-squared testing. For heterogeneity assessment between cases, a composite median absolute deviation (MAD) score was generated for each tumor site by patient and compared using a Wilcoxon paired, two-sided rank test, as previously described [20].

3. Results

To compare MET expression in primary and metastatic RCC tumors and evaluate expression heterogeneity, MET expression was quantitatively assessed on a custom TMA previously described [17, 18]. Briefly, the array was constructed with paired primary tumors and distant sites of metastasis and contained a total of eight cores for each patient (four primary and four metastatic) distributed across two blocks.

As was previously reported, MET staining was predominantly cytoplasmic [11]. To assess the interarray variability of MET expression, the correlation between AQUA scores from corresponding cores (from the same tumor block) from each array was analyzed by linear regression. We found

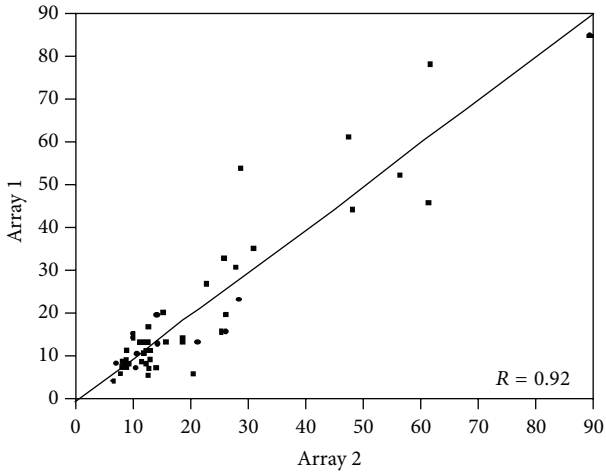

Figure 1: Correlation of MET expression between the two array blocks ($R = 0.92$). Pearson correlation test was used to compare scores from the two tissue microarrays stained for MET ($R = 0.92$).

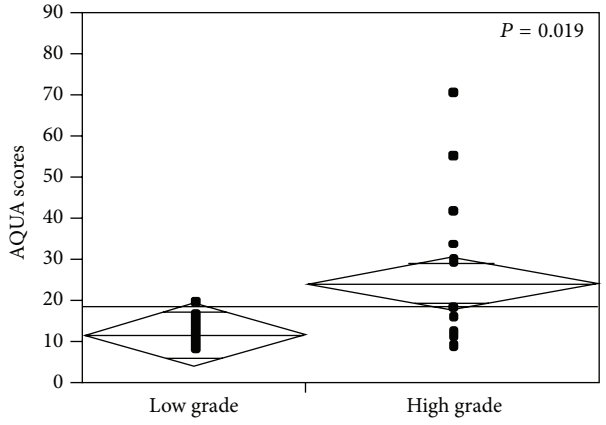

Figure 2: MET expression in low and high Fuhrman grade tumors (1/2 versus 3/4). t-test was used to compare the means of MET expression (AQUA scores) in "low" (1 and 2) versus "high" (3 and 4) Fuhrman grade tumors ($P = 0.019$).

that the scores on the two arrays were highly correlated as demonstrated in Figure 1 ($R = 0.92$).

Using a larger RCC TMA we previously demonstrated an association between MET expression and Fuhrman grade [11]. By using the paired sample t-test, we confirmed this association in this small cohort of predominantly clear cell RCC cases. As shown in Figure 2, the mean expression of MET was over two times greater in high grade tumors (grades 1/2 versus 3/4; mean AQUA scores of 11.825 and 24.258, resp.; $P = 0.019$). For the mixed histology cases, no significant differences were seen between MET expression in tissue with sarcomatoid features and tissue without.

AQUA scores ranged from 7.815 to 87.370 for primary RCC tissue and from 5.705 to 53.843 for metastatic tissue. To compare MET expression between nephrectomy specimens and metastatic RCC tissues, we used t-test. The mean expression of MET in primary tumors (mean AQUA scores for all four cores) was not significantly different when compared to their metastatic counterparts (mean AQUA score of 21.23 versus 15.35, resp., $P = 0.1$, Figure 3(a)).

Table 1: MET expression in primary and metastatic renal cell carcinoma (RCC).

	Primary RCC		
	High MET # (%)	Low MET # (%)	Total cases
Metastatic RCC			
High MET # (%)	10 (58.8%)	6 (42.9%)	16
Low MET # (%)	7 (41.2%)	8 (57.1%)	15
Total cases	17	14	31

Seeing that archival primary RCC tissue is often more readily available to determine patient eligibility for targeted therapy, we studied the correlation of MET expression between primary sites and paired metastatic tissues using the Pearson correlation test. As shown in Figure 3(b), MET expression correlated between the primary and metastatic sites, although the correlation coefficient was modest ($R = 0.5$). While some cases had a low level of discordance, a number of cases exhibited very high levels of discordance. One such example is shown in Figure 4; three out of three assessable primary tumor cores showed either high or moderate staining, while none of the four metastatic cores showed any detectable levels of MET expression. Analysis of scores dichotomized by the median into "high" and "low" showed that in only 58% of cases (18 of 31 assessable cases) scores were concordant, while 42% of the cases (13 of 31) were discordant (Table 1). By chi-square analysis, there was no significant difference between the distribution of high and low MET expression and the two tumor types (primary versus metastatic) (χ^2 $P = 0.375$).

To estimate the degree of heterogeneity of MET expression in primary and metastatic sites, we used the scores from the four cores for each tumor and determined the median absolute deviation (MAD). As seen in Figure 5, a wide range of MAD scores was obtained for each case, indicating wide variability in the degree of heterogeneity. The difference between heterogeneity within nephrectomy specimens compared to the paired metastatic tissues was not statically significant by virtue of a Wilcoxon paired, two-sided rank test ($P = 0.39$).

4. Discussion

With multiple agents now available in the current era of kidney cancer treatment, selection and sequencing is becoming a challenge for clinicians. In order to investigate predictive biomarkers of clinical response, many trials involving targeted agents have incorporated access to resected tissue into the trial eligibility. Two ongoing trials (METEOR, NCT01865747 and CABOSUN, NCT01835158) evaluate XL184 in patients with clear cell RCC, both of which require tissue submission from either the primary tumor or a site of metastasis for retrospective correlative biomarker analysis. As many patients have had a prior nephrectomy, this

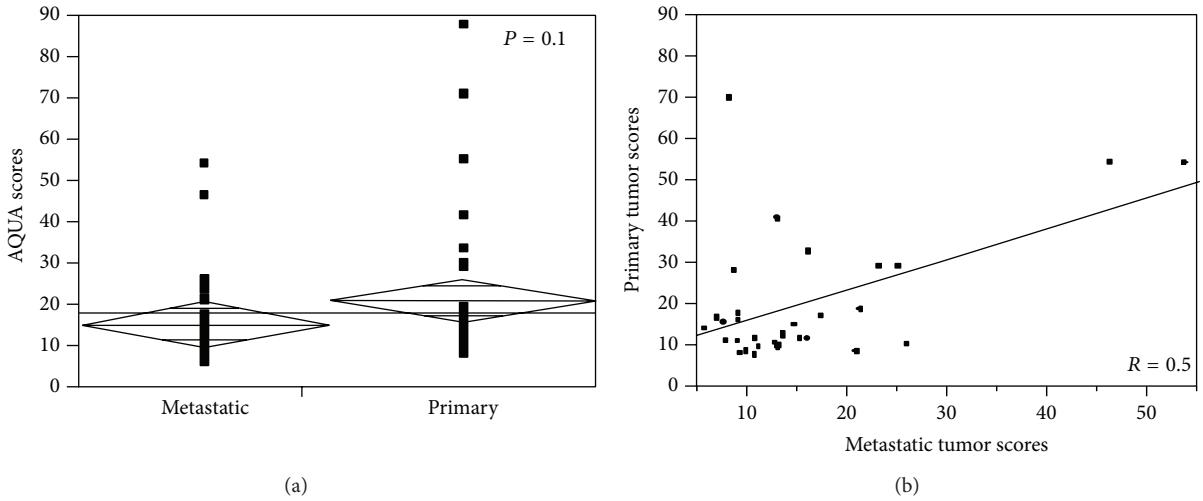

Figure 3: (a) MET expression levels in metastatic versus primary tumors. t-test was used to compare the means of MET expression (AQUA scores) in matched primary and metastatic specimens from the same patients ($P = 0.1$). (b) Correlation of MET expression between primary tumor and matched metastases. Pearson correlation test was used to measure the degree of correlation between MET expressions (AQUA scores) in matched primary versus metastatic specimens ($R = 0.5$).

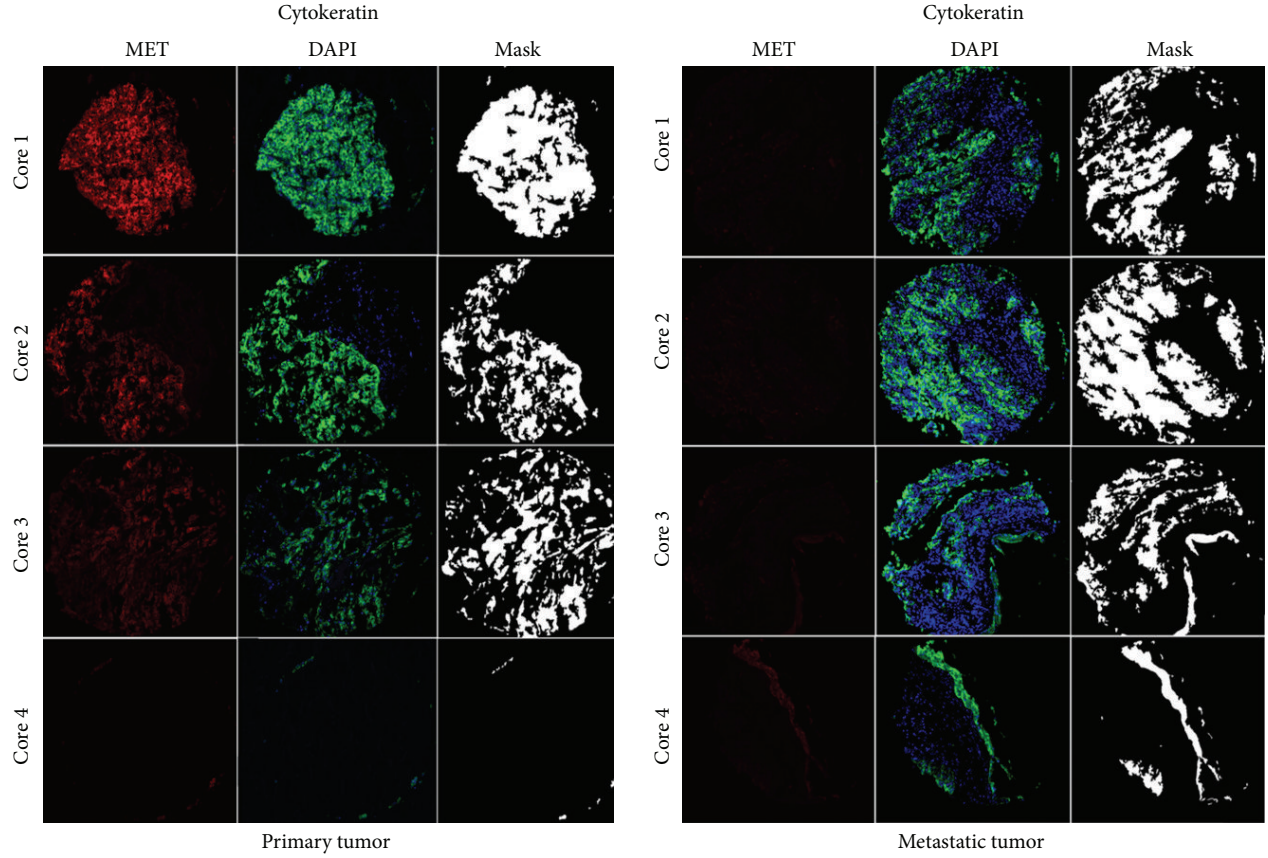

Figure 4: Quantitative immunofluorescent staining of MET in matched primary and metastatic cores. We utilized MET4 antibody to determine expression of MET in a cohort of matched primary and metastatic RCC cases. Cytokeratin (Cy2 signal) was utilized to create a tumor mask. DAPI was used to identify the nuclei. MET signal was visualized by Cy5 and intensities of MET expression were measured within the cytokeratin mask, within the histospot in a quantitative fashion.

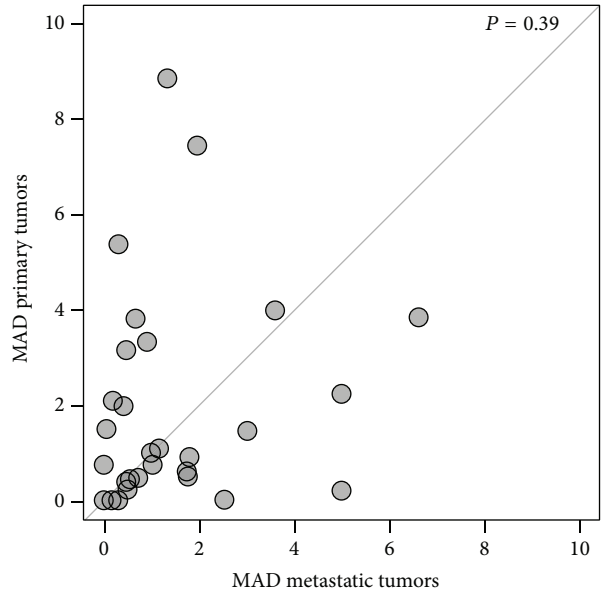

Figure 5: Assessment of MET staining heterogeneity by MAD score for primary and metastatic lesions. We employed the composite median absolute deviation (MAD) to estimate the heterogeneity within primary and metastatic specimens in our cohort. Cases (dots) with larger primary tumor heterogeneity are above the diagonal, while those with a greater heterogeneity in the corresponding metastatic tumors are below the diagonal.

tissue is more readily available for study than a distant site, which is generally assessed with a small core biopsy. With increasing recognition of tumor clonality in kidney cancer, it is necessary to understand if the correlative biomarker analyses should be performed on tissue that represents the metastatic disease. Our data indicate that expression of MET in primary sites does not necessarily correlate with expression at distant sites. While studies have investigated MET expression in the primary clear cell RCC [11, 21], no study to date has evaluated MET expression in a cohort of distant sites or compared matched primary tumor and metastases. We investigated this question using TMAs and a method of quantitated immunohistochemistry (AQUA).

While there are multiple commercially available MET antibodies, many have been reported to have insufficient sensitivity and specificity for biomarker analysis [22]. The antibody we utilized for this study was created by Cao et al. [23]. Knudsen and colleagues interrogated this antibody's performance and found it has excellent technical reproducibility and improved sensitivity when compared to commercially available products [24]. Our analysis of the MET4 antibody confirms the extremely high correlation between arrays ($R = 0.92$).

Limited data exists to demonstrate a correlation between increased MET expression and aggressive pathologic characteristics or/and worse prognosis in RCC. Similar to previous studies, we found that high grade tumors have a greater degree of MET expression ($P = 0.019$). This result supports work from our group and Choi et al. demonstrating tumors with increased MET expression are associated with higher grade and stage disease [11, 25]. While this association has been shown in multiple tumor types, in kidney cancer, there has been some conflicting data including that from Miyata and colleagues [21]. In this analysis, total MET expression was not associated with clinicopathologic characteristics; however pMET was associated with advance stage, higher grade, and the presence of metastatic disease [21]. Differences in these findings could be due to the fact that different antibodies were used between studies. Additionally we did not examine a pMET antibody in our cohort due to the difficulty with signal preservation in formalin-fixed paraffin embedded tissue.

When treating systemic disease with molecular targeted therapy, one would hope the target is highly expressed outside the primary tumor and that the degree of expression would predict response. Our data is the first to evaluate MET expression in sites of distant RCC. We demonstrated that MET expression was not significantly different in metastases when compared to primary sites. For trials involving MET inhibitors, correlative biomarkers are planned on the available tissue, which has generally been submitted from the nephrectomy specimen. While there has been renewed interest in neoadjuvant approaches in locally advanced tumors [26], the majority of systemic therapy in RCC is used to treat distant disease. Therefore correlative biomarker analyses should focus on tissue obtained from distant sites unless the local tumor expression was perfectly correlated with distant disease. In our analysis of the matched sites an important observation was seen; that is, over 40% of specimens had discordant expression when dichotomized to high versus low expression. Also there was only a low level of correlation between MET expressions between the primary and distant tissue ($R = 0.5$). Based on these findings, caution should be used when interpreting correlation of systemic response to

MET therapy if MET expression was generally obtained from tissue from the primary tumor.

Tumor heterogeneity is a concern for any biomarker that may affect treatment, particularly, if the biomarker is to be assessed using tissue from core needle biopsies, which are similar in diameter to our TMA histospots. While the primary tumors often had more MET expression heterogeneity, overall there was no significant difference between sites. We found that MET expression heterogeneity was occasionally high in both the primary tumor and metastatic sites. This raises some concern that sampling expression on limited amount of tissue such as a small core biopsy of either the primary or a distant site may not represent the biology of the majority of the tumor.

Our findings represent the first effort to characterize MET expression patterns in primary and metastatic clear cell RCC. The strengths of this study involve our unique TMA design of matched sites of disease and a novel method of quantitative immunohistochemistry (AQUA). Limitations include the relatively small number of samples, the use of various sites of metastatic disease, and our inability to study pMET in this cohort.

5. Conclusions

MET is a therapeutic target in clear cell RCC and selective inhibitors are currently in clinical trials. Studies of biomarkers predictive of response are planned in many of these trials with the goal of improving the therapeutic window of these inhibitors. Here we demonstrate a weak positive correlation between MET expressions in matched primary and metastatic sites. Moderate concordance of high and low levels of MET expression and significant expression of heterogeneity may be a barrier to the adoption of tissue biomarkers assessing MET expression. Prospective validation of our findings is warranted, as agents targeting the MET pathway appear promising in this disease.

Conflict of Interests

The authors attest that they have no financial or other relationships to declare.

Authors' Contribution

Brian Shuch, Harriet M. Kluger, and Lucia B. Jilaveanu designed and oversaw the research study. Ryan Falbo performed the immunofluorescent staining and data assembly. Adebowale Adeniran performed the pathology review of specimens. Fabio Parisi, Yuval Kluger, Brian Shuch, and Lucia B. Jilaveanu analyzed and interpreted the data. Brian Shuch and Lucia B. Jilaveanu wrote the paper. All authors read and approved the final paper.

Acknowledgments

This publication was made possible by CTSA Grant no. KL2 TR000140 (Lucia B. Jilaveanu, PI) from the National Center for Research Resources (NCRR) and the National Center for Advancing Translational Science (NCATS), components of the National Institutes of Health (NIH), and NIH Roadmap for Medical Research. Its contents are solely the responsibility of the authors and do not necessarily represent the official view of NIH. This work was also supported by NIH Grants R0-1 CA158167 (to Harriet Kluger) and by American Cancer Society Award M130572 (to Harriet Kluger).

References

[1] M. R. Harrison, D. J. George, M. S. Walker et al., "'real world' treatment of metastatic renal cell carcinoma in a joint community-academic cohort: progression-free survival over three lines of therapy," *Clinical Genitourinary Cancer*, vol. 11, no. 4, pp. 441–450, 2013.

[2] R. J. Motzer, T. E. Hutson, P. Tomczak et al., "Sunitinib versus interferon alfa in metastatic renal-cell carcinoma," *The New England Journal of Medicine*, vol. 356, no. 2, pp. 115–124, 2007.

[3] B. Escudier, T. Eisen, W. M. Stadler et al., "Sorafenib in advanced clear-cell renal-cell carcinoma," *The New England Journal of Medicine*, vol. 356, no. 2, pp. 125–134, 2007.

[4] L. Albiges, S. Oudard, S. Negrier et al., "Complete remission with tyrosine kinase inhibitors in renal cell carcinoma," *Journal of Clinical Oncology*, vol. 30, no. 5, pp. 482–487, 2012.

[5] M. Johannsen, A. Flörcken, A. Bex et al., "Can tyrosine kinase inhibitors be discontinued in patients with metastatic renal cell carcinoma and a complete response to treatment? A multicentre, retrospective analysis," *European Urology*, vol. 55, no. 6, pp. 1430–1439, 2009.

[6] N. Nakaigawa, M. Yao, M. Baba et al., "Inactivation of von Hippel-Lindau gene induces constitutive phosphorylation of MET protein in clear cell renal carcinoma," *Cancer Research*, vol. 66, no. 7, pp. 3699–3705, 2006.

[7] M. L. Nickerson, E. Jaeger, Y. Shi et al., "Improved identification of von Hippel-Lindau gene alterations in clear cell renal tumors," *Clinical Cancer Research*, vol. 14, no. 15, pp. 4726–4734, 2008.

[8] Y. Sato, T. Yoshizato, Y. Shiraishi et al., "Integrated molecular analysis of clear-cell renal cell carcinoma," *Nature Genetics*, vol. 45, no. 8, pp. 860–867, 2013.

[9] B. Peruzzi, G. Athauda, and D. P. Bottaro, "The von Hippel-Lindau tumor suppressor gene product represses oncogenic beta-catenin signaling in renal carcinoma cells," *Proceedings of the National Academy of Sciences of the United States of America*, vol. 103, no. 39, pp. 14531–14536, 2006.

[10] F. Shojaei, J. H. Lee, B. H. Simmons et al., "HGF/c-Met acts as an alternative angiogenic pathway in sunitinib-resistant tumors," *Cancer Research*, vol. 70, no. 24, pp. 10090–10100, 2010.

[11] G. T. Gibney, S. A. Aziz, R. L. Camp et al., "C-Met is a prognostic marker and potential therapeutic target in clear cell renal cell carcinoma," *Annals of Oncology*, vol. 24, no. 2, pp. 343–349, 2013.

[12] T. Miyahara, T. Miyata, K. Shigematsu et al., "Clinical outcome and complications of temporary inferior vena cava filter placement," *Journal of Vascular Surgery*, vol. 44, no. 3, pp. 620–624, 2006.

[13] H. Betsunoh, S. Mukai, Y. Akiyama et al., "Clinical relevance of hepsin and hepatocyte growth factor activator inhibitor type 2 expression in renal cell carcinoma," *Cancer Science*, vol. 98, no. 4, pp. 491–498, 2007.

[14] F. Cecchi, D. C. Rabe, and D. P. Bottaro, "Targeting the HGF/Met signalling pathway in cancer," *European Journal of Cancer*, vol. 46, no. 7, pp. 1260–1270, 2010.

[15] P. Schöffski, J. A. Garcia, W. M. Stadler et al., "A phase II study of the efficacy and safety of AMG 102 in patients with metastatic renal cell carcinoma," *BJU International*, vol. 108, no. 5, pp. 679–686, 2011.

[16] T. K. Choueiri, S. Kumar Pal, D. F. McDermott et al., "A phase I study of cabozantinib (XL184) in patients with renal cell cancer," *Annals of Oncology*, 2014.

[17] S. A. Aziz, J. A. Sznol, A. Adeniran et al., "Expression of drug targets in primary and matched metastatic renal cell carcinoma tumors," *BMC Clinical Pathology*, vol. 13, article 3, 2013.

[18] S. A. Aziz, J. Sznol, A. Adeniran, J. W. Colberg, R. L. Camp, and H. M. Kluger, "Vascularity of primary and metastatic renal cell carcinoma specimens," *Journal of Translational Medicine*, vol. 11, no. 1, article 15, 2013.

[19] R. L. Camp, G. G. Chung, and D. L. Rimm, "Automated subcellular localization and quantification of protein expression in tissue microarrays," *Nature Medicine*, vol. 8, no. 11, pp. 1323–1327, 2002.

[20] L. B. Jilaveanu, B. Shuch, C. R. Zito et al., "PD-L1 expression in clear cell renal cell carcinoma: an analysis of nephrectomy and sites of metastases," *Journal of Cancer*, vol. 5, no. 3, pp. 166–172, 2014.

[21] Y. Miyata, H. Kanetake, and S. Kanda, "Presence of phosphorylated hepatocyte growth factor receptor/c-Met is associated with tumor progression and survival in patients with conventional renal cell carcinoma," *Clinical Cancer Research*, vol. 12, no. 16, pp. 4876–4881, 2006.

[22] H. Koeppen, C. Lowe, and S. Rost, "Preclinical evaluation of anti-MET antibodies for immunohistochemical staining," *Journal of Clinical Oncology*, vol. 32, no. 5, supplement, 2014.

[23] B. Cao, Y. Su, M. Oskarsson et al., "Neutralizing monoclonal antibodies to hepatocyte growth factor/scatter factor (HGF/SF) display antitumor activity in animal models," *Proceedings of the National Academy of Sciences of the United States of America*, vol. 98, no. 13, pp. 7443–7448, 2001.

[24] B. S. Knudsen, P. Zhao, J. Resau et al., "A novel multipurpose monoclonal antibody for evaluating human c-Met expression in preclinical and clinical settings," *Applied Immunohistochemistry and Molecular Morphology*, vol. 17, no. 1, pp. 57–67, 2009.

[25] J. S. Choi, M. K. Kim, J. W. Seo et al., "MET expression in sporadic renal cell carcinomas," *Journal of Korean Medical Science*, vol. 21, no. 4, pp. 672–677, 2006.

[26] B. Shuch, S. B. Riggs, J. C. LaRochelle et al., "Neoadjuvant targeted therapy and advanced kidney cancer: observations and implications for a new treatment paradigm," *BJU International*, vol. 102, no. 6, pp. 692–696, 2008.

Hindawi Publishing Corporation
BioMed Research International
Volume 2015, Article ID 215135, 10 pages
http://dx.doi.org/10.1155/2015/215135

Review Article

Molecular Biology in Pediatric High-Grade Glioma: Impact on Prognosis and Treatment

Daniela Rizzo,[1] Antonio Ruggiero,[1] Maurizio Martini,[2] Valentina Rizzo,[1] Palma Maurizi,[1] and Riccardo Riccardi[1]

[1]*Department of Pediatric Oncology, A. Gemelli Hospital, Catholic University of Rome, Largo A Gemelli, 1, 00168 Rome, Italy*
[2]*Anatomic Pathology, Catholic University, "A. Gemelli" Hospital, 00168 Rome, Italy*

Correspondence should be addressed to Antonio Ruggiero; ruggiero@rm.unicatt.it

Received 26 August 2014; Accepted 4 November 2014

Academic Editor: Murat Gokden

High-grade gliomas are the main cause of death in children with brain tumours. Despite recent advances in cancer therapy, their prognosis remains poor and the treatment is still challenging. To date, surgery followed by radiotherapy and temozolomide is the standard therapy. However, increasing knowledge of glioma biology is starting to impact drug development towards targeted therapies. The identification of agents directed against molecular targets aims at going beyond the traditional therapeutic approach in order to develop a personalized therapy and improve the outcome of pediatric high-grade gliomas. In this paper, we critically review the literature regarding the genetic abnormalities implicated in the pathogenesis of pediatric malignant gliomas and the current development of molecularly targeted therapies. In particular, we analyse the impact of molecular biology on the prognosis and treatment of pediatric high-grade glioma, comparing it to that of adult gliomas.

1. Introduction

Brain tumors are the most common solid tumors affecting childhood and the main cause of cancer-related death in children. Gliomas make up approximately 60% of all pediatric brain tumors and about half of these are considered high-grade malignancies. In particular, pediatric glioblastoma (GBM, grade IV WHO) accounts for 15% of all pediatric brain tumours [1]. Despite efforts to improve treatment, children with high-grade glioma (HGG) still have a dismal outcome with a 5-year survival of less than 20% [2].

Surgery followed by radiotherapy (RT) is the standard treatment of patients with HGG. Surgery has prognostic significance in patients with near total resection and at present it is the strongest indicator of prognosis in pediatric HGG. Focal RT is used as first-line therapy except in children under 3 years. Recently, the combination of RT and temozolomide (TMZ) followed by adjuvant TMZ showed a superior outcome compared to RT in the treatment of adults with newly diagnosed GBM [3]. However, several studies on the use of TMZ in the treatment of children with HGG were performed with disappointing results (Table 1) [4–9].

Recognizing the limitations of current standard therapy for HGG, over the past few years substantial advances have been made in molecular biology in identifying new therapeutic approaches. Molecular biological investigations have confirmed that the transformed phenotype of HGG is highly complex and is the result of the dysfunction of a variety of interrelated regulatory pathways (Figure 1) [10]. HGG displays complex chromosomal and genetic alterations leading to the inactivation of various tumor suppressor genes, as well as aberrant activation of protooncogenes. The molecular profiling of HGG in adults has been studied intensively because of its relatively high incidence in this population. Conversely, relatively few studies have been performed on pediatric HGG due to the difficulty in obtaining a large enough series of patient samples. Significant differences exist between adult and pediatric HGG, suggesting that

Table 1: Summary of the main clinical trials in pediatric HGG.

Agent and mechanism of action	Treatment	Study design	Status at diagnosis	Outcome	Reference
Alkylating agent (TMZ)	RT + TMZ	Phase II	Newly diagnosed HGG	EFS3y: 11 ± 3% OS3y: 22 ± 5%	[4]
	TMZ	Phase II	Relapsed or progressive HGG	mOS 4.7 months response rate: 12%	[5]
	RT + TMZ	Phase II	Newly diagnosed HGG	PFS1y: 43% ± 9% PFS2y: 11% ± 5% OS1y: 63% ± 8% OS2y: 21% ± 7%	[6]
	TMZ	Phase II	Relapsed or progressive HGG	mPFS: 3 months PFS6m: 33% mOS: 4 months OS6m: 37.5%	[7]
Receptor tyrosine kinase inhibitors					
EGFR inhibitor (erlotinib)	RT + erlotinib	Phase I	Newly diagnosed HGG	PFS1y: 56% ± 10% PFS2y: 35% ± 12% OS1y:78% ± 9% OS2y: 48% ± 12%	[31]
PDGFR inhibitor (imatinib)	Erlotinib	Phase I	Relapsed or progressive HGG	mPFS: 1.5 months mOS: 4.1 months SD: 28%	[33]
	Imatinib	Phase I	Relapsed or progressive HGG	EFS6m: 17.9% ± 6.6% EFS12m: 0%	[51]
Antiangiogenic agent (BVZ)	BVZ + irinotecan	Phase II	Relapsed or progressive HGG	mPFS: 2.25 months mOS: 6.25 months SD: 33.3%	[65]
	BVZ + irinotecan	Phase II	Relapsed or progressive HGG	mPFS: 4,2 months PFS6m: 41.8%	[64]
	BVZ + irinotecan + TMZ (6 patients) BVZ + irinotecan (1 patient) BVZ + CCNU (1 patient)	Phase II	Relapsed or progressive HGG	mPFS: 15 weeks mOS: 30 weeks	[66]

TMZ: temozolomide; mOS: median overall survival; OS1y: overall survival at 1 year; OS2y: overall survival at 2 years; OS3y: overall survival at 3 years; mPFS: median progression-free survival; PFS1y: progression-free survival at 1 year; PFS2y: progression-free survival at 2 years; SD: stable disease; EFS6m: event-free survival at 6 months; EFS12m: event-free survival at 12 months; EFS3y: event-free survival at 3 years; RT: radiotherapy; CT: chemotherapy; BVZ: bevacizumab; GBM: glioblastoma multiforme.

the pathways and mechanisms of malignant gliomagenesis are molecularly distinct [11, 12]. In this review the genetic abnormalities known to be implicated in the pathogenesis of pediatric HGG are described, underlining their prognostic and predictive role and their main impact on the treatment, including the results achieved with new therapeutic agents directed against rational molecular targets (Table 1).

2. O6-Methylguanine-DNA Methyltransferase (MGMT)

The antitumor activity of TMZ is due to DNA methylation and O6-methylguanine-DNA methyltransferase (MGMT) is one of the suggested mechanisms of chemoresistance [13]. Cytotoxicity of TMZ is initiated by the methylation of the O6

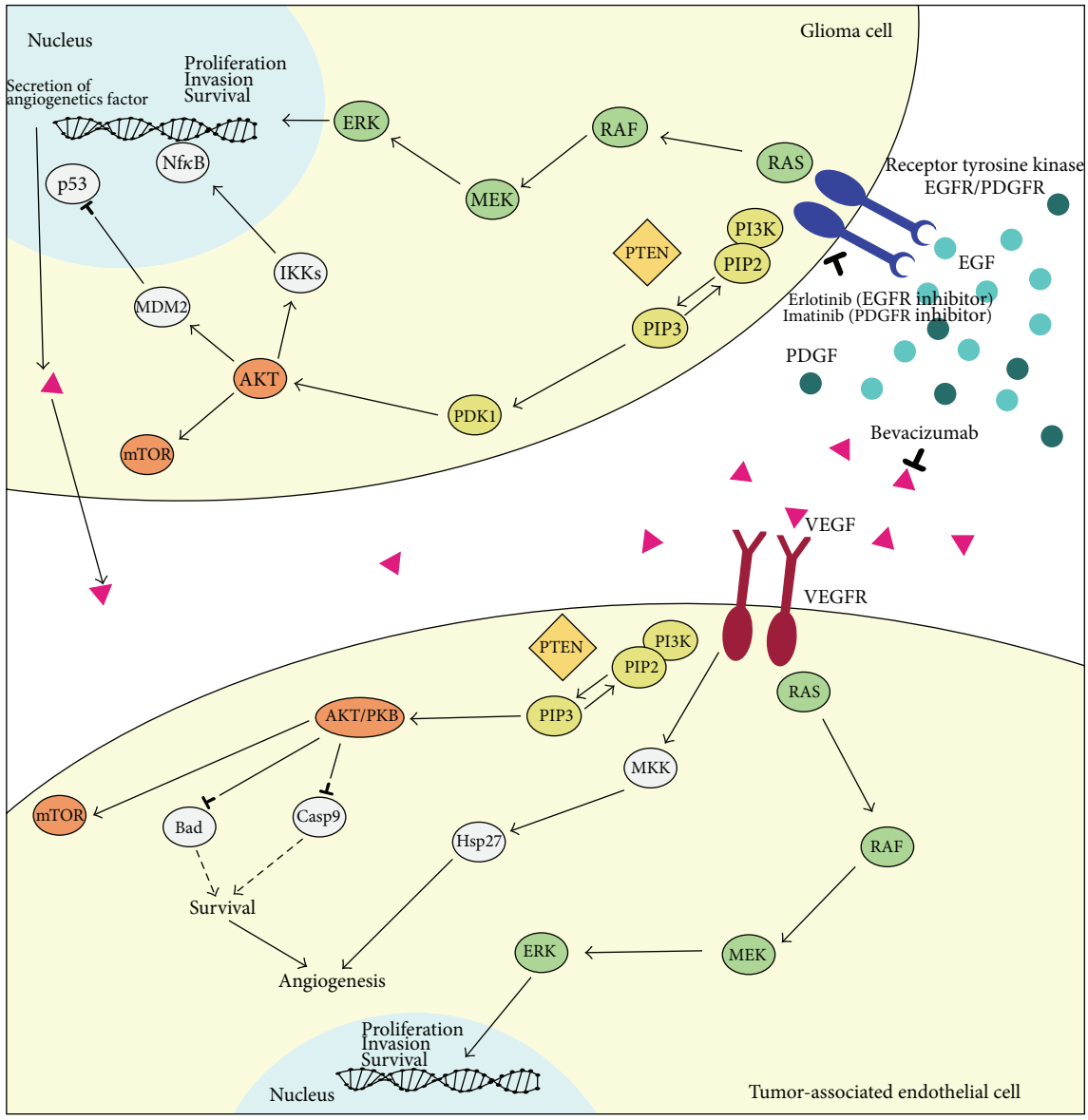

Figure 1: Molecularly targeted therapy for pediatric malignant glioma.

position of guanine which causes mispairing of O6-methylguanine with thymine. The futile repair of this base mismatch by the mismatch repair system generates single- and double-strand DNA breaks that activate cell death. MGMT prevents this process by transferring methylating groups from the O6 position of guanine to one of its internal cysteine residues, neutralizing the cytotoxic effect of alkylating agents. Therefore elevated MGMT activity is associated with enhanced resistance to alkylating agents.

Stupp et al. showed that *MGMT* promoter methylation was associated with loss of MGMT expression and diminished DNA-repair activity. Therefore, *MGMT* promoter methylation represents an independent favorable prognostic factor for GBM patients and a predictive marker of benefit from alkylating agent therapy in GBM [3]. From literature, the percentage of the methylated *MGMT* promoter of adults ranges from 24% to 68%, averaging about 40% [14–16].

Most studies on *MGMT* methylation in HGG have been conducted in adults, probably due to the relatively rare incidence in children. Only few studies in pediatric populations have been reported [17–20], showing a similar methylation status in children and adults and significant correlation between the methylation status and clinical outcome. In particular, a retrospective study of 10 pediatric patients with GBM showed *MGMT* promoter methylation in 4 of 10 patients and revealed a significant association between *MGMT* promoter methylation and prolonged survival ($P = 0.01$) [18]. The average survival time for patients with methylated *MGMT* was 13.7 months as compared to 2.5 months for the patients with unmethylated *MGMT* promoter ($P = 0.01$).

Moreover, the patients receiving TMZ that had the methylated *MGMT* gene promoter responded better to treatment ($P = 0.01$) [18]. In a further study DNA methylation was also associated with increased median event-free survival (EFS) and overall survival (OS) in children with relapsed HGG (5.5 months versus 0.9 months, $P = 0.015$) [21].

Unlike previous studies, recently Lee et al. showed that the incidence of methylation of the *MGMT* promoter in pediatric GBM is rare [22]. In this study the methylation status was assessed using two methods: conventional methylation-specific polymerase chain reaction and, for the first time in pediatric patients, methylation-specific multiplex ligation-dependent probe amplification. Both methods showed a surprisingly low proportion of methylated samples (6% and 16%, resp.). Moreover, there was no difference between the methylated and unmethylated groups in either progression-free survival (PFS) or OS. Based on limitations of this study, such as small number of patients, heterogeneity in terms of adjuvant treatment modality, location of tumor, and extent of resection, the results should be taken with caution and a multicenter collaborative trial with a larger number of patients should be performed.

3. Epidermal Growth Factor Receptor (EGFR)

Epidermal growth factor receptor (EGFR) is a membrane-anchored protein tyrosine kinase that, when phosphorylated, activates a variety of downstream effector molecules regulating cell proliferation and differentiation (Figure 1).

Aberrant cell signaling via the EGFR family has been implicated in the development of several human cancers, including brain tumors. Moreover, recent research has shown a pivotal relationship between EGFR overexpression or *EGFR* amplification and disease progression, poor survival, resistance to chemotherapy, and poor response [23]. *EGFR* amplification and EGFR overexpression affect 30–50% of adult GBM [24]. In pediatric HGGs available data suggest that *EGFR* amplification occurs with low frequency, averaging about 3% [11, 25], although in a recent study Bax et al. found a greater prevalence of *EGFR* gene amplification and *EGFRvIII* mutation in pediatric HGG than had previously been recognized [26]. *EGFRvIII* is the most common mutant of *EGFR* gene reported in GBM. The ability of this variant to "switch on" cell signaling without ligand stimulation, even though it does not dimerize, plays an important role in cancer pathogenesis.

Erlotinib, a small-molecule EGFR inhibitor, has been shown to inhibit EGFRvIII by blocking constitutive EGFRvIII kinase activity and the growth of EGFRvIII transformed cells [27, 28]. However, several clinical trials have demonstrated a limited activity of erlotinib in the treatment of adults and children with recurrent HGG [29–33]. In particular only a subset of patients treated by EGFR inhibitors showed a response to these agents. Mellinghoff et al. demonstrated that coexpression of EGFRvIII and phosphatase and tensin homolog (PTEN) was associated with better response in patients with HGG treated by EGFR inhibitors [27]. Haas-Kogan et al. showed that patients with GBM whose tumors expressed high levels of EGFR and low levels of phosphorylated protein kinase B/Akt responded better to erlotinib therapy [34]. A recent study indicated that 5 genes within the *EGFR* signaling pathway (*STAT1*, *FKBP14*, *RAC1*, *PTGER4*, and *MYC*) may modulate the response of adult GBM to erlotinib [35]. In the study by Bax et al. phosphorylated receptor tyrosine kinase profiling showed a specific activation of platelet-derived growth factor receptor (PDGFR) α/β in EGFRvIII-transduced pediatric GBM cells and targeted coinhibition with erlotinib and imatinib, an inhibitor of the tyrosine kinases Bcr-Abl, Kit, and PDGFR, could lead to enhanced efficacy [26]. This suggests that the erlotinib-associated signaling pathway is a complex one and needs to be taken into account in future trials.

4. Platelet-Derived Growth Factor Receptor (PDGFR)

Platelet-derived growth factor (PDGF) is a major regulator of angiogenesis [36] and is involved in the regulation of proliferation, neuronal differentiation, and motility of cells within the nervous system [37]. PDGF encompasses a family of ligands (AA, AB, BB, CC, and DD) that bind to a pair of receptors (PDGFRα and PDGFRβ) [38]. Concurrent expression of one or more of these ligands and their receptors has been observed in a high percentage of malignant gliomas [38, 39], thus allowing autocrine and paracrine stimulation [38, 40]. In particular, PDGFRA is the most frequent target of focal amplification in pediatric HGGs arising within and outside the brainstem [11, 41–44] and somatic mutations of *PDGFRA* have been recently reported in pediatric HGGs [45, 46]. In contrast, EGFR is the predominant receptor tyrosine kinase targeted by both amplification and mutation in adult GBM [25, 47].

Amplification of wild-type *PDGFRA* occurred more frequently in tumors within the brainstem (26% DIPG versus 11% nonbrainstem HGG, $P = 0.04$), whereas *PDGFRA* sequence mutations were more common in pediatric HGG arising outside the brainstem, although this was not statistically significant (14% nonbrainstem HGG versus 5% DIPG, $P = 0.14$ [11, 41]).

Imatinib (Gleevec) is a molecular targeted drug which selectively inhibits several receptor tyrosine kinases, including PDGFR (Figure 1). Imatinib was evaluated in several clinical trials, with the drug showing limited activity in the monotherapy of adult GBM [48, 49]. Conversely, a substantial antitumor activity of imatinib in combination with hydroxyurea was described in further open-label trials [50]. Nevertheless, the results have been disappointing in pediatric HGG [51] (Table 1) and further trials looking at combination therapy are required. The main reason for the limited activity of imatinib may be that inhibition of PDGFR alone is insufficient to prevent growth of malignant gliomas. Signaling through the Ras-mitogen-activated protein kinase and Akt pathways as a result of *EGFR* amplification and mutation and deletion of *PTEN*, respectively, may result in tumor growth even in the presence of PDGFR inhibition.

5. Phosphatase and Tensin Homolog (PTEN)/Akt

The phosphatidylinositol 3-kinase (PI3K) pathway is involved in several important cellular functions, including growth control, survival, and migration. Following its activation by growth factor receptors, including EGFR, EGFRvIII, and PDGFR, PI3K catalyzes the addition of a phosphate to phosphatidylinositol-4,5,-bisphosphate to form phosphatidylinositol-3,4,5,-triphosphate (PIP3), which initiates many of its tumorigenic activities via Akt (Figure 1). Akt is recruited to the plasma membrane by PI3K mediated formation of PIP3, leading to Akt phosphorylation at thr308 and Ser473 (via phosphoinositide-dependent kinase-1 and phosphoinositide-dependent kinase-2, resp.). Akt phosphorylation at these 2 sites activates its kinase function, leading to downstream signaling promoting proliferation and inhibiting apoptosis.

The *PTEN* gene is an important regulator of the PI3K pathway (Figure 1). It is a tumor suppressor gene which encodes a phosphatase catalyzing the dephosphorylation of PIP3, thus inhibiting activation of the Akt pathway. When *PTEN* is altered, the Akt pathway can become constitutively active. Elevated Akt levels have been associated with loss of PTEN in many GBMs. Moreover, in glial tumors, *PTEN* mutation frequency increases with increasing tumor grade and is associated with poorer outcome [52, 53].

Although *PTEN* mutations are found in approximately 50% of adult HGG, predominantly GBM, a relatively small rate of mutation was found in childhood gliomas [25, 53, 54]. However, in a recent study Pollack et al. observed that activation of Akt is a common finding in pediatric malignant gliomas. In particular, 42 (79%) of the 53 evaluable tumors showed overexpression of activated Akt which was associated with a poor prognosis: 1-year EFS was 59% for patients with Akt overexpression and 91% for those with no overexpression ($P = 0.16$); 1-year OS was 78% and 100%, respectively ($P = 0.06$) [55]. These data were confirmed in a further series of 32 pediatric GBM samples showing an association between Ras/Akt activation and poor survival [1]. In view of the frequency of Akt activation, the evaluation of molecularly targeted therapies that inhibit this pathway warrants consideration as far as these tumors are concerned.

6. Vascular Endothelial Growth Factor (VEGF)

HGGs are some of the most vascularised human tumours and the role of angiogenesis in malignant gliomas has been a very active area of research, with significant impact on the development of targeted therapy [56]. Vascular endothelial growth factor (VEGF) is an important regulator of angiogenesis which is strongly expressed in HGG (Figure 1). The degree of both vasculature density and VEGF expression is associated with the malignancy and aggressiveness of these tumors, as well as with outcomes such as clinical recurrence and survival [57–59]. Recently, data from clinical trials have established antiangiogenic therapy with VEGF targeted agents, with or without cytotoxic chemotherapy, as an active treatment option for patients with recurrent HGG who have failed previous TMZ therapy. Bevacizumab (BVZ) recently received Food and Drug Administration approval as a single agent for the treatment of patients with progressive GBM.

BVZ has been administered with irinotecan, a topoisomerase 1 inhibitor, in patients with recurrent HGG, and this combination has shown activity. BVZ in combination with irinotecan has now been reported in several trials to improve the outcome of recurrent malignant glioma. Both complete and partial responses, as well as disease stabilisation, have been described [60–62]. Moreover, recently, BVZ in combination with standard upfront treatment showed encouraging results [63].

Despite clear evidence of BVZ activity in recurrent HGG, not all patients respond to treatment, and no biomarkers for patients responsive to antiangiogenic therapies have been identified. Moreover, the activity of BVZ was found to be lower in pediatric gliomas, suggesting that genetic differences in pediatric gliomas might account for this difference.

A phase II pediatric brain tumor consortium study of a combination of BVZ and irinotecan was performed in children with recurrent malignant glioma by Gururangan et al., which reported a median PFS of 4.2 months and no sustained responses among the 15 children studied [64]. Similar results were reported in 12 children with recurrent or progressive HGG. Treatment tolerance and toxicity were comparable to adult HGG patients; however, the radiological response rate, response duration, and survival appeared inferior in pediatric patients [65]. Moreover bevacizumab was also investigated in combination with different drugs, such as irinotecan, CCNU, and TMZ, in children with recurrent or progressive WHO grades 3-4 gliomas, and although the combination was well tolerated, it lacked efficacy, with no sustained responses observed [66].

7. TP53

The *TP53* pathway is an important mechanism controlling the cell cycle (Figure 1). Activation of the tumor suppressor p53 by stress signals triggers different cellular programs such as cell cycle arrest, apoptosis, differentiation, DNA repair, autophagy, and senescence through complex network and signaling pathways. Childhood multi-institutional studies have confirmed that p53 overexpression and mutation appear to vary with age, being expressed more strongly in older versus younger children [67, 68]. In the Children's Cancer Group Study, the largest cohort of childhood HGGs analyzed to date, *TP53* mutations were observed in only 2/17 tumors (11.8%) from children <3 years of age at diagnosis versus 24/60 tumors (40%) from older children, a difference that is statistically significant ($P = 0.04$).

Moreover, a significant association has also been found between overexpression of p53, even in the absence of *TP53* mutations, and HGG outcome in children. The rate of PFS at 5 years was 44% in the group of patients whose tumors had low levels of expression of p53 and only 17% in the group of patients whose tumors had overexpression of p53 ($P < 0.001$) [68]. Moreover, overexpression of the p53 protein increases with tumor grade: one-fourth of analyzed AAs and half of GBMs overexpressed this protein.

8. Histone H3.3

Histones are eukaryotic nuclear proteins that play an important role in the regulation of DNA replication, transcription, and storage by changing the nucleosome structure depending on their post translational modifications. H3.3 is a replacement histone subclass that is encoded by 2 distinct genes, *H3.3A* (*H3F3A*) and *H3.3B* [69]. H3.3 is the major histone to be loaded on chromatin during brain development. This histone variant is known to modulate specific chromatin changes and gene expression profiles and to be associated with active chromatin and translation. Recent studies investigated the cancer genome of pediatric diffuse glioma [46, 70]. Exon sequencing identified mutations in histone H3.3 at either aminoacid 27, resulting in replacement of lysine by methionine (K27M), or at aminoacid 34, resulting in replacement of glycine by valine or arginine (G34V/R), as molecular drivers of a subgroup of pediatric and young adult GBMs and pediatric diffuse intrinsic pontine gliomas. In particular one-fourth of pediatric astrocytomas showed somatic mutations in *H3F3A* gene [46, 70–73]. *G34V/R-H3.3* was mainly seen in older patients (median age 20 years) and almost exclusively in hemispheric HGGs [53]. Notably, in GBM patients G34 mutant also showed a trend toward a better OS than wild-type tumor patients, with marginal statistical significance ($P = 0.05$) [55]. In contrast, patients who harbored the *K27M-H3.3* mutation tended toward a worse overall survival when compared to patients who were wild-type for *H3.3*. Moreover, *H3F3A K27* mutation appeared to be exclusive to pediatric high-grade gliomas (median age 11 years) [46, 73] and it was prevalent in diffuse intrinsic pontine glioma [70, 72]. Therefore this mutation defines clinically and biologically distinct subgroup and it is suitable as a molecular marker for pediatric diffuse high-grade astrocytomas with a future impact on therapeutic trial design.

9. Alpha-Thalassemia/Mental-Retardation Syndrome X-Linked (ATRX)

The *ATRX* (alpha-thalassemia/mental-retardation syndrome X-linked) gene is located on chromosome Xq21.1 and encodes a subunit of a chromatin remodelling complex required for H3.3 incorporation at pericentric heterochromatin and telomeres [74]. Mutations that inactivate *ATRX* gene are common in human pancreatic neuroendocrine tumors and central nervous system tumors [70–75]. Loss of ATRX function impairs the heterochromatic state of the telomeres, perhaps because of reduced incorporation of chromatin onto H3.3 histones [75]. This leads to telomere destabilization, which results in a telomerase-independent telomere maintenance mechanism called alternative lengthening of telomeres (ALT).

In 2011, mutations in the *ATRX* gene were described for the first time in a small fraction of adult and pediatric GBM, as well as oligodendrogliomas, and a significant correlation with ALT was demonstrated [75]. Recently, mutations and loss of ATRX have been reported in one-third of pediatric GBMs [46] and 7% of adult GBMs [75]. In gliomas, *ATRX* mutation has been associated with a better prognosis in anaplastic gliomas [76].

Khuong-Quang et al. showed that the presence of *ATRX* mutation significantly overlapped with *TP53* mutations in GBM ($P = 0.01$) regardless of the location within the brain and with G34V/R mutants in supratentorial GBM ($P < 0.0001$). Moreover *ATRX* mutations were infrequent in DIPG and mainly occurred in older children ($P < 0.0001$). The low incidence of this mutation in DIPG could be an age-related phenomenon as the mean age of DIPG cohort was 7 versus 12 years for the supratentorial GBM patient cohort [72]. The requirement for *ATRX* mutations in GBM may thus be due to tumor location and/or the age of the patient. This is potentially indicative of a different cell of origin or age-related plasticity of the tumor.

10. Isocitrate Dehydrogenase (IDH)

Recently a high frequency of mutations of the isocitrate dehydrogenase (*IDH1* and *IDH2*) genes, which encode the IDH enzymes, was detected in adult secondary GBM (85%). These alterations inhibit the normal function of the IDH enzyme in converting isocitrate to α-ketoglutarate [77] and instead drive the conversion of α-ketoglutarate to R(-)-2-hydroxyglutarate [35], a metabolite that may contribute to tumor development. *IDH* mutations likely represent an early step in tumorigenesis because such alterations are also observed commonly in preexisting lower grade lesions [78].

Such alterations are uncommon in pediatric population, highlighting molecular differences with adult secondary GBM.

The series of Balss et al. [79] included 14 pediatric GBMs and only one case had an *IDH1* mutation. In 2 recent studies performed on pediatric malignant gliomas *IDH1* mutations were not detected in any case [80, 81]. Similarly, in a study of 1010 diffuse gliomas that included a small subgroup of children, Hartmann et al. [82] noted that *IDH1* mutations were rare in the pediatric subset, and *IDH2* mutations were absent, although the frequency of mutations as a function of age and histology was not provided.

Based on the molecular similarities that have been noted between primary pediatric malignant gliomas that arise in older children and secondary malignant gliomas that occur in adults, recently Pollack et al. examined the frequency of *IDH* mutations in a cohort of 43 HGG patients aged 3–21 years at the time of diagnosis [83]. *IDH1* mutations were noted in 7 of 20 tumors (35%) from children ≥14 years, but in 0 of 23 (0%) younger children ($P = 0.01$), suggesting that a subset of such lesions may be comparable on a molecular basis to lesions that arise in young adults. In contrast, such alterations were rare in tumors arising in younger children, supporting the existence of age-related pathways of tumorigenesis in childhood. Moreover *IDH*-mutated tumors seemed to be associated with a more favorable prognosis than non mutated tumors as in adult patients [80].

11. Conclusion

HGGs are highly heterogeneous and aggressive brain tumours, requiring a multidisciplinary approach. Recently, molecular research has significantly improved our understanding of glioma pathogenesis and identified key proteins that regulate normal biological processes and cellular pathways associated with pediatric HGG. The identification of agents directed against molecular targets aims at going beyond the traditional therapeutic approach in order to develop a personalized therapy and improve the outcome of pediatric HGG.

Results from adult clinical trials cannot simply be extrapolated to children due to crucial molecular differences between adult and pediatric HGG, drawing attention to the need for exclusively pediatric clinical studies. PDGFRA is the most frequent target of focal amplification in pediatric HGGs; in contrast, EGFR is the predominant receptor tyrosine kinase targeted in adult GBM. No *IDH1* mutations have been found in pediatric tumors, highlighting molecular differences with adult secondary GBM. Activity of bevacizumab is lower in pediatric gliomas than that observed in adult HGG. Recently a central role of *ATRX* and *H3F3A K27* mutations in pediatric HHGs has been described.

Although targeted agents offer great promise, to date the overall response rate has been disappointing, with differences in response not only between children and adults but also within each population. These observations demonstrate that distinct biological profiles can be identified in different subsets of patients; therefore individual targeted therapy based on molecular biology should be investigated in order to define an optimal treatment strategy for each patient.

Conflict of Interests

The authors declare that there is no conflict of interests regarding the publication of this paper.

References

[1] D. Faury, A. Nantel, S. E. Dunn et al., "Molecular profiling identifies prognostic subgroups of pediatric glioblastoma and shows increased YB-1 expression in tumors," *Journal of Clinical Oncology*, vol. 25, no. 10, pp. 1196–1208, 2007.

[2] A. Broniscer and A. Gajjar, "Supratentorial high-grade astrocytoma and diffuse brainstem glioma: two challenges for the pediatric oncologist," *Oncologist*, vol. 9, no. 2, pp. 197–206, 2004.

[3] R. Stupp, W. P. Mason, M. J. van den Bent et al., "Radiotherapy plus concomitant and adjuvant temozolomide for glioblastoma," *The New England Journal of Medicine*, vol. 352, no. 10, pp. 987–996, 2005.

[4] K. J. Cohen, I. F. Pollack, T. Zhou et al., "Temozolomide in the treatment of high-grade gliomas in children: a report from the Children's Oncology Group," *Neuro-Oncology*, vol. 13, no. 3, pp. 317–323, 2011.

[5] L. S. Lashford, P. Thiesse, A. Jouvet et al., "Temozolomide in malignant gliomas of childhood: A United Kingdom Children's Cancer Study Group and French Society for Pediatric Oncology Intergroup Study," *Journal of Clinical Oncology*, vol. 20, no. 24, pp. 4684–4691, 2002.

[6] A. Broniscer, M. Chintagumpala, M. Fouladi et al., "Temozolomide after radiotherapy for newly diagnosed high-grade glioma and unfavorable low-grade glioma in children," *Journal of Neuro-Oncology*, vol. 76, no. 3, pp. 313–319, 2006.

[7] A. Ruggiero, G. Cefalo, M. L. Garré et al., "Phase II trial of temozolomide in children with recurrent high-grade glioma," *Journal of Neuro-Oncology*, vol. 77, no. 1, pp. 89–94, 2006.

[8] H. S. Nicholson, C. S. Kretschmar, M. Krailo et al., "Phase 2 study of temozolomide in children and adolescents with recurrent central nervous system tumors: a report from the Children's Oncology Group," *Cancer*, vol. 110, no. 7, pp. 1542–1550, 2007.

[9] K. J. Cohen, R. L. Heideman, T. Zhou et al., "Temozolomide in the treatment of children with newly diagnosed diffuse intrinsic pontine gliomas: a report from the Children's Oncology Group," *Neuro-Oncology*, vol. 13, no. 4, pp. 410–416, 2011.

[10] E. A. Maher, F. B. Furnari, R. M. Bachoo et al., "Malignant glioma: genetics and biology of a grave matter," *Genes & Development*, vol. 15, no. 11, pp. 1311–1333, 2001.

[11] B. S. Paugh, C. Qu, C. Jones et al., "Integrated molecular genetic profiling of pediatric high-grade gliomas reveals key differences with the adult disease," *Journal of Clinical Oncology*, vol. 28, no. 18, pp. 3061–3068, 2010.

[12] T. J. MacDonald, D. Aguilera, and C. M. Kramm, "Treatment of high-grade glioma in children and adolescents," *Neuro-Oncology*, vol. 13, no. 10, pp. 1049–1058, 2011.

[13] R. Stupp, M. Gander, S. Leyvraz, and E. Newlands, "Current and future developments in the use of temozolomide for the treatment of brain tumours," *The Lancet Oncology*, vol. 2, no. 9, pp. 552–560, 2001.

[14] M. Esteller, J. Garcia-Foncillas, E. Andion et al., "Inactivation of the DNA-repair gene MGMT and the clinical response of gliomas to alkylating agents," *The New England Journal of Medicine*, vol. 343, no. 19, pp. 1350–1354, 2000.

[15] M. E. Hegi, A.-C. Diserens, T. Gorlia et al., "MGMT gene silencing and benefit from temozolomide in glioblastoma," *The New England Journal of Medicine*, vol. 352, no. 10, pp. 997–1003, 2005.

[16] M. Eoli, F. Menghi, M. G. Bruzzone et al., "Methylation of O6-methylguanine DNA methytransferase and loss of heterozygosity on 19q and/or 17p are overlapping features of secondary glioblastomas with prolonged survival," *Clinical Cancer Research*, vol. 13, no. 9, pp. 2606–2613, 2007.

[17] I. F. Pollack, R. L. Hamilton, R. W. Sobol et al., "O6-Methylguanine-DNA methyltransferase expression strongly correlates with outcome in childhood malignant gliomas: results from the CCG-945 cohort," *Journal of Clinical Oncology*, vol. 24, no. 21, pp. 3431–3437, 2006.

[18] A. M. Donson, S. O. Addo-Yobo, M. H. Handler, L. Gore, and N. K. Foreman, "MGMT promoter methylation correlates with survival benefit and sensitivity to temozolomide in pediatric glioblastoma," *Pediatric Blood and Cancer*, vol. 48, no. 4, pp. 403–407, 2007.

[19] F. R. Buttarelli, M. Massimino, M. Antonelli et al., "Evaluation status and prognostic significance of O6-methylguanine-DNA methyltransferase (MGMT) promoter methylation in pediatric high grade gliomas," *Child's Nervous System*, vol. 26, no. 8, pp. 1051–1056, 2010.

[20] A. Srivastava, A. Jain, P. Jha et al., "MGMT gene promoter methylation in pediatric glioblastomas," *Child's Nervous System*, vol. 26, no. 11, pp. 1613–1618, 2010.

[21] S. Schlosser, S. Wagner, J. M. Hlisch et al., "MGMT as a potential stratification marker in relapsed high-grade glioma of children: the HIT-GBM experience," *Pediatric Blood & Cancer*, vol. 54, no. 2, pp. 228–237, 2010.

[22] J. Y. Lee, C.-K. Park, S.-H. Park, K.-C. Wang, B.-K. Cho, and S.-K. Kim, "MGMT promoter gene methylation in pediatric glioblastoma: analysis using MS-MLPA," *Child's Nervous System*, vol. 27, no. 11, pp. 1877–1883, 2011.

[23] N. Shinojima, K. Tada, S. Shiraishi et al., "Prognostic value of epidermal growth factor receptor in patients with glioblastoma multiforme," *Cancer Research*, vol. 63, no. 20, pp. 6962–6970, 2003.

[24] T. A. Libermann, H. R. Nusbaum, N. Razon et al., "Amplification, enhanced expression and possible rearrangement of EGF receptor gene in primary human brain tumours of glial origin," *Nature*, vol. 313, no. 5998, pp. 144–147, 1985.

[25] I. F. Pollack, R. L. Hamilton, C. D. James et al., "Rarity of PTEN deletions and EGFR amplification in malignant gliomas of childhood: results from the Children's Cancer Group 945 cohort," *Journal of Neurosurgery*, vol. 105, no. 5, pp. 418–424, 2006.

[26] D. A. Bax, N. Gaspar, S. E. Little et al., "EGFRvIII deletion mutations in pediatric high-grade glioma and response to targeted therapy in pediatric glioma cell lines," *Clinical Cancer Research*, vol. 15, pp. 5753–5761, 2009.

[27] I. K. Mellinghoff, M. Y. Wang, I. Vivanco et al., "Molecular determinants of the response of glioblastomas to EGFR kinase inhibitors," *The New England Journal of Medicine*, vol. 353, no. 19, pp. 2012–2024, 2005.

[28] I. K. Mellinghoff, T. F. Cloughesy, and P. S. Mischel, "PTEN-mediated resistance to epidermal growth factor receptor kinase inhibitors," *Clinical Cancer Research*, vol. 13, no. 2 I, pp. 378–381, 2007.

[29] M. D. Prados, K. R. Lamborn, S. Chang et al., "Phase 1 study of erlotinib HCl alone and combined with temozolomide in patients with stable or recurrent malignant glioma," *Neuro-Oncology*, vol. 8, no. 1, pp. 67–78, 2006.

[30] W. K. A. Yung, J. J. Vredenburgh, T. F. Cloughesy et al., "Safety and efficacy of erlotinib in first-relapse glioblastoma: a phase II open-label study," *Neuro-Oncology*, vol. 12, no. 10, pp. 1061–1070, 2010.

[31] A. Broniscer, S. J. Baker, C. F. Stewart et al., "Phase Ii and pharmacokinetic studies of erlotinib administered concurrently with radiotherapy for children, adolescents, and young adults with high-grade glioma," *Clinical Cancer Research*, vol. 15, no. 2, pp. 701–707, 2009.

[32] R. I. Jakacki, M. Hamilton, R. J. Gilbertson et al., "Pediatric phase I and pharmacokinetic study of erlotinib followed by the combination of erlotinib and temozolomide: a children's oncology group phase I consortium study," *Journal of Clinical Oncology*, vol. 26, no. 30, pp. 4921–4927, 2008.

[33] B. Geoerger, D. Hargrave, F. Thomas et al., "Innovative therapies for children with cancer pediatric phase I study of erlotinib in brainstem glioma and relapsing/refractory brain tumors," *Neuro-Oncology*, vol. 13, no. 1, pp. 109–118, 2011.

[34] D. A. Haas-Kogan, M. D. Prados, T. Tihan et al., "Epidermal growth factor receptor, protein kinase B/Akt, and glioma response to erlotinib," *Journal of the National Cancer Institute*, vol. 97, no. 12, pp. 880–887, 2005.

[35] M.-E. Halatsch, S. Löw, T. Hielscher, U. Schmidt, A. Unterberg, and V. I. Vougioukas, "Epidermal growth factor receptor pathway gene expressions and biological response of glioblastoma multiforme cell lines to erlotinib," *Anticancer Research*, vol. 28, no. 6A, pp. 3725–3728, 2008.

[36] D. Wang, H.-J. S. Huang, A. Kazlauskas, and W. K. Cavenee, "Induction of vascular endothelial growth factor expression in endothelial cells by platelet-derived growth factor through the activation of phosphatidylinositol 3-kinase," *Cancer Research*, vol. 59, no. 7, pp. 1464–1472, 1999.

[37] A. Erlandsson, M. Enarsson, and K. Forsberg-Nilsson, "Immature neurons from CNS stem cells proliferate in response to platelet-derived growth factor," *Journal of Neuroscience*, vol. 21, no. 10, pp. 3483–3491, 2001.

[38] N. A. Lokker, C. M. Sullivan, S. J. Hollenbach, M. A. Israel, and N. A. Giese, "Platelet-derived growth factor (PDGF) autocrine signaling regulates survival and mitogenic pathways in glioblastoma cells: evidence that the novel PDGF-C and PDGF-D ligands may play a role in the development of brain tumors," *Cancer Research*, vol. 62, no. 13, pp. 3729–3735, 2002.

[39] M. Maxwell, S. P. Naber, H. J. Wolfe et al., "Coexpression of platelet-derived growth factor (PDGF) and PDGF-receptor genes by primary human astrocytomas may contribute to their development and maintenance," *The Journal of Clinical Investigation*, vol. 86, no. 1, pp. 131–140, 1990.

[40] F. S. Vassbotn, A. Östman, N. Langeland et al., "Activated platelet-derived growth factor autocrine pathway drives the transformed phenotype of a human glioblastoma cell line," *Journal of Cellular Physiology*, vol. 158, no. 2, pp. 381–389, 1994.

[41] B. S. Paugh, A. Broniscer, C. Qu et al., "Genome-wide analyses identify recurrent amplifications of receptor tyrosine kinases and cell-cycle regulatory genes in diffuse intrinsic pontine glioma," *Journal of Clinical Oncology*, vol. 29, no. 30, pp. 3999–4006, 2011.

[42] S. Puget, C. Philippe, D. A. Bax et al., "Mesenchymal transition and pdgfra amplification/mutation are key distinct oncogenic events in pediatric diffuse intrinsic pontine gliomas," *PLoS ONE*, vol. 7, no. 2, Article ID e30313, 2012.

[43] M. Zarghooni, U. Bartels, E. Lee et al., "Whole-genome profiling of pediatric diffuse intrinsic pontine gliomas highlights platelet-derived growth factor receptor α and poly (ADP-ribose) polymerase as potential therapeutic targets," *Journal of Clinical Oncology*, vol. 28, no. 8, pp. 1337–1344, 2010.

[44] D. A. Bax, A. Mackay, S. E. Little et al., "A distinct spectrum of copy number aberrations in pediatric high-grade gliomas," *Clinical Cancer Research*, vol. 16, no. 13, pp. 3368–3377, 2010.

[45] B. S. Paugh, X. Zhu, C. Qu et al., "Novel oncogenic PDGFRA mutations in pediatric high-grade gliomas," *Cancer Research*, vol. 73, no. 20, pp. 6219–6229, 2013.

[46] J. Schwartzentruber, A. Korshunov, X.-Y. Liu et al., "Driver mutations in histone H3.3 and chromatin remodelling genes in paediatric glioblastoma," *Nature*, vol. 482, no. 7384, pp. 226–231, 2012.

[47] F. B. Furnari, T. Fenton, R. M. Bachoo et al., "Malignant astrocytic glioma: genetics, biology, and paths to treatment," *Genes and Development*, vol. 21, no. 21, pp. 2683–2710, 2007.

[48] E. Raymond, A. A. Brandes, C. Dittrich et al., "Phase II study of imatinib in patients with recurrent gliomas of various histologies: a European organisation for research and treatment of cancer brain tumor group study," *Journal of Clinical Oncology*, vol. 26, no. 28, pp. 4659–4665, 2008.

[49] P. Y. Wen, W. K. A. Yung, K. R. Lamborn et al., "Phase I/II study of imatinib mesylate for recurrent malignant gliomas: north American brain tumor consortium study 99–08," *Clinical Cancer Research*, vol. 12, no. 16, pp. 4899–4907, 2006.

[50] D. A. Reardon, M. J. Egorin, J. A. Quinn et al., "Phase II study of imatinib mesylate plus hydroxyurea in adults with recurrent glioblastoma multiforme," *Journal of Clinical Oncology*, vol. 23, pp. 9359–9368, 2005.

[51] I. F. Pollack, R. I. Jakacki, S. M. Blaney et al., "Phase I trial of imatinib in children with newly diagnosed brainstem and recurrent malignant gliomas: a Pediatric Brain Tumor Consortium report," *Neuro-Oncology*, vol. 9, no. 2, pp. 145–160, 2007.

[52] J. S. Smith, I. Tachibana, S. M. Passe et al., "PTEN mutation, EGFR amplification, and outcome in patients with anaplastic astrocytoma and glioblastoma multiforme," *Journal of the National Cancer Institute*, vol. 93, no. 16, pp. 1246–1256, 2001.

[53] C. Raffel, L. Frederick, J. R. O'Fallon et al., "Analysis of oncogene and tumor suppressor gene alterations in pediatric malignant astrocytomas reveals reduced survival for patients with PTEN mutations," *Clinical Cancer Research*, vol. 5, no. 12, pp. 4085–4090, 1999.

[54] J. A. Kraus, J. Felsberg, J. C. Tonn, G. Reifenberger, and T. Pietsch, "Molecular genetic analysis of the *TP53*, *PTEN*, *CDKN2A*, *EGFR*, *CDK4* and *MDM2* tumour-associated genes in supratentorial primitive neuroectodermal tumours and glioblastomas of childhood," *Neuropathology and Applied Neurobiology*, vol. 28, no. 4, pp. 325–333, 2002.

[55] I. F. Pollack, R. L. Hamilton, P. C. Burger et al., "Akt activation is a common event in pediatric malignant gliomas and a potential adverse prognostic marker: a report from the Children's Oncology Group," *Journal of Neuro-Oncology*, vol. 99, no. 2, pp. 155–163, 2010.

[56] N. Oka, A. Soeda, A. Inagaki et al., "VEGF promotes tumorigenesis and angiogenesis of human glioblastoma stem cells," *Biochemical and Biophysical Research Communications*, vol. 360, no. 3, pp. 553–559, 2007.

[57] S. P. Leon, R. D. Folkerth, and P. M. Black, "Microvessel density is a prognostic indicator for patients with astroglial brain tumors," *Cancer*, vol. 77, no. 2, pp. 362–372, 1996.

[58] N. O. Schmidt, M. Westphal, C. Hagel et al., "Levels of vascular endothelial growth factor, hepatocyte growth factor/scatter factor and basic fibroblast growth factor in human gliomas and their relation to angiogenesis," *International Journal of Cancer*, vol. 84, pp. 10–18, 1999.

[59] Y.-H. Zhou, F. Tan, K. R. Hess, and W. K. A. Yung, "The expression of PAX6, PTEN, vascular endothelial growth factor, and epidermal growth factor receptor in gliomas: relationship to tumor grade and survival," *Clinical Cancer Research*, vol. 9, no. 9, pp. 3369–3375, 2003.

[60] D. Schiff and B. Purow, "Bevacizumab in combination with irinotecan for patients with recurrent glioblastoma multiforme: commentary," *Nature Clinical Practice Oncology*, vol. 5, no. 4, pp. 186–187, 2008.

[61] M. C. Chamberlain, "Bevacizumab plus irinotecan in recurrent glioblastoma," *Journal of Clinical Oncology*, vol. 26, no. 6, pp. 1012–1013, 2008.

[62] J. J. Vredenburgh, A. Desjardins, J. E. Herndon II et al., "Phase II trial of bevacizumab and irinotecan in recurrent malignant glioma," *Clinical Cancer Research*, vol. 13, no. 4, pp. 1253–1259, 2007.

[63] A. Lai, E. Filka, B. McGibbon et al., "Phase II pilot study of bevacizumab in combination with temozolomide and regional radiation therapy for up-front treatment of patients with newly diagnosed glioblastoma multiforme: interim analysis of safety and tolerability," *International Journal of Radiation Oncology, Biology, Physics*, vol. 71, no. 5, pp. 1372–1380, 2008.

[64] S. Gururangan, S. N. Chi, T. Y. Poussaint et al., "Lack of efficacy of bevacizumab plus irinotecan in children with recurrent malignant glioma and diffuse brainstem glioma: a pediatric brain tumor consortium study," *Journal of Clinical Oncology*, vol. 28, no. 18, pp. 3069–3075, 2010.

[65] A. Narayana, S. Kunnakkat, J. Chacko-Mathew et al., "Bevacizumab in recurrent high-grade pediatric gliomas," *Neuro-Oncology*, vol. 12, no. 9, pp. 985–990, 2010.

[66] C. Parekh, R. Jubran, A. Erdreich-Epstein et al., "Treatment of children with recurrent high grade gliomas with a bevacizumab containing regimen," *Journal of Neuro-Oncology*, vol. 103, no. 3, pp. 673–680, 2011.

[67] I. F. Pollack, S. D. Finkelstein, J. Burnham et al., "Age and TP53 mutation frequency in childhood malignant gliomas: results in a multi-institutional cohort," *Cancer Research*, vol. 61, no. 20, pp. 7404–7407, 2001.

[68] I. F. Pollack, S. D. Finkelstein, J. Woods et al., "Expression of p53 and prognosis in children with malignant gliomas," *The New England Journal of Medicine*, vol. 346, no. 6, pp. 420–427, 2002.

[69] J. A. Simon and R. E. Kingston, "Mechanisms of polycomb gene silencing: knowns and unknowns," *Nature Reviews Molecular Cell Biology*, vol. 10, no. 10, pp. 697–708, 2009.

[70] G. Wu, A. Broniscer, T. A. McEachron et al., "Somatic histone H3 alterations in pediatric diffuse intrinsic pontine gliomas and non-brainstem glioblastomas," *Nature Genetics*, vol. 44, no. 3, pp. 251–253, 2012.

[71] D. Sturm, H. Witt, V. Hovestadt et al., "Hotspot mutations in H3F3A and IDH1 define distinct epigenetic and biological subgroups of glioblastoma," *Cancer Cell*, vol. 22, no. 4, pp. 425–437, 2012.

[72] D.-A. Khuong-Quang, P. Buczkowicz, P. Rakopoulos et al., "K27M mutation in histone H3.3 defines clinically and biologically distinct subgroups of pediatric diffuse intrinsic pontine gliomas," *Acta Neuropathologica*, vol. 124, no. 3, pp. 439–447, 2012.

[73] G. H. Gielen, M. Gessi, J. Hammes, C. M. Kramm, A. Waha, and T. Pietsch, "H3F3A K27M mutation in pediatric CNS tumors: a marker for diffuse high-grade astrocytomas," *The American Journal of Clinical Pathology*, vol. 139, no. 3, pp. 345–349, 2013.

[74] A. Dhayalan, R. Tamas, I. Bock et al., "The ATRX-ADD domain binds to H3 tail peptides and reads the combined methylation state of K4 and K9," *Human Molecular Genetics*, vol. 20, no. 11, pp. 2195–2203, 2011.

[75] C. M. Heaphy, R. F. de Wilde, Y. Jiao et al., "Altered telomeres in tumors with ATRX and DAXX mutations," *Science*, vol. 333, no. 6041, article 425, 2011.

[76] B. Wiestler, D. Capper, T. Holland-Letz et al., "ATRX loss refines the classification of anaplastic gliomas and identifies a subgroup of IDH mutant astrocytic tumors with better prognosis," *Acta Neuropathologica*, vol. 126, no. 3, pp. 443–451, 2013.

[77] S. Zhao, Y. Lin, W. Xu et al., "Glioma-derived mutations in *IDH1* dominantly inhibit *IDH1* catalytic activity and induce HIF-1α," *Science*, vol. 324, no. 5924, pp. 261–265, 2009.

[78] S. Nobusawa, T. Watanabe, P. Kleihues, and H. Ohgaki, "IDH1 mutations as molecular signature and predictive factor of secondary glioblastomas," *Clinical Cancer Research*, vol. 15, no. 19, pp. 6002–6007, 2009.

[79] J. Balss, J. Meyer, W. Mueller, A. Korshunov, C. Hartmann, and A. von Deimling, "Analysis of the IDH1 codon 132 mutation in

brain tumors," *Acta Neuropathologica*, vol. 116, no. 6, pp. 597–602, 2008.

[80] H. Yan, D. W. Parsons, G. Jin et al., "*IDH1* and *IDH2* mutations in gliomas," *The New England Journal of Medicine*, vol. 360, no. 8, pp. 765–773, 2009.

[81] M. Antonelli, F. R. Buttarelli, A. Arcella et al., "Prognostic significance of histological grading, p53 status, YKL-40 expression, and IDH1 mutations in pediatric high-grade gliomas," *Journal of Neuro-Oncology*, vol. 99, no. 2, pp. 209–215, 2010.

[82] C. Hartmann, J. Meyer, J. Balss et al., "Type and frequency of *IDH1* and *IDH2* mutations are related to astrocytic and oligodendroglial differentiation and age: a study of 1,010 diffuse gliomas," *Acta Neuropathologica*, vol. 118, no. 4, pp. 469–474, 2009.

[83] I. F. Pollack, R. L. Hamilton, R. W. Sobol et al., "IDH1 mutations are common in malignant gliomas arising in adolescents: a report from the Children's Oncology Group," *Child's Nervous System*, vol. 27, no. 1, pp. 87–94, 2011.

Hindawi Publishing Corporation
BioMed Research International
Volume 2015, Article ID 712438, 9 pages
http://dx.doi.org/10.1155/2015/712438

Research Article

Overexpression of *GPC6* and *TMEM132D* in Early Stage Ovarian Cancer Correlates with CD8+ T-Lymphocyte Infiltration and Increased Patient Survival

Athanasios Karapetsas,[1] Antonis Giannakakis,[1,2] Denarda Dangaj,[1,3] Evripidis Lanitis,[1,3] Spyridon Kynigopoulos,[4] Maria Lambropoulou,[4] Janos L. Tanyi,[5] Alex Galanis,[1] Stylianos Kakolyris,[6] Gregorios Trypsianis,[7] George Coukos,[3] and Raphael Sandaltzopoulos[1]

[1] *Laboratory of Gene Expression, Molecular Diagnosis and Modern Therapeutics, Department of Molecular Biology and Genetics, Faculty of Health Sciences, Democritus University of Thrace, 68100 Alexandroupolis, Greece*
[2] *Division of Genome and Gene Expression Data Analysis, Bioinformatics Institute, Agency for Science, Technology and Research (A*STAR), Singapore 138671*
[3] *Department of Oncology, University Hospital of Lausanne (CHUV), Ludwig Cancer Research Center, University of Lausanne, 1011 Lausanne, Switzerland*
[4] *Laboratory of Histology and Embryology, School of Medicine, Faculty of Health Sciences, Democritus University of Thrace, 68100 Alexandroupolis, Greece*
[5] *Division of Gynecologic Oncology, University of Pennsylvania, Philadelphia, PA 19014, USA*
[6] *Department of Clinical Oncology, School of Medicine, Faculty of Health Sciences, Democritus University of Thrace, 68100 Alexandroupolis, Greece*
[7] *Medical Statistics Lab, School of Medicine, Faculty of Health Sciences, Democritus University of Thrace, 68100 Alexandroupolis, Greece*

Correspondence should be addressed to Raphael Sandaltzopoulos; rmsandal@mbg.duth.gr

Received 12 January 2015; Revised 27 May 2015; Accepted 28 May 2015

Academic Editor: Beric Henderson

Infiltration of cytotoxic T-lymphocytes in ovarian cancer is a favorable prognostic factor. Employing a differential expression approach, we have recently identified a number of genes associated with CD8+ T-cell infiltration in early stage ovarian tumors. In the present study, we validated by qPCR the expression of two genes encoding the transmembrane proteins GPC6 and TMEM132D in a cohort of early stage ovarian cancer patients. The expression of both genes correlated positively with the mRNA levels of *CD8A*, a marker of T-lymphocyte infiltration [Pearson coefficient: 0.427 ($p = 0.0067$) and 0.861 ($p < 0.0001$), resp.]. *GPC6* and *TMEM132D* expression was also documented in a variety of ovarian cancer cell lines. Importantly, Kaplan-Meier survival analysis revealed that high mRNA levels of GPC6 and/or TMEM132D correlated significantly with increased overall survival of early stage ovarian cancer patients ($p = 0.032$). Thus, *GPC6* and *TMEM132D* may serve as predictors of CD8+ T-lymphocyte infiltration and as favorable prognostic markers in early stage ovarian cancer with important consequences for diagnosis, prognosis, and tumor immunobattling.

1. Introduction

Despite the slight decrease in the incidence and death rates of ovarian cancer over the recent years, it remains the major cause of death due to gynecological malignancies. About 22,000 new cases and 14,000 deaths are expected in the United States alone in 2014 [1]. Because of the lack of obvious and specific symptoms at the onset of the disease, the majority of the cases are diagnosed at a late stage. The five-year overall survival rate of ovarian cancer patients is

approximately 44%. On the contrary, patients with early stage ovarian cancer exhibit significantly higher survival rates [2]. The age at the time of diagnosis, the stage of the disease, the histological subtype, and tumor grade are common prognostic factors used to predict clinical outcome [3]. Similarly, the expression levels of several genes have been found to correlate with patients' survival [4–7]. For instance, patients with low/intermediate levels of *BRCA1* mRNA exhibit higher overall survival following treatment with platinum-based chemotherapy compared to patients with high levels of *BRCA1* mRNA [8]. Thus, characterization of molecular markers with prognostic value is of great importance in order to stratify high-risk ovarian cancer patients and implement the most appropriate therapeutic scheme.

Similar to several other types of solid cancers, ovarian tumors are immunogenic with various immune cell populations infiltrating the tumor sites. Zhang et al. demonstrated that intratumoral infiltration of CD3+ T-lymphocytes correlates significantly with high progression-free and overall survival of ovarian cancer patients [9]. Since then, a number of studies have highlighted the prognostic significance of T-cell infiltration in ovarian cancer [10–13]. For instance, it has been well documented that infiltration with high numbers of CD8+ T-lymphocytes associates positively with survival benefit and favorable clinical outcome [14, 15]. So far, gene expression profiling by microarrays has been employed by three independent research groups in order to elucidate the genes and the underlying molecular mechanisms that govern T-cell infiltration in ovarian cancer [16–18]. All of these studies focused on advanced stage ovarian cancer and each identified a number of differentially expressed genes that were associated with CD8+ T-lymphocyte infiltration and immune responses and even with survival [16–18].

Recently, utilizing a fluorescent version of the ADDER (Amplification of Double-Stranded cDNA End Restriction Fragments) Differential Display methodology, we identified, for the first time, genes overexpressed in early stage ovarian cancer which are associated with CD8+ T-lymphocyte infiltration [19]. For instance, the mRNA levels of one of the identified genes, *SMARCE1*, correlated significantly with the expression of *CD8A*, a marker of T-cell infiltration. Importantly, forced overexpression of *SMARCE1* in ovarian cancer cells induced the expression and secretion of certain chemokines and consequently triggered the chemotaxis of CD8+ T-lymphocytes *in vitro* [19].

In the present study, we evaluated the expression of two other overexpressed genes, *GPC6* and *TMEM132D*, and investigated whether they could represent novel prognostic markers of survival in early stage ovarian cancer. We selected to study these two genes as they are both surface antigens. TMEM132D is a transmembrane protein, while GPC6 is a GPI-anchored protein on the outer surface of the cell which may be cleaved off and released in the extracellular space. Through the heparan sulfate glycosaminoglycan chains GPC6 can interact with other molecules and receptors of the membrane. Moreover, glypicans may regulate Hedgehog, Wnt, BMP, and FGF signaling pathways. On the contrary, the exact biological role of TMEM132D still remains quite elusive. The localization of these proteins suggests that they may be involved in intercellular signalling and cell-cell recognition, aspects critical for the mechanisms of cell attraction and recruitment. We validated with qPCR the expression of *GPC6* and *TMEM132D* in a cohort of stage I-II ovarian cancer patients. The expression of both genes correlated positively with the *CD8A* marker and thus with T-cell infiltration. Furthermore, the expression of both genes was monitored in a variety of ovarian cancer cell lines. Ultimately, we performed a retrospective survival analysis of the early stage ovarian cancer patients and correlated the mRNA levels of *GPC6* and *TMEM132D* with the overall survival. Patients with high mRNA levels of *GPC6* and/or *TMEM132D* exhibited survival benefit compared to patients with low mRNA levels of both genes.

2. Materials and Methods

2.1. Patients and Specimens. Ovarian cancer tumor specimens were obtained from patients undergoing primary debulking surgery by surgeons within the Gynecologic Oncology Division at the University of Pennsylvania. The stage of the disease was determined by the gynecologic oncologists. The histology and grade of the tumor samples were established by the surgical pathologist. Specimens were immediately snap-frozen and stored at −80°C. The tissue collection was approved by the IRB committee of the University of Pennsylvania. The analysis of the samples took place at the Department of Molecular Biology and Genetics, abiding to the guidelines of the Ethics Commission of the Democritus University of Thrace.

2.2. Cell Lines and Culture. Human epithelial ovarian cancer cell lines SKOV3, OVCAR3, OVCAR5, A1847, A2780, and C30 were acquired from ATCC and cultured in RPMI 1640 with stable glutamine, supplemented with 10% FBS, 100 U/mL penicillin, and 100 μg/mL streptomycin (all from Biosera). Mouse ovarian cancer cell line ID8 was originally donated by Drs. Kathy Robby and Paul Terranova and cultured in DMEM high glucose with stable glutamine and sodium pyruvate (Biosera), supplemented with 10% FBS, 100 U/mL penicillin, and 100 μg/mL streptomycin. Cell lines were cultured at 37°C, 5% CO_2, in a humidified atmosphere and passaged for fewer than six months since receipt and stock thawing.

2.3. RNA Isolation and Reverse Transcription. Total RNA was isolated from tissue or from 1×10^6 cells with TRIzol reagent (Life Technologies). The quality, integrity, and quantity of the isolated RNA were assessed spectrophotometrically and by gel electrophoresis. Following treatment with RNase-free DNase, total RNA was reverse-transcribed using Superscript First-Strand Synthesis Kit for RT-PCR (Life Technologies) according to manufacturer's instructions.

2.4. Quantitative PCR. qPCR was performed on a StepOne real-time PCR system (Applied Biosystems) using the KAPA SYBR Fast qPCR kit (KAPA Biosystems) under the following

conditions: 95°C/3 min and then 40 cycles at 95°C/15 seconds and at 59°C/1 min. The housekeeping gene *b-actin* was employed as internal control for normalization. The primers for *CD8A*, *GPC6*, *TMEM132D*, and *b-actin* were as follows:

CD8A forward 5′-CCCTGAGCAACTCCATCATGT-3′ and

reverse 5′-GGCTTCGCTGGCAGGAA-3′,

GPC6 forward 5′-GGGCACAGCAAAGCCAGATA-3′ and

reverse 5′-TGGTTGGTGAGCCCATCAT-3′,

TMEM132D forward 5′-CACTGGTCGCCGGTACTCAT-3′ and

reverse 5′-GACCTTCCGTCACTTTGGAAAA-3′,

b-actin forward 5′-GCGCGGCTACAGCTTCA-3′ and

reverse 5′-CTTAATGTCACGCACGATTTCC-3′.

For relative quantification, the formula $RQ = 2^{-(\Delta\Delta Ct)}$ was used. Prior to using the ΔΔCt method for relative quantification of the transcripts, validation experiments were performed by applying the relative standard curve method in order to demonstrate that the PCR efficiencies of the targets *CD8A*, *GPC6*, and *TMEM132D* and of the housekeeping gene *b-actin* were approximately equal. In general, each reaction was run in triplicate and each PCR experiment included two nontemplate controls.

2.5. ADDER Fluorescent Differential Display. ADDER was adapted from [20] for fluorescent detection as previously described [19].

2.6. Immunohistochemistry. Paraffin embedded tissue samples from ovarian tumors were available from patients who underwent surgery. Four-micron sections (4 μm) of representative blocks from each case were deparaffinized, rehydrated, and treated with 0.3% H_2O_2 for 5 min in methanol to prevent endogenous peroxidase activity and were immunostained by the peroxidase method (Envision System, DAKO, Carpinteria, California, USA) according to the manufacturer's recommendations. After antigen retrieval and endogenous peroxidase blockade, the sections were incubated overnight at 4°C with polyclonal antibodies against Glypican-6 (Acris, Germany) and TMEM132D (Novus Bio, USA) in 1 : 100 and 1 : 80 dilutions, respectively. Then, the sections were incubated with secondary antibody at room temperature for 60 min. Finally, bound antibody complexes were stained for 10 min with 0.05% diaminobenzidine. Sections were then briefly counterstained with Mayer's haematoxylin, mounted, and examined under a Nikon Eclipse 50i microscope. Control slides were incubated for the same period with nonimmunized rabbit serum (negative control). A positive control was always run in the assay. The staining results were evaluated by a pathologist based on the percentage of staining in tumor cells.

2.7. Statistical Analysis. Graphs and statistical analysis of the data were performed with GraphPad Prism 5 and SPSS version 19.0. Correlation of *GPC6* and *TMEM132* mRNA levels with *CD8A* expression levels was examined by Pearson coefficient correlation. The chi-square test was used to assess the association of the expression levels of *GPC6* and *TMEM132D* with patients' clinicopathologic characteristics (stage, grade, and histotype). To study whether mRNA levels of *GPC6* and *TMEM132D* were predictive for overall survival, survival rates were calculated with the Kaplan-Meier method and the statistical difference between survival curves was determined with the log-rank test. Overall survival was defined as the time interval from diagnosis/first surgery to death or last follow-up. Multivariate Cox proportional hazards regression analysis was performed in order to evaluate the independent effect of *GPC6* and *TMEM132D* mRNA levels on overall survival. Multivariate regression models included stage, grade, histotype, and *CD8A* mRNA levels. All tests were two-tailed and statistical significance was considered for p values < 0.05.

3. Results

By employing a fluorescent version of ADDER Differential Display, we have recently reported the identification of 128 genes overexpressed in early stage ovarian tumors enriched with CD8+ T-lymphocytes (TIL+ tumors) [19]. *GPC6* and *TMEM132D*, encoding for the heparan sulfate proteoglycan Glypican-6 and the transmembrane protein 132D, respectively, were included in the identified genes (Figures 1(a) and 2(a), resp.). Here, we further evaluated the expression of these two genes in early stage ovarian cancer.

3.1. GPC6 and TMEM132D Are Differentially Expressed in TIL+ Early Stage Ovarian Cancer and Their Expression Levels Correlate with CD8+ T-Cell Infiltration. In order to validate the expression of *GPC6* and *TMEM132D* in early stage ovarian cancer, we measured by qPCR their mRNA levels in tumor samples from 38 stage I-II ovarian cancer patients (Figures 1(b) and 2(b), resp.). The expression of both genes was detectable in all patient samples analyzed, at various levels. To investigate whether *GPC6* and *TMEM132D* expression correlates with CD8+ T-lymphocyte infiltration in early stage ovarian cancer, we used qPCR to quantify the mRNA levels of the *CD8A* marker in the same cohort of patients. Interestingly, a statistically significant positive correlation between the mRNA levels of *GPC6* or *TMEM132D* and *CD8A* accordingly was observed (Figures 1(c) and 2(c), resp.). Thus, the mRNA expression levels of *GPC6* and *TMEM132D* correlate with CD8+ T-lymphocyte infiltration in early stage ovarian cancer. Moreover, we quantified by qPCR the relative expression of *GPC6* and *TMEM132D* in a variety of ovarian cancer cell lines and demonstrated that the expression of both genes is not restricted to the infiltrating immune cells and may actually originate from the tumor cells. As shown in Figure 1(d), expression of *GPC6* was documented in all cell lines tested except one (i.e., OVCAR5). Similarly, all ovarian cancer cell lines expressed *TMEM132D* (Figure 2(c)). To further validate the expression

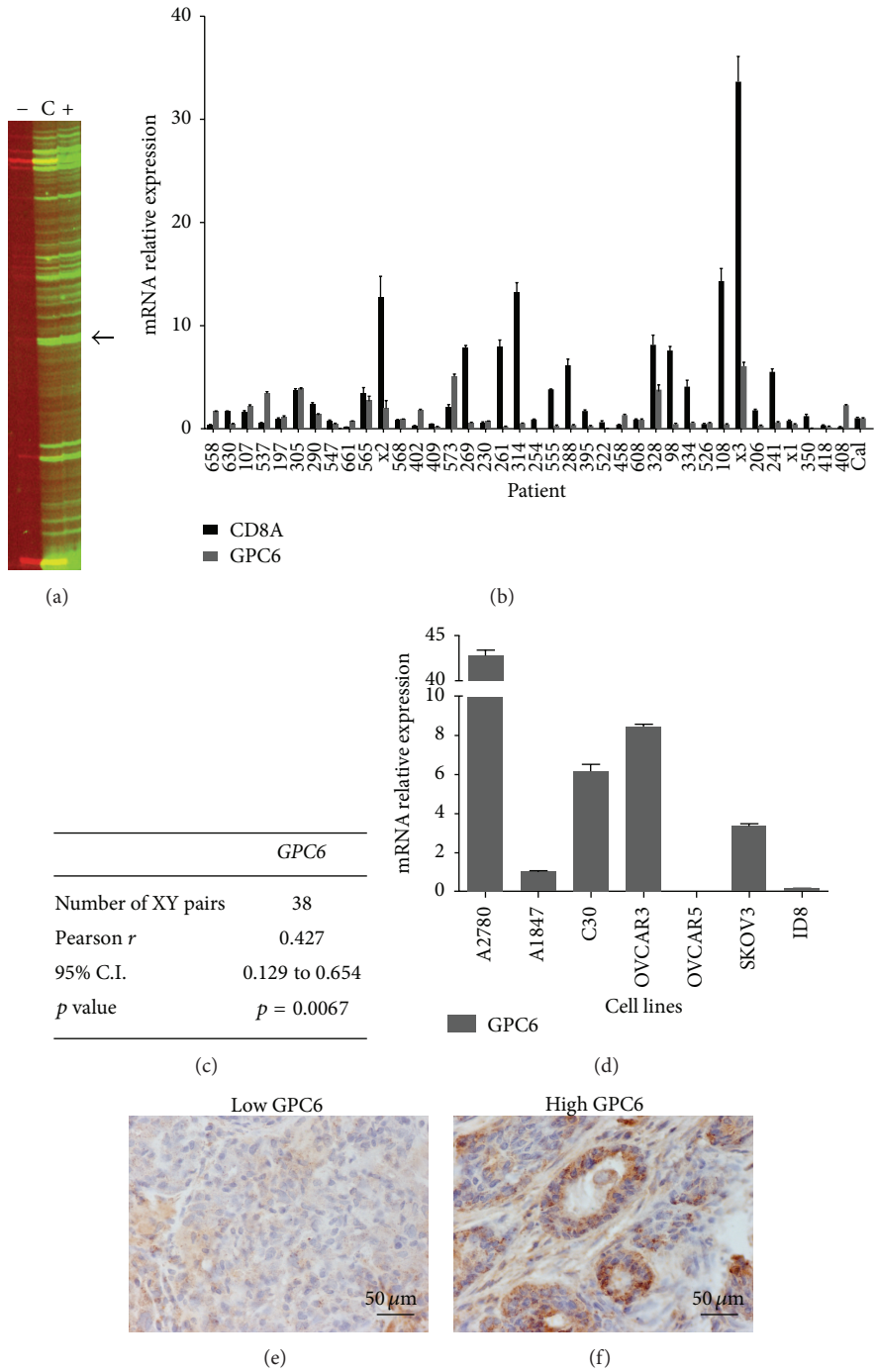

Figure 1: *GPC6* is overexpressed in TIL+ early stage ovarian cancer and its expression correlates positively with CD8+ T-lymphocyte infiltration. (a) *GPC6* was overexpressed in the TIL+ ovarian cancer sample as visualized by fluorescent ADDER (band indicated by an arrow). Lane (+) displays the gene expression profile of the TIL+ sample generated by the corresponding Differential Display primer set; lane (−) displays the expression profile of the TIL− sample and lane (C) displays the combined profile of equal amount of PCR products of both samples. Genes expressed equally in both samples appear as yellow bands in lane (C). (b) The expression of *GPC6* was quantified by qPCR in samples derived from 38 stage I-II ovarian cancer patients. The relative expression of *GPC6* was plotted along with the respective *CD8A* expression levels after normalization to *b-actin*. A pooled mix of equal amounts of all samples served as calibrator (Cal). (c) Pearson correlation coefficient of *CD8A*-*GPC6* expression levels. The correlation is significant ($p = 0.0067$). (d) The relative expression of *GPC6* in 7 ovarian cancer cell lines was estimated by qPCR (normalized to *b-actin*). (e-f) Immunohistochemistry of GPC6 expression in representative early stage ovarian tumor samples. (e) Negative expression of GPC6 protein in the tumor sample 314 with low mRNA levels of the respective gene (see 1(b)). (f) Strong expression of the GPC6 protein in the 408 sample with also high mRNA levels (see 1(b)). Magnification (e-f): ×400. *Columns*: mean, *bars*: SEM.

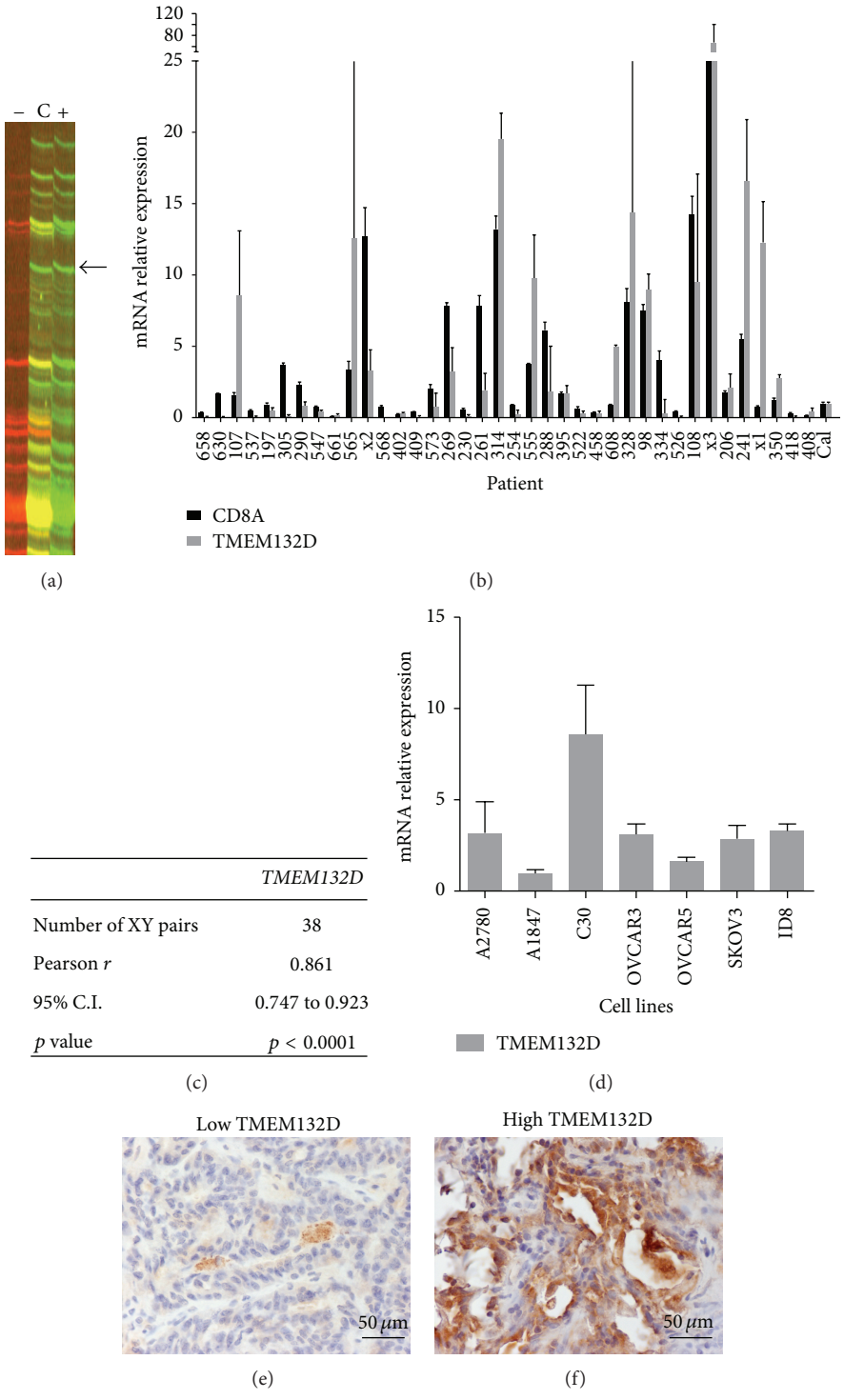

	TMEM132D
Number of XY pairs	38
Pearson *r*	0.861
95% C.I.	0.747 to 0.923
p value	$p < 0.0001$

FIGURE 2: *TMEM132D* is overexpressed in TIL+ early stage ovarian cancer and its expression correlates positively with CD8+ T-lymphocyte infiltration. (a) *TMEM132D* was overexpressed in the TIL+ ovarian cancer sample as visualized by fluorescent ADDER (band indicated by an arrow). (b) The expression of *GPC6* was quantified by qPCR in samples derived from 38 stage I-II ovarian cancer patients. The relative expression of *TMEM132D* was plotted along with the respective *CD8A* expression levels after normalization to *b-actin*. A pooled mix of equal amounts of all samples served as calibrator (Cal). (c) Pearson correlation coefficient of *CD8A*-*TMEM132D* expression levels. The correlation is significant ($p = 0.0067$). (d) The relative expression of *TMEM132D* in 7 ovarian cancer cell lines was estimated by qPCR (normalized to *b-actin*). (e-f) Immunohistochemistry of TMEM132D expression in representative early stage ovarian tumor samples. (e) Negative expression of TMEM132D protein in the tumor sample 408 with low mRNA levels of the respective gene (see 2(b)). (f) Very strong expression of the TMEM132D protein in the 314 sample with also high mRNA levels (see 2(b)). Magnification (e-f): ×400. *Columns*: mean, *bars*: SEM.

Table 1: Clinicopathologic characteristics of the stage I/II ovarian cancer patients.

Characteristic	*N* (%)		
	All stages, $N = 35$	Stage I, $N = 28$ (80%)	Stage II, $N = 7$ (20%)
Age at diagnosis			
Median/mean	59/57.63	59/56.86	59/60.71
Range	(34–83)	(34–78)	(51–83)
Grade			
0	2 (5.7)	2 (7.1)	
1	12 (34.3)	10 (35.7)	2 (28.6)
2	8 (22.9)	5 (17.9)	3 (42.9)
3	13 (37.1)	11 (39.3)	2 (28.6)
Histological subtype			
Serous	11 (31.4)	9 (32.1)	2 (28.5)
Endometrioid	20 (57.2)	16 (57.2)	4 (57.2)
Clear-cell	4 (11.4)	3 (10.7)	1 (14.3)
Debulking status			
Optimal	34 (97.1)	28 (100)	6 (85.7)
Suboptimal	1 (2.9)		1 (14.3)
Response to therapy			
CR[a]	33 (94.3)	27 (96.4)	6 (85.7)
PD[b]	2 (5.7)	1 (3.6)	1 (14.3)
Survival			
Ovarian cancer deaths	6 (17.1)	4 (14.3)	2 (28.5)
Total number of deaths	6 (17.1)	4 (14.3)	2 (28.5)

[a]Complete response.
[b]Progressive disease.

of GPC6 and TMEM132D at protein level in the cancer cells, we performed immunohistochemistry in sections from representative tumor samples with either high or low mRNA levels of *GPC6* and *TMEM132D* as categorized by qPCR (Figures 1(e)-1(f) and 2(e)-2(f)). As depicted in Figure 1(e), the tumors with low mRNA levels of *GPC6* also showed negative expression of the gene at protein level. On the contrary, high expression of the GPC6 protein was observed in tumors with high mRNA levels of the gene. Consistently, the tumors with low mRNA levels of *TMEM132D* showed little expression at protein level, whereas the tumors with high levels of TMEM132D mRNA also showed strong expression at protein level. In conclusion, *GPC6* and *TMEM132D* could serve as potent markers of CD8+ T-cell infiltration in early stage ovarian cancer.

3.2. The mRNA Levels of GPC6 and TMEM132D Correlate with Patients' Overall Survival in Early Stage Ovarian Cancer. In order to evaluate the survival predictive value of *GPC6* and *TMEM132D* mRNA levels in early stage ovarian cancer, we performed a retrospective clinical analysis of the above-studied stage I-II ovarian cancer patients. Patients x1, x2, and x3 were excluded from this analysis due to unavailability of complete data. The clinicopathologic characteristics of the 35 early stage ovarian cancer patients are shown in Table 1. Twenty-eight patients (80%) presented stage I ovarian cancer and seven patients (20%) were stage II. The majority of the patients had endometrioid and clear-cell ovarian tumors (Table 1). All of the clear-cell and more than half of the endometrioid tumors (55%) were high grade. Similarly, about 54% of the serous tumours were also high grade. The median age at diagnosis for all patients was 59 years, while the mean overall survival among the entire cohort was 189 months (95% C.I. 164–213, Table 2). Six patients (17.14%) deceased due to the disease during the study period. There were no statistically significant differences in survival among the two stages or the histological subtypes of the disease (data not shown).

As about 25% of the tumors exhibited abundant T-cell infiltration and both *GPC6* and *TMEM132D* correlated with infiltration, the 75th percentile median mRNA levels of *GPC6* (1.8 relative expression units) or *TMEM132D* (5.0 relative expression units) were selected as the cut-off values to subdivide the patient cohort into two groups: patients with high and patients with low mRNA levels of the relevant gene. There was no significant age difference among the two groups of patients, neither in the case of *GPC6* subdivision nor in the case of *TMEM132D* subdivision. The presence of high levels of *GPC6* and *TMEM132D* was also analysed in relation to stage, grade, and type of the disease. Statistically significant differences were not observed for the mRNA levels of the two genes among different stages, grades, or types of tumors (Tables S1 and S2 in Supplementary Material available online at http://dx.doi.org/10.1155/2015/712438). Kaplan-Meir curves were calculated for the mRNA levels in order to assess whether *GPC6* or *TMEM132D* levels were predictive of

Table 2: Survival characteristics of patients related to their tumoral *GPC6* and *TMEM132D* mRNA levels.

	All	GPC6 mRNA levels		TMEM132D mRNA levels		GPC6/TMEM132D mRNA levels	
		Low	High	Low	High	Both low	High GPC6 and/or TMEM132D
N (%)	35	28 (80)	7 (20)	26 (74.3)	9 (25.7)	22 (62.9)	13 (37.1)
Survival							
5-year survival (%)	91.34 ± 4.78	88.73 ± 6.13	100	88.29 ± 6.36	100	85.45 ± 7.78	100
10-year survival (%)	84.69 ± 6.34	80.06 ± 8.04	100	78.73 ± 8.55	100	73.62 ± 10.27	100
Overall survival (months)							
Mean ± SE	189 ± 12	179 ± 15	Undefined[a]	152 ± 13	Undefined[a]	144 ± 15	Undefined[a]
95% C.I.	164–213	149–209	—	126–177	—	114–174	—
Death cases (%)	6 (17.14%)	6 (21.4)	0 (0)	6 (23.1)	0 (0)	6 (27.3)	0 (0)
p value (log-rank test)		0.214		0.099		0.032	

[a]All subjects alive.

survival (Figures S1(a) and (b), resp.). As shown in Table 2, the analysis suggested a strong trend towards increased survival for patients with high mRNA levels of *GPC6*. Over twenty percent (21.4%) of the patients with low levels deceased due to the disease. Similar results were obtained for *TMEM132D*. Interestingly, all patients with high mRNA levels of *GPC6* or *TMEM132D* were still alive at the end of the study.

We then asked whether the expression of both *GPC6* and *TMEM132D* genes in combination correlated with survival. We divided the patients into 2 groups based on the combined expression of *GPC6* and *TMEM132D*: (i) patients with low levels of both genes ($n = 22$, 62.9%) and (ii) patients with high mRNA levels of *GPC6* and/or *TMEM132D* ($n = 13$, 37.1%). No significant difference in age was observed among the two groups. Patients with low mRNA levels of both *GPC6* and *TMEM132D* had a mean overall survival of 144 months (95% C.I. 114–174). Furthermore, 27.3% of the patients with low mRNA levels deceased due to the disease (Table 2). On the contrary, all the patients with high mRNA levels of *GPC6* and/or *TMEM132D* were alive until the last follow-up (or the end of the study). In conclusion, as shown in Figure 3, high mRNA levels of *GPC6* and/or *TMEM132D* correlate significantly with increased overall survival ($p = 0.032$) in early stage ovarian cancer.

Although CD8A is a classic established marker of T-cell infiltration in ovarian cancer, in our cohort of patients, the prognostic value of *CD8A* mRNA levels was statistically weak ($p = 0.805$) possibly due to the small size of the sample and the low number of deaths. However, in the same cohort of patients, high mRNA levels of *GPC6* and/or *TMEM132* associated significantly with increased survival.

Taken together, our data indicate *GPC6* and *TMEM132D* as potential markers for CD8+ T-lymphocyte infiltration, favorable prognosis, and survival benefit in early stage ovarian cancer.

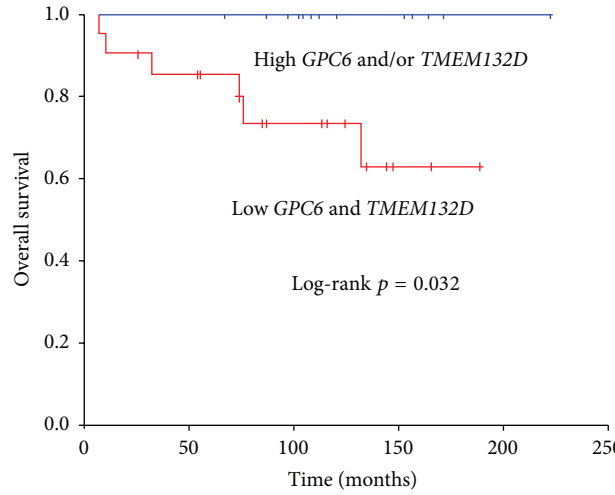

Figure 3: High mRNA levels of *GPC6* and/or *TMEM132D* correlate with increased overall survival of early stage ovarian cancer patients. Kaplan-Meier survival curves calculated for both *GPC6* and *TMEM132D* mRNA levels. Patients were divided into two groups: (i) patients with low mRNA levels of both *GPC6* and *TMEM132D* (cut-off points 1.8 and 5, resp.) and (ii) patients with *GPC6* and/or *TMEM132D* high levels. Patients with high mRNA levels of *GPC6* and/or *TMEM132D* exhibit a favorable overall survival ($p = 0.032$).

4. Discussion

It is well established that the expression of *CD8A* at the transcriptional level is a reliable indicator of CD8+ T-cell infiltration in ovarian cancer [9, 19]. In this study, we documented an association between the expression of *GPC6* and *TMEM132D* with CD8+ T-lymphocyte infiltration and favorable prognosis in early stage ovarian cancer. Both genes were found to be differentially expressed in TIL+ versus the TIL− early stage ovarian cancer [19]. Here we validated by qPCR analysis in a larger group of stage I/II patients ($n = 38$) that the mRNA expression levels of the two genes significantly correlated with the mRNA levels of the T-cell infiltration marker *CD8A*. More importantly, we showed that early stage ovarian cancer patients with high mRNA levels of at least one of the two genes, *GPC6* and *TMEM132D*, exhibited increased overall survival compared to patients with low levels of both genes.

Our results suggest an involvement of *GPC6* in the biology of lymphocyte infiltration in early stage ovarian

tumors. *GPC6* encodes for Glypican-6, a 62.7 kDa heparan sulfate proteoglycan [21, 22]. Glypicans are proteins bearing glycosaminoglycan chains. There are six members of the family (GPC1–GPC6) in mammals, with GPC6 being a close homologue to GPC4 (64% identity). Glypicans are attached to the outer surface of the membrane through a glycosylphosphatidylinositol (GPI) anchor but can also be released to the extracellular space [23, 24]. Their heparan sulfate glycosaminoglycan chains are at the C-terminus of the protein, close to the membrane, and are thought to facilitate the interaction of glypicans with other molecules and receptors of the membrane. It has been shown that glypicans may regulate Hedgehog, Wnt, BMP, and FGF signaling pathways [24]. Interestingly, in *Drosophila* the released glypicans are involved in the transport of Wnts, Hhs, and BMPs by creating a morphogen gradient [25]. Furthermore, GPC6 promotes invasive migration of breast cancer cells through a noncanonical Wnt5A signaling pathway [26]. In particular, NFAT induces the expression of GPC6 which in turn inhibits canonical Wnt and b-catenin signaling and activates Wnt5A signaling that results in activation of JNK and p38α kinases [26]. Further studies are required in order to shed light on the role of GPC6 in ovarian cancer and the mechanism of CD8+ T-lymphocyte infiltration. It is reasonable to anticipate that GPC6 may mediate intercellular interactions with immune cells or that it may be involved in shaping a chemokine gradient, necessary for the CD8+ T-lymphocyte infiltration.

On the other hand, little is known about the biological role of *TMEM132D*. Polymorphisms in *TMEM132D* gene have been associated with panic disorder [27, 28]. *TMEM132D* encodes a single-pass type I transmembrane protein initially discovered in mature oligodendrocytes. *TMEM132D* expression is detectable in brain, lung, pancreas, and testis, but intriguingly not in normal ovaries [29]. Thus, it is possible that the expression of *TMEM132D* is induced in ovarian cancer and by an unknown mechanism becomes implicated in CD8+ T-lymphocyte infiltration. Based on the presence of TMEM132D on the plasma membrane surface, one could hypothesize an involvement in cell-cell interactions or intercellular signaling mechanisms that could be implicated with T-cell recruitment.

According to our results, early stage ovarian cancer patients with low mRNA levels of *GPC6* and *TMEM132D* exhibit significantly reduced overall survival compared to patients with high levels of *GPC6* and/or *TMEM132D*. Therefore, we suggest that *GPC6* and *TMEM132D* mRNA levels could serve as markers of CD8+ T-cell infiltration and survival prognosis in early stage ovarian cancer. For example, monitoring tumoral *GPC6* and *TMEM132D* mRNA levels could facilitate the identification of early stage ovarian cancer patients at high risk. Our conclusions underscore the necessity to elucidate the molecular mechanism of *GPC6* and *TMEM132D* involvement in T-cell infiltration and their impact on cancer progression and also highlight their possible importance as putative diagnostic/therapeutic targets.

Conflict of Interests

The authors declare that there is no conflict of interests regarding the publication of this paper.

Authors' Contribution

Denarda Dangaj and Evripidis Lanitis contributed equally to this work.

Acknowledgment

Athanasios Karapetsas was supported by a Ph.D. scholarship from the State Scholarships Foundation of Greece.

References

[1] R. Siegel, J. Ma, Z. Zou, and A. Jemal, "Cancer statistics, 2014," *CA: A Cancer Journal for Clinicians*, vol. 64, no. 1, pp. 9–29, 2014.

[2] American Cancer Society, *Cancer Facts & Figures 2013*, American Cancer Society, Atlanta, Ga, USA, 2013.

[3] C. H. Holschneider and J. S. Berek, "Ovarian cancer: epidemiology, biology, and prognostic factors," *Seminars in Surgical Oncology*, vol. 19, no. 1, pp. 3–10, 2000.

[4] D. Spentzos, D. A. Levine, M. F. Ramoni et al., "Gene expression signature with independent prognostic significance in epithelial ovarian cancer," *Journal of Clinical Oncology*, vol. 22, pp. 4700–4710, 2004.

[5] M. J. Birrer, M. E. Johnson, K. Hao et al., "Whole genome oligonucleotide-based array comparative genomic hybridization analysis identified fibroblast growth factor 1 as a prognostic marker for advanced-stage serous ovarian adenocarcinomas," *Journal of Clinical Oncology*, vol. 25, no. 16, pp. 2281–2287, 2007.

[6] Y. Tanaka, H. Kobayashi, M. Suzuki et al., "Reduced bikunin gene expression as a factor of poor prognosis in ovarian carcinoma," *Cancer*, vol. 98, no. 2, pp. 424–430, 2003.

[7] A. M. Wolf, H. Rumpold, D. Reimer, C. Marth, A. G. Zeimet, and D. Wolf, "High IL-12 p35 and IL-23 p19 mRNA expression is associated with superior outcome in ovarian cancer," *Gynecologic Oncology*, vol. 118, no. 3, pp. 244–250, 2010.

[8] J. E. Quinn, C. R. James, G. E. Stewart et al., "BRCA1 mRNA expression levels predict for overall survival in ovarian cancer after chemotherapy," *Clinical Cancer Research*, vol. 13, no. 24, pp. 7413–7420, 2007.

[9] L. Zhang, J. R. Conejo-Garcia, D. Katsaros et al., "Intratumoral T cells, recurrence, and survival in epithelial ovarian cancer," *The New England Journal of Medicine*, vol. 348, no. 3, pp. 203–213, 2003.

[10] M. Tomšová, B. Melichar, I. Sedláková, and I. Šteiner, "Prognostic significance of CD3+ tumor-infiltrating lymphocytes in ovarian carcinoma," *Gynecologic Oncology*, vol. 108, no. 2, pp. 415–420, 2008.

[11] N. Leffers, M. J. M. Gooden, R. A. De Jong et al., "Prognostic significance of tumor-infiltrating T-lymphocytes in primary and metastatic lesions of advanced stage ovarian cancer," *Cancer Immunology, Immunotherapy*, vol. 58, no. 3, pp. 449–459, 2009.

[12] L. Han, M. S. Fletcher, D. L. Urbauer et al., "HLA class I antigen processing machinery component expression and intratumoral T-cell infiltrate as independent prognostic markers in ovarian carcinoma," *Clinical Cancer Research*, vol. 14, no. 11, pp. 3372–3379, 2008.

[13] W.-T. Hwang, S. F. Adams, E. Tahirovic, I. S. Hagemann, and G. Coukos, "Prognostic significance of tumor-infiltrating T cells in ovarian cancer: a meta-analysis," *Gynecologic Oncology*, vol. 124, no. 2, pp. 192–198, 2012.

[14] E. Sato, S. H. Olson, J. Ahn et al., "Intraepithelial $CD8^+$ tumor-infiltrating lymphocytes and a high $CD8^+$/regulatory T cell ratio are associated with favourable prognosis in ovarian cancer," *Proceedings of the National Academy of Sciences of the United States of America*, vol. 102, pp. 18538–18543, 2005.

[15] M. Stumpf, A. Hasenburg, M.-O. Riener et al., "Intraepithelial CD8-positive T lymphocytes predict survival for patients with serous stage III ovarian carcinomas: relevance of clonal selection of T lymphocytes," *British Journal of Cancer*, vol. 101, no. 9, pp. 1513–1521, 2009.

[16] M. J. Callahan, Z. Nagymanyoki, T. Bonome et al., "Increased HLA-DMB expression in the tumor epithelium is associated with increased CTL infiltration and improved prognosis in advanced-stage serous ovarian cancer," *Clinical Cancer Research*, vol. 14, no. 23, pp. 7667–7673, 2008.

[17] B. Clarke, A. V. Tinker, C.-H. Lee et al., "Intraepithelial T cells and prognosis in ovarian carcinoma: novel associations with stage, tumor type, and BRCA1 loss," *Modern Pathology*, vol. 22, no. 3, pp. 393–402, 2009.

[18] N. Leffers, R. S. N. Fehrmann, M. J. M. Gooden et al., "Identification of genes and pathways associated with cytotoxic T lymphocyte infiltration of serous ovarian cancer," *British Journal of Cancer*, vol. 103, no. 5, pp. 685–692, 2010.

[19] A. Giannakakis, A. Karapetsas, D. Dangaj et al., "Overexpression of *SMARCE1* is associated with CD8+ T-cell infiltration in early stage ovarian cancer," *The International Journal of Biochemistry & Cell Biology*, vol. 53, pp. 389–398, 2014.

[20] B. Kornmann, N. Preitner, D. Rifat, F. Fleury-Olela, and U. Schibler, "Analysis of circadian liver gene expression by ADDER, a highly sensitive method for the display of differentially expressed mRNAs," *Nucleic acids research*, vol. 29, no. 11, article E51, 2001.

[21] S. Paine-Saunders, B. L. Viviano, and S. Saunders, "GPC6, a novel member of the glypican gene family, encodes a product structurally related to GPC4 and is colocalized with GPC5 on human chromosome 13," *Genomics*, vol. 57, no. 3, pp. 455–458, 1999.

[22] M. Veugelers, B. De Cat, H. Ceulemans et al., "Glypican-6, a new member of the glypican family of cell surface heparan sulfate proteoglycans," *Journal of Biological Chemistry*, vol. 274, no. 38, pp. 26968–26977, 1999.

[23] J. Filmus, M. Capurro, and J. Rast, "Glypicans," *Genome Biology*, vol. 9, article 224, 2008.

[24] J. Filmus and M. Capurro, "The role of glypicans in Hedgehog signaling," *Matrix Biology*, vol. 35, pp. 248–252, 2014.

[25] T. Y. Belenkaya, C. Han, D. Yan et al., "Drosophila Dpp morphogen movement is independent of dynamin-mediated endocytosis but regulated by the glypican members of heparan sulfate proteoglycans," *Cell*, vol. 119, no. 2, pp. 231–244, 2004.

[26] G. K. Yiu, A. Kaunisto, Y. R. Chin, and A. Toker, "NFAT promotes carcinoma invasive migration through glypican-6," *Biochemical Journal*, vol. 440, no. 1, pp. 157–166, 2011.

[27] A. Erhardt, L. Czibere, D. Roeske et al., "TMEM132D, a new candidate for anxiety phenotypes: evidence from human and mouse studies," *Molecular Psychiatry*, vol. 16, no. 6, pp. 647–663, 2011.

[28] A. Erhardt, N. Akula, J. Schumacher et al., "Replication and meta-analysis of *TMEM132D* gene variants in panic disorder," *Translational Psychiatry*, vol. 2, article e156, 2012.

[29] H. Nomoto, T. Yonezawa, K. Itoh et al., "Molecular cloning of a novel transmembrane protein MOLT expressed by mature oligodendrocytes," *The Journal of Biochemistry*, vol. 134, no. 2, pp. 231–238, 2003.

Hindawi Publishing Corporation
BioMed Research International
Volume 2015, Article ID 320214, 14 pages
http://dx.doi.org/10.1155/2015/320214

Review Article

Long Noncoding RNAs as New Architects in Cancer Epigenetics, Prognostic Biomarkers, and Potential Therapeutic Targets

Didier Meseure,[1] Kinan Drak Alsibai,[1] Andre Nicolas,[1] Ivan Bieche,[2] and Antonin Morillon[3]

[1]*Platform of Investigative Pathology, Institute Curie, 75248 Paris, France*
[2]*Department of Pharmacogenomics, Institute Curie and UMR 745 INSERM, University Descartes, 75248 Paris, France*
[3]*UMR 3244, Non-Coding RNA, Epigenetics and Genome Fluidity, Institute Curie, 75248 Paris, France*

Correspondence should be addressed to Didier Meseure; didier.meseure@curie.fr

Received 25 October 2014; Accepted 6 May 2015

Academic Editor: Konstantinos Arnaoutakis

Recent advances in genome-wide analysis have revealed that 66% of the genome is actively transcribed into noncoding RNAs (ncRNAs) while less than 2% of the sequences encode proteins. Among ncRNAs, high-resolution microarray and massively parallel sequencing technologies have identified long ncRNAs (>200 nucleotides) that lack coding protein function. LncRNAs abundance, nuclear location, and diversity allow them to create in association with protein interactome, a complex regulatory network orchestrating cellular phenotypic plasticity via modulation of all levels of protein-coding gene expression. Whereas lncRNAs biological functions and mechanisms of action are still not fully understood, accumulating data suggest that lncRNAs deregulation is pivotal in cancer initiation and progression and metastatic spread through various mechanisms, including epigenetic effectors, alternative splicing, and microRNA-like molecules. Mounting data suggest that several lncRNAs expression profiles in malignant tumors are associated with prognosis and they can be detected in biological fluids. In this review, we will briefly discuss characteristics and functions of lncRNAs, their role in carcinogenesis, and their potential usefulness as diagnosis and prognosis biomarkers and novel therapeutic targets.

1. Long Noncoding RNAs and Functional Organization of the Genome

1.1. Genome and Noncoding RNA. Large-scale genomic technologies (high-resolution microarray, whole genome, and RNA sequencing) combined with bioinformatics analyses have profoundly changed the genome organization understanding. Unexpectedly, these global transcriptional analyses revealed that 66% of the genome is transcribed and 80% presents biochemical marks of active transcription whereas less than 2% encodes proteins [1]. Discovery of a "second genetic code" consisting of ncRNAs has changed traditional concept of genomic organization characterized by presence of genes encoding islets scattered in a sea of repeats and nontranscribed proteins. Recently, high-throughput techniques have identified 58648 human lncRNAs [2].

1.2. Classification of Noncoding RNAs. NcRNAs are classified into two categories according to their structural or regulatory properties and size. This length, arbitrarily set to 200 nucleotides (nt), corresponds to the threshold of sensitivity of RNA extraction methods and can differentiate lncRNAs from short and medium ncRNAs such as microRNAs (miRNAs), small nucleolar RNAs (snoRNAs), and piwi RNAs (piRNAs) [3] (Table 1). Although functions of most ncRNAs are currently still largely uncharacterized, recent studies have involved them in mechanisms implicated in important biological functions and in various pathologic conditions, including neurodegenerative diseases and cancer [4, 5]. It is likely that development of new diagnostic and prognostic classifications involving ncRNAs refine medical practice and that ncRNAs may be useful potential targets for novel anticancer therapies. In this review, we propose to

Table 1: Type and main function of no-coding RNAs.

Type	Size (nt)	Functions
Short ncRNAs	19–31	
miRNAs		Targeting of mRNAs, regulation of proliferation, differentiation, and apoptosis involved in human development
siRNAs		Posttranscriptional gene silencing; defense against pathogenic nucleic acids
tiRNAs		Regulation of transcription by targeting epigenetic silencing complexes
piRNAs		Transposon repression, DNA methylation, development of germ cell, stem self-renewal, and retrotransposon silencing
tel-sRNAs		Epigenetic regulation
Mid-size ncRNAs	≤200	
snoRNAs		rRNA modifications
PASRs		Regulation of the transcription of protein-coding genes
TSSa-RNAs		Maintenance of transcription
PROMPTs		Activation of transcription
crasiRNAs		Recruitment of heterochromatin and/or centromeric proteins
Long ncRNAs	>200	
lincRNAs		Involvement in biological processes such as dosage compensation and/or imprinting
Intronic lncRNAs		Possible link with posttranscriptional gene silencing
T-UCRs		Regulation of miRNA and mRNA levels and antisense inhibitors for protein-coding genes or other ncRNAs
TERRAs		Negative regulation of telomere length and activity through inhibition of telomerase
Pseudogene RNAs		Regulation of tumor suppressors and oncogenes by acting as microRNA decoys
lncRNAs with dual functions		Modulate gene expression through diverse mechanisms

summarize recent literature data on lncRNAs, their involvement in carcinogenesis, and their value as biomarkers and potential therapeutic targets.

1.3. Definition of lncRNAs. LncRNAs transcripts are defined by a length greater than 200 nts without any potential of translation [6]. This definition is however arbitrary and cannot now be based on a set of physical biochemical, structural or functional criteria. Length is not an absolute criterion because ncRNAs smaller than 200 nts (*BC1, snaR*) are included in the lncRNAs subgroup. There is no specific transcription of lncRNAs, the transcriptional machinery being common to lncRNAs and mRNAs. Lack of reading frame cannot also be a discriminating factor between mRNAs and ncRNAs because 50% of lincRNAs contain regions with high translational potential, comparable to those of mRNAs, suggesting that they are actively exported to cytoplasm and translated into short polypeptides, albeit certainly not active. Noncoding characteristic is then not specific to lncRNAs, as bifunctional coding and noncoding lncRNAs and lncRNAs containing other ncRNAs (miRNAs, snoRNAs) have recently been discovered. Several mRNAs lose their ability to encode proteins (*Xist*) while others acquire coding function (*SRA*) [7]. Furthermore, by incorporating multiple exons from coding and noncoding genes, alternative splicing generates ambiguous transcripts beyond all classifications. Nevertheless, this definition appears currently to be the best that could be used waiting for a functional characterization of lncRNAs.

1.4. Investigative Methods and Annotation of lncRNAs. The first lncRNAs were discovered by using functional genetic approaches based on their relation to specific cellular mechanisms: (i) *Ubxn* transcriptional interference-induced repression by trithorax-promoted lncRNA*bdx*, (ii) sex chromosome dosage compensation and *Xist*-induced X chromosome, and (iii) inactivation and genomic imprinting promoted by antisense lncRNAs *Airn* and *Kcnq1*. These seminal studies established the concept of functional lncRNAs acting as transcriptional regulators involved in important and diverse biological processes. Over the past two decades, systematic global sequencing of cDNA libraries yielded comprehensive knowledge of the transcribed but noncoding component of the genome. These transcriptomic analyses have identified numerous lncRNAs. RNA immunoprecipitation and siRNA-induced inactivation techniques led to functional validation of many lncRNAs.

Currently, lncRNAs identification and functional characterization are based on an experimental approach combining (i) discovery of new noncoding transcripts using RNA-seq and ChIP-seq, (ii) annotation of transcribed regions extent and quantity of products transcribed through bioinformatic analysis, (iii) lncRNAs quantification in various cellular and tissue types and conditions, (iv) coexpression or coregulation studies, and (v) gain and loss functional tests on cell lines and xenografts (siRNAs, ASO, TALEN, and CRISPR/CAS9). Advantage of RNA-seq technique resides in its sensibility, allowing most weakly expressed lncRNAs to be identified.

However, due to their frequent very low expression and complex exon/intron structures, it can be difficult to identify different transcripts produced from alncRNA gene. It is then necessary to use other techniques through epigenetic analyses (markers of promoter regions or entire gene), targeted transcripts of interest sequencing after capture on a DNA chip (capture-RNAseq) and 5′ and 3′ extremities identification analyses [8–11].

Systematic large-scale projects have contributed a lot to the systematic characterization of mammalian lncRNAs. For instance, the Fantom (Functional Annotation of the Mammalian genome) is an international project initiated by Japan in 2000 designed to identify and annotate entire transcripts of mouse. Results published identified 15000 lncRNAs in 2002, 23000 in 2005, and 34000 in 2006 with a transcribed genome fraction of 63%. The ENCODE project initiated in 2003 is designed to identify, map, and make public all functional elements of the human genome. This project led to a catalog of lncRNAs with 10000 genes producing 15000 lncRNAs. Very recently, 58648 lncRNAs were identified by using the TCGA database, of which 79% were previously unannotated [2].

1.5. Properties of lncRNAs. LncRNAs genes outnumber those of short ncRNAs and are probably more abundant than mRNA genes. LncRNAs are very heterogeneous in size with some extending over tens of kilobases (kb). They are transcribed in all regions of eukaryotic genome, particularly during development, and are remarkably specific for a given cellular and tissue type.

LncRNAs genes share many biochemical characteristics with proteins coding genes: predominant action of RNA polymerase II, epigenetic profiles, cotranscriptional modifications (5′Cap, pre-lncRNAs alternative splicing, and 3′ polyadenylation), and exons and introns size. However, when lncRNAs are compared to mRNAs, they appear less stable and shorter, with fewer exons, a less well defined reading frame, and many repeat sequences (LINE, SINE). A minority group of poorly characterized lncRNAs is represented by nonpolyadenylated lncRNAs synthesized by RNA polymerase III and lncRNAs synthesized via alternative splicing and snoRNAs.

Depending on their relative position to the nearest coding genes, several categories of lncRNAs can be identified as follows.

(i) Intragenic Regions. Intragenic IncRNAs may be subdivided depending on how they overlap protein-coding genes or their orientation [45].

(a) Long intronic ncRNAs (linRNAs) constitute the major component of ncRNAs transcriptome. Unlike lincRNAs, tens of thousands linRNAs have recently been identified but only few have been analyzed functionally [46].

(b) Sense lncRNAs are transcribed from the sense strand of protein-coding genes containing exons. They may have some overlap with coding genes or cover entire sequence from an intron. If it has been shown that most have no protein-coding potential, several sense lncRNAs can function as both ncRNAs and protein-coding genes (*SRA, ENOD40*).

(c) Antisense lncRNAs (NAT) represent 32% of lncRNAs in humans and are poorly defined. They are transcribed from the antisense strand of protein-coding genes coding. They may also have overlapping with exonic or intronic regions or cover entire sequence from an intron. NATs are observed in many species, including animals, plants, yeasts, prokaryotes, and viruses, but have no sequence or conserved structure that could be indicative of a particular function despite several highly conserved lincRNAs [47].

(ii) Intergenic Regions. *Intergenic lncRNAs (lincRNAs)* are located in unannotated genomic regions and represent the best studied class of lncRNAs. LincRNAs are functional lncRNAs characterized by stability, K4H36 active domain of transcription, and tissue-specific expression. They act in trans and are primarily involved in epigenetic regulation of protein-coding genes expression and maintenance of stem cells pluripotency [48].

(iii) Enhancer ncRNAs (eRNAs). Two types of lncRNA (multiexonic or lacking introns with bidirectional transcription) are derived from enhancer sequences. Enhancer sequences regulate temporal and specific expression of genes via cis or trans mechanisms. The human genome contains approximately one million enhancer sequences most likely controlling the 19000 genes coding for proteins. LncRNAs derived from enhancer sequences play a crucial role in the formation of chromatin loops that allow stabilization and association of enhancer sequences with the promoter regions that initiate transcription of their target genes [49].

(iv) Promoters. PALR (promoter associated long ncRNA).

(v) Telomeric Regions. TERRA (telomeric repeat containing RNAs).

Within cells, lncRNAs are located in the nucleus, according to their main protein-coding genes epigenetic regulatory function. A minority of lncRNAs are involved in nucleocytoplasmic trafficking (*NRON*), mRNA stability, and translational regulation. Several lncRNAs (*MALAT1*) are cleaved by RNase P in a structural and regulatory intranuclear component (speckle) and a small cytoplasmic tRNA-like transcript. LncRNAs topography recognition should help in finding new efficient lncRNAs-based targeted therapies [50]. Finally, lncRNAs can be precursors of ncRNAs (snoRNA, miRNA).

1.6. Modular Organization of the Genome and Structural Plasticity of lncRNAs. The genome has a modular architecture composed of complex transcriptional loci characterized by close links between nucleotide sequences organized in sense/antisense and coding/noncoding transcripts. Thus,

over 50% of protein-coding genes are associated with complementary antisense noncoding transcripts cis-regulating chromatin and adjacent genes expression although no systematic study classified them carefully as lncRNAs. Moreover, combined application of alternative splicing and transcriptional initiation and termination utilizes this modular architecture to ensure transcriptional diversification illustrated by the very large number of lncRNAs isoforms [48]. LncRNAs structural plasticity and biochemical properties better explain the great diversity of their mechanisms of action than their mere nucleotide sequence. Their organization in secondary and tertiary structures contributes to the creation of functional domains interacting with proteins (small ligands, multiprotein complexes) or hybridizing with nucleic acids (mRNA, miRNA, and DNA). Their interactions lead in turn to lncRNAs allosteric conformational changes allowing them to bind to other actors involved in gene expression and mRNA translation. Thus, lncRNAs initiate regulatory networks with high complexity at epigenetic, transcriptional, and posttranscriptional levels, in order to transmit and coordinate information flows in signaling pathways required for eukaryotic cells functioning [51].

1.7. Conservation, Evolution, and Origin of lncRNAs. LncRNAs have been observed in many eukaryotes. Conversely to protein-coding sequences, lncRNAs have rapidly evolved, explaining that lncRNAs orthologues to mammals are only found in vertebrates. Even in vertebrates, DNA sequences conservation is low and suggests that most lncRNAs are not functional due to insufficient selection pressure. Nonetheless, others criteria could be taken into account in assessment of their conservation, including genomic localization, transcriptional profile, and tertiary structure.

Current complexity of human physiology cannot be solely explained by expression of 20000 protein-coding genes, comparable to that observed in Drosophila melanogaster and Caenorhabditis elegans, but rather by parallel development of a noncoding genome. Unlike proteome, amount of ncRNAs has increased during evolution and it seems to be a significant correlation between lncRNAs expression levels and complexity, explaining that primates have most lncRNAs. The number of protein-coding genes cannot explain functioning of very finely regulated organs such as brain. This additional level of complexity observed in vertebrates may be partly related to expression of lncRNAs with a high spatiotemporal specificity and their interactions with DNA, mRNAs, and proteins. LncRNAs could then be considered as molecular sensors of environmental changes conferring evolutional plasticity that contributes to development of life complexity. During environmental changes, lncRNAs located within intergenic sequences may serve as supports for new functions allowing body to adapt new constraints. Protein-coding genes could generate transcripts from lncRNAs genes. Conversely, proteins may be synthesized from lncRNAs. Recent data have identified 24 human protein-coding genes with noncoding homologous genes in other species.

Recent emergence of numerous lncRNAs suggests that they continue to be actively synthesized (i) from ancestral genes that have lost their coding potential, (ii) by genes or other lncRNAs duplication, transposition, and mutation and (iii) de novo from intergenic DNA [52, 53].

1.8. LncRNAs Functions and Mechanisms of Action. Growing data have demonstrated that lncRNAs exhibit the greatest diversity among functional ncRNAs and play regulatory and structural roles in embryogenesis, stem cells pluripotency, allelic expression, protein-coding genes regulation, apoptosis, cycle control, growth, differentiation, and senescence. In practice, only a very limited number of lncRNAs (1%) have been well characterized functionally in humans, including *Xist, KCNQ10T1, AIR, HotAir, ANRIL, HOTTIP, MALAT1, TERRA, and HULC.*

LncRNAs play a role in stem cells and differentiation: maintenance of pluripotency and lineage differentiation in embryonic stem cells (ESCs) and induced pluripotent stem cells (iPSCs). Adult stem cells are finely regulated by lncRNAs networks that are targets of most of master pluripotency transcription factors (Oct4, Sox2, Nanog, cMyc, and KLF4) [54].

LncRNAs are considered as crucial regulators coordinating protein-coding genes expression by numerous mechanisms depending on their cellular localization and leading to modifications of chromatin, transcription, and translation.

These regulatory mechanisms are located at epigenetic, transcriptional, posttranscriptional, and translational levels as follows.

(i) LncRNAs constitute a network of epigenetic modulators, recruiting, guiding, and forming platforms that build ribonucleoprotein complexes at specific genomic sites. 20% of human lncRNAs recruit multimolecular repressor, activator, or chromatin remodeling complexes (PRC1/PRC2 by *ANRIL*, LSD1/PRC2 by *HOTAIR*) whose subcatalytic units (EZH2, EED, BMI1, SUZ12, CBX7, CoREST, and JARID1) interact by altering histone code and methylation profile. Cis-acting lncRNAs adjacent to locus where they are transcribed act by transcriptional interference or by modifying chromatin. Transcriptional interference allows inhibition of preinitialization complexes and interaction with transcription factors. Chromatin modifications result from recruitment of complexes inhibiting (Polycomb by *ANRIL*) or activating (MLL by *HOTTIP*) gene expression. Trans-lncRNAs operate independently of complementarities sequences and act at distance on many genomic loci via specific DNA motifs. They influence genes expression by recruiting modifying chromatin complexes, binding transcriptional elongation factors, and inhibiting RNA polymerase [55].

(ii) LncRNAs associated with promoters (PaRNAs) and lncRNAs of enhancer type (eRNAs) can directly regulate transcription of target genes by transcriptional activation or suppression. PaRNAs function as protein coactivators facilitating gene transcription. PaRNAs of 50–200 nt are involved in repression of polycomb-targeted genes via mechanisms allowing transcription of these lncRNAs from common promoter regions to those of target genes regulated by these noncoding transcripts. Gene cis-repression is the result of PRC2 complex (SUZ12) recruitment by PaRNAs, attachment to promoter regions, and modification of histone methylation (H3K27me3) on target promoters. ERNAs have

transcriptional activation functions of protein-coding genes coding, including genes involved in embryonic development and differentiation (*ncRNAa3 and TAL, ncRNAa7 and SNAI1*) [56–58].

(iii) LncRNAs can also act at posttranscriptional level and are widely involved in biogenesis, stability, and transcriptional activity of mRNAs. They regulate alternative splicing, promote trafficking, direct cellular localization, and promote mRNAs degradation. LncRNAs also synthesize miRNAs and build sponge-like structures to prevent binding of miRNAs to their target mRNAs (*CDR1-as/ciRS-7*, *circular RNA sponge for miR-7*) [59].

(iv) LncRNAs can finally bind to inhibiting factors of translation, interact with ribosomes, and allow transport of proteins.

LncRNAs may participate in assembly of specialized intranuclear functional structures, including speckles (*MALAT1*) paraspeckles (*NEAT1*), and polycomb body (*TUG1*).

Several lncRNAs, particularly lincRNAs, interact with factors (Oct4, Sox2, Nanog, c-Myc, Klf4, Smad, and Tcf3) and play key roles in maintaining stem cells pluripotency.

Moreover, lncRNAs have four known molecular functions (Figure 1): (1) Signal: lncRNAs regulate transcriptional activity or pathways (lincRNA-p21); (2) Guide: lncRNAs link specific proteins belonging to chromatin remodeling complexes and recruit them to homology containing target loci where genes silencing is promoted (HOTTIP, XIST); (3) Decoy: lncRNAs bind and titrate away proteins or RNAs. In the nucleus, they can bind transcription factors or DNA methyltransferase 1 (PANDA, Gas5, MALAT1), whereas in the cytoplasm, they can function like a sponge to attract proteins and miRNA/RISC complexes from their miRNA targets; (4) Scaffold: lncRNAs constitute adaptors that bind molecular complexes and regulate gene expression (HOTAIR, ANRIL, and TERC/TERT) [18, 60].

1.9. lncRNAs and Cancer. Because lncRNAs are involved in various and important physiological processes, their dysfunction should have important consequences for cell homeostasis. Several recent studies have indeed shown that expression of many lncRNAs varies significantly in different conditions compared to healthy tissue. Significance of these deregulations (consequence of a globally altered transcriptional status or causative and driving abnormality) is still a matter of debate. However, transcripts of noncoding genome revealed new dimension of the molecular architecture of cancer and lncRNAs are involved in all stages of oncogenesis. Gene expression profiles analysis of various tumors showed that lncRNAs are deregulated and functional studies have demonstrated that lncRNAs are implicated in general mechanisms of carcinogenesis. Moreover, genetic studies have revealed existence of mutations in their primary sequences. Since most genetic variants identified by genome-wide association studies (GWAS) are located outside coding genes, many of these mutations may therefore affect lncRNAs.

LncRNAs may regulate signaling pathways involved in initiation, tumor progression, and metastatic spread similar to protein-coding oncogenes and oncosuppressors. *PINC* and *PGEM1* were the first oncogenic lncRNAs found overexpressed in breast and prostate carcinomas. Since then, many other lncRNAs have been identified, with oncogenic properties (*KRASP, HULC, HOTAIR, MALAT1, HOTTIP, ANRIL,* and *RICTOR*) or oncosuppressive properties (*MEG3, GAS5, LincRNA-p21, PTENP1, TERRA, CCND1/CyclinD1,* and *TUG1*). Interestingly, several lncRNAs may show both oncogenic and oncosuppressive activities, depending on cellular context. *XIST* noncoding transcript is overexpressed in male tumors and underexpressed in female tumors.

(i) Oncogenic lncRNAs

(a) *SRA* (steroid receptor RNA activator) is a coactivator for steroid receptors and acts as an ncRNA found in the nucleus and cytoplasm. SRA regulates gene expression mediated by steroid receptors through complexing with proteins also containing steroid receptor coactivator 1 (SRC-1). The SRA1 gene can also encode a protein that acts as a coactivator and corepressor. SRA levels have been found to be upregulated in breast tumors where it is assumed that increased SRA levels change the steroid receptors' actions, contributing to breast carcinogenesis. While expression of SRA in normal tissues is low, it is highly upregulated in breast, uterus, and ovary carcinomas [61–63].

(b) *HOTAIR* (HOX antisense intergenic RNA) is a long intergenic noncoding RNA with a length of 2.2 kb in *HOXC* locus and transcribed in antisense manner. HOTAIR regulates gene expression by modulating chromatin structures. It was the first lncRNA discovered to be involved in carcinogenesis. Polycomb group proteins mediate repression of transcription of thousands of genes that control differentiation pathways during development, pluripotency, and cancer progression. Target of PRC2 is *HOXD* locus on chromosome 2 where PRC2 in association with *HOTAIR* promotes transcriptional silencing of metastasis suppressor genes. *HOTAIR* acts as a molecular scaffold remodeling chromatin by causing histone modifications on target genes. *HOTAIR* comprises two known chromatin modification complexes with $5'$ region binding to PRC2 complex responsible for repressive H3K27 methylation and $3'$ region binding to LSD1, which initiates activating H3K4 demethylation [64, 65].

(c) *ANRIL* (antisense ncRNA in the INK4 locus) is a natural antisense transcript, which activates the two polycomb repressor complexes PRC1 and PRC2, resulting in chromatin reorganization with silencing of *INK4b-ARF-INK4a*. This results in p15/INK4b, p14/ARF, and p16INK4a inhibition which are normally implicated in cell cycle negative regulation, senescence, and stress-induced apoptosis. *ANRIL* overexpression in prostate carcinomas has shown silencing of INK4b-ARF-INK4a and p15/CDKN2B.

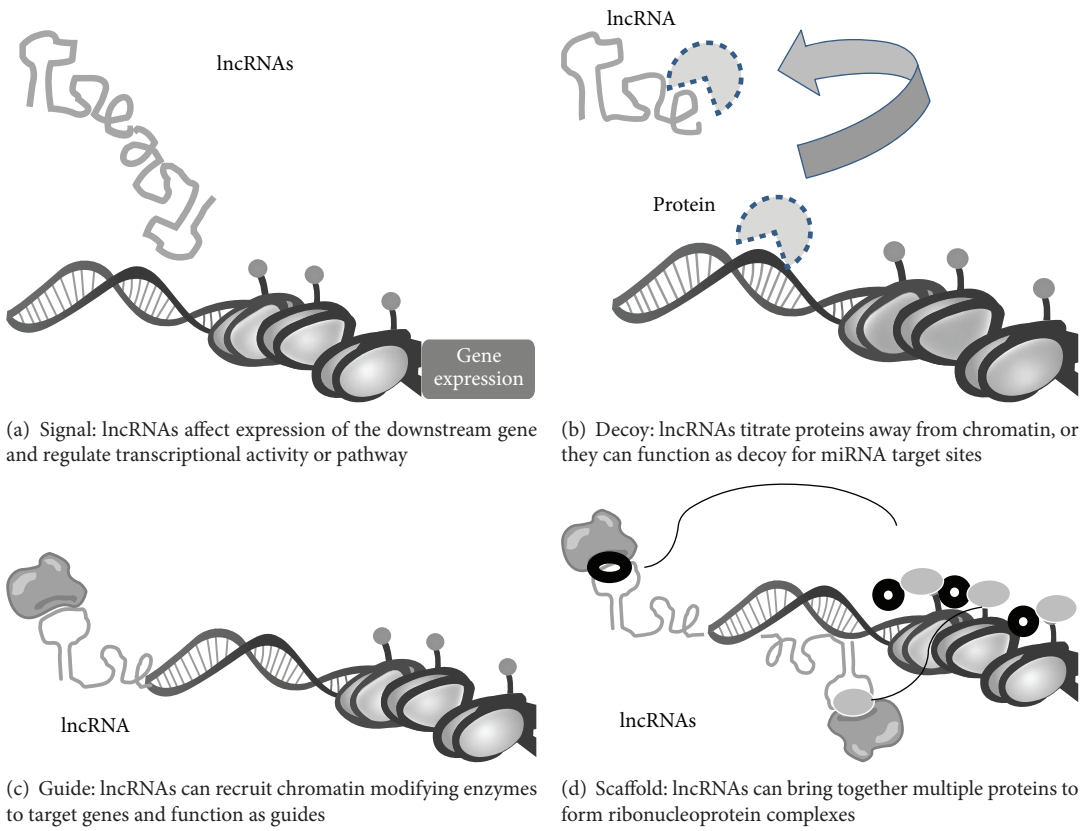

(a) Signal: lncRNAs affect expression of the downstream gene and regulate transcriptional activity or pathway

(b) Decoy: lncRNAs titrate proteins away from chromatin, or they can function as decoy for miRNA target sites

(c) Guide: lncRNAs can recruit chromatin modifying enzymes to target genes and function as guides

(d) Scaffold: lncRNAs can bring together multiple proteins to form ribonucleoprotein complexes

Figure 1: Molecular functions of lncRNAs.

Repression mechanism is mediated by direct binding to CBX 7 and SUZ12, 2 members of PRC1 and PRC2, respectively [66–68].

(d) *MALAT1* (metastasis-associated lung adenocarcinoma transcript 1) is a lincRNA widely expressed in normal human tissues and overexpressed in a variety of breast, colon, liver, pancreas, prostate, and uterus carcinomas. *MALAT1* locus at 11q13.1 has been identified to harbor chromosomal translocation break points and mutations in breast and bladder carcinomas. It is localized in nuclear speckles and recent studies have implicated *MALAT1* in splicing, EMT, cell mobility, ECM remodeling, and metastatic spread [69].

(e) *HULC* (highly upregulated in liver cancer) has been suggested to act as a "sponge" that inhibits miR-372 by sequestering it away from potential mRNA targets [70].

(f) *PCGEM1* (prostate cancer gene expression marker 1) is overexpressed in prostate cancer cells that promotes tumor cells initiation and progression and protects against chemotherapy-induced apoptosis. Moreover, the reciprocal negative control relationship between PCGEM1 and miR-145 regulates both prostate cancer cells proliferation and tumor growth. These results identify PCGEM1 and associated regulators as possible targets for prostate cancer therapy [71].

(ii) Tumor Suppressor lncRNAs

(a) *MEG3* (maternally expressed gene 3) is a transcript of the maternally imprinted gene normally expressed in pituitary cells. *MEG3* loss of expression is observed in pituitary adenomas and meningiomas. *MEG3* acts by regulating p53 pathway. P53 levels are usually extremely low due to its rapid degradation via ubiquitin-proteasome pathway. P53 ubiquitination is mainly mediated by E3 ubiquitin ligase MDM2. *MEG3* downregulates MDM2 expression, increases p53 protein level, stimulates p53-dependent transcription, and enhances p53 binding to target promoters [72].

(b) *GAS5* (growth arrest-specific 5) is widely expressed in embryonic and adult tissues. *GAS5* acts as a starvation or growth arrest-linked riborepressor for glucocorticoid receptors by inhibiting association of these receptors with their DNA recognition sequence. This suppresses several responsive genes activation including gene encoding cellular inhibitor of apoptosis 2 (cIAP2). *GAS5* low expression levels have been observed in prostate and breast carcinomas [73, 74].

(c) *CCND1/Cyclin D1* is transcribed from the promoter region of the Cyclin D1 gene. *Cyclin D1* is a cell cycle regulator frequently mutated, amplified, and overexpressed in carcinomas. *CCND1/Cyclin D1* recruits the RNA-binding protein TLS, which undergoes

allosteric modification, resulting in Cyclin D1 gene inhibition [75, 76].

(d) *LincRNA-p21* expression is directly induced by p53 signaling pathway. This lncRNA is implicated in global repression of genes interfering with p53 function to regulate cellular apoptosis [77].

(e) *TERRA* (telomeric repeat containing RNA) is expressed at chromosome ends. TERRA upregulation upon experimental manipulation or in ICF (immunodeficiency, centromeric instability, and facial anomalies) patients correlates with short telomeres. TERRA transcription facilitates the $5'$-$3'$ nuclease activity of Exo1 at chromosome ends, providing a means to regulate the telomere shortening rate. Thereby, telomere transcription can regulate cellular lifespan through modulation of chromosome end processing activities [78].

(iii) Oncogenic and Tumor Suppressor lncRNAs

(a) *H19* is expressed from the maternal allele and has a pivotal role in genomic imprinting during cell growth and development. The locus contains *H19* and IGF2, which are imprinted. This leads to differential expression of both genes H19 from maternal and IGF2 from paternal allele. This lncRNA presents both oncogenic and suppressive properties although the exact mechanism is still elusive [79].

LncRNAs are implicated in cancer epigenetics. Epigenetics refers to events that modulate activity of the genome without changing its sequence. It provides control of genome expression and establishment of tissular and cellular-type specific genes expression profiles. The main epigenetic mechanisms comprise chemical modifications of DNA and histones (cytosine methylation, posttranslational modifications of histones, chromatin remodeling, and nucleosome positioning). These chemical changes are reversible and controlled by enzyme complexes directly connected to metabolic and signaling pathways as well as sensors of extra- and intracellular microenvironments. Deregulation of these epigenetic mechanisms has been demonstrated in cancer cells which have no transcriptional gene or protein expression while being free of DNA damage. Carcinogenesis is very frequently associated with abnormal signaling and epigenetic abnormalities, most of which are considered as significant oncogenic events (aberrant methylation of oncosuppressor genes). LncRNAs interact with numerous proteins and in particular epigenetic regulators, including DNA methyltransferases and enzymatic complexes modifying chromatin and nucleosomes [80].

(i) Methylation of DNA was first observed in cancer epigenetic alterations. Cancer epigenome is characterized by global hypomethylation leading to genomic instability and hypermethylation of CpG islands which cause inactivation of genes oncosuppressors implicated in signaling pathways (DNA repair, apoptosis, and cycle cell regulation) or transcription factors involved in the control of these genes. LncRNAs bind to DNA methyltransferase, guide it to promoter of oncosuppressor genes, and ensure transcriptional silencing.

(ii) Nucleosomes can be destabilized and restructured by remodeling complexes belonging to 4 families (SWI/SNF, ISWI, CHD, and INO80). Nucleosomes positioning and remodeling regulate gene expression by perturbating accessibility of DNA regulatory sequences by transcription factors and transcription machinery. Mutations and silencing of subunits of these complexes in various types of cancer have been observed. LncRNAs could reposition nucleosomes by interacting and guiding these remodeling complexes to specific genomic regions where nucleosome restructuring would ensure repression of oncosuppressive genes [80].

(iii) LncRNAs recruit histone modifying enzymes acting near the transcription site of lncRNAs. Histones modifying enzymes read, add, or remove covalent links with change in accessibility of chromatin and fixation of nonhistone protein effectors that decode modified histone code. Alterations in the expression of histone-modifying enzymes (mutations, overexpression) were observed in various carcinomas. These alterations inhibit oncosuppressive genes transcription (EZH2 histone methyltransferase responsible for repressive H3K27me3 mark and silencing of p15, p16, and p19; histone deacetylase responsible for loss of lysine acetylated H4) or activate oncogenes transcription (demethylases and deacetylases) [81].

Growing numbers of LncRNAs are implicated in numerous mechanisms characterizing hallmarks of cancer. They can act on proliferation via coactivation (*SRA1*) and inhibition of elongation (*RN7SK*). LncRNAs allow escape mechanisms from suppressor pathways via competition (*PFS*), silencing (*ANRIL*), or ribonucleic repression (*GAS5*). Several lncRNAs are involved in replicative immortality by inhibiting telomerase (*TERRA*). LncRNAs promote neoangiogenesis is by inhibiting HIF1A (*AHIF, MALAT1*). They induce resistance to cell death by acting on p53 and p21 (*PCGEM1*) and by reducing expression of proapoptotic genes (*PANDA*). Finally lncRNAs are involved in mechanisms of invasion and metastasis via deregulation of alternative splicing (*MALAT1*) or trans-silencing of HOXD locus (*HOTAIR*).

2. LncRNAs as Biomarkers and Therapeutic Targets in Future Medical Practice

LncRNAs are emerging as integral functional components of human genome and are now considered as critical regulators in molecular biology of cancer. Recent data have demonstrated that lncRNAs are associated with cancer initiation, tumor progression, and metastatic spread. Unlike mRNAs used as diagnostic and prognostic biomarkers while being expressed by numerous subtypes of malignant tumors, lncRNAs present cellular and tissular specificity and could serve as biomarkers and therapeutic targets in cancer. Furthermore, lncRNAs secreted or released by apoptotic or necrotic tumor cells can be detected in blood, plasma, and urine. There seems to be a significant correlation between levels of circulating nucleic acids and genomic, epigenetic, or transcriptional alterations associated with malignant tumors (Table 2).

(i) Esophagus. Three lncRNA signatures have been identified recently in oesophageal squamous cell carcinoma,

Table 2: Representative lncRNAs involved in carcinogenesis and potential cancer biomarkers.

Cancer type	lncRNAs	References
Esophagus	*ENST00000435885.1, XLOC_013014, ENST00000547963.1*	[12]
Stomach	*GCAT1, H19, SUMO1P3*	[13–17]
Colon and rectum	*HOTAIR, uc.73*	[18, 19]
Liver	*HULC, HOTAIR, MALAT1, HOTTIP, HEIH*	[20–22]
Lung	*MALAT1, TUG1, BANCR, GAS5*	[23–28]
Breast	*HOTAIR, LincRNA-RoR, UCA1*	[29–32]
Ovary	*HOTAIR*	[33]
Bladder	*UCA1, H19, Linc-UBC1, MALAT1*	[34, 35]
Prostate	*PCA3, PCAT1, PCGEM1*	[36–39]
Glioma	*H19*	[40]
Melanoma	*BANCR*	[41]
Oral cavity and nasopharynx	*HOTAIR, lnc-C22orf32-1, lnc-AL355149.1-1 lnc-ZNF674-1*	[4, 42–44]

including ENST00000435885.1, XLOC_013014, and ENST00000547963.1. The expression of these lncRNAs classified the patients into two groups with significantly different overall survival [12].

(ii) Stomach. HOTAIR, GCAT1 (gastric cancer-associated transcript 1), *H19,* and *SUMO1P3* (small ubiquitin-like modifier SUMO 1 pseudogene 3) are the main lncRNAS reported as overexpressed in gastric carcinomas. They are often associated with lymph node and distant metastasis, suggesting that they might serve as potential diagnostic and prognostic biomarker [13–17]. Moreover, CCAT1 expression is closely related to c-Myc activation [14]. *CCAT1* functions as an oncogene and may be used as biomarker and potential therapeutic target in gastric carcinoma [15, 16].

(iii) Lower Digestive Tract. HOTAIR overexpression is observed in colorectal carcinomas with advanced stage and liver metastases [19]. uc.73 lncRNA is also associated with poor overall survival in patient with colorectal carcinomas [18]. These results place HOTAIR and uc.73 lncRNA as reliable biomarkers for poor prognosis in colorectal cancer.

(iv) Liver. In hepatocellular carcinomas (HCC), *HULC* (highly upregulated in liver cancer) was the first lncRNA with highly specific upregulation detected in blood [20]. High plasma *HULC* rates were observed in patients with high grades HCC or with HBV+ status [21]. Recent data have shown that HBx could regulate *HULC* promoter to induce HCC via oncosuppressor *p18* silencing [22]. HBx was found to downregulate lncRNA-*Dreh,* which can inhibit hepatocellular growth and metastasis *in vitro* and *in vivo*.

MALAT-1 and *HOTAIR* have been shown to be overexpressed in large cohorts of HCC patients. Furthermore, *HOTAIR* is a prognostic biomarker for recurrence after liver transplantation. SiRNA-mediated inhibition of *MALAT-1* and *HOTAIR* suppresses cancer cell viability and invasion, sensitizes TNF-α, induces apoptosis, and increases chemotherapeutic sensitivity of HCC to cisplatin and doxorubicin [82, 83]. *HOTTIP* (HOXA transcript at the distal tip) and *HOXA13* were also found to be upregulated in HCC. *HOTTIP* and *HOXA13* levels were associated with HCC tumor progression, metastasis, and survival [84]. *HEIH* (high expression in HCC) is another lncRNA overexpressed in HCC and an independent prognostic factor associated with recurrence [85].

(v) Lung. MALAT1 is a key prognostic biomarker for metastatic spread in lung adenocarcinomas [23]. *TUG1* (taurine upregulated gene 1) is generally downregulated in non-small cell lung carcinomas (NSCLC). In NSCLC patients, *TUG1* low expression was associated with high TNM stage, tumor size, and poorer overall survival. Univariate and multivariate analyses revealed that *TUG1* expression serves as an independent predictor for overall survival [24]. *HOTAIR* was initially reported to be highly expressed in NSCLCs with advanced stage and lymph node metastasis [25]. But more recent meta-analyses study showed that it did not reach statistical significance, and thus it needs further investigations [26]. In NSCLCs, *BANCR* (BRAF activated noncoding RNA) expression is significantly decreased compared to normal tissues. *BANCR* underexpression is considered as an independent prognostic factor and is associated with larger tumor size, advanced pathological stage, metastasis distance, and shorter overall survival. Recently, *BANCR* overexpression was found to play a key role in epithelial-mesenchymal transition [27]. In malignant pleural mesothelioma (MPM), *GAS5* (growth arrest specific transcript 5) underexpression was observed compared to normal mesothelial tissue. Conversely, *GAS5* was upregulated upon growth arrest induced by inhibition of Hedgehog and PI3K/mTOR signaling in MPM models [28].

(vi) Breast. Breast cancer progression is correlated with *HOTAIR* activity in numerous recent studies. The study carried out by Chisholm and colleagues demonstrated *HOTAIR* overexpression in primary and metastatic breast carcinoma tissues by using RNA in situ hybridization technique [29]. Another study focusing on *HOTAIR* revealed the dependence of HOTAIR expression on oestradiol production, due to its promoter region via several estrogen response elements. This study also demonstrated that *HOTAIR* knockdown induced apoptotic pathways in breast cancer cell lines and suggested estrogen receptors as coregulators for *HOTAIR* expression [30]. Conversely, a recent study focusing on 348 primary breast carcinomas revealed that increased DNA methylation led to *HOTAIR* downregulation and an unfavorable disease state, questioning suitability of *HOTAIR* as negative prognostic biomarker in breast carcinomas [31]. *LincRNA-RoR* suppresses p53 in response to DNA damage through interaction with heterogeneous nuclear ribonucleoprotein I (hnRNP I). Recent data demonstrated that hnRNP I can also form a functional ribonucleoprotein complex with *UCA1* (urothelial carcinoma-associated 1) and increase *UCA1* stability. Of interest, the phosphorylated form of hnRNP I, predominantly located in the cytoplasm, is responsible for the interaction with *UCA1*. Although hnRNP I enhances p27 translation through interaction with the 5′-untranslated region of p27 mRNAs, interaction of *UCA1* with hnRNP I suppresses p27 protein expression via competitive inhibition. In support of this finding, *UCA1* seems to have an oncogenic role in breast carcinogenesis both *in vitro* and *in vivo*. Finally, a negative correlation between p27 and *UCA1* was found. Together, these results suggest an important role of UCA1 in breast carcinogenesis [32].

(vii) Glioma. H19/miR-675 signaling was recently identified as a critical pathway in glioma progression. By analyzing gene expression data, *H19* increased levels of expression were found in high grade glioma. SiRNA-induced *H19* depletion inhibited invasion in glioma cells. Furthermore, *H19* expression was positively correlated with miR-675 and *H19* inhibition reduced miR-675 expression. Collectively, these data suggest that *H19* regulates glioma development by deriving miR-675 [40].

(viii) ENT Tumors. Recently, *HOTAIR* was suggested to play a part in nasopharyngeal carcinoma (NPC). *HOTAIR* is implicated in NPC progression and patients with high *HOTAIR* levels have poor clinical outcome with tumor recurrence and distant metastasis [42, 43]. In primary NPCs, upregulation of *lnc-C22orf32-1, lnc-AL355149.1-1, and lnc-ZNF674-1* has been also observed. High levels of *lnc-C22orf32-1* and *lnc-ZNF674-1* are associated with advanced tumor stages. Recurrent NPC displayed a distinctive lncRNA expression pattern with increased expression of *lnc-BCL2L11-3* and decreased expression of *lnc-AL355149.1-1* and *lnc-ZNF674-1* [44]. Interestingly, lncRNAs can be located in whole saliva. *HOTAIR* is differentially expressed in saliva of metastatic oral squamous cell carcinoma patients compared to primary tumors. These findings suggest that detection of lncRNAs in saliva may be used as a noninvasive and rapid diagnostic tool for diagnosis of oral carcinomas [4].

(ix) Bladder. Oncogenic lncRNAs, including *UCA1, H19, MALAT1,* and *linc-UBC1* (upregulated in bladder cancer 1), are overexpressed in bladder carcinomas and activate PI3K-AKT and Wnt/β-catenin pathways. A pilot study took advantage of this to evaluate potential application of *UCA1* in urinary sediments from patients with bladder carcinomas. It turned out to be especially valuable for superficial G2/G3 patients at a high risk for muscular invasion, indicating that *UCA1* may be a new promising urinary biomarker for the diagnosis of bladder cancer. *H19* expression levels are remarkably increased in bladder carcinomas compared to normal tissue and could also serve as another biomarker. More recently, a new lncRNA *linc-UBC1* was found to be overexpressed in 60% of invasive bladder carcinomas and correlated with lymph node metastasis and poor survival. *MALAT1* is upregulated in bladder cancer and its expression level is correlated with tumor grade and metastatic stage [34, 35].

(x) Prostate. Prostate cancer specific lncRNA*DD3/PCA3* was identified fifteen years ago [86]. *PCA3* is a prostate-specific lncRNA markedly overexpressed in prostate carcinomas. It can be detected in prostate cancer tissue, urine, and/or urine sediments. In recent studies, *PCA3* specificity was found even higher than prostate biomarker PSA and *PCA3* score can accurately predict tumor volume and pathological features, which may guide treatment [36, 37]. Therefore, *PCA3* can be used as a noninvasive urine-based test for large-scale screening protocols and for predicting prostate carcinomas aggressiveness. This prominent example of rapid translation of lncRNA research into clinical practice offers a prototype for developing different lncRNAs as biomarkers. Other lncRNAs, such as PCGEM1 and PCAT1 (prostate cancer associated ncRNA transcript 1), are also prostate-specific, posing as attractive biomarkers [38, 39].

(xi) Melanoma. BANCR (lncRNA BRAF-activated noncoding RNA) plays a potentially functional role in melanoma cells proliferation and migration by activating ERK1/2 and JNK MAPK pathways. *BANCR* is upregulated in human malignant melanoma and patients with high levels of expression have a lower survival rate [41].

(xii) Hemopathies. Several recent reports have revealed deregulation of lncRNAs in leukemia, including *ANRIL, lncRNA-P21, MEG3, Dleu2, HOTAIRM1, EGO*, and *lncRNA-a7*. Moreover, *MEG3, UCA1,* and *H19* are upregulated in acute myeloid leukemia [87, 88].

(xiii) Ovary. HOTAIR plays a pivotal role in epithelial ovarian cancer (EOC) metastasis and could represent a novel prognostic marker and potential therapeutic target in patients with EOC. In recent study, *HOTAIR* expression was elevated in EOC tissues, and its level of expression is highly positively

correlated with FIGO stage, histological grade, lymph node metastasis, reduced overall survival, and disease-free survival [33].

Because of their central role in genes expression regulation, lncRNAs could also represent potential therapeutic targets. Better characterization of lncRNAs (structure, functions, polymorphisms, and intracellular topography) could help in faster development of new anticancer strategies modulating expression levels and functions of deregulated lncRNAs. Targeting lncRNAs offers novel exciting opportunity to treat cancer. Currently, nucleic acid-based methods prevail in targeting RNA, by regulating levels of expression and modifying their structures or mature sequences. Among them, RNA interference (RNAi) based techniques are arguably the most popular methods to inhibit lncRNAs in cancer cells. Both siRNAs and shRNAs exhibit great RNA selectivity and knockdown efficiency. Meanwhile, other established methods in inhibiting cancer-associated RNA, including antisense oligonucleotide (ASO), ribozyme, and aptamer, are also effective to modulate lncRNAs, and they show unique features that can have advantages over siRNAs [89].

In principle, targeting of lncRNAs can be achieved using the several approaches, including siRNA-mediated silencing, functional block using small molecules, or oligonucleotide inhibitors to prevent interactions of lncRNAs with proteins and structure disruption via small molecules or oligonucleotide inhibitors to change or mimic their secondary structure to compete for their binding partners [90].

(1) *Small interfering RNAs (siRNA)* are short stretched (19–30 nt) double-stranded RNAs that target RNA molecules via complementary to unpaired lncRNA sequences. The RNA duplex of siRNAs must be unwound into single strands before assembling into the active RNA-induced silencing complex (RISC). SiRNAs are fully complementary to their RNA target that is then cleaved at a single phosphodiester bond located near the centre of the sequence complement to the siRNA sequence [90]. SiRNAs exhibit high knockdown efficiency to many oncogenic lncR-NAs in cancer cells and induce anticancer effects both *in vitro* and *in vivo*. For instance, depletion of *HOTAIR* by siRNAs decreases matrix invasiveness of breast cancer cells and inhibits tumor growth of pancreatic cancer xenograft. *HULC* and *MALAT1* siRNA-induced knockdown inhibits HCC cell proliferation and cell cycle progression [91]. Furthermore, siRNA-mediated knockdown of *H19* induces apoptosis and inactivates p53 [92]. Phase I and II clinical therapeutic trials have been evaluated using siRNAs to inhibit critical cancer-associated genes, including siRNA-EphA2-DOPC (targeting *EphA2*), TKM-080301 (targeting *PLK1*), and CALAA-01 (targeting *RRM2*). Therapy combining siRNA drug siG12D LODER and Atu027 with conventional chemotherapy is studied in phase II for its therapeutic effect in advanced pancreatic cancer patients. However, the main obstacle of siRNAs therapeutics remaining is their delivery. SiRNAs using ribonucleic acid as building block are susceptible to be degraded by nuclease and have poor pharmacokinetics.

(2) *Antisense oligonucleotides (ASO)* are short, single-stranded DNAs or RNAs (between 8 and 50 nt) designed with sequence specific to target lncRNA [90]. ASOs directly hybridize to lncRNA transcripts via base pairing and endogenous RNase H1, which results in cleavage of lncRNA molecules, then recognizes hybrids formed. ASOs modulate lncRNAs function through degradation of lncRNA transcripts. Inhibition of *MALAT1* by ASO attenuates various malignant phenotypes in cancer cells via cycle arrest in cervical cancer cells [93]. Injection of ASO into subcutaneous tumors of nude mice effectively inhibits *MALAT1 in vivo* and blocks metastasis of lung cancer cells [91].

(3) *Ribozymes* are naturally produced RNA molecules that present intracellular catalytic functions. One of their functions is degradation of RNA molecules. Among all types of ribozyme, hammerhead ribozyme (HamRz) has caught major interest as it shows good target inhibitory effect while having the smallest RNA endoribonucleolytic motif as well as function independent to presence of metal ions [94]. HamRz is single-stranded RNA in neutral condition and undergoes folding in cells to expose the binding arms. Binding of HamRz to target sequence depends on complementary match with homologous target site. Both arms of HamRz have to bind with target sites correctly in order to form functional catalytic motif. After binding, HamRz catalyzes cleavage of the flanked RNA region downstream to a NUH site via destabilizing phosphodiester backbone of target RNA [90].

(4) *Aptamers* are short DNA or RNA oligonucleotides or peptides that have a stable 3-dimensional structure *in vivo*. They have broad molecular targets including protein, RNA, and small molecules that rely on fitting 3-dimensional shape of their ligands [95]. They specifically bind to their target lncRNAs that rely on fitting 3-dimensional shape of the lncRNA structures. Aptamers antagonize their lncRNA targets by blocking the interactions between lncRNAs and critical factors [90]. Some reports show promising effects of aptamers to either degrade RNA or inhibit RNA functions, implying the potential of aptamers as therapeutic agents to target lncRNAs. Aptamers are used to modulate viral gene expression by interacting with viral RNAs. A hairpin aptamer is identified to form stable and specific complex with the transactivation response element (TAR) RNA element of HIV-1 mRNA and decrease the TAR-dependent viral protein expression [96]. Another aptamer, selected against TAR element, formed stable loop–loop complexes with the element to regulate the TAR-mediated process [97]. Another study showed that aptamer could target the apical loop domain of pri-microRNA molecules and modulate the biogenesis of mature microRNA [98].

(5) *MicroRNAs (miRNAs)* can interact with lncRNAs. *H19*/miR-675 signaling is critical in glioma progression. By analyzing glioma gene expression data sets, *H19 is* found to be increased in high grade gliomas. *H19* depletion via siRNA inhibits invasion in glioma cells. Further, H19 is positively correlated with its derivate miR-675 expression and reduction of *H19* inhibits miR-675 expression. MiR-675 modulates cadherin 13 expression by directly targeting its binding site within $3'$ UTR. These results demonstrate that *H19* regulates glioma development by deriving miR-675 and provide important clues for understanding key roles of lncRNA-microRNA functional network in glioma.

MicroRNA-based anticancer therapy has great potential as reports show there is apparent lack of adverse event in normal tissues when administrated with microRNA-based agent. Various microRNA delivery strategies, such as cationic lipid and nanoparticle encapsulation, are developed to improve microRNA shuttling into target cancer cells [40, 99, 100]. The potential of microRNA regulation on lncRNAs can be further realized by better understanding of intragenic lncRNA regulating elements.

(6) *Small molecules* are synthesized to specifically bind to RNA binding pockets of lncRNAs. They compete with protein factors or intracellular small ligands for binding lncRNAs. Binding of small molecules may also induce conformational change within lncRNA molecules and disrupt formation of important lncRNA structures [90].

3. Conclusion and Perspectives

Deregulated oncogenic and oncosuppressive lncRNAs are observed at all stages of malignant tumors development of various origins. Mechanisms implicating lncRNAs in carcinogenesis are dominated by deregulation of signaling pathways and altered epigenetic, transcriptional, and post-transcriptional expression of numerous genes. Their use as biomarkers and potential therapeutic targets could appear promising.

Major challenges of the next 10 years remaining are identification, mapping of all lncRNAs belonging to the human genome, and their functional characterization. Although their mechanisms of action are better known, it is still possible that lncRNAs are rather downstream products of particular chromatin structures or deregulated transcriptional processes. Their functionality is currently still debated because of their low level of expression and conservation between species. Unlike proteins, which often have well-defined functional areas, it is currently impossible to predict lncRNAs function from their single sequence. However, many traits exhibited by lncRNAs favor functionality, including 3′polyadenylation, 5′cap, multiple exons, transcriptional activation similar to that of mRNA, K4K36 domain, and alternative splicing. These challenges will only be achieved through combined efforts of functional genomics, epigenomics, and bioinformatics.

Conflict of Interests

No potential conflict of interests was disclosed.

Acknowledgment

This work was supported by Grant INCa-DGOS-4654.

References

[1] S. Djebali, C. A. Davis, A. Merkel et al., "Landscape of transcription in human cells," *Nature*, vol. 489, no. 7414, pp. 101–108, 2012.

[2] M. K. Iyer, Y. S. Niknafs, R. Malik et al., "The landscape of long noncoding RNAs in the human transcriptome," *Nature Genetics*, vol. 47, no. 3, pp. 199–208, 2015.

[3] R. J. Taft, K. C. Pang, T. R. Mercer, M. Dinger, and J. S. Mattick, "Non-coding RNAs: regulators of disease," *Journal of Pathology*, vol. 220, no. 2, pp. 126–139, 2010.

[4] E. A. Gibb, K. S. S. Enfield, G. L. Stewart et al., "Long non-coding RNAs are expressed in oral mucosa and altered in oral premalignant lesions," *Oral Oncology*, vol. 47, no. 11, pp. 1055–1061, 2011.

[5] J. M. Perkel, "Visiting 'Noncodarnia'," *BioTechniques*, vol. 54, no. 6, pp. 301–304, 2013.

[6] K. C. Pang, M. C. Frith, and J. S. Mattick, "Rapid evolution of noncoding RNAs: lack of conservation does not mean lack of function," *Trends in Genetics*, vol. 22, no. 1, pp. 1–5, 2006.

[7] O. Wapinski and H. Y. Chang, "Long noncoding RNAs and human disease," *Trends in Cell Biology*, vol. 21, no. 6, pp. 354–361, 2011.

[8] S. Ye, L. Yang, X. Zhao, W. Song, W. Wang, and S. Zheng, "Bioinformatics method to predict two regulation mechanism: TF–miRNA–mRNA and lncRNA–miRNA–mRNA in pancreatic cancer," *Cell Biochemistry and Biophysics*, vol. 70, no. 3, pp. 1849–1858, 2014.

[9] Q. Jiang, J. Wang, Y. Wang, R. Ma, X. Wu, and Y. Li, "TF2LncRNA: identifying common transcription factors for a list of lncRNA genes from ChIP-seq data," *BioMed Research International*, vol. 2014, Article ID 317642, 5 pages, 2014.

[10] C. Park, N. Yu, I. Choi, W. Kim, and S. Lee, "lncRNAtor: a comprehensive resource for functional investigation of long non-coding RNAs," *Bioinformatics*, vol. 30, no. 17, pp. 2480–2485, 2014.

[11] Z. X. Chen, D. Sturgill, J. Qu et al., "Comparative validation of the D. melanogaster modENCODE transcriptome annotation," *Genome Research*, vol. 24, no. 7, pp. 1209–1223, 2014.

[12] Z. Chen, J. Li, L. Tian et al., "MiRNA expression profile reveals a prognostic signature for esophageal squamous cell carcinoma," *Cancer Letters*, vol. 350, no. 1-2, pp. 34–42, 2014.

[13] M. Hajjari, M. Behmanesh, M. Sadeghizadeh, and M. Zeinoddini, "Up-regulation of HOTAIR long non-coding RNA in human gastric adenocarcinoma tissues," *Medical Oncology*, vol. 30, no. 3, article 670, 2013.

[14] F. Yang, X. Xue, J. Bi et al., "Long noncoding RNA CCAT1, which could be activated by c-Myc, promotes the progression of gastric carcinoma," *Journal of Cancer Research and Clinical Oncology*, vol. 139, no. 3, pp. 437–445, 2013.

[15] W. Sun, Y. Wu, X. Yu et al., "Decreased expression of long noncoding RNA AC096655.1-002 in gastric cancer and its clinical significance," *Tumor Biology*, vol. 34, no. 5, pp. 2697–2701, 2013.

[16] B. Xiao and J. Guo, "Long noncoding RNA AC096655.1-002 has been officially named as gastric cancer-associated transcript 1, GACAT1," *Tumor Biology*, vol. 34, no. 5, p. 3271, 2013.

[17] D. Mei, H. Song, K. Wang et al., "Up-regulation of SUMO1 pseudogene 3 (SUMO1P3) in gastric cancer and its clinical association," *Medical Oncology*, vol. 30, no. 4, article 709, 2013.

[18] J. Sana, P. Faltejskova, M. Svoboda, and O. Slaby, "Novel classes of non-coding RNAs and cancer," *Journal of Translational Medicine*, vol. 10, no. 1, article 103, 2012.

[19] R. Kogo, T. Shimamura, K. Mimori et al., "Long noncoding RNA HOTAIR regulates polycomb-dependent chromatin modification and is associated with poor prognosis in colorectal cancers," *Cancer Research*, vol. 71, no. 20, pp. 6320–6326, 2011.

[20] K. Panzitt, M. M. O. Tschernatsch, C. Guelly et al., "Characterization of HULC, a novel gene with striking up-regulation in

hepatocellular carcinoma, as noncoding RNA," *Gastroenterology*, vol. 132, no. 1, pp. 330–342, 2007.

[21] H. Xie, H. Ma, and D. Zhou, "Plasma HULC as a promising novel biomarker for the detection of hepatocellular carcinoma," *BioMed Research International*, vol. 2013, Article ID 136106, 5 pages, 2013.

[22] J.-F. Huang, Y.-J. Guo, C.-X. Zhao et al., "Hepatitis B virus X protein (HBx)-related long noncoding RNA (lncRNA) down-regulated expression by HBx (Dreh) inhibits hepatocellular carcinoma metastasis by targeting the intermediate filament protein vimentin," *Hepatology*, vol. 57, no. 5, pp. 1882–1892, 2013.

[23] T. Gutschner, M. Hämmerle, M. Eissmann et al., "The noncoding RNA MALAT1 is a critical regulator of the metastasis phenotype of lung cancer cells," *Cancer Research*, vol. 73, no. 3, pp. 1180–1189, 2013.

[24] E. B. Zhang, D. D. Yin, M. Sun et al., "P53-regulated long non-coding RNA TUG1 affects cell proliferation in human non-small cell lung cancer, partly through epigenetically regulating HOXB7 expression," *Cell Death and Disease*, vol. 5, no. 5, Article ID e1243, 2014.

[25] T. Nakagawa, H. Endo, M. Yokoyama et al., "Large noncoding RNA HOTAIR enhances aggressive biological behavior and is associated with short disease-free survival in human non-small cell lung cancer," *Biochemical and Biophysical Research Communications*, vol. 436, no. 2, pp. 319–324, 2013.

[26] J. Yang, J. Lin, T. Liu et al., "Analysis of lncRNA expression profiles in non-small cell lung cancers (NSCLC) and their clinical subtypes," *Lung Cancer*, vol. 85, no. 2, pp. 110–115, 2014.

[27] M. Sun, X.-H. Liu, K.-M. Wang et al., "Downregulation of BRAF activated non-coding RNA is associated with poor prognosis for non-small cell lung cancer and promotes metastasis by affecting epithelial-mesenchymal transition," *Molecular Cancer*, vol. 13, no. 1, article 68, 2014.

[28] A. Renganathan, J. Kresoja-Rakic, N. Echeverry et al., "GAS5 long non-coding RNA in malignant pleural mesothelioma," *Molecular Cancer*, vol. 13, no. 1, article 119, 2014.

[29] K. M. Chisholm, Y. Wan, R. Li, K. D. Montgomery, H. Y. Chang, and R. B. West, "Detection of long non-coding RNA in archival tissue: correlation with polycomb protein expression in primary and metastatic breast carcinoma," *PLoS ONE*, vol. 7, no. 10, Article ID e47998, 2012.

[30] A. Bhan, I. Hussain, K. I. Ansari, S. Kasiri, A. Bashyal, and S. S. Mandal, "Antisense transcript long noncoding RNA (lncRNA) HOTAIR is transcriptionally induced by estradiol," *Journal of Molecular Biology*, vol. 425, no. 19, pp. 3707–3722, 2013.

[31] L. Lu, G. Zhu, C. Zhang et al., "Association of large noncoding RNA HOTAIR expression and its downstream intergenic CpG island methylation with survival in breast cancer," *Breast Cancer Research and Treatment*, vol. 136, no. 3, pp. 875–883, 2012.

[32] J. Huang, N. Zhou, K. Watabe et al., "Long non-coding RNA UCA1 promotes breast tumor growth by suppression of p27 (Kip1)," *Cell Death and Disease*, vol. 5, no. 1, p. e1008, 2014.

[33] J.-J. Qiu, Y.-Y. Lin, L.-C. Ye et al., "Overexpression of long non-coding RNA HOTAIR predicts poor patient prognosis and promotes tumor metastasis in epithelial ovarian cancer," *Gynecologic Oncology*, vol. 134, no. 1, pp. 121–128, 2014.

[34] Q. Zhang, M. Su, G. Lu, and J. Wang, "The complexity of bladder cancer: long noncoding RNAs are on the stage," *Molecular Cancer*, vol. 12, no. 1, article 101, 2013.

[35] L. Wang, D. Fu, Y. Qiu et al., "Genome-wide screening and identification of long noncoding RNAs and their interaction with protein coding RNAs in bladder urothelial cell carcinoma," *Cancer Letters*, vol. 349, no. 1, pp. 77–86, 2014.

[36] G. Ploussard, X. Durand, E. Xylinas et al., "Prostate cancer antigen 3 score accurately predicts tumour volume and might help in selecting prostate cancer patients for active surveillance," *European Urology*, vol. 59, no. 3, pp. 422–429, 2011.

[37] M. J. Roobol, F. H. Schröder, G. L. J. H. Van Leenders et al., "Performance of prostate cancer antigen 3 (PCA3) and prostate-specific antigen in prescreened men: Reproducibility and detection characteristics for prostate cancer patients with high PCA3 scores (≥100)," *European Urology*, vol. 58, no. 6, pp. 893–899, 2010.

[38] A. L. Walsh, A. V. Tuzova, E. M. Bolton, T. H. Lynch, and A. S. Perry, "Long noncoding RNAs and prostate carcinogenesis: the missing 'linc'?" *Trends in Molecular Medicine*, vol. 20, no. 8, pp. 428–436, 2014.

[39] G. O. Ifere and G. A. Ananaba, "Prostate Cancer Gene Expression Marker 1 (PCGEM1): a patented prostate- specific non-coding gene and regulator of prostate cancer progression," *Recent Patents on DNA and Gene Sequences*, vol. 3, no. 3, pp. 151–163, 2009.

[40] Y. Shi, Y. Wang, W. Luan et al., "Long non-coding RNA H19 promotes glioma cell invasion by deriving miR-675," *PLoS ONE*, vol. 9, no. 1, Article ID e86295, 2014.

[41] R. Li, L. Zhang, L. Jia et al., "Long non-coding RNA BANCR promotes proliferation in malignant melanoma by regulating MAPK pathway activation," *PLoS ONE*, vol. 9, no. 6, Article ID e100893, 2014.

[42] R. A. Gupta, N. Shah, K. C. Wang et al., "Long non-coding RNA HOTAIR reprograms chromatin state to promote cancer metastasis," *Nature*, vol. 464, no. 7291, pp. 1071–1076, 2010.

[43] Y. Nie, X. Liu, S. Qu, E. Song, H. Zou, and C. Gong, "Long non-coding RNA HOTAIR is an independent prognostic marker for nasopharyngeal carcinoma progression and survival," *Cancer Science*, vol. 104, no. 4, pp. 458–464, 2013.

[44] W. Gao, J. Y.-W. Chan, and T.-S. Wong, "Differential expression of long noncoding RNA in primary and recurrent nasopharyngeal carcinoma," *BioMed Research International*, vol. 2014, Article ID 404567, 9 pages, 2014.

[45] A. C. Marques, J. Hughes, B. Graham, M. S. Kowalczyk, D. R. Higgs, and C. P. Ponting, "Chromatin signatures at transcriptional start sites separate two equally populated yet distinct classes of intergenic long noncoding RNAs," *Genome Biology*, vol. 14, no. 11, article R131, 2013.

[46] R. Louro, A. S. Smirnova, and S. Verjovski-Almeida, "Long intronic noncoding RNA transcription: expression noise or expression choice?" *Genomics*, vol. 93, no. 4, pp. 291–298, 2009.

[47] T. Kunej, J. Obsteter, Z. Pogacar, S. Horvat, and G. A. Calin, "The decalog of long non-coding RNA involvement in cancer diagnosis and monitoring," *Critical Reviews in Clinical Laboratory Sciences*, vol. 51, no. 6, pp. 344–357, 2014.

[48] A. M. Khalil, M. Guttman, M. Huarte et al., "Many human large intergenic noncoding RNAs associate with chromatin-modifying complexes and affect gene expression," *Proceedings of the National Academy of Sciences of the United States of America*, vol. 106, no. 28, pp. 11667–11672, 2009.

[49] W. Xie and B. Ren, "Enhancing pluripotency and lineage specification," *Science*, vol. 341, no. 6143, pp. 245–247, 2013.

[50] S. Nakagawa, J. Y. Ip, G. Shioi et al., "Malat1 is not an essential component of nuclear speckles in mice," *RNA*, vol. 18, no. 8, pp. 1487–1499, 2012.

[51] I. Ilik, J. Quinn, P. Georgiev et al., "Tandem stem-loops in roX RNAs act together to mediate X Chromosome dosage compensation in *Drosophila*," *Molecular Cell*, vol. 51, no. 2, pp. 156–173, 2013.

[52] Y. A. Sytnikova, R. Rahman, G. Chirn, J. P. Clark, and N. C. Lau, "Transposable element dynamics and PIWI regulation impacts lncRNA and gene expression diversity in *Drosophila ovarian* cell cultures," *Genome Research*, vol. 24, no. 12, pp. 1977–1990, 2014.

[53] J. W. Nam and D. P. Bartel, "Long noncoding RNAs in *C. elegans*," *Genome Research*, vol. 22, no. 12, pp. 2529–2540, 2012.

[54] Y. Zhang, J. Xia, Q. Li et al., "NRF2/long noncoding RNA ROR signaling regulates mammary stem cell expansion and protects against estrogen genotoxicity," *The Journal of Biological Chemistry*, vol. 289, no. 45, pp. 31310–31318, 2014.

[55] S. He, H. Zhang, H. Liu, and H. Zhu, "LongTarget: a tool to predict lncRNA DNA-binding motifs and binding sites via Hoogsteen base-pairing analysis," *Bioinformatics*, vol. 31, no. 2, pp. 178–186, 2015.

[56] J. C. Schwartz, S. T. Younger, N.-B. Nguyen et al., "Antisense transcripts are targets for activating small RNAs," *Nature Structural and Molecular Biology*, vol. 15, no. 8, pp. 842–848, 2008.

[57] R. J. Taft, C. D. Kaplan, C. Simons, and J. S. Mattick, "Evolution, biogenesis and function of promoter-associated RNAs," *Cell Cycle*, vol. 8, no. 15, pp. 2332–2338, 2009.

[58] J. Han, D. Kim, and K. V. Morris, "Promoter-associated RNA is required for RNA-directed transcriptional gene silencing in human cells," *Proceedings of the National Academy of Sciences of the United States of America*, vol. 104, no. 30, pp. 12422–12427, 2007.

[59] S. Memczak, M. Jens, A. Elefsinioti et al., "Circular RNAs are a large class of animal RNAs with regulatory potency," *Nature*, vol. 495, no. 7441, pp. 333–338, 2013.

[60] K. C. Wang and H. Y. Chang, "Molecular mechanisms of long noncoding RNAs," *Molecular Cell*, vol. 43, no. 6, pp. 904–914, 2011.

[61] E. Leygue, H. Dotzlaw, P. H. Watson, and L. C. Murphy, "Expression of the steroid receptor RNA activator in human breast tumors," *Cancer Research*, vol. 59, no. 17, pp. 4190–4193, 1999.

[62] S. Chooniedass-Kothari, E. Emberley, M. K. Hamedani et al., "The steroid receptor RNA activator is the first functional RNA encoding a protein," *FEBS Letters*, vol. 566, no. 1–3, pp. 43–47, 2004.

[63] D. Ulveling, C. Francastel, and F. Hubé, "When one is better than two: RNA with dual functions," *Biochimie*, vol. 93, no. 4, pp. 633–644, 2011.

[64] J. L. Rinn, M. Kertesz, J. K. Wang et al., "Functional demarcation of active and silent chromatin domains in human HOX Loci by noncoding RNAs," *Cell*, vol. 129, no. 7, pp. 1311–1323, 2007.

[65] M.-C. Tsai, O. Manor, Y. Wan et al., "Long noncoding RNA as modular scaffold of histone modification complexes," *Science*, vol. 329, no. 5992, pp. 689–693, 2010.

[66] E. Pasmant, I. Laurendeau, D. Héron, M. Vidaud, D. Vidaud, and I. Bièche, "Characterization of a germ-line deletion, including the entire INK4/ARF locus, in a melanoma-neural system tumor family: identification of ANRIL, an antisense noncoding RNA whose expression coclusters with ARF," *Cancer Research*, vol. 67, no. 8, pp. 3963–3969, 2007.

[67] E. Pasmant, A. Sabbagh, J. Masliah-Planchon et al., "Role of noncoding RNA ANRIL in genesis of plexiform neurofibromas in neurofibromatosis type 1," *Journal of the National Cancer Institute*, vol. 103, no. 22, pp. 1713–1722, 2011.

[68] E. Pasmant, A. Sabbagh, M. Vidaud, and I. Bièche, "ANRIL, a long, noncoding RNA, is an unexpected major hotspot in GWAS," *FASEB Journal*, vol. 25, no. 2, pp. 444–448, 2011.

[69] L. Shen, L. Chen, Y. Wang, X. Jiang, H. Xia, and Z. Zhuang, "Long noncoding RNA MALAT1 promotes brain metastasis by inducing epithelial-mesenchymal transition in lung cancer," *Journal of Neuro-Oncology*, vol. 121, no. 1, pp. 101–108, 2015.

[70] J. Wang, X. Liu, H. Wu et al., "CREB up-regulates long non-coding RNA, HULC expression through interaction with microRNA-372 in liver cancer," *Nucleic Acids Research*, vol. 38, no. 16, pp. 5366–5383, 2010.

[71] J. H. He, J. Z. Zhang, Z. P. Han, L. Wang, Y. Lv, and Y. G. Li, "Reciprocal regulation of PCGEM1 and miR-145 promote proliferation of LNCaP prostate cancer cells," *Journal of Experimental & Clinical Cancer Research*, vol. 33, no. 1, article 72, 2014.

[72] K.-H. Lu, W. Li, X.-H. Liu et al., "Long non-coding RNA MEG3 inhibits NSCLC cells proliferation and induces apoptosis by affecting p53 expression," *BMC Cancer*, vol. 13, article 461, 2013.

[73] M. R. Pickard and G. T. Williams, "Regulation of apoptosis by long non-coding RNA GAS5 in breast cancer cells: implications for chemotherapy," *Breast Cancer Research and Treatment*, vol. 145, no. 2, pp. 359–370, 2014.

[74] M. R. Pickard, M. Mourtada-Maarabouni, and G. T. Williams, "Long non-coding RNA GAS5 regulates apoptosis in prostate cancer cell lines," *Biochimica et Biophysica Acta*, vol. 1832, no. 10, pp. 1613–1623, 2013.

[75] R. Kurokawa, "Promoter-associated long noncoding RNAs repress transcription through a RNA binding protein TLS," *Advances in Experimental Medicine and Biology*, vol. 722, pp. 196–208, 2011.

[76] X. Song, X. Wang, S. Arai, and R. Kurokawa, "Promoter-associated noncoding RNA from the CCND1 promoter," *Methods in Molecular Biology*, vol. 809, pp. 609–622, 2012.

[77] G. Wu, J. Cai, Y. Han et al., "LincRNA-p21 regulates neointima formation, vascular smooth muscle cell proliferation, apoptosis, and atherosclerosis by enhancing p53 activity," *Circulation*, vol. 130, no. 17, pp. 1452–1465, 2014.

[78] V. Pfeiffer and J. Lingner, "TERRA promotes telomere shortening through exonuclease 1-mediated resection of chromosome ends," *PLoS Genetics*, vol. 8, no. 6, Article ID e1002747, 2012.

[79] M. Nordin, D. Bergman, M. Halje, W. Engström, and A. Ward, "Epigenetic regulation of the Igf2/H19 gene cluster," *Cell Proliferation*, vol. 47, no. 3, pp. 189–199, 2014.

[80] S. Marquardt, R. Escalante-Chong, N. Pho et al., "A chromatin-based mechanism for limiting divergent noncoding transcription," *Cell*, vol. 157, no. 7, pp. 1712–1723, 2014.

[81] R. Backofen and T. Vogel, "Biological and bioinformatical approaches to study crosstalk of long-non-coding RNAs and chromatin-modifying proteins," *Cell and Tissue Research*, vol. 356, no. 3, pp. 507–526, 2014.

[82] M.-C. Lai, Z. Yang, L. Zhou et al., "Long non-coding RNA MALAT-1 overexpression predicts tumor recurrence of hepatocellular carcinoma after liver transplantation," *Medical Oncology*, vol. 29, no. 3, pp. 1810–1816, 2012.

[83] Z. Yang, L. Zhou, L.-M. Wu et al., "Overexpression of long non-coding RNA HOTAIR predicts tumor recurrence in hepatocellular carcinoma patients following liver transplantation," *Annals of Surgical Oncology*, vol. 18, no. 5, pp. 1243–1250, 2011.

[84] L. Quagliata, M. S. Matter, S. Piscuoglio et al., "Long noncoding RNA HOTTIP/HOXA13 expression is associated with disease progression and predicts outcome in hepatocellular carcinoma patients," *Hepatology*, vol. 59, no. 3, pp. 911–923, 2014.

[85] S.-X. Yuan, F. Yang, Y. Yang et al., "Long noncoding RNA associated with microvascular invasion in hepatocellular carcinoma promotes angiogenesis and serves as a predictor for hepatocellular carcinoma patients' poor recurrence-free survival after hepatectomy," *Hepatology*, vol. 56, no. 6, pp. 2231–2241, 2012.

[86] M. J. G. Bussemakers, A. Van Bokhoven, G. W. Verhaegh et al., "DD3: a new prostate-specific gene, highly overexpressed in prostate cancer," *Cancer Research*, vol. 59, no. 23, pp. 5975–5979, 1999.

[87] M. Hajjari, A. Khoshnevisan, and Y. K. Shin, "Long noncoding RNAs in hematologic malignancies: road to translational research," *Frontiers in Genetics*, vol. 4, article 250, 2013.

[88] E. F. Heuston, K. T. Lemon, and R. J. Arceci, "The beginning of the road for non-coding RNAs in normal hematopoiesis and hematologic malignancies," *Frontiers in Genetics*, vol. 2, article 94, 2011.

[89] C. H. Li and Y. Chen, "Targeting long non-coding RNAs in cancers: progress and prospects," *International Journal of Biochemistry and Cell Biology*, vol. 45, no. 8, pp. 1895–1910, 2013.

[90] L. Ma, M.-S. Chua, O. Andrisani, and S. So, "Epigenetics in hepatocellular carcinoma: an update and future therapy perspectives," *World Journal of Gastroenterology*, vol. 20, no. 2, pp. 333–345, 2014.

[91] T. Gutschner, M. Hämmerle, and S. Diederichs, "MALAT1—a paradigm for long noncoding RNA function in cancer," *Journal of Molecular Medicine*, vol. 91, no. 7, pp. 791–801, 2013.

[92] F. Yang, J. Bi, X. Xue et al., "Up-regulated long non-coding RNA H19 contributes to proliferation of gastric cancer cells," *FEBS Journal*, vol. 279, no. 17, pp. 3159–3165, 2012.

[93] V. Tripathi, Z. Shen, A. Chakraborty et al., "Long noncoding RNA MALAT1 controls cell cycle progression by regulating the expression of oncogenic transcription factor B-MYB," *PLoS Genetics*, vol. 9, no. 3, Article ID e1003368, 2013.

[94] D. E. Ruffner, G. D. Stormo, and O. C. Uhlenbeck, "Sequence requirements of the hammerhead RNA self-cleavage reaction," *Biochemistry*, vol. 29, no. 47, pp. 10695–10702, 1990.

[95] J. Müller, O. El-Maarri, J. Oldenburg, B. Pötzsch, and G. Mayer, "Monitoring the progression of the in vitro selection of nucleic acid aptamers by denaturing high-performance liquid chromatography," *Analytical and Bioanalytical Chemistry*, vol. 390, no. 4, pp. 1033–1037, 2008.

[96] G. Kolb, S. Reigadas, D. Castanotto et al., "Endogenous expression of an anti-TAR aptamer reduces HIV-1 replication," *RNA Biology*, vol. 3, no. 4, pp. 150–156, 2006.

[97] M. Watrin, F. von Pelchrzim, E. Dausse, R. Schroeder, and J.-J. Toulmé, "In vitro selection of RNA aptamers derived from a genomic human library against the TAR RNA element of HIV-1," *Biochemistry*, vol. 48, no. 26, pp. 6278–6284, 2009.

[98] C. E. Lünse, G. Michlewski, C. S. Hopp et al., "An aptamer targeting the apical-loop domain modulates pri-miRNA processing," *Angewandte Chemie—International Edition*, vol. 49, no. 27, pp. 4674–4677, 2010.

[99] Y. Wu, Y. Xiao, X. Ding et al., "A mir-200b/200c/429-binding site polymorphism in the 3′ untranslated region of the AP-2α gene is associated with cisplatin resistance," *PLoS ONE*, vol. 6, no. 12, Article ID e29043, 2011.

[100] J. Wu, G. Wu, L. Lv et al., "MicroRNA-34a inhibits migration and invasion of colon cancer cells via targeting to Fra-1," *Carcinogenesis*, vol. 33, no. 3, pp. 519–528, 2012.

Hindawi Publishing Corporation
BioMed Research International
Volume 2015, Article ID 294213, 6 pages
http://dx.doi.org/10.1155/2015/294213

Review Article

Inverse Association between Prediagnostic IgE Levels and the Risk of Brain Tumors: A Systematic Review and Meta-Analysis

Chong Ma, Lei Cao, Jianping Zhao, Xing Ming, Ming Shang, Hailiang Zong, Hai Du, Kai Li, Xiaoguang He, and Hongsheng Xu

Department of Neurosurgery, Central Hospital of Xuzhou, Affiliated Hospital of Southeast University, Xuzhou, Jiangsu 221009, China

Correspondence should be addressed to Hongsheng Xu; hongshengxu@sohu.com

Received 16 July 2014; Revised 21 August 2014; Accepted 25 August 2014

Academic Editor: Aurelio Ariza

An inverse association between allergic conditions and glioma risk has been suggested in many epidemiological studies. However, the evidence is inadequate to draw robust conclusions for the association between prediagnostic IgE levels and brain tumors risk. The aim of this study was to provide more precise estimates for this association by meta-analysis of all published studies. Overall, 8 individual studies with 2,461 cases and 3,934 controls were included in our study. A decreased risk of brain tumors (RR = 0.73, 95% CI 0.61–0.86, $P < 0.001$) was observed in relation to elevated level of total IgE. The negative association was significant between elevated total IgE level and the risk of glioma (RR = 0.74, 95% CI 0.62–0.88, $P = 0.001$). However, no significant relationship was demonstrated between testing positive for respiratory allergen-specific IgE and brain tumors risk. In addition, the role of prediagnostic IgE levels in brain tumors risk did not alter in men and women. The present study suggests that increased level of total prediagnostic IgE but not respiratory allergen-specific IgE plays a protective role in brain tumors risk, glioma in particular. More studies are warranted for further elucidation of the meningioma risk related to prediagnostic IgE levels.

1. Introduction

Glioma and meningioma are two common primary brain tumors in adults [1]. Glioma is the most common type representing more than 80% of adult brain tumors [2]. Meningiomas are primarily benign tumors derived from meningothelial cells of the arachnoid membrane [3]. Ionizing radiation and genetic predisposition are well established risk factors for brain tumors [4–6]. However, little is known about the etiology of brain tumors.

The link between allergy and brain tumorigenesis is attracting much attention but remains largely unknown. Allergy is composed of eczema, hay fever, allergic asthma, and other heterogeneous diseases with complicated mechanisms. Some common allergies are characterized by immediate hypersensitivity reactions and mediated by immunoglobulin E (IgE) generated by B cells as well as T helper cells [7, 8]. IgE is a prediagnostic biomarker of allergy [9, 10]. Increased serum IgE is a powerful indication for allergic diseases. Both total serum IgE and allergen-specific IgE participate in the allergic response. Specific serum IgE is indicative of allergic sensitization to specific allergens of respiratory tract, food, or other origins. It is hypothesized that a highly active immune system leads to an enhanced tumor immune surveillance through recognizing and killing tumor cells. Whether prediagnostic IgE levels could modify the risk of brain tumors is currently unclear due to inconsistent and inconclusive findings in previous epidemiological studies. We aim to present more precise estimates for roles of prediagnostic total IgE and respiratory allergen-specific IgE levels in brain tumorigenesis by performing a meta-analysis of all published studies.

2. Materials and Methods

2.1. Search Strategy. A comprehensive literature search was performed in PubMed and Embase databases for eligible studies on the relationship between prediagnostic IgE levels and brain tumors risk. The last search was on June 26, 2014. The following terms were used: immunoglobulin E, IgE, total IgE level, respiratory allergen-specific IgE level, allergic

marker, or allergy and brain tumors, brain cancer, glioma, glioblastoma, or meningioma. The references of retrieved studies were also screened for other relevant articles. No language restriction was imposed.

2.2. Inclusion Criteria. Studies included into our study have to meet the following inclusion criteria: (1) studies on the relationship between prediagnostic IgE levels and brain tumors risk; (2) studies in case-control or cohort design; and (3) studies presenting odds ratio (ORs), relative risks (RRs), or hazard ratios (HRs) with corresponding 95% confidence intervals (95% CIs) for association estimates. Case-only design, case reports, systematic reviews, meta-analysis, animal studies, or studies with duplicated data were all excluded.

2.3. Data Extraction. Two investigators independently extracted data from each eligible study. The following information was extracted: name of first author, publication year, country of origin, characteristics of subjects, study design, type of brain tumors, number of cases and controls, matching criteria, study period, adjusted factors, RRs or HRs or ORs with 95% CIs for assessment of prediagnostic IgE levels, and type of brain tumors. Disagreements on all terms were resolved by discussion.

2.4. Statistical Analysis. The association between prediagnostic IgE levels and brain tumors risk was estimated by calculating the pooled RRs with 95% CIs. Cochran's Q-statistic test and I^2 test were performed to evaluate the between-study heterogeneity, and $P < 0.05$ plus $I^2 > 50\%$ implicated significant between-study heterogeneity among all included studies [11, 12]. The random-effects model by the DerSimonian and Laird method was adopted when the between-study heterogeneity was significant [13]; otherwise, the fixed-effects model by the method of Mantel-Haenszel was used [14]. Stratified analyses by gender and type of brain tumors were also performed. Sensitivity analysis by sequentially omitting single studies one at a time was also carried out to assess the association. Publication bias risk was estimated by Begg's funnel plots and Egger's test [15, 16]. All analyses were performed by use of STATA 12.0 software (StataCorp, College Station, TX, USA). $P < 0.05$ suggested statistical significance.

3. Results

3.1. Characteristics of Studies Included into the Present Meta-Analysis. After a comprehensive literature search, we identified 8 independent studies on the association between prediagnostic IgE levels and brain tumors risk with a total of 2,461 cases and 3,934 controls [17–23]. Table 1 summarized the characteristics of all included studies. The studies were published between 2004 and 2013, which were performed primarily in USA and some European countries including Norway. Among the 8 studies, 6 were about the risk of glioma related to prediagnostic IgE levels, while the other 2 were regarding the meningioma risk.

3.2. Association between Total IgE Level and Brain Tumors Risk. The pooled RRs showed that elevated level of total IgE was associated with a decreased risk of brain tumors (RR = 0.73; 95% CI 0.61–0.86; $P < 0.001$) (Table 2, Figure 1). Besides, elevated total IgE level was negatively related to the risk of glioma (RR = 0.74; 95% CI 0.62–0.88; $P = 0.001$) (Table 2). Sensitivity analysis did not materially alter the combined results (data not shown).

3.3. Association between Respiratory Allergen-Specific IgE Level and Brain Tumors Risk. No significant association was observed between testing positive for respiratory allergen-specific IgE and brain tumors risk (Table 2, Figure 2). Sensitivity analysis confirmed the pooled results (data not shown).

3.4. Stratified Analysis by Gender. As shown in Table 2, no significant relationship of prediagnostic IgE levels (total IgE level and respiratory allergen-specific IgE level) with the risk of overall brain tumors was demonstrated among either men or women. Additionally, the role of prediagnostic IgE levels in glioma development did not change by gender, as suggested by stratified analysis by type of brain tumors in men and women, respectively (Table 2).

3.5. Heterogeneity Analysis and Publication Bias Risk. Results of Cochran's Q-statistic test and I^2 test were presented in Table 2 detailedly. There was no between-study heterogeneity no matter in overall analysis or stratified analyses by type of brain tumors and gender (Table 2). Begg's funnel plots and Egger's test implicated no potential publication bias in our study (data not shown).

4. Discussion

Common allergies consist of eczema, hay fever, and allergic asthma mediated by hypersensitivity reactions and high serum IgE concentrations. However, not all allergic individuals are characteristic of high IgE levels, and increased level of serum IgE cannot reflect all allergic diseases. The modifying effects of prediagnostic IgE levels on diseases initiation and progression alter among different diseases. Epidemiological studies have suggested inverse association between allergic diseases and malignant tumors [10, 24]. Self-reported allergies were shown to be associated with reduced risk of pancreatic cancer [25]. Allergy seems to be strongly and inversely related to childhood non-Hodgkin's lymphomas, as suggested by a recent pooled analysis [26]. Taken together, hypersensitivity was associated with reduced risk of malignancies, implicating an immune surveillance theory in carcinogenesis. Quite the reverse, there was no epidemiological support for the reverse association between allergic diseases and the risk of breast, prostate, and colorectal cancer [27]. Interestingly, a positive relationship between atopy and prostate cancer, but not breast and colorectal cancers, was demonstrated in that study [27]. Thus, despite extensive research, findings for allergy conditions and tumorigenesis warrant further elucidation.

Table 1: Characteristics of all studies.

Study	Year	Brain tumors	Origins	Number of cases	Number of controls	Baseline time	Matching factors
Amirian et al. [17]	2013	Glioma	USA	362	462	2001–2006	Age, sex, and frequency
Schwartzbaum et al. [20]	2012	Glioma	Norway	594	1177	1974–2007	Date of blood collection, 2-year age interval at blood collection, and sex
Schlehofer et al. [19]	2011	Glioma	Europe	275	528	2002–2005	Study centre, gender, data of birth, age, date of blood collection, time of blood collection, and length of followup
Schlehofer et al. [19]	2011	Meningioma	Europe	175	343	2002–2005	Study centre, gender, data of birth, age, date of blood collection, time of blood collection, and length of followup
Calboli et al. [18]	2011	Glioma	USA	169	520	1976–2009	Age, age at blood draw, age at diagnosis, and ethnicity
Wiemels et al. [23]	2011	Meningioma	USA	265	145	2006–2009	Age, frequency, and state of residence
Wiemels et al. [22]	2009	Glioma	USA	393	470	2001–2004	Age, sex, ethnicity, and frequency
Wiemels et al. [21]	2004	Glioma	USA	228	289	1997–2000	Age, sex, ethnicity, and frequency

Table 2: Summary of meta-analysis results.

Comparisons	Number of studies	[a]RR [95% CI]	[b]P value	Tests for heterogeneity	
				I^2 (%)	[c]P
Total IgE level					
Brain tumors	6	0.73 [0.61–0.86]	<0.001	39.5	0.142
Men	2	0.83 [0.63–1.10]	0.202	0.0	0.602
Women	2	0.69 [0.43–1.11]	0.125	0.0	0.450
Glioma	5	0.74 [0.62–0.88]	0.001	50.6	0.088
Men	2	0.83 [0.63–1.10]	0.202	0.0	0.602
Women	2	0.69 [0.43–1.11]	0.125	0.0	0.450
Respiratory allergen-specific IgE level					
Brain tumors	6	0.88 [0.77–1.00]	0.055	0.0	0.527
Men	4	0.96 [0.78–1.19]	0.744	0.0	0.770
Women	4	0.87 [0.67–1.15]	0.331	51.6	0.103
Glioma	5	0.87 [0.76–1.00]	0.051	0.0	0.407
Men	3	0.99 [0.80–1.23]	0.923	0.0	0.878
Women	3	0.81 [0.59–1.10]	0.172	60.3	0.081

[a]RR: relative risk; 95% CI: 95% confidence interval; [b]P: P values for pooled analysis; [c]P: P values for heterogeneity analysis.

IgE is a critical atopic marker linking allergy and cancer. Jensen-Jarolim et al. elaborated an evolving new field called AllergoOncology, which gave new insights into the role of IgE-mediated allergy in malignancies [28]. Due to its capacity of destroying tumor cells, IgE antibodies specifically targeting overexpressed tumor antigens have been identified as useful immunological agents. Besides, IgE nonspecifically binding to tumor cells has also been demonstrated to be a powerful adjuvant establishing tumor-specific immune memory [29, 30]. Moreover, IgE antibodies not only play critical roles in natural tumor surveillance, but also participate in active and adaptive immune responses involved in antitumor immunotherapy [28]. Additionally, macrophages, mast cells, and other IgE-receptor-expressed immune cells can become potent effectors in antitumor immunity by the bridge IgE. A number of epidemiological studies have been performed to estimate the association between prediagnostic IgE levels and brain tumors risk [17–23]. Nevertheless, the findings were inconsistent and inconclusive. Calboli et al. reported that total IgE levels were inversely associated with glioma risk [18].

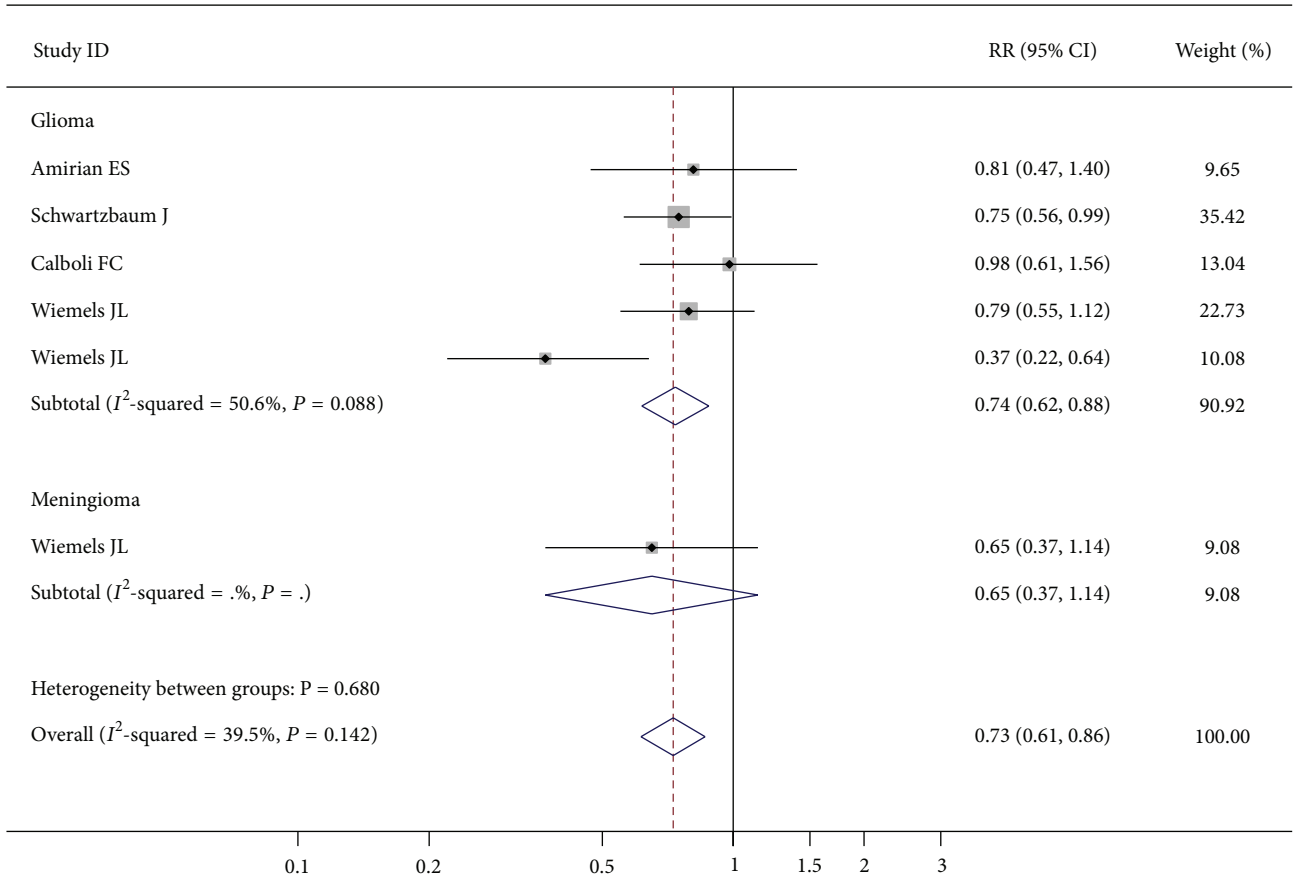

Figure 1: Forest plot for total IgE level and brain tumors risk.

However, no such association was observed for either respiratory allergen-specific or food allergen-specific IgE levels [18]. On the contrary, individuals with high levels of respiratory allergen-specific IgE were at decreased risk of glioma, but not meningioma [19]. As suggested by the study by Wiemels et al., increased serum total IgE concentrations were negatively related to the development of meningioma, indicating a protective role of atopic marker IgE in meningioma risk [23]. Taken together, the modifying effect of serum IgE level on brain tumors risk appears different with diverse types of brain cancer and the source of determined IgE. Up till now, no meta-analysis has been conducted to precisely estimate roles of prediagnostic IgE levels (total IgE level and/or allergen-specific IgE level) in brain tumorigenesis. A recent meta-analysis supported the evidence that allergic conditions were negatively related to the risk of glioma, suggesting a protective role of allergy in glioma development [31]. Nonetheless, the authors failed to assess the influence of specific allergies such as hay fever, eczema as well as allergic asthma, and allergic biomarker IgE in brain cancer risk. The association between different source of serum IgE and brain tumors risk, meningioma in particular, remains obscure and warrants further investigation. Our study firstly showed that increased level of total prediagnostic IgE but not respiratory allergen-specific IgE played a protective role in the risk of brain tumors, particularly glioma. It must be mentioned that the relationship of meningioma risk with prediagnostic IgE levels needs to be elucidated by more relevant epidemiological studies.

SNPs are supported to be important risk factors in brain tumorigenesis [5, 6, 32]. They can confer modifying effects on brain tumors risk independently or in combination with other factors, for instance, smoking and ionizing radiation. Interestingly, allergy-related SNPs can influence the development of brain tumors by interacting with immunological factors like prediagnostic IgE levels, which implicates critical roles of immune susceptibility factors in the etiology of brain cancers [32]. Gene polymorphisms of IL-4, IL-4R, and IL-13 represent promising immune factors in regulating IgE levels and tumorigenesis [32–34]. Unfortunately, we failed to investigate roles of such allergy-related SNPs in brain cancer risk in combination with prediagnostic IgE levels, in that very few studies have elucidated this issue up to date. The interaction between SNPs and serum IgE levels warrants further investigation to provide more support for the link between allergies and risk of brain tumors.

Findings in our study should be interpreted cautiously because of some limitations. Firstly, the strength of our study especially in relation to the meningioma risk was insufficient due to limited eligible studies published to date. Besides, only studies clearly presenting information about the detection of prediagnostic IgE levels were included into our study. More

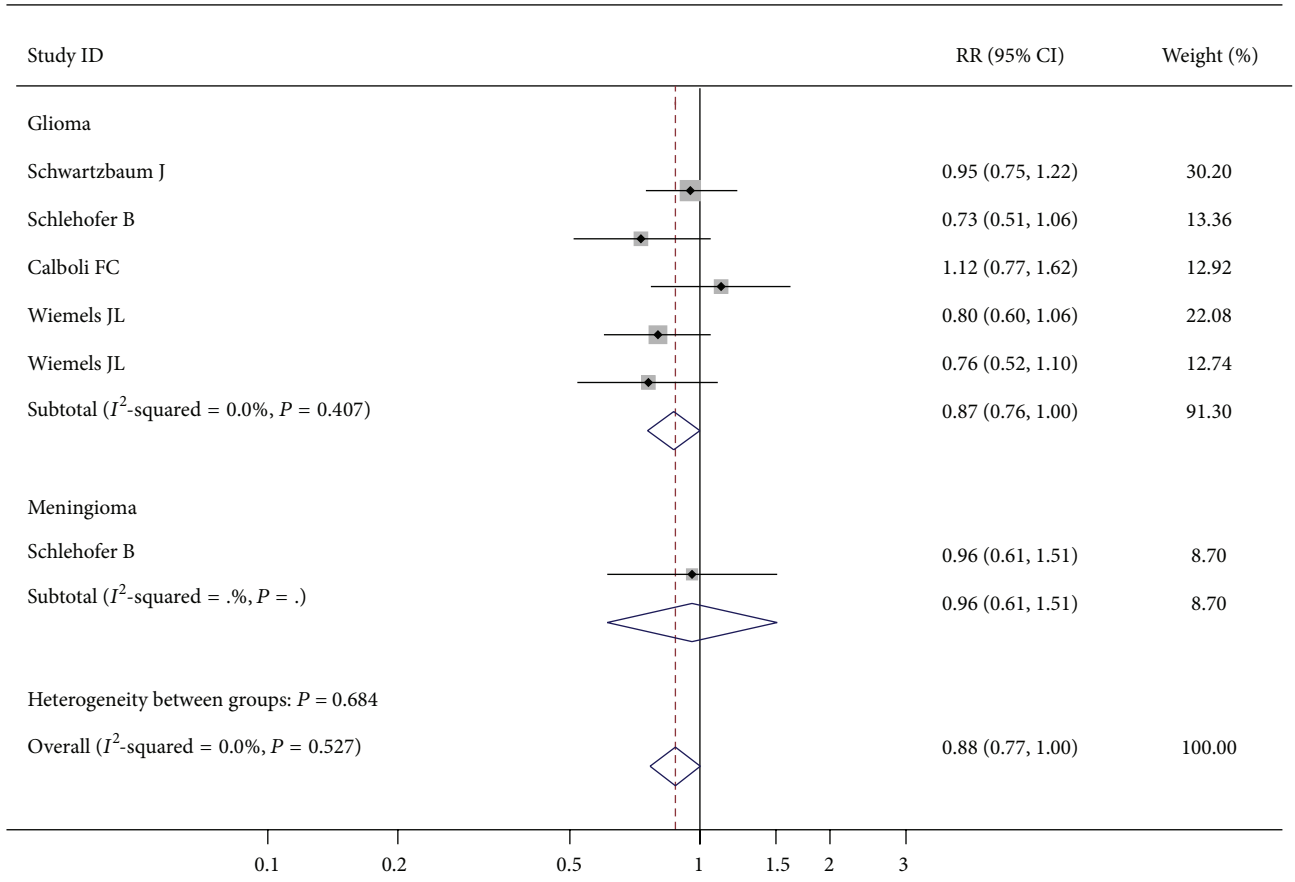

Figure 2: Forest plot for respiratory allergen-specific IgE level and brain tumors risk.

relevant studies with enough statistical power are encouraged in the future. Secondly, IgE levels were significantly associated with gender, age, smoking status, and ethnicity in glioma risk [21]. Apart from gender and type of brain tumors, we did not perform other stratified analyses by smoking, age, and so on, for lack of available published data. More studies with high quality are warranted for more precise estimates. Thirdly, inverse association was identified between elevated respiratory allergen-specific IgE level and high-grade glioma risk rather than low-grade glioma [19]. The effect of prediagnostic IgE levels on different subtypes of glioma was not estimated due to insufficient included publications. Lastly, the pooled analysis was based on unadjusted estimates, which might introduce bias. Some confounding factors including age, sex, IgE detection methods, smoking status, and education level of subjects should be considered in future studies.

5. Conclusions

A significant inverse association between total IgE levels and brain tumors risk is suggested in the present meta-analysis. The measurement of allergic biomarker IgE is valuable in targeting brain tumors, particularly glioma. In addition, the association between prediagnostic IgE levels and meningioma risk warrants further investigation. The study implicates that IgE monoclonal antibodies directing specifically against tumor-associated antigens can be a promising way of passive immunotherapy in brain cancer treatment.

Conflict of Interests

There was no conflict of interests to declare.

Authors' Contribution

Chong Ma and Lei Cao contributed equally to this work.

References

[1] Q. T. Ostrom, H. Gittleman, P. Farah et al., "CBTRUS statistical report: Primary brain and central nervous system tumors diagnosed in the United States in 2006–2010," *Neuro-Oncology*, vol. 15, supplement 2, pp. ii1–ii56, 2013.

[2] H. Ohgaki and P. Kleihues, "Epidemiology and etiology of gliomas," *Acta Neuropathologica*, vol. 109, no. 1, pp. 93–108, 2005.

[3] S. Saraf, B. J. McCarthy, and J. L. Villano, "Update on meningiomas," *The Oncologist*, vol. 16, no. 11, pp. 1604–1613, 2011.

[4] Q. T. Ostrom and J. S. Barnholtz-Sloan, "Current state of our knowledge on brain tumor epidemiology," *Current Neurology and Neuroscience Reports*, vol. 11, no. 3, pp. 329–335, 2011.

[5] J. Guo, L. Shi, M. Li et al., "Association of the interleukin-4Rα rs1801275 and rs1805015 polymorphisms with glioma risk," *Tumor Biology*, vol. 35, no. 1, pp. 573–579, 2014.

[6] H. Zong, L. Cao, C. Ma et al., "Association between the G870A polymorphism of Cyclin D1 gene and glioma risk," *Tumour Biology*, 2014.

[7] R. G. Hamilton, D. W. MacGlashan Jr., and S. S. Saini, "IgE antibody-specific activity in human allergic disease," *Immunologic Research*, vol. 47, no. 1–3, pp. 273–284, 2010.

[8] W. E. Paul and J. Zhu, "How are T(H)2-type immune responses initiated and amplified?" *Nature Reviews Immunology*, vol. 10, no. 4, pp. 225–235, 2010.

[9] D. H. Josephs, J. F. Spicer, C. J. Corrigan, H. J. Gould, and S. N. Karagiannis, "Epidemiological associations of allergy, IgE and cancer," *Clinical and Experimental Allergy*, vol. 43, no. 10, pp. 1110–1123, 2013.

[10] M. C. Turner, "Epidemiology: allergy history, IgE, and cancer," *Cancer Immunology, Immunotherapy*, vol. 61, no. 9, pp. 1493–1510, 2012.

[11] W. G. Cochran, "The comparison of percentages in matched samples," *Biometrika*, vol. 37, no. 3-4, pp. 256–266, 1950.

[12] J. P. T. Higgins, S. G. Thompson, J. J. Deeks, and D. G. Altman, "Measuring inconsistency in meta-analyses," *British Medical Journal*, vol. 327, no. 7414, pp. 557–560, 2003.

[13] R. DerSimonian and N. Laird, "Meta-analysis in clinical trials," *Controlled Clinical Trials*, vol. 7, no. 3, pp. 177–188, 1986.

[14] N. Mantel and W. Haenszel, "Statistical aspects of the analysis of data from retrospective studies of disease," *Journal of the National Cancer Institute*, vol. 22, no. 4, pp. 719–748, 1959.

[15] M. Egger, G. D. Smith, M. Schneider, and C. Minder, "Bias in meta-analysis detected by a simple, graphical test," *British Medical Journal*, vol. 315, no. 7109, pp. 629–634, 1997.

[16] A. E. Stuck, L. Z. Rubenstein, and D. Wieland, "Bias in meta-analysis detected by a simple, graphical test. Asymmetry detected in funnel plot was probably due to true heterogeneity," *British Medical Journal*, vol. 316, no. 7129, pp. 469–471, 1998.

[17] E. S. Amirian, D. Marquez-Do, M. L. Bondy, and M. E. Scheurer, "Antihistamine use and immunoglobulin E levels in glioma risk and prognosis," *Cancer Epidemiology*, vol. 37, no. 6, pp. 908–912, 2013.

[18] F. C. F. Calboli, D. G. Cox, J. E. Buring et al., "Prediagnostic plasma IgE levels and risk of adult glioma in four prospective cohort studies," *Journal of the National Cancer Institute*, vol. 103, no. 21, pp. 1588–1595, 2011.

[19] B. Schlehofer, B. Siegmund, J. Linseisen et al., "Primary brain tumours and specific serum immunoglobulin E: a case-control study nested in the European prospective investigation into cancer and nutrition cohort," *Allergy*, vol. 66, no. 11, pp. 1434–1441, 2011.

[20] J. Schwartzbaum, B. Ding, T. B. Johannesen et al., "Association between prediagnostic IgE levels and risk of glioma," *Journal of the National Cancer Institute*, vol. 104, no. 16, pp. 1251–1259, 2012.

[21] J. L. Wiemels, J. K. Wiencke, J. Patoka et al., "Reduced immunoglobulin E and allergy among adults with glioma compared with controls," *Cancer Research*, vol. 64, no. 22, pp. 8468–8473, 2004.

[22] J. L. Wiemels, D. Wilson, C. Patil et al., "IgE, allergy, and risk of glioma: update from the San Francisco Bay Area Adult Glioma Study in the temozolomide era," *International Journal of Cancer*, vol. 125, no. 3, pp. 680–687, 2009.

[23] J. L. Wiemels, M. Wrensch, J. D. Sison et al., "Reduced allergy and immunoglobulin e among adults with intracranial meningioma compared to controls," *International Journal of Cancer*, vol. 129, no. 8, pp. 1932–1939, 2011.

[24] D. Rittmeyer and A. Lorentz, "Relationship between allergy and cancer: an overview," *International Archives of Allergy and Immunology*, vol. 159, no. 3, pp. 216–225, 2012.

[25] S. H. Olson, M. Hsu, J. L. Wiemels et al., "Serum immunoglobuline and risk of pancreatic cancer in the prostate, lung, colorectal, and ovarian cancer screening trial," *Cancer Epidemiology, Biomarkers & Prevention*, vol. 23, no. 7, pp. 1414–1420, 2014.

[26] S. K. Dikalioti, E. T. Chang, N. Dessypris et al., "Allergy-associated symptoms in relation to childhood non-Hodgkin's as contrasted to Hodgkin's lymphomas: a case-control study in Greece and meta-analysis," *European Journal of Cancer*, vol. 48, no. 12, pp. 1860–1866, 2012.

[27] P. Vojtechova and R. M. Martin, "The association of atopic diseases with breast, prostate, and colorectal cancers: a meta-analysis," *Cancer Causes and Control*, vol. 20, no. 7, pp. 1091–1105, 2009.

[28] E. Jensen-Jarolim, G. Achatz, M. C. Turner et al., "AllergoOncology: the role of IgE-mediated allergy in cancer," *Allergy*, vol. 63, no. 10, pp. 1255–1266, 2008.

[29] S. N. Karagiannis, D. H. Josephs, P. Karagiannis et al., "Recombinant IgE antibodies for passive immunotherapy of solid tumours: From concept towards clinical application," *Cancer Immunology, Immunotherapy*, vol. 61, no. 9, pp. 1547–1564, 2012.

[30] J. Singer and E. Jensen-Jarolim, "IgE-based immunotherapy of cancer: challenges and chances," *Allergy*, vol. 69, no. 2, pp. 137–149, 2014.

[31] H. Zhao, W. Cai, S. Su, D. Zhi, J. Lu, and S. Liu, "Allergic conditions reduce the risk of glioma: a meta-analysis based on 128,936 subjects," *Tumor Biology*, vol. 35, no. 4, pp. 3875–3880, 2014.

[32] J. L. Wiemels, J. K. Wiencke, K. T. Kelsey et al., "Allergy-related polymorphisms influence glioma status and serum IgE levels," *Cancer Epidemiology Biomarkers and Prevention*, vol. 16, no. 6, pp. 1229–1235, 2007.

[33] T. D. Howard, G. H. Koppelman, J. Xu et al., "Gene-gene interaction in asthma: Il4ra and il13 in a dutch population with asthma," *The American Journal of Human Genetics*, vol. 70, no. 1, pp. 230–236, 2002.

[34] D. M. Backes, A. Siddiq, D. G. Cox et al., "Single-nucleotide polymorphisms of allergy-related genes and risk of adult glioma," *Journal of Neuro-Oncology*, vol. 113, no. 2, pp. 229–238, 2013.

Hindawi Publishing Corporation
BioMed Research International
Volume 2015, Article ID 209745, 9 pages
http://dx.doi.org/10.1155/2015/209745

Research Article

Plasma Protein Biomarker Candidates for Myelodysplastic Syndrome Subgroups

Pavel Majek,[1] Klara Pecankova,[1] Jaroslav Cermak,[2] and Jan E. Dyr[1]

[1]*Department of Biochemistry, Institute of Hematology and Blood Transfusion, U Nemocnice 1, 128 20 Prague 2, Czech Republic*
[2]*Clinical Department, Institute of Hematology and Blood Transfusion, U Nemocnice 1, 128 20 Prague 2, Czech Republic*

Correspondence should be addressed to Pavel Majek; pavel.majek@uhkt.cz

Received 31 August 2014; Revised 19 December 2014; Accepted 13 January 2015

Academic Editor: Konstantinos Arnaoutakis

In recent years the plasma proteomes of several different myelodysplastic syndrome (MDS) subgroups have been investigated and compared with those of healthy donors. However, the resulting data do not facilitate a direct and statistical comparison of the changes among the different MDS subgroups that would be useful for the selection and proposal of diagnostic biomarker candidates. The aim of this work was to identify plasma protein biomarker candidates for different MDS subgroups by reanalyzing the proteomic data of four MDS subgroups: refractory cytopenia with multilineage dysplasia (RCMD), refractory anemia or refractory anemia with ringed sideroblasts (RA-RARS), refractory anemia with excess blasts subtype 1 (RAEB-1), and refractory anemia with excess blasts subtype 2 (RAEB-2). Reanalysis of a total of 47 MDS patients revealed biomarker candidates, with alpha-2-HS-glycoprotein and leucine-rich alpha-2-glycoprotein as the most promising candidates.

1. Introduction

Myelodysplastic syndrome (MDS) is a group of heterogeneous oncohematological bone marrow disorders characterized by peripheral blood cytopenias, ineffective hematopoiesis, bone marrow hypercellularity, and so forth [1]. MDS classification covers a range from low-risk subgroups with good patient outlook and survival, to high-risk subgroups characterized by a progression of the disease toward acute myeloid leukemia and a poor outcome [2, 3]. The molecular mechanisms that lead to the genesis of MDS and its development are not yet fully understood. Moreover, our knowledge of the changes occurring in MDS remains limited. Some findings at the DNA (chromosomal aberrations [4], up- or downregulation of genes [5], DNA methylation changes [6], single nucleotide polymorphisms [7], etc.) and RNA levels (altered expression of microRNAs in CD34+ cells [8, 9]) have been observed; however, there is a lack of detailed characterization of the changes at the protein level. Protein changes, whether in protein levels or posttranslational modifications, are expected to play a crucial role in the modern diagnostic toolkit. Considerable effort has been expended in the preparation of such tools in recent years (from the studies of plasma protein interactions with antifouling surfaces [10] to the preparation of low- or even nonfouling surfaces suitable for biochip construction [11, 12]); the topic of clinical applications in oncohematology has been reviewed by Fracchiolla et al. [13]; however, the first step has to be the identification of protein biomarker candidates. In our previous studies, we used a proteomic approach to investigate plasma proteome changes in the different MDS subgroups, covering the range from low- to high-risk subgroups: refractory cytopenia with multilineage dysplasia [14], refractory anemia with excess blasts subtype 1 [15], refractory anemia and refractory anemia with ringed sideroblasts [16], and refractory anemia with excess blasts subtype 2 [17]. Several proteins were proposed as potential biomarkers of different MDS subgroups in comparison with control groups of healthy donors. Although the control group study designs were kept similar to maintain consistency in the interpretation of the results and to facilitate comparison of the changes among the different MDS subgroups, only rough estimation may be obtained on this basis. Moreover, some criteria (statistical significance) cannot be estimated by this method

at all. Therefore, the goal of this work was to reanalyze the data from our four proteomic studies of different MDS subgroups in order to evaluate the protein biomarker candidates of these different MDS subgroups.

2. Methods

In this work, the data from four previous proteomic studies of different MDS subgroups has been reanalyzed: refractory cytopenia with multilineage dysplasia [14], refractory anemia with excess blasts subtype 1 [15], refractory anemia and refractory anemia with ringed sideroblasts [16], and refractory anemia with excess blasts subtype 2 [17]; only patient data (no healthy control donors) were used. There were 47 myelodysplastic syndrome patients: 22 patients with refractory cytopenia with multilineage dysplasia (RCMD), 10 patients with refractory anemia or refractory anemia with ringed sideroblasts (RA-RARS), 7 patients with refractory anemia with excess blasts subtype 1 (RAEB-1), and 8 patients with refractory anemia with excess blasts subtype 2 (RAEB-2). The median of age was 57, 71.5, 68, and 63.5 years, and the patient make-up was 50%, 40%, 57%, and 38% male in RCMD, RA-RARS, RAEB-1, and RAEB-2, respectively. Patients' characteristics are summarized in Table 1. Diagnoses were established according to the WHO classification criteria [2]. All individuals tested agreed to participate in the study on the basis of an informed consent. All samples were obtained and analyzed in accordance with the Ethical Committee regulations of the Institute of Hematology and Blood Transfusion in Prague.

Scanned gel images obtained from our previous four proteomic studies were used in this study; blood collection, sample preparation, high-abundance plasma protein depletion, 2D SDS-PAGE protein separation, protein visualization, and gel digitization have been described in detail [14, 18]. Digitized gel images were processed with Progenesis SameSpots software (Nonlinear Dynamics, Newcastle upon Tyne, UK); images were divided into four groups according to MDS diagnoses, and the fold and P values of all spots were computed by the software using one-way ANOVA analysis. Protein identification was performed for spots (proteins within the spots) that were not submitted for protein identification in the previous studies. An HCT ultra ion-trap mass spectrometer with nanoelectrospray ionization (Bruker Daltonics, Bremen, Germany) coupled to a nanoLC system UltiMate 3000 (Dionex, Sunnydale, CA, USA) was used to perform MS analysis. Mascot (Matrix Science, London, UK) was used for database searching (Swiss-Prot). Two unique peptides (with a higher Mascot score than the minimum for identification, $P < 0.05$) were necessary to identify a protein. The procedure was described in detail previously [18]. Western blot analysis was performed as previously described in detail [19]. Briefly, 6 samples (3 males and 3 females) were used for each MDS subgroup as a pooled sample. Proteins of pooled samples were precipitated with acetone, protein pellets were diluted in a sample buffer, and SDS-PAGE was performed, followed by protein transfer to a PVDF membrane. The following primary antibodies were used: monoclonal mouse anti-leucine-rich alpha-2-glycoprotein (ab57992), 1 : 400 (Abcam, Cambridge, UK); monoclonal mouse antialbumin (A6684), 1 : 2000 (Sigma-Aldrich, Prague, Czech Republic); polyclonal rabbit anti-alpha-2-HS-glycoprotein (ab112528), 1 : 1000 (Abcam); and polyclonal mouse antiapolipoprotein A-I (H00000335-B01P), 1 : 1000 (Abnova, Taipei, Taiwan). The following secondary antibodies were utilized: rabbit anti-mouse IgG antibody conjugated with peroxidase (A9044), 1 : 80000 (Sigma-Aldrich) and goat anti-rabbit IgG antibody conjugated with peroxidase (A0545), 1 : 80000 (Sigma-Aldrich). Protein bands were visualized using a 1-Step Ultra TMB-Blotting Solution (Thermo Scientific, Waltham, MA, USA).

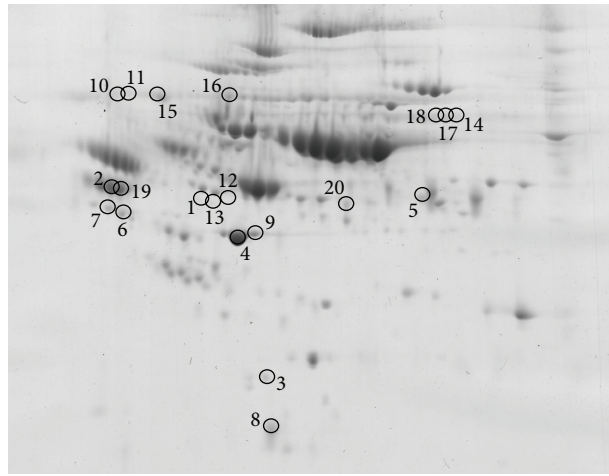

Figure 1: Positions of the spots. Positions of the spots with identified proteins were displayed on an illustrative 2D gel of a patient sample. For better clarity the gel image is shown as highlighted by brightness and contrast image adjustment.

3. Results and Discussion

The aim of this work was to evaluate plasma protein biomarker candidates of myelodysplastic syndrome subgroups by reanalyzing previously published proteomic data to allow direct and statistical comparisons. In order to select the most promising protein candidates, a two-step selection process was applied. In the first step, all four MDS subgroups were compared together and spots that were found to significantly differ (ANOVA $P < 0.05$) among the groups were selected; 42 different spots were found. In the second step, all the groups were compared mutually (each to each other), and the only spots selected in the first step were considered. In order to maintain the same level of significance, a Bonferroni correction was applied in the second step selection [20]. Therefore, the P value threshold for the second step comparison was lowered to $P < 0.00833$. As an additional criterion, only spots with at least a 50% change of their normalized spot volumes were accepted. There were then 23 different spots found which satisfied these criteria; proteins in 20 spots (Figure 1) were identified by mass spectrometry. The numbers of spots that were found to differ between the compared

Table 1: Patients' characteristics.

Patient	Sex	Age	Diagnosis	Karyotype	WBC [10^9/L]	PLT [10^9/L]	Blasts in PB [%]	NS [%]	IPSS	IPSS-R
1	f	21	RCMD	46, XX	3.51	31	0	22.9	Good	Very good
2	f	24	RCMD	46, XX	4.79	238	0	52	Good	Very good
3	f	29	RCMD	46, XX	3.93	19	0	27	Good	Very good
4	m	29	RCMD	46, XY-polyploidy	3.81	50	0	73	Good	Very good
5	f	30	RCMD	46, XX	2.53	134	0	36	Good	Very good
6	m	30	RCMD	46, XY	7.96	107	0	69	Good	Very good
7	m	49	RAEB2	46, XY	4.34	15	3	23	Good	Very good
8	f	50	RA	46, XX	3.64	184	0	59	Good	Very good
9	f	50	RCMD	46, XX, inv(9)	1.81	108	0	48	Intermediate	Intermediate
10	f	51	RCMD	46, XX, 9qh+	3.80	20	0	58	Intermediate	Intermediate
11	m	55	RCMD	46, XY	2.19	236	0	25	Good	Very good
12	f	56	RCMD	46, XX	3.90	129	0	39	Good	Very good
13	f	56	RCMD	46, XX	4.15	211	0	71	Good	Very good
14	m	58	RAEB1	45, XY, −18, multiple aberrations	1.26	28	0	30	Poor	Very poor
15	f	58	RAEB2	42~47, XX, del(5)(q?), −7, +8, der(12)t(7; 12)(?; p?13)ins(12; 7)(q?12; ?)ins(12; 7)(q?13; ?), der(17)t(17; 20)(p11.2; ?)	1.57	310	5.2	43.2	Poor	Very poor
16	m	58	RCMD	46, XY −46, XY, del(20)(q12)	2.00	211	0	56	Good	Good
17	m	58	RCMD	46, XY	2.48	153	0	55	Good	Very good
18	m	59	RAEB2	46, XY −43~44, XY, multiple changes	2.30	110	14	18	Poor	Very poor
19	m	59	RCMD	46, XY	2.81	103	0	50	Good	Very good
20	f	60	RA	46, XX	7.41	149	0	60	Good	Very good
21	m	60	RAEB1	46, XY	0.65	88	0	34	Good	Very good
22	f	60	RAEB2	46, XX	5.36	39	11	46	Good	Very good
23	m	61	RARS	46, XY	5.84	218	0	67	Good	Very good
24	m	62	RCMD	46, XY −45, X, −Y	6.82	89	0	65	Good	Very good
25	f	62	RCMD	46, XX	2.58	28	0	51	Good	Very good
26	m	62	RCMD	46, XY	4.49	56	0	61	Good	Very good
27	f	63	RA	46, XX −46, XX, del(5)(q13q13)	3.54	146	0	52	Good	Good
28	f	64	RAEB1	46, XX, t(2; 12)(p22; q13)	5.91	121	1	44	Intermediate	Intermediate
29	f	65	RA	46, XX −46, XX, del(5)(q15q33)	3.20	192	1	29	Good	Good
30	m	65	RCMD	46, XY −43~46, XY, der(2)t(2; 12)(q37; ?), del(11)(q13)	2.93	297	0	43	Poor	Very poor
31	m	66	RCMD	46, XY, 21ps+	6.74	81	0	52	Intermediate	Intermediate
32	f	66	RCMD	46, XX	2.79	16	0	84.3	Good	Very good
33	f	67	RAEB2	—	3.93	22	14	28	—	—
34	f	68	RAEB1	46, XX −46, XX, del(5)(q22q33)	3.80	412	0	50	Good	Good
35	m	68	RCMD	46, XY −45, X, −Y	19.94	399	3	51	Good	Very good
36	f	70	RAEB1	46, XX	1.13	150	0	46	Good	Very good
37	m	70	RAEB2	5q31 deletion (8 of 11 tests)	3.70	156	8	73	Good	Good
38	m	71	RAEB1	46, XY	4.25	85	3	17	Good	Very good
39	m	71	RAEB1	46, XY	1.39	21	0	20	Good	Very good
40	f	72	RCMD	46, XX, del(5)(q13.3q33.3)	4.18	119	0	47	Good	Good
41	f	76	RAEB2	47–51, XX-multiple changes	1.52	8	2	42	Poor	Very poor

Table 1: Continued.

Patient	Sex	Age	Diagnosis	Karyotype	WBC [10^9/L]	PLT [10^9/L]	Blasts in PB [%]	NS [%]	IPSS	IPSS-R
42	m	78	RA	46, XY	8.65	162	0	75	Good	Very good
43	f	78	RA	46, XX, del(5)(q13q33)	3.77	288	0	67	Good	Good
44	m	78	RA	46, XY	5.36	243	1	68	Good	Very good
45	f	79	RAEB2	46, XX -46, XX, del(5)(q13q33)	0.43	6	38	8	Good	Good
46	f	86	RARS	46, XX	8.86	375	0	55	Good	Very good
47	m	89	RARS	46, XY	6.44	155	0	40	Good	Very good

WBC: white blood cells; PLT: platelets; PB: peripheral blood; NS: neutrophil segments.

Table 2: The numbers of spots found to differ between the compared pairs of MDS subgroups.

	RCMD	RA-RARS	RAEB-1	RAEB-2
RCMD	—	—	—	—
RA-RARS	6	—	—	—
RAEB-1	11	0	—	—
RAEB-2	6	5	0	—

Table 3: Brief characterization of the identified spots.

RCMD versus RA-RARS					
Increase in RCMD			Increase in RA-RARS		
Spot	*P*	*r*	Spot	*P*	*r*
8	0.00117	1.6	3	0.00002	2.3
15	0.00061	1.7	14	0.00534	1.6
—	—	—	17	0.00107	1.6
—	—	—	18	0.00093	1.6
RCMD versus RAEB-1					
Increase in RCMD			Increase in RAEB-1		
Spot	*P*	*r*	Spot	*P*	*r*
2	0.0032	1.8	1	0.00074	6.4
5	0.00382	1.6	12	0.00177	4.7
8	0.00011	2.0	13	0.00232	5.2
19	0.00124	1.6	14	0.00093	1.7
20	0.0035	1.5	16	0.00274	1.7
—	—	—	18	0.00519	1.6
RCMD versus RAEB-2					
Increase in RCMD			Increase in RAEB-2		
Spot	*P*	*r*	Spot	*P*	*r*
8	0.00392	1.6	6	0.00787	1.6
9	0.00335	1.6	7	0.00525	1.7
—	—	—	10	0.00659	1.6
—	—	—	18	0.00701	1.6
RA-RARS versus RAEB-2					
Increase in RA-RARS			Increase in RAEB-2		
Spot	*P*	*r*	Spot	*P*	*r*
3	0.00538	2.1	10	0.00435	1.8
4	0.00348	1.5	11	0.00104	1.6
9	0.00008	1.8	—	—	—

P: *t*-test *P* value, *r*: fold change value.

pairs of MDS subgroups are summarized in Table 2. A brief characterization of these spots (*P* value and the relative change between the groups) with regard to the compared pairs of MDS subgroups is shown in Table 3. Identification of the proteins, together with the number of unique identified peptides, accession numbers, and protein sequence coverage, is summarized in Table 4. From the results in Table 2 there is no direct correlation between the number of differences and the severity of the subgroups. Although the patient cohort is relatively small, the results support the notion proposed in our previous studies that "a degree of change" is the principal factor affecting proteome alterations observed for different MDS subgroups [16, 17]. Therefore, when protein posttranslational modifications are taken into consideration, it is not surprising that several proteins found to differ in this work were also identified to differentiate between MDS subgroups and the healthy control groups: alpha-2-HS-glycoprotein, leucine-rich alpha-2-glycoprotein, retinol-binding protein 4, hemopexin, apolipoprotein A-I, and so forth. These observations suggest that it is unlikely to find a single protein as a diagnostic MDS biomarker when only considering its plasma level change. However, finding a single protein biomarker with respect to its plasma level change can be possible for potential prognostic MDS biomarkers, as previously indicated for alpha-2-HS-glycoprotein [16, 17]. This protein seemed to decrease its plasma level relative to the severity of the MDS subgroups studied; and moreover, it was also shown that its plasma level decrease reflected the degree of malignancy found in other different tumor types [21].

In order to estimate whether the changes determined by 2D SDS-PAGE reflect the plasma level changes or posttranslational modifications of proteins, we performed western blot analysis for the selected proteins. Alpha-2-HS-glycoprotein and leucine-rich alpha-2-glycoprotein were selected as previously proposed MDS biomarker candidates (differentiating MDS subgroups from healthy controls), as well as due to their possible role in MDS pathophysiology as previously described in detail in [16] and [15], respectively. Apolipoprotein A1 was selected as it was identified in all four of the MDS subgroups studied and because it has been observed to form posttranslationally modified isoforms in cardiovascular disease patients [19, 22]. Serum albumin was selected as a control protein of the acute phase reaction to reflect a possible inflammation influence. Our findings are illustrated in Figure 2.

Western blotting of alpha-2-HS-glycoprotein showed several bands of approximately 50 kDa with a trend of decreasing intensity in advanced MDS subgroups. This result is in agreement with our electrophoretic data; however, it is apparent from the western blot that the representation of individual bands differs more substantially relative to total protein levels. The most obvious change can be observed for the bottom band, whose intensity increases substantially in the RAEB-1 subgroup. This supports the need for precise characterization of A2HSG posttranslational modifications and their quantification. Western blot analysis of leucine-rich alpha-2-glycoprotein revealed two bands of approximately 48 and 60 kDa. The lower 48 kDa band corresponds to that identified in 2D electrophoresis and shows the trend of increasing its intensity in advanced MDS subgroups. This is in agreement with the data obtained by 2D electrophoresis. As in the case of alpha-2-HS-glycoprotein, the modifications need to be characterized. Apolipoprotein A1 was shown to increase the spot volume in RA-RARS compared to RCMD and RAEB-2. It is clear from the western blot that the highest intensities were observed for both the RA-RARS and RAEB-1 subgroups. The fact that the changes were found for RA-RARS by 2D electrophoresis and not for RAEB-1 was most probably caused by the low number of RAEB-1 samples. No obvious changes were observed for albumin; therefore, we assume a minimal influence of the acute phase reaction on the results. Nevertheless, it has been recently shown that there are many other factors (genetic, clinical, or lifestyle factors) that

Table 4: Protein identification.

Spot	Protein identification	Peptides	AN	SC (%)
1	Alpha-1-antitrypsin	12	P01009	38
2	Alpha-2-HS-glycoprotein	2	P02765	13
3	Apolipoprotein A-I	6	P02647	25
4	Apolipoprotein A-IV	10	P06727	44
5	Hemopexin	3	P02790	11
6	Leucine-rich alpha-2-glycoprotein	4	P02750	23
7	Leucine-rich alpha-2-glycoprotein	3	P02750	18
8	Retinol-binding protein 4	2	P02753	16
9	Actin, cytoplasmic 1; 2	4; 4	P60709; P63261	22; 22
	Apolipoprotein A-IV	5	P06727	21
10	Alpha-1-antichymotrypsin	6	P01011	23
	Plasma protease C1 inhibitor	4	P05155	13
11	Alpha-1-antichymotrypsin	4	P01011	14
	Plasma protease C1 inhibitor	4	P05155	18
12	Alpha-1-antitrypsin	10	P01009	29
	Antithrombin-III	2	P01008	8
13	Alpha-1-antitrypsin	9	P01009	28
	Antithrombin-III	2	P01008	8
14	Ig mu chain C region	2	P01871	17
	Prothrombin	3	P00734	20
15	Plasma protease C1 inhibitor	3	P05155	13
	Alpha-1-antichymotrypsin	2	P01011	10
16	Alpha-1-antitrypsin	3	P01009	24
	Prothrombin	4	P00734	24
	Complement C4-A; B	4	P0C0L4; P0C0L5	4
17	Prothrombin	3	P00734	25
	Serum albumin	3	P02768	11
	Ig mu chain C region	2	P01871	13
18	Serum albumin	3	P02768	8
	Ig mu chain C region	2	P01871	19
	Prothrombin	3	P00734	27
19	Alpha-1-antichymotrypsin	3	P01011	11
	Alpha-2-HS-glycoprotein	2	P02765	9
	Kininogen-1	3	P01042	8
	Corticosteroid-binding globulin	2	P08185	14
20	Pigment epithelium-derived factor	4	P36955	16
	Complement factor I	4	P05156	10
	Beta-2-glycoprotein 1	3	P02749	26
	Alpha-1-antichymotrypsin	2	P01011	14

AN: protein accession number (UniProt), SC: sequence coverage in %.

can strongly affect protein plasma levels [23]. Moreover, the alterations in plasma protein levels may be affected by defects in cells' functions. For example, Blalock et al. [24] reported that phosphorylated form (on Thr451) of the dsRNA-dependent kinase accumulates in the cell nucleus of high-risk MDS patients and thus probably alters nuclear signaling. The implications of this finding on the disease or plasma protein changes are not known. A study by Aivado et al. [25] showed that CXC chemokine ligands 4 and 7 decreased their serum levels in advanced MDS patients compared to non-MDS cytopenia patients. The authors also showed that this serum decrease was related to platelets and, therefore, both the chemokines should be considered as platelet-derived markers. That platelet function impaired in MDS patients was recently confirmed in the study by Fröbel et al. [26]. In our study, the CXCL4 and CXCL7 were not identified; this is, however, not surprising when considering their low plasma (serum) levels. Aivado et al. used mass spectrometry-based detection which is capable of detecting proteins of lower concentrations compared to

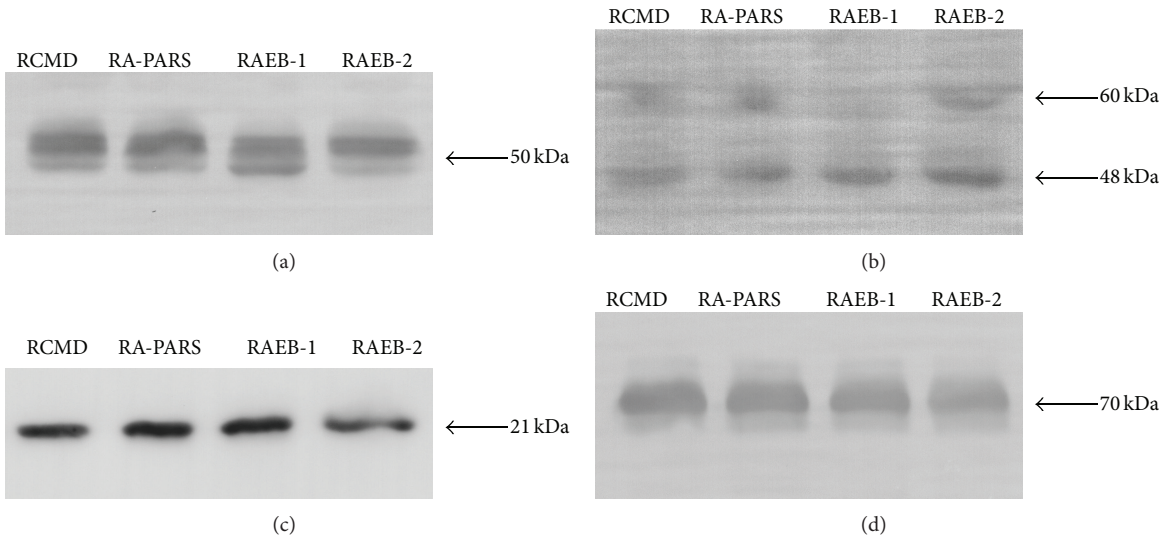

Figure 2: Western blot analysis. Western blot analysis was performed for alpha-2-HS-glycoprotein (a), leucine-rich alpha-2-glycoprotein (b), apolipoprotein A1 (c), and serum albumin (d) using pooled plasma samples of patients with four different MDS subgroups: refractory cytopenia with multilineage dysplasia (RCMD), refractory anemia or refractory anemia with ringed sideroblasts (RA-RARS), refractory anemia with excess blasts subtype 1 (RAEB-1), and refractory anemia with excess blasts subtype 2 (RAEB-2). For better clarity the western blot analysis results are shown as highlighted by brightness and contrast image adjustment.

electrophoresis-based studies; the advantages and limitations of this approach have been reviewed in literature [27]. Unfortunately, there is no all-purpose proteomic method and a subset of proteins can be observed at once using a specific proteomic method. In the study by Chen et al. [28] ProteinChip array technology and mass spectrometry were used to investigate disease-associated and therapy-associated differences in sera of del(5q) MDS patients. Platelet factor 4 (also known as CXCL4) was found to be a potential therapy-associated marker; therefore, the results supported the observation by Aivado et al. [25]. Several proteins were proposed to be potential disease-associated markers (e.g., ITIH4, transferrin, transthyretin); these proteins were not identified in our reanalysis; however, it is not surprising as there were no non-MDS control samples used in our reanalysis contrary to the work by Chen et al. [28]. Nevertheless, when the results obtained by Chen et al. are compared to our previous protemic studies (which were used for this reanalysis) investigating different MDS subgroup patients with the healthy control samples, there were the same proteins identified. Since the proteins are altered between MDS and control samples but seem to be unaltered among MDS subgroups as shown in our reanalysis, these results indicate that the protein changes may be related to other (patho)physiological processes and not to be specific to MDS.

Identifying new biomarkers could have a significant impact on the clinical practice. While for diagnostics it is important to investigate the differences between the healthy (or nondisease) and patient cohorts, it is essential to identify alterations in the disease progression for prognosis and therapy monitoring. Considering MDS, it is important to describe the changes among different subgroups (as was the aim of our study), alterations related to the therapy (e.g., the study by Chen et al.), or specific changes during the disease progression. The changes related to MDS progression toward acute myeloid leukemia were investigated in work by Braoudaki et al. [29] in plasma, bone marrow, and cell lysate samples of pediatric patients. The most promising protein candidates observed in our reanalysis were also identified by Braoudaki et al.: leucine-rich alpha-2-glycoprotein and alpha-2-HS-glycoprotein. This observation further highlights the potential and importance of those protein candidates. Moreover, another protein coidentified in two spots (antithrombin-III) in our reanalysis was also observed in the study by Braoudaki et al.; antithrombin-III was found to be differentially expressed in both bone marrow and peripheral blood plasma samples and it was shown to be altered after 3 months of treatment. Thus, antithrombin-III could be another promising target of future proteomic investigations.

4. Conclusions

In conclusion, plasma protein biomarker candidates have been presented in this work with respect to different MDS subgroups. Alpha-2-HS-glycoprotein and leucine-rich alpha-2-glycoprotein appear to be the most promising candidates with regard to western blot observations, as well as our previous results detailing the differences in plasma proteome patterns between MDS subgroups and healthy donors. The presented results should be a catalyst for further MDS biomarker validation requiring precise protein posttranslational modification characterization, profiling of the changes in MDS subgroups, and extended statistical validation with large patient cohorts.

Conflict of Interests

The authors declare that there is no conflict of interests regarding the publication of this paper.

Acknowledgments

This study was supported by the Czech Science Foundation P205/12/G118 and by the Ministry of Health of the Czech Republic project for the conceptual development of the research organization (Institute of Hematology and Blood Transfusion).

References

[1] L. Malcovati, E. Hellström-Lindberg, D. Bowen et al., "Diagnosis and treatment of primary myelodysplastic syndromes in adults: recommendations from the European LeukemiaNet," *Blood*, vol. 122, no. 17, pp. 2943–2964, 2013.

[2] J. W. Vardiman, N. L. Harris, and R. D. Brunning, "The World Health Organization (WHO) classification of the myeloid neoplasms," *Blood*, vol. 100, no. 7, pp. 2292–2302, 2002.

[3] J. W. Vardiman, J. Thiele, D. A. Arber et al., "The 2008 revision of the World Health Organization (WHO) classification of myeloid neoplasms and acute leukemia: rationale and important changes," *Blood*, vol. 114, no. 5, pp. 937–951, 2009.

[4] Z. Zemanova, K. Michalova, H. Buryova et al., "Involvement of deleted chromosome 5 in complex chromosomal aberrations in newly diagnosed myelodysplastic syndromes (MDS) is correlated with extremely adverse prognosis," *Leukemia Research*, vol. 38, no. 5, pp. 537–544, 2014.

[5] A. Vasikova, M. Belickova, E. Budinska, and J. Cermak, "A distinct expression of various gene subsets in CD34+ cells from patients with early and advanced myelodysplastic syndrome," *Leukemia Research*, vol. 34, no. 12, pp. 1566–1572, 2010.

[6] H. Cechova, P. Lassuthova, L. Novakova et al., "Monitoring of methylation changes in 9p21 region in patients with myelodysplastic syndromes and acute myeloid leukemia," *Neoplasma*, vol. 59, no. 2, pp. 168–174, 2012.

[7] M. Belickova, M. D. Merkerova, E. Stara et al., "DNA repair gene variants are associated with an increased risk of myelodysplastic syndromes in a Czech population," *Journal of Hematology and Oncology*, vol. 6, no. 1, article 9, 2013.

[8] M. D. Merkerova, Z. Krejcik, H. Votavova, M. Belickova, A. Vasikova, and J. Cermak, "Distinctive microRNA expression profiles in CD34+ bone marrow cells from patients with myelodysplastic syndrome," *European Journal of Human Genetics*, vol. 19, no. 3, pp. 313–319, 2011.

[9] H. Votavova, M. Grmanova, M. Dostalova Merkerova et al., "Differential expression of MicroRNAs in CD34+ cells of 5q-syndrome," *Journal of Hematology and Oncology*, vol. 4, article 1, 2011.

[10] C. R. Emmenegger, E. Brynda, T. Riedel, Z. Sedlakova, M. Houska, and A. B. Alles, "Interaction of blood plasma with antifouling surfaces," *Langmuir*, vol. 25, no. 11, pp. 6328–6333, 2009.

[11] T. Riedel, E. Brynda, J. E. Dyr, and M. Houska, "Controlled preparation of thin fibrin films immobilized at solid surfaces," *Journal of Biomedical Materials Research A*, vol. 88, no. 2, pp. 437–447, 2009.

[12] C. Rodriguez-Emmenegger, E. Brynda, T. Riedel et al., "Polymer brushes showing non-fouling in blood plasma challenge the currently accepted design of protein resistant surfaces," *Macromolecular Rapid Communications*, vol. 32, no. 13, pp. 952–957, 2011.

[13] N. S. Fracchiolla, S. Artuso, and A. Cortelezzi, "Biosensors in clinical practice: focus on oncohematology," *Sensors*, vol. 13, no. 5, pp. 6423–6447, 2013.

[14] P. Májek, Z. Reicheltová, J. Suttnar, J. Čermák, and J. E. Dyr, "Plasma proteome changes associated with refractory cytopenia with multilineage dysplasia," *Proteome Science*, vol. 9, article 64, 2011.

[15] P. Májek, Z. Reicheltová, J. Suttnar, J. Čermák, and J. E. Dyr, "Plasma protein alterations in the refractory anemia with excess blasts subtype 1 subgroup of myelodysplastic syndrome," *Proteome Science*, vol. 10, no. 1, article 31, 2012.

[16] P. Májek, Z. Riedelová-Reicheltová, J. Suttnar, K. Pečánková, J. Čermák, and J. E. Dyr, "Plasma proteome changes associated with refractory anemia and refractory anemia with ringed sideroblasts in patients with myelodysplastic syndrome," *Proteome Science*, vol. 11, no. 1, article 14, 2013.

[17] P. Majek, Z. Riedelova-Reicheltova, J. Suttnar, K. Pecankova, J. Cermak, and J. E. Dyr, "Proteome changes in the plasma of myelodysplastic syndrome patients with refractory anemia with excess blasts subtype 2," *Disease Markers*, vol. 2014, Article ID 178709, 8 pages, 2014.

[18] P. Májek, Z. Reicheltová, J. Štikarová, J. Suttnar, A. Sobotková, and J. E. Dyr, "Proteome changes in platelets activated by arachidonic acid, collagen, and thrombin," *Proteome Science*, vol. 8, article 56, 2010.

[19] P. Májek, Z. Reicheltová, J. Suttnar et al., "Plasma proteome changes in cardiovascular disease patients: novel isoforms of apolipoprotein A1," *Journal of Translational Medicine*, vol. 9, article 84, 2011.

[20] S. Holm, "A simple sequentially rejective multiple test procedure," *Scandinavian Journal of Statistics*, vol. 6, no. 2, pp. 65–70, 1979.

[21] V. Petrik, S. Saadoun, A. Loosemore et al., "Serum α2-HS glycoprotein predicts survival in patients with glioblastoma," *Clinical Chemistry*, vol. 54, no. 4, pp. 713–722, 2008.

[22] J. Cubedo, T. Padró, and L. Badimon, "Glycoproteome of human apolipoprotein A-I: *N*- and *O*-glycosylated forms are increased in patients with acute myocardial infarction," *Translational Research*, vol. 164, no. 3, pp. 209–222, 2014.

[23] S. Enroth, Å. Johansson, S. B. Enroth, and U. Gyllensten, "Strong effects of genetic and lifestyle factors on biomarker variation and use of personalized cutoffs," *Nature Communications*, vol. 5, article 4684, 2014.

[24] W. L. Blalock, A. Bavelloni, M. Piazzi et al., "Multiple forms of PKR present in the nuclei of acute leukemia cells represent an active kinase that is responsive to stress," *Leukemia*, vol. 25, no. 2, pp. 236–245, 2011.

[25] M. Aivado, D. Spentzos, U. Germing et al., "Serum proteome profiling detects myelodysplastic syndromes and identifies CXC chemokine ligands 4 and 7 as markers for advanced disease," *Proceedings of the National Academy of Sciences of the United States of America*, vol. 104, no. 4, pp. 1307–1312, 2007.

[26] J. Fröbel, R.-P. Cadeddu, S. Hartwig et al., "Platelet proteome analysis reveals integrin-dependent aggregation defects in patients with myelodysplastic syndromes," *Molecular and Cellular Proteomics*, vol. 12, no. 5, pp. 1272–1280, 2013.

[27] S. Beranova-Giorgianni, "Proteome analysis by two-dimensional gel electrophoresis and mass spectrometry: strengths and limitations," *TrAC—Trends in Analytical Chemistry*, vol. 22, no. 5, pp. 273–281, 2003.

[28] C. Chen, D. T. Bowen, A. A. N. Giagounidis, B. Schlegelberger, S. Haase, and E. G. Wright, "Identification of disease- and therapy-associated proteome changes in the sera of patients with myelodysplastic syndromes and del(5q)," *Leukemia*, vol. 24, no. 11, pp. 1875–1884, 2010.

[29] M. Braoudaki, F. Tzortzatou-Stathopoulou, A. K. Anagnostopoulos et al., "Proteomic analysis of childhood de novo acute myeloid leukemia and myelodysplastic syndrome/AML: correlation to molecular and cytogenetic analyses," *Amino Acids*, vol. 40, no. 3, pp. 943–951, 2011.

Hindawi Publishing Corporation
BioMed Research International
Volume 2015, Article ID 303987, 9 pages
http://dx.doi.org/10.1155/2015/303987

Review Article

Potential Role of MicroRNA-210 as Biomarker in Human Cancers Detection: A Meta-Analysis

Jiongjiong Lu, Feng Xie, Li Geng, Weifeng Shen, Chengjun Sui, and Jiamei Yang

Department of Special Treatment, Eastern Hepatobiliary Surgery Hospital, Second Military Medical University, No. 225, Changhai Road, Shanghai 200438, China

Correspondence should be addressed to Jiamei Yang; jmyang_smmu@hotmail.com

Received 23 August 2014; Accepted 13 November 2014

Academic Editor: Aurelio Ariza

We conducted this meta-analysis aimed to evaluate diagnostic accuracy of miR-210 in human cancers. A total of 673 cancer patients and 606 cancer-free individuals from 13 studies were contained in this meta-analysis. The overall diagnostic results in our study showed that the pooled sensitivity was 0.70, specificity was 0.76, and the AUC was 0.80. In addition, the PLR and NLR were 2.9 and 0.39, with DOR of 8. After the outliner exclusion detected by sensitivity analysis, these parameters had minimal change, which confirmed the stability of our work. The results in our studies showed that the miR-210 assay yielded relatively moderate accuracy in cancer patients and cancer-free individual differentiation. More basic researches are needed to highlight its role as supplement in clinical treatment.

1. Introduction

Cancer, with an estimate of millions of deaths each year, is considered as one of the highest mortalities worldwide [1–3]. The complex and progressive molecular progress involved in cancer development made it a challenge in clinic, bringing the early stage treatment to the front as it seems easier to control the disease. For example, 5-year survival rate is approximately 98% for renal cancer stage I patients, while survival drops to 50% for patients in stage III [4, 5]. For instance, 5-year survival rate of 80% for stage I but only 10% for stage IV patients with lung cancer also accounts for the importance of early detection [6, 7]. Thus, the most effective way to improve the disease outcomes and therefore reduce the worldwide health burden is the development of diagnostic tool for early detection.

Nowadays, the gold standard for cancer detection is the histological evaluation of biopsy. Though it is the most reliable way in cancer prediction with relatively high sensitivity and specificity, its usage is still restricted in clinic for the suffering of patients resulting from the invasive nature [8]. Several currently blood-based biomarkers may enhance the early cancer detection without the unpleasant procedure, including carcinoembryonic antigen (CEA), carbohydrate antigen 19-9, alphafetoprotein (AFP), and prostate specific antigen (PSA), but the low accuracy makes them minimally useful for the supplement of existing screening methods [9–12]. Therefore, although the diagnostic tool for early cancer detection could reduce the mortality, the effective biomarkers are still absent.

The discovery of microRNAs (miRNAs), a group of regulatory RNAs with 22 nucleotides in length, has opened up a new field in molecular diagnosis of cancer at early stage [13]. miRNAs have proven to be involved in the initiation and progression of human malignancy by influencing the degradation or translation of hundreds of mRNAs [13–15]. Further, their abnormally expression levels are found to be associated with a variety of diseases, including pancreatic cancer, lung cancer, and breast cancer [16–18]. What is more, miRNAs, present in human body matrix like plasma, sputum, feces, and serum, are resistant to RNase activity and keep stable even in extreme environment, which is the evidence of its stability [19, 20]. For instance, reproducibility is another advantage of miRNAs as they are stable and easy to be accessed by quantitative reverse transcription polymerase chain reaction (qTR-PCR) methods [21, 22]. Therefore, miRNAs may be

the promising candidate as invasive biomarkers for early cancer detection.

MicroRNA-210 (miRNA-210, miR-210), a member of miRNAs, has been largely studied in the past several years and has been identified as a major induced miRNA under hypoxia [23, 24]. Thus, unusual expression of hypoxia-inducible miR-210 may link to cancer, as hypoxia is a common feature of the neoplastic microenvironment [25]. Since Wang et al. firstly demonstrated the miR-210 might have a prediction value for pancreatic cancer with sensitivity 0.42 and specificity 0.73, more researches have been done to explore the possible clinical usage of miR-210 [16, 26–28]. For example, Anjuman et al. found that miR-210 were present in considerably higher levels in sputum of lung cancer patients than cancer-free individuals and yielded diagnostic accuracy of 0.77 in lung cancer detection [28]. For instance, the improvement in diagnostic performance of miR-210 with sensitivity 0.84 and specificity 0.82 in the diagnosis of breast cancer was pronounced by Madhavan et al., which lightens the potential value of miR-210 with relatively better accuracy in supplement of the current screening tools [29]. Though other single studies as well investigated the important diagnostic role of miR-210 in various cancers, the limited sample size, different study design, and lack of unified standard resulted in conflicting results. And notably two meta-analyses have already been conducted to evaluate the performance of miR-210 as a prognostic factor in breast cancer, but the there is no meta-analysis focusing on the diagnostic value of miR-210 and systematically pooling all the relative published studies of miR-210 in a series of cancers [30, 31]. Thus, we performed the present meta-analysis to summarize the overall accuracy of miR-210 in cancer detection and further identify its value in clinical use.

2. Methods

2.1. Search Strategy. We conducted a literature research in database including PubMed, EMBASE, CNKI, Wan Fang library before August 6, 2014, in order to identify the relevant records about miR-210 in cancer. The key words we used in the research were "cancer" or "tumor" or "neoplasm" or "malignancy" or "neoplasia" and "microRNA-210" or "miR-210" or "has-miR-210" and "sensitivity" or "specificity" or "ROC curve" or "accuracy."

Two reviewers checked the abstract of the studies and read the full-text if necessary to identify the final included studies based on the following included criteria: (1) studies which evaluated the diagnostic value of miR-210 for detecting cancer, (2) case-control design with control group of benign disease or healthy people, and (3) studies providing sufficient data to calculate diagnostic parameters.

2.2. Data Extraction and Quality Assessment. The necessary information of the included studies was extracted by two reviewers and filled onto standardized data forms. The data extracted were (1) first author, (2) year of publication, (3) country, (4) ethnicity, (5) number, age, and male ratio of the case and control groups, (6) cancer type, (7) specimen, and (8) the diagnostic parameters including sensitivity and specificity. We also scored each of the included studies according to the QUADAS-2 (quality assessment of diagnostic accuracy studies-2) tool. With the max score of 7, the quality of the included studies can be judged by the results.

2.3. Statistical Analysis. The random-effects model was used in our analysis to summarize the sensitivity, specificity, and other parameters [37]. The SROC curve (summary receiver operating characteristic) and its under area AUC were also gathered to evaluate the accuracy of miR-210 in cancer [38]. In addition, we performed metaregression to investigate the heterogeneity between the included studies with $P < 0.05$ considered statistically significant [39]. Confirming the stability of our study, we also conducted the sensitivity analysis and further performed the outliner exclusion in our work. For instance, Deeks et al.'s funnel plot was employed to assess the potential publication bias [40]. All the statistical analyses were undertaken using Stata 12.0.

3. Results

3.1. Study Research. 110 manuscripts were identified from the initial search including PubMed, EMBASE, CNKI, and Wan Fang databases. After 8 records were excluded for duplications, totals of 102 records were left for the next step judgment. Then, 82 records were excluded as unrelated studies by reviewing the abstract and keywords. After full-text reading of the remaining 20 records, 8 of them were rejected due to the unavailable data. Thus, 12 records related to miR-210 in cancer detection were finally included in the meta-analysis [5, 16–18, 26–28, 32–36]. The flow diagram for literature research processes is shown in Figure 1.

The characteristics of studies included in this analysis are summarized in Table 1. 673 cancer patients and 606 cancer-free individuals from 13 studies published from 2009 to 2014 were contained in this meta-analysis. All the 13 studies tested miR-210s expression using qRT-PCR methods based on plasma ($n = 5$), sputum ($n = 3$), serum ($n = 4$), and fecal ($n = 1$). Six of the studies were conducted in Caucasian and African population, 4 of them conducted in Asian population, and 4 of them performed in Caucasian population. Among the 13 studies, 6 explore the association between miR-210 expression and lung cancer, 2 investigated that in breast cancer, and the other 5 focused on pancreatic cancer ($n = 2$), renal cancer ($n = 2$), and leukemia ($n = 1$). In addition, two reviews independently scored the included studies based on QUADAS-2 score system. All of them had relatively high quality with scores between 4 and 7 (Table 1), indicating the reliable foundation of our analysis.

3.2. Outcomes of miR-210 Assay. Considering the significant heterogeneity observed among the included studies ($I^2 = 79.35\%$ for sensitivity and $I^2 = 64.95$ for specificity, resp.) (Figure 2), the random-effect model was chosen in our analysis. As the SROC curve shown in Figure 3(a), the overall diagnostic results showed that the pooled sensitivity was

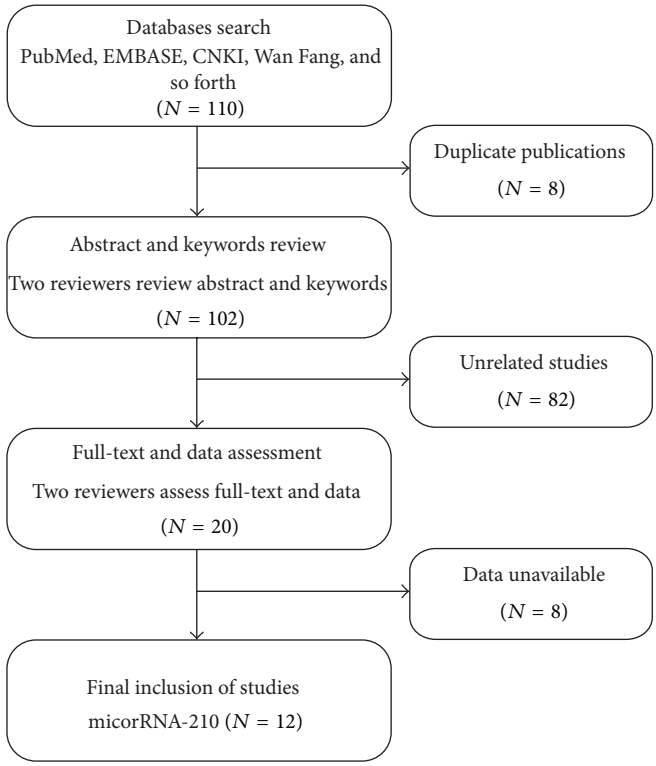

Figure 1: Flow diagram of publications research process.

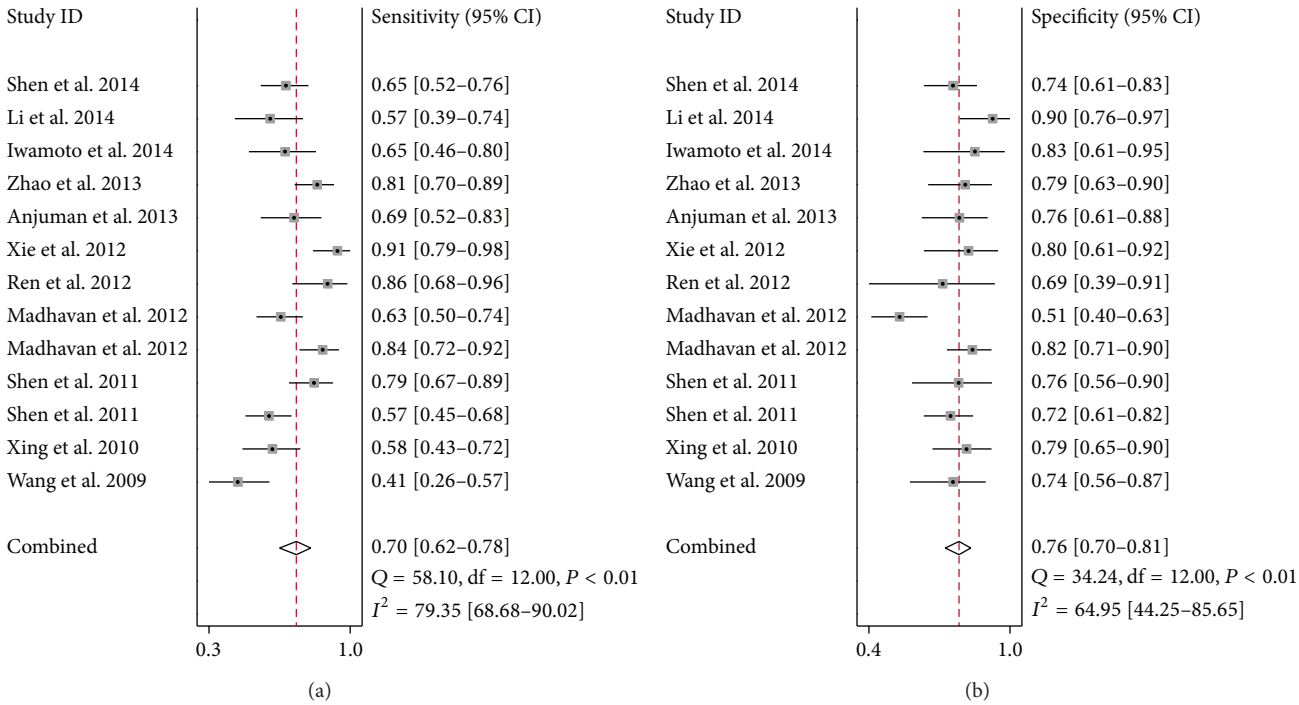

Figure 2: Forest plots of sensitivity (a) and specificity (b) of the overall 12 included publications.

Table 1: Characteristics of the included studies.

First author	Year	Country	Ethnicity	Sample size		Male		Cancer	Specimen	Diagnostic power				QUADAS
				Control	Case	Control	Case			TP	FP	FN	TN	
Wang [16]	2009	USA	Caucasian	44	34	0.51	n.a.	Pancreatic cancer	Plasma	18	9	26	25	4
Xing [17]	2010	USA	Caucasian/African	48	48	0.68	0.54	Lung cancer	Sputum	28	10	20	38	5
Shen [18]	2011	USA	Caucasian/African	76	80	0.55	0.63	Lung cancer	Plasma	43	22	33	58	5
Shen [26]	2011	USA	Caucasian/African	58	29	0.68	0.66	Lung cancer	Plasma	46	7	12	22	6
Madhavan [32]	2012	Germany	Caucasian	61	76	n.a.	n.a.	Breast cancer	Plasma	51	14	10	62	7
				72	76	n.a.	n.a.	Breast cancer	Plasma	45	37	27	39	
Ren [33]	2012	China	Asian	29	13	0.66	0.62	Pancreatic cancer	Fecal	25	4	4	9	6
Xie [27]	2012	China	Asian	45	30	0.62	0.57	Leukemia	Serum	41	6	4	24	4
Anjuman [28]	2013	USA	Caucasian/African	39	42	0.59	0.61	Lung cancer	Sputum	27	10	12	32	5
Zhao [34]	2013	France	Caucasian	68	42	0.68	0.52	Renal cancer	Serum	55	9	13	33	6
Iwamoto [5]	2014	Japan	Asian	34	23	0.76	0.48	Renal cancer	Serum	22	4	12	19	4
Li [35]	2014	USA	Caucasian/African	35	40	0.63	0.65	Lung cancer	Sputum	20	4	15	36	6
Shen [36]	2014	USA	Caucasian/African	64	73	0.64	0.66	Lung cancer	Sputum	43	18	23	50	5

n.a.: not available; TP: true positive; FP: false positive; FN: false negative; TN: true negative; QUADAS: quality assessment of diagnostic accuracy studies.

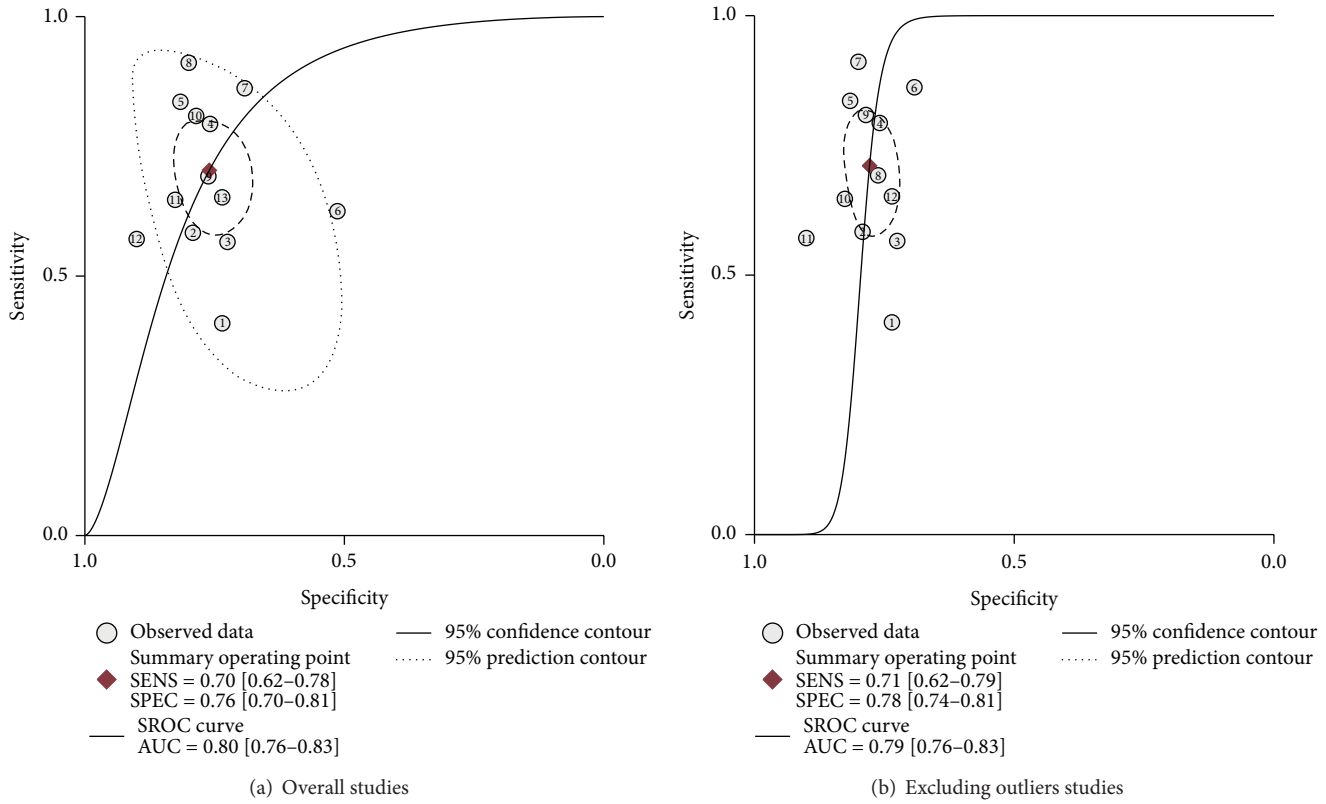

Figure 3: The SROC curves containing mean operating sensitivity and specificity point with AUC (a) overall and (b) after exclusion.

0.70 (95% CI: 0.62–0.78), specificity was 0.76 (95% CI: 0.70–0.81), and the AUC was 0.80 (95% CI: 0.70–0.83). The pooled positive likelihood ratios (PLR) and negative likelihood ratios (NLR) were also calculated by the bivariate meta-analysis with values of 2.9 (95% CI: 2.3–3.8) and 0.39 (95% CI: 0.29–0.52), respectively. The overall diagnostic odds ratio (DOR), ratio of PLR and NLR, was 8 (95% CI: 4–13). The results all together indicated a relatively moderate diagnostic accuracy of miR-210 in distinguishing cancer patients and cancer-free individuals.

3.3. Metaregression and Sensitivity Analyses. In order to find potential sources of heterogeneity, we performed the metaregression based on the variables including number of case and control, age of case and control, cancer type, and specimen. The results in Figure 4 suggested that cancer type ($P < 0.05$) had an effect on sensitivity, while the cancer type ($P < 0.05$) and the specimen ($P < 0.001$) contributed to interstudy heterogeneity for specificity. We also conducted sensitivity analyses and further excluded 1 outliner found by influence analysis and outlier detection in Figure 5. After exclusion, the sensitivity increased from 0.70 to 0.71, specificity increased from 0.76 to 0.78, the PLR increased from 2.9 to 3.2, the NLR dropped from 0.39 to 0.37, DOR improved from 8 to 9, and AUC decreased from 0.80 to 0.79, showing minimal change with our overall analysis (Figure 3(b)). Combined with goodness of fit and bivariate normality analyses, we confirmed the robustness of our meta-analysis.

3.4. Publication Bias. Fagan's nomogram in Figure 6 describes the association between miR-210 assays results and the probability of cancer. For instance, when miR-210 assays were tested for any people with a pretest probability of 25% to have cancer, a positive result would improve posttest probability having cancer to 50%, while a negative result would drop the posttest probability to 12%. Thus, the miR-210 may serve as a noninvasive biomarker to supply the existing diagnostic methods. In addition, we conducted Deeks et al.'s funnel plot asymmetry test and found no significant publication bias in our study with P value of 0.22 (Figure 7).

4. Discussion

Cancer is a worldwide health problem due to the complex and progressive molecular procedure and the absence of effective diagnostic tool at cancer early stage [2]. Though the development of such invasive and effective biomarkers has been investigated for decades, little progress has been made until the discovery of miRNAs. miRNAs have been reported to associate with the development of tumor as a regulator in gene expression [13]. Large efforts have been made to investigate the link between abnormal miRNA expression and cancer, including the miR-210, the most consistently hypoxia-induced miRNA [41]. However, the diagnostic accuracy of miR-210 was inconsistent in literature due to the inescapable limitation of single study. Thus, we conducted the present

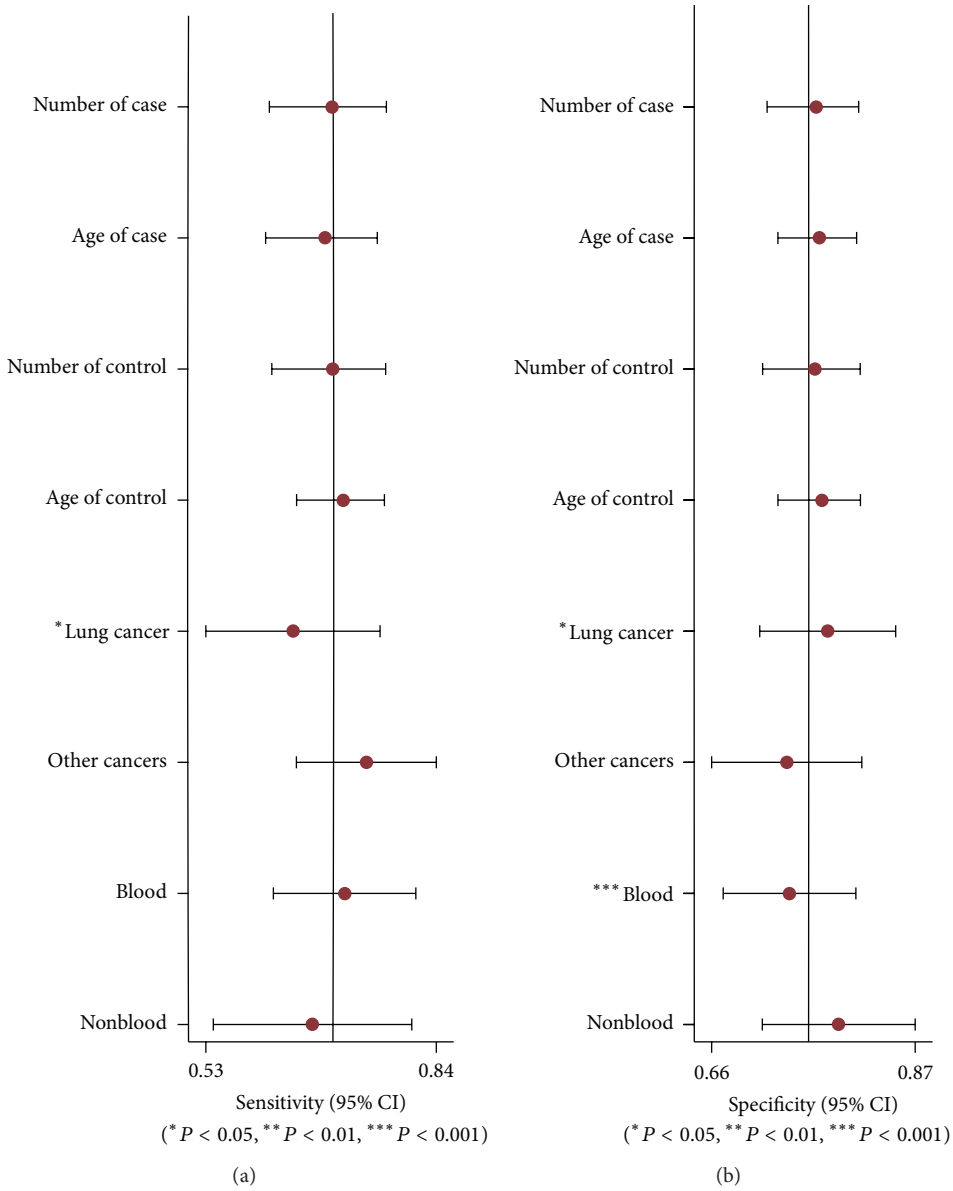

Figure 4: Multivariable metaregression (a) sensitivity and (b) specificity.

meta-analysis to evaluate the diagnostic performance of miR-210 in cancer detection.

The pooled results in our study were sensitivity of 0.70 (95% CI: 0.62–0.78), specificity of 0.76 (95% CI: 0.70–0.81), and the AUC of 0.80 (95% CI: 0.70–0.83), indicating a moderate diagnostic efficiency of miR-210 in diagnosis of cancer. The pooled PLR and NLR were 2.9 (95% CI: 2.3–3.8) and 0.39 (95% CI: 0.29–0.52), respectively, with DOR of 8 (95% CI: 4–13), suggesting the relatively low level of miR-210 assay to identify or exclude cancer patients. Thus, due to the moderate accuracy, the application of miR-210 serving as a clinical biomarker still has a long way to go.

As the results in our analysis, a single miR-210 in cancer detection may lack sensitivity and specificity, but there are several areas we need to focus on in the future research in order to promote the usage of miR-210 in clinical treatment. Firstly, the mechanism of miR-210 abnormally expressed in cancer is not completely understood; more scientific and technological methods should be used in future basic research to provide better understanding of biological roles of miR-210 in cancer, hence lightening up the diagnostic value of miR-210. Recent studies suggested that hypoxic condition, which is a feature for solid tumor, may increase the level of miR-210 as miR-210 is related to the hypoxia-inducible factor-(HIF-) 1a and HIF-2a [41–43]. Although such connection of miR-210 and cancer highlights the function of miR-210 in cancer detection, the exact mechanism of it in tumor development needs further investigation.

Secondly, plenty of studies have demonstrated the advantages of multiple miRNAs combined assays, which may be the solution for the lack of accuracy of miR-210 in our analysis. For example, Shen et al. explored the prediction

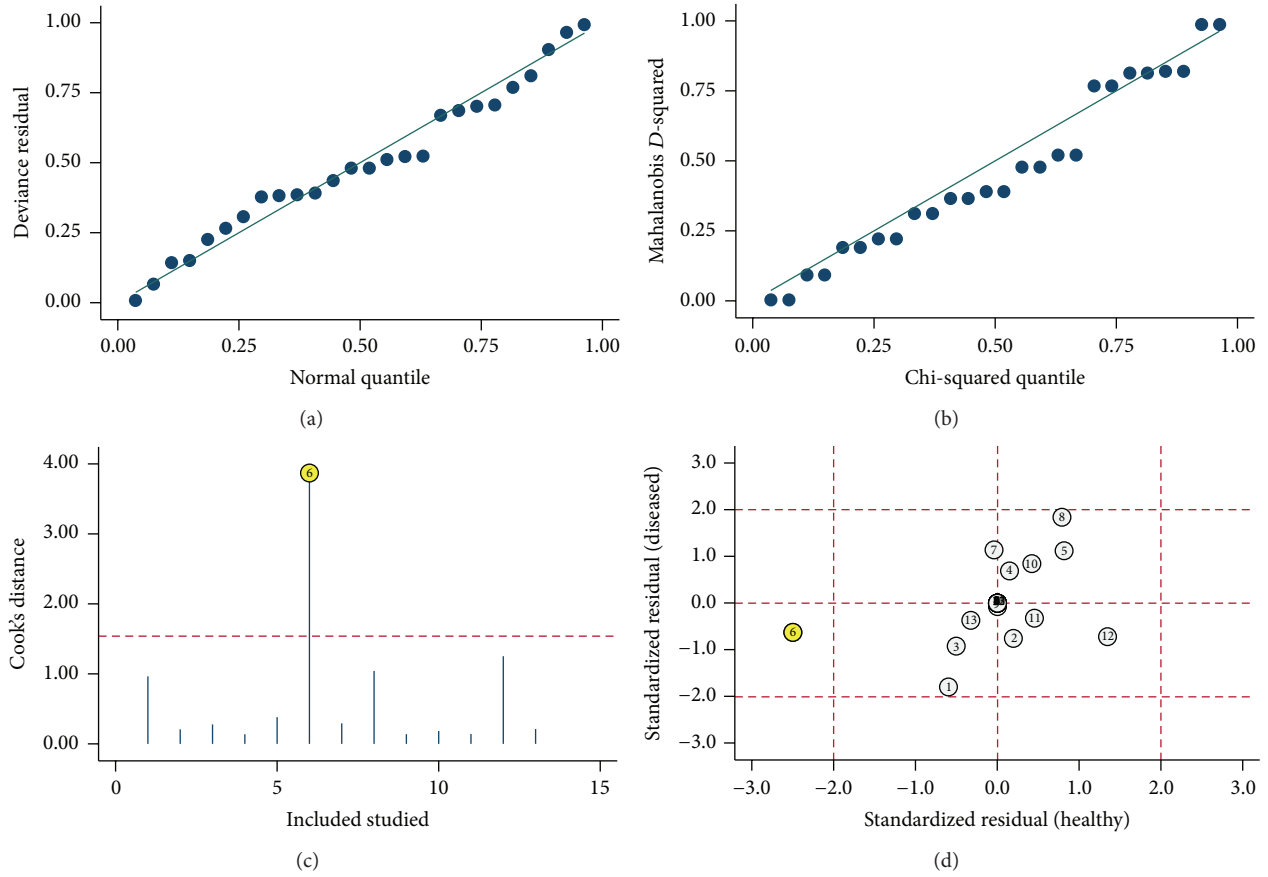

FIGURE 5: Influence analysis and outlier detection: (a) goodness of fit, (b) bivariate normality, (c) influence analysis, and (d) outlier detection.

ability of miR-210 and miR-31 for lung cancer; combined use of the two miRNAs yielded 65.2% sensitivity and 89.7% specificity versus sensitivity of 67.2% and specificity of 31.5% of single miR-210 assay [36]. Not happening singly but in pairs, Anjuman et al. also found that single miR-210 test generated 0.77 accuracy in diagnosis of lung cancer, while the combined analysis of miR-210 and miR-31 had a better overall diagnostic performance with 0.83 [28]. For instance, we know that single miR-210 can cover a broad spectrum of cancers and the combination of miR-210 and other miRNAs may contribute to the accuracy improvement, but the combination way, as well as the unique group for specific cancer, needs to be further clarified.

Thirdly, although the ethnicity is not the source of heterogeneity according to the metaregression in the present analysis, cancer prediction based on population is still an important task in the future as different ethic patient may have specific characteristics of their tumors. What is more, the sample size was too small in our study with only 3 studies focused on the miR-210 expression in cancer in Asian population and no study explored the miR-210 function in only African populations, which resulted in unavoidable limitations. Actually, the included studies showed that the serum-based miR-210 assay in renal cancer yielded 81% sensitivity and 79.4% specificity in Caucasian populations but 65% sensitivity and 83% specificity in Asian populations [5, 34]. Thus, more fundamental research with long follow-up period should pay attention to the heterogeneity of miR-210 in cancer based on populations.

Fourthly, data normalization is currently a problem we need to deal with. For example, when we demonstrated that miR-210 was highly expressed in cancer, infeasible comparison can be done between studies as no reference substance can be found in the existing included studies, such as a miRNA sharing the same expression in cancer patients and cancer-free individuals. In addition, the cut-off values of miR-210 were varied in different studies and different cancers, which may result in the higher accuracy from lower cut-off value. Therefore, the standard should be set up in order to avoid the systemic differences.

5. Conclusion

In conclusion, the results in current meta-analysis showed that the application of miR-210 as the first-line screening tool in clinical treatment was immature due to lack of accuracy. However, the miR-210 assay showed potential used as a supplement for the existing diagnostic methods to improve accuracy. What is more, future research should focus on the combined usage of miR-210 with other miRNAs and make improvement in technic consensus such as data normalization.

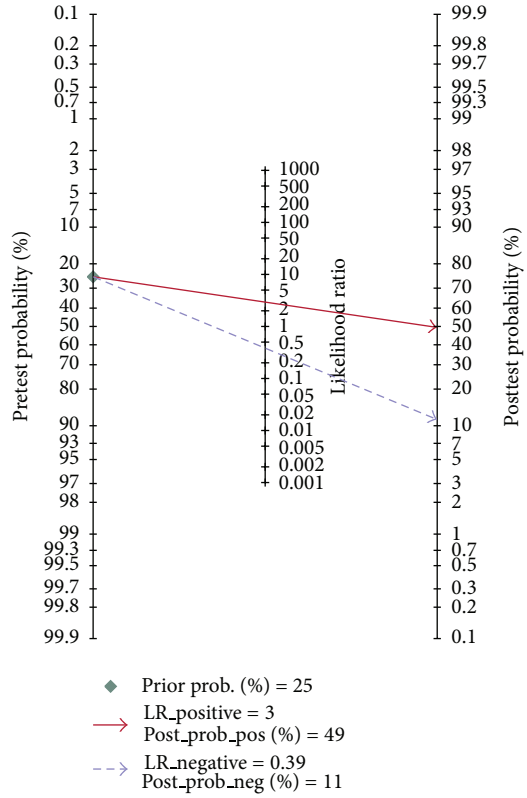

Figure 6: Fagan's nomogram in assessment of the test probabilities after miR-210 assay.

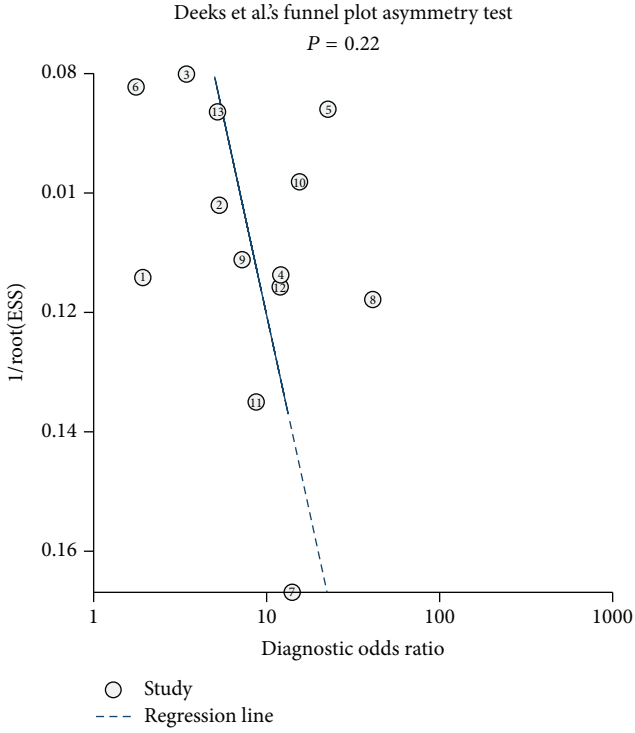

Figure 7: Deeks et al.'s funnel plots asymmetry test with regression line to explore publication bias.

Conflict of Interests

The authors declare that there is no conflict of interests regarding the publication of this paper.

References

[1] A. Jemal, R. Siegel, E. Ward et al., "Cancer statistics, 2008," *CA: A Cancer Journal for Clinicians*, vol. 58, no. 2, pp. 71–96, 2008.

[2] X. Li, K. Wu, and D. Fan, "CIAPIN1 as a therapeutic target in cancer," *Expert Opinion on Therapeutic Targets*, vol. 14, no. 6, pp. 603–610, 2010.

[3] A. Jemal, F. Bray, M. M. Center, J. Ferlay, E. Ward, and D. Forman, "Global cancer statistics," *CA: A Cancer Journal for Clinicians*, vol. 61, no. 2, pp. 69–90, 2011.

[4] R. J. Motzer, M. Mazumdar, J. Bacik, W. Berg, A. Amsterdam, and J. Ferrara, "Survival and prognostic stratification of 670 patients with advanced renal cell carcinoma," *Journal of Clinical Oncology*, vol. 17, no. 8, pp. 2530–2540, 1999.

[5] H. Iwamoto, Y. Kanda, T. Sejima, M. Osaki, F. Okada, and A. Takenaka, "Serum miR-210 as a potential biomarker of early clear cell renal cell carcinoma," *International Journal of Oncology*, vol. 44, no. 1, pp. 53–58, 2014.

[6] J. K. Frost, W. C. Ball Jr., M. L. Levin et al., "Early lung cancer detection: results of the initial (prevalence) radiologic and cytologic screening in the Johns Hopkins Study," *American Review of Respiratory Disease*, vol. 130, no. 4, pp. 549–554, 1984.

[7] F. R. Hirsch, W. A. Franklin, A. F. Gazdar, and Jr. Bunn P. A., "Early detection of lung cancer: clinical perspectives of recent advances in biology and radiology," *Clinical Cancer Research*, vol. 7, no. 1, pp. 5–22, 2001.

[8] J. Wittmann and H.-M. Jäck, "Serum microRNAs as powerful cancer biomarkers," *Biochimica et Biophysica Acta—Reviews on Cancer*, vol. 1806, no. 2, pp. 200–207, 2010.

[9] F. Lumachi, A. A. Brandes, M. Ermani, G. Bruno, and P. Boccagni, "Sensitivity of serum tumor markers CEA and CA 15–3 in breast cancer recurrences and correlation with different prognostic factors," *Anticancer Research*, vol. 20, no. 6C, pp. 4751–4755, 2000.

[10] J. Schneider, H.-G. Velcovsky, H. Morr, N. Katz, K. Neu, and E. Eigenbrodt, "Comparison of the tumor markers Tumor M2-PK, CEA, CYFRA 21-1, NSE and SCC in the diagnosis of lung cancer," *Anticancer Research*, vol. 20, no. 6 D, pp. 5053–5058, 2000.

[11] H. A. Dbouk, A. Tawil, F. Nasr et al., "Significance of CEA and VEGF as diagnostic markers of colorectal cancer in Lebanese patients," *The Open Clinical Cancer Journal*, vol. 1, pp. 1–5, 2007.

[12] S. M. Hanash, C. S. Baik, and O. Kallioniemi, "Emerging molecular biomarkers-blood-based strategies to detect and monitor cancer," *Nature Reviews Clinical Oncology*, vol. 8, no. 3, pp. 142–150, 2011.

[13] G. Hutvágner and P. D. Zamore, "A microRNA in a multiple-turnover RNAi enzyme complex," *Science*, vol. 297, no. 5589, pp. 2056–2060, 2002.

[14] A. Esquela-Kerscher and F. J. Slack, "Oncomirs—microRNAs with a role in cancer," *Nature Reviews Cancer*, vol. 6, no. 4, pp. 259–269, 2006.

[15] B. Zhang, X. Pan, G. P. Cobb, and T. A. Anderson, "microRNAs as oncogenes and tumor suppressors," *Developmental Biology*, vol. 302, no. 1, pp. 1–12, 2007.

[16] J. Wang, J. Chen, P. Chang et al., "MicroRNAs in plasma of pancreatic ductal adenocarcinoma patients as novel blood-based biomarkers of disease," *Cancer Prevention Research*, vol. 2, no. 9, pp. 807–813, 2009.

[17] L. Xing, N. W. Todd, L. Yu, H. Fang, and F. Jiang, "Early detection of squamous cell lung cancer in sputum by a panel of microRNA markers," *Modern Pathology*, vol. 23, no. 8, pp. 1157–1164, 2010.

[18] J. Shen, Z. Liu, N. W. Todd et al., "Diagnosis of lung cancer in individuals with solitary pulmonary nodules by plasma microRNA biomarkers," *BMC Cancer*, vol. 11, article 374, 2011.

[19] P. S. Mitchell, R. K. Parkin, E. M. Kroh et al., "Circulating microRNAs as stable blood-based markers for cancer detection," *Proceedings of the National Academy of Sciences of the United States of America*, vol. 105, no. 30, pp. 10513–10518, 2008.

[20] J. A. Weber, D. H. Baxter, S. Zhang et al., "The microRNA spectrum in 12 body fluids," *Clinical Chemistry*, vol. 56, no. 11, pp. 1733–1741, 2010.

[21] X. Chen, Y. Ba, L. Ma et al., "Characterization of microRNAs in serum: a novel class of biomarkers for diagnosis of cancer and other diseases," *Cell Research*, vol. 18, no. 10, pp. 997–1006, 2008.

[22] A. Turchinovich, L. Weiz, A. Langheinz, and B. Burwinkel, "Characterization of extracellular circulating microRNA," *Nucleic Acids Research*, vol. 39, no. 16, pp. 7223–7233, 2011.

[23] R. Kulshreshtha, M. Ferracin, S. E. Wojcik et al., "A microRNA signature of hypoxia," *Molecular and Cellular Biology*, vol. 27, no. 5, pp. 1859–1867, 2007.

[24] A. Osman, "MicroRNAs in health and disease—basic science and clinical applications," *Clinical Laboratory*, vol. 58, no. 5-6, pp. 393–402, 2012.

[25] M. E. Crosby, C. M. Devlin, P. M. Glazer, G. A. Calin, and M. Ivan, "Emerging roles of microRNAs in the molecular responses to hypoxia," *Current Pharmaceutical Design*, vol. 15, no. 33, pp. 3861–3866, 2009.

[26] J. Shen, N. W. Todd, H. Zhang et al., "Plasma microRNAs as potential biomarkers for non-small-cell lung cancer," *Laboratory Investigation*, vol. 91, no. 4, pp. 579–587, 2011.

[27] H. Xie, Z. Chu, and H. Wang, "Serum microRNA expression profile as a biomarker in diagnosis and prognosis of acute myeloid leukemia," *Journal of Clinical Pediatric Dentistry*, vol. 30, no. 5, pp. 421–424, 2012.

[28] N. Anjuman, N. Li, M. Guarnera, S. A. Stass, and F. Jiang, "Evaluation of lung flute in sputum samples for molecular analysis of lung cancer," *Clinical and Translational Medicine*, vol. 2, article 15, 2013.

[29] D. Madhavan, K. Cuk, B. Burwinkel, and R. Yang, "Cancer diagnosis and prognosis decoded by blood-based circulating micro RNA signatures," *Frontiers in Genetics*, vol. 4, article 116, 2013.

[30] L. Hong, J. Yang, Y. Han, Q. Lu, J. Cao, and L. Syed, "High expression of miR-210 predicts poor survival in patients with breast cancer: a meta-analysis," *Gene*, vol. 507, no. 2, pp. 135–138, 2012.

[31] Y. Li, X. Ma, J. Zhao, B. Zhang, Z. Jing, and L. Liu, "microRNA-210 as a prognostic factor in patients with breast cancer: meta-analysis," *Cancer Biomarkers*, vol. 13, no. 6, pp. 471–481, 2013.

[32] D. Madhavan, M. Zucknick, M. Wallwiener et al., "Circulating miRNAs as surrogate markers for circulating tumor cells and prognostic markers in metastatic breast cancer," *Clinical Cancer Research*, vol. 18, no. 21, pp. 5972–5982, 2012.

[33] Y. Ren, J. Gao, J.-Q. Liu et al., "Differential signature of fecal microRNAs in patients with pancreatic cancer," *Molecular Medicine Reports*, vol. 6, no. 1, pp. 201–209, 2012.

[34] A. Zhao, G. Li, M. Péoc'h, C. Genin, and M. Gigante, "Serum miR-210 as a novel biomarker for molecular diagnosis of clear cell renal cell carcinoma," *Experimental and Molecular Pathology*, vol. 94, no. 1, pp. 115–120, 2013.

[35] N. Li, J. Ma, M. A. Guarnera, H. Fang, L. Cai, and F. Jiang, "Digital PCR quantification of miRNAs in sputum for diagnosis of lung cancer," *Journal of Cancer Research and Clinical Oncology*, vol. 140, no. 1, pp. 145–150, 2014.

[36] J. Shen, J. Liao, M. A. Guarnera et al., "Analysis of microRNAs in sputum to improve computed tomography for lung cancer diagnosis," *Journal of Thoracic Oncology*, vol. 9, no. 1, pp. 33–40, 2014.

[37] E. C. Vamvakas, "Meta-analyses of studies of the diagnostic accuracy of laboratory tests: a review of the concepts and methods," *Archives of Pathology & Laboratory Medicine*, vol. 122, no. 8, pp. 675–686, 1998.

[38] A. J. Mitchell, A. Vaze, and S. Rao, "Clinical diagnosis of depression in primary care: a meta-analysis," *The Lancet*, vol. 374, no. 9690, pp. 609–619, 2009.

[39] J. Dinnes, J. Deeks, J. Kirby, and P. Roderick, "A methodological review of how heterogeneity has been examined in systematic reviews of diagnostic test accuracy," *Health Technology Assessment*, vol. 9, no. 12, pp. 1–113, 2005.

[40] J. J. Deeks, P. Macaskill, and L. Irwig, "The performance of tests of publication bias and other sample size effects in systematic reviews of diagnostic test accuracy was assessed," *Journal of Clinical Epidemiology*, vol. 58, no. 9, pp. 882–893, 2005.

[41] C. Devlin, S. Greco, F. Martelli, and M. Ivan, "MiR-210: more than a silent player in hypoxia," *IUBMB Life*, vol. 63, no. 2, pp. 94–100, 2011.

[42] R. H. Wenger and M. Gassmann, "Oxygen(es) and the hypoxia-inducible factor-1," *Biological Chemistry*, vol. 378, no. 7, pp. 609–616, 1997.

[43] C. S. Neal, M. Z. Michael, L. H. Rawlings, M. B. van der Hoek, and J. M. Gleadle, "The VHL-dependent regulation of microRNAs in renal cancer," *BMC Medicine*, vol. 8, article 64, 2010.

Hindawi Publishing Corporation
BioMed Research International
Volume 2015, Article ID 618924, 13 pages
http://dx.doi.org/10.1155/2015/618924

Research Article

Long Noncoding RNA Expression Signatures of Metastatic Nasopharyngeal Carcinoma and Their Prognostic Value

Wei Zhang,[1,2] Lin Wang,[3,4] Fang Zheng,[5] Ruhai Zou,[6] Changqing Xie,[7] Qiannan Guo,[1,2] Qian Hu,[8] Jianing Chen,[1,2] Xing Yang,[8] Herui Yao,[8] Erwei Song,[1,2] and Yanqun Xiang[3,4]

[1]*Breast Tumor Center, Sun Yat-Sen Memorial Hospital, Sun Yat-Sen University, 107 Yanjiang West Road, Guangzhou, Guangdong 510120, China*
[2]*Key Laboratory of Malignant Tumor Gene Regulation and Target Therapy of Guangdong Higher Education Institutes, Sun Yat-Sen Memorial Hospital, Sun Yat-Sen University, 107 Yanjiang West Road, Guangzhou, Guangdong 510120, China*
[3]*Department of Nasopharyngeal Carcinoma, Sun Yat-Sen University Cancer Center, 651 Dongfeng East Road, Guangzhou, Guangdong 510060, China*
[4]*State Key Laboratory of Oncology in Southern China, Guangzhou, China*
[5]*Medical Research Center, Sun Yat-Sen Memorial Hospital, Sun Yat-Sen University, 107 Yanjiang West Road, Guangzhou, Guangdong 510120, China*
[6]*Department of Ultrasonography, Sun Yat-Sen University Cancer Center, 651 Dongfeng East Road, Guangzhou, Guangdong 510060, China*
[7]*Department of Internal Medicine, Brody School of Medicine, Vidant Medical Center, East Carolina University, Greenville, NC, USA*
[8]*Department of Oncology, Sun Yat-Sen Memorial Hospital of Sun Yat-Sen University, 107 Yanjiang West Road, Guangzhou, Guangdong 510120, China*

Correspondence should be addressed to Herui Yao; yaoherui@163.com, Erwei Song; songew@mail.sysu.edu.cn, and Yanqun Xiang; yanqun.xiang@gmail.com

Received 24 June 2014; Accepted 2 September 2014

Academic Editor: Murat Gokden

Long noncoding RNAs (lncRNAs) have recently been found to play important roles in various cancer types. The elucidation of genome-wide lncRNA expression patterns in metastatic nasopharyngeal carcinoma (NPC) could reveal novel mechanisms underlying NPC carcinogenesis and progression. In this study, lncRNA expression profiling was performed on metastatic and primary NPC tumors, and the differentially expressed lncRNAs between these samples were identified. A total of 33,045 lncRNA probes were generated for our microarray based on authoritative data sources, including RefSeq, UCSC Knowngenes, Ensembl, and related literature. Using these probes, 8,088 lncRNAs were found to be significantly differentially expressed (≥2-fold). To identify the prognostic value of these differentially expressed lncRNAs, four lncRNAs (LOC84740, ENST00000498296, AL359062, and ENST00000438550) were selected; their expression levels were measured in an independent panel of 106 primary NPC samples via QPCR. Among these lncRNAs, ENST00000438550 expression was demonstrated to be significantly correlated with NPC disease progression. A survival analysis showed that a high expression level of ENST00000438550 was an independent indicator of disease progression in NPC patients ($P = 0.01$). In summary, this study may provide novel diagnostic and prognostic biomarkers for NPC, as well as a novel understanding of the mechanism underlying NPC metastasis and potential targets for future treatment.

1. Introduction

Nasopharyngeal carcinoma (NPC), a squamous cell carcinoma that occurs in the epithelial lining of the nasopharynx, displays a characteristic geographic and racial distribution worldwide. NPC is a rare malignant tumor in Western countries with an incidence of less than 1/100,000; however, the incidence of NPC was reported to be greater than

20/100,000 in southern China, especially among the Cantonese population living in the central region of Guangdong Province [1, 2]. The histological profile of NPC varies between endemic and nonendemic areas. For example, the tumors from more than 95% of NPC patients in high-incidence areas of China are undifferentiated nonkeratinizing carcinoma, whereas those from patients of Western descent, such as Caucasian, African-American, and Hispanic patients, are predominantly keratinizing squamous cell carcinoma [3–5]. According to the WHO histological profile, NPC among Chinese patients accounts for the majority of nonkeratinizing carcinomas, including 55.9% of the differentiated nonkeratinizing carcinomas and 58.0% of the undifferentiated nonkeratinizing carcinomas. This difference is attributed to the multifactorial etiology of NPC, which includes genetic factors, viral infection, the environment, and dietary habits [5–12]. The cure rate of NPC has improved significantly since the development of radiation technology and chemotherapy. However, distant metastasis remains the primary reason for treatment failure [3, 11, 13]. It is necessary to identify the specific molecular mechanisms that contribute to the pathogenesis and progression of NPC metastasis.

Recent studies suggest that noncoding RNAs (ncRNAs) constitute a large proportion of genome-encoded transcripts [14–16]. There is increasing evidence confirming that ncRNA performs biological functions in both *cis*- and *trans*-gene regulation, especially among higher eukaryotes [16–19]. Due to their functional relevance, ncRNAs have been categorized into housekeeping and regulatory ncRNAs [15]. Long noncoding RNAs (lncRNAs with a length of more than 200 nucleotides) comprise a majority of regulatory ncRNAs [15, 16, 20]. Many lncRNAs are highly conserved and are involved in diverse cellular functions, such as epigenetic regulation [21–23]. lncRNAs have been demonstrated to play crucial roles in dosage compensation, genome imprinting, X chromosome inactivation, chromatin modification, and whole-genome rearrangement [17, 18, 21, 24, 25]. The dysregulated expression of lncRNAs has been identified in a variety of diseases, including different types of cancer [26]; this observation suggests that aberrant lncRNA expression may represent a major contributor to carcinogenesis and cancer progression [17, 27]. For example, HOTAIR and ANRIL act as cancer regulators in carcinogenesis and cancer progression [17, 28]. HOTAIR expression levels increase with clinical stage progression in NPC; NPC patients with high HOTAIR levels have a poor prognosis for overall survival [29]; metastasis-associated lung adenocarcinoma transcript (MALAT-1), PANDA, and ncRNA-DHFR regulate DNA damage, the cell cycle, alternative splicing, and tumor progression [30, 31]. Based on microarray analysis, the H19 gene is strongly expressed in undifferentiated NPC. Furthermore, H19 is highly expressed in an undifferentiated human NPC cell line. H19 plays a role in the differentiation of human NPC cells and the transcriptional silencing of imprinted genes [32]. LINC00312, also named NAG7 (NPC-associated gene 7), is a lincRNA expressed in the cytoplasm of nasopharyngeal epithelial cells. LINC00312 is expressed in 51.4% of NPC samples and 78.4% of noncancerous nasopharyngeal epithelia samples ($P < 0.001$) [33]. Compared with noncancerous nasopharyngeal epithelial tissues, LINC00312 is significantly downregulated in NPC tissues. LINC00312 could be used as a biomarker for NPC metastasis, progression, and prognosis. Based on rematching and reannotation of the existing microarray datasets, five lncRNAs were selected to validate the differential expression of lncRNAs in both primary and recurrent nasopharyngeal carcinoma compared with noncancerous nasopharyngeal epithelia [34]. However, most of the differentially expressed lncRNAs have not been functionally characterized. We suspect that some of these lncRNAs play roles in NPC progression and that some are candidate biomarkers for the diagnosis or prognosis of NPC. The novel molecular mechanisms by which lncRNAs regulate carcinogenesis and metastasis are expected to be elucidated.

In the present study, we performed lncRNA expression profiling on metastatic and primary NPC tumors and identified differentially expressed lncRNAs that could show altered expression prior to or during the invasion-metastasis process. Further investigation validated that the expression level of the lncRNA ENST00000438550 was an independent prognostic marker in NPC patients.

2. Materials and Methods

2.1. Patients and Tissue Specimens. From July 2010 to November 2012, a total of 110 primary NPC samples and 3 metastatic NPC samples with confirmed pathology were collected from Sun Yat-Sen University Cancer Center. All of the samples were excess discarded tissues from diagnostic procedures. Three NPC metastatic tissue samples were collected via needle biopsy of bone metastatic sites of NPC patients. Among the 110 primary NPC samples, 4 of them were randomly selected for lncRNA microarray analysis. The remaining 106 primary NPC samples underwent QPCR. The tumor tissues from each subject were snap-frozen in liquid nitrogen immediately after biopsy. Written informed consent was obtained from all patients. The research ethics committee of Sun Yat-Sen University Cancer Center approved this study. No patients had received therapy prior to biopsy. The TNM classification of the patients was determined according to the criteria of the American Joint Committee on Cancer (AJCC 7th edition). The detailed clinical information corresponding to the seven NPC patient samples used for microarray analysis is presented in Table S01 in the Supplementary Material available online at http://dx.doi.org/10.1155/2015/618924.

2.2. RNA Extraction. Total RNA was extracted from 113 snap-frozen samples using TRIzol reagent (Invitrogen) according to the manufacturer's protocol. The sample quality was evaluated using a Nano Drop ND-1000 spectrophotometer and standard denaturing agarose gel electrophoresis.

2.3. Microarray and Computational Analyses. For microarray analysis, the previously prepared total RNA from each sample was purified after rRNA removal (mRNA-ONLY Eukaryotic mRNA Isolation Kit, Epicentre) and then amplified and transcribed into fluorescent cRNA along the entire length of

the transcripts without 3′ bias utilizing a random priming method. The labeled cRNAs were hybridized to the Human lncRNA Array v2.0 (8 × 60 K, Arraystar). After washing the slides, the arrays were scanned using the Agilent Scanner G2505C.

Agilent Feature Extraction software (version 11.0.1.1) was used to analyze the acquired array images. Quantile normalization and subsequent data processing were performed using the GeneSpring GX v11.5.1 software package (Agilent Technologies). After quantile normalization of the raw data, lncRNAs in which all 7 samples displayed flags corresponding to Present or Marginal ("All Targets Value") were selected for further data analysis. The differentially expressed lncRNAs displaying statistical significance between the two groups were identified via Volcano Plot filtering. Finally, hierarchical clustering was performed to elucidate the differentially expressed lncRNA expression profile in the samples.

The experimental protocol was as follows: (1) RNA extraction and RNA QC (described previously); (2) labeling and hybridization (the Agilent Quick Amp Labeling Kit was used for sample labeling and hybridization was performed in Agilent Sure Hyb Hybridization Chambers); (3) data collection and normalization; (4) further data analysis (using Agilent Gene Spring GX v11.5.1 software); and (5) lncRNA classification and subgroup analysis (using homemade scripts). The microarray was performed by KangChen Bio-tech, Shanghai, China.

2.4. Quantitative RT-PCR. Real-time PCR was performed using a LightCycler 480 (Roche, Basel, Switzerland). The reactions were performed in triplicate, and the relative expression of lncRNAs (LOC84740, ENST00000498296, AL359062, and ENST00000438550) was normalized to that of the internal control GAPDH. The primer sequences are presented in Supplementary Table S02.

2.5. Statistics. Statistical analyses were performed using SPSS version 16.0. Receiver operating characteristic (ROC) curve analysis was used to select the threshold expression levels of the lncRNAs detected via QPCR for disease-free survival (DFS). The survival curves were plotted using the Kaplan-Meier method and were compared using the log-rank test. A multivariate survival analysis was performed using a Cox proportional hazards model (forward). The statistical tests were two-sided, and $P < 0.05$ was considered to be significant.

3. Results

3.1. Overview of the lncRNA Expression Profiles. Using the lncRNA expression profiles, differentially expressed lncRNAs were determined between the metastatic and primary NPC tumor tissues. The differences in lncRNA expression were evaluated by calculating the normalized fold-change in lncRNA expression between the metastatic/primary tumor (M/T) samples. The selection criterion was a fold-change threshold of 2.0. A positive fold-change indicated upregulation, whereas a negative fold-change indicated downregulation. Log fold-change corresponded to the log2 value of the absolute fold-change. Both the fold-change and the *P* value were normalized. Thousands of lncRNAs were found to be differentially expressed between the metastatic and primary NPC tumors according to UCSC-known gene, Ensemble, RefSeq_NR, H-invDB, NRED, RNAdb, lincRNA, RNAdb, HOX cluster, misc_RNA, UCR, and lncRNAdb.

A total of 33,045 lncRNA probes were used in our lncRNA microarray. Up to 30,610 lncRNAs were detected in all seven samples (Table S03). Thousands of lncRNAs were found to be differentially expressed, and samples in the same group shared many differentially expressed lncRNAs (Figure 1, Table 1, Table S04). A total of 8,088 lncRNAs were identified to be significantly differentially expressed (≥2-fold) between the metastatic and primary NPC tumors (Table 1, Table S04). Among these, 3,778 lncRNAs were found to be consistently upregulated; 4,310 lncRNAs were downregulated. Additionally, H19 was found to be 2.2-fold upregulated in the metastatic tissue, which could be related to metastasis (Figure 1, Tables S03-S04). CR620154 (log2 fold-change M/T = 94.02) was the most significantly upregulated lncRNA, and TUBA4B (log2 fold-change M/T = −1,364.72) was the most significantly downregulated lncRNA (Table 2).

3.2. lncRNA Classification and Subgroup Analysis. According to the function and locus of each lncRNA and its association with protein-encoding RNA, Gibb et al. separated lncRNAs into several categories, such as long intronic ncRNAs, antisense RNAs, and promoter-associated long RNAs [35]. In our microarray study, the lncRNAs were classified into four subgroups: enhancer lncRNAs acting on a nearby coding gene, HOX cluster, lncRNAs near a coding gene, and Rinn lincRNAs [23, 36–38]. The expression levels of the lncRNAs in these subgroups were different between the metastatic and primary NPC tumors (Figure 2, Table 1).

In our study, we found that 477 transcribed regions in HOX loci; of these, 257 were ncRNAs and 220 were HOX coding transcripts (Table S05). In the four randomly paired groups, the number of differentially expressed lncRNAs differed, but several lncRNAs displayed similar changes in expression. Compared with the NPC primary tumors, 70 lncRNAs were found to be differentially expressed in metastatic tissues; 51 coding transcripts were differentially expressed (Table S06, Figure 3(a)). According to the comparative analysis of the four randomly paired groups, 33 lncRNAs were upregulated and 37 lncRNAs were downregulated in the metastatic NPC samples compared with the primary NPC tumor samples (Figure 3(b)). Interestingly, HOTAIR, a known regulatory lncRNA located at the HOX locus, was among the 33 upregulated lncRNAs (Figure 3(c)). HOTAIR has been demonstrated to be an oncogene to modulate the metastasis of breast cancer and NPC [17, 39].

Rinn lincRNAs, a type of lincRNAs identified by Rinn, were also detected in our study [23, 38]. A total of 4,199 Rinn lincRNAs were detected in our microarray (Table S07). The number of upregulated and downregulated Rinn lincRNAs

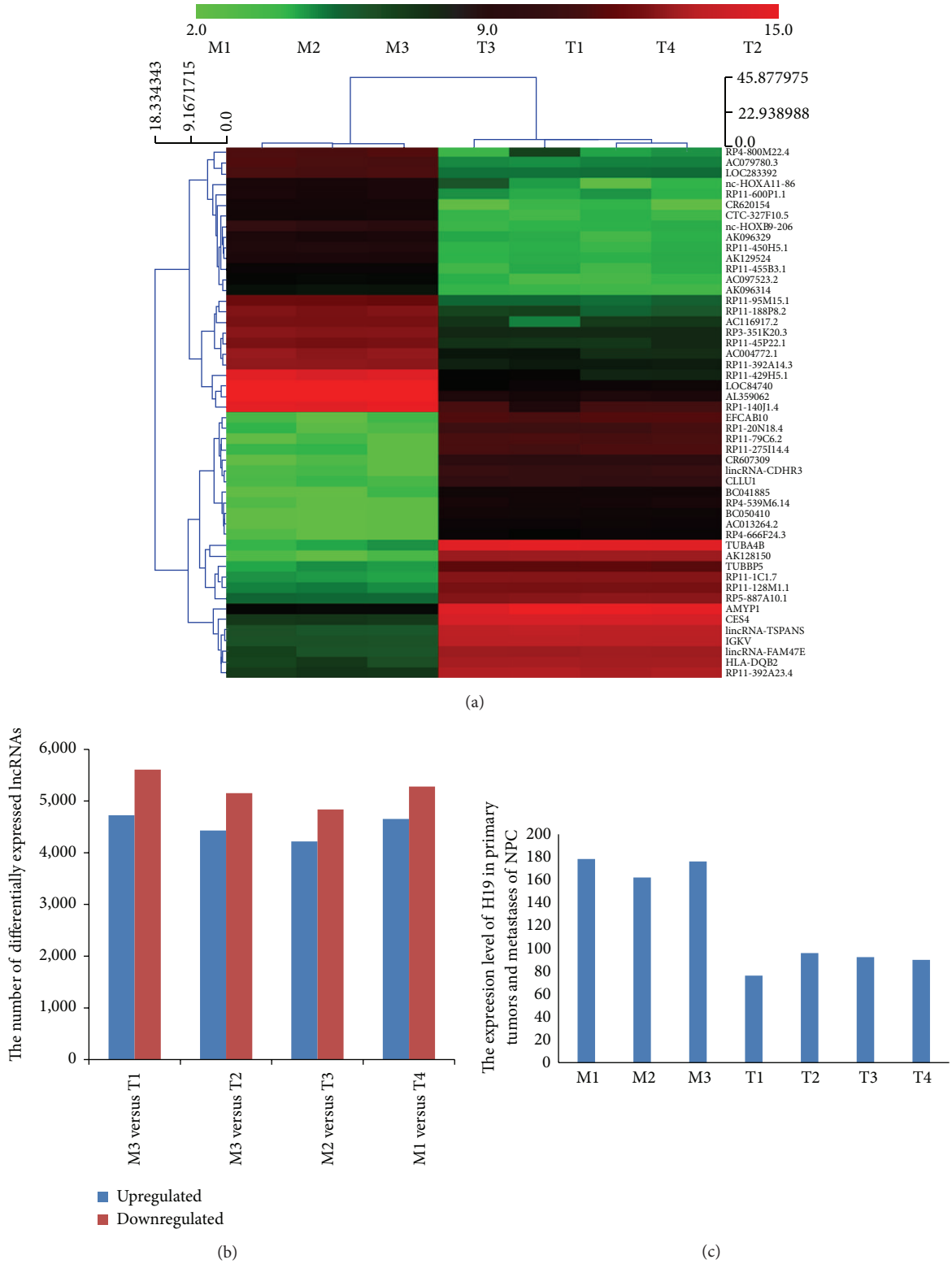

Figure 1: The number of upregulated and downregulated lncRNAs. (a) Hierarchical clustering was performed based on "All Targets Value-lncRNAs." The results of hierarchical clustering revealed distinct lncRNA expression profiles between the samples. (b) Thousands of lncRNAs were found to be significantly upregulated or downregulated in metastatic NPC tumors compared with primary NPC tumors in seven NPC patients based on microarray analysis. The number of upregulated and downregulated lncRNAs varied between the seven patients. In the four randomly paired M and T groups, downregulated lncRNAs were more common than upregulated lncRNAs. (c) H19 was found to be upregulated in all metastatic samples ($P < 0.001$); the expression levels of H19 were 1.8- to 3-fold higher in the metastatic tumors than in the primary tumors.

Table 1: Summary of the microarray data for the metastatic and primary NPC tumors.

Gene type	RNA expression	Fold-change (n)				Differentially expressed RNAs (n)
		>20	10–20	2–10	Total	
lncRNA	Upregulated	65	191	3,522	3,778	8,088
	Downregulated	198	225	3,887	4,310	
Enhancer lncRNAs regulating a nearby coding gene	Upregulated	4	5	94	103	462
	Downregulated	17	20	322	359	
HOX cluster	Upregulated	15	5	51	71	121
	Downregulated	1	3	46	50	
lncRNAs regulating a nearby coding gene	Upregulated	4	5	94	103	462
	Downregulated	17	20	322	359	
Rinn lincRNAs	Upregulated	6	14	328	348	1,069
	Downregulated	33	28	660	721	

NPC: nasopharyngeal carcinoma; lncRNA: long noncoding RNA; lincRNA: long intergenic noncoding RNA.

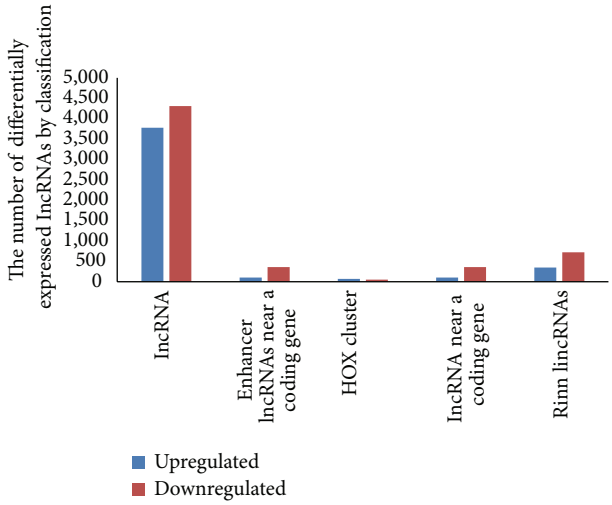

Figure 2: The number of upregulated and downregulated lncRNAs in each subgroup. The lncRNAs were classified into four subgroups based on microarray analysis, including enhancer lncRNAs regulating a nearby coding gene, HOX cluster, lincRNAs regulating a nearby coding gene, and Rinn lincRNAs. The number of lncRNAs that were consistently upregulated or downregulated in the metastatic tumors compared with the primary tumors was calculated for each subgroup.

Table 2: A collection of significantly differentially expressed lncRNAs detected via microarray analysis in seven NPC patients.

Upregulated		Downregulated	
lncRNA	log2 fold-change (M/T)	lncRNA	log2 fold-change (M/T)
CR620154	94.02	TUBA4B	1,364.72
LOC84740	92.86	AK128150	1,120.20
nc-HOXB9-206	87.55	RP11-79C6.2	303.82
RP4-800M22.4	67.25	EFCAB10	274.84
RP11-450H5.1	65.75	RP11-1C1.7	208.11
RP11-429H5.1	64.15	RP11-275I14.4	206.67
CTC-327F10.5	62.57	CR607309	197.51
AK096329	58.19	RP1-20N18.4	196.02
AC079780.3	55.47	lincRNA-CDHR3	195.01
AK129524	53.04	BC041885	141.04
AL359062	50.10	lincRNA-TSPAN8	137.80
RP11-95M15.1	46.94	BC050410	131.80
RP11-455B3.1	45.48	RP4-539M6.14	130.89
RP11-188P8.2	41.74	IGKV	125.27
AC097523.2	41.72	AC013264.2	122.93
nc-HOXA11-86	41.48	CES4	120.27
RP11-600P1.1	38.72	CLLU1	108.35
LOC283392	33.97	TUBBP5	108.01
AK096314	33.87	RP11-128M1.1	105.58
AC116917.2	33.61	RP4-666F24.3	100.17

NPC: nasopharyngeal carcinoma; M: metastatic NPC tissue; T: primary NPC tissue.
False discovery rate (FDR) < 0.1%, $P < 0.01$.

varied between the seven patients. A total of 1,069 Rinn lincRNAs were found to be differentially expressed between the patient samples (Figure 4, Table S08). As shown in Figure 4, the downregulation of the lncRNAs was more common than the upregulation. Among the four paired samples, we found 348 lncRNAs that were consistently upregulated and 721 lncRNAs that were consistently downregulated. The consistently dysregulated lncRNAs in the four groups may function as oncogenes or tumor suppressor genes; this merits further investigation.

Enhancer lncRNAs acting on a nearby coding gene were first found in human cell lines [37]. The present study revealed an unanticipated role of this subgroup of lncRNAs in the activation of critical development and differentiation regulators. In this study, many enhancer lncRNAs were found to display increased or decreased expression in M/T. Enhancer lncRNA profiling contained the profiling data of all lncRNAs displaying enhancer-like function (Table S09). A total of

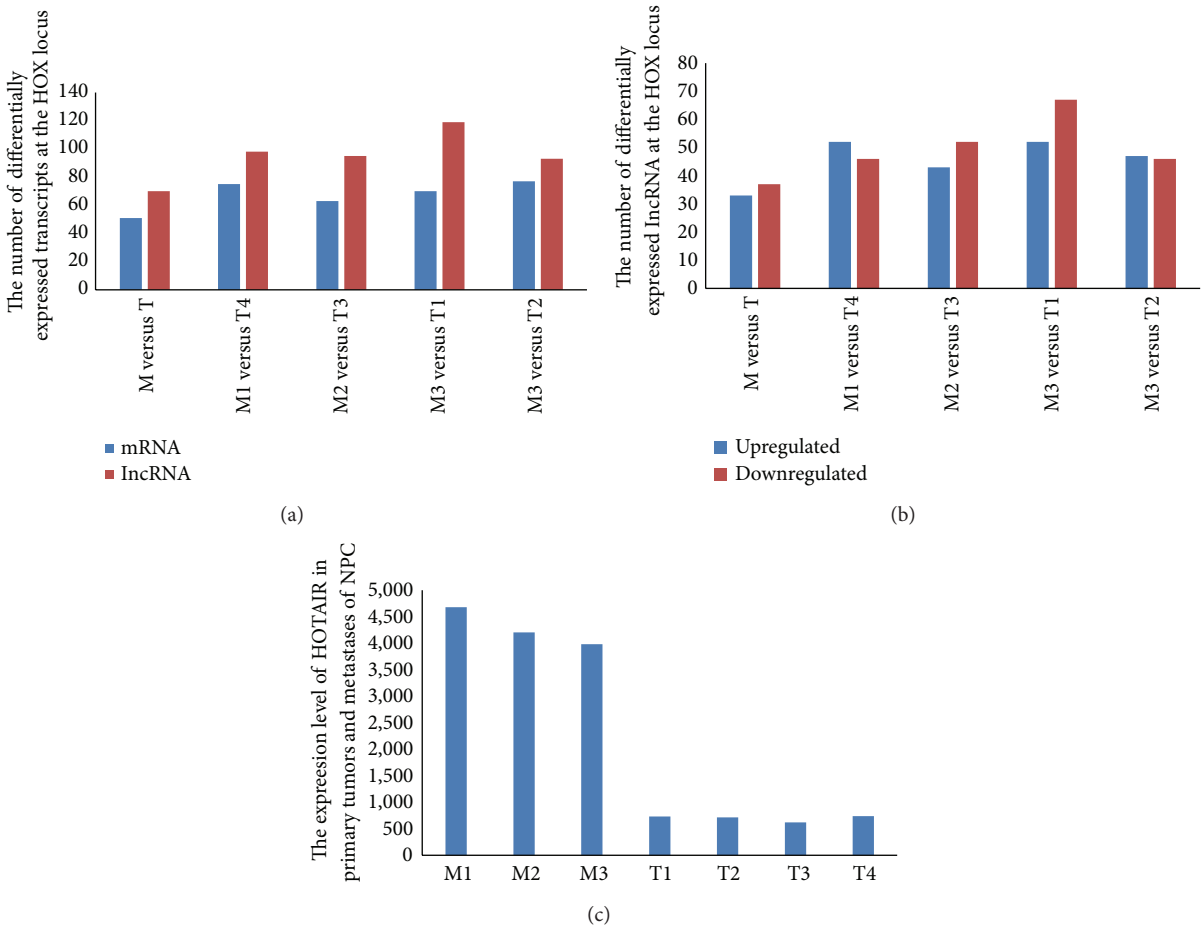

Figure 3: The number of differentially expressed lncRNAs at the HOX locus. (a) The transcripts at the HOX locus varied between the four randomly paired M and T groups. A total of 70 lncRNAs were found to be differentially expressed in the metastatic tissues, and 51 coding transcripts were differentially expressed. (b) Different numbers of lncRNAs were detected in the four randomly paired M and T groups. A total of 33 lncRNAs at the HOX locus were found to be upregulated in all groups, and 37 lncRNAs were downregulated. (c) HOTAIR was found to be upregulated in the metastatic tumor samples from all of the groups ($P < 0.001$); the expression levels of HOTAIR in the metastatic tumors were 4- to 6-fold higher than those in the primary tumors.

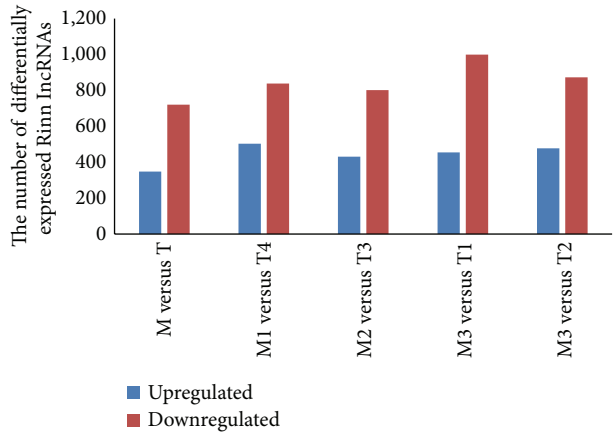

Figure 4: The number of differentially expressed Rinn lincRNAs. Rinn lincRNAs are a type of lincRNAs termed based on studies by Rinn. A total of 4,199 Rinn lincRNAs were detected in our microarray analysis. The number of downregulated Rinn lincRNAs was greater than the number of upregulated Rinn lincRNAs. According to the expression levels of all detected Rinn lincRNAs in metastatic and primary NPC tumors, 348 of these lncRNAs displayed consistent upregulation and 721 of these lncRNAs displayed consistent downregulation in the four randomly paired M and T groups.

Table 3: The clinicopathological characteristics and their association with the expression levels of four lncRNAs (LOC84740, ENST00000498296, AL359062, and ENST00000438550) in NPC patients.

	LOC84740 (n = 105)			ENST00000498296 (n = 106)			AL359062 (n = 106)			ENST00000438550 (n = 106)		
	L	H	P	L	H	P	L	H	P	L	H	P
Age (years)												
<50	53	14	0.81	25	43	0.54	34	34	0.23	12	56	0.06
≥50	29	9		17	21		14	24		13	25	
Gender												
Male	66	15	0.15	32	49	1.00	37	44	0.82	11	70	0.00
Female	15	8		9	15		10	14		14	10	
Histological type												
D	2	0	0.00	0	2	0.52	1	1	1.00	1	1	0.42
U	80	23		42	62		47	57		24	80	
T classification												
T1-2	7	0	0.34	4	3	0.43	5	2	0.24	1	6	1.00
T3-4	75	23		38	61		43	56		24	75	
N classification												
N0-1	51	16	0.63	26	41	0.84	28	39	0.42	15	52	0.81
N2-3	31	7		16	23		20	19		10	29	
Distant metastasis												
No	73	18	0.18	36	56	0.78	44	48	0.25	24	68	0.18
Yes	9	5		6	8		4	10		1	13	
Local-regional relapse												
No	74	21	1.00	40	56	0.31	45	51	0.34	25	71	0.11
Yes	8	2		2	8		3	7		0	10	
Disease progression												
No	65	17	0.58	34	49	0.64	41	42	0.16	24	59	0.01
Yes	17	6		8	15		7	16		1	22	

L: low level; H: high level; P: P value; D: differentiated nonkeratinized carcinoma; U: undifferentiated nonkeratinized carcinoma.

1,598 enhancer lncRNAs were detected, of which 468 were differentially expressed. The differentially expressed enhancer lncRNAs and their nearby coding genes (distance < 300 kb) are presented in Table S10. As shown in Figure 5, the enhancer lncRNAs were located either upstream or downstream of the coding genes. Some of the enhancer lncRNAs shared the same change in expression with their nearby coding genes, while the others displayed the opposite changes; this was helpful for the identification of functional enhancer lncRNAs.

We performed a further analysis of the lincRNA profiles to identify additional potential regulatory lncRNAs and their target genes among the lincRNAs. The differentially expressed lincRNAs and nearby coding gene pairs (distance < 300 kb) are provided in Table S11 ($P < 0.05$).

3.3. Real-Time Quantitative PCR Validation. Based on this microarray analysis and according to the baseline and fold-change in the expression levels, four different lncRNA members (LOC84740, ENST00000498296, AL359062, and ENST00000438550) were selected to verify their expression levels via QPCR. The results revealed strong consistency among the QPCR results and the microarray data (Figures 6(a)-6(b)). Additionally, the expression levels of the four lncRNAs (LOC84740, ENST00000498296, AL359062, and ENST00000438550) were measured in an independent panel of 106 primary NPC samples via QPCR; however, the sample from one patient did not show expression of LOC84740 (Figure 6(c), Table 3). The clinicopathological characteristics of these 106 patients and the associations between these characteristics and the expression levels of LOC84740, ENST00000498296, AL359062, and ENST00000438550 are presented in Table 3. According to their respective ROC curves, the fold-change cutoff points in the expression thresholds for LOC84740, ENST00000498296, AL359062, and ENST00000438550 were 5.54, 0.37, 3.76, and 0.43, respectively. The expression levels of the lncRNAs were categorized into high and low levels accordingly. A high ENST00000438550 expression level was associated with disease progression among NPC patients ($P = 0.01$).

3.4. Prognosis of NPC Patients Displaying Differentially Expressed lncRNAs. To further confirm the prognostic value of these lncRNAs for NPC, the DFS of the four lncRNAs was analyzed. Among them, only ENST00000438550 was a

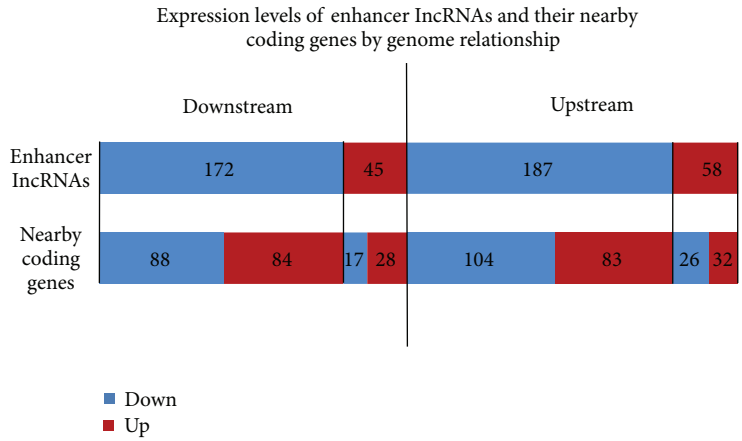

Figure 5: Expression levels of enhancer lncRNAs and their nearby coding genes based on genome relationship analysis. A total of 245 enhancer lncRNAs upstream of their nearby coding genes were differentially expressed; 58 of these enhancer lncRNAs were upregulated and 187 were downregulated. Additionally, 217 enhancer lncRNAs downstream of their nearby coding genes were differentially expressed; 45 of these enhancer lncRNAs were upregulated and 172 were downregulated. Some of the nearby coding genes displayed consistent upregulation or downregulation in concert with that of their corresponding enhancer lncRNAs, whereas other nearby coding genes displayed opposite differences.

significant predictor of disease progression in NPC patients (3-year DFS of 96% and 73% for the low and high level groups, respectively, $P = 0.02$, Figure 7). A multivariate analysis was performed using the COX proportional hazards model to analyze the prognostic values of age, gender, T classification, N classification, and the expression levels of LOC84740, ENST00000498296, AL359062, and ENST00000438550. The results revealed that only the expression level of ENST00000438550 was an independent prognostic indicator of disease progression in NPC patients (*Chi* square = 6.64, $P = 0.01$). These results suggested that ENST00000438550 could serve as a prognostic marker in NPC patients.

4. Discussion

The present study was the first to demonstrate that lncRNAs are differentially expressed between metastatic and primary NPC tumors. There have been no previous reports describing lncRNA expression profiles of NPC samples that also performed a differential expression analysis. Furthermore, this study was the first to demonstrate that a high expression level of ENST00000438550 is an independent indicator of disease progression in NPC patients.

Epstein-Barr virus (EBV) plays very important roles in the carcinogenesis of NPC. EBV exhibits tumorigenic potential due to a unique set of latent genes. Latent membrane protein-1 (LMP1) is the principal oncogene, and its expression level is a prognostic marker of NPC [40]. With the development of microarray technology, novel potential therapeutic targets as well as diagnostic and prognostic biomarkers have been identified based on gene expression array analyses. lncRNA expression array analysis has been used in oncology studies in recent years. A variety of lncRNAs, including ANRIL, MEG3 and HULC, either promote or suppress the development of cancer [41–44]. Among these, XIST is a well-known imprinted lncRNA that is abnormally expressed in ovarian and breast cancers [45, 46]. MALAT-1 was the first lncRNA that was found to be associated with high metastatic potential and poor patient prognosis in non-small-cell lung cancer patients [47]. MALAT-1 is also upregulated in other human cancers, such as breast cancer, prostate cancer, colorectal cancer, liver cancer, and uterine cancer [48–51]. These findings imply an association between lncRNAs and carcinogenesis.

The altered expression of many genes has been reported to be associated with the development of NPC [52, 53]. HOTAIR, a lincRNA in the mammalian HOXC locus, was the first lincRNA that was found to be systematically dysregulated during breast cancer progression via microarray analysis [17]. Further evidence indicates that HOTAIR reprograms the chromatin state to promote cancer metastasis and primary tumor growth *in vivo* [17]. HOTAIR has been proposed as a putative biomarker for metastasis of human malignant tumors, and it is a powerful predictor of eventual metastasis and death [17, 29]. HOTAIR is aberrantly expressed in several carcinomas, including NPC [29, 39, 54–56]. HOTAIR is upregulated in cases of NPC at more advanced clinical stage and with increased lymph node tumor burden [29]. In our study, HOTAIR was also consistently upregulated in metastatic samples, indicating that increased HOTAIR expression is associated with the progression and development of NPC. H19, another imprinted lncRNA gene with high expression levels during vertebrate embryo development, is downregulated in most tissues shortly after birth [57]. Its loss of imprinting and aberrant expression has been detected in various cancers and has been demonstrated to play a key role in oncogenesis and tumor suppression [18, 32, 58–61]. H19 expression is induced by hypermethylation of its promoter region. H19 is significantly upregulated in the undifferentiated human NPC cell line CNE-2, but it is not expressed in well-differentiated human HK1 NPC cells [32].

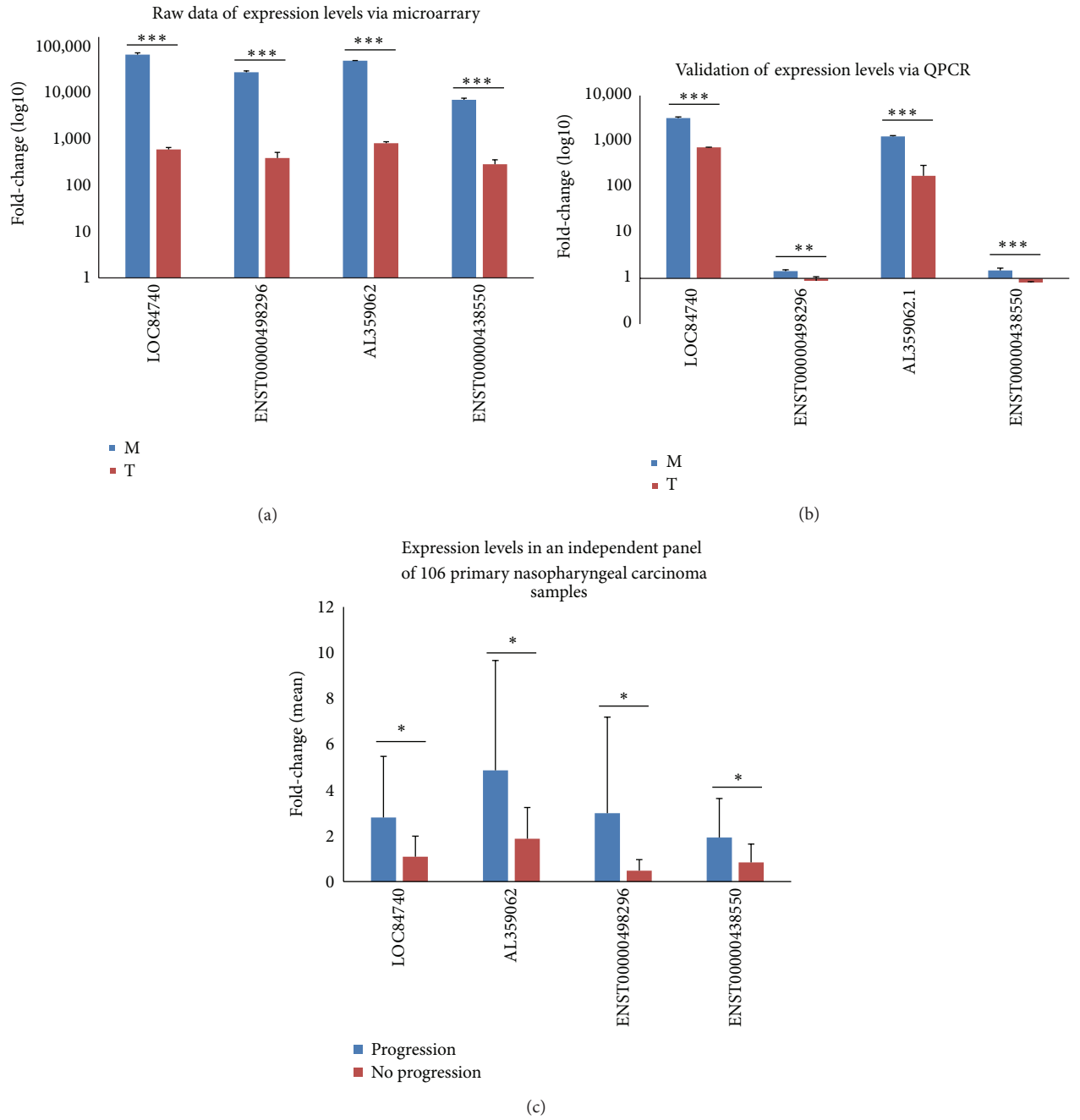

Figure 6: Real-time quantitative PCR validation. (a) Raw data of the expression levels of the four lncRNAs (LOC84740, ENST00000498296, AL359062, and ENST00000438550) based on microarray analysis. All four of these lncRNAs displayed a high basal expression level in metastatic and primary NPC tumors, but their expression levels significantly differed between the two groups. $^{***}P < 0.001$. (b) Validation of the microarray data. All four lncRNAs (LOC84740, ENST00000498296, AL359062, and ENST00000438550) were differentially expressed in the metastatic and primary NPC tumors based on microarray analysis, which was validated via QPCR using the same tissues. The validation results of the four lncRNAs indicated that the microarray data strongly correlated with the QPCR results. $^{***}P < 0.001$ and $^{**}P < 0.01$. (c) The expression levels of four lncRNAs (LOC84740, ENST00000498296, AL359062, and ENST00000438550) were measured in an independent panel of 106 primary NPC samples via QPCR. These lncRNAs displayed higher expression levels in NPC primary tumors with progression than in those without progression. $^{*}P < 0.05$.

Our study observed that H19 expression was upregulated in metastatic NPC tumors compared with primary NPC tumors; this result suggests that H19 expression is related to NPC progression.

lincRNA LINC00312 is significantly downregulated in NPC tissues compared with noncancerous nasopharyngeal epithelial tissues as assessed by a NPC tissue microarray [33]. However, we did not find LINC00312 in our differentially

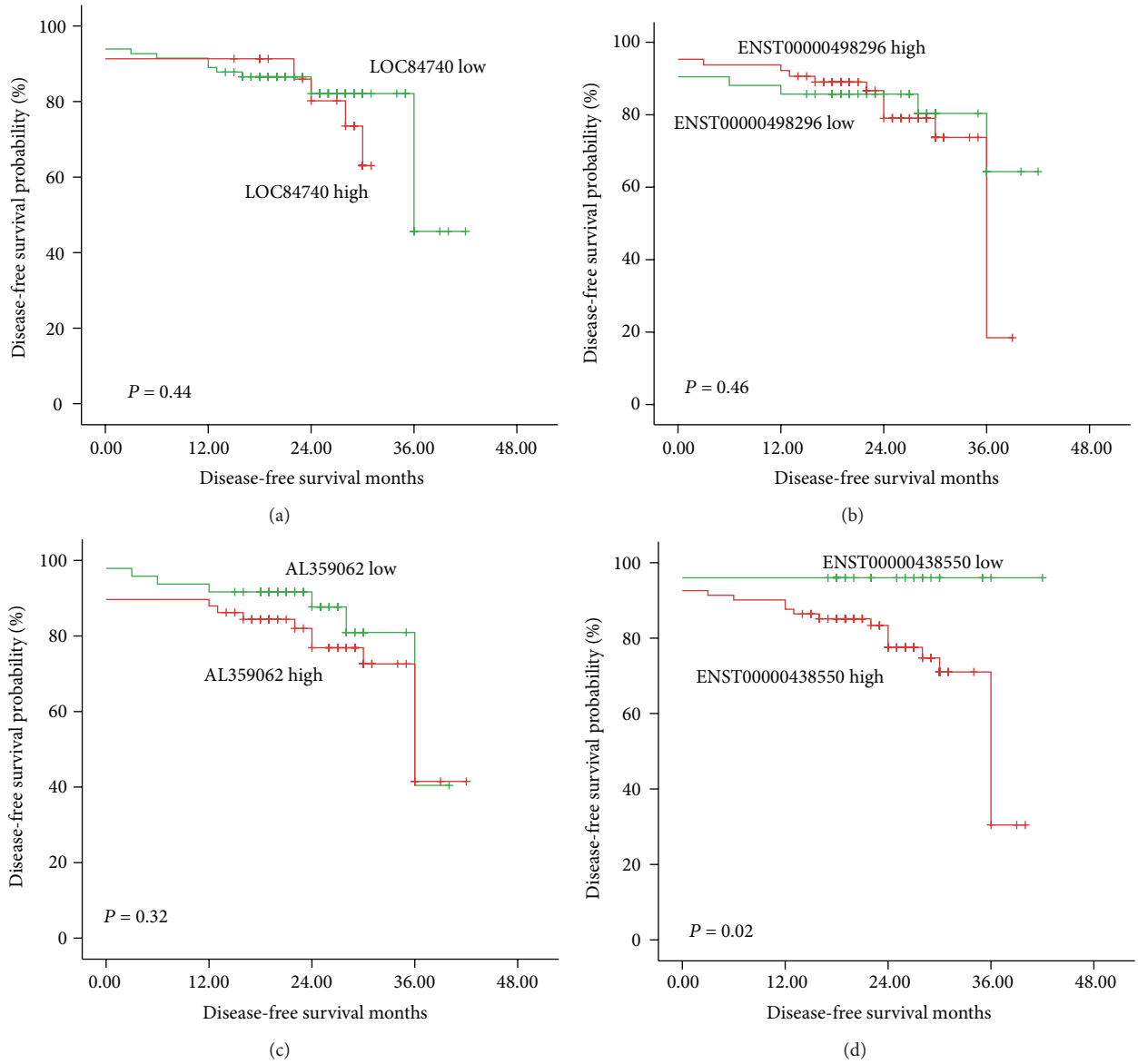

Figure 7: DFS. The expression level of ENST00000438550 correlated with disease progression in NPC patients; those displaying a high ENST00000438550 expression level experienced a significantly shorter DFS (d). However, the expression levels of LOC84740, ENST00000498296, and AL359062 were not correlated with the DFS of the NPC patients ((a)–(c)).

expressed lncRNAs. The expression of LINC00312 decreased with NPC progression. In addition, only half of the NPC samples express LINC00312, and the number of samples used in our microarray study is limited. Five lncRNAs (lnc-C22orf32-1, lnc-TLR4-1, lnc-BCL2L11-3, lnc-AL355149.1-1, and lnc-ZNF674-1) were differentially expressed in NPC compared with normal nasopharyngeal epithelial tissues in the microarray data set GSE12452 [34]. Four of these lncRNAs (lnc-C22orf32-1, lncTLR4-1, lnc-AL355149.1-1, and lnc-ZNF674-1) demonstrated significant expression differences between primary NPC and normal nasopharyngeal samples via QPCR. Only lnc-BCL2L11-3 was upregulated in the recurrent NPC tissues compared with the paired normal tissues. lnc-AL355149.1-1 and lnc-ZNF674-1 were downregulated compared with primary NPC. Unfortunately, none of the five lncRNAs were identified among the differentially expressed lncRNAs based on our microarray data. Our research focuses on NPC metastasis, and the expression of the five lncRNAs varied during carcinogenesis and recurrence.

Based on this microarray analysis and according to the baseline and fold-change in the expression levels, four lncRNAs (LOC84740, ENST00000498296, AL359062, and ENST00000438550) were selected to validate the microarray results and to evaluate their roles as biomarkers in NPC patients. Consistent with the microarray results, the four lncRNAs were differentially expressed based on QPCR. To

further illustrate the relationship between these four lncRNAs and NPC prognosis, we analyzed the expression levels of these four lncRNAs via QPCR and evaluated their potential values as prognostic indicators of NPC. We found that, among these four lncRNAs, only ENST00000438550 was an independent prognostic indicator of disease progression in NPC patients. The expression level of ENST00000438550 was negatively correlated with the prognosis of NPC patients; this suggests that elucidating the role of ENST00000438550 in NPC progression may contribute to understanding of the mechanism of NPC metastasis.

5. Conclusion

To the best of our knowledge, few differentially expressed lncRNAs have been reported in NPC, and this is the first report elucidating the lncRNA expression profiles of metastatic and primary NPC tumor tissues. Further investigation is required in the search for additional functional lncRNAs in NPC. This study has limitations, including the limited sample number for microarray analysis, which was partially due to the difficulty in conducting bone metastases biopsies. In brief, our finding provides new insights into understanding NPC. lncRNAs may underlie novel mechanisms of NPC and may represent potential targets for NPC treatment and prognostic factors for NPC, which are expected to be elucidated in the near future.

Conflict of Interests

The authors declare that there is no conflict of interests regarding the publication of this study.

Authors' Contribution

Wei Zhang and Lin Wang contributed equally to this paper.

Acknowledgments

This work was supported by grants from 973 Projects (2010CB912800, 2011CB504203) from Ministry of Science and Technology of China, the National Nature Science Foundation of China (81172041, 81472525, 81372819, 81230060, and 81261140373), the Specialized Research Fund for the Doctoral Program of Higher Education (20120171110075), Science Foundation of Guangdong Province (S2012030006287), the Guangzhou Science and Technology Bureau (2014J4100170), and Sun Yat-Sen University (13ykzd14).

References

[1] K. Shanmugaratnam, "Nasopharyngeal carcinoma: epidemiology, histopathology and aetiology," *Annals of the Academy of Medicine Singapore*, vol. 9, no. 3, pp. 289–295, 1980.

[2] M. C. Yu and J.-M. Yuan, "Epidemiology of nasopharyngeal carcinoma," *Seminars in Cancer Biology*, vol. 12, no. 6, pp. 421–429, 2002.

[3] S.-H. Ou, J. A. Zell, A. Ziogas, and H. Anton-Culver, "Epidemiology of nasopharyngeal carcinoma in the United States: improved survival of Chinese patients within the keratinizing squamous cell carcinoma histology," *Annals of Oncology*, vol. 18, no. 1, pp. 29–35, 2007.

[4] Y. S. Zong, R. F. Zhang, S. Y. He, and H. Qiu, "Histopathologic types and incidence of malignant nasopharyngeal tumors in Zhongshan county," *Chinese Medical Journal*, vol. 96, no. 7, pp. 511–516, 1983.

[5] T. L. Vaughan, J. A. Shapiro, R. D. Burt et al., "Nasopharyngeal cancer in a low-risk population: defining risk factors by histological type," *Cancer Epidemiology Biomarkers & Prevention*, vol. 5, no. 8, pp. 587–593, 1996.

[6] A. Mutirangura, W. Pornthanakasem, A. Theamboonlers et al., "Epstein-Barr viral DNA in serum of patients with nasopharyngeal carcinoma," *Clinical Cancer Research*, vol. 4, no. 3, pp. 665–669, 1998.

[7] J.-C. Lin, K. Y. Chen, W.-Y. Wang et al., "Detection of Epstein-Barr virus DNA in the peripheral-blood cells of patients with nasopharyngeal carcinoma: relationship to distant metastasis and survival," *Journal of Clinical Oncology*, vol. 19, no. 10, pp. 2607–2615, 2001.

[8] J. C. Lin, W. Y. Wang, K. Y. Chen et al., "Quantification of plasma Epstein-Barr virus DNA in patients with advanced nasopharyngeal carcinoma," *The New England Journal of Medicine*, vol. 350, pp. 2461–2470, 2004.

[9] E.-L. Tan, S.-C. Peh, and C.-K. Sam, "Analyses of Epstein-Barr virus latent membrane protein-1 in Malaysian nasopharyngeal carcinoma: high prevalence of 30-bp deletion, Xho1 polymorphism and evidence of dual infections," *Journal of Medical Virology*, vol. 69, no. 2, pp. 251–257, 2003.

[10] W.-H. Jia, X.-Y. Luo, B.-J. Feng et al., "Traditional Cantonese diet and nasopharyngeal carcinoma risk: a large-scale case-control study in Guangdong, China," *BMC Cancer*, vol. 10, article 446, 2010.

[11] E. E. Vokes, D. N. Liebowitz, and R. R. Weichselbaum, "Nasopharyngeal carcinoma," *The Lancet*, vol. 350, no. 9084, pp. 1087–1091, 1997.

[12] J. Polesel, S. Franceschi, R. Talamini et al., "Tobacco smoking, alcohol drinking, and the risk of different histological types of nasopharyngeal cancer in a low-risk population," *Oral Oncology*, vol. 47, no. 6, pp. 541–545, 2011.

[13] A. W. M. Lee, Y. F. Poon, W. Foo et al., "Retrospective analysis of 5037 patients with nasopharyngeal carcinoma treated during 1976–1985: overall survival and patterns of failure," *International Journal of Radiation Oncology Biology Physics*, vol. 23, no. 2, pp. 261–270, 1992.

[14] J. S. Mattick, "The genetic signatures of noncoding RNAs," *PLoS Genetics*, vol. 5, Article ID e1000459, 2009.

[15] K. V. Prasanth and D. L. Spector, "Eukaryotic regulatory RNAs: an answer to the "genome complexity" conundrum," *Genes & Development*, vol. 21, no. 1, pp. 11–42, 2007.

[16] J. S. Mattick and I. V. Makunin, "Non-coding RNA," *Human Molecular Genetics*, vol. 15, pp. R17–R29, 2006.

[17] M. Chaudhary, S. Gupta, S. Khare, and S. Lal, "Diagnosis of tuberculosis in an era of HIV pandemic: a review of current status and future prospects," *Indian Journal of Medical Microbiology*, vol. 28, no. 4, pp. 281–289, 2010.

[18] A. Gabory, M.-A. Ripoche, T. Yoshimizu, and L. Dandolo, "The H19 gene: regulation and function of a non-coding RNA," *Cytogenetic and Genome Research*, vol. 113, no. 1–4, pp. 188–193, 2006.

[19] S. Lottin, E. Adriaenssens, T. Dupressoir et al., "Overexpression of an ectopic H19 gene enhances the tumorigenic properties of breast cancer cells," *Carcinogenesis*, vol. 23, no. 11, pp. 1885–1895, 2002.

[20] J. E. Wilusz, H. Sunwoo, and D. L. Spector, "Long noncoding RNAs: functional surprises from the RNA world," *Genes & Development*, vol. 23, no. 13, pp. 1494–1504, 2009.

[21] P. P. Amaral and J. S. Mattick, "Noncoding RNA in development," *Mammalian Genome*, vol. 19, no. 7-8, pp. 454–492, 2008.

[22] M. E. Dinger, P. P. Amaral, T. R. Mercer, and J. S. Mattick, "Pervasive transcription of the eukaryotic genome: functional indices and conceptual implications," *Briefings in Functional Genomics and Proteomics*, vol. 8, no. 6, Article ID elp038, pp. 407–423, 2009.

[23] M. Guttman, I. Amit, M. Garber et al., "Chromatin signature reveals over a thousand highly conserved large non-coding RNAs in mammals," *Nature*, vol. 458, no. 7235, pp. 223–227, 2009.

[24] T. R. Mercer, M. E. Dinger, and J. S. Mattick, "Long non-coding RNAs: insights into functions," *Nature Reviews Genetics*, vol. 10, no. 3, pp. 155–159, 2009.

[25] J. Zhao, B. K. Sun, J. A. Erwin, J.-J. Song, and J. T. Lee, "Polycomb proteins targeted by a short repeat RNA to the mouse X chromosome," *Science*, vol. 322, no. 5902, pp. 750–756, 2008.

[26] O. Wapinski and H. Y. Chang, "Long noncoding RNAs and human disease," *Trends in Cell Biology*, vol. 21, no. 6, pp. 354–361, 2011.

[27] M. Huarte and J. L. Rinn, "Large non-coding RNAs: missing links in cancer?" *Human Molecular Genetics*, vol. 19, no. 2, pp. R152–R161, 2010.

[28] K. L. Yap, S. Li, A. M. Muñoz-Cabello et al., "Molecular interplay of the noncoding RNA *ANRIL* and methylated histone H3 lysine 27 by polycomb CBX7 in transcriptional silencing of *INK4a*," *Molecular Cell*, vol. 38, no. 5, pp. 662–674, 2010.

[29] Y. Nie, X. Liu, S. Qu, E. Song, H. Zou, and C. Gong, "Long non-coding RNA *HOTAIR* is an independent prognostic marker for nasopharyngeal carcinoma progression and survival," *Cancer Science*, vol. 104, no. 4, pp. 458–464, 2013.

[30] V. Tripathi, J. D. Ellis, Z. Shen et al., "The nuclear-retained noncoding RNA MALAT1 regulates alternative splicing by modulating SR splicing factor phosphorylation," *Molecular Cell*, vol. 39, no. 6, pp. 925–938, 2010.

[31] T. Hung, Y. Wang, M. F. Lin et al., "Extensive and coordinated transcription of noncoding RNAs within cell-cycle promoters," *Nature Genetics*, vol. 43, no. 7, pp. 621–629, 2011.

[32] A. Ng, J. P. Tang, C. H. K. Goh, and K. M. Hui, "Regulation of the H19 imprinting gene expression in human nasopharyngeal carcinoma by methylation," *International Journal of Cancer*, vol. 104, no. 2, pp. 179–187, 2003.

[33] W. Zhang, C. Huang, Z. Gong et al., "Expression of LINC00312, a long intergenic non-coding RNA, is negatively correlated with tumor size but positively correlated with lymph node metastasis in nasopharyngeal carcinoma," *Journal of Molecular Histology*, vol. 44, pp. 545–554, 2013.

[34] W. Gao, J. Y. Chan, and T.-S. Wong, "Differential expression of long noncoding RNA in primary and recurrent nasopharyngeal carcinoma," *BioMed Research International*, vol. 2014, Article ID 404567, 9 pages, 2014.

[35] E. A. Gibb, C. J. Brown, and W. L. Lam, "The functional role of long non-coding RNA in human carcinomas," *Molecular Cancer*, vol. 10, article 38, 2011.

[36] J. L. Rinn, M. Kertesz, J. K. Wang et al., "Functional demarcation of active and silent chromatin domains in human HOX loci by noncoding RNAs," *Cell*, vol. 129, no. 7, pp. 1311–1323, 2007.

[37] U. A. Ørom, T. Derrien, M. Beringer et al., "Long noncoding RNAs with enhancer-like function in human cells," *Cell*, vol. 143, no. 1, pp. 46–58, 2010.

[38] A. M. Khalil, M. Guttman, M. Huarte et al., "Many human large intergenic noncoding RNAs associate with chromatin-modifying complexes and affect gene expression," *Proceedings of the National Academy of Sciences of the United States of America*, vol. 106, no. 28, pp. 11667–11672, 2009.

[39] T. Chiyomaru, S. Yamamura, S. Fukuhara et al., "Genistein inhibits prostate cancer cell growth by targeting miR-34a and oncogenic HOTAIR," *PLoS ONE*, vol. 8, Article ID e70372, 2013.

[40] J. Chou, Y.-C. Lin, J. Kim et al., "Nasopharyngeal carcinoma—review of the molecular mechanisms of tumorigenesis," *Head and Neck*, vol. 30, no. 7, pp. 946–963, 2008.

[41] K. Panzitt, M. M. O. Tschernatsch, C. Guelly et al., "Characterization of HULC, a novel gene with striking up-regulation in hepatocellular carcinoma, as noncoding RNA," *Gastroenterology*, vol. 132, no. 1, pp. 330–342, 2007.

[42] X. Zhang, Y. Zhou, K. R. Mehta et al., "A pituitary-derived MEG3 isoform functions as a growth suppressor in tumor cells," *Journal of Clinical Endocrinology & Metabolism*, vol. 88, no. 11, pp. 5119–5126, 2003.

[43] W. Yu, D. Gius, P. Onyango et al., "Epigenetic silencing of tumour suppressor gene p15 by its antisense RNA," *Nature*, vol. 451, no. 7175, pp. 202–206, 2008.

[44] N. Popov and J. Gil, "Epigenetic regulation of the *INK4B-ARF-INK4a* locus: in sickness and in health," *Epigenetics*, vol. 5, no. 8, pp. 685–690, 2010.

[45] K.-C. Huang, P. H. Rao, C. C. Lau et al., "Relationship of XIST expression and responses of ovarian cancer to chemotherapy," *Molecular Cancer Therapeutics*, vol. 1, no. 10, pp. 769–776, 2002.

[46] S. M. Sirchia, S. Tabano, L. Monti et al., "Misbehaviour of *XIST* RNA in breast cancer cells," *PLoS ONE*, vol. 4, Article ID e5559, 2009.

[47] P. Ji, S. Diederichs, W. Wang et al., "MALAT-1, a novel noncoding RNA, and thymosin β4 predict metastasis and survival in early-stage non-small cell lung cancer," *Oncogene*, vol. 22, no. 39, pp. 8031–8041, 2003.

[48] A. Guffanti, M. Iacono, P. Pelucchi et al., "A transcriptional sketch of a primary human breast cancer by 454 deep sequencing," *BMC Genomics*, vol. 10, article 163, 2009.

[49] K. Yamada, J. Kano, H. Tsunoda et al., "Phenotypic characterization of endometrial stromal sarcoma of the uterus," *Cancer Science*, vol. 97, no. 2, pp. 106–112, 2006.

[50] R. Lin, S. Maeda, C. Liu, M. Karin, and T. S. Edgington, "A large noncoding RNA is a marker for murine hepatocellular carcinomas and a spectrum of human carcinomas," *Oncogene*, vol. 26, no. 6, pp. 851–858, 2007.

[51] J.-H. Luo, B. Ren, S. Keryanov et al., "Transcriptomic and genomic analysis of human hepatocellular carcinomas and hepatoblastomas," *Hepatology*, vol. 44, no. 4, pp. 1012–1024, 2006.

[52] J. Lu, G. Getz, E. A. Miska et al., "MicroRNA expression profiles classify human cancers," *Nature*, vol. 435, no. 7043, pp. 834–838, 2005.

[53] S.-L. Yu, H.-Y. Chen, G.-C. Chang et al., "MicroRNA signature predicts survival and relapse in lung cancer," *Cancer Cell*, vol. 13, no. 1, pp. 48–57, 2008.

[54] C. J. Woo and R. E. Kingston, "HOTAIR lifts noncoding RNAs to new levels," *Cell*, vol. 129, no. 7, pp. 1257–1259, 2007.

[55] K. Kim, I. Jutooru, G. Chadalapaka et al., "HOTAIR is a negative prognostic factor and exhibits pro-oncogenic activity in pancreatic cancer," *Oncogene*, vol. 32, no. 13, pp. 1616–1625, 2013.

[56] X.-B. Lv, G.-Y. Lian, H.-R. Wang, E. Song, H. Yao, and M.-H. Wang, "Long noncoding RNA HOTAIR is a prognostic marker for esophageal squamous cell carcinoma progression and survival," *PLoS ONE*, vol. 8, Article ID e63516, 2013.

[57] O. Lustig, I. Ariel, J. Ilan, E. Lev-Lehman, N. de-Groot, and A. Hochberg, "Expression of the imprinted gene H19 in the human fetus," *Molecular Reproduction and Development*, vol. 38, no. 3, pp. 239–246, 1994.

[58] I. Ariel, N. de Groot, and A. Hochberg, "Imprinted H19 gene expression in embryogenesis and human cancer: the oncofetal connection," *The American Journal of Medical Genetics*, vol. 91, pp. 46–50, 2000.

[59] K. Hashimoto, C. Azuma, Y. Tokugawa et al., "Loss of *H19* imprinting and up-regulation of *H19* and *SNRPN* in a case with malignant mixed müllerian tumor of the uterus," *Human Pathology*, vol. 28, no. 7, pp. 862–865, 1997.

[60] K. Hibi, H. Nakamura, A. Hirai et al., "Loss of *H19* imprinting in esophageal cancer," *Cancer Research*, vol. 56, no. 3, pp. 480–482, 1996.

[61] Y. Fellig, I. Ariel, P. Ohana et al., "*H19* expression in hepatic metastases from a range of human carcinomas," *Journal of Clinical Pathology*, vol. 58, no. 10, pp. 1064–1068, 2005.

Hindawi Publishing Corporation
BioMed Research International
Volume 2015, Article ID 670691, 13 pages
http://dx.doi.org/10.1155/2015/670691

Review Article

Statistical Methods for Establishing Personalized Treatment Rules in Oncology

Junsheng Ma, Brian P. Hobbs, and Francesco C. Stingo

Department of Biostatistics, The University of Texas MD Anderson Cancer Center, Unit 1411, 1400 Pressler Street, Houston, TX 77030, USA

Correspondence should be addressed to Francesco C. Stingo; fstingo@mdanderson.org

Received 25 November 2014; Accepted 9 February 2015

Academic Editor: Aurelio Ariza

The process for using statistical inference to establish personalized treatment strategies requires specific techniques for data-analysis that optimize the combination of competing therapies with candidate genetic features and characteristics of the patient and disease. A wide variety of methods have been developed. However, heretofore the usefulness of these recent advances has not been fully recognized by the oncology community, and the scope of their applications has not been summarized. In this paper, we provide an overview of statistical methods for establishing optimal treatment rules for personalized medicine and discuss specific examples in various medical contexts with oncology as an emphasis. We also point the reader to statistical software for implementation of the methods when available.

1. Introduction

Cancer is a set of diseases characterized by cellular alterations the complexity of which is defined at multiple levels of cellular organization [1, 2]. Personalized medicine attempts to combine a patient's genomic and clinical characteristics to devise a treatment strategy that exploits current understanding of the biological mechanisms of the disease [3, 4]. Recently the field has witnessed successful development of several molecularly targeted medicines, such as Trastuzumab, a drug developed to treat breast cancer patients with *HER2* amplification and overexpression [5, 6]. However, successes have been limited. Only 13% of cancer drugs that initiated phase I from 1993 to 2004 attained final market approval by the US Food and Drug Administration (FDA) [7]. Moreover, from 2003 to 2011, 71.7% of new agents failed in phase II, and only 10.5% were approved by the FDA [8]. The low success rate can be partially explained by inadequate drug development strategies [3] and an overreliance on univariate statistical models that fail to account for the joint effects of multiple candidate genes and environmental exposures [9]. For example, in colorectal cancer there have been numerous attempts to develop treatments that target a single mutation, yet only one, an EGFR-targeted therapy for metastatic disease, is currently used in clinical practice [10].

In oncology, biomarkers are typically classified as either predictive or prognostic. Prognostic biomarkers are correlates for the extent of disease or extent to which the disease is curable. Therefore, prognostic biomarkers impact the likelihood of achieving a therapeutic response regardless of the type of treatment. By way of contrast, predictive biomarkers select patients who are likely or unlikely to benefit from a particular class of therapies [3]. Thus, predictive biomarkers are used to guide treatment selection for individualized therapy based on the specific attributes of a patient's disease. For example, BRAF V600-mutant is a widely known predictive biomarker which is used to guide the selection of Vemurafenib for treatment metastatic melanoma [11]. Biomarkers need not derive from single genes as those aforementioned and yet may arise from the combination of a small set of genes or molecular subtypes obtained from global gene expression profiles [6]. Recently, studies have shown that the Oncotype DX recurrence score, which is based on 21 genes, can predict a woman's therapeutic response to adjuvant chemotherapy for estrogen receptor-positive tumors [12, 13]. Interestingly, Oncotype DX was originally developed as a

prognostic biomarker. In fact, prognostic gene expression signatures are fairly common in breast cancer [12, 14]. The reader may note that Oncotype DX was treated as a single biomaker and referred to as a gene expression based predictive classifier [3].

Statistically, predictive associations are identified using models with an interaction between a candidate biomarker and targeted therapy [15], whereas prognostic biomarkers are identified as significant main effects [16]. Thus, analysis strategies for identifying prognostic markers are often unsuitable for personalized medicine [17, 18]. In fact, the discovery of predictive biomarkers requires specific statistical techniques for data-analysis that optimize the combination of competing therapies with candidate genetic features and characteristics of the patient and disease. Recently, many statistical approaches have been developed providing researchers with new tools for identifying potential biomarkers. However, the usefulness of these recent advances has not been fully recognized by the oncology community, and the scope of their applications has not been summarized.

In this paper, we provide an overview of statistical methods for establishing optimal treatment rules for personalized medicine and discuss specific examples in various medical contexts with oncology as an emphasis. We also point the reader to statistical software when available. The various approaches enable investigators to ascertain the extent to which one should expect a new untreated patient to respond to each candidate therapy and thereby select the treatment that maximizes the expected therapeutic response for the specific patient [3, 19]. Section 2 discusses the limitations of conventional approaches based on post hoc stratified analysis. Section 3 offers an overview of the process for the development of personalized regimes. Section 4 discusses the selection of an appropriate statistical method for different types of clinical outcomes and data sources. Section 5 presents technical details for deriving optimal treatment selection rules. In Section 6, we discuss approaches for evaluating model performance and assessing the extent to which treatment selection using the derived optimal rule is likely to benefit future patients.

2. Limitations of Subgroup Analysis

Cancer is an inherently heterogeneous disease. Yet, often efforts to personalize therapy rely on the application of analysis strategies that neglect to account for the extent of heterogeneity intrinsic to the patient and disease and therefore are too reductive for personalizing treatment in many areas of oncology [20–23]. Subgroup analysis is often used to evaluate treatment effects among stratified subsets of patients defined by one or a few baseline characteristics [23–26]. For example, Thatcher et al. [21] conducted a series of preplanned subgroup analyses for refractory advanced non-small-cell lung cancer patients treated with Gefitinib plus best supportive care against placebo. Heterogeneous treatment effects were found in subgroups defined by smoking status; that is, significant prolonged survival was observed for nonsmokers, while no treatment benefit was found for smokers.

Though very useful when well planned and properly conducted, the reliance on subgroup analysis for developing personalized treatment has been criticized [24, 25]. Obviously, a subgroup defined by a few factors is inadequate for characterizing individualized treatment regimes that depends on multivariate synthesis. Moreover, post hoc implementation of multiple subgroup analyses considers a set of statistical inferences simultaneously (multiple testing), and errors, such as incorrectly rejecting the null hypothesis, are likely to occur. The extent to which the resulting inference inflates the risk of a false positive finding can be dramatic [23]. Take, for example, a recent study that concluded that chemotherapy followed by tamoxifen promises substantial clinical benefit for postmenopausal women with ER negative, lymph node-negative breast cancer [27] through post hoc application subgroup analysis. Subsequent studies failed to reproduce this result, concluding instead that the regime's clinical effects were largely independent of ER status [28], but may depend on other factors including age.

3. Personalized Medicine from a Statistical Perspective

From a statistical perspective, personalized medicine is a process involving six fundamental steps provided in Figure 1 [20, 29, 30]. Intrinsic to any statistical inference, initially one must select an appropriate method of inference based on the available source of training data and clinical endpoints (e.g., steps (1) and (2)). Step (3) is the fundamental component of personalized treatment selection, deriving the individualized treatment rule (ITR) for the chosen method of inference. An ITR is a decision rule that identifies the optimal treatment given patient/disease characteristics [31, 32]. Section 5 is dedicated to the topic of establishing ITRs for various statistical models and types of clinical endpoints that are commonly used to evaluate treatment effectiveness in oncology.

Individualized treatment rules are functions of model parameters (usually treatment contrasts reflecting differences in treatment effects) which must be estimated from the assumed statistical model and training data. Statistical estimation takes place in step 4. The topic is quite general, and it thus is not covered in detail owning to the fact that other authors have provided several effective expositions on model building strategies in this context [29, 33]. After estimating the optimal treatment rule in step (4), the resulting estimated ITR's performance and reliability must be evaluated before the model can be used to guide treatment selection [34]. The manner in which one assesses the performance of the derived ITR depends on the appropriate clinical utility (i.e., increased response rate or prolonged survival duration). Evaluation of model goodness-of-fit and appropriate summary statistics that use the available information to measure the extent to which future patients would benefit from application of the ITR is conducted in step (5) and will be discussed in Section 6. The ITR is applied to guide treatment selection for a future patient based on his/her baseline clinical and genetic characteristics as the final step.

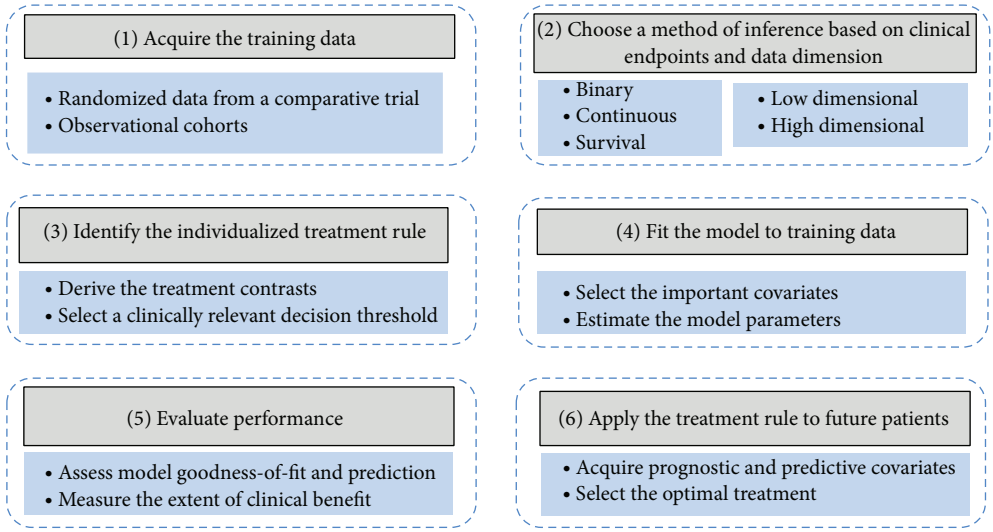

Figure 1: The process for using statistical inference to establish personalized treatment rules.

4. Selecting an Appropriate Method of Inference

The quality of a treatment rule depends on the aptness of the study design used to acquire the training data, clinical relevance of the primary endpoints, statistical analysis plans for model selection and inference, and quality of the data. *Randomized clinical trials* (RCT) remain the gold standard study design for treatment comparison, since randomization mitigates bias arising from treatment selection. Methods for deriving ITRs using data from RCTs are described in Section 5.1. Data from well conducted observational studies provide useful sources of information as well, given that the available covariates can be used to account for potential sources of confounding due to selection bias. Predominately, methods based on propensity scores are used to adjust for confounding [35, 36]. Approaches for establishing ITRs using observational studies are discussed in Section 5.2.

The predominate statistical challenge pertaining to the identification of predictive biomarkers is the high-dimensional nature of molecular derived candidate features. Classical regression models cannot be directly applied since the number of covariates, for example, genes, is much larger than number of samples. Many approaches have been proposed to analyze high-dimensional data for prognostic biomarkers. Section 5.3 discusses several that can be applied to detect predictive biomarkers under proper modification.

In oncology, several endpoints are used to compare clinical effectiveness. However, the primary therapeutic goal is to extend survivorship or delay recurrence/progression. Thus, time-to-event endpoints are often considered to be the most representative of clinical effectiveness [37]. The approaches aforementioned were developed for ordinal or continuous outcomes and were thus not directly applicable for survival analysis. Methods for establishing ITRs from time-to-event endpoints often use Cox regression or accelerated failure time models [38, 39]. The later approach is particularly appealing in this context since the clinical benefits of prolonged survival time can be easily obtained [40, 41]. In Section 5.4, we will discuss both models.

The performance of ITRs for personalized medicine is highly dependent upon the extent to which the model assumptions are satisfied and/or the posited model is correctly specified. Specifically, performances may suffer from misspecification of main effects and/or interactions, random error distribution, violation of linear assumptions, sensitivity to outliers, and other potential sources of inadequacy [42]. Some advanced methodologies have been developed to overcome these issues [43], including semiparametric approaches that circumvent prespecification of the functional form of the relationship between biomarker and expected clinical response [32, 40]. In addition, optimal treatment rules can be defined without regression models, using classification approaches where patients are assigned to the treatment that provides the highest expected clinical benefit. Appropriate class labels can be defined by the estimated treatment difference (e.g., >0 versus ≤ 0), thereby enabling the use of machine learning and data mining techniques [42, 44, 45]. These will be discussed in Section 5.5.

5. Methods for Identifying Individualized Treatment Rules

This section provides details of analytical approaches that are appropriate identifying ITRs using a clinical data source. The very nature of treatment benefit is determined by the clinical endpoint. While extending overall survival is the ultimate therapeutic goal, often the extent of reduction in tumor size as assessed by RECIST criteria (http://www.recist.com/) is used as a categorical surrogate for long-term response. Alternatively, oncology trials often compare the extent to which the treatment delays locoregional recurrence or disease progression. Therefore, time-to-event and binary (as in absence/presence of partial or complete response) are the

most commonly used endpoints in oncologic drug development [37, 46].

Let Y denote the observed outcome such as survival duration or response to the treatment, and let $A \in \{0, 1\}$ denote the treatment assignment with 0 indicating standard treatment and 1 for a new therapy. Denote the collection of observable data for a previously treated patient by $(Y, A, \mathbf{X})$, where $\mathbf{X} = X_1, X_2, \ldots, X_p$, represents a vector of values for the p biomarkers under study. Quantitatively, the optimal ITR derives from the following equation relating the observed response to the potential outcome attained under the alternative treatment

$$Y = AY^{(1)} + (1 - A)\, Y^{(0)}, \tag{1}$$

where $Y^{(1)}$ and $Y^{(0)}$ denote the potential outcomes that would be observed if the subject had been assigned to the new therapy or the standard treatment, respectively [32, 43]. Let $E(Y \mid A, \mathbf{X}) = \mu(A, \mathbf{X})$ denote the expected value of Y given A and $\mathbf{X}$. The optimal treatment rule follows as

$$g^{\text{opt}}(\mathbf{X}) = I\left\{\mu(A = 1, \mathbf{X}) - \mu(A = 0, \mathbf{X}) > 0\right\}, \tag{2}$$

where $I(\cdot)$ is the indicator function. For instance, if $I\{\mu(1, \text{age} > 50) - \mu(0, \text{age} > 50) > 0\} = 1$, then the optimal rule would assign patients who are older than 50 to the new treatment. However, $E(Y \mid A, \mathbf{X})$ is actually a function of parameters, $\mu(A, \mathbf{X}; \boldsymbol{\beta})$, denoted by $\boldsymbol{\beta}$. The model needs to be "fitted" to the training data to obtain estimates of $\boldsymbol{\beta}$, which we denote by $\widehat{\boldsymbol{\beta}}$. Hence for a patient with observed biomarkers $\mathbf{X} = \mathbf{x}$, the estimated optimal treatment rule is

$$\begin{aligned}\widehat{g}^{\text{opt}}\left(\mathbf{X} = \mathbf{x}, \widehat{\boldsymbol{\beta}}\right) \\ = I\left\{\mu\left(A = 1, \mathbf{X} = \mathbf{x}; \widehat{\boldsymbol{\beta}}\right) - \mu\left(A = 0, \mathbf{X} = \mathbf{x}; \widehat{\boldsymbol{\beta}}\right)\right\}.\end{aligned} \tag{3}$$

The above equation pertains to steps (3) and (4) in Figure 1; that is, the parameter estimates from a fitted model are used to construct the personalized treatment rule. The remainder of this section instructs the readers how to identify ITRs for the various data types.

We classify the statistical methods presented in this section into five categories: methods based on multivariate and generalized linear regression for analysis of data acquired from RCT (Section 5.1) and observational studies (Section 5.2); methods based on penalized regression techniques for high-dimensional data (Section 5.3); methods for survival data (Section 5.4); and advanced methods based on robust estimation and machine learning techniques (Section 5.5).

5.1. Multiple Regression for Randomized Clinical Trial Data. Classical generalized linear models (GLM) can be used to develop ITRs in the presence of training data derived from randomized clinical study. The regression framework assumes that the outcome Y is a linear function of prognostic covariates, X_1; putative predictive biomarkers, X_2; the treatment indicator, A; and treatment-by-predictive interaction, AX_2:

$$\begin{aligned}\mu(A, \mathbf{X}) &= E(Y \mid A, \mathbf{X}) \\ &= \beta_0 + \beta_1 X_1 + \beta_2 X_2 + A\left(\beta_3 + \beta_4 X_2\right).\end{aligned} \tag{4}$$

Let $\Delta(\mathbf{X}) = E(Y \mid A = 1, X) - E(Y \mid A = 0, X) = \mu(A = 1, X) - \mu(A = 0, X)$ denote the treatment contrast. The optimal treatment rule assigns a patient to the new treatment if $\Delta(\mathbf{X}) > 0$. For binary endpoints, the logistic regression model for $\mu(A, \mathbf{X}) = P(Y = 1 \mid A, \mathbf{X})$ is defined such that

$$\begin{aligned}\log\left\{\frac{\mu(A, \mathbf{X})}{1 - \mu(A, \mathbf{X})}\right\} &= \omega(A, \mathbf{X}) \\ &= \beta_0 + \beta_1 X_1 + \beta_2 X_2 + A\left(\beta_3 + \beta_4 X_2\right).\end{aligned} \tag{5}$$

The treatment contrast $\Delta(\mathbf{X})$ can be calculated using $E(Y \mid A = a, X) = P(Y = 1 \mid A = a, \mathbf{X}) = e^{\omega(A,\mathbf{X})}/(1 + e^{\omega(A,\mathbf{X})})$ for $a = 0, 1$, respectively. Similarly, an optimal ITR assigns a patient to the new treatment if $\Delta(\mathbf{X}) > 0$. This optimal treatment rule can be alternatively defined as $g^{\text{opt}}(\mathbf{X}) = I\{(\beta_3 + \beta_4 X_2) > 0\}$ without the need to calculate the treatment contrast $\Delta(\mathbf{X})$ [43, 45].

Often one might want to impose a clinically meaningful minimal threshold, $\Delta(\mathbf{X}) > \delta$, on the magnitude of treatment benefit before assigning patients to a novel therapy [45, 47]. For example, it may be desirable to require at least a 0.1 increase in response rate before assigning a therapy for which the long-term safety profile has yet to be established. The use of a threshold value can be applied to all methods. Without loss of generality, we assume $\delta = 0$ unless otherwise specified. In addition, the reader should note that the approaches for constructing an ITR described above can be easily applied to linear regression models for continuous outcomes.

This strategy was used to develop an ITR for treatment of depression [19] using data collected from a RCT of 154 patients. In this case, the continuous outcome was based on posttreatment scores from the Hamilton Rating Scale for Depression. The authors constructed a personalized advantage index using the estimated treatment contrasts $\Delta(\mathbf{X})$, derived from five predictive biomarkers. A clinically significant threshold was selected, $\delta = 3$, based on the National Institute for Health and Care Excellence criterion. The authors identified that 60% of patients in the sample would obtain a clinically meaningful advantage if their therapy decision followed the proposed treatment rule. The approaches discussed in this section can be easily implemented with standard statistical software, such as the *R* (http://www.r-project.org/) using the functions *lm* and *glm* [48].

5.2. Methods for Observational Data. Randomization attenuates bias arising from treatment selection, thereby providing the highest quality data for comparing competing interventions. However, due to ethical or financial constraints RCTs are often infeasible, thereby necessitating an observational study. Treatment selection is often based on a patient's prognosis. In the absence of randomization, the study design fails to ensure that patients on competing arms exhibit similar clinical and prognostic characteristics, thereby inducing bias.

However, in the event that the available covariates capture the sources of bias, a well conducted observational study can also provide useful information for constructing ITRs. For example, the two-gene ratio index (HOXB13:IL17BR)

was first discovered as an independent prognostic biomarker for ER+ node-negative patients using retrospective data from 60 patients [49]. These findings were confirmed on an independent data set comprising 852 tumors, which was acquired from a tumor bank at the Breast Center of Baylor College of Medicine [50]. Interestingly, the two-gene ratio index (HOXB13:IL17BR) was reported to predict the benefit of treatment with letrozole in one recent independent study [51].

Methods based on propensity scores are commonly used to attenuate selection bias [35]. In essence, these approaches use the available covariates to attempt to diminish the effects of imbalances among variables that are not of interest for treatment comparison. Moreover, they have been shown to be robust in the presence of multiple confounders and rare events [52]. Generally, after adjusting for bias using propensity scores, the same principles for deriving ITRs from RCTs may be applied to the observational cohort.

The propensity score characterizes the probability of assigning a given treatment A from the available covariates, $\mathbf{X}$ [35]. Using our notation, the propensity score is $\pi(\mathbf{X}, \boldsymbol{\xi}) = P(A = 1 \mid \mathbf{X}, \boldsymbol{\xi})$, which can be modeled using logistic regression

$$\log\left\{\frac{\pi(\mathbf{X})}{1-\pi(\mathbf{X})}\right\} = \xi_0 + \xi_1 X_1 + \xi_2 X_2 + \xi_3 X_3 + \cdots + \xi_p X_p, \tag{6}$$

where p is the number of independent variables used to construct the propensity score and ξ_j represents the jth regression coefficient, which characterizes the jth covariate's partial effect. After fitting the data to obtain estimates for the regression coefficients, $\widehat{\boldsymbol{\xi}}$, the estimated probability of receiving new treatment can be obtained for each patient, $\widehat{\pi}(\mathbf{X_i}) = \pi(\mathbf{X_i}, \widehat{\boldsymbol{\xi}})$, by inverting the logit function. The event that $\widehat{\boldsymbol{\xi}} \approx \mathbf{0}$ implies that the measured independent variables are reasonably "balanced" between treatment cohorts. In practice, one often includes as many baseline covariates into the propensity score model as permitted by the sample size.

Methods that use propensity scores can be categorized into four categories: matching, stratification, adjusting, and inverse probability weighted estimation [36, 53]. Matching and stratification aim to mimic RCTs by defining a new dataset using propensity scores such that outcomes are directly comparable between treatment cohorts [53]. These two approaches are well suited for conventional subgroup analysis but their application to personalized medicine has been limited. Regression adjustment or simply adjusting can be used to reduce bias due to residual differences in observed baseline covariates between treatment groups. This method incorporates the propensity scores as an independent variable in a regression model and therefore can be used in conjunction with all regression-based methods [36]. Methods involving inverse probability weighted estimators will be discussed in Section 5.5.1 [43].

Of course, propensity scores methods may only attenuate the effects of the important confounding variables that have been acquired by the study design. Casual inference in general is not robust to the presence of unmeasured confounders that influenced treatment assignment [35, 54, 55]. For the development of ITRs, predictive and important prognostic covariates can be incorporated in the regression model for the clinical outcome Y along with the propensity scores, while other covariates may be utilized only in the model for estimating the propensity scores. Hence, propensity score methods may offer the researcher a useful tool for controlling for potential confounding due to selection bias and maintaining a manageable number of prognostic and predictive covariates.

5.3. Methods for High-Dimensional Biomarkers. The methods presented in the previous sections are appropriate for identifying an ITR using a small set of biomarkers (low-dimensional). However, recent advances in molecular biology in oncology have enabled researchers to acquire vast amounts of genetic and genomic characteristics on individual patients. Often the number of acquired genomic covariates will exceed the sample size. Proper analysis of these high-dimensional data sources poses many analytical challenges. Several methods have been proposed specifically for analysis of high-dimensional covariates [56], although the majority of these methods are well suited only for the analysis of prognostic biomarkers. In what follows, we introduce variable selection methods that were developed to detect predictive biomarkers from high-dimensional sources as well as describing how to construct optimal ITRs from the final set of biomarkers.

An appropriate regression model can be defined generally as $E(Y \mid A, \mathbf{X}) = h_0(\mathbf{X}) + A(\widetilde{\mathbf{X}}\boldsymbol{\beta})$, where $h_0(\mathbf{X})$ is an unspecified baseline mean function, $\boldsymbol{\beta} = (\beta_0, \beta_1, \ldots, \beta_q)^T$ is a column vector of regression coefficients, and $\widetilde{\mathbf{X}} = (1, \mathbf{X})$ the design matrix. Subscript q denotes the total number of biomarkers, which may be larger than the sample size n. An ITR derives from evaluating the interactions in $A(\widetilde{\mathbf{X}}\boldsymbol{\beta})$, not the baseline effect of the high-dimensional covariates $h_0(\mathbf{X})$ [32]. Technically, function $A(\widetilde{\mathbf{X}}\boldsymbol{\beta}) = A(\beta_0 + \beta_1 X_1 + \beta_2 X_2 + \cdots + \beta_q X_q)$ cannot be uniquely estimated using traditional maximum likelihood-based methods when $q > n$ [57]. Yet, practically, many of the available biomarkers may not influence the optimal ITR [31]. Thus, the process for identify ITRs from a high-dimensional source requires that we first identify a sparse subset of predictive biomarkers that can be utilized for constructing the ITR.

Parameters for the specified model can be estimated using the following loss function:

$$L_{n,\phi}(\boldsymbol{\beta}, \boldsymbol{\gamma}) = \frac{1}{n}\sum_{i=1}^{n}\left[Y_i - \phi(\mathbf{X}_i; \boldsymbol{\gamma}) - \widetilde{\mathbf{X}}\boldsymbol{\beta}\{A_i - \pi(\mathbf{X}_i)\}\right]^2, \tag{7}$$

where $\phi(\mathbf{X}; \boldsymbol{\gamma})$ represents any arbitrary function characterizing the "baseline" relationship between $\mathbf{X}$ and $\mathbf{Y}$ (e.g., an intercept or an additive model). Here we let $\pi(\mathbf{X}_i) = P(A_i = 1 \mid \mathbf{X}_i)$ denote either a propensity score (for observational data) or a randomization probability (e.g., 0.5 given 1:1 randomization) for RCT data. If $\pi(\mathbf{X})$ is known, estimation using this model yields unbiased estimates (asymptotically consistent) of the interaction effects $\boldsymbol{\beta}$ even if the main effects are not correctly specified, providing a robustness [32].

Penalized estimation provides the subset of relevant predictive markers that are extracted from the nonzero coefficients of the corresponding treatment-biomarker interaction terms of

$$\widehat{\boldsymbol{\beta}} = \arg\min_{\boldsymbol{\beta}} \left\{ L_{n,\phi}(\boldsymbol{\beta}, \boldsymbol{\gamma}) + \lambda_n \sum_{j=1}^{p+1} J\left|\beta_j\right| \right\}, \tag{8}$$

where λ_n is a tuning parameter which is often selected via cross validation and J is a shrinkage penalty. Different choices of J lead to different types of estimators. For example, the lasso penalized regression corresponds to $J = 1$ [58] and the adaptive lasso to $J = \omega_j = 1/|\widehat{\beta}_{\text{init},j}|$, where $\widehat{\beta}_{\text{init},j}$ is an initial estimate of β_j [59]. With little modification, (8) can be solved using the LARS algorithm implemented with the *R* package of *lars* [32, 60, 61]. As we have shown before, a treatment rule can be defined from the parameter estimates as $I\{\beta_0 + \beta_1 X_1 + \beta_2 X_2 + \cdots + \beta_q X_q > 0\}$. *Note* this generic form may have zero estimates for some coefficients (e.g., $\widehat{\beta}_2 = \widehat{\beta}_5 = \cdots = \widehat{\beta}_q = 0$); hence an ITR can be equivalently constructed from the final estimated nonzero coefficients and the corresponding covariates.

Alternative penalized regression approaches include SCAD [62] and elastic-net [63]. All penalized approaches produce sparse solutions (i.e., identifying a small subset of predictive biomarkers); however the adaptive lasso is less effective when $p > n$. Methods that produce nonsparse models, such as ridge regression [57], are less preferable since ITRs based on many biomarkers are often unstable and less useful in practice [31]. Several packages in *R* offer implementation of penalized regression, such as *parcor* for ridge, lasso and adaptive lasso, and *ncvreg* for SCAD [64, 65].

Lu et al. [32] used a penalized regression approach to analyze data from the AIDS Clinical Trials Group Protocol 175 (ACTG175) [66]. In this protocol, 2,000 patients were equally randomized to one of four treatments: zidovudine (ZDV) monotherapy, ZDV + didanosine (ddI), ZDV + zalcitabine, and ddI monotherapy. CD4 count at 15–25 weeks postbaseline was the primary outcome and 12 baseline covariates were included in the analysis. The resulting treatment rule favored the combined regimes over ZDV monotherapy. Moreover, the treatment rule determined that ZDV + ddI should be preferred to ddI when $I(71.59 + 1.07 \times \text{age} - 0.18 \times \text{CD40} - 33.57 \times \text{homo}) = 1$, where CD40 represents baseline CD4 counts and homo represents homosexual activity. Based on this treatment rule, 878 patients would have benefited from treatment with ZDV + ddI.

5.4. Survival Analysis. Heretofore, we have discussed methods for continuous or binary outcomes, yet often investigators want to discern the extent to which a therapeutic intervention may alter the amount of time required before an event occurs. This type of statistical inference is referred to broadly as survival analysis. One challenge for survival analysis is that the outcomes may be only partially observable at the time of analysis due to censoring or incomplete follow-up. Survival analysis has been widely applied in cancer studies, often in association studies aimed to identify prognostic biomarkers [56, 67]. Here we discuss two widely used models for deriving ITRs using time-to-event data, namely, Cox regression and accelerated failure time models.

The Cox regression model follows as

$$\lambda(t \mid \mathbf{X}, A) = \lambda_0(t) \exp\left\{\beta_1 X_1 + \beta_2 X_2 + A(\beta_4 + \beta_5 X_2)\right\}, \tag{9}$$

where t is the survival time, $\lambda_0(t)$ is an arbitrary baseline hazard function, and X_1, X_2 represent prognostic and predictive biomarkers, respectively. Each β characterizes the multiplicative effect on the hazard associated with a unit increase in the corresponding covariate. Therefore, Cox models are referred to as proportional hazards (PH) models.

Several authors have provided model building strategies [29] and approaches for treatment selection [20, 30, 68]. Following the previously outlined strategy, a naive approach for deriving an ITR uses the hazard ratio (new treatment versus the standard) as the treatment contrast, which can be calculated as $\Delta(\mathbf{X}) = \exp(\beta_4 + \beta_5 X_2)$. The ITR therefore is $I\{(\beta_4 + \beta_5 X_2) < 0\}$. There are obvious limitations to this approach. First, violations of the PH assumption yield substantially misleading results [69]. Moreover, even when the PH assumption is satisfied, because the Cox model does not postulate a direct relationship between the covariate (treatment) and the survival time, the hazard ratio fails to measure the extent to which the treatment is clinically valuable [38, 70].

Accelerated failure time (AFT) models provide an alternative semiparametric model. Here we introduce its application for high-dimensional data. Let T and C denote the survival and censoring times, and denote the observed data by $(\widetilde{T}, \delta, A, \mathbf{X})$ where $\widetilde{T} = \min(T, C)$ and $\delta = I(T < C)$. Define the log survival time as $Y = \log(T)$; a semiparametric regression model is given as $E(Y \mid A, \mathbf{X}) = h_0(\mathbf{X}) + A(\widetilde{\mathbf{X}}\boldsymbol{\beta})$, where $h_0(\mathbf{X})$ is the unspecified baseline mean function. Similar to the previous section, the treatment rule is $I\{(\beta_0 + \beta_1 X_1 + \beta_2 X_2 + \cdots + \beta_q X_q) > 0\}$. Under the assumption of independent censoring, the AFT model parameters can be estimated by minimizing the following loss function:

$$L_{n,\phi}(\boldsymbol{\beta}) = \frac{1}{n} \sum_{i=1}^{n} \frac{\delta_i}{\widehat{G}(\widetilde{T}_i)} \left[\widetilde{Y}_i - \phi(\mathbf{X}_i; \boldsymbol{\gamma}) - \widetilde{\mathbf{X}}\boldsymbol{\beta}\{A_i - \pi(\mathbf{X}_i)\}\right]^2, \tag{10}$$

where $\widetilde{Y}_i = \log(\widetilde{T}_i)$, $\pi(\mathbf{X}_i) = P(A_i = 1 \mid \mathbf{X}_i)$ is the propensity score or randomization probability, $\widehat{G}(\cdot)$ is the Kaplan-Meier estimator of the survival function of the censoring time, and $\phi(\mathbf{X}; \boldsymbol{\gamma})$ characterizes any arbitrary function.

This method can be extended to accommodate more than two treatments simultaneously by specifying appropriate treatment indicators. For instance, the mean function can be modeled as $E(Y \mid A, \mathbf{X}) = h_0(\mathbf{X}) + A_{(1)}\{\widetilde{\mathbf{X}}\boldsymbol{\beta}_{(1)}\} + A_{(2)}\{\widetilde{\mathbf{X}}\boldsymbol{\beta}_{(2)}\}$ for two treatment drugs versus the standard care. The ITR assigns the winning drug. Note this work was proposed by [40] and is an extension of [32] to the survival setting. Hence, it shares the robustness property and can be applied to observational data. For implementation, the same procedure can be followed to obtain estimates, with one addition step of calculating $\widehat{G}(\widetilde{T}_i)$. There are several *R* packages for Kaplan-Meier

estimates and Cox regression models. These sources can be found at http://cran.r-project.org/web/views/Survival.html. More details pertaining to statistical methods for survival analysis can be found here [71]. To compare treatment rules constructed from Cox and AFT models, for example, methods for measuring the extent of clinical effectiveness for an ITR will be discussed in Section 6.

We here present an example when an AFT model was used to construct an ITR for treatment of HIV [40]. The example derives from the AIDS Clinical Trials Group Protocol 175 that was discussed in Section 5.3 [32, 66]. In this case, the primary outcome variable was time (in days) to first ≥50% decline in CD4 count or an AIDS-defining event or death. A total of 12 covariates and four treatments (ZDV, ZDV + ddI, ZDV + zalcitabine, and ddI) were included. The four treatments were evaluated simultaneously. Patients receiving the standard care of ZDV monotherapy were considered as the reference group. Hence, three treatment contrasts ($I_{\text{ZDV+ddI}}$, $I_{\text{ZDV+zalcitabine}}$, and I_{ddI}) were combined with various putative predictive covariates and compared with ZDV monotherapy. For example, gender was detected as the predictive covariate only for ddI monotherapy. The investigators assumed $\phi(\mathbf{X};\boldsymbol{\gamma}) = \gamma_0$. The treatment rule recommended 1 patient for ZDV monotherapy, while 729, 1216, and 193 patients were recommended for ZDV + ddI, ZDV + zalcitabine, and ddI, respectively.

5.5. Advanced Methods

5.5.1. Robust Inference. The performances of ITRs heretofore presented depend heavily on whether the statistical models were correctly specified. Recently there has been much attention focused on the development of more advanced methods and modeling strategies that are robust to various aspects of potential misspecification. We have already presented a few robust models that avoid specification of functional parametric relationships for main effects [32, 40]. Here, we introduce two more advanced methods widely utilized for ITRs that are robust to the type of misspecification issues commonly encountered in practice [42, 43].

Recall that the ITR for a linear model $E(Y \mid A = a, \mathbf{X}) = \mu(A = a, \mathbf{X}; \boldsymbol{\beta})$ with two predictive markers follows as $g(\mathbf{X}, \boldsymbol{\beta}) = I\{(\beta_4 + \beta_5 X_2 + \beta_6 X_3) > 0\}$, where $a = 0, 1$. The treatment rule of $g(\mathbf{X}, \boldsymbol{\beta})$ may use only a subset of the high-dimensional covariates (e.g., $\{X_2, X_3\}$), but it always depends on the correct specification of $E(Y \mid A = a, \mathbf{X})$. Defining a scaled version of β as $\eta(\beta)$, the corresponding ITR is $g(\boldsymbol{\eta}, \mathbf{X}) = g(\mathbf{X}, \boldsymbol{\beta}) = I(X_3 > \eta_0 + \eta_1 X_2)$, where $\eta_0 = -\beta_4/\beta_6$ and $\eta_1 = \beta_5/\beta_6$. If the model for $\mu(A, \mathbf{X}; \boldsymbol{\beta})$ is indeed correctly specified, the treatment rules of $g(\mathbf{X}, \boldsymbol{\beta})$ and $g(\boldsymbol{\eta}, \mathbf{X})$ lead to the same optimal ITR. Hence, the treatment rule parameterized by $\boldsymbol{\eta}$ can be derived from a regression model or may be based on some key clinical considerations which enable evaluation of $g(\boldsymbol{\eta}, \mathbf{X})$ directly without reference to the regression model for $\mu(A, \mathbf{X}; \boldsymbol{\beta})$.

Let $C_\eta = Ag(\boldsymbol{\eta}, \mathbf{X}) + (1 - A)\{1 - g(\boldsymbol{\eta}, \mathbf{X})\}$, where $C_\eta = 1$ indicates random assignment to an intervention that is recommended by the personalized treatment rule $g(\boldsymbol{\eta}, \mathbf{X})$. Let $\pi(\mathbf{X}; \widehat{\boldsymbol{\gamma}})$ denote the randomization ratio or the estimated propensity score (as in previous section), and $m(\mathbf{X}; \boldsymbol{\eta}, \widehat{\boldsymbol{\beta}})$ denote the potential outcome under the treatment rule estimated from the following model $E(Y \mid A = a, \mathbf{X}) = \mu(A, \mathbf{X}; \boldsymbol{\beta})$. For example, if the treatment rule $g(\boldsymbol{\eta}, \mathbf{X}) = 1$, then $m(\mathbf{X}; \boldsymbol{\eta}, \widehat{\boldsymbol{\beta}}) = g(\boldsymbol{\eta}, \mathbf{X})\mu(A = 1, \mathbf{X}; \widehat{\boldsymbol{\beta}}) + \{1 - g(\boldsymbol{\eta}, \mathbf{X})\}\mu(A = 0, \mathbf{X}; \widehat{\boldsymbol{\beta}}) = \mu(A = 1, \mathbf{X}; \widehat{\boldsymbol{\beta}})$. Two estimators of the expected response to treatment, the inverse probability weighted estimator (IPWE) and doubly robust AIPWE, are given as follows:

$$\begin{aligned}
\text{IPWE}(\boldsymbol{\eta}) &= \frac{1}{n}\sum_{i=1}^{n} \frac{C_{\boldsymbol{\eta}\cdot i} Y_i}{\pi_c(\mathbf{X}_i; \boldsymbol{\eta}, \widehat{\boldsymbol{\gamma}})} \\
&= \frac{1}{n}\sum_{i=1}^{n} \frac{C_{\boldsymbol{\eta}\cdot i} Y_i}{\pi(\mathbf{X}_i; \widehat{\boldsymbol{\gamma}})^{A_i}\{1 - \pi(\mathbf{X}_i; \widehat{\boldsymbol{\gamma}})\}^{1 - A_i}}, \\
\text{AIPWE}(\boldsymbol{\eta}) &= \frac{1}{n}\sum_{i=1}^{n} \left\{ \frac{C_{\boldsymbol{\eta}\cdot i} Y_i}{\pi_c(\mathbf{X}_i; \boldsymbol{\eta}, \widehat{\boldsymbol{\gamma}})} \right. \\
&\qquad \left. - \frac{C_{\boldsymbol{\eta}\cdot i} Y_i - \pi_c(\mathbf{X}_i; \boldsymbol{\eta}, \widehat{\boldsymbol{\gamma}})}{\pi_c(\mathbf{X}_i; \boldsymbol{\eta}, \widehat{\boldsymbol{\gamma}})} m\left(\mathbf{X}_i; \boldsymbol{\eta}, \widehat{\boldsymbol{\beta}}\right) \right\},
\end{aligned} \tag{11}$$

where $\pi_c(\mathbf{X}_i; \boldsymbol{\eta}, \widehat{\boldsymbol{\gamma}}) = \pi(\mathbf{X}; \widehat{\boldsymbol{\gamma}})g(\boldsymbol{\eta}, \mathbf{X}) + \{1 - \pi(\mathbf{X}; \widehat{\boldsymbol{\gamma}})\}\{1 - g(\boldsymbol{\eta}, \mathbf{X})\}$. The optimal treatment rule follows as $\widehat{g}(\widehat{\boldsymbol{\eta}}, \mathbf{X} = \mathbf{x})$, where $\widehat{\boldsymbol{\eta}}$ is estimated from the above models; a constraint, such as $\|\boldsymbol{\eta}\| = 1$, is imposed to obtain a unique solution $\widehat{\boldsymbol{\eta}}$ [43]. If the propensity score is correctly specified, the IPWE estimator yields robust (consistent) estimates; AIPWE is considered a doubly robust estimator since it produces consistent estimates when either propensity score or the model $E(Y \mid A = a, \mathbf{X})$ is misspecified, but not both [42, 43]. The companion *R* code is publicly available at http://onlinelibrary.wiley.com/doi/10.1111/biom.12191/suppinfo.

5.5.2. Data Mining and Machine Learning. The methods presented in Section 5.5.1 are robust against misspecification of regression models. Yet, they often require prespecification of the parametric form for the treatment rule (e.g., $I(X_3 > \eta_0 + \eta_1 X_2)$), which can be practically challenging [44]. Well established classification methods and other popular machine learning techniques can alternatively be customized to define treatment selection rules [44, 72, 73]; these methods avoid prespecification of the parametric form of the ITR. An ITR can be defined following a two-step approach: in the first step, treatment contrasts are estimated from a posited model and in the second step classification techniques are applied to determine the personalized treatment rules. For example, when only two treatments are considered, a new variable Z can be defined based on the treatment contrast; that is, $Z = 1$ if $\Delta(\mathbf{X}) = \{\mu(A = 1, \mathbf{X}) - \mu(A = 0, \mathbf{X})\} > 0$ and $Z = 0$ otherwise. The absolute value of the treatment contrast $W_i = |\Delta(\mathbf{X})|$ can be used in conjunction with a classification technique to define an appropriate ITR [44].

Unlike classification problems wherein the class labels are observed for the training data, the binary "response" variable Z, which serves as the class label, is not available in practice. Specifically, patients who are in the class $Z = 1$

have $\{\mu(A = 1, \mathbf{X}) > \mu(A = 0, \mathbf{X})\}$ and should therefore be treated with the new therapy; however these quantities need to be estimated, since patients are typically assigned to only one of the available treatments. This imparts flexibility for estimation of the optimal treatment regimes, since any of the previously discussed regression models and even some ensemble prediction methods such as random forest [74] can be used to construct the class labels $\widehat{Z}_i$ and weights $\widehat{W}_i$ [44]. An ITR can be estimated from the dataset $\{\widehat{Z}_i, \mathbf{X}_i, \widehat{W}_i\}$ using any classification approach, where $\widehat{W}_i$ are subject specific misclassification weights [44, 45]. This includes popular classification methods such as adaptive boosting [75], support vector machines [76], and classification and regression trees (CART) [77]. At least one study has suggested that SVM outperforms other classification methods in this context, whereas random forest and boosting perform comparatively better than CART [78]. However, the performances of these classification algorithms are data dependent. Definitive conclusion pertaining to their comparative effectiveness in general has yet to be determined [78]. It shall be also noted that these classification methods can be also applied to high-dimensional data [45, 72].

One special case of this framework is the "virtue twins" approach [45]. Specifically, in the first step a random forest approach [74] is used to obtain the treatment contrasts. Then in the second step CART is used to classify subjects to the optimal treatment regime. The approach can be easily implemented in *R* using packages of *randomForest* [79] and *rpart* [80]. Very recently, Kang et al. [42] proposed a modified version of the adaptive boosting technique of Friedman et al. [75]. The algorithm iteratively fits a simple logistic regression model ("working model") to estimate $P(Y = 1 \mid A, \mathbf{X})$ and at each stage assigns higher weights to subjects whose treatment contrast is near zero. After a prespecified stopping criterion is met, an average of the treatment contrasts $\overline{\Delta}(\mathbf{X})$ is calculated for each patient using all models fitted at each iteration. A subject is assigned to the new therapy if $\overline{\Delta}(\mathbf{X}) > 0$. The *R* code for the aforementioned boosting methods is publicly available at http://onlinelibrary.wiley.com/doi/10.1111/biom.12191/suppinfo.

Lastly, we present a breast cancer example where several biomarkers were combined to construct an optimal ITR. The data was collected in the Southwest Oncology Group (SOWG)-SS8814 trial [13] and analyzed with the machine learning approach of Kang et al. [42]. Three hundred and sixty-seven node-positive, ER-positive breast cancer patients were selected from the randomized trial of SOWG. A total of 219 received tamoxifen plus adjuvant chemotherapy and 148 was given tamoxifen alone. The outcome variable was defined as breast cancer recurrence at 5 years. The authors selected three genes, which had presented treatment-biomarker interactions in a multivariate linear logistic regression model [42]. Data were analyzed with logistic models, IPWE, AIPWE, logistic boosting, a single classification tree with treatment-biomarker interactions, and the proposed boosting approach with a classification tree as the working model. Each method identified different patient cohorts that could benefit from tamoxifen alone: these cohorts consisted of 184, 183, 128, 86, 263, and 217 patients, respectively (see Table 5 in [42]). In this analysis, the clinical benefits provided by these 6 treatment rules were not statistically different. Hence, investigators need to evaluate and compare ITRs in terms of the extent of expected clinical impact. This is considered in the next section.

6. Performance Evaluation for Individualized Treatment Rules

Heretofore, we have discussed various methodologies for the construction of ITR, while their performances need to be assessed before these rules can be implemented in clinical practice. Several aspects pertaining to the performance of a constructed ITR need to be considered. The first one is how well the ITR fits the data, and the second is how well the ITR performs compared with existing treatment allocation rules. The former is related to the concept of goodness-of-fit or predictive performance [34]. As the true optimal treatment groups are hidden, model fits may be evaluated by measuring the congruity between observed treatment contrasts and predicted ones [34, 47]. More details can be found in a recent paper by Janes et al. [47]. Performances of ITRs can be compared via assessment of a global summary measure, for example, prolonged survival time or reduced disease rate [40, 42]. Summary measures are also very useful for evaluating the extent to which an ITR may benefit patients when applied in practice. Moreover, it is essential that performance of an ITR is considered in comparison to business-as-usual procedures such as a naive rule that randomly allocates patients to treatment [81]. Summary measures will be discussed in Section 6.1. The effectiveness of an ITR should go beyond the training data set used to construct a treatment rule; cross-validation and bootstrapping techniques are often employed to assess the impact of ITRs on future patients [81] and will be discussed in Section 6.2.

6.1. Summary Measures. ITRs may be derived from different methodologies, and comparisons should be conducted with respect to the appropriate clinically summaries. A few summary measures for different types of outcomes have been proposed [19, 40, 42]; these measures quantify the direct clinical improvements obtained by applying an ITR in comparison with default methods for treatment allocation.

Binary Outcomes. Clinical effectiveness for binary clinical response is represented by the difference in disease rates (or treatment failure) induced by ITR versus a default strategy that allocates all patients to a standard treatment [42, 47, 82]. Let $g^{\text{opt}}(\mathbf{X}) = I\{\mu(A = 1, \mathbf{X}) - \mu(A = 0, \mathbf{X}) < 0\}$, be an optimal ITR. This difference is formally defined as

$$\begin{aligned}\Theta_B &\left\{g^{\text{opt}}(\mathbf{X})\right\} \\ &= P(Y = 1 \mid A = 0) \\ &\quad - \sum_{a=0}^{1} \left[P\left\{Y = 1 \mid A = a, g^{\text{opt}}(\mathbf{X}) = a\right\} P\left\{g^{\text{opt}}(\mathbf{X}) = a\right\}\right]\end{aligned}$$

$$= \left[P\left\{Y = 1 \mid A = 0, g^{\text{opt}}(\mathbf{X}) = 1\right\} - P\left\{Y = 1 \mid A = 1, g^{\text{opt}}(\mathbf{X}) = 1\right\}\right] P\left\{g^{\text{opt}}(\mathbf{X}) = 1\right\}. \quad (12)$$

Note $\mu(A, \mathbf{X})$ needs to be estimated to construct the ITR yet parameters $\boldsymbol{\beta}$ are omitted for simplicity. Larger values of $\Theta_B\{g^{\text{opt}}(\mathbf{X})\}$ indicate increased clinical value for the biomarker driven ITR. A subset of patients that are recommended for new treatment ($A = 1$) under an ITR may have been randomly selected to receive it, while the remaining subset of "unlucky" patients would have received the standard treatment [19]. The summary measure of $\Theta_B\{g^{\text{opt}}(\mathbf{X})\}$ characterizes a weighted difference in the disease rates between the standard and the new treatments in a population wherein the constructed optimal ITR would recommend the new treatment $g^{\text{opt}}(\mathbf{X} = 1)$. The weight is the proportion of patients identified by the optimal ITR for the new treatment and can be empirically estimated using the corresponding counts. For example, $P\{g^{\text{opt}}(\mathbf{X}) = 1\}$ can be estimated using the number of patients recommended for the new treatment divided by the total sample size. A similar summary statistic can be derived for an alternative strategy allocating all patients to the new treatment. The summary could be applied to the aforementioned breast cancer example [42], for example, with the aim of finding a subgroup of patients who were likely to benefit from adjuvant chemotherapy, while those unlikely to benefit would be assigned tamoxifen alone to avoid the unnecessary toxicity and inconvenience of chemotherapy.

Continuous Variables. Another strategy for continuous data compares outcomes observed for "lucky" subjects, those who received the therapy that would have been recommended by the ITR based [81]. Further, one business-as-usual drug allocation procedure is randomizing treatment and standard care at the same probability of 0.5. A summary statistic is to measure the mean outcome under ITR compared to that obtained under random assignment, for instance, the mean decrease in Hamilton Rating Scale for Depression as discussed in Section 5.1 [19]. Define the summary measure as $\Theta_C\{g^{\text{opt}}(\mathbf{X})\} = \mu\{g^{\text{opt}}(\mathbf{X}), \mathbf{X}\} - \mu\{g^{\text{rand}}(\mathbf{X}), \mathbf{X}\}$, where $g^{\text{rand}}(\mathbf{X})$ represents the randomization allocation procedure. The quantity of $\mu\{g^{opt}(\mathbf{X}), \mathbf{X}\}$ represents the mean outcome under the constructed IRT that can be empirically estimated from the "lucky" subjects, and $\mu\{g^{\text{rand}}(\mathbf{X}), \mathbf{X}\}$ can be estimated empirically from the sample means.

Alternatively, an ITR may be compared to an "optimal" drug that has showed universal benefits (a better drug on average) in a controlled trial. The clinical benefits of an "optimal" drug can be defined as $\mu\{g^{\text{best}}(\mathbf{X}), \mathbf{X}\} = \max\{\mu(A = 0, \mathbf{X}), \mu(A = 1, \mathbf{X})\}$; $\mu(A = a, \mathbf{X})$, and can be empirically estimated from the sample means of the new and standard treatments, respectively. Then the alternative summary measure is defined as $\Theta_{\text{Calt}} = \{g^{\text{opt}}(\mathbf{X})\} = \mu\{g^{\text{opt}}(\mathbf{X}), \mathbf{X}\} - \mu\{g^{\text{best}}(\mathbf{X}), \mathbf{X}\}$.

Survival Data. For survival data, a clinically relevant measure is mean overall (or progression free) survival time. As survival time is continuous in nature, the identical strategy provided above for continuous outcomes can be employed here. However, because the mean survival time may not be well estimated from the observed data due to a high percentage of censored observations [40], an alternative mean restricted survival duration was proposed and defined as the population average event-free durations for a restricted time of t^* [41, 83]. Often t^* is chosen to cover the trial's follow-up period. Mathematically, it can be calculated by integrating the survival function of $S(t)$ over the domain of $(0, t^*)$, that is, $\mu\{g^{\text{opt}}(\mathbf{X}), \mathbf{X}, t^*\} = \int_0^{t^*} S(t)dt$, and often estimated by the area under the Kaplan-Meier curve up to t^* [84]. Thus, an ITR's potential to prolong survival can be calculated as $\Theta_S\{g^{\text{opt}}(\mathbf{X}), t^*\} = \mu\{g^{\text{opt}}(\mathbf{X}), \mathbf{X}, t^*\} - \mu\{g^{\text{rand}}(\mathbf{X}), \mathbf{X}, t^*\}$.

6.2. Assessing Model Performance. The summaries heretofore discussed evaluate an optimal ITR for a given model and estimating procedure. Because these quantities are estimated conditionally given the observed covariates, they neglect to quantify the extent of marginal uncertainty for future patients. Hence an ITR needs to be internally validated if external data is not available [34]. Cross-validation (CV) and bootstrap resampling techniques are commonly used for this purpose [19, 42, 45, 81], and expositions on both approaches are well described elsewhere [33, 85, 86].

We here briefly introduce a process that was proposed by Kapelner et al. [81] in the setting of personalized medicine. Tenfold CV is commonly used in practice, where the whole data is randomly partitioned into 10 roughly equal-sized exclusive subsamples. All methods under consideration are applied to 9/10 of the data, excluding 1/10 as an independent testing data set. The process is repeated 10 times for each subsample. Considering the assignments recommended by the optimal ITRs, the summary measures can be calculated using results from each testing fold [45]. The CV process gives the estimated summary measures, and its variation can be evaluated using bootstrap procedures. Specifically, one draws a sample with replacement from the entire data and calculates the summary measure from 10-fold CV. This process will be repeated B times, where B is chosen for resolution of the resulting confidence intervals [81]. Using the summary measures as B new random samples, the corresponding mean and variances can be calculated empirically. Note that the summary measures compare two treatment rules, one for the optimal ITR and another naive rule (e.g., randomization).

The above procedure can be applied to all the methods we have discussed so far. The *R* software package *TreatmentSelection* (http://labs.fhcrc.org/janes/index.html) can be used to implement these methods for evaluating and comparing biomarkers for binary outcomes [47]. Very recently, an inferential procedure was proposed for continuous outcomes that is implemented in the publicly available *R* package "Personalized Treatment Evaluator" [81, 87]. Both methods consider data from RCTs with two arms for comparative treatments. These methods are, in general, applicable to regression model based methods but are not suitable for approaches based on classification techniques or penalized regression.

Next we present two examples. Recall in Section 5.5 that Kang et al. [42] reported the estimated clinical benefits of an ITR for breast cancer when compared to the default strategy of assigning all patients to adjuvant chemotherapy. The proposed approach (based on boosting and classification trees) achieved the highest value of the summary measure at 0.081 with 95% confidence interval (CI) $(0.000, 0.159)$ [42]. In the second example, introduced in Section 5.1 [19], the authors calculated the mean score of the Hamilton Rating Scale for Depression for two groups of subjects; groups were defined by randomly assigning patients to the "optimal" and "nonoptimal" therapy as defined by the ITR. The reported difference between the two groups was -1.78 with a P value of 0.09, which fails to attain a clinical significant difference of 3 [19]. The same data was analyzed by Kapelner et al. [81]. Following the discussed procedure, the authors reported the estimated values (and 95% CI) of $\Theta_C\{g^{\text{opt}}(\mathbf{X})\}$ and $\Theta_{\text{Calt}}\{g^{\text{opt}}(\mathbf{X})\}$ as $-0.842(-2.657, -0.441)$ and $-0.765(-2.362, 0.134)$, respectively. The results, which fail to achieve clinical significance, were based on rigorous statistical methods and thus can be considered reliable estimates of the ITR's performance.

7. Discussion

As our understanding tumor heterogeneity evolves, personalized medicine will become standard medical practice in oncology. Therefore, it is essential that the oncology community uses appropriate analytical methods for identifying and evaluating the performance of personalized treatment rules. This paper provided an exposition of the process for using statistical inference to establish optimal individualized treatment rules using data acquired from clinical study. The quality of an ITR depends on the quality of the design used to acquire the data. Moreover, an ITR must be properly validated before it is integrated into clinical practice. Personalized medicine in some areas of oncology may be limited by the fact that biomarkers arising from a small panel of genes may never adequately characterize the extent of tumor heterogeneity inherent to the disease. Consequently, the available statistical methodology needs to evolve in order to optimally exploit global gene signatures for personalized medicine.

The bulk of our review focused on statistical approaches for treatment selection at a single time point. The reader should note that another important area of research considers optimal dynamic treatment regimes (DTRs) [88, 89], wherein treatment decisions are considered sequentially over the course of multiple periods of intervention using each patient's prior treatment history. Zhao and Zeng provide a summary of recent developments in this area [90].

Conflict of Interests

The authors declare that there is no conflict of interests regarding the publication of this paper.

Acknowledgments

Junsheng Ma was fully funded by the University of Texas MD Anderson Cancer Center internal funds. Brian P. Hobbs and Francesco C. Stingo were partially supported by the Cancer Center Support Grant (CCSG) (P30 CA016672).

References

[1] J. Reimand, O. Wagih, and G. D. Bader, "The mutational landscape of phosphorylation signaling in cancer," *Scientific Reports*, vol. 3, article 2651, 2013.

[2] D. Hanahan and R. A. Weinberg, "Hallmarks of cancer: the next generation," *Cell*, vol. 144, no. 5, pp. 646–674, 2011.

[3] R. Simon, "Clinical trial designs for evaluating the medical utility of prognostic and predictive biomarkers in oncology," *Personalized Medicine*, vol. 7, no. 1, pp. 33–47, 2010.

[4] P. L. Bedard, A. R. Hansen, M. J. Ratain, and L. L. Siu, "Tumour heterogeneity in the clinic," *Nature*, vol. 501, no. 7467, pp. 355–364, 2013.

[5] M. D. Pegram, G. Pauletti, and D. J. Slamon, "Her-2/neu as a predictive marker of response to breast cancer therapy," *Breast Cancer Research and Treatment*, vol. 52, no. 1–3, pp. 65–77, 1998.

[6] G. J. Kelloff and C. C. Sigman, "Cancer biomarkers: selecting the right drug for the right patient," *Nature Reviews Drug Discovery*, vol. 11, no. 3, pp. 201–214, 2012.

[7] J. A. DiMasi, J. M. Reichert, L. Feldman, and A. Malins, "Clinical approval success rates for investigational cancer drugs," *Clinical Pharmacology and Therapeutics*, vol. 94, no. 3, pp. 329–335, 2013.

[8] M. Hay, D. W. Thomas, J. L. Craighead, C. Economides, and J. Rosenthal, "Clinical development success rates for investigational drugs," *Nature Biotechnology*, vol. 32, no. 1, pp. 40–51, 2014.

[9] S. S. Knox, "From 'omics' to complex disease: a systems biology approach to gene-environment interactions in cancer," *Cancer Cell International*, vol. 10, article 11, 2010.

[10] V. Deschoolmeester, M. Baay, P. Specenier, F. Lardon, and J. B. Vermorken, "A review of the most promising biomarkers in colorectal cancer: one step closer to targeted therapy," *The Oncologist*, vol. 15, no. 7, pp. 699–731, 2010.

[11] J. A. Sosman, K. B. Kim, L. Schuchter et al., "Survival in braf V600–mutant advanced melanoma treated with vemurafenib," *The New England Journal of Medicine*, vol. 366, no. 8, pp. 707–714, 2012.

[12] S. Paik, S. Shak, G. Tang et al., "A multigene assay to predict recurrence of tamoxifen-treated, node-negative breast cancer," *The New England Journal of Medicine*, vol. 351, no. 27, pp. 2817–2826, 2004.

[13] K. S. Albain, W. E. Barlow, S. Shak et al., "Prognostic and predictive value of the 21-gene recurrence score assay in postmenopausal women with node-positive, oestrogen-receptor-positive breast cancer on chemotherapy: a retrospective analysis of a randomised trial," *The Lancet Oncology*, vol. 11, no. 1, pp. 55–65, 2010.

[14] J. E. Lang, J. S. Wecsler, M. F. Press, and D. Tripathy, "Molecular markers for breast cancer diagnosis, prognosis and targeted therapy," *Journal of Surgical Oncology*, vol. 111, no. 1, pp. 81–90, 2015.

[15] W. Werft, A. Benner, and A. Kopp-Schneider, "On the identification of predictive biomarkers: detecting treatment-by-gene interaction in high-dimensional data," *Computational Statistics and Data Analysis*, vol. 56, no. 5, pp. 1275–1286, 2012.

[16] M. Jenkins, A. Flynn, T. Smart et al., "A statistician's perspective on biomarkers in drug development," *Pharmaceutical Statistics*, vol. 10, no. 6, pp. 494–507, 2011.

[17] A. J. Vickers, M. W. Kattan, and D. J. Sargent, "Method for evaluating prediction models that apply the results of randomized trials to individual patients," *Trials*, vol. 8, no. 1, article 14, 2007.

[18] H. Janes, M. S. Pepe, P. M. Bossuyt, and W. E. Barlow, "Measuring the performance of markers for guiding treatment decisions," *Annals of Internal Medicine*, vol. 154, no. 4, pp. 253–259, 2011.

[19] R. J. DeRubeis, Z. D. Cohen, N. R. Forand, J. C. Fournier, L. A. Gelfand, and L. Lorenzo-Luaces, "The personalized advantage index: translating research on prediction into individualized treatment recommendations. A demonstration," *PLoS ONE*, vol. 9, no. 1, Article ID e83875, 2014.

[20] D. P. Byar and D. K. Corle, "Selecting optimal treatment in clinical trials using covariate information," *Journal of Chronic Diseases*, vol. 30, no. 7, pp. 445–459, 1977.

[21] N. Thatcher, A. Chang, P. Parikh et al., "Gefitinib plus best supportive care in previously treated patients with refractory advanced non-small-cell lung cancer: results from a randomised, placebo-controlled, multicentre study (iressa survival evaluation in lung cancer)," *The Lancet*, vol. 366, no. 9496, pp. 1527–1537, 2005.

[22] A. J. Vickers, "Prediction models in cancer care," *CA: A Cancer Journal for Clinicians*, vol. 61, no. 5, pp. 315–326, 2011.

[23] R. M. Simon, "Subgroup analysis," in *Wiley Encyclopedia of Clinical Trials*, John Wiley & Sons, Hoboken, NJ, USA, 2007.

[24] S. J. Pocock, S. E. Assmann, L. E. Enos, and L. E. Kasten, "Subgroup analysis, covariate adjustment and baseline comparisons in clinical trial reporting: current practice and problems," *Statistics in Medicine*, vol. 21, no. 19, pp. 2917–2930, 2002.

[25] P. M. Rothwell, Z. Mehta, S. C. Howard, S. A. Gutnikov, and C. P. Warlow, "From subgroups to individuals: general principles and the example of carotid endarterectomy," *The Lancet*, vol. 365, no. 9455, pp. 256–265, 2005.

[26] R. Wang, S. W. Lagakos, J. H. Ware, D. J. Hunter, and J. M. Drazen, "Statistics in medicine—reporting of subgroup analyses in clinical trials," *The New England Journal of Medicine*, vol. 357, no. 21, pp. 2108–2194, 2007.

[27] International Breast Cancer Study Group, "Endocrine responsiveness and tailoring adjuvant therapy for postmenopausal lymph node-negative breast cancer: a randomized trial," *Journal of the National Cancer Institute*, vol. 94, no. 14, pp. 1054–1065, 2002.

[28] Early Breast Cancer Trialists' Collaborative Group (EBCTCG), "Effects of chemotherapy and hormonal therapy for early breast cancer on recurrence and 15-year survival: an overview of the randomised trials," *The Lancet*, vol. 365, no. 9472, pp. 1687–1717, 2005.

[29] F. E. Harrell, K. L. Lee, and D. B. Mark, "Tutorial in biostatistics multivariable prognostic models: issues in developing models, evaluating assumptions and adequacy, and measuring and reducing errors," *Statistics in Medicine*, vol. 15, no. 4, pp. 361–387, 1996.

[30] S. Gill, C. L. Loprinzi, D. J. Sargent et al., "Pooled analysis of fluorouracil-based adjuvant therapy for stage II and III colon cancer: who benefits and by how much?" *Journal of Clinical Oncology*, vol. 22, no. 10, pp. 1797–1806, 2004.

[31] M. Qian and S. A. Murphy, "Performance guarantees for individualized treatment rules," *The Annals of Statistics*, vol. 39, no. 2, pp. 1180–1210, 2011.

[32] W. Lu, H. H. Zhang, and D. Zeng, "Variable selection for optimal treatment decision," *Statistical Methods in Medical Research*, vol. 22, no. 5, pp. 493–504, 2013.

[33] R. Kohavi, "A study of cross-validation and bootstrap for accuracy estimation and model selection," in *Proceedings of the 14th International Joint Conference on Artificial Intelligence (IJCAI '95)*, vol. 2, pp. 1137–1145, 1995.

[34] E. W. Steyerberg, A. J. Vickers, N. R. Cook et al., "Assessing the performance of prediction models: a framework for traditional and novel measures," *Epidemiology*, vol. 21, no. 1, pp. 128–138, 2010.

[35] P. R. Rosenbaum and D. B. Rubin, "The central role of the propensity score in observational studies for causal effects," *Biometrika*, vol. 70, no. 1, pp. 41–55, 1983.

[36] R. B. d'Agostino Jr., "Tutorial in biostatistics: propensity score methods for bias reduction in the comparison of a treatment to a non-randomized control group," *Statistics in Medicine*, vol. 17, no. 19, pp. 2265–2281, 1998.

[37] R. Pazdur, "Endpoints for assessing drug activity in clinical trials," *The Oncologist*, vol. 13, supplement 2, pp. 19–21, 2008.

[38] S. L. Spruance, J. E. Reid, M. Grace, and M. Samore, "Hazard ratio in clinical trials," *Antimicrobial Agents and Chemotherapy*, vol. 48, no. 8, pp. 2787–2792, 2004.

[39] J. D. Kalbeisch and R. L. Prentice, *The Statistical Analysis of Failure Time Data*, vol. 360, John Wiley & Sons, 2011.

[40] Y. Geng, *Flexible Statistical Learning Methods for Survival Data: Risk Prediction and Optimal Treatment Decision*, North Carolina State University, 2013.

[41] J. Li, L. Zhao, L. Tian et al., *A Predictive Enrichment Procedure to Identify Potential Responders to a New Therapy for Randomized, Comparative, Controlled Clinical Studies*, Harvard University Biostatistics Working Paper Series, Working Paper 169, Harvard University, 2014.

[42] C. Kang, H. Janes, and Y. Huang, "Combining biomarkers to optimize patient treatment recommendations," *Biometrics*, vol. 70, no. 3, pp. 695–720, 2014.

[43] B. Zhang, A. A. Tsiatis, E. B. Laber, and M. Davidian, "A robust method for estimating optimal treatment regimes," *Biometrics*, vol. 68, no. 4, pp. 1010–1018, 2012.

[44] B. Zhang, A. A. Tsiatis, M. Davidian, M. Zhang, and E. Laber, "Estimating optimal treatment regimes from a classification perspective," *Stat*, vol. 1, no. 1, pp. 103–114, 2012.

[45] J. C. Foster, J. M. G. Taylor, and S. J. Ruberg, "Subgroup identification from randomized clinical trial data," *Statistics in Medicine*, vol. 30, no. 24, pp. 2867–2880, 2011.

[46] US Food and Drug Administration, *Guidance for Industry: Clinical Trial Endpoints for the Approval of Cancer Drugs and Biologics*, US Food and Drug Administration, Washington, DC, USA, 2007.

[47] H. Janes, M. D. Brown, M. Pepe, and Y. Huang, "Statistical methods for evaluating and comparing biomarkers for patient treatment selection," UW Biostatistics Working Paper Series, Working Paper 389, 2013.

[48] R Development Core Team, R: a language and environment for statistical computing, 2008, http://www.R-project.org/.

[49] X.-J. Ma, Z. Wang, P. D. Ryan et al., "A two-gene expression ratio predicts clinical outcome in breast cancer patients treated with tamoxifen," *Cancer Cell*, vol. 5, no. 6, pp. 607–616, 2004.

[50] X.-J. Ma, S. G. Hilsenbeck, W. Wang et al., "The HOXB13:IL17BR expression index is a prognostic factor in early-stage breast cancer," *Journal of Clinical Oncology*, vol. 24, no. 28, pp. 4611–4619, 2006.

[51] D. C. Sgroi, E. Carney, E. Zarrella et al., "Prediction of late disease recurrence and extended adjuvant letrozole benefit by

the HOXB13/IL17BR biomarker," *Journal of the National Cancer Institute*, vol. 105, no. 14, pp. 1036–1042, 2013.

[52] M. S. Cepeda, R. Boston, J. T. Farrar, and B. L. Strom, "Comparison of logistic regression versus propensity score when the number of events is low and there are multiple confounders," *The American Journal of Epidemiology*, vol. 158, no. 3, pp. 280–287, 2003.

[53] P. C. Austin, "An introduction to propensity score methods for reducing the effects of confounding in observational studies," *Multivariate Behavioral Research*, vol. 46, no. 3, pp. 399–424, 2011.

[54] G. Heinze and P. Jüni, "An overview of the objectives of and the approaches to propensity score analyses," *European Heart Journal*, vol. 32, no. 14, Article ID ehr031, pp. 1704–1708, 2011.

[55] L. E. Braitman and P. R. Rosenbaum, "Rare outcomes, common treatments: analytic strategies using propensity scores," *Annals of Internal Medicine*, vol. 137, no. 8, pp. 693–695, 2002.

[56] D. M. Witten and R. Tibshirani, "Survival analysis with high-dimensional covariates," *Statistical Methods in Medical Research*, vol. 19, no. 1, pp. 29–51, 2010.

[57] A. E. Hoerl and R. W. Kennard, "Ridge regression: biased estimation for nonorthogonal problems," *Technometrics*, vol. 42, no. 1, pp. 80–86, 2000.

[58] R. Tibshirani, "Regression shrinkage and selection via the lasso," *Journal of the Royal Statistical Society. Series B. Methodological*, vol. 58, no. 1, pp. 267–288, 1996.

[59] H. Zou, "The adaptive lasso and its oracle properties," *Journal of the American Statistical Association*, vol. 101, no. 476, pp. 1418–1429, 2006.

[60] B. Efron, T. Hastie, I. Johnstone, and R. Tibshirani, "Least angle regression," *The Annals of Statistics*, vol. 32, no. 2, pp. 407–499, 2004.

[61] T. Hastie and B. Efron, "lars: Least angle regression, lasso and forward stagewise," R package version 1.2, 2013, http://cran.r-project.org/web/packages/lars/index.html.

[62] J. Fan and R. Li, "Variable selection via nonconcave penalized likelihood and its oracle properties," *Journal of the American Statistical Association*, vol. 96, no. 456, pp. 1348–1360, 2001.

[63] H. Zou and T. Hastie, "Regularization and variable selection via the elastic net," *Journal of the Royal Statistical Society. Series B. Statistical Methodology*, vol. 67, no. 2, pp. 301–320, 2005.

[64] N. Krämer, J. Schäfer, and A.-L. Boulesteix, "Regularized estimation of large-scale gene association networks using graphical gaussian models," *BMC Bioinformatics*, vol. 10, no. 1, article 384, 2009.

[65] P. Breheny and J. Huang, "Coordinate descent algorithms for nonconvex penalized regression, with applications to biological feature selection," *The Annals of Applied Statistics*, vol. 5, no. 1, pp. 232–253, 2011.

[66] S. M. Hammer, D. A. Katzenstein, M. D. Hughes et al., "A trial comparing nucleoside monotherapy with combination therapy in HIV-infected adults with CD4 cell counts from 200 to 500 per cubic millimeter," *The New England Journal of Medicine*, vol. 335, no. 15, pp. 1081–1090, 1996.

[67] H. M. Bøvelstad, S. Nygård, H. L. Størvold et al., "Predicting survival from microarray data—a comparative study," *Bioinformatics*, vol. 23, no. 16, pp. 2080–2087, 2007.

[68] V. Kehl and K. Ulm, "Responder identification in clinical trials with censored data," *Computational Statistics and Data Analysis*, vol. 50, no. 5, pp. 1338–1355, 2006.

[69] P. Royston and M. K. Parmar, "The use of restricted mean survival time to estimate the treatment effect in randomized clinical trials when the proportional hazards assumption is in doubt," *Statistics in Medicine*, vol. 30, no. 19, pp. 2409–2421, 2011.

[70] P. Royston and M. K. B. Parmar, "Restricted mean survival time: an alternative to the hazard ratio for the design and analysis of randomized trials with a time-to-event outcome," *BMC Medical Research Methodology*, vol. 13, no. 1, article 152, 2013.

[71] E. T. Lee and J. W. Wang, *Statistical Methods for Survival Data Analysis*, John Wiley & Sons, Hoboken, NJ, USA, 2013.

[72] Y. Zhao, D. Zeng, A. J. Rush, and M. R. Kosorok, "Estimating individualized treatment rules using outcome weighted learning," *Journal of the American Statistical Association*, vol. 107, no. 499, pp. 1106–1118, 2012.

[73] D. B. Rubin and M. J. van der Laan, "Statistical issues and limitations in personalized medicine research with clinical trials," *The International Journal of Biostatistics*, vol. 8, no. 1, pp. 1–20, 2012.

[74] L. Breiman, "Random forests," *Machine Learning*, vol. 45, no. 1, pp. 5–32, 2001.

[75] J. Friedman, T. Hastie, and R. Tibshirani, "Additive logistic regression: a statistical view of boosting," *The Annals of Statistics*, vol. 28, no. 2, pp. 337–407, 2000.

[76] C. Cortes and V. Vapnik, "Support-vector networks," *Machine Learning*, vol. 20, no. 3, pp. 273–297, 1995.

[77] L. Breiman, J. Friedman, C. J. Stone, and R. A. Olshen, *Classification and Regression Trees*, CRC Press, New York, NY, USA, 1984.

[78] S. Dudoit, J. Fridlyand, and T. P. Speed, "Comparison of discrimination methods for the classification of tumors using gene expression data," *Journal of the American Statistical Association*, vol. 97, no. 457, pp. 77–87, 2002.

[79] A. Liaw and M. Wiener, "Classification and regression by randomforest," *R News*, vol. 2, no. 3, pp. 18–22, 2002, http://CRAN.R-project.org/doc/Rnews/.

[80] T. Therneau, B. Atkinson, and B. Ripley, "rpart: Recursive Partitioning and Regression Trees," R package version 4.1-3, http://cran.r-project.org/web/packages/rpart/index.html.

[81] A. Kapelner, J. Bleich, Z. D. Cohen, R. J. DeRubeis, and R. Berk, "Inference for treatment regime models in personalized medicine," http://arxiv.org/abs/1404.7844.

[82] X. Song and M. S. Pepe, "Evaluating markers for selecting a patient's treatment," *Biometrics*, vol. 60, no. 4, pp. 874–883, 2004.

[83] T. Karrison, "Restricted mean life with adjustment for covariates," *Journal of the American Statistical Association*, vol. 82, no. 400, pp. 1169–1176, 1987.

[84] C. Barker, "The mean, median, and confidence intervals of the kaplan-meier survival estimate—computations and applications," *Journal of the American Statistical Association*, vol. 63, no. 1, pp. 78–80, 2009.

[85] B. Efron and R. J. Tibshirani, *An Introduction to the Bootstrap*, vol. 57, CRC Press, 1994.

[86] S. Arlot and A. Celisse, "A survey of cross-validation procedures for model selection," *Statistics Surveys*, vol. 4, pp. 40–79, 2010.

[87] A. Kapelner and J. Bleich, "PTE: Personalized Treatment Evaluator," 2014, R package version 1.0, http://CRAN.R-project.org/package=PTE.

[88] S. A. Murphy, "Optimal dynamic treatment regimes," *Journal of the Royal Statistical Society, Series B: Statistical Methodology*, vol. 65, no. 2, pp. 331–355, 2003.

[89] J. M. Robins, "Optimal structural nested models for optimal sequential decisions," in *Proceedings of the Second Seattle Symposium in Biostatistics*, vol. 179 of *Lecture Notes in Statistics*, pp. 189–326, Springer, Berlin, Germany, 2004.

[90] Y. Zhao and D. Zeng, "Recent development on statistical methods for personalized medicine discovery," *Frontiers of Medicine in China*, vol. 7, no. 1, pp. 102–110, 2013.

Hindawi Publishing Corporation
BioMed Research International
Volume 2015, Article ID 641023, 9 pages
http://dx.doi.org/10.1155/2015/641023

Research Article

The Diagnostic Ability of Follow-Up Imaging Biomarkers after Treatment of Glioblastoma in the Temozolomide Era: Implications from Proton MR Spectroscopy and Apparent Diffusion Coefficient Mapping

Martin Bulik,[1,2] Tomas Kazda,[3,4,5] Pavel Slampa,[4,5] and Radim Jancalek[3,6,7]

[1]*Department of Diagnostic Imaging, Faculty of Medicine, Masaryk University, 625 00 Brno, Czech Republic*
[2]*Department of Diagnostic Imaging, St. Anne's University Hospital Brno, 656 91 Brno, Czech Republic*
[3]*International Clinical Research Center, St. Anne's University Hospital Brno, 656 91 Brno, Czech Republic*
[4]*Department of Radiation Oncology, Faculty of Medicine, Masaryk University, 625 00 Brno, Czech Republic*
[5]*Department of Radiation Oncology, Masaryk Memorial Cancer Institute, 656 53 Brno, Czech Republic*
[6]*Department of Neurosurgery, St. Anne's University Hospital Brno, Faculty of Medicine, Masaryk University, 625 00 Brno, Czech Republic*
[7]*Department of Neurosurgery, St. Anne's University Hospital Brno, 656 91 Brno, Czech Republic*

Correspondence should be addressed to Radim Jancalek; radim.jancalek@fnusa.cz

Received 23 January 2015; Revised 25 April 2015; Accepted 27 April 2015

Academic Editor: Murat Gokden

Objective. To prospectively determine institutional cut-off values of apparent diffusion coefficients (ADCs) and concentration of tissue metabolites measured by MR spectroscopy (MRS) for early differentiation between glioblastoma (GBM) relapse and treatment-related changes after standard treatment. *Materials and Methods*. Twenty-four GBM patients who received gross total resection and standard adjuvant therapy underwent MRI examination focusing on the enhancing region suspected of tumor recurrence. ADC maps, concentrations of *N*-acetylaspartate, choline, creatine, lipids, and lactate, and metabolite ratios were determined. Final diagnosis as determined by biopsy or follow-up imaging was correlated to the results of advanced MRI findings. *Results*. Eighteen (75%) and 6 (25%) patients developed tumor recurrence and pseudoprogression, respectively. Mean time to radiographic progression from the end of chemoradiotherapy was 5.8 ± 5.6 months. Significant differences in ADC and MRS data were observed between those with progression and pseudoprogression. Recurrence was characterized by *N*-acetylaspartate ≤ 1.5 mM, choline/*N*-acetylaspartate ≥ 1.4 (sensitivity 100%, specificity 91.7%), *N*-acetylaspartate/creatine ≤ 0.7, and ADC ≤ 1300×10^{-6} mm^2/s (sensitivity 100%, specificity 100%). *Conclusion*. Institutional validation of cut-off values obtained from advanced MRI methods is warranted not only for diagnosis of GBM recurrence, but also as enrollment criteria in salvage clinical trials and for reporting of outcomes of initial treatment.

1. Introduction

High-grade gliomas (HGG) are the most common and the most serious of primary brain tumors. Despite significant improvements in patient outcomes associated with the introduction of temozolomide (TMZ) into treatment protocols, prognosis remains dismal. The median progression-free survival of glioblastoma (GBM), the most common and lethal HGG, is still only 6.9 months [1]. Unfortunately, with conventional MRI, recurrences often have similar radiologic characteristics as therapy-related changes such as pseudoprogression (PsP) or radionecrosis, and its mutual differentiation remains challenging [2].

Routinely available structural MRI utilizing T2- and gadolinium-enhanced T1-weighted sequences has insufficient sensitivity and specificity for differentiation between

recurrence and radionecrosis or PsP, due to their similar imaging patterns characterized by contrast-enhancing lesion(s) surrounded by edema [3, 4]. PsP can develop after radiotherapy alone but more frequently is present after concomitant radiotherapy and TMZ with occurrence in up to 30% of patients, especially those with O(6)-methylguanine-DNA methyltransferase (MGMT) promoter methylation [5, 6]. Even higher incidence of unclear early radiographic progression at the first postradiotherapy imaging was reported [7]. Nevertheless, in the most recent and robust analysis performed by researchers from Heidelberg, PsP incidence was indicative of prolonged overall survival, despite quite low overall (11.4% of 79 patients) [8]. Thus, the valid and accurate differentiation of follow-up lesions becomes increasingly important for the proper indication of subsequent management, especially in countries with regulatory approval of bevacizumab for salvage treatment [9].

Modern multiparametric MRI techniques such as diffusion-weighted imaging (DWI) with apparent diffusion coefficient (ADC) mapping, dynamic susceptibility-weighted contrast-enhanced (DSC) perfusion imaging, and MR spectroscopy (MRS) allow a much deeper and still noninvasive insight into interpretation of brain lesions, resulting in greater specificity of diagnostic imaging, especially when in combination with amino acid PET imaging [10–14].

However, in routine practice, availability of advanced MRI as well as PET methods is limited with exception of DWI/ADC and MRS. DWI reflects changes in water diffusion as a result of changed tissue microarchitecture due to tumor infiltration and can be quantitatively assessed with the ADC. MRS enables noninvasive examination of the spatial distribution of multiple metabolite concentrations in normal and pathological tissues. The goals of the present prospective study are to verify whether combination of ADC values and concentrations of tissue metabolites measured by proton MRS enable early differentiation between GBM relapse and treatment-related changes in the era of routinely used TMZ and to set institutional cut-off values for increasing accurate diagnosis.

2. Materials and Methods

2.1. Patient Selection and Treatment. Consecutive series of patients with GBM underwent standard treatment consisting of maximal safe resection at the Department of Neurosurgery at St. Anne's University Hospital Brno followed by adjuvant concurrent chemotherapy and radiation therapy (RT). Only patients with MRI-proven gross total resection were eligible. TMZ was administered daily during RT and 5 days every 4 weeks for six cycles as adjuvant treatment. RT was delivered by linear accelerator to the standard dose of 60 Gy in 30 fractions to the clinical target volume defined as the resection cavity with a margin of 1-2 cm. The T2/FLAIR signal abnormality received 40–50 Gy while meeting dose constraints for adjacent organs at risk. Patients underwent structural MRI 6 weeks after the end of RT and then every 3 months thereafter. After radiographic progression was determined with structural MRI, patients became eligible for receiving MRS and DWI. At the treating physician's discretion, biopsy/resection or repeated structural MRI was performed in the final determination of progression. The protocol for this prospective study was approved by St. Anne's University Hospital Brno Institutional Review Board and informed consent was signed by all enrolled patients.

2.2. Advanced MRI. Advanced MRI and proton MR spectroscopy examinations were performed using a 3.0T clinical MR scanner (GE Medical Systems Discovery MR750). Due to the signal heterogeneity and irregular shape of observed MRI lesions, 2D proton MR spectroscopy maps covering the gadolinium-enhanced regions on MRI were performed by means of chemical shift imaging (CSI) technique in two orthogonal planes respecting long axis of the lesion and proximity to structures increasing noise in MR spectra (e.g., bone tissue). All voxels covering the region marked by experienced neuroradiologist as suspected of GBM relapse or PsP were analyzed and the representative ones with the lowest signal-to-noise ratio on each MR spectroscopy map were chosen for further analysis. This procedure led to two spatially independent concentrations of measured metabolites in each patient and resulted in a total of 48 original values for each metabolite in the cohort of 24 patients.

The following parameters were used for proton MR spectroscopy: a point-resolved spectroscopy sequence (PRESS), TR/TE 1800/144 ms, 16-cm FOV, 15-mm slice thickness, and voxel size $10 \times 10 \times 15$ mm. The volume of interest (VOI) encompassed the contrast-enhancing region in contrast-enhanced axial T1-weighted images. Automatic prescanning was performed prior to each spectroscopic scan to ensure adequate water suppression.

MR spectroscopy data were evaluated using LCModel version 6.3 [15] and the concentration of each metabolite was measured. The LCModel data were further postprocessed by jSIPRO 1.0_beta [16]. Metabolite peaks were identified for *N*-acetylaspartate, *N*-acetylaspartylglutamate (tNAA), choline-containing compounds (tCho), (phospho-)creatine (tCr), lipid-containing compounds at 1.3–0.9 ppm (Lip), and lactate (Lac). Metabolite ratios were calculated manually. A routine water unsuppressed spectrum obtained at each examination was used to evaluate the spectrum quality.

The DWI scans were obtained by using an axial echo-planar SE sequence (TR/TE 6000/100 ms), 5-mm slice thickness, diffusion gradient encoding in three orthogonal directions, $b = 0$ and $1000\,\text{mm}^2/\text{s}$, and 240-mm FOV. Postprocessing of DWI data with calculation of ADC maps was performed by using OsiriX software version 6.0.2 64-bit (Pixmeo SARL, Switzerland) with ADC Map Calculation plugin version 1.9 (Stanford University). Regions of interest (ROIs) were drawn manually onto the ADC maps and corresponded to the MRS voxels covering areas with contrast enhancement on T1-weighted images. The mean ADC value (ADCmean) in the voxel corresponding with the measured MRS voxel was calculated automatically by OsiriX software.

2.3. Data Analysis. The metabolite concentrations, their ratios, and ADCmean values were further evaluated using

Table 1: Demographic and clinical characteristics: T = temporal, F = frontal, P = parietal, O = occipital, F-P = frontoparietal, 3D-CRT = three-dimensional conformal radiotherapy, and IMRT = intensity-modulated radiotherapy.

Characteristic	$n = 24$
Age at initial diagnosis (years)	
Median	52.5
Range	29–66
Sex (n)	
Men	17 (65%)
GBM location (%)	
T/F/P/O/F-P	36/28/21/7/8
Radiotherapy	
Median dose (Gy)	60
Technique 3D-CRT/IMRT (%)	50/50
Cycles of adjuvant TMZ	
Median	6
Range	4–10
Time to graphic progression (months)	
Mean	5.8
SD	5.6
Diagnosis validation	
Biopsy/subsequent imaging (%)	67/33
Final diagnosis	
Tumor recurrence	18 (75%)
Pseudoprogression	6 (25%)

statistical software STATISTICA 12 (StatSoft, Inc.) and expressed as medians. Fisher's exact test for categorical data and Mann-Whitney U test for continuous variables were used for estimation of significance of measured differences. ROC analysis was used for definition of the optimal diagnostic cut-offs and description of their sensitivity and specificity for the final diagnosis. The area under the ROC curve (AUC) expressed a measure of how well a parameter can distinguish between the two diagnostic groups (GBM relapse and PsP). Probability value $p < 0.05$ was considered significant in all tests.

3. Results

3.1. Patient Characteristics. Twenty-four patients (mean age 52 years) were enrolled between May 2013 and August 2014. Their characteristics are summarized in Table 1. Sixteen (67%) and 8 (33%) patients had their final diagnosis made by biopsy/resection and by imaging findings on subsequent structural MRI, respectively. Eighteen (75%) patients developed tumor recurrence, 6 (25%) developed PsP, and none developed radionecrosis. Representative imaging data of patients are shown in Figure 1. With 13.8 months of median overall survival, the mean time to radiographic progression from the end of chemoradiotherapy was 5.8 ± 5.6 months. Zero and 9 (37%) patients developed radiographic progression during the first 6 weeks and during the first 3 months after the end of RT, respectively.

3.2. ADC and MRS. Relapse of GBM was characterized by a significantly lower concentration of tNAA as compared to PsP ($p < 0.001$; Table 2), with a cut-off of 1.5 mM (sensitivity 75%, specificity 100%). While only 25% of the patients with a GBM relapse had a concentration of tNAA > 1.5 mM, all of the patients with PsP had [tNAA] > 1.5 mM (Table 3). GBM relapse was also characterized by a higher concentration of Lip + Lac compared to PsP with a cut-off 4.8 mM (sensitivity 100.0, specificity 66.7) ($p = 0.004$; Table 2). Although 33.3% of patients with PsP had a Lip + Lac concentration ≥ 4.8 mM, all patients with GBM relapse had a Lip + Lac concentration ≥ 4.8 mM (Table 3). Concentrations of tCho and tCr did not reach statistical significance between the two groups of patients.

The findings from the individual metabolites were also seen in their ratios. The tCho/tNAA, tNAA/tCr, and Lip + Lac/tCr ratios showed significant differences between GBM relapse and PsP ($p < 0.001$, $p < 0.001$, and $p = 0.004$, resp.) (Table 2). GBM relapse was characterized by a lower tNAA/tCr ratio with a cut-off of 0.7 (sensitivity 94.4%, specificity 91.7%) and higher Lip + Lac/tCr ratio with a cut-off of 1.9 (sensitivity 91.7%, specificity 75.0%; Table 2). Moreover, the GBM relapse group had higher tCho/tNAA ratio values (cut-off 1.4; sensitivity 100.0%, specificity 91.7%; Table 2). Whereas a tCho/tNAA ratio < 1.4 was not specific for PsP, all patients with GBM relapse had a tCho/tNAA ratio ≥ 1.4 (Table 3). The tCho/tCr ratio did not reach statistical significance between both groups of patients.

The calculated ADCmean value was significantly lower in the GBM relapse group than in the PsP group ($p < 0.001$) with a cut-off of 1300×10^{-6} mm^2/s (sensitivity 100.0%, specificity 100.0%; Table 2). All patients with GBM relapse had an ADCmean ≤ 1300×10^{-6} mm^2/s and all patients with PsP had an ADCmean > 1300×10^{-6} mm^2/s.

4. Discussion

Accurate and timely identification of progression is essential for appropriate salvage management for patients with primary brain tumors. Development of response assessment tools is an ongoing process. Currently the most reliable and robust criteria for disease progression are the Response Assessment in Neuro-Oncology (RANO) 2D criteria established in 2010, updated from the earlier established McDonald criteria [17, 18]. In particular, the newly recognized phenomenon of PsP (the transient treatment-related increase of contrast enhancement suggestive of tumor progression) and pseudoresponse (the early and rapid decrease of contrast enhancement without a true tumoricidal effect) are addressed in the RANO criteria. This pseudoresponse is most likely related to the introduction of TMZ and antiangiogenic targeted therapies in treatment protocols [19, 20]. Still, many questions remain for the clear and safe clinical use of TMZ and antiangiogenic targeted therapies. With developments in RT techniques and with the standard administration of TMZ in all GBM patients, radionecrosis has become more infrequent in contrast to the increasing incidence of PsP in therapy-related imaging patterns. Increased incidence of

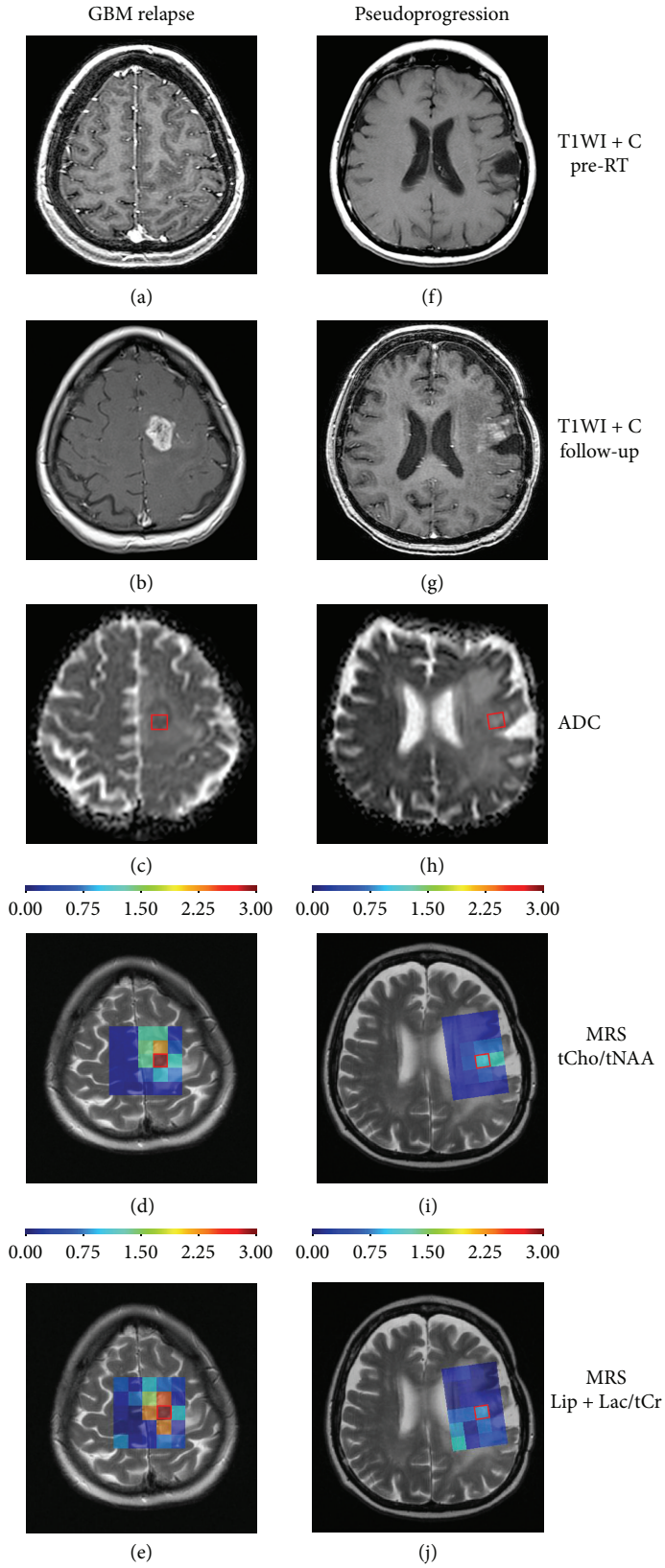

Figure 1: Representative MRI examples of glioblastoma relapse ((a)–(e)) and pseudoprogression ((f)–(j)): (a) + (f) show T1WI with gadolinium after surgical resection before radiotherapy, (b) + (g) show follow-up T1WI with gadolinium after 3 months from radiotherapy, (c) + (h) show ADC maps with marked VOI (ADCmean values for VOI: 848×10^{-6} mm^2/s in GBM relapse and 1355×10^{-6} mm^2/s in PsP), (d) + (i) show proton MR spectroscopy maps focused on tCho/tNAA ratio with marked VOI (peak values: 2.98 in GBM relapse and 1.33 in PsP), and (e) + (j) show proton MR spectroscopy maps focused on Lip + Lac/tCr ratio with marked VOI (peak values: 2.93 in GBM relapse and 0.83 in PsP).

Table 2: The cut-offs, sensitivity, and specificity of the metabolite concentrations, their ratios, and ADCmean values in a GBM relapse. AUC, area under the curve for each ROC analysis with appropriate statistical significance (p).

	AUC (95% CI)	p	Cut-off	Sensitivity	Specificity
Metabolite/MRS			[mM]		
tCho	0.532 (0.325; 0.740)	0.739	≤2.9	69.4	41.7
tNAA	0.970 (0.926; 1.000)	<0.001	≤1.5	75.0	100.0
tCr	0.613 (0.426; 0.801)	0.243	≤2.6	55.6	66.7
Lip + Lac	0.782 (0.574; 0.991)	0.004	≥4.8	100.0	66.7
tCho/tNAA	0.991 (0.970; 1.000)	<0.001	≥1.4	100.0	91.7
tCho/tCr	0.597 (0.388; 0.806)	0.317	≥0.7	83.3	41.7
tNAA/tCr	0.926 (0.786; 1.000)	<0.001	≤0.7	94.4	91.7
Lip + Lac/tCr	0.782 (0.574; 0.990)	0.004	≥1.9	91.7	75.0
ADC/DWI			$[10^{-6}\,mm^2/s]$		
ADCmean	1.000 (1.000; 1.000)	<0.001	≤1300	100.0	100.0

PsP has been proven by several authors especially in tumors with hypermethylation of the O(6)-methylguanine-DNA methyltransferase (MGMT) promoter gene [6] confirming greater activity of the combined treatment in this subset of patients with a favorable prognosis and longer progression and survival times [21]. MGMT is involved in the repair of DNA damage caused by alkylating agents such as TMZ. Methylation of MGMT promoter alters transcription of this gene and inhibits the repair mechanism. According to Kong's results, dynamic susceptibility-weighted contrast-enhanced perfusion MRI can be used for PsP development prediction and for its differentiation from tumor progression in GBM patients. Its value was significantly higher in the patients with an unmethylated MGMT promoter, compared with tumors with a hypermethylated MGMT status [22].

In our series, radionecrosis was not observed in any patients whereas PsP was documented in 25%. However, the RANO definition of PsP, which includes new enhancement within the radiation field within the first 12 weeks after completion of RT, is currently being challenged by Radbruch's observations of considerably lower incidence in PsP compared to previous reports [8]. Furthermore, in 30% of patients PsP developed later than during the first 12 weeks [8]. Taken together, standard follow-up MR imaging of GBM patients has its inherent limitations in identifying PsP with the recommended RANO criteria. The incorporation of advanced MRI techniques into MRI response assessment tools may be warranted for increased sensitivity and specificity in distinguishing between true tumor recurrence and treatment-related changes [10, 23].

Although advanced imaging modalities such as multiparametric MRI and PET have potential for further improvement in evaluation of brain lesions, their limited availability limits their routine use in worldwide clinical practice. For example, the most studied PET tracer for brain tumors, L-[methyl-11C]methionine, has sufficient tumor to normal brain uptake ratio for the recurrence diagnosis, but the short physical half-life of 11C restricts its clinical use to PET facilities that operate a cyclotron for on-site manufacturing of 11C [24]. In contrast, DWI and MRS are becoming a part of standard protocols. These methods enable further brain imaging beyond structural T1 or T2/FLAIR weighted imaging. By measurement of Brownian random motion of water molecules, DWI identifies changes in water diffusivity as a function of surrounding micro architecture such as increases in cell density, a histopathologic characteristic of a tumor recurrence. Decreased diffusivity is reflected in lower ADC values, which are a quantitative parameter of DWI independent of magnetic field strength. In our study, the upper threshold for GBM relapse determined was $1300 \times 10^{-6}\,mm^2/s$. All patients with PsP had ADCmean values above this cut-off value, yielding 100% sensitivity as well as specificity. This high sensitivity and specificity may be related to the lack of radionecrosis cases in our cohort and its small sample size. It may be assumed that, in PsP cases, the treatment-related tumor vasculature permeability and blood brain barrier instability responsible for temporary contrast enhancement lead to increased intercellular edema (and thus to high ADCs) as compared to radionecrotic cases, where release of products of cell death into the extracellular space may limit water diffusion (and lead to lower ADCs compared to PsP). Thus, it may not be possible to distinguish between recurrence and radionecrosis with 100% specificity and sensitivity utilizing only DWI. The combination of ADC values with MRS focused mainly on tNAA concentration, as a biomarker of neuronal density and viability, may aid in resolving these obscure cases. In our cohort, all PsP patients had tNAA concentration higher than calculated cut-off value, 1.5 mM. However, there are some limitations in the reproducibility and application of absolute metabolite concentrations because of their interpersonal variability [25]. Moreover, a significant regional variability in the absolute metabolite concentrations of different brain regions has to be also taken into consideration [26]. We recommend use of metabolite ratios that have generally lower intrasubject coefficient of variation and thus they can serve as feasible biomarkers for differentiation of PsP and tumor recurrence. Apart from the most common metabolite ratios as tCho/tNAA and tNAA/tCr, which can be correlated with other institutional data (Table 4), we have also documented Lac + Lip/tCr ratio as a new statistically significant parameter ($p = 0.004$) for differentiation between GBM relapse and PsP. GBM relapse was characterized by a higher Lac + Lip/tCr ratio with a cut-off of 1.9 (sensitivity 91.7%, specificity 75.0%;

Table 3: Comparison of MRS and DWI/ADCmean results between the patients (n = 24) with a pseudoprogression and glioblastoma relapse. Two spatially independent values corresponding with two perpendicular planes on MRI were analyzed in each patient (n = 48 analyzed samples).

	Pseudoprogression (N = 12)	GBM relapse (N = 36)	p
tCho [mM]			
>2.9	5 (41.7%)	11 (30.6%)	0.500
≤2.9	7 (58.3%)	25 (69.4%)	
Median (min; max)	**2.88 (0.86; 3.73)**	**2.41 (1.26; 4.40)**	**0.739**
tNAA [mM]			
>1.5	12 (100.0%)	9 (25.0%)	<0.001
≤1.5	0 (0.0%)	27 (75.0%)	
Median (min; max)	**2.88 (1.52; 5.13)**	**1.19 (0.44; 2.22)**	**<0.001**
tCr [mM]			
>2.6	8 (66.7%)	16 (44.4%)	0.318
≤2.6	4 (33.3%)	20 (55.6%)	
Median (min; max)	**2.74 (1.71; 7.53)**	**2.49 (1.46; 5.86)**	**0.243**
Lip + Lac			
<4.8	8 (66.7%)	0 (0.0%)	<0.001
≥4.8	4 (33.3%)	36 (100.0%)	
Median (min; max)	**3.50 (0.31; 26.76)**	**10.77 (5.14; 37.23)**	**0.004**
tCho/tNAA			
<1.4	11 (91.7%)	0 (0.0%)	<0.001
≥1.4	1 (8.3%)	36 (100.0%)	
Median (min; max)	**0.77 (0.38; 1.77)**	**2.00 (1.63; 3.93)**	**<0.001**
tCho/tCr			
<0.7	5 (41.7%)	6 (16.7%)	0.113
≥0.7	7 (58.3%)	30 (83.3%)	
Median (min; max)	**0.82 (0.30; 1.37)**	**0.86 (0.54; 1.64)**	**0.317**
tNAA/tCr			
>0.7	11 (91.7%)	2 (5.6%)	<0.001
≤0.7	1 (8.3%)	34 (94.4%)	
Median (min; max)	**0.99 (0.28; 1.59)**	**0.45 (0.24; 0.72)**	**<0.001**
Lip + Lac/tCr			
<1.9	9 (75.0%)	3 (8.3%)	<0.001
≥1.9	3 (25.0%)	33 (91.7%)	
Median (min; max)	**0.88 (0.08; 12.35)**	**4.43 (1.33; 17.42)**	**0.004**
ADCmean [10^{-6} mm^2/s]			
>1300	12 (100.0%)	0 (0.0%)	<0.001
≤1300	0 (0.0%)	36 (100.0%)	
Median (min; max)	**1373 (1317; 1463)**	**1160 (1011; 1276)**	**<0.001**

Table 2). This finding indicates lactate and lipid accumulation that is the typical feature of high-grade gliomas documented, in line with our results, by other authors [27].

This small prospective imaging study has two main limitations. One is the lack of standardized MR image acquisition parameters at different institutions which precludes direct comparison with other studies (Table 4). As expected, greater similarity is observed between cross-institutional ADC values than between MRS metabolite concentrations and ratios, which are more sensitive to institutional setup of acquisition parameters. Another limitation is missing biopsy data of suspected lesions in 33% of patients. Imaging of this subgroup of patients with no resolving contrast enhancement may represent a local mixture of PsP patterns and growing recurrent tumor leading to relatively low ADC values, but still MRS characteristics favoring diagnosis of PsP. Unfortunately, this subgroup of patients where biopsy is risky forms the group of patients that would benefit most from the noninvasive nature of advanced MRI. However, care must be taken in the case where different MRI methods point towards different diagnoses. Thus, combination of multiple MRI methods is warranted. Close follow-up with early repeated imaging is recommended for these patients.

The accurate determination of progression is important not only for the individual care of each patient but also for correct enrollment in clinical trials investigating salvage

Table 4: Comparison of MRS and ADC results with other studies focusing on differentiation of GBM recurrence and treatment-related changes: No. pt. = number of patients, Dg = diagnosis, RI = radiation injury, GR = glioma recurrence, Tu = tumor, and RN = radiation necrosis.

Authors	Primary grade [No. pt.]	MR [T]	Dg	*N*	Cho/Cr	Cho/NAA	NAA/Cr	ADC [10^{-3} m^2/s]
Hein et al. [30]	III/10	1.5	GR	12				1.18 ± 0.13
	IV/8		RI	6				1.40 ± 0.17
Weybright et al. [31]	II–IV/24	1.5	GR	16	2.52 (1.66–4.26)	3.48 (1.70–6.47)	0.79 (0.47–1.15)	
	Other/5		RI	13	1.57 (0.72–1.76)	1.31 (0.83–1.78)	1.22 (0.94–1.69)	
Zeng et al. [32]	III/36	3.0	Tu	32	2.82 ± 0.65	3.52 ± 0.98	0.84 ± 0.23	1.20 ± 0.08
	IV/19		RI	23	1.61 ± 0.34	1.55 ± 0.54	1.10 ± 0.26	1.39 ± 0.09
Nakajima et al. [33]	II/4	1.5	GR	7	3.17 ± 0.83			
	III/6, IV/8		RN	11	2.25 ± 0.80			
Bobek-Billewicz et al. [34]	III/6	1.5/3.0	GR	5	2.16 (1.67–3.15)	1.9 (0.86–2.36)		1.06 ± 0.18
	IV/2		RI	6	1.34 (1.13–2.37)	2.1 (0.97–2.87)		1.13 ± 0.13
Amin et al. [35]	II/5	1.5	GR	18	2.00 ± 0.20	1.60 ± 0.27		
	III/12, IV/7		RN	6		0.94 ± 0.3		
Present study, 2015	IV/24	3.0	GR	18	0.95 ± 0.27	2.20 ± 0.55	0.45 ± 0.13	1.152 ± 0.064
			RI	6	0.82 ± 0.34	0.86 ± 0.37	1.03 ± 0.38	1.383 ± 0.045

treatment and reporting results of trials investigating initial treatment. While overall survival is generally the most well-established outcome of oncologic clinical trials, time to progression, progression-free survival, and progression-free survival at 6 months are becoming more reasonable endpoints in evaluating brain tumor response [7, 28, 29]. For evaluation of initial treatment (surgery or concurrent chemoradiation), progression is a more accurately representative endpoint compared to overall survival, which may be biased by different salvage treatments. The appropriate and correct determination of progression continues to be essential as well for correct patient enrollment and treatment within salvage treatment clinical trials. Care must be taken in the case of a suspected treatment-related change, which typically results in termination of ongoing effective adjuvant treatment and if misidentified would bias results of the investigated salvage agent. We suggest that institutions involved in clinical research of new agents for patients suffering from brain tumors consider establishing their own institutional validation using advanced MRI methods with institutionally determined cut-off values as in our presented study. Particularly for MRS values, institutionally determined threshold values may be necessary to account for variability between different institutions as summarized in Table 4. Thus, the ratio of concentrations of representative metabolites (e.g., tCho/tNAA) is preferred in comparing the absolute concentration of a metabolite.

In summary, more accessible advanced MRI methods such as diffusion-weighted and spectroscopic imaging may further improve sensitivity and specificity of standard imaging in diagnosing recurrence of brain tumors. ADCmean values $\leq 1300 \times 10^{-6}\,mm^2/s$ and tCho/tNAA ratio ≥ 1.4 are strongly associated with differentiating GBM recurrence from treatment-related changes indicative of PsP. Institutional validation of thresholds for advanced MRI methods is warranted especially for appropriate enrollment into salvage clinical trials and reporting of outcomes of initial treatment.

Conflict of Interests

The authors declare that there is no conflict of interests regarding the publication of this paper.

Acknowledgments

This paper is supported by Grants IGA NT/14600, NT/14120 of the Czech Ministry of Health, supported by European Regional Development Fund, Project FNUSA-ICRC (no. CZ.1.05/1.1.00/02.0123), and supported by MH CZ-DRO (MMCI, 00209805). The authors thank Seaberg, Maasa H., Ph.D., for revision of paper.

References

[1] R. Stupp, W. P. Mason, M. J. van den Bent et al., "Radiotherapy plus concomitant and adjuvant temozolomide for glioblastoma," *The New England Journal of Medicine*, vol. 352, no. 10, pp. 987–996, 2005.

[2] D. Brandsma, L. Stalpers, W. Taal, P. Sminia, and M. J. van den Bent, "Clinical features, mechanisms, and management of pseudoprogression in malignant gliomas," *The Lancet Oncology*, vol. 9, no. 5, pp. 453–461, 2008.

[3] A. J. Kumar, N. E. Leeds, G. N. Fuller et al., "Malignant gliomas: MR imaging spectrum of radiation therapy- and chemotherapy-induced necrosis of the brain after treatment," *Radiology*, vol. 217, no. 2, pp. 377–384, 2000.

[4] A. A. Brandes, A. Tosoni, F. Spagnolli et al., "Disease progression or pseudoprogression after concomitant radiochemotherapy treatment: pitfalls in neurooncology," *Neuro-Oncology*, vol. 10, no. 3, pp. 361–367, 2008.

[5] A. Chakravarti, M. G. Erkkinen, U. Nestler et al., "Temozolomide-mediated radiation enhancement in glioblastoma: a report on underlying mechanisms," *Clinical Cancer Research*, vol. 12, no. 15, pp. 4738–4746, 2006.

[6] A. A. Brandes, E. Franceschi, A. Tosoni et al., "MGMT promoter methylation status can predict the incidence and outcome of pseudoprogression after concomitant radiochemotherapy in newly diagnosed glioblastoma patients," *Journal of Clinical Oncology*, vol. 26, no. 13, pp. 2192–2197, 2008.

[7] K. R. Lamborn, W. K. A. Yung, S. M. Chang et al., "Progression-free survival: an important end point in evaluating therapy for recurrent high-grade gliomas," *Neuro-Oncology*, vol. 10, no. 2, pp. 162–170, 2008.

[8] A. Radbruch, J. Fladt, P. Kickingereder et al., "Pseudoprogression in patients with glioblastoma: clinical relevance despite low incidence," *Neuro-Oncology*, vol. 17, no. 1, pp. 151–159, 2014.

[9] H. S. Friedman, M. D. Prados, P. Y. Wen et al., "Bevacizumab alone and in combination with irinotecan in recurrent glioblastoma," *Journal of Clinical Oncology*, vol. 27, no. 28, pp. 4733–4740, 2009.

[10] H.-W. Kao, S.-W. Chiang, H.-W. Chung, F. Y. Tsai, and C.-Y. Chen, "Advanced MR imaging of gliomas: an update," *BioMed Research International*, vol. 2013, Article ID 970586, 14 pages, 2013.

[11] M. Bulik, R. Jancalek, J. Vanicek, A. Skoch, and M. Mechl, "Potential of MR spectroscopy for assessment of glioma grading," *Clinical Neurology and Neurosurgery*, vol. 115, no. 2, pp. 146–153, 2013.

[12] B. Roy, R. K. Gupta, A. A. Maudsley et al., "Utility of multiparametric 3-T MRI for glioma characterization," *Neuroradiology*, vol. 55, no. 5, pp. 603–613, 2013.

[13] R. Ahmed, M. J. Oborski, M. Hwang, F. S. Lieberman, and J. M. Mountz, "Malignant gliomas: current perspectives in diagnosis, treatment, and early response assessment using advanced quantitative imaging methods," *Cancer Management and Research*, vol. 6, no. 1, pp. 149–170, 2014.

[14] A. Ion-Margineanu, S. van Cauter, D. M. Sima et al., "Tumour relapse prediction using multiparametric MR data recorded during follow-up of GBM patients," *BioMed Research International*. In press.

[15] S. W. Provencher, "Automatic quantitation of localized *in vivo* ^{1}H spectra with LCModel," *NMR in Biomedicine*, vol. 14, no. 4, pp. 260–264, 2001.

[16] F. Jiru, A. Skoch, D. Wagnerova, M. Dezortova, and M. Hajek, "jSIPRO—analysis tool for magnetic resonance spectroscopic imaging," *Computer Methods and Programs in Biomedicine*, vol. 112, no. 1, pp. 173–188, 2013.

[17] P. Y. Wen, D. R. Macdonald, D. A. Reardon et al., "Updated response assessment criteria for high-grade gliomas: response assessment in neuro-oncology working group," *Journal of Clinical Oncology*, vol. 28, no. 11, pp. 1963–1972, 2010.

[18] D. R. Macdonald, T. L. Cascino, S. C. Schold Jr., and J. G. Cairncross, "Response criteria for phase II studies of supratentorial malignant glioma," *Journal of Clinical Oncology*, vol. 8, no. 7, pp. 1277–1280, 1990.

[19] E. R. Gerstner, M. B. McNamara, A. D. Norden, D. LaFrankie, and P. Y. Wen, "Effect of adding temozolomide to radiation therapy on the incidence of pseudo-progression," *Journal of Neuro-Oncology*, vol. 94, no. 1, pp. 97–101, 2009.

[20] L. C. H. da Cruz Jr., I. Rodriguez, R. C. Domingues, E. L. Gasparetto, and A. G. Sorensen, "Pseudoprogression and pseudoresponse: imaging challenges in the assessment of posttreatment glioma," *American Journal of Neuroradiology*, vol. 32, no. 11, pp. 1978–1985, 2011.

[21] A. Fabi, M. Russillo, G. Metro, A. Vidiri, S. Di Giovanni, and F. Cognetti, "Pseudoprogression and MGMT status in glioblastoma patients: implications in clinical practice," *Anticancer Research*, vol. 29, no. 7, pp. 2607–2610, 2009.

[22] D.-S. Kong, S. T. Kim, E.-H. Kim et al., "Diagnostic dilemma of pseudoprogression in the treatment of newly diagnosed glioblastomas: the role of assessing relative cerebral blood flow volume and oxygen-6-methylguanine-DNA methyltransferase promoter methylation status," *American Journal of Neuroradiology*, vol. 32, no. 2, pp. 382–387, 2011.

[23] D. Wagnerova, V. Herynek, A. Malucelli et al., "Quantitative MR imaging and spectroscopy of brain tumours: a step forward?" *European Radiology*, vol. 22, no. 11, pp. 2307–2318, 2012.

[24] M. M. D'Souza, R. Sharma, A. Jaimini et al., "11C-MET PET/CT and advanced MRI in the evaluation of tumor recurrence in high-grade gliomas," *Clinical Nuclear Medicine*, vol. 39, no. 9, pp. 791–798, 2014.

[25] O. T. Wiebenga, A. M. Klauser, G. J. Nagtegaal et al., "Longitudinal absolute metabolite quantification of white and gray matter regions in healthy controls using proton MR spectroscopic imaging," *NMR in Biomedicine*, vol. 27, no. 3, pp. 304–311, 2014.

[26] L. Minati, D. Aquino, M. G. Bruzzone, and A. Erbetta, "Quantitation of normal metabolite concentrations in six brain regions by in-vivoH-MR spectroscopy," *Journal of Medical Physics*, vol. 35, no. 3, pp. 154–163, 2010.

[27] S. Chawla, Y. Zhang, S. Wang et al., "Proton magnetic resonance spectroscopy in differentiating glioblastomas from primary cerebral lymphomas and brain metastases," *Journal of Computer Assisted Tomography*, vol. 34, no. 6, pp. 836–841, 2010.

[28] M.-Y. C. Polley, K. R. Lamborn, S. M. Chang, N. Butowski, J. L. Clarke, and M. Prados, "Six-month progression-free survival as an alternative primary efficacy endpoint to overall survival in newly diagnosed glioblastoma patients receiving temozolomide," *Neuro-Oncology*, vol. 12, no. 3, pp. 274–282, 2010.

[29] L. Trippa, P. Y. Wen, G. Parmigiani, D. A. Berry, and B. M. Alexander, "Combining progression-free survival and overall survival as a novel composite endpoint for glioblastoma trials," *Neuro-Oncology*, 2015.

[30] P. A. Hein, C. J. Eskey, J. F. Dunn, and E. B. Hug, "Diffusion-weighted imaging in the follow-up of treated high-grade gliomas: tumor recurrence versus radiation injury," *The American Journal of Neuroradiology*, vol. 25, no. 2, pp. 201–209, 2004.

[31] P. Weybright, P. C. Sundgren, P. Maly et al., "Differentiation between brain tumor recurrence and radiation injury using MR spectroscopy," *American Journal of Roentgenology*, vol. 185, no. 6, pp. 1471–1476, 2005.

[32] Q.-S. Zeng, C.-F. Li, H. Liu, J.-H. Zhen, and D.-C. Feng, "Distinction between recurrent glioma and radiation injury using magnetic resonance spectroscopy in combination with diffusion-weighted imaging," *International Journal of Radiation, Oncology, Biology, Physics*, vol. 68, no. 1, pp. 151–158, 2007.

[33] T. Nakajima, T. Kumabe, M. Kanamori et al., "Differential diagnosis between radiation necrosis and glioma progression using sequential proton magnetic resonance spectroscopy and methionine positron emission tomography," *Neurologia Medico-Chirurgica*, vol. 49, no. 9, pp. 394–401, 2009.

[34] B. Bobek-Billewicz, G. Stasik-Pres, H. Majchrzak, and Ł. Zarudzki, "Differentiation between brain tumor recurrence and

radiation injury using perfusion, diffusion-weighted imaging and MR spectroscopy," *Folia Neuropathologica*, vol. 48, no. 2, pp. 81–92, 2010.

[35] A. Amin, H. Moustafa, E. Ahmed, and M. El-Toukhy, "Glioma residual or recurrence versus radiation necrosis: accuracy of pentavalent technetium-99m-dimercaptosuccinic acid [Tc-99m (V) DMSA] brain SPECT compared to proton magnetic resonance spectroscopy (1H-MRS): initial results," *Journal of Neuro-Oncology*, vol. 106, no. 3, pp. 579–587, 2012.

Hindawi Publishing Corporation
BioMed Research International
Volume 2015, Article ID 108458, 9 pages
http://dx.doi.org/10.1155/2015/108458

Research Article

Long Noncoding RNA KIAA0125 Potentiates Cell Migration and Invasion in Gallbladder Cancer

Wenjie Lv, Lei Wang, Jianhua Lu, Jiasheng Mu, Yingbin Liu, and Ping Dong

Department of General Surgery, Xinhua Hospital Affiliated to School of Medicine, Shanghai Jiao Tong University, 1665 Kongjiang Road, Shanghai 200092, China

Correspondence should be addressed to Ping Dong; pingdongdr@163.com

Received 29 May 2014; Revised 15 August 2014; Accepted 20 August 2014

Academic Editor: Aurelio Ariza

Gallbladder cancer (GBC) is one of the mostly aggressive diseases with poor prognosis due to the lack of severe symptoms. To date, little is known about the potential roles and underlying mechanisms of long noncoding RNAs (lncRNAs) in GBC initiation and progression. Thus, it provides us with a novel insight into the contribution of lncRNAs to GBC development. Remarkably, we found the differential expression of a lncRNA, namely, KIAA0125, in a pair of GBC cell sublines which possess different metastatic potentials. Then the effects of KIAA0125 on GBC cell migration, invasion, and epithelial-mesenchymal transitions (EMT) were investigated by using a lentivirus-mediated RNA interference (RNAi) system. Notably, cell migration and invasion were strongly inhibited by KIAA0125 suppression. Moreover, the expression of β-Catenin was increased and the expression of Vimentin was decreased in GBC-SD/M cells after KIAA0125 knockdown. Thus, our findings suggested that KIAA0125 promoted the migration and invasion of GBC cells and could serve as a potential therapeutic target in advanced GBC.

1. Introduction

Gallbladder cancer (GBC) is one of the most lethal malignancies and the fifth common neoplasm of gastrointestinal tract [1–3]. The 5-year survival rate is extremely low, possibly due to the lack of severe symptoms and thus it is hard to make a diagnosis at an early stage [4]. Moreover, treatment approaches such as cholecystectomy, chemotherapy, or radiotherapy in advanced cases did not yield favorable outcomes [4–8]. Hence, exploring novel signal molecules involved in GBC metastasis may provide new effective therapeutic strategies.

Recently, an increasing number of investigations have shown that long noncoding RNAs (lncRNAs), a group of newly identified noncoding RNA molecules, are emerging as key players in the regulation of multiple stages of many cancers, such as colorectal cancers, prostate cancer, hepatocellular carcinomas, and breast cancers [9–15]. For instance, the aberrant expression of Hox transcript antisense intergenic RNA (HOTAIR) has been identified in some cancers, which has been shown to correlate with cellular proliferation, metastasis, and clinical relapse [10, 16, 17]. The human metastasis associated lung adenocarcinoma transcript 1 (MALAT-1) is known to be misregulated in several cancers and usually acts as a critical regulator of cancer metastasis and epithelial-mesenchymal transitions (EMT) [18–20]. Yet, it is still obscure whether lncRNAs are involved in GBC progression.

Intriguingly, a novel lncRNA, namely, KIAA0125, draws our attention. The *KIAA0125* gene is localized on chromosome 14q32.33. A recent study reported that *KIAA0125* might play a role in neurogenesis, maybe in preventing the generation of dopaminergic neurons, or it could also be involved in inducing astrocytosis. However, the functional role of KIAA0125 in cancer has not been determined yet. In the present study, we investigated whether KIAA0125 is involved in GBC progression. We found KIAA0125 expression is incredibly elevated in a GBC cell subline GBC-SD/M with higher metastatic potentials as compared to the other subline GBC-SD cells [21]. A lentivirus-mediated RNA interference (RNAi) system was thus employed to knock down KIAA0125 expression in GBC-SD/M cells. Moreover, the effects of KIAA0125 on GBC cell migration and invasion were further evaluated.

2. Materials and Methods

2.1. Cell Culture. Two human GBC cell sublines, GBC-SD and GBC-SD/M, which possess lower and higher metastatic potential, respectively [21], were obtained from the Type Culture Collection of the Chinese Academy of Sciences (Shanghai, China). The two cell sublines were cultured in DMEM (# 11995065; Gibco Life Technology, Gaithersburg, MD) supplemented with 10% fetal bovine serum (FBS; Biowest, Nuaille, France). HEK293T cells were grown in DMEM (# SH30243.01B+; HyClone, Logan, Utah, USA) containing 10% FBS. All cells were grown at 37°C in an incubator with 5% CO_2.

2.2. Lentivirus Construction. An shRNA sequence (5′-GCAAGGCCAGTGGAGTTAATCCTCGAGGATTAACTCCACTGGCCTTGC-3′) was designed based on human lncRNA gene KIAA0125 (NR_026800). The nontargeting shRNA (5′-GCGGAGGGTTTGAAAGAATATCTCGAGATATTCTTTCAAACCCTCCGCTTTTTT-3′) was used as control. Then two shRNA sequences were cloned into pFH-L vectors (Shanghai Hollybio, China), which contain green fluorescent protein (GFP) as the detectable marker. The two reconstructed vectors were then transfected into HEK293T cells to generate lentiviruses, along with pCMVΔR8.92 and pVSVG-I as packing vectors (Shanghai Hollybio, China). Supernatants containing either the lentivirus expressing the KIAA0125 shRNA (Lv-shKIAA0125) or the control shRNA (Lv-shCon) were harvested 96 h after transfection.

2.3. Lentivirus Infection. GBC-SD/M cells were applied for KIAA0125 knockdown, which were cultured in 6-well plates at a density of 5×10^4 cells/well. Then GBC-SD/M cells were subjected to Lv-shKIAA0125 and Lv-shCon treatment for 96 h, with a multiplicity of infection (MOI) of 50. To evaluate the infection efficiency, cells were observed under fluorescence microscope and the percentage of GFP positive cells was counted.

2.4. Quantitative Real-Time PCR. Total RNA was extracted from GBC-SD/M cells using the Trizol reagent (Invitrogen, Carlsbad, CA, USA). For each sample, 2 μg of total RNA was subjected to reverse transcription by using Mu-MLV (MBI Fermentas, Euromedex, Souffelweyersheim, France). Then the expression levels of four candidate genes (KIAA0125, α-Catenin, β-Catenin, and Vimentin) in each cDNA sample were analyzed using primers listed below. Beta-actin and GAPDH were used as internal control genes. For each 20 μL PCR reaction, we added SYBR Premix Ex Taq (10 μL), forward and reverse primers (2.5 μM, 0.8 μL), cDNA sample (5 μL), and ddH_2O (4.2 μL). The Bio-Rad Connect real-time PCR platform was applied to run PCR reactions for 40 cycles under the following conditions: (1) initial denaturation at 95°C for 1 min, (2) denaturation at 95°C for 5 s, and (3) annealing extension at 60°C for 20 s. Mathematical model for relative quantification in real-time PCR was $2^{-\Delta\Delta CT}$ method [22]. Data were presented as CT values, which were defined as the threshold PCR cycle number at which an amplified product is first detected: ΔCT = Avg. CT (target gene) – Avg. CT (housekeeping gene), and ΔΔCT = Avg. ΔCT – Avg. ΔCT (control). Results presented in histogram are the normalized target gene amount relative to control $2^{-\Delta\Delta CT}$. Primers are listed as follows:

KIAA0125 (*KIAA0125*, ID: 9834):
5′-CCTCTCAGCCTCCAGCGTTG-3′ (forward)
5′-TGCTCTTGCTCACTCACACTCC-3′ (reverse)
Vimentin (*VIM*, ID: 7431):
5′-ATTCCACTTTGCGTTCAAGG-3′ (forward)
5′-CTTCAGAGAGAGGAAGCCGA-3′ (reverse)
α-Catenin (*CTNNA1*, ID: 1495):
5′-GAGCTGTCTACGCAAGTCCC-3′ (forward)
5′-TTTCGGAGTACATGGGCAAT-3′ (reverse)
β-Catenin (*CTNNB1*, ID: 1499):
5′-AGCTACTGCCTCCGGTCTTC-3′ (forward)
5′-GTGGTCAACAGCCAGCTCA-3′ (reverse)
β-actin (*ACTB*, ID: 60):
5′-GTGGACATCCGCAAAGAC-3′ (forward)
5′-AAAGGGTGTAACGCAACTA-3′ (reverse)
GAPDH (*GAPDH*, ID: 2597):
5′-GGAAGCTTGTCATCAATGGAA-3′ (forward)
5′-TGGACTCCACGACGTACTCA-3′ (reverse).

2.5. The Scratch Test. Random migration was determined by the scratch test assay, in which cells were grown to 90% confluency in 96-well plates, streaked with a 200 μL sterile pipette tip, and allowed to recover in an incubator at 37°C in the next 36 h. The plates were visualized under light microscope and fluorescence microscope (×40 magnification) at 24 h and 36 h. Random migration was evaluated by measuring the area of occupancy via an image-analysis program (Image-Pro Plus, Media Cybernetics, MD).

2.6. Transwell Assay. Transwell chambers and Matrigel Invasion Chambers (Corning, NY, USA) were used for transwell assay and transwell invasion assay, respectively. For transwell assay, cells were harvested and suspended in serum-free medium. Then 200 μL cell suspension was added to the upper chamber at a density of 3×10^4 cells/well, and 500 μL of serum-rich medium was added to the lower chamber. The transwell chambers were cultured for 6 h. For transwell invasion assay, the Matrigel Invasion Chambers were incubated for 16 h. In both analyses, the chambers were collected for the following treatment. The surface of the upper chamber was swabbed with cotton-tipped applicators to remove the cells that did not migrate. The lower compartment was fixed with methanol and stained by crystal violet. Distilled water was then applied to wash off excess stain materials. For data analysis, migrating cells and the amount of dissolved crystal violet were both measured by using a light microscope and spectrophotometer.

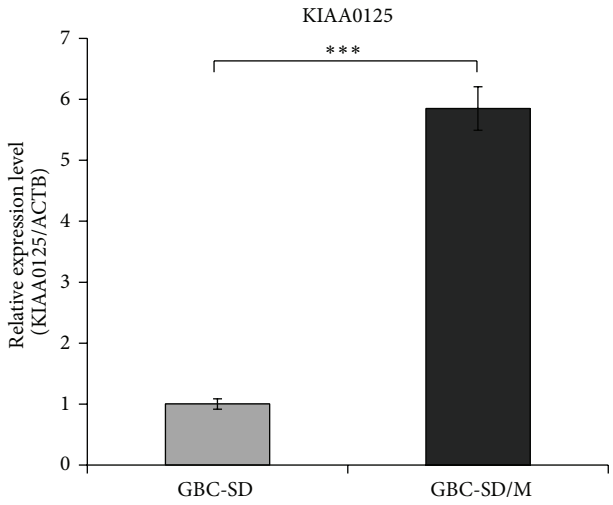

Figure 1: KIAA0125 expression in human GBC cells. The mRNA expression levels of KIAA0125 in GBC-SD and GBC-SD/M cells were determined by qRT-PCR. β-Actin was used as an internal control gene. $^{***}P < 0.001$, compared to GBC-SD.

2.7. Statistical Analysis. All assays were performed in triplicate and the data were expressed as mean ± standard deviation (SD). The Student's t-test was applied for statistical analysis and a P value of less than 0.05 was considered significant.

3. Results

3.1. Suppression of KIAA0125 by Lentivirus-Mediated RNAi. Here we firstly detected the expression of KIAA0125 in human GBC-SD and GBC-SD/M cells using qRT-PCR analysis. As shown in Figure 1, the relative expression level of KIAA0125 was remarkably upregulated in GBC-SD/M cells (5.85 ± 0.357), compared to GBC-SD cells (1.003 ± 0.087). As previously described by Liu and his colleagues, GBC-SD and GBC-SD/M had relative lower and higher metastatic potential, respectively. The GBC-SD/M subline was established by isolating a subpopulation with high metastatic potential from an experimental liver metastatic model of GBC [21]. Hence, our data strongly suggest that KIAA0125 is involved in the regulation of GBC metastasis. To verify the role of KIAA0125 in GBC, we employed a lentivirus-mediated RNAi system to specifically knock down the expression of KIAA0125 in GBC-SD/M cells. Our constructed lentiviruses could successfully infect GBC-SD/M cells, with an infection efficiency more than 80% (Figure 2(a)). The relative expression level of KIAA0125 in Lv-shKIAA0125 infected cells was much lower than in Lv-shCon infected cells, with a knockdown efficiency more than 60% (Figure 2(b)). These results indicated that Lv-shKIAA0125 could specifically knock down KIAA0125 in GBC-SD/M cells.

3.2. Suppression of KIAA0125 Inhibited GBC Cell Migration. To testify our hypothesis that KIAA0125 may contribute to GBC migration, we performed the scratch test and transwell assay in GBC-SD/M cells treated with Lv-shKIAA0125. Compared with Lv-shCon group, the "wound healing" ability of Lv-shKIAA0125 treated cells was significantly inhibited as shown by the reduced areas of occupancy at indicated time points (Figures 3(a) and 3(b)). Moreover, we observed remarkable reduction of cells that migrated to the lower compartment in Lv-shKIAA0125 group (Figure 4(a)). The number of migrating cells was reduced in Lv-shKIAA0125 group by 67%, as compared to Lv-shCon group (Figure 4(b)). The amount of crystal violet was also decreased by 55% after KIAA0125 suppression ($P < 0.001$, Figure 4(c)). However, the impact of KIAA0125 knockdown on GBC-SD cell migration was negligible, as determined by transwell assay (Figure S1(A) in Supplementary Material available online at http://dx.doi.org/10.1155/2015/108458). As shown in Figure S1(B), the number of migrating cells was reduced in Lv-shKIAA0125 group by 29%, as compared to Lv-shCon group. Also, the amount of crystal violet was decreased by only 7% (Figure S1(C)). These results strongly indicate that KIAA0125 is a key regulator of GBC cell motility and migration.

3.3. Suppression of KIAA0125 Inhibited GBC Cell Invasion. Furthermore, the invasive potential of Lv-shKIAA0125 treated cells was evaluated by transwell assay using Matrigel Invasion Chambers. As shown in Figures 5(a) and 5(b), the number of cells that invaded to the lower compartment was markedly reduced after KIAA0125 suppression (164.9 ± 6.5), as compared to Lv-shCon group (205.9 ± 2.4), which was confirmed by the amount of crystal violet (Figure 5(c)). These results indicate that KIAA0125 also facilitates GBC cell invasion.

3.4. Effect of KIAA0125 Suppression on EMT. To determine the underlying molecular mechanism by which KIAA0125 controls GBC metastasis, we analyzed the effect of KIAA0125 knockdown on EMT, which has been shown to play a key role in promoting the aggressiveness of GBC [23]. Three EMT markers, Vimentin, α-Catenin, and β-Catenin, were selected for qRT-PCR analysis. As shown in Figure 6, the relative expression level of Vimentin in Lv-shKIAA0125 infected cells was much lower than in Lv-shCon infected cells, with a reduction by over 10%. The relative expression level of β-Catenin was remarkably elevated by about 40% after KIAA0125 knockdown. However, the expression of α-Catenin was not significantly changed. Our data suggest that KIAA0125 is essential for GBC metastasis possibly due to the induction of EMT.

4. Discussion

LncRNAs can be classified into several subtypes including intergenic, intronic, sense, antisense, and bidirectional according to their genomic relationship with coding genes [24, 25]. In the present study, we found a differentially expressed lncRNA named KIAA0125 in GBC-SD and GBC-SD/M using qRT-PCR analysis. KIAA0125 was upregulated in a highly metastatic GBC cell subline GBC-SD/M, in contrast

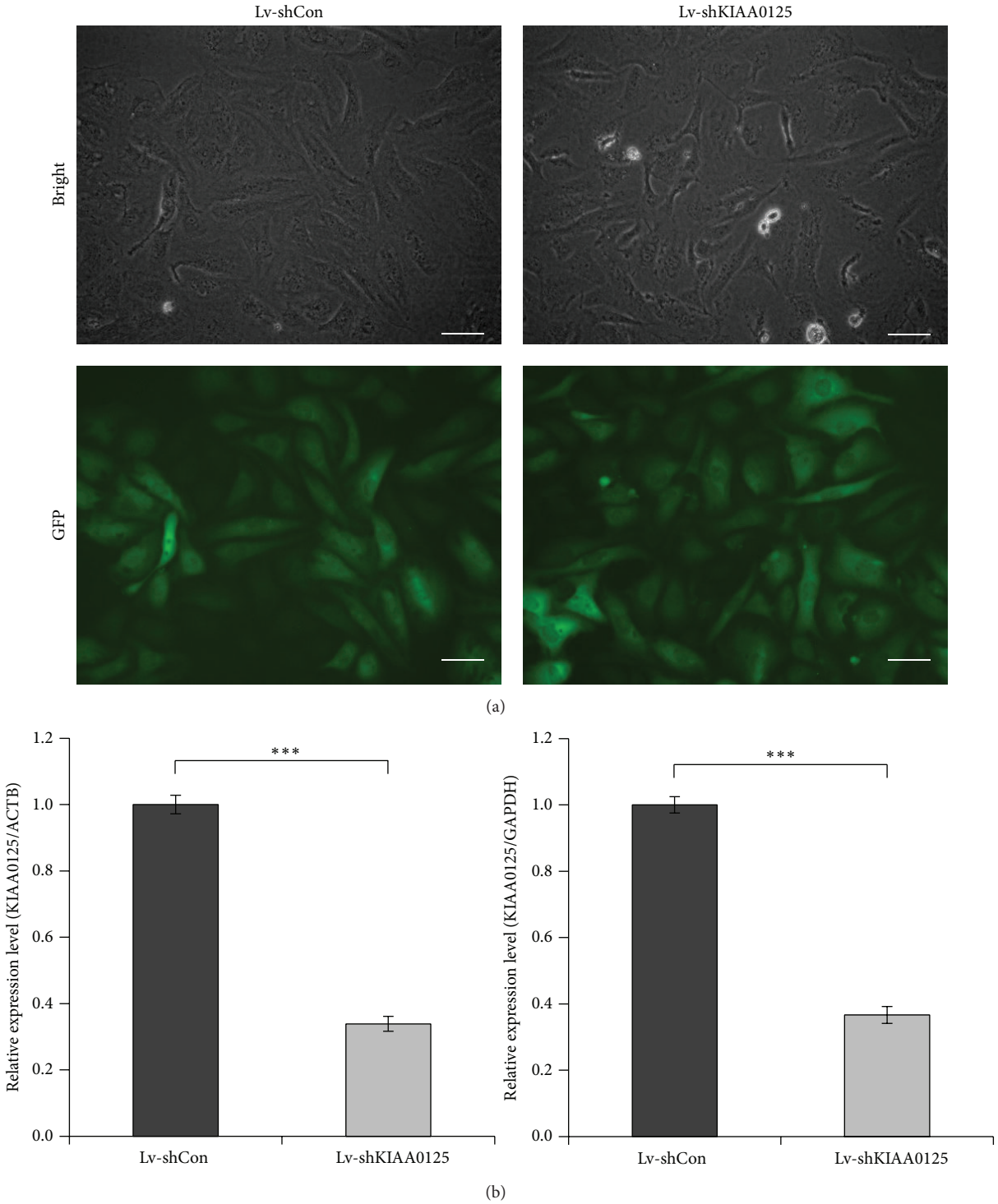

Figure 2: Knockdown of KIAA0125 by lentivirus-mediated RNAi. (a) GBC-SD/M cells were infected with Lv-shKIAA0125 or Lv-shCon, and the infection efficiency was monitored by fluorescence microscopy after 96 h. Scale bar: 100 μm. (b) The knockdown efficiency of KIAA0125 targeting lentivirus-mediated RNAi was determined by qRT-PCR. β-Actin and GAPDH were used as internal control genes. $^{***}P < 0.001$, compared to Lv-shCon.

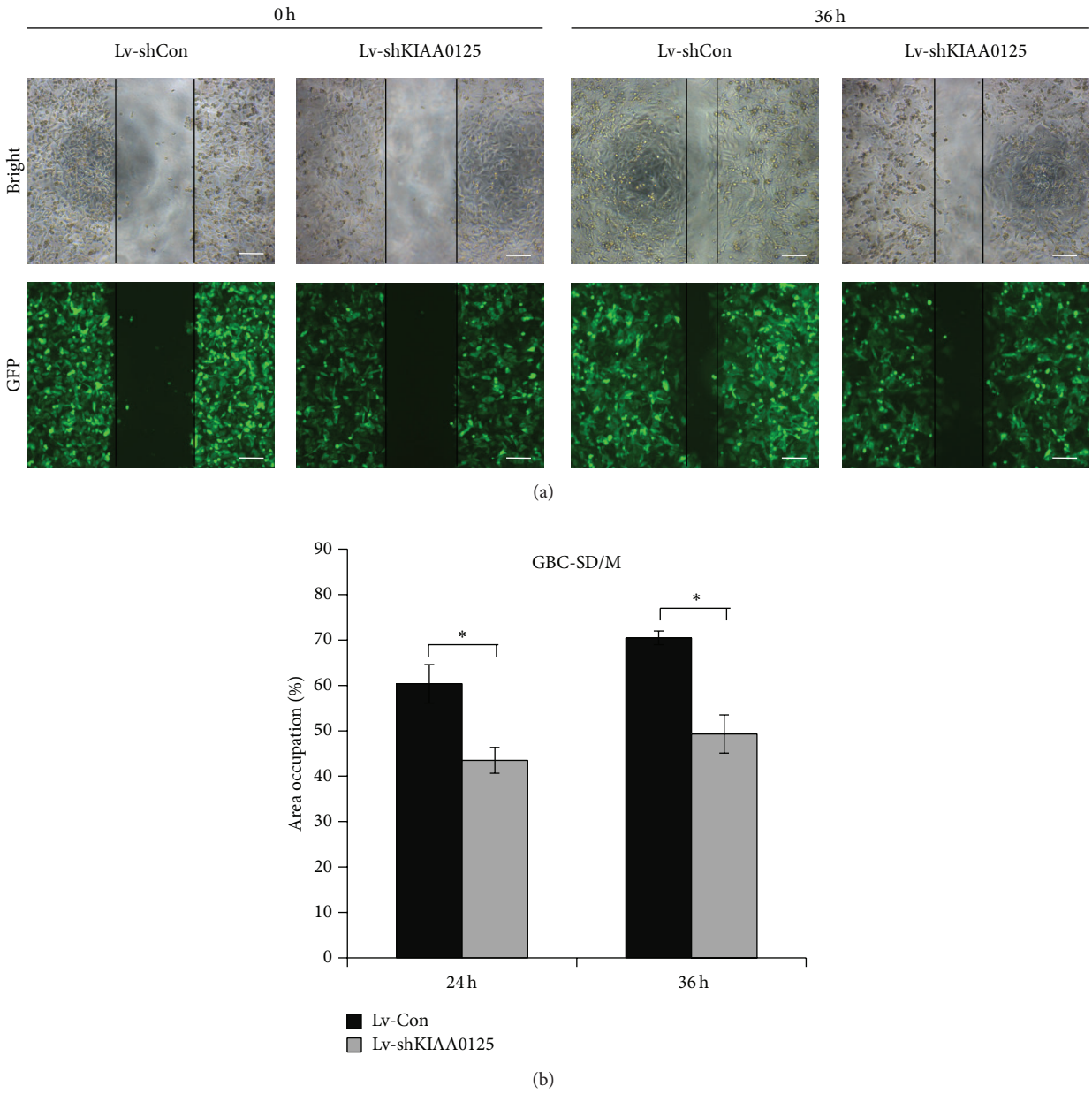

Figure 3: Effect of KIAA0125 knockdown on wound healing. (a, b) The wound healing ability of GBC-SD/M cells was evaluated by using the scratch test after Lv-shKIAA0125 or Lv-shCon treatment at 24 h and 36 h after wound. Scale bar: 250 μm. $^{*}P < 0.05$, compared to Lv-shCon.

to GBC-SD cell subline with a relative lower metastatic potential. More importantly, *in vitro* studies revealed that knockdown of KIAA0125 had an inhibitory effect on GBC cell motility, migration, and invasion. So far, little is known about the biological roles of lncRNAs in GBC initiation and progression, even though many of them are known to be misregulated in various cancer types and involved as a key regulator during carcinogenesis [10, 16–20]. Hence, the present study presents us with a novel insight into the contribution of lncRNAs in GBC metastasis.

EMT, originally viewed as a phenotype switch in developmental biology, has been linked to carcinoma invasion and metastasis in recent years. EMT can be recognized as a manifestation of extreme epithelial cell plasticity, which involves derangement of apicobasal polarity, regulation of cell-to-cell adhesive architecture, loss of basal lamina integrity, and lack of cell shape plasticity [26, 27]. In many circumstances, EMT leads to increased translocation (migration) ability and participates in cancer metastasis [28–30]. In GBC, EMT also plays an important role in promoting the aggressiveness of cancer cells [4]. A great number of molecules change in expression and distribution during the EMT, including Catenins, Cadherins, Vimentin, and integrins [31]. Remarkably, we observed that after KIAA0125 knockdown,

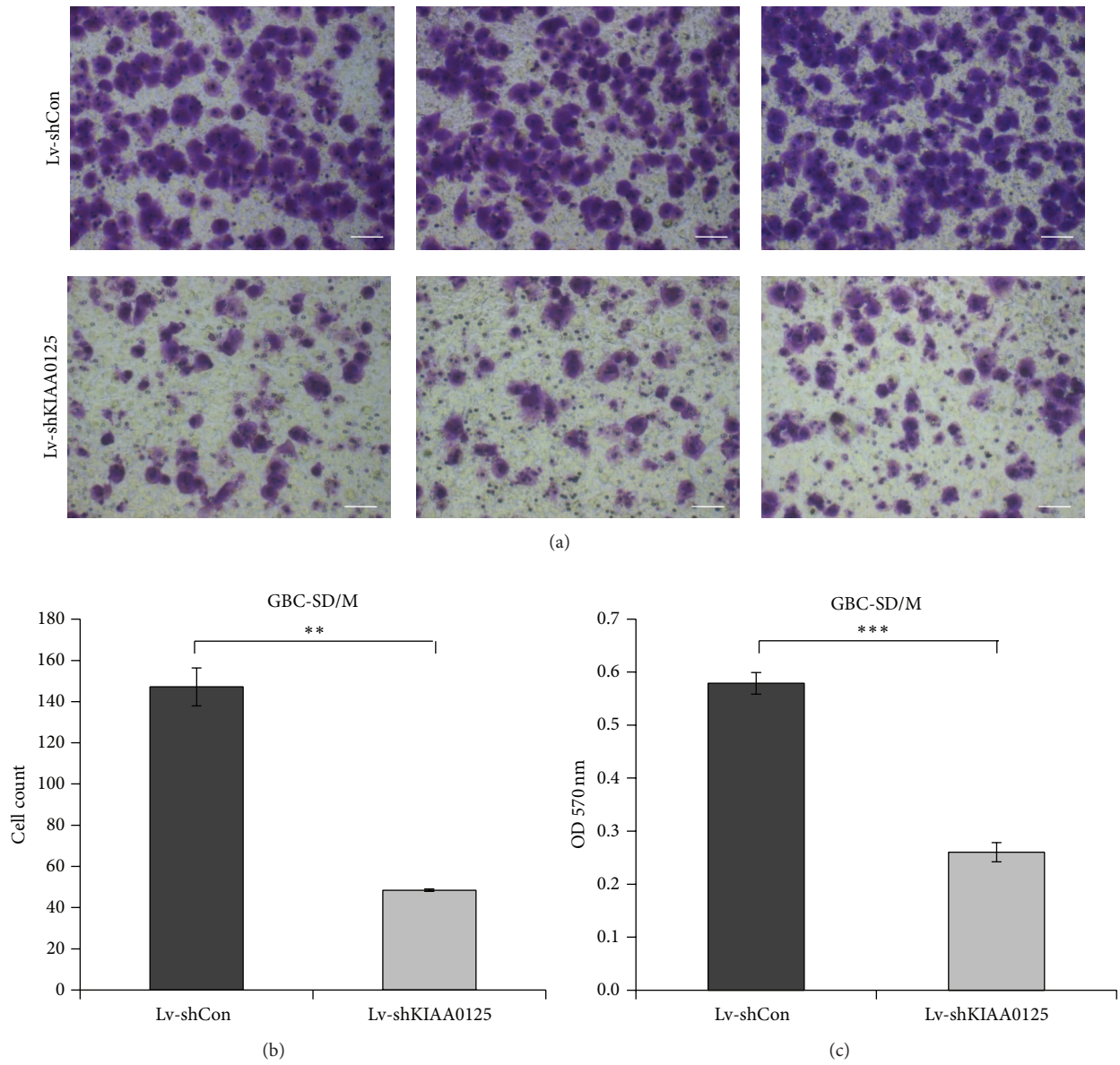

Figure 4: Effect of KIAA0125 knockdown on cell migration. The migration of Lv-shKIAA0125 or Lv-shCon treated cells was evaluated using the transwell assay. (a) Cells migrating to the lower chamber were stained by crystal violet and photographed. Scale bar: 100 μm. (b) The number of migrating cells and (c) the amount of crystal violet in both groups were measured. $^{**}P < 0.01$, $^{***}P < 0.001$, compared to Lv-shCon.

the expression of Vimentin was downregulated and the expression of β-Catenin was upregulated. Vimentin, a major component of the intermediate filament family, is known to maintain cellular integrity and thus its overexpression may result in accelerated cell growth, invasion, and poor prognosis in many cancers [32]. β-Catenin is typically more abundant in epithelial-like cells, and loss of β-Catenin is a hallmark of EMT [33]. Taken together, we may infer that KIAA0125 promotes GBC cell migration and invasion partly via induction of Vimentin and suppression of β-Catenin. However, further investigation is needed to clarify the sophisticated regulatory mechanism underlying this process.

In all, we described for the first time the function of KIAA0125 in GBC cell migration, invasion, and EMT. Our findings suggest that KIAA0125 may serve as a potential therapeutic target for advanced GBC cases. More detailed research would be crucial to evaluate the biological function of KIAA0125 in tumor samples from GBC cases.

Conflict of Interests

The authors declare that there is no conflict of interests regarding the publication of this paper.

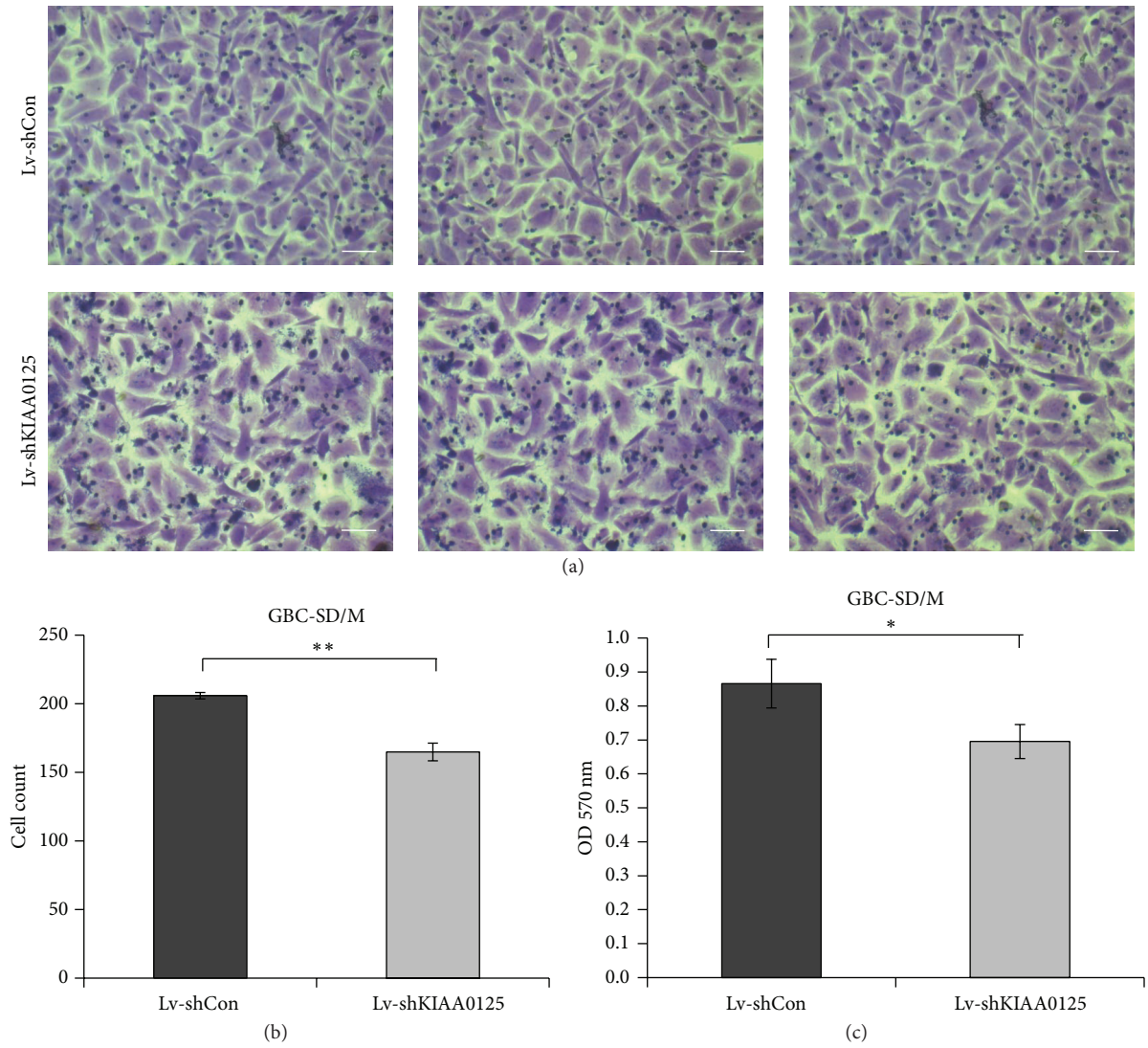

Figure 5: Effect of KIAA0125 knockdown on cell invasion. The invasive ability of Lv-shKIAA0125 or Lv-shCon treated cells was evaluated using the Matrigel Invasion Chambers. (a) Cells invading to the lower chamber were stained by crystal violet and photographed. Scale bar: 100 μm. (b) The number of migrating cells and (c) the amount of crystal violet in both groups were measured. $^{*}P < 0.05$, $^{**}P < 0.01$, compared to Lv-shCon.

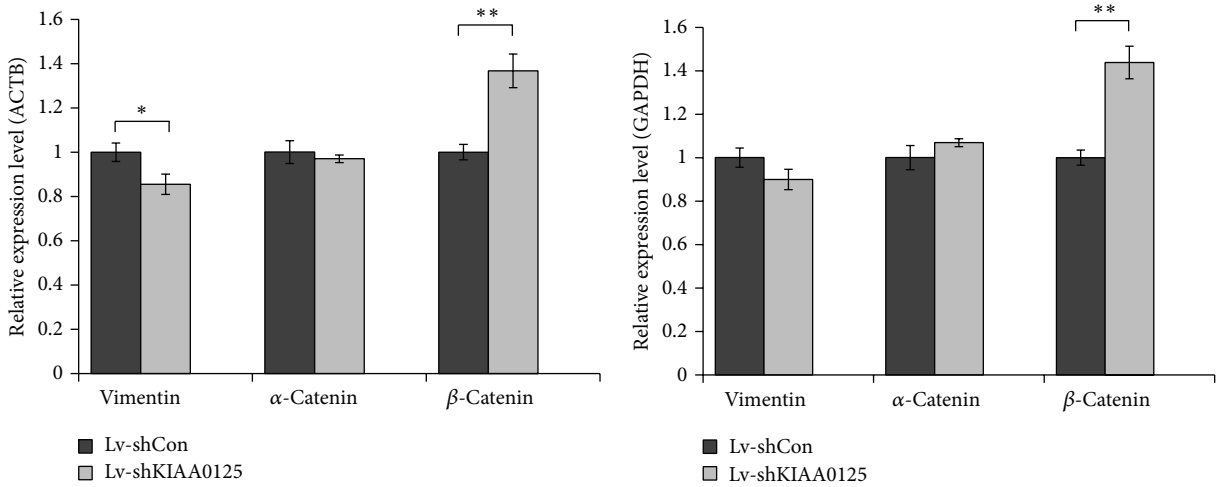

Figure 6: Effect of KIAA0125 knockdown on EMT. The mRNA expression levels of molecules (Vimentin, α-Catenin, and β-Catenin) involved in EMT was examined in Lv-shKIAA0125 or Lv-shCon treated groups. β-Actin and GAPDH were used as internal control genes. $^{*}P < 0.05$, $^{**}P < 0.01$, compared to Lv-shCon.

Acknowledgment

This study was supported by the National Natural Science Foundation of China (Grant nos. 81172026, 81272402, and 81172029).

References

[1] Z. Tan, M. Li, W. Wu et al., "NLK is a key regulator of proliferation and migration in gallbladder carcinoma cells," *Molecular and Cellular Biochemistry*, vol. 369, no. 1-2, pp. 27–33, 2012.

[2] S. Gourgiotis, H. M. Kocher, L. Solaini, A. Yarollahi, E. Tsiambas, and N. S. Salemis, "Gallbladder cancer," *American Journal of Surgery*, vol. 196, no. 2, pp. 252–264, 2008.

[3] Z. Tan, S. Zhang, M. Li et al., "Regulation of cell proliferation and migration in gallbladder cancer by zinc finger X-chromosomal protein," *Gene*, vol. 528, no. 2, pp. 261–266, 2013.

[4] H. Zong, B. Yin, H. Zhou, D. Cai, B. Ma, and Y. Xiang, "Inhibition of mTOR pathway attenuates migration and invasion of gallbladder cancer via EMT inhibition," *Molecular Biology Reports*, vol. 41, no. 7, pp. 4507–4512, 2014.

[5] I. H. Jeong, S. U. Choi, S. R. Lee et al., "Outcomes after combined laparoscopic gastrectomy and laparoscopic cholecystectomy in gastric cancer patients," *European Surgical Research*, vol. 42, no. 4, pp. 203–208, 2009.

[6] G. Miller and W. R. Jarnagin, "Gallbladder carcinoma," *European Journal of Surgical Oncology*, vol. 34, no. 3, pp. 306–312, 2008.

[7] A. X. Zhu, T. S. Hong, A. F. Hezel, and D. A. Kooby, "Current management of gallbladder carcinoma," *Oncologist*, vol. 15, no. 2, pp. 168–181, 2010.

[8] X. Wang, S. Arai, X. Song et al., "Induced ncRNAs allosterically modify RNA-binding proteins in cis to inhibit transcription," *Nature*, vol. 454, no. 7200, pp. 126–130, 2008.

[9] T. R. Mercer, M. E. Dinger, and J. S. Mattick, "Long non-coding RNAs: insights into functions," *Nature Reviews Genetics*, vol. 10, no. 3, pp. 155–159, 2009.

[10] H. Ono, N. Motoi, H. Nagano et al., "Long noncoding RNA HOTAIR is relevant to cellular proliferation, invasiveness, and clinical relapse in small-cell lung cancer," *Cancer Medicine*, vol. 3, no. 3, pp. 632–642, 2014.

[11] C. P. Ponting, P. L. Oliver, and W. Reik, "Evolution and functions of long noncoding RNAs," *Cell*, vol. 136, no. 4, pp. 629–641, 2009.

[12] K. Takahashi, I. Yan, H. Haga, and T. Patel, "Long non-coding RNA in liver diseases," *Hepatology*, vol. 60, no. 2, pp. 744–753, 2014.

[13] S. Chung, H. Nakagawa, M. Uemura et al., "Association of a novel long non-coding RNA in 8q24 with prostate cancer susceptibility," *Cancer Science*, vol. 102, no. 1, pp. 245–252, 2011.

[14] H. Ling, R. Spizzo, Y. Atlasi et al., "CCAT2, a novel noncoding RNA mapping to 8q24, underlies metastatic progression and chromosomal instability in colon cancer," *Genome Research*, vol. 23, no. 9, pp. 1446–1461, 2013.

[15] L. Lu, G. Zhu, C. Zhang et al., "Association of large noncoding RNA HOTAIR expression and its downstream intergenic CpG island methylation with survival in breast cancer," *Breast Cancer Research and Treatment*, vol. 136, no. 3, pp. 875–883, 2012.

[16] C. P. Alves, A. S. Fonseca, B. R. Muys et al., "Brief report: the lincRNA hotair is required for epithelial-to-mesenchymal transition and stemness maintenance of cancer cell lines," *Stem Cells*, vol. 31, no. 12, pp. 2827–2832, 2013.

[17] X.-B. Lv, G.-Y. Lian, H.-R. Wang, E. Song, H. Yao, and M.-H. Wang, "Long noncoding RNA HOTAIR is a prognostic marker for esophageal squamous cell carcinoma progression and survival," *PLoS ONE*, vol. 8, no. 5, Article ID e63516, 2013.

[18] C. Xu, M. Yang, J. Tian, X. Wang, and Z. Li, "MALAT-1: a long non-coding RNA and its important 3' end functional motif in colorectal cancer metastasis," *International Journal of Oncology*, vol. 39, no. 1, pp. 169–175, 2014.

[19] P. Ji, S. Diederichs, W. Wang et al., "MALAT-1, a novel noncoding RNA, and thymosin β4 predict metastasis and survival in early-stage non-small cell lung cancer," *Oncogene*, vol. 22, no. 39, pp. 8031–8041, 2003.

[20] L. Ying, Q. Chen, Y. Wang, Z. Zhou, Y. Huang, and F. Qiu, "Upregulated MALAT-1 contributes to bladder cancer cell migration by inducing epithelial-to-mesenchymal transition," *Molecular BioSystems*, vol. 8, no. 9, pp. 2289–2294, 2012.

[21] Y.-B. Liu, X.-W. He, J.-W. Wang et al., "Establishment of liver metastasis model of human gallbladder cancer and isolation of the subpopulation with high metastatic potential," *National Medical Journal of China*, vol. 86, no. 30, pp. 2117–2121, 2006.

[22] K. J. Livak and T. D. Schmittgen, "Analysis of relative gene expression data using real-time quantitative PCR and the 2-$\Delta\Delta$CT method," *Methods*, vol. 25, no. 4, pp. 402–408, 2001.

[23] F. Schulze, K. Schardt, I. Wedemeyer et al., "Epithelial-mesenchymal transition of biliary epithelial cells in advanced liver fibrosis," *Verhandlungen der Deutschen Gesellschaft für Pathologie*, vol. 91, pp. 250–256, 2007.

[24] M. D. Paraskevopoulou, G. Georgakilas, N. Kostoulas et al., "DIANA-LncBase: experimentally verified and computationally predicted microRNA targets on long non-coding RNAs," *Nucleic Acids Research*, vol. 41, no. 1, pp. D239–D245, 2013.

[25] H. Yang, Y. Zhong, H. Xie et al., "Induction of the liver cancer-down-regulated long noncoding RNA uc002mbe.2 mediates trichostatin-induced apoptosis of liver cancer cells," *Biochemical Pharmacology*, vol. 85, no. 12, pp. 1761–1769, 2013.

[26] E. D. Hay and A. Zuk, "Transformations between epithelium and mesenchyme: normal, pathological, and experimentally induced," *American Journal of Kidney Diseases*, vol. 26, no. 4, pp. 678–690, 1995.

[27] E. W. Thompson and D. F. Newgreen, "Carcinoma invasion and metastasis: a role for epithelial-mesenchymal transition?" *Cancer Research*, vol. 65, no. 14, pp. 5991–5995, 2005.

[28] J. P. Thiery, "Epithelial-mesenchymal transitions in tumour progression," *Nature Reviews Cancer*, vol. 2, no. 6, pp. 442–454, 2002.

[29] D. A. Zajchowski, M. F. Bartholdi, Y. Gong et al., "Identification of gene expression profiles that predict the aggressive behavior of breast cancer cells," *Cancer Research*, vol. 61, no. 13, pp. 5168–5178, 2001.

[30] J. A. Davies, "Mesenchyme to epithelium transition during development of the mammalian kidney tubule," *Acta Anatomica*, vol. 156, no. 3, pp. 187–201, 1996.

[31] A. Bonnomet, A. Brysse, A. Tachsidis et al., "Epithelial-to-mesenchymal transitions and circulating tumor cells," *Journal of Mammary Gland Biology and Neoplasia*, vol. 15, no. 2, pp. 261–273, 2010.

[32] A. Satelli and S. Li, "Vimentin in cancer and its potential as a molecular target for cancer therapy," *Cellular and Molecular Life Sciences*, vol. 68, no. 18, pp. 3033–3046, 2011.

[33] R. Kalluri and R. A. Weinberg, "The basics of epithelial-mesenchymal transition," *The Journal of Clinical Investigation*, vol. 119, no. 6, pp. 1420–1428, 2009.

Hindawi Publishing Corporation
BioMed Research International
Volume 2015, Article ID 131547, 8 pages
http://dx.doi.org/10.1155/2015/131547

Review Article

The Fine LINE: Methylation Drawing the Cancer Landscape

Isabelle R. Miousse and Igor Koturbash

Department of Environmental and Occupational Health, Fay W. Boozman College of Public Health, University of Arkansas for Medical Sciences, 4301 W. Markham Street, Little Rock, AR 72205-7199, USA

Correspondence should be addressed to Isabelle R. Miousse; iracinemiousse@uams.edu and Igor Koturbash; ikoturbash@uams.edu

Received 23 October 2014; Revised 17 November 2014; Accepted 25 November 2014

Academic Editor: Aurelio Ariza

LINE-1 (L1) is the most abundant mammalian transposable element that comprises nearly 20% of the genome, and nearly half of the mammalian genome has stemmed from L1-mediated mobilization. Expression and retrotransposition of L1 are suppressed by complex mechanisms, where the key role belongs to DNA methylation. Alterations in L1 methylation may lead to aberrant expression of L1 and have been described in numerous diseases. Accumulating evidence clearly indicates that loss of global DNA methylation observed in cancer development and progression is tightly associated with hypomethylation of L1 elements. Significant progress achieved in the last several years suggests that such parameters as L1 methylation status can be potentially utilized as clinical biomarkers for determination of the disease stage and in predicting the disease-free survival in cancer patients. In this paper, we summarize the current knowledge on L1 methylation, with specific emphasis given to success and challenges on the way of introduction of L1 into clinical practice.

1. Introduction

Only about 1% of the genome is comprised of genes while the vast majority is comprised of repetitive elements—retrotransposons, transposons, satellite, and tandem repeats. The first two are also known as mobile or transposable elements, since they are capable of moving within the genome. While the more ancient class—transposons—uses the "cut-and-paste" mechanisms, retrotransposons relocate via an RNA intermediate in a "copy-and-paste" mechanism.

It is becoming increasingly evident that transposable elements are tightly associated with the generation of genetic diversity and can influence the expression of numerous genes. Specifically, transposable elements can affect the integrity of the genome by retrotransposition, resulting in potential insertions and deletions within the coding sequences, as well as genomic rearrangements—by shuffling genomic fragments by 5′ and 3′ transduction and recombination between the homologous elements. Additionally, transposable elements have capacity to affect gene expression by numerous mechanisms, such as providing alternative promoters, silencing by transcriptional or RNA interference (RNAi), and creating cryptic splice sites and polyadenylation signals [1–4].

Two major classes of retrotransposons are long-terminal repeats (LTR) and non-LTR elements. The former are named for their long-terminal repeats flanking the internal proviral sequence on both sides. LTRs are structurally related to exogenous retroviruses, although lacking the ability to move from one cell to another. Two families of these endogenous retroviruses are known to be currently active in mice [5]. Activity of LTR in humans remains controversial, with some reports suggesting that HERV-K is active in the human genome (reviewed in [6]). Non-LTR retrotransposons are presented as autonomous long interspersed nuclear elements (LINE), which include low-copy archaic inactive elements, such as LINE-2 (L2 and LINE-3), and active elements, such as LINE-1 (L1), as well as short interspersed nuclear elements (SINE; Alu—in humans) and SVA [7, 8] that utilize LINE machinery for their mobilization, thus, called nonautonomous.

There are about 516,000 copies of LINE-1 (L1) in the human genome prevalently located within its gene-poor regions, reaching up to 20% of the human genome [9]. However, the vast majority of them are 5′-truncated (0.9 Kb in length on average), contain internal deletions or other mutations, and are thus incapable of retrotransposition. There

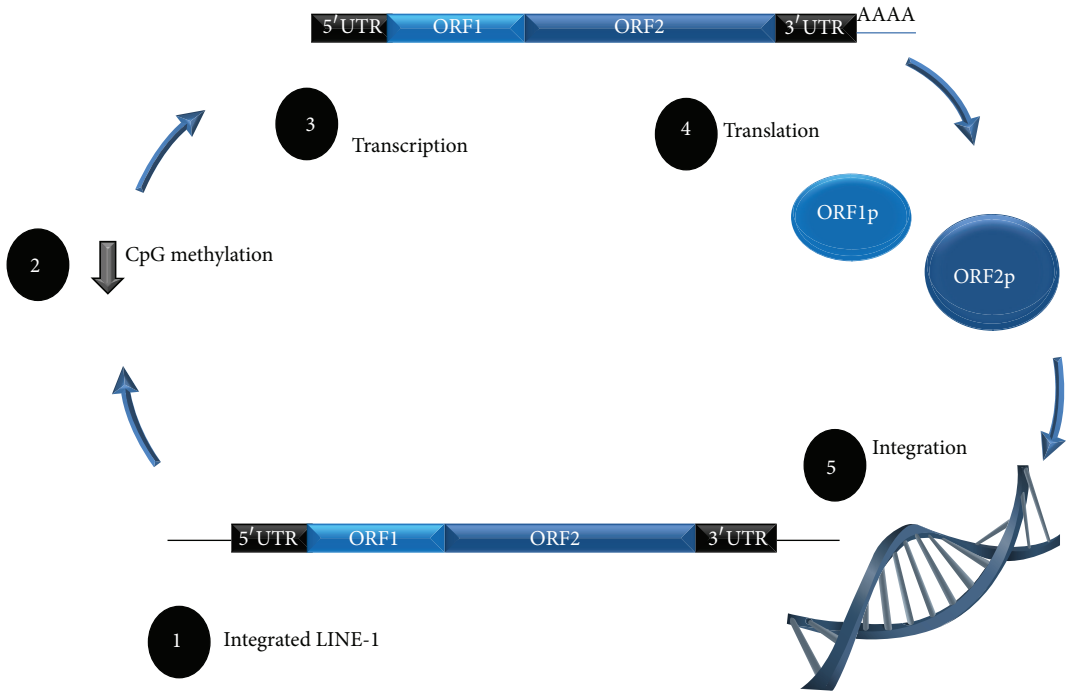

Figure 1: Biology of the LINE-1 element. The LINE-1 element is composed of four units (1). A decrease in silencing methylation marks at CpG dinucleotides (2) may induce an increase in LINE-1 transcription (3). The proteins ORF1p and ORF2p (4) encoded in LINE-1 contribute to its reinsertion in the genome (5).

are, however, ~100 functional full-length L1 in the human genome. They are about 6 Kb in length and contain a 5′-untranslated region (UTR), a bicistronic open reading frame that encodes two proteins—ORF1p and ORF2p—and a 3′-UTR with a poly(A) tail [1] (Figure 1). ORF1p is a 40 kDa protein and is a nucleic acid-binding chaperone. ORF2p is a 150 kDa protein responsible for retrotranspositioning, encoding an endonuclease, reverse transcriptase, and zinc finger-like protein [10, 11]. Earlier studies considered that only ORF2 was needed for successful retrotransposition; however, recent reports clearly demonstrated that both ORF1 and ORF2 are vital for L1 mobilization. The 5′-UTR of L1 contains sense and antisense promoters and binding sites for several transcription factors, including p53, YY1, Runx, SRY, and Socs1 [12–14]. The sense promoter regulates the expression of L1. Although the role of the antisense promoter is still largely unknown, the most recent studies indicate its role in the regulation of transcription of neighboring genes [15] and even those located up to 300 Kb from L1 [16]. Furthermore, the most recent studies show that the L1 antisense promoter is also involved in downregulation of transcription from the L1 sense promoter since the resultant bidirectional transcripts are processed into small interfering RNAs [17], as well as in control over L1 retrotransposition [18].

2. Biology of L1

2.1. Mechanisms of L1 Mobilization. Propagation of L1 in mammalian genomes occurs via the process of autonomous retrotransposition. Current endogenous retrotransposition activity of some recent L1 elements determines the widespread genomic structural variations within and between populations and variations in normal development, neuronal differentiation, and human cancers [2, 19–22].

Transcription of the L1 full-length mRNA from the internal promoter, mediated by the RNA polymerase II, initiates L1 retrotransposition. This mRNA then is transported to the cytoplasm, where it is translated to ORF1p and ORF2p—L1-encoded proteins that preferentially associate with their encoding RNA [23]. The L1 ribonucleoprotein particle (RNP) is formed then in a *cis*-preference followed by the entrance of RNP into the nucleus [24]. Next, a target-primed reverse transcription (PPRT) occurs. During the TPRT, a single-stranded nick is produced in genomic DNA due to the ORF2p endonuclease activity. This allows for exposing a free 3′-hydroxyl residue that serves as a primer, and a cDNA copy of the associated L1 mRNA is synthesized [1].

Mobilization of L1, thus, occurring via a "copy-paste" mechanism is associated with a number of events, including the development of novel gene promoters, splice sites, polyadenylation signals, dispersing transcription binding splice sites, linking genes in transcriptional networks, and facilitating the evolution of novel traits (reviewed in [3]).

2.2. Regulation of L1 (Retrotransposition) Activity. DNA methylation is one of the most important mechanisms for the regulation of genetic information and one of the key mechanisms for silencing repetitive elements (reviewed in [25]). It is a covalent addition of a methyl group to the 5th position of carbon on the cytosine ring in CpG dinucleotides,

called CpG sites. It has been estimated that about 56% of these CpG sites are located within repetitive sequences [26]. Taking into account that L1 is the most abundant repetitive element in the genome and that it is heavily methylated in normal somatic cells, one can assume that L1 accounts for the largest portion of methylation.

Silent transcriptional status of L1 has been associated with DNA methylation, specifically within the 5′-UTR, that contains both L1 promoters and is rich in CpG sites. Demethylation of L1 by exogenous stressors, DNA demethylating agents (5-azacytidine), or in disease has been associated with its aberrant transcription [27–29]. DNA methylation, therefore, is considered as a key mechanism for L1 silencing. It has been shown, using embryonic stem cells, that inherited L1 methylation patterns are maintained via utilization of DNA methylation machinery—methyltransferases DNMT1, DNMT3A, and DNMT3B [30].

Other epigenetic mechanisms have also been reported to be involved in the regulation of L1 expression. For example, acetylation and methylation of histones have been implicated in silencing of L1 retrotransposition in embryonic carcinoma cell lines [31]. Accumulating evidence also suggests the role of noncoding RNAs, including Piwi-interacting RNAs (piRNAs), siRNA, and miRNA regulation of L1 [32, 33]. Additionally, a number of other mechanisms, including self-regulation by the L1 antisense promoter, have been proposed and described [18].

3. LINE-1 in Cancer

3.1. Retrotransposition. When the regulation of normal L1 activity is impaired, retrotransposition events may result in numerous deleterious effects. For instance, it can result in disruption of the ORF of the functional gene, genome amplification, and the development of genomic instability. The first human disease associated with L1 retrotransposition was haemophilia A, stemmed from the independent mutagenic L1 insertions into exon 14 of the *Factor VIII* gene that prevented synthesis of functional coagulation factor [34]. To date, about 100 diseases are known that are associated with L1 retrotransposition, including chronic granulomatous disease, β-thalassemia, and diabetes [2, 35, 36].

It has also been hypothesized for a long time that L1 retrotransposition may be associated with cancer development and progression, but the lack of tools needed to detect novel retrotransposition events in human cancers did not allow the support of this hypothesis. The first L1 retrotransposition in cancer was reported by Miki et al. in colorectal cancer and was characterized by insertion of the 3′ portion of L1 into the last exon of the *APC* gene, leading to the disruption of its function [37]. A number of robust and sensitive techniques have been developed since that time to detect retrotransposition events and, up to date, several human cancers have been characterized by the presence of somatic L1 retrotransposition, including colorectal, lung, prostate, and ovarian cancers [38, 39]. However, it still remains largely unknown whether retrotransposition is the driving force of tumorigenesis or merely occurs after tumor initiation. It is certainly without a doubt that a retrotransposition event that occurs within a critical gene, like in the case of *APC* in colorectal cancer [37], can be considered as a driving mechanism. On the other hand, some studies have indicated that L1 insertions may differ in different sections of the same tumor. For instance, the study by Solyom et al. [40] reported that, in about 60% of cases, L1 insertion identified in the first section was not identified in the second section of the same tumor.

3.2. Methylation. Loss of global DNA methylation was the first epigenetic alteration demonstrated in human cancers [41, 42]. Subsequent studies have shown that this hypomethylation is not primarily associated with gene-specific methylation, as numerous tumor-suppressor genes in cancers were found in hypermethylated (an often inactivated) status [43, 44]. The following studies clearly demonstrated that global genomic hypomethylation in cancer is associated with the loss of methylation within the TEs, particularly L1 and Alu. Since then, numerous studies were performed demonstrating the loss of L1 methylation in human cancers, and, as of today, L1 hypomethylation has been reported in virtually all human cancers [45].

This hypomethylation can result in a number of unwanted effects associated with aberrant L1 activity and retrotransposition. Also, while L1 is interspersed primarily within gene-poor regions of the genome, its presence within or neighboring the coding sequences can be detrimental. For instance, loss of L1 methylation within its 5′-UTR may result in its aberrant activation and affect the expression of neighboring genes. Hypomethylation of L1 element insertions within the promoters and introns of coding genes may result in aberrant expression of these genes [46]. On the other hand, it has been demonstrated that the presence of repetitive elements facilitates the spreading of methylation into a promoter-CpG island [47]. Altogether, taking into account that about 25% of mammalian promoter regions contain repetitive sequences [48], alterations in DNA methylation within L1 elements may have significant effects on expression of genetic information.

4. LINE-1 as a Biomarker

Significant alterations of L1 in human cancers, associated primarily with its increased expression, elevated protein levels, and hypomethylation, together with the very high copy numbers of L1 in the genome, suggest that L1 can be potentially utilized as a diagnostic modality. It is becoming increasingly evident that the methylation status of L1 can be utilized as a prognostic marker in cancer. Indeed, loss of L1 methylation is usually found to be more pronounced in advanced stages of cancer and in metastasis than in the early stages of cancer, or in primary tumors, respectively.

4.1. Methylation of L1 as a Prognostic Tool. Growing evidence clearly demonstrates that hypomethylation of L1 is usually associated with poor prognosis and shorter disease-free survival. For instance, a study of 211 lung adenocarcinoma patients concluded that disease-free survival in the group with hypomethylated L1 was significantly shorter than that of the nonhypomethylated group [49]. The results from

several studies using cohorts of patients with hepatocellular carcinomas show that hypomethylation of L1 is also inversely correlated with disease-free survival and is associated with poor prognosis [50–52]. Interestingly, the hypomethylated status of L1 was also correlated with higher expression of the *c-MET* oncogene, the gene that contains an L1 insertion within its intron [52].

Importantly, the study by Benard et al. [53] shows that L1 methylation status can serve as an independent clinical prognostic marker in patients with early-stage cancers (stage I-II), as evident from the cohort of patients with rectal cancer.

While, for the vast majority of human cancers, L1 demethylation was associated with poor prognosis, some controversial results exist for melanoma, where L1 hypomethylation was associated with favorable prognosis in stage IIIc patients [54]. However, more recent studies report loss of L1 methylation in regard to poor prognosis and survival in melanoma patients [55, 56].

4.2. LINE-1 and Cancer Stage. Accumulating evidence suggests that the methylation status of L1 cannot only be utilized as a prognostic marker but also discriminate between the earlier and later stages of cancer. Extensive research performed in several cohorts of colorectal cancer (CRC) patients indicates that methylation of L1 not only is considerably lower in the tumor compared to adjacent stromal and normal mucosal epithelial cells [57, 58] but notably correlates with the tumor stage in CRC, where the stage 3-4 tumors were characterized by a higher degree of L1 hypomethylation than stage 1-2 tumors [57].

Another study by Park et al. [59], performed on two cohorts of 145 and 179 patients, revealed that decreased levels of L1 can already be identified in human breast samples with atypical ductal hyperplasia/flat epithelial atypia. This suggests that the methylation of L1 can be considered as an early biomarker in cancer diagnosis, as well as clearly providing further evidence of the driving role L1 plays in carcinogenesis. The authors also noted that L1 hypomethylation was associated with negative ER status, *ERBB2(HER2)* amplification, and *p53* overexpression [59]. Similarly, data obtained from the cohort of ovarian cancer patients suggests that L1 hypomethylation is an early molecular event involved in ovarian endometrioid adenocarcinoma and clear cell carcinoma malignant transformation [60].

4.3. L1 and the Field for Cancerization. Field for cancerization is the phenomenon characterized by "the occurrence of multifocal and recurrent epithelial tumors that are preceded by and associated with widespread changes of surrounding tissue or organ fields [61]." The role of epigenetic alterations in field or cancerization is well recognized [62–64]. Therefore, hypomethylation of L1, as one of the most frequently observed epigenetic alterations in cancer, may be an important player in the development of field for cancerization. Indeed, the abovementioned study [59] demonstrated that L1 hypomethylation can be detected in breast atypical ductal hyperplasia/flat epithelial atypia. Another study reported correlation between the loss of L1 methylation in normal colon tissue and increased risk for multiple colorectal cancers [65]. Another example of data supporting involvement of L1 in the field for cancerization comes from the study that, among others, evaluated the levels of L1 methylation in normal colorectal mucosa in patients with Lynch syndrome, sporadic colorectal cancer, and familial colorectal cancer [66]. The lowest L1 methylation levels were detected in normal mucosa of patients with familial colorectal cancer, suggesting that L1 methylation status may predispose normal tissue to cancer development [66]. Also, significantly lower levels of L1 were detected in normal mucosa of esophageal squamous cell carcinoma patients with the history of tobacco smoking in comparison with nonsmokers [67].

4.4. It Is Better Than the Gene(s)! It is becoming increasingly evident that the prognostic value of the L1 methylation status might exhibit higher potential than the methylation status of individual tumor-suppressor genes characteristic of a specific cancer. In the recent study, Saito et al. [68] reported that while methylation levels of *APC* and *RASSF1* were significant prognostic factors only in univariate analysis in non-small cell lung cancer, the methylation status of L1 remained significant prognostic factor in multivariate analysis that included age, gender, smoking history, histologic type, and pathologic stage. Moreover, in the same study, L1 methylation also revealed a significant prognostic value for stage IA NSCLC patients in multivariate analysis [68].

Similar findings were reported from the cohort of 217 patients with curatively resected esophageal squamous cell carcinoma, where L1 hypomethylation was significantly associated with shorter survival, while the methylation status of *MGMT* and *MLH1* genes was not associated with patient prognosis [69].

4.5. LINE-1 and Metastasis. The role of L1 in tumor's metastatic potential is becoming increasingly recognized [16]. Several recent studies have investigated the L1 methylation status in primary tumors and its distant metastasis. The study by Matsunoki et al. performed in CRC patients did not identify any differences in L1 methylation between the primary tumor and lymph node or distant metastasis [58]. However, the later study by Hur et al. [46], using a larger sample size and more sensitive techniques, reported significantly lower levels of L1 methylation in distant (liver) metastasis, compared to matched primary CRC tissue [46]. Interestingly, they have also shown that the loss of L1 methylation within the intronic region of protooncogenes *MET*, *RAB3IP*, and *CHRMP* results in their reactivation and aberrant expression in CRC metastasis. The recent study by Ikeda et al. [49] reported that vascular invasion in lung adenocarcinoma patients was significantly associated with lower methylation levels of L1.

4.6. LINE-1 as a Biomarker in Biological Fluids. Ideal biomarkers should be low-invasive and reflect the pathomorphological changes in the target organs. In this regard, determination of L1 methylation status in biological fluids, such as blood and saliva, is of particular interest. Up to date, a number of studies have attempted to determine the association between the methylation of L1 in leukocytes,

peripheral blood mononuclear cells, and buccal DNA and the risk for certain cancers [70–73]. Despite the significant progress achieved in this field in the last year, the results of these studies do not provide a clear picture of L1 methylation status in biological fluids and its association with certain human cancers. For instance, while L1 hypomethylation was detected in peripheral blood leukocytes in patients with gastric cancer [72], L1 hypermethylation in white blood cells DNA was significantly associated with pancreatic cancer [73]. No significant associations in L1 methylation in peripheral blood between melanoma patients and a healthy cohort were found [71]. The most recent meta-analysis performed on 2554 samples from cancer patients and 3553 control specimens identified that although there was a significant association between lower L1 methylation and tumor versus normal DNA, no association for L1 methylation levels in the blood of control and cancer patients was found [74].

4.7. LINE-1 as a Biomarker and Prognostic Tool: Expression. While normal adult human tissues usually do not express L1 (or express at very low levels), considerable levels of L1 RNA and protein are found in cancerous tissues [75]. Importantly, several studies report that the extent of L1 expression or protein levels is inversely correlated with the prognosis in pancreatic ductal carcinoma [76] and high-grade breast carcinomas [77], respectively. Another study reports that nuclear expression of both ORF1p and ORF2p is associated with lymph node metastasis in breast cancer and poor patient survival [78].

5. Challenges

One of the major challenges is the high degree of variability in L1 methylation between the evaluated samples [57]. Interestingly, the authors extended these findings to include a number of established colon cancer cell lines and have shown that these cancer cell lines also exhibited a large variation in demethylation. This variability was also reported in other studies [79, 80].

Another challenge is variability and certain discrepancies between the studies. For instance, while some studies report L1 hypomethylation in leukemia patients [81], others report no such changes in L1 methylation [82]. Similarly, while one study indicates unfavorable prognosis in melanoma patients associated with L1 hypomethylation [55], another study reports favorable prognosis associated with L1 hypomethylation [54]. These differences can be attributable to a number of factors, including the heterogeneity in human populations involved in these studies; the high degree of tumor heterogeneity, where striking differences in expression and methylation of L1 can be detected in different samples obtained from the same tumor; different assays utilized for the analysis—from COBRA to pyrosequencing and array-based analysis; different L1 regions assayed—5′-UTR, ORF1, and ORF2; and differences in the number of CpG sites analyzed in a given assay. Studies also indicate the possibility of evolutionary age of L1 families influence on the degree of L1 demethylation, where the youngest L1 elements undergo the most dramatic loss of methylation [83, 84]. Also, the most recent report indicates significant differences in L1 methylation from samples collected from the left or right side of the bowel [85], adding an extra level of complexity.

6. Concluding Remarks

In the last two decades, L1, the most abundant repetitive element in the human genome, experienced a dramatic switch from being "junk DNA" to being "an important player in the mammalian genomes [86]." Its involvement in numerous important biological processes, and in both health and disease, makes it one of the most interesting subjects. Significant progress is achieved in our understanding of L1 biology and the effects this retrotransposon can exert. L1's role in cancer development and progression is becoming increasingly recognized, given its contribution to global genomic alterations in DNA methylation, expression of genetic information, and retrotransposition. Accumulating evidence suggests that such parameters as L1 methylation status can be potentially utilized as clinical biomarkers for determination of the disease stage and predicting the disease-free survival in cancer patients. However, certain challenges need to be overcome before the introduction of L1 into clinical practice. Additionally, while genetic alterations, such as mutations, are usually irreversible, epigenetic alterations, such as DNA methylation, are potentially reversible and, thus, can provide possible molecular targets for successful cancer therapy.

Conflict of Interests

The authors declare that there is no conflict of interests regarding the publication of this paper.

Acknowledgments

The authors are thankful to Dr. Kristy Kutanzi and Dr. Rebecca Helm for critical reading and editing this paper. The research in Koturbash' Lab is supported, in part, by the NIH/UAMS Clinical and Translational Science Award (UL1TR000039 and KL2TR000063) and the Arkansas Biosciences Institute.

References

[1] E. M. Ostertag and H. H. Kazazian Jr., "Biology of mammalian L1 retrotransposons," *Annual Review of Genetics*, vol. 35, pp. 501–538, 2001.

[2] K. H. Burns and J. D. Boeke, "Human transposon tectonics," *Cell*, vol. 149, no. 4, pp. 740–752, 2012.

[3] M. Cowley and R. J. Oakey, "Transposable elements re-wire and fine-tune the transcriptome," *PLoS Genetics*, vol. 9, no. 1, Article ID e1003234, 2013.

[4] E. Belan, "LINEs of evidence: noncanonical DNA replication as an epigenetic determinant," *Biology Direct*, vol. 8, article 22, 2013.

[5] Y. Zhang, I. A. Maksakova, L. Gagnier, L. N. van de Lagemaat, and D. L. Mager, "Genome-wide assessments reveal extremely high levels of polymorphism of two active families of mouse

endogenous retroviral elements," *PLoS Genetics*, vol. 4, no. 2, Article ID e1000007, 2008.

[6] R. E. Mills, E. A. Bennett, R. C. Iskow, and S. E. Devine, "Which transposable elements are active in the human genome?" *Trends in Genetics*, vol. 23, no. 4, pp. 183–191, 2007.

[7] H. S. Malik, W. D. Burke, and T. H. Eickbush, "The age and evolution of non-LTR retrotransposable elements," *Molecular Biology and Evolution*, vol. 16, no. 6, pp. 793–805, 1999.

[8] A. F. Smit, "Interspersed repeats and other mementos of transposable elements in mammalian genomes," *Current Opinion in Genetics and Development*, vol. 9, no. 6, pp. 657–663, 1999.

[9] E. S. Lander, L. M. Linton, B. Birren et al., "Initial sequencing and analysis of the human genome," *Nature*, vol. 409, no. 6822, pp. 860–921, 2001.

[10] Q. Feng, J. V. Moran, H. H. Kazazian Jr., and J. D. Boeke, "Human L1 retrotransposon encodes a conserved endonuclease required for retrotransposition," *Cell*, vol. 87, no. 5, pp. 905–916, 1996.

[11] G. J. Cost, Q. Feng, A. Jacquier, and J. D. Boeke, "Human L1 element target-primed reverse transcription *in vitro*," *The EMBO Journal*, vol. 21, no. 21, pp. 5899–5910, 2002.

[12] T. Tchénio, J.-F. Casella, and T. Heidmann, "Members of the SRY family regulate the human LINE retrotransposons," *Nucleic Acids Research*, vol. 28, no. 2, pp. 411–415, 2000.

[13] N. Yang, L. Zhang, Y. Zhang, and H. H. Kazazian Jr., "An important role for RUNX3 in human L1 transcription and retrotransposition," *Nucleic Acids Research*, vol. 31, no. 16, pp. 4929–4940, 2003.

[14] C. R. Harris, A. Dewan, A. Zupnick et al., "P53 responsive elements in human retrotransposons," *Oncogene*, vol. 28, no. 44, pp. 3857–3865, 2009.

[15] K. Mätlik, K. Redik, and M. Speek, "L1 antisense promoter drives tissue-specific transcription of human genes," *Journal of Biomedicine and Biotechnology*, vol. 2006, Article ID 71753, 16 pages, 2006.

[16] H. A. Cruickshanks, N. Vafadar-Isfahani, D. S. Dunican et al., "Expression of a large LINE-1-driven antisense RNA is linked to epigenetic silencing of the metastasis suppressor gene TFPI-2 in cancer," *Nucleic Acids Research*, vol. 41, no. 14, pp. 6857–6869, 2013.

[17] N. Yang and H. H. Kazazian Jr., "L1 retrotransposition is suppressed by endogenously encoded small interfering RNAs in human cultured cells," *Nature Structural & Molecular Biology*, vol. 13, no. 9, pp. 763–771, 2006.

[18] J. Li, M. Kannan, A. L. Trivett et al., "An antisense promoter in mouse L1 retrotransposon open reading frame-1 initiates expression of diverse fusion transcripts and limits retrotransposition," *Nucleic Acids Research*, vol. 42, no. 7, pp. 4546–4562, 2014.

[19] A. R. Muotri, M. C. N. Marchetto, N. G. Coufal et al., "L1 retrotransposition in neurons is modulated by MeCP2," *Nature*, vol. 468, no. 7322, pp. 443–446, 2010.

[20] J. K. Baillie, M. W. Barnett, K. R. Upton et al., "Somatic retrotransposition alters the genetic landscape of the human brain," *Nature*, vol. 479, no. 7374, pp. 534–537, 2011.

[21] A. D. Ewing and H. H. Kazazian Jr., "Whole-genome resequencing allows detection of many rare LINE-1 insertion alleles in humans," *Genome Research*, vol. 21, no. 6, pp. 985–990, 2011.

[22] J. Xing, Y. Zhang, K. Han et al., "Mobile elements create structural variation: analysis of a complete human genome," *Genome Research*, vol. 19, no. 9, pp. 1516–1526, 2009.

[23] H. Hohjoh and M. F. Singer, "Cytoplasmic ribonucleoprotein complexes containing human LINE-1 protein and RNA," *The EMBO Journal*, vol. 15, no. 3, pp. 630–639, 1996.

[24] D. A. Kulpa and J. V. Moran, "Cis-preferential LINE-1 reverse transcriptase activity in ribonucleoprotein particles," *Nature Structural and Molecular Biology*, vol. 13, no. 7, pp. 655–660, 2006.

[25] P. A. Jones and G. Liang, "Rethinking how DNA methylation patterns are maintained," *Nature Reviews Genetics*, vol. 10, no. 11, pp. 805–811, 2009.

[26] R. A. Rollins, F. Haghighi, J. R. Edwards et al., "Large-scale structure of genomic methylation patterns," *Genome Research*, vol. 16, no. 2, pp. 157–163, 2006.

[27] I. Koturbash, A. Boyko, R. Rodriguez-Juarez et al., "Role of epigenetic effectors in maintenance of the long-term persistent bystander effect in spleen in vivo," *Carcinogenesis*, vol. 28, no. 8, pp. 1831–1838, 2007.

[28] B. Weber, S. Kimhi, G. Howard, A. Eden, and F. Lyko, "Demethylation of a LINE-1 antisense promoter in the cMet locus impairs Met signalling through induction of illegitimate transcription," *Oncogene*, vol. 29, no. 43, pp. 5775–5784, 2010.

[29] J. M. Tubio, Y. Li, Y. S. Ju et al., "Mobile DNA in cancer. Extensive transduction of nonrepetitive DNA mediated by L1 retrotransposition in cancer genomes," *Science*, vol. 345, no. 6196, Article ID 1251343, 2014.

[30] G. Liang, M. F. Chan, Y. Tomigahara et al., "Cooperativity between DNA methyltransferases in the maintenance methylation of repetitive elements," *Molecular and Cellular Biology*, vol. 22, no. 2, pp. 480–491, 2002.

[31] J. L. Garcia-Perez, M. Morell, J. O. Scheys et al., "Epigenetic silencing of engineered L1 retrotransposition events in human embryonic carcinoma cells," *Nature*, vol. 466, no. 7307, pp. 769–773, 2010.

[32] M. A. Carmell, A. Girard, H. J. G. van de Kant et al., "MIWI2 is essential for spermatogenesis and repression of transposons in the mouse male germline," *Developmental Cell*, vol. 12, no. 4, pp. 503–514, 2007.

[33] J. P. Ross, K. N. Rand, and P. L. Molloy, "Hypomethylation of repeated DNA sequences in cancer," *Epigenomics*, vol. 2, no. 2, pp. 245–269, 2010.

[34] H. H. Kazazian Jr., C. Wong, H. Youssoufian, A. F. Scott, D. G. Phillips, and S. E. Antonarakis, "Haemophilia A resulting from de novo insertion of L1 sequences represents a novel mechanism for mutation in man," *Nature*, vol. 332, no. 6160, pp. 164–166, 1988.

[35] C. R. Beck, J. L. Garcia-Perez, R. M. Badge, and J. V. Moran, "LINE-1 elements in structural variation and disease," *Annual Review of Genomics and Human Genetics*, vol. 12, pp. 187–215, 2011.

[36] D. C. Hancks and H. H. Kazazian, "Active human retrotransposons: variation and disease," *Current Opinion in Genetics and Development*, vol. 22, no. 3, pp. 191–203, 2012.

[37] Y. Miki, I. Nishisho, A. Horii et al., "Disruption of the APC gene by a retrotransposal insertion of L1 sequence in a colon cancer," *Cancer Research*, vol. 52, no. 3, pp. 643–645, 1992.

[38] R. C. Iskow, M. T. McCabe, R. E. Mills et al., "Natural mutagenesis of human genomes by endogenous retrotransposons," *Cell*, vol. 141, no. 7, pp. 1253–1261, 2010.

[39] E. Lee, R. Iskow, L. Yang et al., "Landscape of somatic retrotransposition in human cancers," *Science*, vol. 337, no. 6097, pp. 967–971, 2012.

[40] S. Solyom, A. D. Ewing, E. P. Rahrmann et al., "Extensive somatic L1 retrotransposition in colorectal tumors," *Genome Research*, vol. 22, no. 12, pp. 2328–2338, 2012.

[41] A. P. Feinberg and B. Vogelstein, "Hypomethylation distinguishes genes of some human cancers from their normal counterparts," *Nature*, vol. 301, no. 5895, pp. 89–92, 1983.

[42] M. Ehrlich, M. A. Gama-Sosa, L.-H. Huang et al., "Amount and distribution of 5-methylcytosine in human DNA from different types of tissues or cells," *Nucleic Acids Research*, vol. 10, no. 8, pp. 2709–2721, 1982.

[43] S. B. Baylin, J. W. M. Hoppener, A. de Bustros, P. H. Steenbergh, C. J. Lips, and B. D. Nelkin, "DNA methylation patterns of the calcitonin gene in human lung cancers and lymphomas," *Cancer Research*, vol. 46, no. 6, pp. 2917–2922, 1986.

[44] P. A. Jones, M. J. Wolkowicz, W. M. Rideout III et al., "De novo methylation of the MyoD1 CpG island during the establishment of immortal cell lines," *Proceedings of the National Academy of Sciences of the United States of America*, vol. 87, no. 16, pp. 6117–6121, 1990.

[45] A. Portela and M. Esteller, "Epigenetic modifications and human disease," *Nature Biotechnology*, vol. 28, no. 10, pp. 1057–1068, 2010.

[46] K. Hur, P. Cejas, J. Feliu et al., "Hypomethylation of long interspersed nuclear element-1 (LINE-1) leads to activation of proto-oncogenes in human colorectal cancer metastasis," *Gut*, vol. 63, pp. 635–646, 2014.

[47] Y. Zhang, J. Shu, J. Si, L. Shen, M. R. H. Estecio, and J.-P. J. Issa, "Repetitive elements and enforced transcriptional repression co-operate to enhance DNA methylation spreading into a promoter CpG-island," *Nucleic Acids Research*, vol. 40, no. 15, pp. 7257–7268, 2012.

[48] I. K. Jordan, I. B. Rogozin, G. V. Glazko, and E. V. Koonin, "Origin of a substantial fraction of human regulatory sequences from transposable elements," *Trends in Genetics*, vol. 19, no. 2, pp. 68–72, 2003.

[49] K. Ikeda, K. Shiraishi, A. Eguchi et al., "Long interspersed nucleotide element 1 hypomethylation is associated with poor prognosis of lung adenocarcinoma," *Annals of Thoracic Surgery*, vol. 96, no. 5, pp. 1790–1794, 2013.

[50] K. Harada, Y. Baba, T. Ishimoto et al., "LINE-1 methylation level and patient prognosis in a database of 208 hepatocellular carcinomas," *Annals of Surgical Oncology*, 2014.

[51] X.-D. Gao, J.-H. Qu, X.-J. Chang et al., "Hypomethylation of long interspersed nuclear element-1 promoter is associated with poor outcomes for curative resected hepatocellular carcinoma," *Liver International*, vol. 34, no. 1, pp. 136–146, 2014.

[52] C. Zhu, T. Utsunomiya, T. Ikemoto et al., "Hypomethylation of long interspersed nuclear element-1 (LINE-1) is associated with poor prognosis via activation of c-MET in hepatocellular carcinoma," *Annals of Surgical Oncology*, vol. 21, no. 4, supplement, pp. 729–735, 2014.

[53] A. Benard, C. J. H. Van De Velde, L. Lessard et al., "Epigenetic status of LINE-1 predicts clinical outcome in early-stage rectal cancer," *British Journal of Cancer*, vol. 109, no. 12, pp. 3073–3083, 2013.

[54] L. Sigalotti, E. Fratta, E. Bidoli et al., "Methylation levels of the "long interspersed nucleotide element-1" repetitive sequences predict survival of melanoma patients," *Journal of Translational Medicine*, vol. 9, article 78, 2011.

[55] S. Hoshimoto, C. T. Kuo, K. K. Chong et al., "*AIM1* and LINE-1 epigenetic aberrations in tumor and serum relate to melanoma progression and disease outcome," *Journal of Investigative Dermatology*, vol. 132, no. 6, pp. 1689–1697, 2012.

[56] S. I. Ecsedi, H. Hernandez-Vargas, S. C. Lima, Z. Herceg, R. Adany, and M. Balazs, "Transposable hypomethylation is associated with metastatic capacity of primary melanomas," *International Journal of Clinical and Experimental Pathology*, vol. 6, no. 12, pp. 2943–2948, 2013.

[57] M. R. H. Estécio, V. Gharibyan, L. Shen et al., "LINE-1 hypomethylation in cancer is highly variable and inversely correlated with microsatellite instability," *PLoS ONE*, vol. 2, no. 5, article e399, 2007.

[58] A. Matsunoki, K. Kawakami, M. Kotake et al., "LINE-1 methylation shows little intra-patient heterogeneity in primary and synchronous metastatic colorectal cancer," *BMC Cancer*, vol. 12, article 574, 2012.

[59] S. Y. Park, A. N. Seo, H. Y. Jung et al., "Alu and LINE-1 hypomethylation is associated with HER2 enriched subtype of breast cancer," *PLoS ONE*, vol. 9, no. 6, Article ID e100429, 2014.

[60] A. Senthong, N. Kitkumthorn, P. Rattanatanyong, N. Khemapech, S. Triratanachart, and A. Mutirangura, "Differences in LINE-1 methylation between endometriotic ovarian cyst and endometriosis-associated ovarian cancer," *International Journal of Gynecological Cancer*, vol. 24, no. 1, pp. 36–42, 2014.

[61] G. P. Dotto, "Multifocal epithelial tumors and field cancerization: stroma as a primary determinant," *Journal of Clinical Investigation*, vol. 124, no. 4, pp. 1446–1453, 2014.

[62] Y. Luo, M. Yu, and W. M. Grady, "Field cancerization in the colon: a role for aberrant DNA methylation?" *Gastroenterology Report (Oxford)*, vol. 2, pp. 16–20, 2014.

[63] T. Ushijima, "Epigenetic field for cancerization: its cause and clinical implications," *BMC Proceedings*, vol. 7, supplement 2, article K22, 2013.

[64] T. Ushijima, "Epigenetic field for cancerization," *Journal of Biochemistry and Molecular Biology*, vol. 40, no. 2, pp. 142–150, 2007.

[65] H. Kamiyama, K. Suzuki, T. Maeda et al., "DNA demethylation in normal colon tissue predicts predisposition to multiple cancers," *Oncogene*, vol. 31, no. 48, pp. 5029–5037, 2012.

[66] W. Pavicic, E. I. Joensuu, T. Nieminen, and P. Peltomäki, "LINE-1 hypomethylation in familial and sporadic cancer," *Journal of Molecular Medicine*, vol. 90, no. 7, pp. 827–835, 2012.

[67] H. Shigaki, Y. Baba, M. Watanabe et al., "LINE-1 hypomethylation in noncancerous esophageal mucosae is associated with smoking history," *Annals of Surgical Oncology*, vol. 19, no. 13, pp. 4238–4243, 2012.

[68] K. Saito, K. Kawakami, I. Matsumoto, M. Oda, G. Watanabe, and T. Minamoto, "Long interspersed nuclear element 1 hypomethylation is a marker of poor prognosis in stage IA non-small cell lung cancer," *Clinical Cancer Research*, vol. 16, no. 8, pp. 2418–2426, 2010.

[69] S. Iwagami, Y. Baba, M. Watanabe et al., "LINE-1 hypomethylation is associated with a poor prognosis among patients with curatively resected esophageal squamous cell carcinoma," *Annals of Surgery*, vol. 257, no. 3, pp. 449–455, 2013.

[70] S. M. Tajuddin, A. F. Amaral, A. F. Fernandez et al., "Malats N: LINE-1 methylation in leukocyte DNA, interaction with phosphatidylethanolamine N-methyltransferase variants and bladder cancer risk," *British Journal of Cancer*, vol. 110, pp. 2123–2130, 2014.

[71] L. Pergoli, C. Favero, R. M. Pfeiffer et al., "Blood DNA methylation, nevi number, and the risk of melanoma," *Melanoma Research*, vol. 24, pp. 480–487, 2014.

[72] A. Dauksa, A. Gulbinas, Z. Endzinas, J. Oldenburg, and O. El-Maarri, "DNA methylation at selected CpG sites in peripheral blood leukocytes is predictive of gastric cancer," *Anticancer Research*, vol. 34, no. 10, pp. 5381–5388, 2014.

[73] R. E. Neale, P. J. Clark, J. Fawcett et al., "Association between hypermethylation of DNA repetitive elements in white blood cell DNA and pancreatic cancer," *Cancer Epidemiology*, vol. 38, no. 5, pp. 576–582, 2014.

[74] M. Barchitta, A. Quattrocchi, A. Maugeri, M. Vinciguerra, and A. Agodi, "LINE-1 hypomethylation in blood and tissue samples as an epigenetic marker for cancer risk: a systematic review and meta-analysis," *PLoS ONE*, vol. 9, no. 10, Article ID e109478, 2014.

[75] V. P. Belancio, A. M. Roy-Engel, R. R. Pochampally, and P. Deininger, "Somatic expression of LINE-1 elements in human tissues," *Nucleic Acids Research*, vol. 38, no. 12, pp. 3909–3922, 2010.

[76] D. T. Ting, D. Lipson, S. Paul et al., "Aberrant overexpression of satellite repeats in pancreatic and other epithelial cancers," *Science*, vol. 331, no. 6017, pp. 593–596, 2011.

[77] C. R. Harris, R. Normart, Q. Yang et al., "Association of nuclear localization of a long interspersed nuclear element-1 protein in breast tumors with poor prognostic outcomes," *Genes & Cancer*, vol. 1, no. 2, pp. 115–124, 2010.

[78] L. Chen, J. E. Dahlstrom, A. Chandra, P. Board, and D. Rangasamy, "Prognostic value of LINE-1 retrotransposon expression and its subcellular localization in breast cancer," *Breast Cancer Research and Treatment*, vol. 136, no. 1, pp. 129–142, 2012.

[79] C. Phokaew, S. Kowudtitham, K. Subbalekha, S. Shuangshoti, and A. Mutirangura, "LINE-1 methylation patterns of different loci in normal and cancerous cells," *Nucleic Acids Research*, vol. 36, no. 17, pp. 5704–5712, 2008.

[80] A. Daskalos, G. Nikolaidis, G. Xinarianos et al., "Hypomethylation of retrotransposable elements correlates with genomic instability in non-small cell lung cancer," *International Journal of Cancer*, vol. 124, no. 1, pp. 81–87, 2009.

[81] S. Fabris, V. Bollati, L. Agnelli et al., "Biological and clinical relevance of quantitative global methylation of repetitive DNA sequences in chronic lymphocytic leukemia," *Epigenetics*, vol. 6, no. 2, pp. 188–194, 2011.

[82] H. C. Si, S. Worswick, H.-M. Byun et al., "Changes in DNA methylation of tandem DNA repeats are different from interspersed repeats in cancer," *International Journal of Cancer*, vol. 125, no. 3, pp. 723–729, 2009.

[83] S. Szpakowski, X. Sun, J. M. Lage et al., "Loss of epigenetic silencing in tumors preferentially affects primate-specific retroelements," *Gene*, vol. 448, no. 2, pp. 151–167, 2009.

[84] H.-M. Byun, V. Motta, T. Panni et al., "Evolutionary age of repetitive element subfamilies and sensitivity of DNA methylation to airborne pollutants," *Particle and Fibre Toxicology*, vol. 10, no. 1, article 28, 2013.

[85] J. C. Figueiredo, M. V. Grau, K. Wallace et al., "Global DNA hypomethylation (LINE-1) in the normal colon and lifestyle characteristics and dietary and genetic factors," *Cancer Epidemiology Biomarkers and Prevention*, vol. 18, no. 4, pp. 1041–1049, 2009.

[86] R. Rebollo, M. T. Romanish, and D. L. Mager, "Transposable elements: an abundant and natural source of regulatory sequences for host genes," *Annual Review of Genetics*, vol. 46, pp. 21–42, 2012.

Hindawi Publishing Corporation
BioMed Research International
Volume 2015, Article ID 812027, 5 pages
http://dx.doi.org/10.1155/2015/812027

Research Article

Collagen Type XI Alpha 1 Expression in Intraductal Papillomas Predicts Malignant Recurrence

Javier Freire,[1,2] Lucia García-Berbel,[3] Pilar García-Berbel,[1,2] Saray Pereda,[1,2] Ainara Azueta,[1,2] Pilar García-Arranz,[1] Ana De Juan,[4] Alfonso Vega,[5] Ángela Hens,[6] Ana Enguita,[7] Pedro Muñoz-Cacho,[8] and Javier Gómez-Román[1,2]

[1]*Anatomía Patológica, Hospital Universitario Marqués de Valdecilla, 39008 Santander, Spain*
[2]*IDIVAL, 39011 Santander, Spain*
[3]*Ginecología y Obstetricia, Hospital Universitario de Puerto Real, 11510 Puerto Real, Spain*
[4]*Oncología Médica, Hospital Universitario Marqués de Valdecilla, 39008 Santander, Spain*
[5]*Radiodiagnóstico, Hospital Universitario Marqués de Valdecilla, 39008 Santander, Spain*
[6]*Anatomía Patológica, Hospital Universitario de Puerto Real, 11510 Puerto Real, Spain*
[7]*Anatomía Patológica, Hospital Universitario 12 de Octubre, 28041 Madrid, Spain*
[8]*Gerencia Atención Primaria, Servicio Cántabro de Salud, 39011 Santander, Spain*

Correspondence should be addressed to Javier Freire; javifreiresalinas@gmail.com

Received 14 January 2015; Accepted 17 February 2015

Academic Editor: Konstantinos Arnaoutakis

Despite the progress achieved in the treatment of breast cancer, there are still many unsolved clinical issues, being the diagnosis, prognosis, and treatment of papillary diseases, one of the highest challenges. Because of its unpredictable clinical behavior, treatment of intraductal papilloma has generated a great controversy. Even though considered as a benign lesion, it presents high rate of malignant recurrence. This is the reason why there are clinicians supporting a complete excision of the lesion, while others support an only expectant follow-up. Previous results of our group suggested that procollagen 11 alpha 1 (pro-COL11A1) expression correlates with infiltrating phenotype in breast lesions. We analyzed the correlation between expression of pro-COL11A1 in intraductal papilloma and their risk of malignant recurrence. Immunohistochemistry of pro-COL11A1 was performed in 62 samples of intraductal papilloma. Ten out 11 cases relapsed as carcinoma presents positive staining for COL11A1, while just 17 out of 51 cases with benign behaviour present immunostaining. There were significant differences ($P < 0.0001$) when comparing patients with malignant recurrence versus nonmalignant relapse patients. These data suggest that pro-COL11A1 expression is a highly sensitive biomarker to predict malignant relapse of intraductal papilloma and it can be used as indicative factor for prevention programs.

1. Background

Breast cancer is the first tumor disease among women, causing more than 600000 new cases per year [1]. Furthermore it is also the second cause of cancer death among women, causing more than 39,000 deaths each year only in United States [2]. Although in the last years the early detection of this disease has improved overall survival [3], breast cancer remains a very serious problem for public health and there are still open many research areas.

Papillary lesions (intraductal papilloma, papillomatosis, atypical papilloma, and intraductal papillary carcinoma) are controversial and continuously generate problems in diagnosis and clinical management [4]. Because of their similarity, the accurate diagnosis of these lesions only by morphology may be complex, so pathologist requires the use of ancillary techniques. The main indicator of malignancy of papillary lesion is the absence of myoepithelial cells [5] which can be revealed by immunohistochemistry for p63 protein, smooth muscle actin (SMM-HC), or calponin [6]. Other biomarkers have been used as estrogen receptor or cytokeratins [6] CK5/6 and CK8 [7] for differential diagnosis but there is a no clear consensus to determine the sensitivity and accuracy of these markers in routine [5, 8].

Intraductal papilloma is the most controversial papillary lesion relating diagnosis and treatment [6]. While intraductal papilloma *per se* behaves like a benign lesion, the association between intraductal papilloma and malignant recurrence is fairly high, reaching up to 33% of the cases [5, 9, 10]. Indeed, there is a great controversy on how to act when a new case of intraductal papilloma is diagnosed. In fact there are papers suggesting a radical excision of the lesion in all cases [11, 12], while others support only an expectant follow-up [13–15]. An accurate diagnosis pointing to cases amenable of a malignant behavior is essential [6, 16, 17], not only for the benefit of the patient, as it would avoid unnecessary interventions, but also because of its economic impact [8].

It has been shown that the extracellular matrix plays an essential role in breast tumor development and progression, being collagens its main component. Collagen type XI alpha 1 (COL11A1) has been shown to be a marker of malignancy in different tumors including pancreas [18], lung [19], stomach [20], and colon [21–23]. Previous work from our group has demonstrated that pro-COL11A1 expression in cancer associated fibroblasts is a powerful marker of invasive growth in breast carcinomas, with sensitivity and specificity rates higher than 90% [24]. COL11A1 is not present in benign lesions so we thought it can be a predictable marker for malign behavior of intraductal papilloma.

2. Mat and Meth

2.1. Tissue Samples. Sixty-two patients with a clinicopathological diagnosis of breast intraductal papilloma from the University Hospital Marqués de Valdecilla (Santander, Spain), University Hospital of Puerto Real (Puerto Real, Spain) and University Hospital 12 de Octubre (Madrid, Spain) were enrolled for this work. All the samples examined were core needle biopsies from 18G gauge.

Patients were diagnosed by two independent pathologists following the standard work routine. All patients recruited for the study had a minimum follow-up of 5 years. Patient recruitment was conducted under approvement by the Clinical Research Ethics Committee of Cantabria.

Five cases of encapsulated papillary carcinoma were also selected as positive control of malignant lesion.

2.2. Immunohistochemical Analysis. Formalin fixed, paraffin embedded biopsies were stained by using proCol11a1 monoclonal antibody clone 1E8.33 (ONCOMATRYX, Bilbao, SPAIN) as previously described [24, 25]. Samples were considered as positive when a clear cytoplasmic labeling of at least one tumor-associated fibroblast was observed. Staining was separately evaluated by two independent pathologists.

2.3. Statistical Methods. Nonparametric Fisher exact test was performed, using SPSS 20 suite, to analyze difference of COL11A1 expression between intraductal papilloma with or without malignant relapse. Survival analyses were performed using Kaplan-Meier curves, and hazard ratio (HR) and corresponding 95% confident interval (95% CI) were estimated using Cox proportional hazards regression of recurrence for positive staining for COL11A1.

3. Results

Out of 62 cases studied, 11 presented recurrence as an infiltrative carcinoma, 7 presented further nonmalignant proliferative lesion (papilloma, columnar hyperplasia…) while 44 remaining cases showed no recurrence. Benign relapsed or no recurrence samples were considered as a single group for comparing with those which presented as a malignant relapse. Immunolabeling of pro-COL11A1 was observed in fibroblasts surrounding central fibrovascular stalks.

Among papillomas with malignant relapse 91% showed positive staining (Figure 1(b)), whereas those papillomas with benign or not recurrence present only 33% of immunostaining ($P < 0.0001$) (Figure 1(a)). All five encapsulated papillary carcinoma were positive for COL11A1 staining (Figure 1(C)).

Pro-COL11A1 staining showed sensitivity of 91% and a specificity of 67% when compared intraductal papilloma malignant relapsed samples with those not recurrent. Moreover, Cox regression analysis for recurrence risk presents highly statistical significance ($P = 0.0008$) while comparing positive and negative staining, with a HR of 12.6 (3.8–41.4) (Figure 1 sup data) (see Supplementary Material available online at http://dx.doi.org/10.1155/2015/812027).

4. Discussion

The present work demonstrates that the presence of COL11A1 in the stroma of breast intraductal papillomas could be a potential marker of malignant behavior.

Breast intraductal papillomas are considered as benign indolent lesions but a significant number of patients are suitable to develop a malignant recurrence [26] something that explain the huge controversy over the treatment to be applied in these kind of lesions [4, 27–30].

Several clinical groups argue for an aggressive complete excisional treatment when an intraductal papilloma is diagnosed, going from a tumorectomy whether solitary papillomas to a radical mastectomy in the case of diffuse lesions [11, 12, 31–33]. On the other hand there are works suggesting the treatment of breast intraductal papilloma to be not so invasive and based in a conservative image-controlled follow-up [13–15, 34]. The possibility of making a recommendation for excision only in specific cases where an uncertain degree of malignancy is present is also discussed [35]. This could be a nice approach but, how is the malignancy probability of a pure intraductal papilloma determined [8]? The answer must be coming from morphology and characteristics of neoplastic as well as stromal cells.

Breast intraductal papilloma presents a high rate of underestimation (12–19%) when it is diagnosed in Core-Needle Biopsy [10, 29, 36] mainly due to small sample and to indefinite histopathological features [29]. This is why a reliable system for classifying papillary lesions according to malignant potential is required.

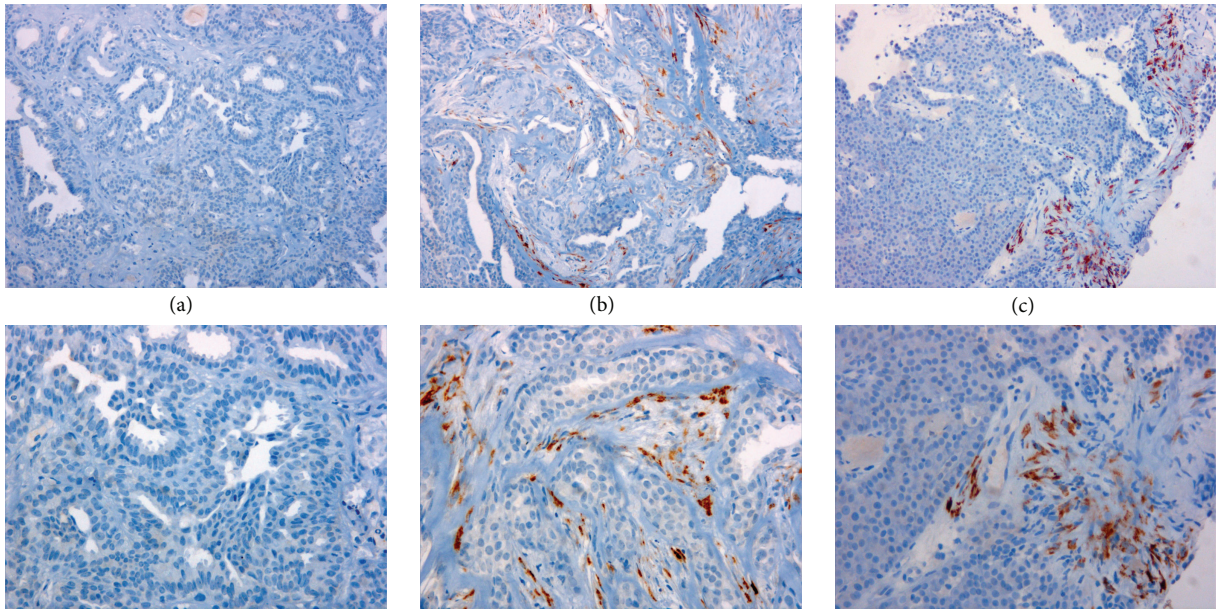

Figure 1: Pro-COL11A1 expression in breast papillary lesions. Immunostaining for pro-COL11A1 in: (a) benign intraductal papilloma, (b) malignant relapse intraductal papilloma, (c) encapsulated papillary carcinoma. Counterstain with Hematoxilin. Lowercase letters images magnification ×200, uppercase letters images magnification ×400.

Although several biomarkers have been suggested for differentiating potential malignant phenotype of benign intraductal papillomas, none has been demonstrated as an accurate predictive factor of malignancy. Markers as the CD44 [37] or cyclin D1 [38] have been proposed as differentially expressed genes between malignant and benign papillary lesions, but there is no correlation with malignant recurrence of intraductal papillomas. Some genetic alterations, such as loss of heterozygosity of chromosome 16 [39], have also been proposed as capable of predicting an increased susceptibility for malignant recurrence of intraductal papillomas, but accuracy has not been demonstrated [38, 39].

Our work is in the cutting edge for classification of intraductal papillomas because it is based on tumor associated fibroblasts and not in the neoplastic cells by itself or in the presence or absence of myoepithelial cells. COL11A1 expression in fibroblast surrounding central fibrovascular stalks of intraductal papillomas can predict future malignant relapse with a sensitivity of 91%. Although the specificity derived from our data is not so high (65%) it can be explained primarily because the elective treatment for intraductal papillomas in Spain is the complete excision of the lesion, which prevents secondary recurrence.

Positive staining in all encapsulated papillary carcinoma suggests what has been discussed for some time that these lesions, long considered variations of DCIS, may in fact be a form of low-grade invasive carcinoma with an expansile growth pattern [40, 41]. This fact supports our hypothesis of a dual nature of intraductal papillomas: malignant papillary carcinomas or intraductal papillomas with benign prognosis.

This marker combined with other prognostic events such as size larger than 1.5 cm, location [28], or presence of microcalcifications [42] can assist when deciding the possibility of an aggressive treatment versus a conservative follow-up. In any case, the absence of COL11A1 in a biopsy can predict with a high probability that an intraductal papilloma will present a benign behavior since it presents a recurrence HR value of 0.0793 (0.02–0.26), although changing in therapeutic behavior seems complicated without further studies.

Given that this injury occurs predominantly in pre- and postmenopausal [30] women and that breast intraductal papillary lesions are usually hormone-dependent [43] (in our series more than 85% estrogens positive), these patients may be susceptible to receive an chemoprevention with hormone inhibitors. It has been demonstrated in different studies that the inhibition of both estrogen receptors (tamoxifen and raloxifene) [44–46] and aromatase pathway (exametasane) [47] reduces contralateral breast cancer relapse. The major problem of these therapies is the election of patients to receive treatment, we propose that COL11A1 positive biopsy should be a new factor to ponder besides a Gail 5-year risk score greater than 1.66% and prior preneoplastic lesion [47] to select candidates for this chemoprevention as these lesions have a high susceptibility to malignant relapse.

To conclude, the expression of COL11A1 in breast intraductal papillomas is an optimal prognostic biomarker, and we propose that patients with positive staining for this protein should be given further evaluation of both surgical treatment and preventive adjuvant chemotherapy.

Conflict of Interests

The authors declare that there is no conflict of interests regarding the publication of this paper.

Acknowledgments

The authors are grateful to the nursing unit of radiodiagnosis service for their selfless help in the patient recruitment. This study was supported by grants from the Government of Spain through the INNPACTO program, Project Mamacan IPT 2011-1817-900000.

References

[1] R. Siegel, D. Naishadham, and A. Jemal, "Cancer statistics, 2012," *CA Cancer Journal for Clinicians*, vol. 62, no. 1, pp. 10–29, 2012.

[2] C. DeSantis, R. Siegel, P. Bandi, and A. Jemal, "Breast cancer statistics, 2011," *CA: A Cancer Journal for Clinicians*, vol. 61, no. 6, pp. 409–418, 2011.

[3] M. T. Tirona, "Breast cancer screening update," *American Family Physician*, vol. 87, no. 4, pp. 274–278, 2013.

[4] L. C. Collins and S. J. Schnitt, "Papillary lesions of the breast: selected diagnostic and management issues," *Histopathology*, vol. 52, no. 1, pp. 20–29, 2008.

[5] S.-H. Ueng, T. Mezzetti, and F. A. Tavassoli, "Papillary neoplasms of the breast: a review," *Archives of Pathology and Laboratory Medicine*, vol. 133, no. 6, pp. 893–907, 2009.

[6] A. M. Mulligan and F. P. O'Malley, "Papillary lesions of the breast: a review," *Advances in Anatomic Pathology*, vol. 14, no. 2, pp. 108–119, 2007.

[7] M. Moumen, A. Chiche, S. Cagnet et al., "The mammary myoepithelial cell," *International Journal of Developmental Biology*, vol. 55, no. 7–9, pp. 763–771, 2011.

[8] D. Shouhed, F. F. Amersi, R. Spurrier et al., "Intraductal papillary lesions of the breast: clinical and pathological correlation," *The American Surgeon*, vol. 78, no. 10, pp. 1161–1165, 2012.

[9] P. P. Rosen, "Papilloma and related benign tumors," in *Rosen's Breast Pathology*, P. P. Rosen, Ed., pp. 85–136, Lippincott Williams & Wilkins, Philadelphia, Pa, USA, 2009.

[10] E. K. Valdes, P. I. Tartter, E. Genelus-Dominique, D.-A. Guilbaud, S. Rosenbaum-Smith, and A. Estabrook, "Significance of papillary lesions at percutaneous breast biopsy," *Annals of Surgical Oncology*, vol. 13, no. 4, pp. 480–482, 2006.

[11] M. Rizzo, M. J. Lund, G. Oprea, M. Schniederjan, W. C. Wood, and M. Mosunjac, "Surgical follow-up and clinical presentation of 142 breast papillary lesions diagnosed by ultrasound-guided core-needle biopsy," *Annals of Surgical Oncology*, vol. 15, no. 4, pp. 1040–1047, 2008.

[12] A. R. Skandarajah, L. Field, A. Yuen Larn Mou et al., "Benign papilloma on core biopsy requires surgical excision," *Annals of Surgical Oncology*, vol. 15, no. 8, pp. 2272–2277, 2008.

[13] S. N. Agoff and T. J. Lawton, "Papillary lesions of the breast with and without atypical ductal hyperplasia: can we accurately predict benign behavior from core needle biopsy," *The American Journal of Clinical Pathology*, vol. 122, no. 3, pp. 440–443, 2004.

[14] E. L. Rosen, R. C. Bentley, J. A. Baker, and M. S. Soo, "Imaging-guided core needle biopsy of papillary lesions of the breast," *American Journal of Roentgenology*, vol. 179, no. 5, pp. 1185–1192, 2002.

[15] V. Sohn, J. Keylock, Z. Arthurs et al., "Breast papillomas in the era of percutaneous needle biopsy," *Annals of Surgical Oncology*, vol. 14, no. 10, pp. 2979–2984, 2007.

[16] Y. D. Choi, G. Y. Gong, M. J. Kim et al., "Clinical and cytologic features of papillary neoplasms of the breast," *Acta Cytologica*, vol. 50, no. 1, pp. 35–40, 2006.

[17] V. Gomez-Aracil, E. Mayayo, J. Azua, and A. Arraiza, "Papillary neoplasms of the breast: clues in fine needle aspiration cytology," *Cytopathology*, vol. 13, no. 1, pp. 22–30, 2002.

[18] M. Erkan, N. Weis, Z. Pan et al., "Organ-, inflammation- and cancer specific transcriptional fingerprints of pancreatic and hepatic stellate cells," *Molecular Cancer*, vol. 9, article 88, 2010.

[19] I.-W. Chong, M.-Y. Chang, H.-C. Chang et al., "Great potential of a panel of multiple hMTH1, SPD, ITGA11 and COL11A1 markers for diagnosis of patients with non-small cell lung cancer," *Oncology Reports*, vol. 16, no. 5, pp. 981–988, 2006.

[20] Y. Zhao, T. Zhou, A. Li et al., "A potential role of collagens expression in distinguishing between premalignant and malignant lesions in stomach," *Anatomical Record (Hoboken)*, vol. 292, no. 5, pp. 692–700, 2009.

[21] K. B. Bowen, A. P. Reimers, S. Luman, J. D. Kronz, W. E. Fyffe, and J. Thom, "Immunohistochemical localization of collagen type XI α1 and α2 chains in human colon tissue," *Journal of Histochemistry & Cytochemistry*, vol. 56, no. 3, pp. 275–283, 2008.

[22] H. Fischer, S. Salahshor, R. Stenling et al., "*COL11A1* in FAP polyps and in sporadic colorectal tumors," *BMC Cancer*, vol. 1, article 17, 2001.

[23] H. Fischer, R. Stenling, C. Rubio, and A. Lindblom, "Colorectal carcinogenesis is associated with stromal expression of COL11A1 and COL5A2," *Carcinogenesis*, vol. 22, no. 6, pp. 875–878, 2001.

[24] J. Freire, "Collagen, type XI, alpha 1: an accurate marker for differential diagnosis of breast carcinoma invasiveness in core needle biopsies," *Pathology—Research and Practice*, vol. 210, no. 12, pp. 879–884, 2014.

[25] M. García-Ocaña, F. Vázquez, C. García-Pravia et al., "Characterization of a novel mouse monoclonal antibody, clone 1E8.33, highly specific for human procollagen 11A1, a tumor-associated stromal component," *International Journal of Oncology*, vol. 40, no. 5, pp. 1447–1454, 2012.

[26] J. A. Ibarra, "Papillary lesions of the breast," *Breast Journal*, vol. 12, no. 3, pp. 237–251, 2006.

[27] L. E. Bennett, S. V. Ghate, R. Bentley, and J. A. Baker, "Is surgical excision of core biopsy proven benign papillomas of the breast necessary?" *Academic Radiology*, vol. 17, no. 5, pp. 553–557, 2010.

[28] W.-H. Kil, E. Y. Cho, J. H. Kim, S.-J. Nam, and J.-H. Yang, "Is surgical excision necessary in benign papillary lesions initially diagnosed at core biopsy?" *Breast*, vol. 17, no. 3, pp. 258–262, 2008.

[29] Q. Lu, E. Y. Tan, B. Ho, J. J. C. Chen, and P. M. Y. Chan, "Surgical excision of intraductal breast papilloma diagnosed on core biopsy," *ANZ Journal of Surgery*, vol. 82, no. 3, pp. 168–172, 2012.

[30] T. C. Putti, S. E. Pinder, C. W. Elston, A. H. S. Lee, and I. O. Ellis, "Breast pathology practice: most common problems in a consultation service," *Histopathology*, vol. 47, no. 5, pp. 445–457, 2005.

[31] K. Irfan and R. F. Brem, "Surgical and mammographic follow-up of papillary lesions and atypical lobular hyperplasia diagnosed with stereotactic vacuum-assisted biopsy," *Breast Journal*, vol. 8, no. 4, pp. 230–233, 2002.

[32] T. W. Jacobs, J. L. Connolly, and S. J. Schnitt, "Nonmalignant lesions in breast core needle biopsies: to excise or not to excise?" *The American Journal of Surgical Pathology*, vol. 26, no. 9, pp. 1095–1110, 2002.

[33] F. Puglisi, C. Zuiani, M. Bazzocchi et al., "Role of mammography, ultrasound and large core biopsy in the diagnostic evaluation of papillary breast lesions," *Oncology*, vol. 65, no. 4, pp. 311–315, 2003.

[34] N. Ahmadiyeh, M. A. Stoleru, S. Raza, S. C. Lester, and M. Golshan, "Management of intraductal papillomas of the breast: an analysis of 129 cases and their outcome," *Annals of Surgical Oncology*, vol. 16, no. 8, pp. 2264–2269, 2009.

[35] P. J. Carder, J. Garvican, I. Haigh, and J. C. Liston, "Needle core biopsy can reliably distinguish between benign and malignant papillary lesions of the breast," *Histopathology*, vol. 46, no. 3, pp. 320–327, 2005.

[36] X. Wen and W. Cheng, "Nonmalignant breast papillary lesions at core-needle biopsy: a meta-analysis of underestimation and influencing factors," *Annals of Surgical Oncology*, vol. 20, no. 1, pp. 94–101, 2013.

[37] G. M. K. Tse, P.-H. Tan, T. K. F. Ma, C. B. Gilks, C. S. P. Poon, and B. K. B. Law, "CD44s is useful in the differentiation of benign and malignant papillary lesions of the breast," *Journal of Clinical Pathology*, vol. 58, no. 11, pp. 1185–1188, 2005.

[38] M. Saddik, R. Lai, L. J. Medeiros, A. McCourty, and R. K. Brynes, "Differential expression of cyclin D1 in breast papillary carcinomas and benign papillomas: an immunohistochemical study," *Archives of Pathology and Laboratory Medicine*, vol. 123, no. 2, pp. 152–156, 1999.

[39] M. Yoshida, H. Tsuda, S. Yamamoto et al., "Loss of heterozygosity on chromosome 16q suggests malignancy in core needle biopsy specimens of intraductal papillary breast lesions," *Virchows Archiv*, vol. 460, no. 5, pp. 497–504, 2012.

[40] C. A. Wynveen, T. Nehhozina, M. Akram et al., "Intracystic papillary carcinoma of the breast: an in situ or invasive tumor? results of immunohistochemical analysis and clinical follow-up," *American Journal of Surgical Pathology*, vol. 35, no. 1, pp. 1–14, 2011.

[41] E. A. Rakha, N. Gandhi, F. Climent et al., "Encapsulated papillary carcinoma of the breast: an invasive tumor with excellent prognosis," *The American Journal of Surgical Pathology*, vol. 35, no. 8, pp. 1093–1103, 2011.

[42] X. Li, O. Weaver, M. M. Desouki et al., "Microcalcification is an important factor in the management of breast intraductal papillomas diagnosed on core biopsy," *The American Journal of Clinical Pathology*, vol. 138, no. 6, pp. 789–795, 2012.

[43] F. O'Malley, D. Visscher, G. MacGrogan, P. H. Tan, and S. Ichihara, "Intraductal papilloma," in *WHO Classification of Tumours of the Breast*, S. R. Lakhani, I. O. Ellis, S. J. Schnitt, P. H. Tan, and M. J. van de Vijver, Eds., pp. 99–105, International Agency of Research on Cancer (IARC), Lyon, France, 2012.

[44] J. Cuzick, T. Powles, U. Veronesi et al., "Overview of the main outcomes in breast-cancer prevention trials," *The Lancet*, vol. 361, no. 9354, pp. 296–300, 2003.

[45] B. Fisher, J. P. Costantino, D. L. Wickerham et al., "Tamoxifen for the prevention of breast cancer: current status of the National Surgical Adjuvant Breast and Bowel Project P-1 study," *Journal of the National Cancer Institute*, vol. 97, no. 22, pp. 1652–1662, 2005.

[46] V. G. Vogel, J. P. Costantino, D. L. Wickerham et al., "Effects of tamoxifen vs raloxifene on the risk of developing invasive breast cancer and other disease outcomes: the NSABP study of tamoxifen and raloxifene (STAR) P-2 trial," *The Journal of the American Medical Association*, vol. 295, no. 23, pp. 2727–2741, 2006.

[47] P. E. Goss, J. N. Ingle, J. Ales-Martinez et al., "Exemestane for breast-cancer prevention in postmenopausal women," *The New England Journal of Medicine*, vol. 364, no. 25, pp. 2381–2391, 2011.

Hindawi Publishing Corporation
BioMed Research International
Volume 2015, Article ID 306964, 7 pages
http://dx.doi.org/10.1155/2015/306964

Research Article

Circulating Galectin-1 and 90K/Mac-2BP Correlated with the Tumor Stages of Patients with Colorectal Cancer

Keng-Liang Wu,[1,2] Hong-Hwa Chen,[3,4] Chen-Tzi Pen,[5] Wen-Ling Yeh,[5] Eng-Yen Huang,[4,6,7] Chang-Chun Hsiao,[2] and Kuender D. Yang[8,9]

[1]*Division of Hepatogastroenterology, Department of Internal Medicine, Kaohsiung Chang Gung Memorial Hospital, Kaohsiung 83301, Taiwan*
[2]*Graduate Institute of Clinical Medical Sciences, Chang Gung University, Taoyuan 33302, Taiwan*
[3]*Division of Colonic and Rectal Surgery, Department of Surgery, Kaohsiung Chang Gung Memorial Hospital, Kaohsiung 83301, Taiwan*
[4]*College of Medicine, Chang Gung University, Taoyuan 33302, Taiwan*
[5]*Department of Medical Research, Kaohsiung Chang Gung Memorial Hospital, Kaohsiung 83301, Taiwan*
[6]*Department of Radiation Oncology, Kaohsiung Chang Gung Memorial Hospital, Kaohsiung 83301, Taiwan*
[7]*School of Traditional Chinese Medicine, Chang Gung University College of Medicine, Taoyuan 33302, Taiwan*
[8]*Institute of Clinical Medicine, National Yang Ming University, Taipei 11221, Taiwan*
[9]*Department of Medical Research and Development, Chang Bing Show Chwan Memorial Hospital, Changhua 50544, Taiwan*

Correspondence should be addressed to Eng-Yen Huang; huangengyen@gmail.com
and Kuender D. Yang; yangkd.yeh@msa.hinet.net

Received 15 September 2014; Revised 3 December 2014; Accepted 17 December 2014

Academic Editor: Aurelio Ariza

Background. The simultaneous correlation of serum galectin-1, galectin-3, and 90K/Mac-2BP levels with clinical stages of patients with colorectal cancer has not yet been clarified. We plan to measure the serum levels of galectin-1, galectin-3, and 90K/Mac-2BP of patients at different stages of colorectal cancer and analyze the correlation of these galectins with stages of colorectal cancers. *Methods*. 198 colorectal cancer patients (62 ± 13 (range 31–85) years old, 43.6% female) were recruited for this study. Subjects' blood samples were checked for serum galectin-1, galectin-3, 90K/Mac-2BP, and carcinoembryonic antigen by sandwich enzyme-linked immunosorbent assay. We determined the correlation between plasma concentrations with clinical tumor stages. *Results*. Colorectal cancer patients with larger cancer sizes (stages T3, T4 rather than T1, T2) have higher serum 90K/Mac-2BP ($P = 0.014$) and patients with lymph node metastasis have higher serum galectin-1 ($P = 0.002$) but there was not a significant correlation between galectin-3 and tumor staging of colon cancer. In colorectal cancer patients even with normal carcinoembryonic antigen, serum galectin-1 could predict more lymph node metastasis. *Conclusions*. We found 90K/Mac-2BP correlated with the size of colorectal cancer. Galectin-1 but not galectin-3 was associated with lymph node metastasis. Galectin-1 could predict more lymph node metastasis in colorectal cancer patients with normal serum carcinoembryonic antigen.

1. Introduction

Carcinoembryonic antigen (CEA) was one of the first serological tumor markers to be discovered and has contributed significantly to the prediction of colorectal cancer and its recurrence. Several other serum markers in addition to CEA, such as carbohydrate antigen 19-9 (CA19-9), carbohydrate antigen 242, and tissue inhibitor of metalloproteinases type 1, have been reported and evaluated for various clinical uses in colorectal cancer (CRC) management. These serum markers may contribute to the prediction of prognosis or relapse after therapy, but high-powered, controlled studies are still needed to assess potential biomarkers for prognosis and recurrence of CRC. Serum markers for CRC are preferred over tissue- or stool-based assays, especially for screening and monitoring purposes, which require repeat testing. Blood-based tests

have a better acceptance level and provide increased patient compliance.

Galectins are β-galactoside-binding proteins possibly involved in tumor prognosis. Four galectins, galectin-1, galectin-3, galectin-4, and galectin-8, are expressed in the human colon and rectum and their expressions show significant changes during colorectal cancer development and metastasis [1]. In particular, galectin-1 and galectin-3 play a role in the regulation of cell migration. Galectin-1, galectin-3, and their binding protein 90K/Mac-2BP are reported to be correlated and modulated with the malignancy prognosis and distal metastasis of colon cancer [2–4], but clinically the correlation between these serum galectins and prognosis of patients with colorectal cancer is less studied, especially 90K/Mac-2BP. Galectin-3 is also known to maintain epidermal growth factor receptor lattice formation on colon cancer cells for enhancing growth and epithelial mesenchymal transition that is implicated in cancer stem cells formation, resulting in the progression, and metastasis [5]. 90K/Mac-2BP, a tumor-associated glycoprotein, interacts with galectins and has roles in host defense by augmenting the immune response, but serum 90K/Mac-2BP level was suggested to indicate poor prognosis in several cancers [6–9]. There are few studies regarding serum 90K/Mac-2BP concentration on colon cancer prognosis reported to date. The aim of our study was to identify whether galectin-1, galectin-3, and/or 90K/Mac-2BP correlates with tumor staging in patients with CRC and to investigate their possible clinical role in the prediction of patients with CRC.

2. Methods

2.1. Subjects. One hundred ninety-eight patients with colorectal cancer who received surgical resection were enrolled in this study. Exclusion criteria included no well-defined pathology and no adequate clinical document available. The study was conducted at the Kaohsiung Chang Gung Memorial Hospital between May 2008 and June 2011, after the study protocol was approved by the Institutional Review Board of the hospital. All patients received surgical resection for CRC. Clinical data about age, gender, size of cancer, lymph node metastasis, and pathologic reports (vascular invasion, lymph node invasion, and well/poor differentiation) and clinical stage by TNM (tumor, nodes, and metastasis) system of the American Joint Committee on Cancer (AJCC 7th edition) were recorded as shown in Table 1. Blood samples were taken before the surgery and stored at −80°C until ELISA.

2.2. Serum Samples Studied. Serum samples were from the same patients who underwent colon cancer resection. These serum samples studied were obtained from the tissue bank of the Kaohsiung Chang Gung Memorial Hospital. One hundred ninety-eight consecutively decoded CRC patients (105 males and 93 females, 62±13 years) who received surgery during May 2008 to June 2011 were enrolled in this study. Of the 198 patients, 174 had no clinically detectable metastasis (94 males and 80 females) and 24 had liver metastasis (11 males and 13 females). Serum galectin-1 and galectin-3 levels were assessed by a microplate immunoenzymatic method (Bender MedSystems, Vienna, Austria), and concentration of 90K/Mac-2BP molecule was evaluated using a commercial enzyme-linked immunosorbent assay kit (DIESSE, Siena, Italy) according to the manufacturer instructions.

Table 1: Baseline characteristics of patients of the study.

	Number
Gender (male/female)	105/93
Age (mean [range])	62 ± 13 [31–85] years
Site (A/T/D/S/R)	33/15/12/38/100
Histopathology (well/moderate/poor differentiation)	5/176/17
Stage (TNM) (I/II/III/IV)	45/62/67/24
Vascular invasion	39/198 (19.7%)

Note: A: cecum and ascending; T: transverse colon; D: descending colon; S: sigmoid colon; R: rectum.

2.3. Determination of Serum Galectins and 90K/Mac-2BP Concentrations. The 96-well plates were coated with anti-galectin antibody at 2.5 mg/mL in coating buffer (15 mmol/L Na_2CO_3 and 17 mmol/L $NaHCO_3$, pH: 9.6) overnight at 4°C. The plates were washed with a washing buffer (0.05% Tween-20 in PBS) and incubated with blocking buffer (1% bovine serum albumin in PBS) for 1 hour at room temperature. Serum samples or standard recombinant galectins were introduced to the plates for 2 hours before the application of biotinylated anti-galectin antibody (1.25 mg/mL in blocking buffer) for 1 hour at room temperature. After introduction of ExtrAvidin peroxidase (1 : 10,000 dilution in blocking buffer) for 1 hour, the plates were developed with Sigma FAST OPD for 10 minutes. The reaction was stopped by adding 4 mol/L sulfuric acid, and the absorbance was read at 492 nm by a microplate reader. We measured the exact concentration of galectin-1 (R&D), galectin-3 (R&D), and 90K/Mac-2BP (Bender MedSystems) by intrapolation of a standard curve made by a series of well-known concentrations as per manufacturer's instruction.

2.4. Statistical Analysis. Data were reported as means ± standard errors of the mean unless otherwise indicated. Continuous and categorical variables were compared by using Student's t-test and χ^2 or Fisher's exact test, respectively. Spearman's rank correlation coefficient was used to explore relationships among variables. Predictability for an inadequate outcome when additional risk factors ($P < 0.05$ on multivariate logistic regression) were individually added was further determined.

3. Results

3.1. Serum Concentrations of Galectin-1, Galectin-3, and 90K/Mac-2BP. The 198 consecutive patients were male-predominant (105/198). Of the patients studied, more than one-half of the patients (100/198, 51%) had rectal cancer.

Table 2: Levels of galectin-1, galectin-3, 90K/Mac-2BP, and CEA in the sera of colon cancer patients.

	All patients	Stages I and II	Stages III and IV	P
Galectin-1 (ng/mL)	14.33 ± 1.67	8.73 ± 1.08	20.93 ± 3.77	0.002*
Galectin-3 (ng/mL)	1.54 ± 0.10	1.44 ± 0.11	1.65 ± 0.17	0.320
90K/Mac-2BP (μg/mL)	6.77 ± 0.25	6.87 ± 0.36	6.65 ± 0.36	0.665
CEA (ng/mL)	153.19 ± 66.31	26.30 ± 19.89	302.39 ± 140.43	0.055

CEA: carcinoembryonic antigen; * significant difference.
The continuous variables were described by mean ± SEM.

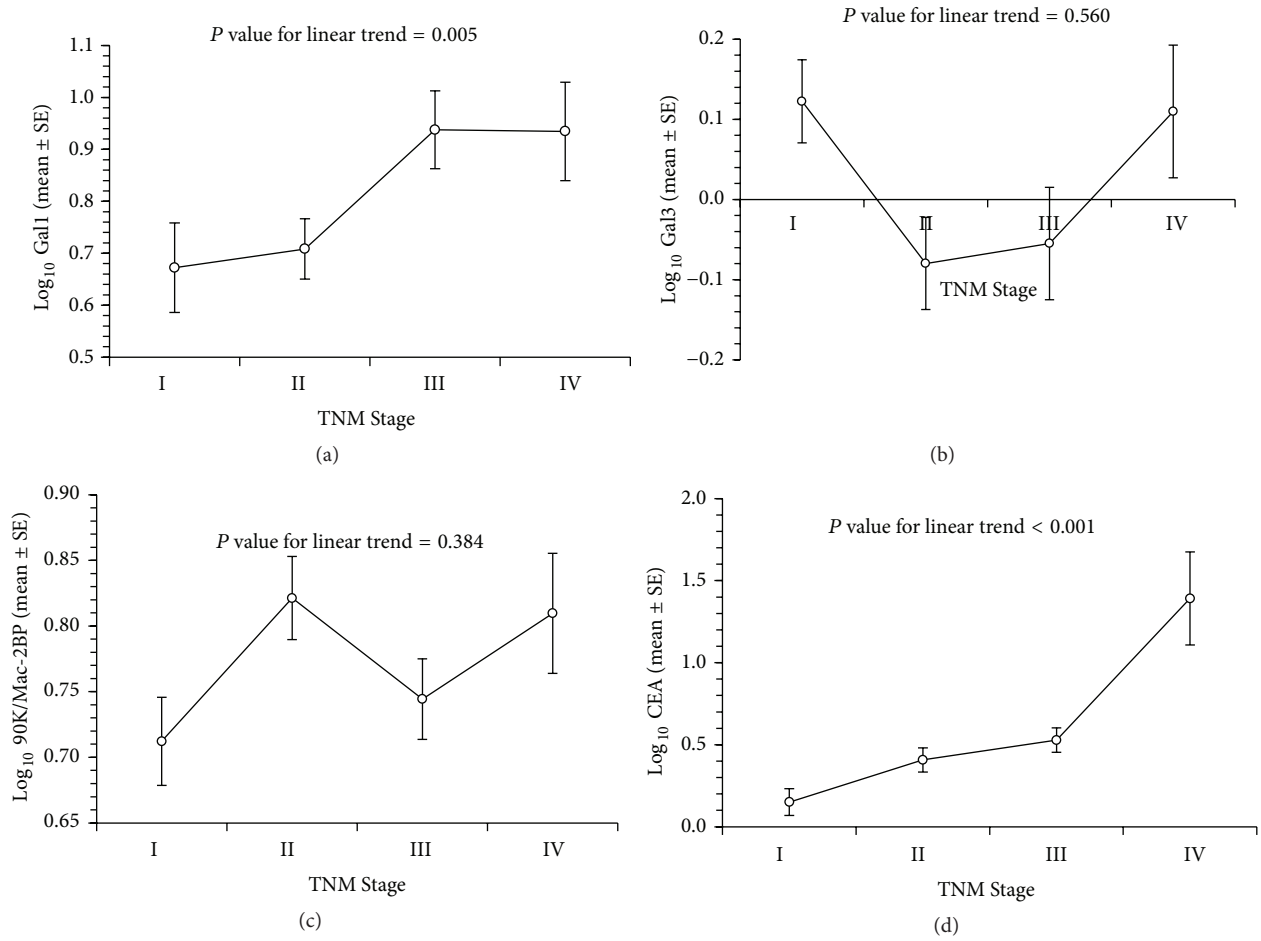

Figure 1: The correlation of galectin-1, galectin-3, 90K/Mac-2BP, and carcinoembryonic antigen with TNM system score. Galectin-1 levels were associated with advanced TNM Stages (III and IV, $P = 0.005$). Carcinoembryonic antigen levels were significantly associated with advanced stage of TNM system ($P < 0.001$). (d) Gal1: galectin-1; Gal3: galectin-3; Gal3BP: 90K/Mac-2BP; CEA: carcinoembryonic antigen.

Approximately one-half (46%, 91/198) had advanced cancer TNM systems III and IV and 44% (87/198) had lymph node metastasis.

3.2. Serum Galectin-1 and CEA Levels Associated with TNM System. Serum galectin-1 levels in CRC patients ranged from 0.14 to 198.34 (average 14.19 ± 2.63) ng/mL. Patients with TNM Stage III or IV revealed significantly higher galectin-1 levels (20.93 ± 3.77 ng/mL versus 8.73 ± 1.08 ng/mL). Galectin-3 and 90K/Mac-2BP levels were not significantly different between patients with lower (I or II) and advanced stages (Table 2). CEA levels had a higher trend in patients with advanced TNM Stage (26.3 ± 19.89 versus 302.39 ± 140.43 ng/mL). As shown in Figure 1, galectin-1 but not galectin-3 or 90K/Mac-2BP levels were significantly higher in CRC patients with TNM Stage III/IV. Higher galectin-1 levels were found in patients with Stage III/IV rather than Stage I and Stage II ($P = 0.005$) (Figure 1(a)). In addition, we also found that CEA concentrations were significantly correlated with TNM Stage of colon cancer ($P < 0.0001$) (Figure 1(d)).

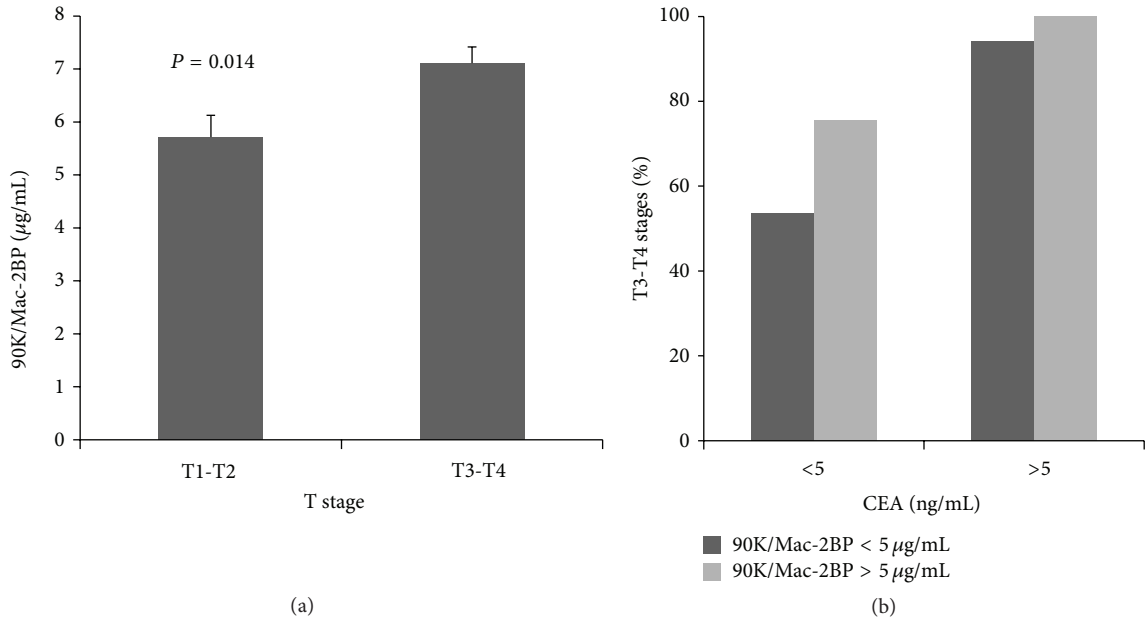

Figure 2: Patients with larger cancer sizes of stages T3, T4 rather than T1, T2 have more serum 90K/Mac-2BP levels which were significantly associated with tumor size (T3 or T4) ($P = 0.014$). Galectin-3 or galectin-1 levels were not significantly associated with tumor size. In colon cancer patients with normal serum carcinoembryonic antigen, advanced T stage had higher serum 90K/Mac-2BP levels. (b) CEA: carcinoembryonic antigen.

3.3. 90K/Mac-2BP Levels Associated with Tumor Size (T Stage). The patients with advanced T stage (stages T3-T4) had higher serum 90K/Mac-2BP levels than those with small tumor size (stages T1-T2) ($P = 0.014$) as shown in Figure 2(a). In contrast, galectin-3 and galectin-1 levels were not significantly associated with tumor size (data not shown). Interestingly, we found that CRC patients with normal serum CEA and higher serum 90K/Mac-2BP levels were associated with tumor size (T3 or T4) (Figure 2(b)). Analyses of linear correlation between galectins levels and tumor size also found that tumor size was significantly correlated with 90K/Mac-2BP concentrations ($r = 0.264$, $P < 0.001$) (Figure 3(a)) and with CEA levels ($r = 0.208$, $P = 0.005$) (Figure 3(b)), but no significant correlation was found with galectin-1 or galectin-3 levels (Figures 3(c) and 3(d)).

3.4. Lymph Node Metastasis Associated with Galectin-1 and CEA Levels. Patients with lymph node metastasis had higher serum galectin-1 levels ($P = 0.002$, Figure 4). However, galectin-3 or 90K/Mac-2BP levels were not correlated with lymph node metastasis (data not shown). Further analysis found that, in patients with normal CEA concentration, galectin-1 levels predicted positive lymph node metastasis of colon cancer (Figure 5(a)). Analysis of Receiver Operating Characteristic (ROC) curves of galectins and CEA concentrations for CRC with LN metastasis found that galectin-1 and CEA levels could predict lymph node metastasis at good sensitivity and specificity, showing area under the curve (AUC) at 0.627 for galectin-1 and at 0.638 for CEA (Figure 5(b)).

4. Discussion

Galectin-3 and galectin-1 are members of the galectins gene family that are expressed at elevation in a variety of neoplastic cell types and have been associated with cell growth, apoptosis, cellular adhesion process, cell proliferation, transformation, invasiveness, and metastasis. Some galectins (such as galectin-1 and galectin-3) and their binding proteins such as 90K/Mac-2BP are reported to be correlated with the malignancy prognosis and distant metastasis of colon cancer [2–4, 10–12]; Nakamura et al. had clarified that strong expression of galectin-3 in colorectal cancer correlated with cancer progression, liver metastasis, and poor prognosis [13]. Several reports have indicated its involvement in carcinogenesis of certain cancers [14, 15], but we did not find any correlation between serum galectin-3 levels and progression of colon cancer in our study. Thijssen et al. showed that galectin-3 expression on epithelium of colon cancer was unaltered [16] and Sanjuán et al. found that galectin-3 expression is downregulated in the initial stages of neoplastic progression, whereas a dissociated cytoplasmic expression increases in later phases of tumor progression [3]. Galectin-3 was a cytosolic and secretary protein but was less detected in the extracellular medium during primary cancer cell culture [17], indicating that cancer cells alone do not secrete galectin-3 into extracellular medium and this could be the reason why the present result, serum galectin-3, was not correlated with prognosis of colon cancer. Further studies to clarify are necessary.

We found that 90K/Mac-2BP could be a predictor for the advanced invasion of colorectal cancer. Greco et al. showed that galectin-3 ligand, 90K/Mac-2BP molecule, was

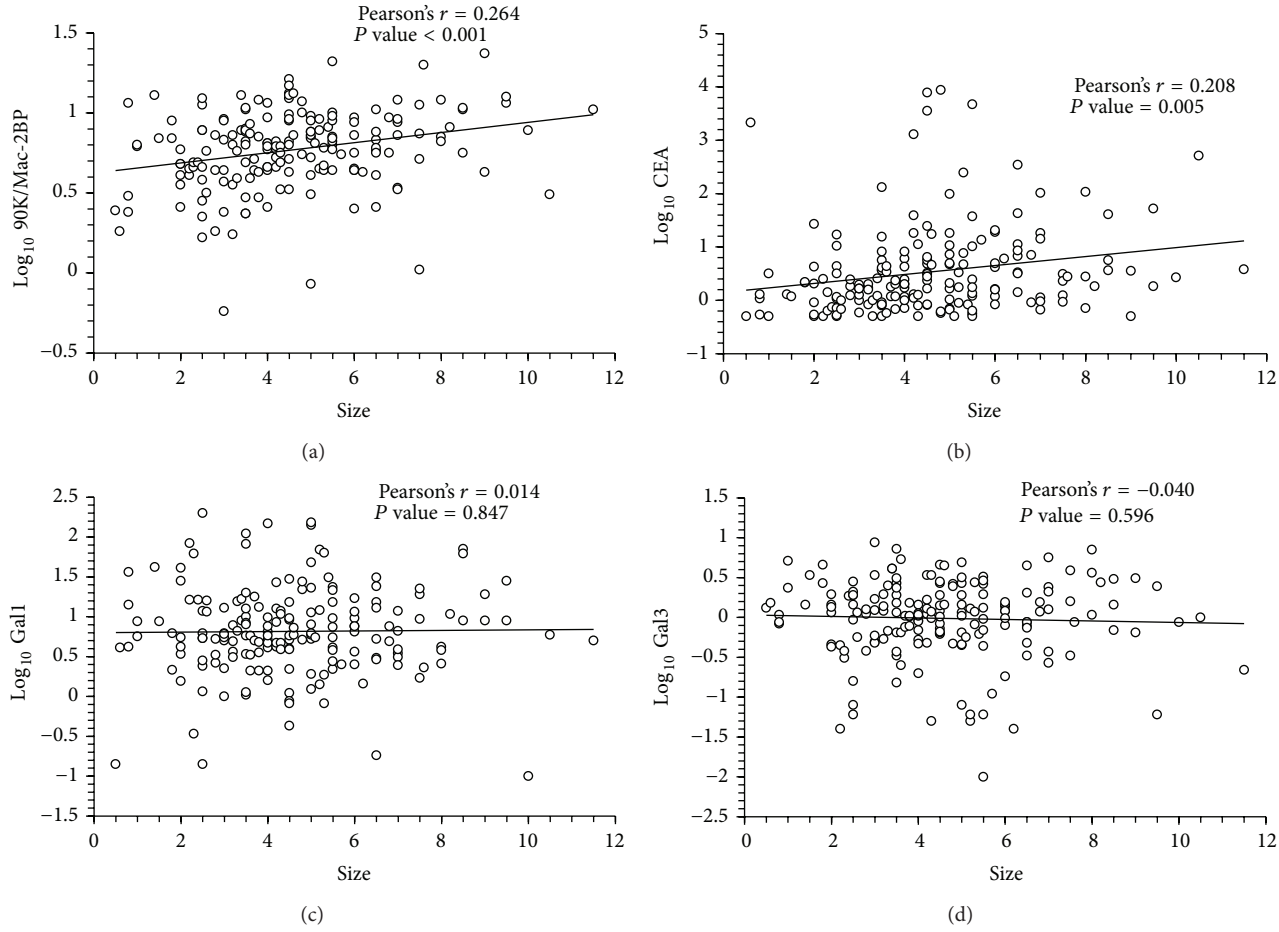

Figure 3: Linear correlation between tumor size of colon tumors and 90K/Mac-2BP levels ($r = 0.264$, $P < 0.001$) or carcinoembryonic antigen levels ($r = 0.208$, $P = 0.005$) but no significant correlation with galectin-1 or galectin-3 levels. Gal1: galectin-1; Gal3: galectin-3; Gal3BP: 90K/Mac-2BP; CEA: carcinoembryonic antigen.

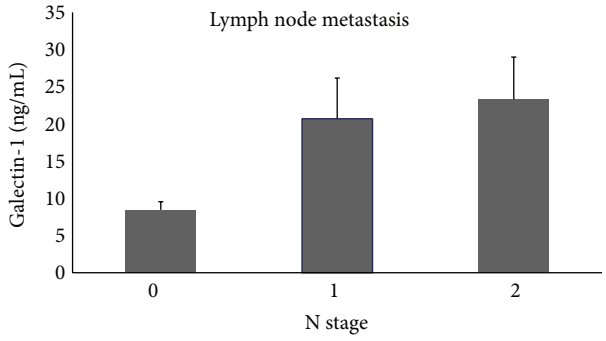

Figure 4: Serum galectin-1 concentrations were significantly increased in patients with lymph node metastasis ($P = 0.002$).

increased in the blood plasma from patients with both adenomatous and adenocarcinomatous lesions [18]. Iacovazzi et al. also clarified the correlation prognosis of colon cancer with 90K/Mac-2BP [6], the same result as our present study, but we did not find that 90K/Mac-2BP mean values ranged higher in right-side than in left-side colon cancer although they hypothesized that this could be due to the better blood and lymph supply that can provide a more efficient local tumor defense. Natoli et al. showed that the increase of 90K/Mac-2BP after r-IFN-alpha-2b administration might be of importance for the early detection of disease recurrence in breast and colon cancer patients without evidence of disease [19]. In contrast, Lee et al. clarified that 90K/Mac-2BP itself has antitumor activity in CRC cells via suppression of Wnt signaling with a novel mechanism of ISGylation-dependent ubiquitination of beta-catenin when it interacts with CD9/CD82 but is downregulated in advanced CRC tissues [20]. To date, the effect of 90K/Mac-2BP on colon cancer prognosis is not well studied.

In this study, we found that galectin-1 could be a marker for prediction of lymph node metastasis. Barrow et al. showed that the concentrations of galectin-1 were not significantly increased in patients with colorectal cancer [12] but Thijssen et al. showed that endothelial cells express galectin-1 and that the expression and distribution change on cell activation, resulting in a different profile in the tumor vasculature [16]. The expression of galectin-1 significantly increased with the degree of dysplasia from Hittelet A study [21].

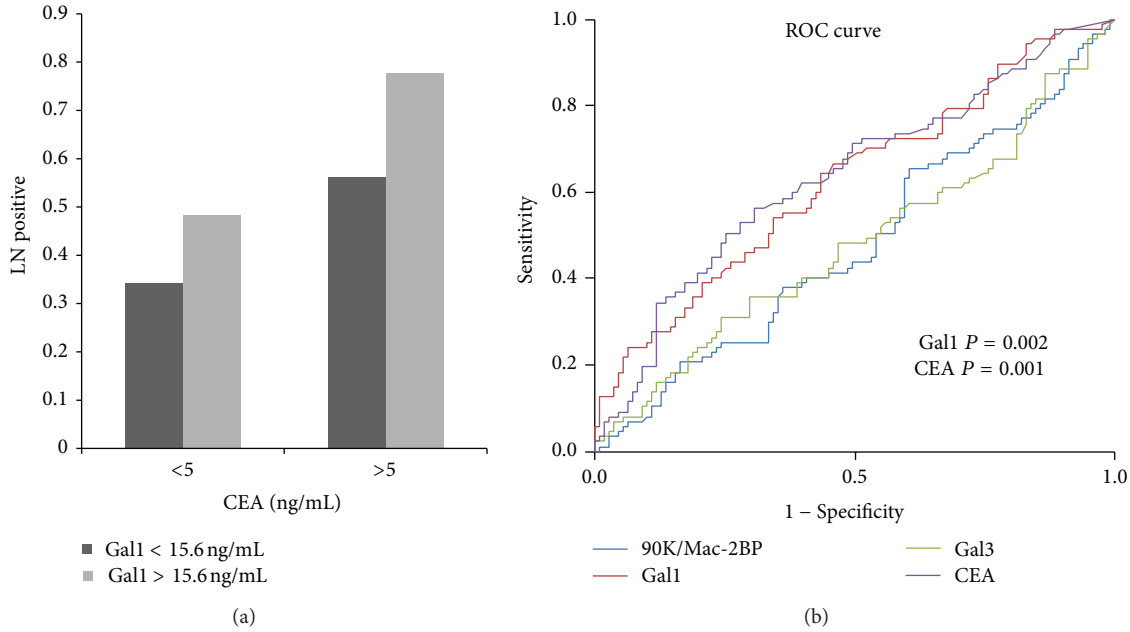

Figure 5: Galectin-1 levels predicted positive lymph node metastasis of colon cancer. (a) Analysis of Receiver Operating Characteristic curves found that galectin-1 and carcinoembryonic antigen levels could predict good sensitivity and specificity, showing area under the curve (AUC) at 0.627 for galectin-1 and at 0.638 for carcinoembryonic antigen. (b) Gal1: galectin-1; Gal3: galectin-3; 90K: 90K/Mac-2BP; CEA: carcinoembryonic antigen; ROC: Receiver Operating Characteristic.

Nagy et al. observed a significant prognostic value associated with galectin-1 in Dukes A and B colon tumors [4] and our study showed different result. From André et al.'s study, histopathological analysis of lymph node carcinomas indicated a correlation of either increased galectin-1 binding or reduced binding of both galectins with the occurrence of lymph node lesions [22]. It could be that galectin-1 in colorectal mucosa is predominant in stromal cells whose overexpression is associated with the neoplastic progression of colorectal cancer as told by Sanjuán et al. [3]. We also found that, in colon cancer patients with normal CEA, galectin-1 could predict more lymph node metastasis.

In conclusion, serum 90K/Mac-2BP concentrations in colorectal cancer patients at an advanced stage were significantly higher than those at an early stage. Higher galectin-1 concentration was correlated with lymph node metastasis, especially in colorectal cancer patients with normal CEA. These results suggest that the measurement of serum 90K/Mac-2BP and galectin-1 concentration is helpful to predict patients with advanced colorectal cancer.

Conflict of Interests

The authors declare that there is no conflict of interests regarding the publication of this paper.

Authors' Contribution

Keng-Liang Wu and Hong-Hwa Chen equally contributed to this work.

Acknowledgments

The authors thank the Tissue Bank of Kaohsiung Chang Gung Memorial Hospital (CLRPG870463) for providing the decoded materials for this study. The study was supported by Grants CMRPG880622 and CMRPG880623 from the Chang Gung Memorial Hospital, Taiwan, and NSC101-2325-B-182A-002 and NSC102-2325-B-182A-002 from the National Science Council, Taiwan, for Keng-Liang Wu, Grant no. MOST103-2325-B-758-001 for Kuender D. Yang, and Grant no. NSC102-2325-B-182A-014 for Eng-Yen Huang.

References

[1] H. Barrow, J. M. Rhodes, and L.-G. Yu, "The role of galectins in colorectal cancer progression," *International Journal of Cancer*, vol. 129, no. 1, pp. 1–8, 2011.

[2] H. L. Schoeppner, A. Raz, S. B. Ho, and R. S. Bresalier, "Expression of anendogenous galactose-binding lectin correlates with neoplastic progression in the colon," *Cancer*, vol. 75, no. 12, pp. 2818–2826, 1995.

[3] X. Sanjuán, P. L. Fernández, A. Castells et al., "Differential expression of galectin 3 and galectin 1 in colorectal cancer progression," *Gastroenterology*, vol. 113, no. 6, pp. 1906–1915, 1997.

[4] N. Nagy, H. Legendre, O. Engels et al., "Refined prognostic evaluation in colon carcinoma using immunohistochemical galectin fingerprinting," *Cancer*, vol. 97, no. 8, pp. 1849–1858, 2003.

[5] J. Merlin, L. Stechly, S. de Beaucé et al., "Galectin-3 regulates MUC1 and EGFR cellular distribution and EGFR downstream pathways in pancreatic cancer cells," *Oncogene*, vol. 30, no. 22, pp. 2514–2525, 2011.

[6] P. A. Iacovazzi, M. Notarnicola, M. G. Caruso et al., "Serum levels of galectin-3 and its ligand 90k/Mac-2BP in colorectal cancer patients," *Immunopharmacology and Immunotoxicology*, vol. 32, no. 1, pp. 160–164, 2010.

[7] S. J. Kim, S. J. Lee, H. J. Sung et al., "Increased serum 90K and galectin-3 expression are associated with advanced stage and a worse prognosis in diffuse large B-cell lymphomas," *Acta Haematologica*, vol. 120, no. 4, pp. 211–216, 2008.

[8] C.-C. Wu, Y.-S. Huang, L.-Y. Lee et al., "Overexpression and elevated plasma level of tumor-associated antigen 90K/Mac-2 binding protein in colorectal carcinoma," *Proteomics—Clinical Applications*, vol. 2, no. 12, pp. 1586–1595, 2008.

[9] Y. Ozaki, K. Kontani, K. Teramoto et al., "Involvement of 90K/Mac-2 binding protein in cancer metastases by increased cellular adhesiveness in lung cancer," *Oncology Reports*, vol. 12, no. 5, pp. 1071–1077, 2004.

[10] K. Endo, S. Kohnoe, E. Tsujita et al., "Galectin-3 expression is a potent prognostic marker in colorectal cancer," *Anticancer Research*, vol. 25, no. 4, pp. 3117–3122, 2005.

[11] L. Z. Povegliano, C. T. F. Oshima, F. de Oliveira Lima, P. L. A. Scherholz, and N. M. Forones, "Immunoexpression of galectin-3 in colorectal cancer and its relationship with survival," *Journal of Gastrointestinal Cancer*, vol. 42, no. 4, pp. 217–221, 2011.

[12] H. Barrow, X. Guo, H. H. Wandall et al., "Serum galectin-2, -4, and -8 are greatly increased in colon and breast cancer patients and promote cancer cell adhesion to blood vascular endothelium," *Clinical Cancer Research*, vol. 17, no. 22, pp. 7035–7046, 2011.

[13] M. Nakamura, H. Inufusa, T. Adachi et al., "Involvement of galectin-3 expression in colorectal cancer progression and metastasis," *International Journal of Oncology*, vol. 15, no. 1, pp. 143–148, 1999.

[14] Y. Takenaka, H. Inohara, T. Yoshii et al., "Malignant transformation of thyroid follicular cells by galectin-3," *Cancer Letters*, vol. 195, no. 1, pp. 111–119, 2003.

[15] T. Yoshii, H. Inohara, Y. Takenaka et al., "Galectin-3 maintains the transformed phenotype of thyroid papillary carcinoma cells," *International Journal of Oncology*, vol. 18, no. 4, pp. 787–792, 2001.

[16] V. L. Thijssen, S. Hulsmans, and A. W. Griffioen, "The galectin profile of the endothelium: altered expression and localization in activated and tumor endothelial cells," *The American Journal of Pathology*, vol. 172, no. 2, pp. 545–553, 2008.

[17] A. Satelli, P. S. Rao, P. K. Gupta, P. R. Lockman, K. S. Srivenugopal, and U. S. Rao, "Varied expression and localization of multiple galectins in different cancer cell lines," *Oncology Reports*, vol. 19, no. 3, pp. 587–594, 2008.

[18] C. Greco, R. Vona, M. Cosimelli et al., "Cell surface overexpression of galectin-3 and the presence of its ligand 90K in the blood plasma as determinants in colon neoplastic lesions," *Glycobiology*, vol. 14, no. 9, pp. 783–792, 2004.

[19] C. Natoli, C. Garufi, N. Tinari et al., "Dynamic test with recombinant interferon-alpha-2b: effect on 90K and other tumour-associated antigens in cancer patients without evidence of disease," *British Journal of Cancer*, vol. 67, no. 3, pp. 564–567, 1993.

[20] J. H. Lee, J. A. Bae, Y.-W. Seo et al., "Glycoprotein 90K, downregulated in advanced colorectal cancer tissues, interacts with CD9/CD82 and suppresses the Wnt/β-catenin signal via ISGylation of β-catenin," *Gut*, vol. 59, no. 7, pp. 907–917, 2010.

[21] A. Hittelet, H. Legendre, N. Nagy et al., "Upregulation of galectins-1 and -3 in human colon cancer and their role in regulating cell migration," *International Journal of Cancer*, vol. 103, no. 3, pp. 370–379, 2003.

[22] S. André, S. Kojima, N. Yamazaki et al., "Galectins-1 and -3 and their ligands in tumor biology. Non-uniform properties in cell-surface presentation and modulation of adhesion to matrix glycoproteins for various tumor cell lines, in biodistribution of free and liposome-bound galectins and in their expression by breast and colorectal carcinomas with/without metastatic propensity," *Journal of Cancer Research and Clinical Oncology*, vol. 125, no. 8-9, pp. 461–474, 1999.

Hindawi Publishing Corporation
BioMed Research International
Volume 2015, Article ID 486391, 7 pages
http://dx.doi.org/10.1155/2015/486391

Clinical Study

BRAF Testing in Multifocal Papillary Thyroid Carcinoma

Hillary Z. Kimbrell,[1] Andrew B. Sholl,[1] Swarnamala Ratnayaka,[1] Shanker Japa,[1] Michelle Lacey,[2] Gandahari Carpio,[3] Parisha Bhatia,[4] and Emad Kandil[4]

[1]*Department of Pathology and Laboratory Medicine, Tulane University, 1430 Tulane Avenue SL-79, New Orleans, LA 70112, USA*
[2]*Department of Mathematics, Tulane University, 6823 St. Charles Avenue, New Orleans, LA 70118, USA*
[3]*Department of Medicine, Tulane University, 1430 Tulane Avenue SL-12, New Orleans, LA 70112, USA*
[4]*Department of Surgery, Tulane University, 1430 Tulane Avenue SL-22, New Orleans, LA 70112, USA*

Correspondence should be addressed to Hillary Z. Kimbrell; hillarykimbrell@gmail.com

Received 6 January 2015; Revised 3 March 2015; Accepted 8 March 2015

Academic Editor: Aurelio Ariza

Background. *BRAF* V600E mutation is associated with poor prognosis in patients with papillary thyroid carcinoma (PTC). PTC is often multifocal, and there are no guidelines on how many tumors to test for *BRAF* mutation in multifocal PTC. *Methods*. Fifty-seven separate formalin-fixed and paraffin-embedded PTCs from twenty-seven patients were manually macrodissected and tested for *BRAF* mutation using a commercial allele-specific real-time polymerase chain reaction-based assay (Entrogen, Woodland Hills, CA). Data related to histologic characteristics, patient demographics, and clinical outcomes were collected. *Results*. All mutations detected were *BRAF* V600E. Seventeen patients (63%) had concordant mutation status in the largest and second-largest tumors (i.e., both were positive or both were negative). The remaining ten patients (37%) had discordant mutation status. Six of the patients with discordant tumors (22% overall) had a *BRAF*-negative largest tumor and a *BRAF*-positive second-largest tumor. No histologic feature was found to help predict which cases would be discordant. *Conclusions*. Patients with multifocal PTC whose largest tumor is *BRAF*-negative can have smaller tumors that are *BRAF*-positive. Therefore, molecular testing of more than just the dominant tumor should be considered. Future studies are warranted to establish whether finding a *BRAF* mutation in a smaller tumor has clinical significance.

1. Introduction

Papillary thyroid carcinoma (PTC) is often a multifocal disease, with rates as high as 80% in the literature [1]. Despite multiple studies using different methodologies [1–11] it remains an unsettled question as to whether the multifocality represents separate primary tumors or intraglandular metastasis, or a combination of both. It seems likely from prior studies that a subset of cases represent separate primaries, or at the very least have molecularly distinct tumors. The question then arises, how many tumors should be tested for *BRAF* mutation in multifocal PTC? A recent very large retrospective study found that patients with multifocal disease and a *BRAF* V600E mutation had a significantly higher rate of mortality than patients with multifocal disease without a *BRAF* mutation, but the study did not elaborate on how many or which tumors were tested for each patient [12]. Our study attempts to further the data on *BRAF* mutation status in patients with multifocal disease and to find the optimal strategy for *BRAF* testing in these patients.

2. Materials and Methods

The study protocol was approved by the IRB at Tulane University. The laboratory information system was searched for cases of multifocal papillary thyroid carcinoma in patients with all thyroid tissue removed, either as a single surgery or two separate surgeries, since January 1, 2006. Thirty-three cases were identified, and the slides from each case were reviewed by the study pathologists (H.Z.K. and A.B.S.). In all but one case, the entire thyroid was submitted. The following histologic features were recorded for each tumor: size, laterality, histologic variant, and the presence or absence

of additional features such as irregular border, location close to the capsule, extrathyroidal extension, satellite nodules, and isolated psammoma bodies. Satellite nodules were defined as tumor foci less than 0.5 mm that were within one section of a larger tumor nodule but not directly attached to the larger nodule. Isolated psammoma bodies were defined as psammoma bodies within the thyroid parenchyma and separate from any tumor nodules. The histologic variant was decided by each pathologist separately, based on the predominant pattern seen in the tumor; discrepancies were resolved by viewing the case together at a multiheaded scope.

The study pathologists marked the two largest tumors in each case, and the tissue was manually macrodissected and placed into tubes. DNA was extracted using the EZ1 DNA Tissue kit (Qiagen, Valencia, CA). *BRAF* mutational status was tested using a commercial allele-specific real-time polymerase chain reaction-based assay that can detect five point mutations in codon 600 (V600E, V600K, V600R, V600D, and V600M) when present in as little as 1% of the tissue (Entrogen, Woodland Hills, CA). Overall, six of the original thirty-three cases were excluded because of insufficient DNA (either a tumor focus was gone on deeper levels or the DNA was of poor quality), leaving a total of twenty-seven cases for the study (see Table 1). Two of the cases where both the largest and second-largest tumors were *BRAF*-negative had additional tumors (see Patients 24 and 25 in Table 1); three of these additional tumors had adequate DNA and were tested for *BRAF* mutation (two additional tumors for Patient 24 and one additional tumor for Patient 25). In all, a total of fifty-seven tumors were tested for *BRAF* mutation. Clinical data related to patient demographics, tumor stage, months of followup, and outcome was collected for these twenty-seven patients. Statistical calculations were performed using *R*, with the Student's *t*-test and Fisher's exact test used to calculate significance. To assess whether *BRAF* status was associated with positive lymph nodes independently of size, multivariate analysis was carried out using logistic regression and the corresponding likelihood ratio test. Additionally, a model was made to predict the size of each tumor (on the log scale) as a function of *BRAF* status and size.

3. Results

There were 17 women and 10 men included in the study with an average age at diagnosis of 52 (range: 26 to 78). The average number of tumor nodules rounded to the nearest whole number was 3, ranging from 2 to 9. Overall, 34 of the 57 tumors (60%) were *BRAF*-positive and all mutations were V600E. Figure 1 illustrates the histologic variants and their respective rates of *BRAF* mutation. Notably, the tall cell variant had the highest rate of positivity for *BRAF* mutation (3 of 3 cases), and the encapsulated follicular variant had the lowest rate (1 of 6 cases). The one *BRAF*-positive encapsulated follicular variant showed focal invasion through the capsule and therefore should probably have been considered along with the other follicular variant tumors that showed an infiltrative growth pattern, as in Walts et al. [13]. There was no significant correlation between *BRAF*-positivity and the presence of an irregular border ($P = 0.6$), location close to the capsule ($P = 0.8$), or extrathyroidal extension ($P = 1$).

The overall average size of the largest nodule was 1.6 cm, ranging from 0.2 cm to 3.6 cm. There was no significant difference in size between the *BRAF*-negative and *BRAF*-positive largest nodules (average sizes 1.8 cm and 1.5 cm, $P = 0.3$). The overall average size of the second-largest nodule was 0.5 cm, ranging from 0.1 cm to 2.2 cm. There was no significant difference in size between the *BRAF*-negative and *BRAF*-positive second-largest nodules (average sizes 0.5 cm and 0.6 cm, $P = 0.7$).

A mutation was present in at least 1 nodule in 22 of the 27 cases (81.4%). In 17 patients, both the largest and second-largest nodules had concordant *BRAF* status; that is, they were both either positive or negative. The remaining ten patients had discordant mutation status; that is, one tumor was positive and one tumor was negative. No histologic features were significantly different between the concordant and discordant cases. The tumors were of the same histologic variant in 11 (65%) of the concordant cases, compared with 7 (70%) of the discordant cases ($P = 1$), as illustrated in Figure 2. Satellite nodules were present in 53% of the concordant cases and 20% of the discordant cases ($P = 0.1$). Isolated psammoma bodies were present in 41% of the concordant cases and 20% of the discordant cases ($P = 0.4$). The largest tumor had irregular borders in 65% of concordant cases and 70% of discordant cases ($P = 1$). Both the largest and second-largest tumors had smooth borders in 12% of the concordant cases and 10% of the discordant cases ($P = 1$).

Similarly, there was no significant correlation between concordant mutation status and laterality: the largest and second-largest tumors were in the same lobe in 6 of the 17 concordant cases (35%), compared to 2 of the 10 discordant cases (20%, $P = 0.7$). The two largest tumors were concordant in 4 of the 5 cases where the disease was unilateral (80%), compared to 13 of the 22 cases that were bilateral (59%, $P = 0.6$).

Cases with 4 or more nodules tended to have concordant mutation status (8 of 9, or 89%) compared to cases with fewer than 4 nodules (9 of 18, or 50%) but this did not reach statistical significance ($P = 0.09$).

Lymph node dissection was performed at the discretion of the surgeon (E.K.) who was not aware of the *BRAF* status preoperatively. There was a significant difference in nodal stage between the patients with a *BRAF*-positive largest tumor and a *BRAF*-negative largest tumor: 11 of the 16 patients (69%) with a *BRAF*-positive largest tumor had cervical lymph node metastases (either N1a or N1b) compared to 2 of the 11 patients (18%) with a *BRAF*-negative largest tumor ($P = 0.02$). This association remained significant when a multivariate analysis was done to account for tumor size ($P = 0.005$). With regards to the largest tumors, the smallest of these were the *BRAF*-negative tumors with positive lymph nodes ($P = 0.04$), followed by the *BRAF*-positive tumors with negative lymph nodes ($P = 0.06$). There was no significant size difference between the *BRAF*-negative tumors with negative lymph nodes and the *BRAF*-positive tumors with positive lymph nodes. Of note, none of the six patients with a *BRAF*-negative

Table 1: Patient characteristics.

Patient number	Age	Sex	Months of Followup	Initial pTN	Number of nodules	Size of largest nodule (cm)	Histologic variant of largest nodule	BRAF status of largest nodule	Size of second-largest nodule (cm)	Histologic variant of second-largest nodule	BRAF status of second-largest nodule
1	40	F	34	T1b N1a	4	1.4	Fol	Positive	0.8	Fol	Positive
2	64	M	40	T3 N1b	2	1.2	TC	Positive	0.5	Clas	Positive
3	74	M	1	T3 N1b	4	1.1	Clas	Positive	0.3	Clas	Positive
4*	58	M	13	T3 N1b	2	1.3	Clas	Positive	0.4	Fol	Positive
5	65	M	2	T1a N1a	5	1.0	Clas	Positive	0.9	Clas	Positive
6	78	M	9	T1a N0	4	0.5	Clas	Positive	0.2	Clas	Positive
7	55	F	29	T2 N0	6	2.5	TC	Positive	0.4	War	Positive
8	59	F	4	T1b N1b	2	1.5	Fol	Positive	0.2	Fol	Positive
9*	50	M	50	T1a N0	3	0.9	Clas	Positive	0.8	Clas	Positive
10	28	F	6	T3 N1a	8	2.2	Clas	Positive	2.2	Clas	Positive
11	63	M	3	T1b N1a	2	1.2	Clas	Positive	0.2	Fol	Positive
12	26	F	3	T1b N1a	2	1.4	Clas	Positive	0.3	Fol	Positive
13	43	M	23	T2 N1b	3	3.6	TC	Positive	0.2	Fol	Negative
14	50	F	22	T3 N0	3	0.4	Clas	Positive	0.1	Fol	Negative
15	42	F	22	T2 N1a	2	2.6	Clas	Positive	0.2	Clas	Negative
16	44	F	11	T1a N0	2	0.7	Onc	Positive	0.4	Onc	Negative
17	37	F	10	T1a N0	2	1.0	Clas	Negative	0.3	Clas	Positive
18	45	F	8	T2 N0	9	2.4	Fol	Negative	0.5	Fol	Positive
19‡	49	F	56	T2 N0	2	2.4	Fol	Negative	0.6	Fol	Positive
20	53	M	6	T2 N0	2	2.4	Fol	Negative	0.2	Fol	Positive
21	49	F	20	T1a N0	2	0.2	Fol	Negative	0.1	Fol	Positive
22	76	F	1	T3 N0	2	1.2	Fol	Negative	0.9	Clas	Positive
23	53	F	79	T3 N0	2	2.0	Fol	Negative	2.0	Fol	Negative
24**	32	F	4	T1b N1b	4	2.0	Clas	Negative	0.2	Clas	Negative
25**	67	F	<1	T1b N1a	5	1.1	Onc	Negative	0.2	Fol	Negative
26	48	F	81	T2 N0	2	3.5	Fol	Negative	0.7	Fol	Negative
27	60	M	<1	T1b N0	2	1.9	Fol	Negative	0.5	Fol	Negative

The ∗ indicates that the patient experienced a recurrence (Patient 4 at 7 months postsurgery/3 months post-radioactive iodine and Patient 9 at 19 months postsurgery/16 months post-radioactive iodine). The ‡ indicates a patient who had a possible recurrence that could not be biopsied and was treated with radioiodine. The ∗∗ indicates that additional tumors were tested for these patients (Patient 24: two additional nodules, Patient 25: one additional nodule); the additional nodules were all negative. Fol = follicular variant, TC = tall cell variant, Clas = classic variant, Onc = oncocytic variant, War = Warthin-like variant.

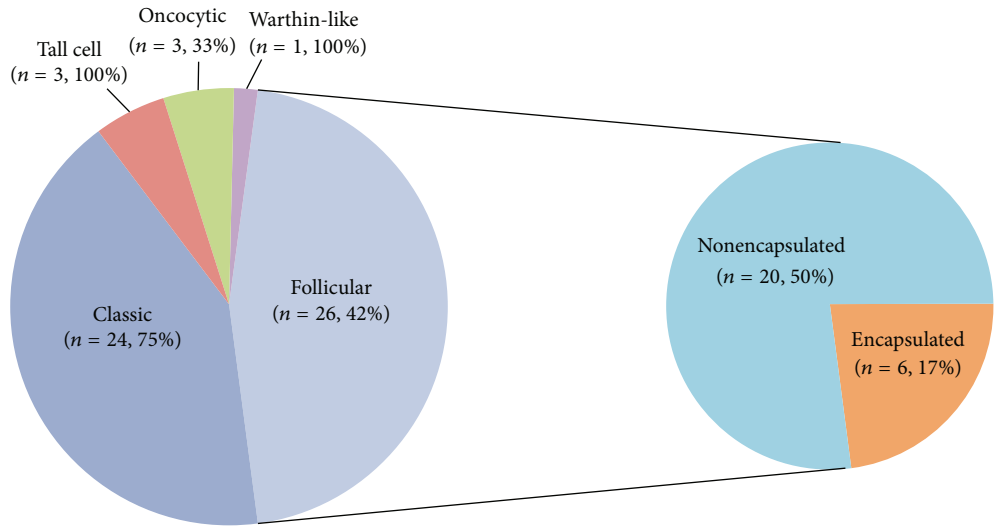

Figure 1: Histologic variants and rates of *BRAF* mutation. The percentage given after the number of cases indicates the rate of *BRAF* mutation for that particular variant. Follicular variant is broken down into encapsulated and nonencapsulated.

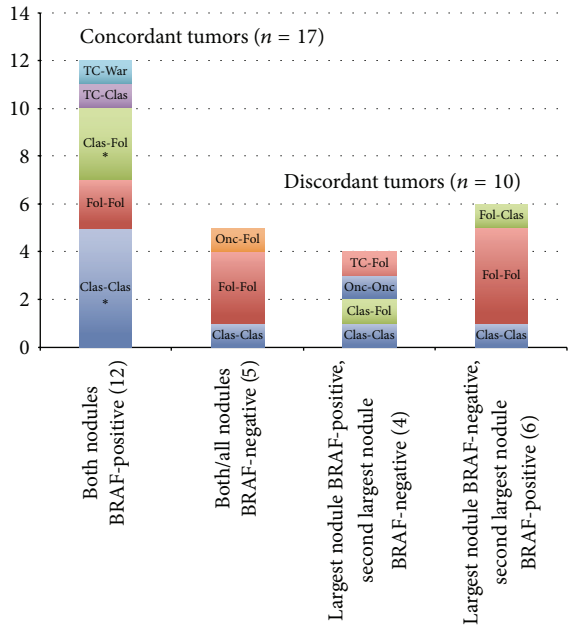

Figure 2: Breakdown of cases relative to mutation concordance and histologic variant(s) of the largest and second-largest tumors. The number in parentheses indicates the number of cases. Clas = classic variant, Fol = follicular variant, TC = tall cell variant, War = Warthin-like variant, Onc = oncocytic variant, and ∗ = one patient in this subgroup experienced a recurrence.

largest tumor and *BRAF*-positive second-largest tumor had positive lymph nodes.

None of the patients presented with or experienced distant metastases. Overall, the average amount of clinical followup was 20 months (range <1 month to 81 months). Two of the 27 patients (7.4%) had recurrence in the cervical lymph nodes, one at 7 months postsurgery/3 months post-radioactive iodine and one at 19 months postsurgery/16 months post-radioactive iodine. These two patients were *BRAF*-positive in both the largest and the second-largest tumors. None of the remaining patients had a definitive recurrence. One patient with a *BRAF*-negative largest tumor and a *BRAF*-positive second-largest tumor did have positive radioactive iodine uptake in the mediastinum after surgery, but it was unclear whether this represented ectopic thyroid tissue or recurrent disease and the area was not amenable to biopsy.

4. Discussion

In this study, we attempted to find the optimal approach for *BRAF* mutation testing in multifocal PTC. One hypothetical strategy would be to test each tumor sequentially, starting with the largest tumor and working towards the smallest until a mutation is found; however, this would require strong coordination between the surgical pathologist and molecular pathologist and would not be the most timely or cost-effective strategy, given that each tumor would be tested on a separate run. At the other extreme, another strategy would be to test all of the tumors up front, but since twelve of our patients (44%) had three or more tumors, testing every single nodule may be costly with overuse of resources. We sought an approach somewhere in between these two extremes.

Not surprisingly, all of our tall cell variants were *BRAF*-positive, which is consistent with the generally accepted idea that tall cell variant has the highest rate of *BRAF* positivity (around 80% [14]). This indicates that tumors with tall cell histology should be prioritized in any testing algorithm.

The follicular variant had the lowest rate of *BRAF*-positivity at 42%. This percentage is high relative to the generally accepted value of around 10% [14], but is in line with more recent studies that used more sensitive molecular techniques and found *BRAF*-positivity in 21% to 54% of follicular variants [13, 15–17]. Additionally, in the current

study, three of the follicular variants that were positive were in the same gland as a *BRAF*-positive classic variant (see Table 1) and therefore could have been intraglandular metastases. Walts et al. specifically excluded cases like this from their study of follicular variants and were very strict on the definition of follicular variant (requiring 95% or more of the tumor to have follicular architecture); their study had a rate of 33.3% *BRAF*-positivity (16 of 48 cases, which included both unifocal and multifocal cases) [13]. Therefore, follicular variant tumors should not be excluded from the testing algorithm, with the caveat that tumors that are completely encapsulated have a very low chance of being positive.

In this study, 10 cases (37%) had tumors with discordant *BRAF* mutation status. This is in line with other studies that have reported discordant *BRAF* mutation status in 14% to 39% of multifocal PTC cases [2, 3, 8, 10, 11]. Ideally, there would be some histologic feature to help identify which cases are likely to have discordant mutation status and therefore indicate that more than just the largest tumor should be tested. We first looked at whether discordant tumors tended to be of different histologic variants because in Park et al. tumors were of different histologic variants in 58.3% of discordant cases compared to 32.4% of concordant cases ($P = 0.047$) [8]; similar observations were made by Bansal et al. [1] and Giannini et al. [2]. We did not find this in our study, however, as discordant tumors were statistically equally likely to be of the same or different histologic variants.

Another variable we examined was whether concordant tumors were more often in the same lobe. In Bansal et al., tumors with the same mutation (*BRAF*, *RAS,* or *RET/PTC*) were statistically more likely to be in the same lobe when compared to those with different mutations (60% versus 22.2%, $P = 0.04$) [1]. Similarly, Kuhn et al. found that tumors with concordant X chromosome inactivation patterns tended to be in the same lobe and discordant tumors were in contralateral lobes [4]. However, Park et al. did not find a correlation between *BRAF* mutation concordance and laterality: 9 of 24 unilateral cases (37.5%) had mixed *BRAF* status compared to 15 of 37 bilateral cases (40.5%, $P > 0.05$) [8]. Our findings were similar to Park et al. in that tumors with concordant mutations were not more likely to be in the same lobe, and tumors with discordant mutations were not more likely to be in opposite lobes.

We next examined whether the presence of satellite nodules indicated a concordant mutation status. In theory, satellite nodules should result from intraglandular metastasis and therefore all tumors would have the same mutational status. In Bansal et al., microscopic peritumoral dissemination (which is similar to what we are calling satellite nodules) was seen at a significantly lower rate in cases with different mutations ($P = 0.029$) [1]. We found a similar trend: cases with satellite tumors did tend to have concordant mutation status, but this did not reach statistical significance. Isolated psammoma bodies, which again should indicate intraglandular metastasis, also did not correlate significantly with concordant mutation status.

Bansal et al. noted that >60% of tumors with different mutations had smooth borders, with the idea that a smooth border indicates a less aggressive tumor that would be unlikely to develop intraglandular metastasis. In other words, multiple tumors with smooth borders would more likely represent separate primaries, and tumors with irregular borders would more likely represent intraglandular metastasis [1]. We did not find any significant association between smooth borders and discordant mutation status, or irregular borders and concordant mutation status, however.

Cases with more than three tumor foci were more likely to have discordant *BRAF* status in Park et al. [8], but our study found a trend in the opposite direction: cases with more nodules tended to be concordant, but this did not reach statistical significance.

In summary, there does not seem to be a reliable way to predict which cases will have tumors with discordant *BRAF* status. However, from our limited data it does seem that testing more than two tumors may not be necessary: of the five cases where the two largest tumors were both negative, two cases had additional nodules with adequate DNA for testing, and these three additional nodules were all *BRAF*-negative. In other words, although our numbers were limited, we did not find any cases where a third-largest or fourth-largest tumor was *BRAF*-positive when the largest and second-largest tumors were *BRAF*-negative.

Importantly, six of our cases (22%) had a *BRAF* mutation in the second-largest tumor when the largest tumor was *BRAF*-negative. This is similar to Ahn et al., where thirteen out of eighty-five patients with multifocal PTC (15%) had a *BRAF* mutation in a smaller nodule when the largest was *BRAF*-negative [18]. Therefore, if only the largest tumor is tested, a substantial number of patients would be considered *BRAF*-negative even though they harbor a smaller tumor that is *BRAF*-positive.

The clinical significance of finding a *BRAF* mutation in a nondominant tumor, however, is unknown. Among our cohort, none of the six patients with a *BRAF*-negative largest tumor and *BRAF*-positive second-largest tumor presented with positive lymph nodes or had a definitive recurrence, although one patient had a small area of positivity on a radioiodine scan that was either a positive mediastinal lymph node or ectopic thyroid tissue (the area was not amenable to biopsy and the patient was given adjuvant radioiodine). Our study is too small and the followup is too short to draw further conclusions, but the two patients who experienced a definite recurrence had a *BRAF* mutation in both their largest and second-largest nodules. This finding is of interest, since Ahn et al. found that the patients who were *BRAF*-positive in all of their nodules had significantly higher rates of extrathyroidal invasion, lymph node metastases, and postoperative radioactive iodine therapy, when compared to the group with mixed mutation status. Thus, having a *BRAF* mutation in all nodules likely indicates more aggressive disease, probably because the tumors represent intraglandular spread from the same primary [18].

We note that this study had a relatively high rate of *BRAF* mutation (42% of the follicular variants, as described above, and 60% of the tumors overall), which may be due to two factors: first, *BRAF* mutation may be more frequent in multifocal disease [18, 19] and second, our *BRAF* assay has high analytic sensitivity. Recent studies have found that

BRAF mutation is most likely not present in every cell of a given tumor and that the percentage of mutated alleles may vary regionally within the tumor. Thus, an assay that can detect a smaller percentage of mutated alleles will call more tumors positive [20–24]. One excellent example of how analytic sensitivity can affect the rate of *BRAF* mutations is seen in Guerra et al., who used two different assays in their study: BigDye Terminator sequencing (PE Applied Biosystems, Foster City, CA) and pyrosequencing. By BigDye Terminator sequencing, *BRAF* mutation was identified in 62 of 168 (36.9%) cases of unifocal papillary thyroid carcinoma and by pyrosequencing, it was identified in 90 of 168 (53.6%). This resulted in differences in the clinical variables that were significantly associated with the presence of *BRAF* mutation. For example, lymph node metastasis and AJCC stage I disease had positive associations with *BRAF* mutation by BigDye Terminator sequencing ($P = 0.012$ and $P = 0.016$, resp.) but neither had significant associations by pyrosequencing. Recurrence was 2.1 times more likely in *BRAF*-positive patients by BigDye Terminator sequencing ($P = 0.040$), but there was no significant difference in recurrence by pyrosequencing [24]. Clearly, the choice of assay can affect both the rate of *BRAF* mutation and its clinical utility. This means that the results from our study may not be generalizable to labs that use a less sensitive assay.

We also note that the study cohort contained a high number of male patients (10 out of 27, or 37%). One possibility for this is that the percentage of men might be higher among patients with multifocal disease as was found in Huang et al. [25], who studied 648 patients with PTC in China. In their study, 49 of 168 patients with multifocal disease were male (29%) compared to 89 of 480 patients with unifocal disease (19%, $P = 0.004$). However, other studies have found nearly equal percentages of males in both multifocal and unifocal cases, ranging from 16% to 24% [11, 26, 27]. Therefore, it is more likely that the high number of male patients reflects some bias in the types of patients referred to the study surgeon. Since the percentage of cases with discordant *BRAF* mutations is in line with previous studies, as discussed above, it is unlikely that this bias had a great effect on our results.

5. Conclusions

Patients with multifocal PTC whose largest tumor is *BRAF*-negative can have smaller tumors that are *BRAF*-positive. Therefore, molecular testing of more than just the dominant nodule should be considered, especially if a smaller tumor has tall cell features. Future larger studies are warranted to establish whether finding a *BRAF* mutation in a smaller tumor correlates with more aggressive disease.

Conflict of Interests

The authors declare that there is no conflict of interests regarding the publication of this paper.

Acknowledgments

The authors would like to thank Tulane University's Department of Pathology and Laboratory Medicine for funding this study, and Darl D. Flake II, MS, for additional statistical calculations. The abstract was previously presented as a poster at the American Thyroid Association's annual meeting in 2014 (no. 2036822).

References

[1] M. Bansal, M. Gandhi, R. L. Ferris et al., "Molecular and histopathologic characteristics of multifocal papillary thyroid carcinoma," *The American Journal of Surgical Pathology*, vol. 37, no. 10, pp. 1586–1591, 2013.

[2] R. Giannini, C. Ugolini, C. Lupi et al., "The heterogeneous distribution of BRAF mutation supports the independent clonal origin of distinct tumor foci in multifocal papillary thyroid carcinoma," *Journal of Clinical Endocrinology and Metabolism*, vol. 92, no. 9, pp. 3511–3516, 2007.

[3] L. Jovanovic, B. Delahunt, B. McIver, N. L. Eberhardt, and S. K. G. Grebe, "Most multifocal papillary thyroid carcinomas acquire genetic and morphotype diversity through subclonal evolution following the intra-glandular spread of the initial neoplastic clone," *Journal of Pathology*, vol. 215, no. 2, pp. 145–154, 2008.

[4] E. Kuhn, L. Teller, S. Piana, J. Rosai, and M. J. Merino, "Different clonal origin of bilateral papillary thyroid carcinoma, with a review of the literature," *Endocrine Pathology*, vol. 23, no. 2, pp. 101–107, 2012.

[5] X. Lin, S. D. Finkelstein, B. Zhu, and J. F. Silverman, "Molecular analysis of multifocal papillary thyroid carcinoma," *Journal of Molecular Endocrinology*, vol. 41, no. 3-4, pp. 195–203, 2008.

[6] R. P. McCarthy, M. Wang, T. D. Jones, R. W. Strate, and L. Cheng, "Molecular evidence for the same clonal origin of multifocal papillary thyroid carcinomas," *Clinical Cancer Research*, vol. 12, no. 8, pp. 2414–2418, 2006.

[7] S. Moniz, A. L. Catarino, A. R. Marques, B. Cavaco, L. Sobrinho, and V. Leite, "Clonal origin of non-medullary thyroid tumours assessed by non-random X-chromosome inactivation," *European Journal of Endocrinology*, vol. 146, no. 1, pp. 27–33, 2002.

[8] S. Y. Park, Y. J. Park, Y. J. Lee et al., "Analysis of differential BRAF V600E mutational status in multifocal papillary thyroid carcinoma: evidence of independent clonal origin in distinct tumor foci," *Cancer*, vol. 107, no. 8, pp. 1831–1838, 2006.

[9] T. M. Shattuck, W. H. Westra, P. W. Ladenson, and A. Arnold, "Independent clonal origins of distinct tumor foci in multifocal papillary thyroid carcinoma," *The New England Journal of Medicine*, vol. 352, no. 23, pp. 2406–2412, 2005.

[10] W. Wang, H. Wang, X. Teng et al., "Clonal analysis of bilateral, recurrent, and metastatic papillary thyroid carcinomas," *Human Pathology*, vol. 41, no. 9, pp. 1299–1309, 2010.

[11] X. Zheng, T. Xia, L. Lin et al., "BRAF V600E status and clinical characteristics in solitary and multiple papillary thyroid carcinoma: experience of 512 cases at a clinical center in China," *World Journal of Surgical Oncology*, vol. 10, article 104, 2012.

[12] M. M. Xing, A. S. Alzahrani, K. A. Carson et al., "Association between BRAF V600E mutation and mortality in patients with papillary thyroid cancer," *Journal of the American Medical Association*, vol. 309, no. 14, pp. 1493–1501, 2013.

[13] A. E. Walts, J. M. Mirocha, and S. Bose, "Follicular variant of papillary thyroid carcinoma (FVPTC): histological features, BRAF V600E mutation, and lymph node status," *Journal of Cancer Research and Clinical Oncology*, 2015.

[14] Y. E. Nikiforov, "Molecular diagnostics of thyroid tumors," *Archives of Pathology and Laboratory Medicine*, vol. 135, no. 5, pp. 569–577, 2011.

[15] Y. Y. Jung, J. H. Yoo, E. S. Park et al., "Clinicopathologic correlations of the $BRAF^{V600E}$ mutation, BRAF V600E immunohistochemistry, and *BRAF* RNA *in situ* hybridization in papillary thyroid carcinoma," *Pathology—Research and Practice*, vol. 211, pp. 162–170, 2015.

[16] R. K. Virk, A. L. van Dyke, A. Finkelstein et al., "$BRAF^{V600E}$ mutation in papillary thyroid microcarcinoma: a genotype-phenotype correlation," *Modern Pathology*, vol. 26, no. 1, pp. 62–70, 2013.

[17] H. S. Min, C. Lee, and K. C. Jung, "Correlation of immunohistochemical markers and BRAF mutation status with histological variants of papillary thyroid carcinoma in the Korean population," *Journal of Korean Medical Science*, vol. 28, no. 4, pp. 534–541, 2013.

[18] H. Y. Ahn, Y. J. Chung, B. S. Kim et al., "Clinical significance of the BRAF V600E mutation in multifocal papillary thyroid carcinoma in Korea," *Surgery*, vol. 155, no. 4, pp. 689–695, 2014.

[19] C. Li, K. C. Lee, E. B. Schneider, and M. A. Zeiger, "BRAF V600E mutation and its association with clinicopathological features of papillary thyroid cancer: a meta-analysis," *Journal of Clinical Endocrinology and Metabolism*, vol. 97, no. 12, pp. 4559–4570, 2012.

[20] S. P. Cheng, Y. C. Hsu, C. L. Liu et al., "Significance of allelic percentage of *BRAF* c.1799T > A (V600E) mutation in papillary thyroid carcinoma," *Annals of Surgical Oncology*, vol. 21, no. 4, pp. 619–626, 2014.

[21] D. de Biase, V. Cesari, M. Visani et al., "High-sensitivity BRAF mutation analysis: BRAF V600E is acquired early during tumor development but is heterogeneously distributed in a subset of papillary thyroid carcinomas," *The Journal of Clinical Endocrinology & Metabolism*, vol. 99, no. 8, pp. E1530–E1538, 2014.

[22] G. Gandolfi, V. Sancisi, F. Torricelli et al., "Allele percentage of the *BRAF* V600E mutation in papillary thyroid carcinomas and corresponding lymph node metastases: no evidence for a role in tumor progression," *The Journal of Clinical Endocrinology and Metabolism*, vol. 98, no. 5, pp. E934–E942, 2013.

[23] A. Guerra, M. R. Sapio, V. Marotta et al., "The primary occurrence of $BRAF^{V600E}$ is a rare clonal event in papillary thyroid carcinoma," *The Journal of Clinical Endocrinology & Metabolism*, vol. 97, no. 2, pp. 517–524, 2012.

[24] A. Guerra, L. Fugazzola, V. Marotta et al., "A high percentage of BRAFV600E alleles in papillary thyroid carcinoma predicts a poorer outcome," *Journal of Clinical Endocrinology and Metabolism*, vol. 97, no. 7, pp. 2333–2340, 2012.

[25] G. Huang, X. Tian, Y. Li, and F. Ji, "Clinical characteristics and surgical resection of multifocal papillary thyroid carcinoma: 168 cases," *International Journal of Clinical and Experimental Medicine*, vol. 7, no. 12, pp. 5802–5807, 2014.

[26] H. Mazeh, Y. Samet, D. Hochstein et al., "Multifocality in well-differentiated thyroid carcinomas calls for total thyroidectomy," *The American Journal of Surgery*, vol. 201, no. 6, pp. 770–775, 2011.

[27] K.-J. Kim, S.-M. Kim, Y. S. Lee, W. Y. Chung, H.-S. Chang, and C. S. Park, "Prognostic significance of tumor multifocality in papillary thyroid carcinoma and its relationship with primary tumor size: a retrospective study of 2,309 consecutive patients," *Annals of Surgical Oncology*, vol. 22, no. 1, pp. 125–131, 2015.

Hindawi Publishing Corporation
BioMed Research International
Volume 2015, Article ID 421747, 7 pages
http://dx.doi.org/10.1155/2015/421747

Research Article

LINE-1 Methylation Patterns as a Predictor of Postmolar Gestational Trophoblastic Neoplasia

Ruangsak Lertkhachonsuk,[1] Krissada Paiwattananupant,[1] Patou Tantbirojn,[2] Prakasit Rattanatanyong,[3] and Apiwat Mutirangura[3]

[1]*Division of Gynecologic Oncology, Department of Obstetrics and Gynecology, Faculty of Medicine, Chulalongkorn University, King Chulalongkorn Memorial Hospital, Bangkok 10330, Thailand*
[2]*Division of Gynecologic Pathology, Department of Obstetrics and Gynecology, Faculty of Medicine, Chulalongkorn University, King Chulalongkorn Memorial Hospital, Bangkok 10330, Thailand*
[3]*Center of Excellence in Molecular Genetic of Cancer and Human Disease, Department of Anatomy, Faculty of Medicine, Chulalongkorn University, King Chulalongkorn Memorial Hospital, Bangkok 10330, Thailand*

Correspondence should be addressed to Ruangsak Lertkhachonsuk; drruang9@yahoo.com

Received 21 January 2015; Revised 4 March 2015; Accepted 29 March 2015

Academic Editor: Murat Gokden

Objective. To study the potential of long interspersed element-1 (LINE-1) methylation change in the prediction of postmolar gestational trophoblastic neoplasia (GTN). *Methods*. The LINE-1 methylation pattern from first trimester placenta, hydatidiform mole, and malignant trophoblast specimens were compared. Then, hydatidiform mole patients from 11999 to 2010 were classified into the following 2 groups: a remission group and a group that developed postmolar GTN. Specimens were prepared for a methylation study. The methylation levels and percentages of LINE-1 loci were evaluated for their sensitivity, specificity, and accuracy for the prediction of postmolar GTN. *Results*. First, 12 placentas, 38 moles, and 19 malignant trophoblast specimens were compared. The hydatidiform mole group had the highest LINE-1 methylation level ($p = 0.003$) and the $^{u}C^{u}C$ of LINE-1 increased in the malignant trophoblast group ($p \leq 0.001$). One hundred forty-five hydatidiform mole patients were classified as 103 remission and 42 postmolar GTN patients. The $\%^{m}C^{u}C$ and $\%^{u}C^{m}C$ of LINE-1 showed the lowest p value for distinguishing between the two groups ($p < 0.001$). The combination of the pretreatment β-hCG level (≥100,000 mIU/mL) with the $\%^{m}C^{u}C$ and $\%^{u}C^{m}C$, sensitivity, specificity, PPV, NPV, and accuracy modified the levels to 60.0%, 92.2%, 77.4%, 83.8%, and 82.3%, respectively. *Conclusions*. A reduction in the partial methylation of LINE-1 occurs early before the clinical appearance of malignant transformation. The $\%^{m}C^{u}C$ and $\%^{u}C^{m}C$ of LINE-1s may be promising markers for monitoring hydatidiform moles before progression to GTN.

1. Introduction

Hydatidiform mole, a genetic imprinting disease [1–3], is caused by fertilization abnormalities such as androgenetic (monospermic and dispermic) diploid or biparental triploid [4]. The incidence of this disease varies around the world. However, Southeast Asia still has a higher incidence than Western countries [5]. Most hydatidiform mole patients reach remission after primary treatment; however, 8–30% [6, 7] of patients develop postmolar gestational trophoblastic neoplasm (GTN). A high-risk hydatidiform mole is characterized by a human chorionic gonadotropin level (hCG) >100,000 mIU/mL, excessive uterine enlargement, and theca lutein cysts that are >6 cm in diameter. However, these clinical features are only able to predict 40% of postmolar GTN [8]. Currently, there is still no appropriate method for predicting malignant changes in hydatidiform moles.

Although hydatidiform moles can now be diagnosed earlier than in previous decades [9], the incidence of postmolar GTN is still unchanged from these earlier times. This suggests

that the malignant potential of hydatidiform moles begin when the moles form. Thus, genetic factors may play a crucial role in the malignant transformation of hydatidiform moles. Investigation of molecular markers in hydatidiform moles may aid in the early prediction of postmolar GTN. Epigenetic change in cancer is an event that causes abnormal gene expression and promotes carcinogenesis, even when the DNA sequences do not change [10–14]. DNA methylation is one of the mechanisms in which methylated cytosines precede guanine areas, which are called CpG island. Two common methylation changes in cancer are promoter hypermethylation and genome-wide hypomethylation at interspersed repetitive sequences (IRS) or transposon-derived sequences. The role of promoter hypermethylation is to inhibit tumor suppressor gene functions. Loss of IRS methylation leads to several consequences including genomic instability and genome-wide gene expression changes [15–18].

The methylation status of long interspersed element-1 (LINE-1) in cancer has been reported in many cancers [15]. LINE-1 is an interspersed repetitive sequence in the human genome, and elements of methylation have been used to represent genome-wide methylation [18]. Recent evidence has demonstrated LINE-1 hypomethylation in several cancers including head and neck cancer, breast cancer, bladder cancer, hepatic cancer, lung cancer, prostate cancer, colon cancer, and gynecologic cancer [8, 19–23]. In most cancers, LINE-1 methylation levels are lower than in normal tissues. Interestingly, alterations in DNA methylation are not randomly distributed in partial hydatidiform moles (PHMs). Perrin et al. reported global hypomethylation, LINE-1 hypermethylation, and unchanged methylation in PHMs [24]. We aimed to explore the IRS methylation levels and patterns of GTN as well as investigate the role of LINE-1 methylation in the prediction of postmolar GTN in hydatidiform mole patients.

For this reason, we evaluated the methylation statuses of IRS using Combined Bisulfite Restriction Analysis (COBRA). Unlike other techniques, COBRA differentiates IRS sequences into the following 4 methylation-status categories: hypermethylated, hypomethylated, and 2 forms of partially methylated loci. COBRA also provides information on the methylation levels [25, 26]. These subclassifications improved the sensitivity of the test in early cancer detection over other techniques, revealing only the overall methylation levels such as pyrosequencing. Recently, we reported that the LINE-1 hypomethylated loci distinguish tumor DNA more efficiently than the overall methylation levels [27, 28]. Moreover, while there were no LINE-1 methylation level changes in the oral epithelium of smokers, LINE-1s of partially methylated loci were different [29]. Therefore, the alteration in the percentage of the LINE-1 partially methylated loci may indicate early genome-wide hypomethylation in the multistep process of carcinogenesis.

2. Materials and Methods

This study was approved by the institutional review board of the Faculty of Medicine, Chulalongkorn University, Bangkok, Thailand. Pathological specimens were retrieved between 1999 and 2010. Patients' demographic and clinical data were reviewed from medical records.

2.1. Collection of Specimens. First, we studied the differences in the LINE-1 methylation levels among first trimester placenta ($n = 12$), hydatidiform moles ($n = 38$), and malignant trophoblasts (invasive mole and choriocarcinoma) ($n = 19$). Formalin-fixed, paraffin-embedded (FFPE) specimens were randomly collected from the Gynecologic Pathology Unit, King Chulalongkorn Memorial Hospital. Then, patients with hydatidiform moles who had been treated between 1999 and 2010 were recruited, and we reviewed these patients' medical records. The demographic data of the patients, including age, obstetrics history, histology, serum hCG level, and treatment outcomes, were collected. Postmolar GTN was defined by the FIGO criteria [30]. FFPE specimens from these patients were processed to analyze the methylation levels and patterns to be used as diagnostic tool for the malignant transformation of hydatidiform moles.

One gynecologic pathologist reviewed the hematoxylin and eosin-stained slides for all the sections, verified the quality of tissue, and mapped the studied areas. The expression of p57, observed by immunohistochemistry, was determined to differentiate between complete and partial mole. Unavailable paraffin-embedded specimens and degenerated tissue were excluded from this study. Paraffin-embedded specimens were collected and prepared at a 5 μm thickness on the slides. The slides were deparaffinized with xylene solution and absolute alcohol. Microdissection was then performed by the laser caper technique. Lysis buffer was added to mix the microdissected tissues in micropipette tubes. DNA was then separated from other proteins by using phenol-chloroform-isoamyl alcohol.

2.2. DNA Extraction and COBRA LINE-1 PCR. DNA extraction and PCR were performed by the COBRA LINE-1 protocol [20, 31]. Briefly, 22 M NaOH was used for the denaturing of genomic DNA at 37°C for 10 minutes. DNA was then treated with 20 μL of 10 mM hydroquinone and 520 μL of 3 M sodium bisulfite at 50°C for 16–20 hours to convert the unmethylated cytosine to uracil. DNA was purified and incubated in 0.33 M NaOH at 25°C for 3 min, ethanol precipitated, washed with 70% ethanol, and resuspended in 20 μL of H_2O. Two microliters of bisulfite DNA was annealed with two added primers for COBRA LINE-1, 5-CCGTAAGGGGTTAGGGAGTTTTT-3 and 5-RTAAAACCCTCCRAACCAAATATAAA-3, at 50°C. Amplification of PCR was conducted for 40 cycles. LINE-1 amplicons (160 bp) were digested in 10 μL reaction volumes with 8 U of *TasI* in 1x *TaqI* buffer (MBI Fermentas, Burlington, ON, Canada) at 65°C overnight and were then electrophoresed in 8% nondenaturing polyacrylamide gel. There were 4 bands on the electrophoresis of LINE-1: 160 bp ($^{m}C^{u}C$), 98 bp ($^{u}C^{u}C$), 80 bp (^{m}C), and 62 bp (^{u}C) (Figure 1). The intensities of the DNA fragments were measured twice by PhosphorImager using

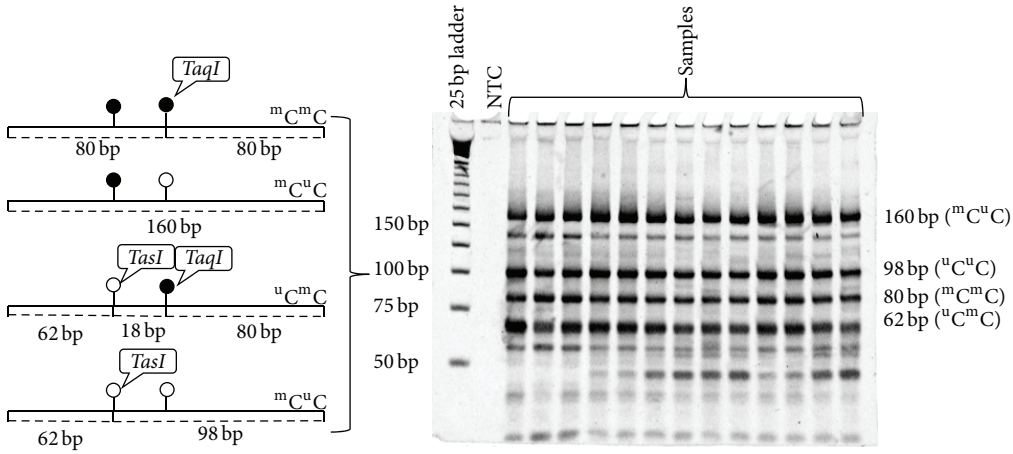

Figure 1: Methylation patterns of the LINE-1 methylation patterns of COBRA LINE-1. The following four patterns of methylated CpGs were demonstrated: hypermethylation ($^{m}C^{m}C$), hypomethylation ($^{u}C^{u}C$), and two forms of partial methylation ($^{m}C^{u}C$ and $^{u}C^{m}C$).

Image-Quant software (Molecular Dynamics, Sunnyvale, CA).

Recently, Pobsook et al. [25] found that the 160 bp uncut band is one of the partially methylated bands. Therefore, this study improved the LINE-1 methylation formula for COBRA LINE-1. The percentage of LINE-1 hypomethylated loci ($^{u}C^{u}C$) was calculated by LINE-1 formulas. The intensity of each band was divided by the length (bp) of the double-stranded DNA before the calculations were performed (A = %160/160, B = %98/94, C = %80/78, and D = %62/62).

The LINE-1 formula was calculated as the $\%^{m}C$ (total methylation) = $100 \times (C + A)/(C + A + A + B + D)$, % number of $^{m}C^{m}C$ (hypermethylated loci) = $100 \times ((C - D + B)/2/(C - D + B/2) + D + A)$, %PM (partial methylation) = $100 \times (A + D - B)/((C - D + B)/2 + A + D)$, $\%^{m}C^{u}C$ (partial methylated loci) = $100 \times (A/((C - D + B)/2) + D + A)$, $\%^{u}C^{m}C$ (partial methylated loci) = $100 \times ((D - B)/((C - D + B)/2) + D + A)$, and $\%^{u}C^{u}C$ (hypomethylated loci) = $100 \times (B/((C - D + B)/2) + D + A)$. The same preparations of DNA from *HeLa*, *Daudi*, and *Jurkat* cell lines were used as positive controls in every experiment to adjust for interassay variation.

2.3. Statistical Analysis. The mean difference in the percentage of LINE-1 among the normal first trimester placenta, hydatidiform mole, and cancer group (invasive mole and choriocarcinoma) was analyzed using a one-way ANOVA. In the latter portion of the study, an ROC curve was created according to each group's percentage of methylation (^{m}C), percentage of partially methylated loci ($^{m}C^{u}C$, $^{u}C^{m}C$), and percentage of the hypomethylated loci ($^{u}C^{u}C$) to estimate the respective cut-off points. The sensitivity, specificity, positive predictive value (PPV), negative predictive value (NPV), and accuracy were calculated. The mean differences in the percentage levels between the remission group and malignant transformation group were analyzed by independent samples t-test. Statistical analysis was performed by SPSS software for Windows version 17.0 (SPSS Inc., Chicago, IL), and statistical significance was set at p values of less than 0.05.

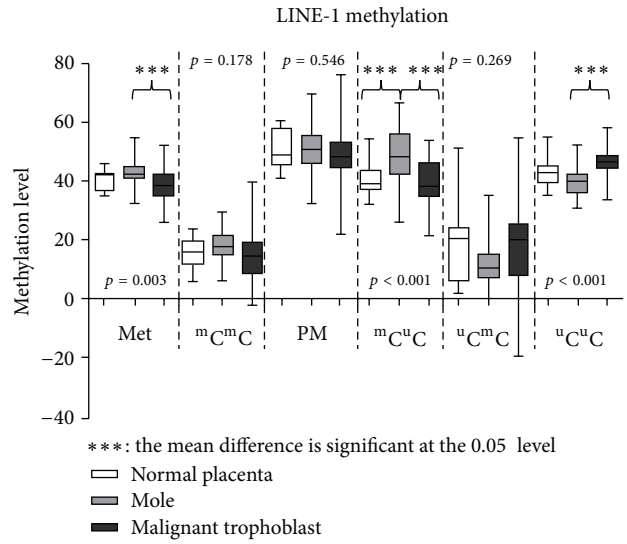

Figure 2: LINE-1 methylation in normal placenta, hydatidiform mole, and malignant trophoblast samples. Hydatidiform moles had the highest value in the mean total methylation ($\%^{m}C$) ($p = 0.003$) and hypermethylation ($\%^{m}C^{m}C$) ($p = 0.178$). Malignant trophoblasts had significantly higher mean hypomethylation ($\%^{u}C^{u}C$) ($p < 0.001$).

3. Results

3.1. LINE-1 Methylation in 3 Different Trophoblastic Tissues (First Trimester Placenta, Hydatidiform Moles, and Malignant Trophoblast). The differences in the LINE-1 methylation levels among the first trimester placenta group ($n = 12$), hydatidiform mole group ($n = 38$), and malignant trophoblast group (invasive mole and choriocarcinoma) ($n = 19$) are shown in Figure 2. The hydatidiform mole group had the highest value in the mean $\%^{m}C$ (LINE-1 43.0% ± 3.8%, $p = 0.003$) and $\%^{m}C^{m}C$ (LINE-1 18.1% ± 5.1%, $p = 0.178$). The malignant trophoblast group had a significantly higher

Table 1: Association of clinicopathologic variables and LINE-1 methylation level.

LINE-1 level (mean ± SD)	Parameters					
	^{m}C	$^{m}C^{m}C$	PM	$^{m}C^{u}C$	$^{u}C^{m}C$	$^{u}C^{u}C$
Age (years)						
≤40	40.6 ± 4.0	17.2 ± 6.3	48.5 ± 8.1	42.1 ± 10.0	18.7 ± 14.7	45.5 ± 5.9
>40	39.7 ± 4.7	18.7 ± 5.4	44.2 ± 9.4	45.0 ± 7.8	9.1 ± 7.9	49.0 ± 7.9
p value	0.484	0.296	0.086	0.169	<0.001	0.094
Pretreatment βhCG level (mIU/mL)*						
<100,000	40.9 ± 4.1	16.1 ± 5.9	50.7 ± 7.7	43.3 ± 10.8	19.6 ± 14.8	44.1 ± 5.3
≥100,000	39.9 ± 3.7	17.7 ± 6.4	46.5 ± 8.9	42.1 ± 9.3	16.4 ± 14.7	47.2 ± 6.4
p value	0.173	0.133	0.005	0.544	0.234	0.004
Pathological diagnosis						
Complete hydatidiform mole	40.5 ± 4.0	17.5 ± 6.2	47.7 ± 8.1	43.0 ± 9.5	16.7 ± 13.7	46.0 ± 6.1
Partial hydatidiform mole	40.6 ± 4.8	16.5 ± 6.6	49.6 ± 10.3	38.7 ± 11.4	23.0 ± 17.8	45.4 ± 7.3
p value	0.939	0.565	0.463	0.137	0.158	0.748
Metastasis						
No metastasis	40.5 ± 4.2	20.0 ± 8.9	44.6 ± 10.7	47.0 ± 7.4	9.9 ± 16.1	47.3 ± 7.4
Metastasis	39.5 ± 2.5	18.9 ± 5.3	43.8 ± 7.2	46.2 ± 4.5	9.3 ± 6.0	48.8 ± 4.6
p value	0.304	0.578	0.806	0.660	0.860	0.415

PM = percentage of LINE-1 partial methylation.
$^{m}C^{u}C$, $^{u}C^{m}C$ = percentage of LINE-1 partially methylated loci.
$^{m}C^{m}C$ = percentage of LINE-1 hypermethylated loci number.
$^{u}C^{u}C$ = percentage of LINE-1 hypomethylated loci number.
^{m}C = percentage of LINE-1 methylation.
*Incomplete data for 15 patients.

%$^{u}C^{u}C$ than the hydatidiform mole group (LINE-1 47.2% ± 6.7% versus 40.0% ± 4.7%, $p < 0.001$).

3.2. LINE-1 Methylation in the Hydatidiform Mole, Comparing the Remission and Postmolar GTN Groups. In the study period, 145 hydatidiform mole patients were classified as 103 patients in the remission group and 42 patients in the postmolar GTN group. The ages in most cases were ≤40 years (128 cases, 88.30%). Pretreatment hCG levels over 100,000 mIU/mL were found in 82 cases (63.10%). Most (86.90%) cases were diagnosed with a complete hydatidiform mole (CHM). The incidence rates of malignant transformation were 33.33% and 5.27% for CHM and PHM cases, respectively. The mean age in the postmolar GTN group was older than the remission group (31.5 versus 27.8, $p = 0.04$). All postmolar GTN cases reached remission. Among these, 35 cases (87.50%) achieved successful treatment with single-agent chemotherapy. According to LINE-1 methylation, no significant difference was found with regard to patient age, pathological diagnosis, and metastasis. Only the pretreatment βhCG ≥ 100,000 mIU/mL group had a significantly higher %$^{u}C^{u}C$ of LINE-1 than the pretreatment βhCG < 100,000 mIU/mL (47.2% ± 6.4% versus 44.1% ± 5.3%, $p = 0.004$) and a lower %PM (46.5% ± 8.9% versus 50.7% ± 7.7%, $p = 0.005$). The association of clinicopathologic variables and LINE-1 methylation level were demonstrated in Table 1.

When focused on the LINE-1 methylation levels between the remission hydatidiform mole and postmolar GTN, there were significant differences in these 2 groups with regard to the %PM (LINE-1 49.4% ± 7.5% versus 44.4% ± 9.5%, $p = 0.003$), %$^{m}C^{m}C$ (LINE-1 16.4% ± 5.1% versus 19.8% ± 7.8%, $p = 0.010$), and %$^{u}C^{u}C$ (LINE-1 45.2% ± 5.9% versus 47.7% ± 6.5%, $p = 0.036$). Furthermore, we found significant differences in the %$^{m}C^{u}C$ (40.7% ± 10.4% versus 46.6% ± 6.6%, $p < 0.001$) and %$^{u}C^{m}C$ (20.7% ± 13.6% versus 9.9% ± 13.5%, $p < 0.001$) in LINE-1 (Figure 3).

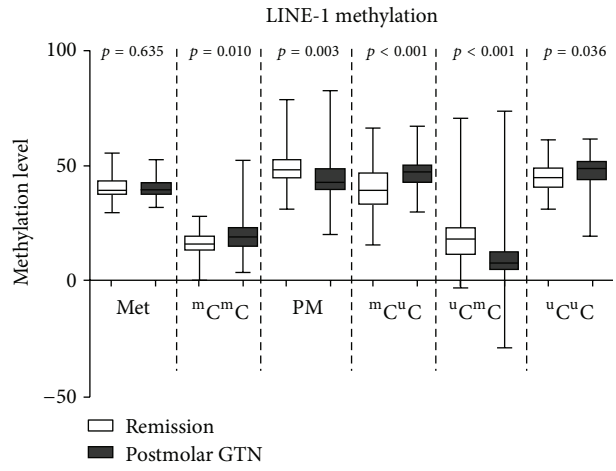

Figure 3: LINE-1 methylation patterns in the remission and postmolar GTN groups. The postmolar GTN group demonstrated a higher % hypermethylation ($^{m}C^{m}C$) (16.4% versus 19.8%, $p = 0.010$), % hypomethylation ($^{u}C^{u}C$) (45.2% versus 47.7%, $p = 0.036$), and %$^{u}C^{m}C$ (20.7% versus 9.9%, $p < 0.001$). However, the remission group showed higher % partial methylation (49.4% versus 44.4%, $p = 0.003$) and %$^{m}C^{u}C$ (40.7% versus 46.6%, $p < 0.001$).

Table 2: Diagnostic power of the methylation levels combined with βhCG.

Diagnostic tools	PM	$^{m}C^{u}C$	$^{u}C^{m}C$	$^{m}C^{u}C + {}^{u}C^{m}C$	$^{m}C^{u}C + {}^{u}C^{m}C + \beta$hCG*
Sensitivity	60.9%	88.1%	71.1%	69.0%	60.0%
Specificity	84.5%	55.3%	81.6%	85.4%	92.2%
PPV	64.4%	44.5%	61.2%	65.9%	77.4%
NPV	87.0%	91.9%	87.5%	87.1%	83.8%
Accuracy	80.0%	64.8%	78.6%	80.7%	82.3%

βhCG-pretreatment βhCG: positive if ≥100,000 IU/mL.
PM-partial methylation: positive if ≤44.0%, $^{m}C^{u}C$-partially methylated loci: positive if ≥40.9%, $^{u}C^{m}C$-partially methylated loci: positive if ≤10.7%, and *incomplete data in 15 patients.

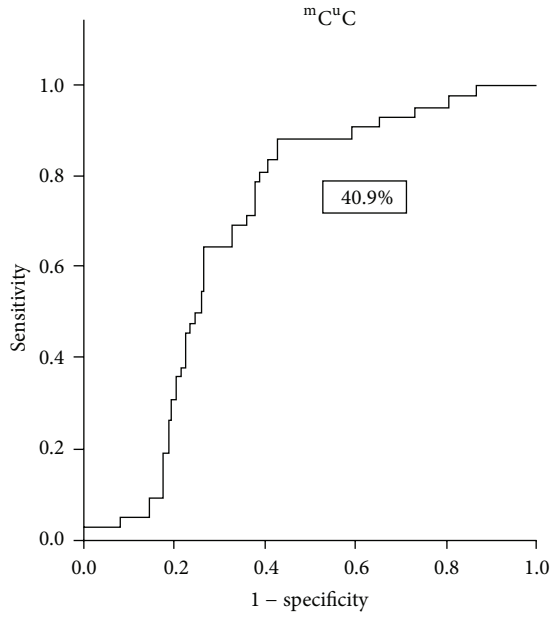

Figure 4: The ROC curve demonstrates $\%^{m}C^{u}C$ in LINE-1 if defined to positively test at ≥40.9%.

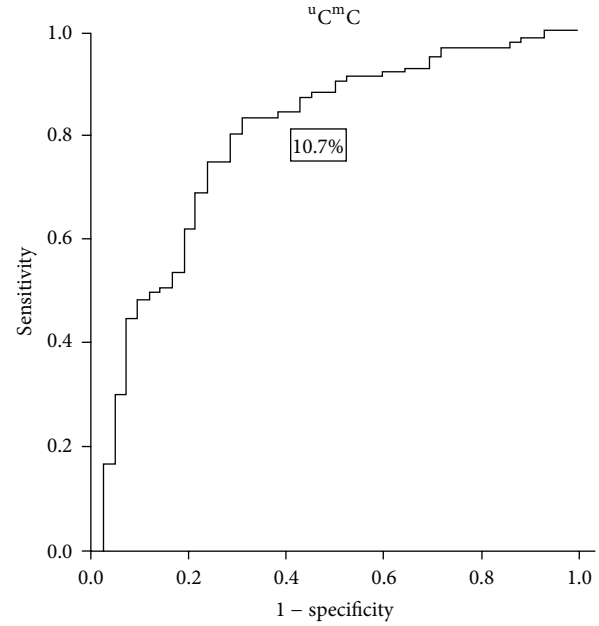

Figure 5: The ROC curve demonstrates the $\%^{u}C^{m}C$ in LINE-1 with cut-off level ≤10.7%.

The ROC curve of the %PM, $\%^{m}C^{u}C$, and $^{u}C^{m}C$ in LINE-1 proved to be useful as a diagnostic tool. If the $\%^{m}C^{u}C$ in LINE-1 was defined to positively test at ≥40.9%, the sensitivity, specificity, PPV, NPV, and accuracy were 88.1%, 55.3%, 44.5%, 91.9%, and 64.8%, respectively (Figure 4). When the defined criterion of the $\%^{u}C^{m}C$ in LINE-1 was ≤10.7%, the sensitivity, specificity, PPV, NPV, and accuracy were 71.1%, 81.6%, 61.2%, 87.5%, and 78.6%, respectively (Figure 5). When the diagnosis was defined by both $\%^{m}C^{u}C$ and $\%^{u}C^{m}C$ as positive, the results were 69.0%, 85.4%, 65.9%, 87.1%, and 80.7% for the sensitivity, specificity, PPV, NPV, and accuracy, respectively. Furthermore, pretreatment with βhCG ≥ 100,000 mIU/mL had a significant difference in this study when the $\%^{m}C^{u}C$ and $\%^{u}C^{m}C$ were combined as a diagnostic tool plotted in an ROC curve. To be considered as a positive test, all pretreatment βhCG ≥ 100,000 mIU/mL and both $\%^{m}C^{u}C$ and $\%^{u}C^{m}C$ conditions had the same criteria. The sensitivity, specificity, PPV, NPV, and accuracy were then modified to 60.0%, 92.2%, 77.4%, 83.8%, and 82.3%, respectively (Table 2).

4. Discussion

Hydatidiform moles, particularly complete hydatidiform moles, have a risk of subsequent development of postmolar GTN. The mechanisms of this process are unknown. Many studies have demonstrated that an epigenetic mechanism may play a role in the malignant transformation of hydatidiform moles [6, 32]. Xue et al. [6] reported a study of 54 hydatidiform moles, 5 choriocarcinomas, and 10 first trimester placenta samples. Both hydatidiform mole and choriocarcinoma cases showed hypermethylation of the p16 gene, indicating that aberrant CpG island methylation is a frequent and likely disease-restricted occurrence in GTD. Li et al. [32] demonstrated hypermethylation of the SOX2 gene in 31/55 of hydatidiform mole cases and 4/4 of choriocarcinoma cases. Chen et al. [33] showed that both PHM and CHM have PTEN hypermethylation. Perrin et al. [24] also found LINE-1 hypermethylation in PHM. This study revealed results that LINE-1 hypomethylated loci ($^{u}C^{u}C$) levels were

higher in choriocarcinoma and invasive moles, which was comparable with previous studies [8, 19–23].

In addition to genomic DNA mutation, amplifications, and deletions, DNA methylation also plays an important role in the process of carcinogenesis [34–36]. LINE-1 hypomethylation is a common epigenetic process in many cancer cells [21, 22, 37, 38]. The mechanisms of LINE-1 hypomethylation induce carcinogenesis, influence gene expression over the entire genome, and promote genomic instability. Hypomethylated intragenic LINE-1s are nuclear siRNA mediated cis-regulatory elements that can repress genes. This epigenetic regulation of retrotransposons likely influences many aspects of genomic biology [16]. In this study, we divided the partially methylated loci into two classes: $^{m}C^{u}C$ and $^{u}C^{m}C$. The LINE-1 hypomethylation levels corresponded to significantly higher in cancer cells than in normal placenta and hydatidiform mole samples. The partially methylated loci numbers of $^{m}C^{u}C$ had significantly higher in hydatidiform moles than the normal placenta and malignant trophoblast samples. These findings suggest that methylation may play a role in multistep carcinogenesis. Interestingly, when we compared the LINE-1 expression between the remission hydatidiform mole group and postmolar GTN group, the percentage of LINE-1 overall partial methylation (PM) in the remission group was higher than the postmolar GTN group. However, there was a significantly higher $^{m}C^{u}C$ percentage of LINE-1 in the postmolar group. In contrast, the $^{u}C^{m}C$ percentage of LINE-1 was significantly higher in the remission group (Figure 2). Therefore, the loss of LINE-1 methylation in malignancy appears to be a multistep pattern.

Because prophylaxis chemotherapy showed a positive outcome for high-risk hydatidiform mole [39, 40], identifying patients with a higher risk of developing postmolar GTN is necessary. However, clinical indices were only 40–50% accurate [39, 40]. Therefore, more than half of these patients experienced toxicity from chemotherapy without any benefits. In the current study, we set up the ROC of the $\%^{m}C^{u}C$ and $\%^{u}C^{m}C$ to predict whether postmolar GTN would occur. Using a $\%^{m}C^{u}C$ level ≥40.9% and $\%^{u}C^{m}C$ level ≤10.7% combined with a pretreatment βhCG level (considering the pretreatment hCG level ≥100,000 mIU/mL as positive) has promising diagnostic power (sensitivity 60.0%, specificity 92.2%, PPV 77.4%, NPV 83.8%, and accuracy 82.3%). This diagnostic test may allow for the early detection of postmolar GTN and improve the quality of treatment.

In conclusion, a high level of $\%^{m}C^{u}C$ and a low level of $\%^{u}C^{m}C$ in LINE-1 were found in the postmolar GTN group. These findings occur early, before the clinical manifestations of malignant transformation, in hydatidiform moles. The precise measurement of the LINE-1 methylation level may be a promising marker in monitoring hydatidiform moles before progression to GTN.

Conflict of Interests

The authors declare that there is no conflict of interests regarding the publication of this paper.

Acknowledgments

This study was supported by the Ratchadaphiseksompotch Fund, Faculty of Medicine, Chulalongkorn University, and a 2011 Research Chair Grant from the National Science and Technology Development Agency (NSTDA) of Thailand.

References

[1] H. Judson, B. E. Hayward, E. Sheridan, and D. T. Bonthron, "A global disorder of imprinting in the human female germ line," *Nature*, vol. 416, no. 6880, pp. 539–542, 2002.

[2] R. A. Fisher and M. D. Hodges, "Genomic imprinting in gestational trophoblastic disease—a review," *Placenta*, vol. 24, supplement, pp. S111–S118, 2003.

[3] T. Matsuda and N. Wake, "Genetics and molecular markers in gestational trophoblastic disease with special reference to their clinical application," *Best Practice & Research Clinical Obstetrics & Gynaecology*, vol. 17, no. 6, pp. 827–836, 2003.

[4] M. J. Seckl, N. J. Sebire, and R. S. Berkowitz, "Gestational trophoblastic disease," *The Lancet*, vol. 376, no. 9742, pp. 717–729, 2010.

[5] E. I. O. Garner, D. P. Goldstein, C. M. Feltmate, and R. S. Berkowitz, "Gestational trophoblastic disease," *Clinical Obstetrics and Gynecology*, vol. 50, no. 1, pp. 112–122, 2007.

[6] W.-C. Xue, K. Y. K. Chan, H.-C. Feng et al., "Promoter hypermethylation of multiple genes in hydatidiform mole and choriocarcinoma," *The Journal of Molecular Diagnostics*, vol. 6, no. 4, pp. 326–334, 2004.

[7] C. P. Morrow, O. A. Kletzky, P. J. Disaia, D. E. Townsend, D. R. Mishell, and R. M. Nakamura, "Clinical and laboratory correlates of molar pregnancy and trophoblastic disease," *American Journal of Obstetrics and Gynecology*, vol. 128, no. 4, pp. 424–430, 1977.

[8] C. M. Suter, D. I. Martin, and R. I. Ward, "Hypomethylation of L1 retrotransposons in colorectal cancer and adjacent normal tissue," *International Journal of Colorectal Disease*, vol. 19, no. 2, pp. 95–101, 2004.

[9] V. Soto-Wright, M. Bernstein, D. P. Goldstein, and R. S. Berkowitz, "The changing clinical presentation of complete molar pregnancy," *Obstetrics and Gynecology*, vol. 86, no. 5, pp. 775–779, 1995.

[10] K. Grønbæk, C. Hother, and P. A. Jones, "Epigenetic changes in cancer," *APMIS*, vol. 115, no. 10, pp. 1039–1059, 2007.

[11] A. Bird, "DNA methylation patterns and epigenetic memory," *Genes & Development*, vol. 16, no. 1, pp. 6–21, 2002.

[12] A. P. Feinberg, "A genetic approach to cancer epigenetics," *Cold Spring Harbor Symposia on Quantitative Biology*, vol. 70, pp. 335–341, 2005.

[13] B. K. Dunn, "Hypomethylation: one side of a larger picture," *Annals of the New York Academy of Sciences*, vol. 983, pp. 28–42, 2003.

[14] R. Cordaux and M. A. Batzer, "The impact of retrotransposons on human genome evolution," *Nature Reviews Genetics*, vol. 10, no. 10, pp. 691–703, 2009.

[15] N. Kitkumthorn and A. Mutirangura, "Long interspersed nuclear element-1 hypomethylation in cancer: biology and clinical applications," *Clinical Epigenetics*, vol. 2, no. 2, pp. 315–330, 2011.

[16] C. Aporntewan, C. Phokaew, J. Piriyapongsa et al., "Hypomethylation of intragenic LINE-1 represses transcription in

cancer cells through AGO2," *PLoS ONE*, vol. 6, no. 3, Article ID e17934, 2011.

[17] N. Kongruttanachok, C. Phuangphairoj, A. Thongnak et al., "Replication independent DNA double-strand break retention may prevent genomic instability," *Molecular Cancer*, vol. 9, article 70, 2010.

[18] W. Pornthanakasem, N. Kongruttanachok, C. Phuangphairoj et al., "LINE-1 methylation status of endogenous DNA double-strand breaks," *Nucleic Acids Research*, vol. 36, no. 11, pp. 3667–3675, 2008.

[19] A. N. Carnell and J. I. Goodman, "The long (LINEs) and the short (SINEs) of it: altered methylation as a precursor to toxicity," *Toxicological Sciences*, vol. 75, no. 2, pp. 229–235, 2003.

[20] G. Alves, A. Tatro, and T. Fanning, "Differential methylation of human LINE-1 retrotransposons in malignant cells," *Gene*, vol. 176, no. 1-2, pp. 39–44, 1996.

[21] K. Chalitchagorn, S. Shuangshoti, N. Hourpai et al., "Distinctive pattern of LINE-1 methylation level in normal tissues and the association with carcinogenesis," *Oncogene*, vol. 23, no. 54, pp. 8841–8846, 2004.

[22] P. Tangkijvanich, N. Hourpai, P. Rattanatanyong, N. Wisedopas, V. Mahachai, and A. Mutirangura, "Serum LINE-1 hypomethylation as a potential prognostic marker for hepatocellular carcinoma," *Clinica Chimica Acta*, vol. 379, no. 1-2, pp. 127–133, 2007.

[23] J. Pattamadilok, N. Huapai, P. Rattanatanyong et al., "LINE-1 hypomethylation level as a potential prognostic factor for epithelial ovarian cancer," *International Journal of Gynecological Cancer*, vol. 18, no. 4, pp. 711–717, 2008.

[24] D. Perrin, E. Ballestar, M. F. Fraga et al., "Specific hypermethylation of LINE-1 elements during abnormal overgrowth and differentiation of human placenta," *Oncogene*, vol. 26, no. 17, pp. 2518–2524, 2007.

[25] T. Pobsook, K. Subbalekha, P. Sannikorn, and A. Mutirangura, "Improved measurement of LINE-1 sequence methylation for cancer detection," *Clinica Chimica Acta*, vol. 412, no. 3-4, pp. 314–321, 2011.

[26] A. S. Yang, M. R. H. Estécio, K. Doshi, Y. Kondo, E. H. Tajara, and J.-P. J. Issa, "A simple method for estimating global DNA methylation using bisulfite PCR of repetitive DNA elements," *Nucleic Acids Research*, vol. 32, no. 3, p. e38, 2004.

[27] N. Kitkumthorn, T. Tuangsintanakul, P. Rattanatanyong, D. Tiwawech, and A. Mutirangura, "LINE-1 methylation in the peripheral blood mononuclear cells of cancer patients," *Clinica Chimica Acta*, vol. 413, no. 9-10, pp. 869–874, 2012.

[28] N. Kitkumthorn, S. Keelawat, P. Rattanatanyong, and A. Mutirangura, "LINE-1 and alu methylation patterns in lymph node metastases of head and neck cancers," *Asian Pacific Journal of Cancer Prevention*, vol. 13, no. 9, pp. 4469–4475, 2012.

[29] S. Wangsri, K. Subbalekha, N. Kitkumthorn, and A. Mutirangura, "Patterns and possible roles of LINE-1 methylation changes in smoke-exposed epithelia," *PLoS ONE*, vol. 7, no. 9, Article ID e45292, 2012.

[30] H. Y. S. Ngan, H. Bender, J. L. Benedet, H. Jones, G. C. Montruccoli, and S. Pecorelli, "Gestational trophoblastic neoplasia, FIGO 2000 staging and classification," *International Journal of Gynecology and Obstetrics*, vol. 83, supplement 1, pp. 175–177, 2003.

[31] Z. Xiong and P. W. Laird, "COBRA: a sensitive and quantitative DNA methylation assay," *Nucleic Acids Research*, vol. 25, no. 12, pp. 2532–2534, 1997.

[32] A. S. M. Li, M. K. Y. Siu, H. Zhang et al., "Hypermethylation of SOX2 gene in hydatidiform mole and choriocarcinoma," *Reproductive Sciences*, vol. 15, no. 7, pp. 735–744, 2008.

[33] H. Chen, D. Ye, X. Xie, W. Lu, C. Zhu, and X. Chen, "PTEN promoter methylation and protein expression in normal early placentas and hydatidiform moles," *Journal of the Society for Gynecologic Investigation*, vol. 12, no. 3, pp. 214–217, 2005.

[34] M. P. Lambert and Z. Herceg, "Epigenetics and cancer, 2nd IARC meeting, Lyon, France, 6 and 7 December 2007," *Molecular Oncology*, vol. 2, no. 1, pp. 33–40, 2008.

[35] P. A. Jones and S. B. Baylin, "The epigenomics of cancer," *Cell*, vol. 128, no. 4, pp. 683–692, 2007.

[36] M. Esteller, "Epigenetics in cancer," *The New England Journal of Medicine*, vol. 358, no. 11, pp. 1148–1159, 2008.

[37] C. Phokaew, S. Kowudtitham, K. Subbalekha, S. Shuangshoti, and A. Mutirangura, "LINE-1 methylation patterns of different loci in normal and cancerous cells," *Nucleic Acids Research*, vol. 36, no. 17, pp. 5704–5712, 2008.

[38] S. Shuangshoti, N. Hourpai, U. Pumsuk, and A. Mutirangura, "Line-1 hypomethylation in multistage carcinogenesis of the uterine cervix," *Asian Pacific Journal of Cancer Prevention*, vol. 8, no. 2, pp. 307–309, 2007.

[39] S. Limpongsanurak, "Prophylactic actinomycin D for high-risk complete hydatidiform mole," *The Journal of Reproductive Medicine*, vol. 46, no. 2, pp. 110–116, 2001.

[40] D. S. Kim, H. Moon, K. T. Kim, and Y. Y. Hwang, "Effects of prophylactic chemotherapy for persistent trophoblastic disease in patients with complete hydatidiform mole," *Obstetrics and Gynecology*, vol. 67, no. 5, pp. 690–694, 1986.

Hindawi Publishing Corporation
BioMed Research International
Volume 2015, Article ID 340732, 10 pages
http://dx.doi.org/10.1155/2015/340732

Review Article

The Emergent Landscape of Detecting EGFR Mutations Using Circulating Tumor DNA in Lung Cancer

Wei-Lun Huang,[1,2] Fang Wei,[3] David T. Wong,[3] Chien-Chung Lin,[1,4] and Wu-Chou Su[1,4]

[1] *Department of Internal Medicine, National Cheng Kung University Hospital, College of Medicine, National Cheng Kung University, No. 138, Shengli Road, North District, Tainan City 704, Taiwan*
[2] *Institute of Oral Medicine, College of Medicine, National Cheng Kung University, No. 1, University Road, East District, Tainan City 704, Taiwan*
[3] *UCLA School of Dentistry, 10833 Le Conte, CHS-Box 951668, Los Angeles, CA 90095-1668, USA*
[4] *Institute of Clinical Medicine, National Cheng Kung University Hospital, College of Medicine, National Cheng Kung University, No. 35, Xiaodong Road, North District, Tainan City 704, Taiwan*

Correspondence should be addressed to Chien-Chung Lin; joshcclin@gmail.com and Wu-Chou Su; sunnysu@mail.ncku.edu.tw

Received 29 January 2015; Accepted 18 March 2015

Academic Editor: Aurelio Ariza

The advances in targeted therapies for lung cancer are based on the evaluation of specific gene mutations especially the epidermal growth factor receptor (EGFR). The assays largely depend on the acquisition of tumor tissue via biopsy before the initiation of therapy or after the onset of acquired resistance. However, the limitations of tissue biopsy including tumor heterogeneity and insufficient tissues for molecular testing are impotent clinical obstacles for mutation analysis and lung cancer treatment. Due to the invasive procedure of tissue biopsy and the progressive development of drug-resistant EGFR mutations, the effective initial detection and continuous monitoring of EGFR mutations are still unmet requirements. Circulating tumor DNA (ctDNA) detection is a promising biomarker for noninvasive assessment of cancer burden. Recent advancement of sensitive techniques in detecting EGFR mutations using ctDNA enables a broad range of clinical applications, including early detection of disease, prediction of treatment responses, and disease progression. This review not only introduces the biology and clinical implementations of ctDNA but also includes the updating information of recent advancement of techniques for detecting EGFR mutation using ctDNA in lung cancer.

1. Introduction

Lung cancer is the leading cause of cancer death since most patients are diagnosed at advanced stage [1, 2]. The identification of oncogenic driver mutations in lung cancer has led to the rapid rise of genotype-directed target therapy such as EGFR tyrosine kinase inhibitors (TKIs) and has shown dramatic clinical benefits [3]. EGFR mutation analysis is performed on tumor cells in biopsy or cytology specimens obtained from bronchoscopy, computed tomography- (CT-) guided biopsy, surgical resection, or drainage from malignant pleural effusions. Sampling tumor tissue other than surgical resection has inevitable limitations. Tumor heterogeneity in single snapshot in time may lead to selection bias. And it may be difficult to obtain enough DNA for EGFR mutation test if biopsy tissue lacks tumor cells [4]. Since initial detection and continuous monitoring of EGFR mutations are needed, the less invasive procedures are still unmet requirements. Blood-borne biomarkers such as circulating tumor cells (CTCs) and circulating tumor DNA (ctDNA) are promising for the detection of somatic mutations derived from malignant tumors [5], since they harbor the same genetic lesions as the primary tumor. Limitation exists on the uncertainty of collection and diversity of phenotypes from CTCs in blood [6]. ctDNA genotyping has the potential to be more widely used than many CTC capture technologies in development for specific purposes because of important advantages of ctDNA genotyping over CTCs for specimen processing. Firstly, CTCs must be separated from the much more abundant hematologic cells in the blood requiring significant

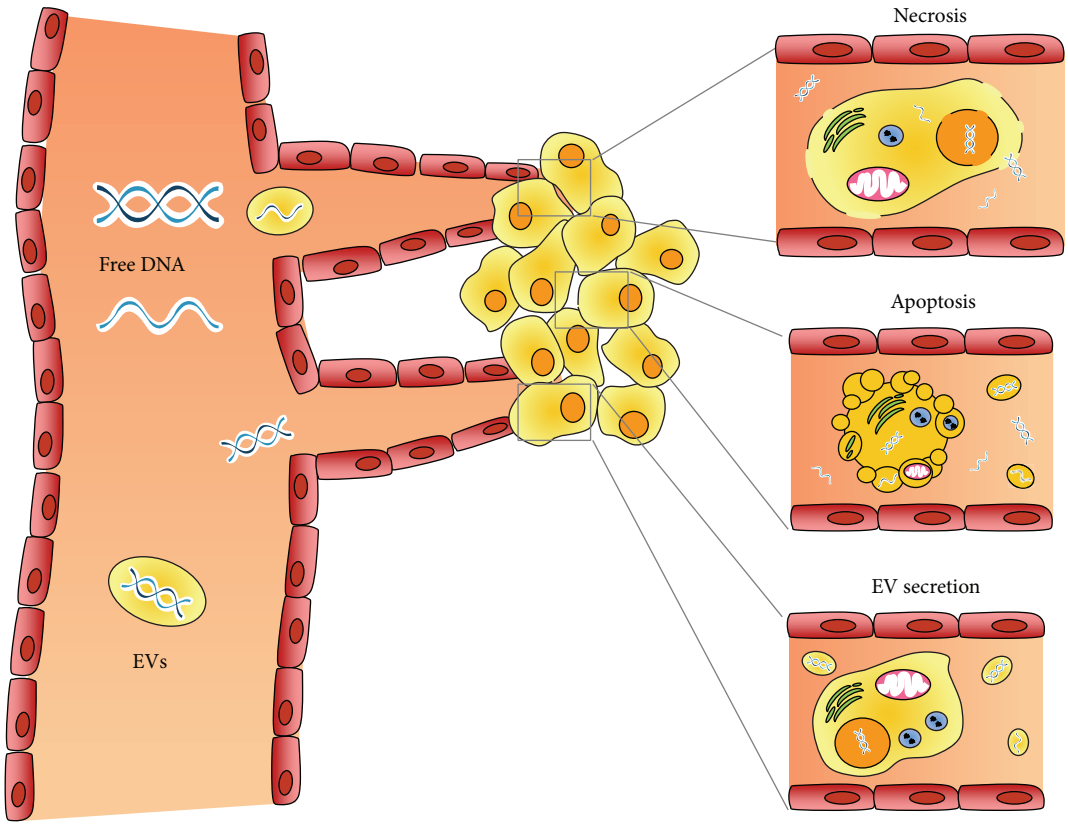

Figure 1: Source and biology of ctDNA.

laboratory infrastructure to obtain a viable population of CTCs for study. CTCs in circulation encounter substantial apoptosis and fragility leading to variability between different CTC assays. In contrast, most of the ctDNA genotyping methods require a minimum of special handling and do not depend on special equipment. Furthermore, ctDNA could be analyzed together with plasma DNA from normal cells, which is always present in the circulation. Current technologies are sensitive enough to detect tumor-specific somatic mutations, even if the ctDNA fragments represent only a minority of all DNA fragments in the circulation. In this review, we not only introduce the biology and clinical implementations of ctDNA but also include the updating information of recent advancement of techniques for detecting EGFR mutation using ctDNA in lung cancer.

2. Source and Biology of ctDNA

2.1. Apoptotic and Necrotic Cells. The finding of circulating extracellular DNA in the bloodstream was first reported at 1948 [7] and the correlation between cell-free nucleic acid levels in plasma and cancer was initially researched in 1977 [8]. It was the first study demonstrating that the plasma levels of circulating free DNA (cfDNA) were much higher in cancer patients than in healthy controls. Tumor cells release small fragments of cfDNA into circulation by multiple mechanisms (Figure 1). The apoptosis and necrosis of cancer cells in the tumor microenvironment are the main explanations for the release of the nucleic acids into the blood [3]. The cellular turnover leads to the increase of apoptotic and necrotic cells as the tumor increases in volume. The apoptotic and necrotic cells are engulfed by macrophages and the digested DNA was released into circulation [9, 10]. When double-stranded ctDNA in plasma is separated and visualized by gel electrophoresis, the fragments with a 180 to 1000 bp size ladder are likely to be formed by apoptosis. In contrast, DNA released by necrosis is nonspecifically digested and thus exhibits smears on electrophoretic separation with fragment sizes about 10,000 bp [10].

2.2. Secretion of Extracellular Vesicles. Cells release different types of membrane vesicles of endosomal and plasma membrane origin called exosomes and microvesicles, respectively, into the extracellular environment called extracellular vesicles (EVs) [11]. EVs play an important role of intercellular communication by serving as vehicles for transferring cytosolic proteins, lipids, and nucleic acids between cells. Thus, DNA secreted by EVs has also been suggested as a potential source of ctDNA. Recent investigations provide further evidence that EVs carry not only proteins, mRNA, microRNA, mitochondrial DNA [12], and single-stranded DNA, but also large fragments (>10 kb) of double-stranded carrying mutated KRAS, p53 and EGFR sequences [13, 14]. There are many attractive advantages of EV DNA as a

marker. First, EVs are very stable under different conditions that they can protect the DNA cargo against degradation and denaturation in the extracellular environment including the circulation [15]. Second, EVs can be collected from complex plasma samples via various isolating methods such as ultracentrifugation and immunoaffinity isolation based on specific EV surface markers. Thirdly, EVs can be transported via circulation and are found in all kinds of cancer associated body fluids such as pleural effusion, ascites, saliva, and urine [16]. They provide other sources for ctDNA detection other than serum.

3. Assays for EGFR Mutations Using ctDNA in Plasma Samples

Since ctDNA often represents a small fraction (<1.0%) of total cfDNA, its detection remains challenging [4]. Thus, direct sequencing approaches like Sanger sequencing or pyrosequencing are not suitable for detecting EGFR mutations using ctDNA. Several different types of PCR-based assays have been explored for ctDNA genotyping including amplification-refractory mutation system (ARMS)/Scorpion assay, digital PCR, mutant-enriched PCR, peptide nucleic acid- (PNA-) mediated PCR, PNA-locked nucleic acid (LNA) PCR clamp, and BEAMing (beads, emulsions, amplification, and magnetics). In addition to the PCR-based assays, mass spectrometry genotyping, high-resolution melting (HRM) analysis, denaturing high performance liquid chromatography (DHPLC), next-generation sequencing (NGS), and electric field-induced release and measurement (EFIRM) were also extensively developed for detecting EGFR mutations in various ctDNA containing cancer associated biofluids including plasma, malignant pleural effusion, and saliva. Here, we review the technical characteristics of these existing technologies shortly and compare their sensitivity, specificity, and predictive value (Table 1).

3.1. ARMS/Scorpion Assay. ARMS, also known as allele-specific polymerase chain reaction (ASPCR), is a reliable method for detecting single base mutations or small deletions which is based on the use of sequence-specific PCR primers [17]. This allows amplification of only DNA containing target allele and will not amplify the nontarget allele. Because Taq DNA polymerase is effective at distinguishing between a match and a mismatch at the $3'$ end of a primer, specific mutated sequences are selectively amplified. The amplification proceeds with full efficiency, when the primer is fully matched. In contrast, only low-level background amplification occurs when the $3'$ base is mismatched. Scorpions are tailed primers containing a PCR primer covalently linked to a probe. The fluorophore in this probe interacts with a quencher which also incorporated in the probe and reduces fluorescence. The fluorophore and quencher become separated when the probe binds to the amplicon during PCR that leads to an increase in fluorescence from the reaction tube [18]. Specific Scorpion ARMS primers have been designed and optimized for detecting various EGFR mutations and have been widely used for ctDNA based assays [19–25].

3.2. Digital PCR. Digital PCR is a refinement of conventional PCR that can be used to directly quantify and clonally amplify nucleic acids [26, 27]. It is to amplify a single DNA template from minimally diluted samples and generate amplicons that are exclusively derived from one template. It can be detected with different fluorophores or sequencing to distinguish different alleles. Thus, digital PCR transforms the exponential, analog nature of the conventional PCR into a linear, digital signal, suitable for statistical analysis. Digital PCR has been applied in quantification of EGFR mutants in clinical specimens, providing a promising molecular diagnostic tool [28].

3.3. Mutant-Enriched PCR. Mutant-enriched PCR is a sensitive assay that can detect one mutant gene among as many as 10^3 to 10^4 copies of the wild-type gene. The sensitivity is achieved by selective PCR amplification of mutant gene sequences with a two stage procedure. The first stage entails the amplification of both mutant and wild-type sequences, followed by selective digestion of only wild-type sequences with thermostable restriction enzymes during PCR. A subsequent step then amplifies the undigested fragments, enriched in mutant sequences [29]. This method has been shown to detect EGFR mutations in various kinds of clinical samples including pleural fluid and surgically resected tissues from patients with NSCLC [30–33].

3.4. PNA-Mediated PCR and PNA-LNA PCR Clamp. The assay uses PNA as both PCR clamp and sensor probe. It is a synthetic DNA analog in which the phosphodiester backbone is replaced by a peptide-like repeat [34, 35]. Since PNA contains no charged phosphate groups, the binding between PNA and DNA is stronger than that between DNA and DNA. Since PNA/DNA duplexes are more stable than the relevant DNA-DNA duplexes, PNA will not bind to a not perfectly matched DNA strand. In addition, PNA oligomers are not recognized by DNA polymerases and will not be utilized as primers in subsequence real-time PCR. Thus, the PNA probe binds tightly to perfectly matched wild-type DNA templates but not to mismatched mutant DNA templates and specifically inhibits the PCR amplification of wild-type alleles without interfering with the amplification of mutant DNA. A fluorescein tag also allows the PNA probe to generate unambiguous melting curves for real-time fluorescent monitoring [36]. Oligonucleotides containing LNA hybridize to complementary DNA with an increased affinity compared to oligonucleotide DNA. Thus, the incorporation of LNA residues increases the melting temperature of the oligonucleotide and allows the use of shorter LNA probes as allele-specific tools in genotyping [37]. In PNA clamp PCR, amplification of the wild-type sequences is suppressed and only amplification of the mutant sequences is enhanced. In combination, LNA probes specifically detect mutant sequences in the presence of wild-type sequences. Because PNA clamp primers have wild-type sequences and LNA probes have mutant sequences, they are located in the same position. PNA clamp primers competitively inhibit mutant LNA probes to bind to the wild type, further increasing

Table 1: Recent advancement of techniques for detecting EGFR mutation using ctDNA in lung cancer.

Study team	Sample	Oncogene mutation	Sample size	Method	Conclusion
Wang et al.	Plasma	EGFR	68 (III/IV)	ARMS/Scorpion assay	Sensitivity (22.06%), specificity (96.97%), positive predictive value (88.24%), and negative predictive value (54.70%) [20]
Liu et al.	Plasma	EGFR	86 (III/IV)	ARMS	Sensitivity (67.5%), specificity (100%), and concordance rate was 84.9% [21].
Goto et al.	Plasma	EGFR	86 (III/IV)	ARMS/Scorpion assay	Sensitivity (43.1%), specificity (100%), positive predictive value (100%), negative predictive value (54.7%), and concordance ratio (66.3%) [22]
Kimura et al.	Plasma	EGFR	42 (advanced stage)	ARMS/Scorpion assay	Sensitivity (85.7%), specificity (94.2%), and concordance ratio (92.9%) [23]
Kimura et al.	Plasma	EGFR	27 (III/IV)	ARMS/Scorpion	Detection rate 48.1% [24]
Yung et al.	Plasma	EGFR	35 (III/IV)	Digital PCR	Sensitivity (92%) and specificity (100%) [28]
Brevet et al.	Plasma	EGFR	34 (III/IV)	Mass spectrometry genotyping	Detection rate 61% [51]
Hu et al.	Plasma	EGFR	24 (I/II/III/IV)	High-resolution melting analysis	Positive rate was 100% for patients in stages II–IV, 81.8% (9/11) for stage I. The sensitivity was 91.67% and specificity was 100% [52].
Zhao et al.	Plasma	EGFR	111 (I/II/III/IV)	Mutant-enriched PCR	Concordance ratio (71.2%), sensitivity (35.6%), and specificity (95.5%). Sensitivity varied according to the disease stage and pathological differentiation; early stage (10%) versus advanced stage (56%). Highly differentiated (20%) patients and moderately differentiated (19%) and poorly differentiated subgroup (77.8%) [31].
Jiang et al.	Plasma	EGFR	58 (III/IV)	Mutant-enriched PCR	Sensitivity (77.8%), specificity (100%), and concordance rate (93.1%), more sensitive than the nonenriched assay [32].
Bai et al.	Plasma	EGFR	230 (III/IV)	DHPLC	Sensitivity 81.8% and specificity 89.5% [57]
Kim et al.	Plasma	EGFR	35 (III/IV)	PNA-mediated PCR	Concordance in the serum and tumor samples was 17% [42].
Kim et al.	Plasma	EGFR	57 (III/IV)	PNA–LNA PCR clamp	Concordance in the serum and tumor samples was 87.7% [43].
Xu et al.	Plasma	EGFR	51 (III/IV)	ARMS/Scorpion assay	Sensitivity (50.0%) Specificity (100%) [25]
				Mutant-enriched PCR	Sensitivity (25.0%) Specificity (96.2%)
				DHPLC	Sensitivity (25.0%) Specificity (92.3%)
			60 (III/IV)	Direct sequencing versus Mutant-enriched PCR	Sensitivity 18.3% versus 55.0% [33]
Kuang et al.	Plasma	EGFR –T790M	54 (III/IV)	ARMS/Scorpion assay	Detected in 54% of patients with prior clinical response to TKI and 29% of prior stable disease [19]
Taniguchi et al.	Plasma	EGFR –T790M	44 (III/IV)	BEAMing	82.6% detection rate in patient who developed PD after EGFR TKI and 43.5% detection rate in patients were never treated with EGFR TKI [48]
Sakai et al.	Plasma	EGFR –T790M	75 (III/IV)	Mass spectrometry genotyping	28% detection rate in patient who developed PD after EGFR TKI [50].
Kukita et al.	Plasma	EGFR	144 (III/IV)	Next-generation sequencers: Ion Torrent PGM	72.7% detection rate in exon 19 deletion, 78.2% detection rate in L858R or L861Q [66]

Table 1: Continued.

Study team	Sample	Oncogene mutation	Sample size	Method	Conclusion
Couraud et al.	Plasma	EGFR (exons 18, 19, 20, and 21)	68 (I/II/III/IV)	Next-generation sequencers: Ion Torrent PGM	Sensitivity ranged from 55% (EGFR exon 19) to 100% (EGFR exon 18) Considering all amplicons, the sensitivity was 58% and the concordance rate was 68% [67].
Wei et al.	Saliva	EGFR	40 (III/IV)	EFIRM	Exon 19 Del (AUCs = 0.94, 95% CI, 0.82–1) and L858R (AUCs = 0.96, 95% CI, 0.90–1) [80]

ARMS: amplification-refractory mutation system; DHPLC: denaturing high performance liquid chromatography; PNA: peptide nucleic acid; PNA-LNA: peptide nucleic acid-locked nucleic acid; BEAMing: beads, emulsions, amplification, and magnetics; NGS: next-generation sequencing; Ion Torrent PGM: Ion Torrent Personal Genome Machine (PGM) System; EFIRM: electric field-induced release and measurement.

the specificity of detection. In this way, EGFR mutations can be detected in the presence of 100- to 1,000-fold wild-type EGFR background [38, 39]. Because of its high sensitivity and specificity, PNA-LNA PCR clamp was considered suitable to detect EGFR mutations in histological samples such as surgical specimens as well as in cytological samples such as sputum and pleural effusions [40–43].

3.5. BEAMing. BEAMing is a process built on the basis of four of its principal components-beads, emulsion, amplification, and magnetics. BEAMing relies on single-molecule PCR at a massively parallel scale that millions of individual DNA molecules can be assessed in this fashion with standard laboratory equipment, similar to next-generation DNA sequencing technologies [44, 45]. Briefly, BEAMing starts with conventional PCR of a predetermined locus and the PCR product is added to millions of oligonucleotide-coupled beads in oil. An emulsion is then created that most of the beads bind only a single DNA molecule followed by the second round PCR. After the deemulsification and magnetic capture step, single-base primer extension or hybridization with mutant-specific probes is performed with different fluorescent probs. Finally, the detection and quantification of wild-type or mutant alleles are done by flow cytometry analysis of the beads. Moreover, specific variants can be isolated by flow cytometry sorting and used for further analysis. Because BEAMing analyzes one allele at a time, it is highly sensitive for the detection of rare mutant allele which is the exact molecular environment found in ctDNA cases. It has been shown to be potential for detecting PIK3CA and EGFR mutations using ctDNA [46–48].

3.6. Mass Spectrometry. In combination with base extension after PCR, mass spectrometry allows ctDNA detection with single-base specificity and single DNA molecule sensitivity [49]. Briefly, DNA is first amplified by PCR and then linear amplification with base extension reaction which is designed to anneal to the region upstream of the mutation site. Few bases are added to the extension primer to produce different extension products from wild-type DNA and mutant DNA. Mass spectrometry has been applied in detection of EGFR mutations in plasma DNA from lung cancer patients [50, 51].

3.7. High-Resolution Melting Analysis. HRM analysis is a powerful technique for the detection of mutations, polymorphisms, and epigenetic differences using double-stranded DNA samples. Typically PCR will be used prior to HRM analysis to amplify the DNA region in which their mutation of interest lies. The HRM process is simply a precise warming of the amplicon DNA from around 50°C up to around 95°C. When the melting temperature of the amplicon is reached and the two strands of DNA separate or "melt" apart, the HRM is to monitor this melting process happening in real time. This is achieved by using fluorescent dyes that bind specifically to double-stranded DNA. When the dyes are bound, they fluoresce brightly and they only fluoresce at a low level in the absence of double-stranded DNA. The melting temperature of double-stranded DNA molecules is influenced by several factors such as the length, GC content, and sequence, which are properties of the individual molecule. Thus, the difference on DNA sequences on various mutants determines the different melting temperature and will show different HRM signatures and it was shown to be suitable for serum EGFR mutation screening for NSCLC patients [52, 53].

3.8. DHPLC. DHPLC uses heteroduplex formation between wild-type and mutated DNA strands to identify mutations. Heteroduplex molecules could be separated from homoduplex molecules by ion-pair, reverse-phase liquid chromatography on a special column matrix with partial heat denaturation of the DNA strands [54]. In EGFR mutation analysis, mutations in exons 18 to 21 were analyzed using a DNA endonuclease, SURVEYOR assay, which cleaved mismatched heteroduplexed DNA [55]. For these analyses DNA could be prepared from both frozen and formalin-fixed, paraffin-embedded (FFPE) tumor specimens as well as ctDNA from plasma [38, 56, 57]. Furthermore, a partially denaturing HPLC (pDHPLC) assay was developed to detect a large range of sequence variants with high sensitivity and low detection limits for minority alleles which could be a useful approach for routine detection of EGFR variants [58].

3.9. Next-Generation Sequencing (NGS). Over the past years, there has been a dramatically shift away from automated Sanger sequencing to the NGS platform for genome analysis [59]. The NGS technologies include a number of methods

grouped broadly as template preparation, sequencing and imaging, and data analysis. The combination of specific protocols distinguishes one platform from another that determines the data output from each platform as well as their quality and cost [60]. In addition to the pure genomic studies, the NGS technology has also been used to characterize the evolutionary relationships of ancient genomes, to elucidate the role of noncoding RNAs in disease, and to detect oncogenic mutations as well [61–64]. For the oncogenic detection application, it has been introduced into the clinical analysis and was further designed as streamlined commercial products with targeted panels which cover the main genetic alterations with predictive value, including EGFR mutations [61, 63–65]. In addition, it has been shown that NGS could also be used for ctDNA based EGFR mutation analysis [66, 67]. However, the cost is relatively higher than the PCR-based methods and the clinical usage is still limited.

4. Assays for EGFR Mutations Using ctDNA in Other Biofluid Samples

There are limited studies of using other noninvasive biofluid samples for detecting oncogenic mutations in lung cancer until recent studies using urine and saliva. Although somatic mutation detection in urine has previously been performed in patients with cancer, nearly all prior studies were restricted to patients with genitourinary malignancies [68–70]. Hyman and colleagues demonstrated that there was 100% concordance between tissue and urinary cfDNA genotype in treatment naïve samples from patients with systemic Histiocytic disorders using a droplet-digital PCR assay for quantitative detection of the BRAFV600E mutation [71]. Janku, one of the colleagues, further implied urinary cfDNA might have utility in detecting advanced cancer patients with BRAF-mutant tumors for treatment response [72]. They enrolled 17 patients with advanced, biopsy-proven BRAF-mutant cancers, including melanoma, nonsmall cell lung cancer, and colorectal cancer. Of these patients, 88% had the same mutation in urinary cfDNA. Longitudinal analysis further showed that changes in the amount of BRAF V600E cfDNA correlated with response to BRAF/MEK targeted therapy. Mutation detection in urine not only provides convenience for disease monitoring on an outpatient basis without the need for blood sampling but also provides flexibility of storage since DNA in urine can be stabilized for at least 9 days compared to the only 6-hour limit for accurate assessment of cfDNA in plasma [73].

Saliva contains a variety of biomolecules, including DNA, mRNA, miRNA, protein, metabolites, and microbiota. The changes in their salivary concentration can be applied to develop potential biomarkers for detecting early oral and systemic diseases including oral cancer, lung cancer, and ovary cancer as well as evaluating disease prognosis and monitoring the response to treatment [74, 75]. The salivary genome consists of both human and microbial DNAs. Nearly 70% of the salivary genome is of human origin, while the remaining 30% is from the oral microbiota [76]. The quality of salivary DNA is good that 72% to 96% of samples can be genotyped; 84% can be amplified; and 67% can be sequenced [77, 78]. In addition, it can be stored for long term without significant degradation [79]. However, no oncogene mutated DNA was identified in saliva previously. Recently, we explored the clinical utility of saliva to detect EGFR mutations in NSCLC patients by developing a core technology, electric field-induced release and measurement (EFIRM) [80]. We termed the Saliva-Based EFIRM detection of EGFR mutation as SABER. The detection of EGFR mutations by SABER was developed from cell line and validated in lung cancer xenograph model and clinical sample. And finally, a blinded test was performed on saliva from 40 late-stage NSCLC patient saliva samples. The receiver operating characteristic analysis indicated that EFIRM detected the exon 19 deletion with an area under the curve (AUC) of 0.94 and the L858R mutation with an AUC of 0.96.

5. Clinical Implementation of Detecting EGFR Mutations Using ctDNA in Biofluid

5.1. Concordance with Tissue Biopsy. When ctDNA was used to detecting EGFR mutations in NSCLC patients, one key concern was whether or not the genetic variation within ctDNA was consistent with tumor tissue. Many studies have demonstrated that blood samples could be used to reflect genetic changes in tumor of NSCLC patients (Table 1). Another key issue was what would be the best method for detecting EGFR mutations using ctDNA. For ctDNA based EGFR mutation assay, the most commonly used method is ARMS/Scorpion assay. In average, this method provided very high specificity but its sensitivity performance varied largely. Other methods such HRM and Digital PCR seemed to had better sensitivity [28, 52]. In these studies, due to different sample cohorts recruited, the results should be further verified by more comprehensive comparison studies. Concerning the comparison of the sensitivity of these methods, recently a meta-analysis study demonstrated that DHPLC and HRM showed higher sensitivity than ARMS in subgroup analyses [81]. However, in another report, DHPLC and mutant-enriched PCR showed lower sensitivity than ARMS [25]. In addition, another study also emphasized that different stage and different differentiation of cancer cell may affect the sensitivity [31]. Thus, more studies are needed to further clarify this issue.

5.2. Monitoring Drug Resistance. Despite good responses to EGFR TKIs in the majority of lung cancer patients carrying sensitive EGFR mutations, most of these patients eventually become resistant to EGFR TKIs within 1 year [82]. Since patients at this stage are often too weak to receive second biopsy, a noninvasive method for detecting T790M mutation remains an unmet need for directing patient treatment strategy. Though T790M mutation was identified at 2005 [83, 84], it is not until 2009 that T790M mutation was proved being identified from plasma DNA in 54% (15 of 28) of patients with prior clinical response to gefitinib/erlotinib, 29% (4 of 14) with prior stable disease, and in 0% (0 of 12) that had primary progressive disease or were untreated with gefitinib/erlotinib [19]. In other studies, activating T790M

mutation was detected in 72.7% and 28% of plasma DNA using different methods [50, 85]. The progression free survival of the T790M-positive patients was proved significantly shorter than that of the T790M-negative patients [50]. However, unlike the study in using ctDNA to detect EGFR 19Del or L858R, these studies did not investigate the concordance with tumor tissue since most of these patients did not receive second biopsy.

5.3. Early Detection. Surgery is the most effective treatment for lung cancer but only one-third of lung cancer patients were diagnosed at early stage and amenable to surgery. Early-stage detection has the theoretical potential to reduce lung cancer mortality. Recently, National Lung Screening Trial (NLST) demonstrated that low-dose computed tomography screening (LDCT) is an effective way of detecting early lung cancer and reducing lung cancer mortality [50] compared to conventional chest X ray image. However, the study also raised two major unmet needs including the identification of nonsmoker subjects who carry the highest likelihood of developing lung cancer and which nodules are likely to be cancerous before sending patients into surgery. The NLST eligibility criteria did not clearly identify all the high-risk subjects for lung cancer who will be most likely to benefit from LDCT screening and the false positive findings confer potential harm from unnecessary interventions and undue anxiety for patients [86, 87]. Recently, using an ultrasensitive method for quantitating methods, ctDNA was detected in 100% of patients with stage II–IV NSCLC and in 50% of patients with stage I, with 96% specificity for mutant allele fractions down to ~0.02% [88]. Another study also demonstrated that EGFR DNA can be detected in early-stage lung cancer ranging from 10% to 81%. However, the application of circulating EGFR DNA for lung cancer screening should be limited on certain high risk groups. According to the International Cancer Advocacy Network (ICAN) study (NCT01106781) investigating EGFR gene mutation status in early-stage Chinese NSCLC patients with adenocarcinoma (ADC) histology, 55.1% patients were EGFR mutation positive [89]. The mutation rate is quite similar to the pioneer study, a prospective, molecular epidemiology study of EGFR mutations in Asian patients with advanced NSCLC of adenocarcinoma histology [90]. Though the detection of EGFR DNA in early lung cancer remains rare and the detection rate is lower than late stage, it remains a promising tool for screening lung cancer in combination with LDCT in Asian area.

6. Conclusion

ctDNA and CTC for detecting EGFR mutation have received more and more interest since a feasible, reliable, and minimally invasive approach is needed for clinical research and practice. ctDNA analysis is likely to be the preferred option for genotyping, monitoring treatment response, and early detection with no need to enrich and isolate a rare population of cells. However, optimizing and standardizing new technologies with appropriate analytical and clinical validity remained to be great challenges. In addition, other biofluids such as saliva and urine also have the potential for detecting EGFR mutations but large prospective clinical trials are needed for establishing the clinical utility. Finally, the combination of LDCT and EGFR mutation detection using ctDNA may provide an attractive method for screening early-stage lung cancer which could be the best way to decrease the high mortality of lung cancer.

Conflict of Interests

David Wong is co-founder of RNAmeTRIX Inc., a molecular diagnostic company. He holds equity in RNAmeTRIX, and serves as a company Director and Scientific Advisor. The University of California also holds equity in RNAmeTRIX. Intellectual property that David Wong invented and which was patented by the University of California has been licensed to RNAmeTRIX. Additionally, he is a consultant to PeriRx.

Acknowledgments

This work was supported by MOHW104-TDU-B-211-124-003 and MOHW104-TDU-B-211-113002 from the Ministry of Health and Welfare, Taiwan, MOST103-2120-M-006-002 and MOST103-2314-B-006-064 from the Ministry of Science and Technology, Taiwan. The authors thank Professor Yi-Lin Chen (Department of Pathology National Cheng Kung University Hospital, Tainan, Taiwan) for her advice on NGS associated parts in this paper.

References

[1] R. Siegel, J. Ma, Z. Zou, and A. Jemal, "Cancer statistics, 2014," *CA Cancer Journal for Clinicians*, vol. 64, no. 1, pp. 9–29, 2014.

[2] "Targeting resistance in lung cancer," *Cancer Discovery*, vol. 3, no. 12, article OF9, 2013.

[3] T. J. Lynch, D. W. Bell, R. Sordella et al., "Activating mutations in the epidermal growth factor receptor underlying responsiveness of non-small-cell lung cancer to Gefitinib," *The New England Journal of Medicine*, vol. 350, no. 21, pp. 2129–2139, 2004.

[4] L. A. Diaz Jr. and A. Bardelli, "Liquid biopsies: genotyping circulating tumor DNA," *Journal of Clinical Oncology*, vol. 32, no. 6, pp. 579–586, 2014.

[5] F.-C. Bidard, B. Weigelt, and J. S. Reis-Filho, "Going with the flow: from circulating tumor cells to DNA," *Science Translational Medicine*, vol. 5, no. 207, p. 207ps14, 2013.

[6] M. S. Wicha and D. F. Hayes, "Circulating tumor cells: not all detected cells are bad and not all bad cells are detected," *Journal of Clinical Oncology*, vol. 29, no. 12, pp. 1508–1511, 2011.

[7] P. Mandel and P. Metais, "Les acides nucleiques du plasma sanguin chez l'homme," *Comptes Rendus des Séances de la Société de Biologie et de ses Filiales*, vol. 142, no. 3-4, pp. 241–243, 1948.

[8] S. A. Leon, B. Shapiro, D. M. Sklaroff, and M. J. Yaros, "Free DNA in the serum of cancer patients and the effect of therapy," *Cancer Research*, vol. 37, no. 3, pp. 646–650, 1977.

[9] H. Schwarzenbach, D. S. B. Hoon, and K. Pantel, "Cell-free nucleic acids as biomarkers in cancer patients," *Nature Reviews Cancer*, vol. 11, no. 6, pp. 426–437, 2011.

[10] M. Stroun, J. Lyautey, C. Lederrey, A. Olson-Sand, and P. Anker, "About the possible origin and mechanism of circulating DNA: apoptosis and active DNA release," *Clinica Chimica Acta*, vol. 313, no. 1-2, pp. 139–142, 2001.

[11] G. Raposo and W. Stoorvogel, "Extracellular vesicles: exosomes, microvesicles, and friends," *The Journal of Cell Biology*, vol. 200, no. 4, pp. 373–383, 2013.

[12] M. Guescini, D. Guidolin, L. Vallorani et al., "C2C12 myoblasts release micro-vesicles containing mtDNA and proteins involved in signal transduction," *Experimental Cell Research*, vol. 316, no. 12, pp. 1977–1984, 2010.

[13] C. Kahlert, S. A. Melo, A. Protopopov et al., "Identification of double-stranded genomic dna spanning all chromosomes with mutated KRAS and P53 DNA in the serum exosomes of patients with pancreatic cancer," *The Journal of Biological Chemistry*, vol. 289, no. 7, pp. 3869–3875, 2014.

[14] B. K. Thakur, H. Zhang, A. Becker et al., "Double-stranded DNA in exosomes: a novel biomarker in cancer detection," *Cell Research*, vol. 24, no. 6, pp. 766–769, 2014.

[15] D. D. Taylor and C. Gercel-Taylor, "MicroRNA signatures of tumor-derived exosomes as diagnostic biomarkers of ovarian cancer," *Gynecologic Oncology*, vol. 110, no. 1, pp. 13–21, 2008.

[16] D. Duijvesz, T. Luider, C. H. Bangma, and G. Jenster, "Exosomes as biomarker treasure chests for prostate cancer," *European Urology*, vol. 59, no. 5, pp. 823–831, 2011.

[17] C. R. Newton, A. Graham, L. E. Heptinstall et al., "Analysis of any point mutation in DNA. The amplification refractory mutation system (ARMS)," *Nucleic Acids Research*, vol. 17, no. 7, pp. 2503–2516, 1989.

[18] D. Whitcombe, J. Theaker, S. P. Guy, T. Brown, and S. Little, "Detection of PCR products using self-probing amplicons and fluorescence," *Nature Biotechnology*, vol. 17, no. 8, pp. 804–807, 1999.

[19] Y. Kuang, A. Rogers, B. Y. Yeap et al., "Noninvasive detection of EGFR T790M in gefitinib or erlotinib resistant non-small cell lung cancer," *Clinical Cancer Research*, vol. 15, no. 8, pp. 2630–2636, 2009.

[20] S. Wang, X. Han, X. Hu et al., "Clinical significance of pre-treatment plasma biomarkers in advanced non-small cell lung cancer patients," *Clinica Chimica Acta*, vol. 430, pp. 63–70, 2014.

[21] X. Liu, Y. Lu, G. Zhu et al., "The diagnostic accuracy of pleural effusion and plasma samples versus tumour tissue for detection of EGFR mutation in patients with advanced non-small cell lung cancer: comparison of methodologies," *Journal of Clinical Pathology*, vol. 66, no. 12, pp. 1065–1069, 2013.

[22] K. Goto, Y. Ichinose, Y. Ohe et al., "Epidermal growth factor receptor mutation status in circulating free DNA in serum: from IPASS, a phase III study of gefitinib or carboplatin/paclitaxel in non-small cell lung cancer," *Journal of Thoracic Oncology*, vol. 7, no. 1, pp. 115–121, 2012.

[23] H. Kimura, M. Suminoe, K. Kasahara et al., "Evaluation of epidermal growth factor receptor mutation status in serum DNA as a predictor of response to gefitinib (IRESSA)," *British Journal of Cancer*, vol. 97, no. 6, pp. 778–784, 2007.

[24] H. Kimura, K. Kasahara, M. Kawaishi et al., "Detection of epidermal growth factor receptor mutations in serum as a predictor of the response to gefitinib in patients with non-small-cell lung cancer," *Clinical Cancer Research*, vol. 12, no. 13, pp. 3915–3921, 2006.

[25] F. Xu, J. Wu, C. Xue et al., "Comparison of different methods for detecting epidermal growth factor receptor mutations in peripheral blood and tumor tissue of non-small cell lung cancer as a predictor of response to gefitinib," *OncoTargets and Therapy*, vol. 5, pp. 439–447, 2012.

[26] G. Pohl and L.-M. Shih, "Principle and applications of digital PCR," *Expert Review of Molecular Diagnostics*, vol. 4, no. 1, pp. 41–47, 2004.

[27] B. Vogelstein and K. W. Kinzler, "Digital PCR," *Proceedings of the National Academy of Sciences of the United States of America*, vol. 96, no. 16, pp. 9236–9241, 1999.

[28] T. K. F. Yung, K. C. A. Chan, T. S. K. Mok, J. Tong, K.-F. To, and Y. M. D. Lo, "Single-molecule detection of epidermal growth factor receptor mutations in plasma by microfluidics digital PCR in non-small cell lung cancer patients," *Clinical Cancer Research*, vol. 15, no. 6, pp. 2076–2084, 2009.

[29] S. M. Kahn, W. Jiang, T. A. Culbertson, I. B. Weinstein, G. M. Williams, and N. Z. Tomita Ronai, "Rapid and sensitive nonradioactive detection of mutant K-ras genes via 'enriched' PCR amplification," *Oncogene*, vol. 6, no. 6, pp. 1079–1083, 1991.

[30] H. Asano, S. Toyooka, M. Tokumo et al., "Detection of EGFR gene mutation in lung cancer by mutant-enriched polymerase chain reaction assay," *Clinical Cancer Research*, vol. 12, no. 1, pp. 43–48, 2006.

[31] X. Zhao, R.-B. Han, J. Zhao et al., "Comparison of epidermal growth factor receptor mutation statuses in tissue and plasma in stage I-IV non-small cell lung cancer patients," *Respiration*, vol. 85, no. 2, pp. 119–125, 2013.

[32] B. Jiang, F. Liu, L. Yang et al., "Serum detection of epidermal growth factor receptor gene mutations using mutant-enriched sequencing in Chinese patients with advanced non-small cell lung cancer," *Journal of International Medical Research*, vol. 39, no. 4, pp. 1392–1401, 2011.

[33] C. He, M. Liu, C. Zhou et al., "Detection of epidermal growth factor receptor mutations in plasma by mutant-enriched PCR assay for prediction of the response to gefitinib in patients with non-small-cell lung cancer," *International Journal of Cancer*, vol. 125, no. 10, pp. 2393–2399, 2009.

[34] A. Ray and B. Nordén, "Peptide nucleic acid (PNA): its medical and biotechnical applications and promise for the future," *The FASEB Journal*, vol. 14, no. 9, pp. 1041–1060, 2000.

[35] P. Wittung, P. E. Nielsen, O. Buchardt, M. Egholm, and B. Nordén, "DNA-like double helix formed by peptide nucleic acid," *Nature*, vol. 368, no. 6471, pp. 561–563, 1994.

[36] C.-C. Chiou, J.-D. Luo, and T.-L. Chen, "Single-tube reaction using peptide nucleic acid as both PCR clamp and sensor probe for the detection of rare mutations," *Nature Protocols*, vol. 1, no. 6, pp. 2604–2612, 2007.

[37] L. A. Ugozzoli, D. Latorra, R. Pucket, K. Arar, and K. Hamby, "Real-time genotyping with oligonucleotide probes containing locked nucleic acids," *Analytical Biochemistry*, vol. 324, no. 1, pp. 143–152, 2004.

[38] J. Obradovic and V. Jurisic, "Evaluation of current methods to detect the mutations of epidermal growth factor receptor in non-small cell lung cancer patients," *Multidisciplinary Respiratory Medicine*, vol. 7, no. 7, article 52, 2012.

[39] Y. Nagai, H. Miyazawa, T. Tanaka et al., "Genetic heterogeneity of the epidermal growth factor receptor in non-small cell lung cancer cell lines revealed by a rapid and sensitive detection system, the peptide nucleic acid-locked nucleic acid PCR clamp," *Cancer Research*, vol. 65, no. 16, pp. 7276–7282, 2005.

[40] T. Tanaka, Y. Nagai, H. Miyazawa et al., "Reliability of the peptide nucleic acid-locked nucleic acid polymerase chain

reaction clamp-based test for epidermal growth factor receptor mutations integrated into the clinical practice for non-small cell lung cancers," *Cancer Science*, vol. 98, no. 2, pp. 246–252, 2007.

[41] A. Sutani, Y. Nagai, K. Udagawa et al., "Gefitinib for non-small-cell lung cancer patients with epidermal growth factor receptor gene mutations screened by peptide nucleic acid-locked nucleic acid PCR clamp," *British Journal of Cancer*, vol. 95, no. 11, pp. 1483–1489, 2006.

[42] H.-R. Kim, S. Y. Lee, D.-S. Hyun et al., "Detection of EGFR mutations in circulating free DNA by PNA-mediated PCR clamping," *Journal of Experimental & Clinical Cancer Research*, vol. 32, no. 1, article 50, 2013.

[43] S. T. Kim, J. S. Sung, U. H. Jo, K. H. Park, S. W. Shin, and Y. H. Kim, "Can mutations of EGFR and KRAS in serum be predictive and prognostic markers in patients with advanced non-small cell lung cancer (NSCLC)?" *Medical Oncology*, vol. 30, no. 1, article 328, 2013.

[44] D. Dressman, H. Yan, G. Traverso, K. W. Kinzler, and B. Vogelstein, "Transforming single DNA molecules into fluorescent magnetic particles for detection and enumeration of genetic variations," *Proceedings of the National Academy of Sciences of the United States of America*, vol. 100, no. 15, pp. 8817–8822, 2003.

[45] F. Diehl, K. Schmidt, K. H. Durkee et al., "Analysis of mutations in DNA isolated from plasma and stool of colorectal cancer patients," *Gastroenterology*, vol. 135, no. 2, pp. 489.e7–498.e7, 2008.

[46] J. Lauring and B. H. Park, "BEAMing sheds light on drug resistance," *Clinical Cancer Research*, vol. 17, no. 24, pp. 7508–7510, 2011.

[47] A. L. Richardson and J. D. Iglehart, "BEAMing up personalized medicine: mutation detection in blood," *Clinical Cancer Research*, vol. 18, no. 12, pp. 3209–3211, 2012.

[48] K. Taniguchi, J. Uchida, K. Nishino et al., "Quantitative detection of EGFR mutations in circulating tumor DNA derived from lung adenocarcinomas," *Clinical Cancer Research*, vol. 17, no. 24, pp. 7808–7815, 2011.

[49] C. Ding, R. W. K. Chiu, T. K. Lau et al., "MS analysis of single-nucleotide differences in circulating nucleic acids: application to noninvasive prenatal diagnosis," *Proceedings of the National Academy of Sciences of the United States of America*, vol. 101, no. 29, pp. 10762–10767, 2004.

[50] K. Sakai, A. Horiike, D. L. Irwin et al., "Detection of epidermal growth factor receptor T790M mutation in plasma DNA from patients refractory to epidermal growth factor receptor tyrosine kinase inhibitor," *Cancer Science*, vol. 104, no. 9, pp. 1198–1204, 2013.

[51] M. Brevet, M. L. Johnson, C. G. Azzoli, and M. Ladanyi, "Detection of EGFR mutations in plasma DNA from lung cancer patients by mass spectrometry genotyping is predictive of tumor EGFR status and response to EGFR inhibitors," *Lung Cancer*, vol. 73, no. 1, pp. 96–102, 2011.

[52] C. Hu, X. Liu, Y. Chen et al., "Direct serum and tissue assay for EGFR mutation in non-small cell lung cancer by high-resolution melting analysis," *Oncology Reports*, vol. 28, no. 5, pp. 1815–1821, 2012.

[53] C. F. Taylor, "Mutation scanning using high-resolution melting," *Biochemical Society Transactions*, vol. 37, no. 2, pp. 433–437, 2009.

[54] G. Keller, A. Hartmann, J. Mueller, and H. Höfler, "Denaturing high pressure liquid chromatography (DHPLC) for the analysis of somatic p53 mutations," *Laboratory Investigation*, vol. 81, no. 12, pp. 1735–1737, 2001.

[55] P. A. Jänne, A. M. Borras, Y. Kuang et al., "A rapid and sensitive enzymatic method for epidermal growth factor receptor mutation screening," *Clinical Cancer Research*, vol. 12, no. 3, pp. 751–758, 2006.

[56] V. Cohen, J. S. Agulnik, J. Jarry et al., "Evaluation of denaturing high-performance liquid chromatography as a rapid detection method for identification of epidermal growth factor receptor mutations in nonsmall-cell lung cancer," *Cancer*, vol. 107, no. 12, pp. 2858–2865, 2006.

[57] H. Bai, L. Mao, H. S. Wang et al., "Epidermal growth factor receptor mutations in plasma DNA samples predict tumor response in Chinese patients with stages IIIB to IV non-small-cell lung cancer," *Journal of Clinical Oncology*, vol. 27, no. 16, pp. 2653–2659, 2009.

[58] T. M. Chin, D. Anuar, R. Soo et al., "Detection of epidermal growth factor receptor variations by partially denaturing HPLC," *Clinical Chemistry*, vol. 53, no. 1, pp. 62–70, 2007.

[59] E. R. Mardis, "Next-generation sequencing platforms," *Annual Review of Analytical Chemistry*, vol. 6, pp. 287–303, 2013.

[60] M. L. Metzker, "Sequencing technologies the next generation," *Nature Reviews Genetics*, vol. 11, no. 1, pp. 31–46, 2010.

[61] H. L. Rehm, "Disease-targeted sequencing: a cornerstone in the clinic," *Nature Reviews Genetics*, vol. 14, no. 4, pp. 295–300, 2013.

[62] J. C. Mwenifumbo and M. A. Marra, "Cancer genome-sequencing study design," *Nature Reviews Genetics*, vol. 14, no. 5, pp. 321–332, 2013.

[63] M. T. Lin, S. L. Mosier, M. Thiess et al., "Clinical validation of KRAS, BRAF, and EGFR mutation detection using next-generation sequencing," *American Journal of Clinical Pathology*, vol. 141, no. 6, pp. 856–866, 2014.

[64] D. de Biase, M. Visani, U. Malapelle et al., "Next-generation sequencing of lung cancer EGFR exons 18-21 allows effective molecular diagnosis of small routine samples (cytology and biopsy)," *PLoS ONE*, vol. 8, no. 12, Article ID e83607, 2013.

[65] H. S. Kim, J. S. Sung, S.-J. Yang et al., "Predictive efficacy of low burden EGFR mutation detected by next-generation sequencing on response to EGFR tyrosine kinase inhibitors in non-small-cell lung carcinoma," *PLoS ONE*, vol. 8, no. 12, Article ID e81975, 2013.

[66] Y. Kukita, J. Uchida, S. Oba et al., "Quantitative identification of mutant alleles derived from lung cancer in plasma cell-free DNA via anomaly detection using deep sequencing data," *PLoS ONE*, vol. 8, no. 11, Article ID e81468, 2013.

[67] S. Couraud, F. Vaca-Paniagua, S. Villar et al., "Noninvasive diagnosis of actionable mutations by deep sequencing of circulating free DNA in lung cancer from never-smokers: a proof-of-concept study from BioCAST/IFCT-1002," *Clinical Cancer Research*, vol. 20, no. 17, pp. 4613–4624, 2014.

[68] V. Casadio, D. Calistri, S. Salvi et al., "Urine cell-free DNA integrity as a marker for early prostate cancer diagnosis: a pilot study," *BioMed Research International*, vol. 2013, Article ID 270457, 5 pages, 2013.

[69] V. Casadio, D. Calistri, M. Tebaldi et al., "Urine cell-free DNA integrity as a marker for early bladder cancer diagnosis: preliminary data," *Urologic Oncology: Seminars and Original Investigations*, vol. 31, no. 8, pp. 1744–1750, 2013.

[70] S. H. Zhang, S. M. Zhao, Z. M. Zhao, and C. T. Li, "Genotyping of urinary samples stored with EDTA for forensic applications," *Genetics and Molecular Research*, vol. 11, no. 3, pp. 3007–3012, 2012.

[71] D. M. Hyman, E. L. Diamond, C. R. Vibat et al., "Prospective blinded study of $BRAF^{V600E}$ mutation detection in cell-free DNA of patients with systemic histiocytic disorders," *Cancer Discovery*, vol. 5, no. 1, pp. 64–71, 2015.

[72] F. Janku, C. R. T. Vibat, G. S. Falchook et al., "Longitudinal monitoring of BRAF V600E mutation in urinary cell-free DNA of patients with metastatic cancers," *ASCO Annual Meeting*, abstract e22175, 2014.

[73] K. C. A. Chan, S.-W. Yeung, W.-B. Lui, T. H. Rainer, and Y. M. D. Lo, "Effects of preanalytical factors on the molecular size of cell-free DNA in blood," *Clinical Chemistry*, vol. 51, no. 4, pp. 781–784, 2005.

[74] P. Denny, F. K. Hagen, M. Hardt et al., "The proteomes of human parotid and submandibular/sublingual gland salivas collected as the ductal secretions," *Journal of Proteome Research*, vol. 7, no. 5, pp. 1994–2006, 2008.

[75] N. Spielmann and D. Wong, "Saliva: diagnostics and therapeutic perspectives," *Oral Diseases*, vol. 17, no. 4, pp. 345–354, 2011.

[76] T. Rylander-Rudqvist, N. Håkansson, G. Tybring, and A. Wolk, "Quality and quantity of saliva DNA obtained from the self-administrated oragene method—a pilot study on the cohort of Swedish men," *Cancer Epidemiology, Biomarkers & Prevention*, vol. 15, no. 9, pp. 1742–1745, 2006.

[77] M.-L. Looi, H. Zakaria, J. Osman, and R. Jamal, "Quantity and quality assessment of DNA extracted from saliva and blood," *Clinical Laboratory*, vol. 58, no. 3-4, pp. 307–312, 2012.

[78] T. V. O. Hansen, M. K. Simonsen, F. C. Nielsen, and Y. A. Hundrup, "Collection of blood, saliva, and buccal cell samples in a pilot study on the Danish nurse cohort: comparison of the response rate and quality of genomic DNA," *Cancer Epidemiology Biomarkers and Prevention*, vol. 16, no. 10, pp. 2072–2076, 2007.

[79] N. J. Bonne and D. T. W. Wong, "Salivary biomarker development using genomic, proteomic and metabolomic approaches," *Genome Medicine*, vol. 4, no. 10, article 82, 2012.

[80] F. Wei, C. Lin, A. Joon et al., "Noninvasive saliva-based EGFR gene mutation detection in patients with lung cancer," *The American Journal of Respiratory and Critical Care Medicine*, vol. 190, no. 10, pp. 1117–1126, 2014.

[81] J. Luo, L. Shen, and D. Zheng, "Diagnostic value of circulating free DNA for the detection of EGFR mutation status in NSCLC: a systematic review and meta-analysis," *Scientific Reports*, vol. 4, article 6269, 2014.

[82] S. Kobayashi, T. J. Boggon, T. Dayaram et al., "EGFR mutation and resistance of non-small-cell lung cancer to gefitinib," *The New England Journal of Medicine*, vol. 352, no. 8, pp. 786–792, 2005.

[83] W. Pao, V. A. Miller, K. A. Politi et al., "Acquired resistance of lung adenocarcinomas to gefitinib or erlotinib is associated with a second mutation in the EGFR kinase domain," *PLoS Medicine*, vol. 2, no. 3, article e73, 2005.

[84] R. K. Thomas, H. Greulich, Y. Yuza et al., "Detection of oncogenic mutations in the EGFR gene in lung adenocarcinoma with differential sensitivity to EGFR tyrosine kinase inhibitors," *Cold Spring Harbor Symposia on Quantitative Biology*, vol. 70, pp. 73–81, 2005.

[85] K. Taniguchi, J. Uchida, K. Nishino et al., "Quantitative detection of EGFR mutations in circulating tumor DNA derived from lung adenocarcinomas," *Clinical Cancer Research*, vol. 17, no. 24, pp. 7808–7815, 2011.

[86] D. R. Aberle, A. M. Adams, C. D. Berg et al., "Reduced lung-cancer mortality with low-dose computed tomographic screening," *The New England Journal of Medicine*, vol. 365, no. 5, pp. 395–409, 2011.

[87] K. Courtright and S. Manaker, "Counterpoint: should lung cancer screening by chest CT scan be a covered benefit? No," *Chest*, vol. 147, no. 2, pp. 289–292, 2015.

[88] A. M. Newman, S. V. Bratman, J. To et al., "An ultrasensitive method for quantitating circulating tumor DNA with broad patient coverage," *Nature Medicine*, vol. 20, no. 5, pp. 548–554, 2014.

[89] X. Zhang, Y. L. Wu, J. Wang et al., "A prospective comparison study on EGFR mutations by direct sequencing and ARMS in completely resected Chinese non-small cell lung cancer with adenocarcinoma histology (ICAN)," in *Proceedings of the ASCO Annual Meeting*, European Society for Medical Oncology, 2014.

[90] Y. Shi, J. S.-K. Au, S. Thongprasert et al., "A prospective, molecular epidemiology study of EGFR mutations in Asian patients with advanced non-small-cell lung cancer of adenocarcinoma histology (PIONEER)," *Journal of Thoracic Oncology*, vol. 9, no. 2, pp. 154–162, 2014.

Hindawi Publishing Corporation
BioMed Research International
Volume 2015, Article ID 476508, 22 pages
http://dx.doi.org/10.1155/2015/476508

Review Article

Genetic and Chromosomal Aberrations and Their Clinical Significance in Renal Neoplasms

Ning Yi Yap,[1] Retnagowri Rajandram,[1,2,3] Keng Lim Ng,[1,2] Jayalakshmi Pailoor,[4] Ahmad Fadzli,[1] and Glenda Carolyn Gobe[2]

[1]*Department of Surgery, Faculty of Medicine, University of Malaya, Jalan Universiti, Kuala Lumpur, Malaysia*
[2]*Centre for Kidney Disease Research, University of Queensland, Translational Research Institute, 37 Kent Street, Brisbane QLD 4102, Australia*
[3]*University of Malaya Cancer Research Institute, University of Malaya, Jalan Universiti, Kuala Lumpur, Malaysia*
[4]*Department of Pathology, Faculty of Medicine, University of Malaya, Jalan Universiti, Kuala Lumpur, Malaysia*

Correspondence should be addressed to Retnagowri Rajandram; rretnagowri@gmail.com

Received 23 January 2015; Revised 23 May 2015; Accepted 25 May 2015

Academic Editor: Konstantinos Arnaoutakis

The most common form of malignant renal neoplasms is renal cell carcinoma (RCC), which is classified into several different subtypes based on the histomorphological features. However, overlaps in these characteristics may present difficulties in the accurate diagnosis of these subtypes, which have different clinical outcomes. Genomic and molecular studies have revealed unique genetic aberrations in each subtype. Knowledge of these genetic changes in hereditary and sporadic renal neoplasms has given an insight into the various proteins and signalling pathways involved in tumour formation and progression. In this review, the genetic aberrations characteristic to each renal neoplasm subtype are evaluated along with the associated protein products and affected pathways. The potential applications of these genetic aberrations and proteins as diagnostic tools, prognostic markers, or therapeutic targets are also assessed.

1. Introduction

The incidence of kidney cancers has been increasing steadily in developed countries over the past decade and new reports show similar trends in developing countries [1–3]. Renal cell carcinoma (RCCs) form the majority of malignant kidney neoplasms and are grouped into a few different subtypes based on their histomorphological features. The most common subtype is clear cell RCC (ccRCC), followed by papillary (pRCC), chromophobe (chRCC), and collecting duct RCC (CDRCC). Renal oncocytoma (RO) is a benign renal neoplasm with histological similarities to chRCC [4]. Accurate identification of these subtypes is important for disease management as each subtype has a different biological and clinical behaviour. Cancer is often described as a genetic disease, caused by genetic alterations which regulate cell growth [5–7]. Hence, distinctive genetic aberrations in each RCC subtype affect the clinical course and prognosis of the tumour. The majority of RCCs are sporadic while only approximately <3% are hereditary [8, 9]. Although less frequently encountered, hereditary RCCs play a significant role in the understanding of genetic changes and pathways affecting tumour progression (Table 2).

Genetic alterations such as duplication, deletion, translocation, hypermethylation, or mutations result in the activation or inactivation of genes and the over- or underexpression of the corresponding proteins in RCCs. Genetics analysis helps in the identification of tumours in situations where histology and immunohistochemistry (IHC) profiles do not provide a clear distinction between the subtypes. Conventional methods for analysis include chromosomal comparative genomic hybridization (CGH), fluorescent in situ hybridization (FISH), G banding, and polymerase chain reaction (PCR) based loss of heterozygosity (LOH) analysis. Newer technologies such as array CGH (aCGH), single nucleotide polymorphisms (SNP) arrays, and next generation sequencing (NGS) have allowed for high throughput analyses

of known aberrations as well as identification of novel genetic alterations.

In this review, the various genetic aberrations associated with familial and sporadic clear cell, papillary, chromophobe, collecting duct RCCs, and oncocytoma will be explored, along with the prognostic, diagnostic, and therapeutic implications of these genes.

2. Clear Cell Renal Cell Carcinoma (ccRCC)

Clear cell RCC is the most frequent subtype of renal cancer, accounting for 80–90% of all RCCs [10]. Originating from renal proximal tubules, ccRCC cells have abundant clear cytoplasm, a result of high glycogen and lipid content. Eosinophilic or granular cells may be present, due to a higher number of mitochondria [11]. Clear cell RCC has a metastatic rate of 15.3–21.5% at presentation and a 5-year cancer specific survival of 71–81.3% [12–14].

2.1. Von Hippel-Lindau (VHL) Gene. The most common and characteristic genetic changes in ccRCCs are aberrations such as LOH, hypermethylation, or mutation in 3p chromosome region, which are found in up to 91% of the tumours [15–17]. The *VHL* gene, a tumour suppressor gene (TSG) located at 3p25 loci, is one of the earlier genes associated with ccRCC. This gene was first discovered in patients with VHL disease, an autosomal dominant hereditary syndrome that predisposes affected individuals to cancers such as pheochromocytomas, hemangioblastomas, and ccRCC [18]. Up to 75% of patients with VHL syndrome develop ccRCC, a leading cause of death in these patients [19, 20]. However, only approximately 1.6% of all ccRCC cases are associated with hereditary VHL syndrome [21]. Interest in *VHL* grew when the majority of sporadic ccRCC cases were also found to contain *VHL* aberrations.

The VHL protein (pVHL) functions to ubiquitinate proteins and mark them for degradation, with hypoxia inducible factor α (HIFα) being a well-researched target involved in tumourigenesis [22–24]. HIFα is a transcription factor controlling angiogenesis, glucose uptake, cell proliferation, and apoptosis through downstream targets like vascular endothelial growth factor (VEGF), platelet-derived growth factor (PDGF), transforming growth factor alpha (TGFα), and C-X-C chemokine receptor type 4 (CXCR4) [25–27]. Under normal oxygen conditions, HIFα is degraded by pVHL but when oxygen is low, HIFα is allowed to accumulate, inducing transcription of genes that improve cell proliferation, oxygen delivery, and angiogenesis [22–24]. Inactivation of *VHL*, which occurs through mutation, deletion, or methylation, causes the accumulation of HIFα under normal oxygen conditions and encourages tumour growth. Individuals with VHL disease have one wild type *VHL* allele and one inactivated *VHL* allele [28]. According to the Knudson two-hit model, biallelic VHL inactivation is achieved when the remaining copy is inactivated by spontaneous mutation [28, 29]. Sporadic renal tumours require spontaneous mutation of two wild type *VHL* alleles [30].

VHL genetic changes are believed to be exclusively associated with ccRCC but van Houwelingen and colleagues have detected *VHL* mutations in 15% of non-ccRCCs from a cohort of sporadic RCC patients in Netherlands. They noted that the percentage of patients with *VHL* mutation was significantly higher for ccRCC compared to RCCs of other histological types [31]. Other studies however found no *VHL* mutation in other subtypes [32–34].

Inactivation of *VHL* may play an important role in the pathogenesis of ccRCC, but the association of *VHL* status with clinicopathological parameters and disease progression is still unclear and contradictory. Some studies showed that the presence or absence of *VHL* alterations does not affect tumour stage, grade, or prognosis [35–37]. It has also been shown that there is no correlation between *VHL* mutation or methylation status with angiogenesis and proliferation of ccRCC [35, 38]. Brauch et al. and Schraml et al. reported an association of tumour *VHL* alterations with advanced stage and adverse prognosis [35, 39]. In contrast, several other studies revealed favourable prognosis for tumours with *VHL* inactivation or alteration [40–44]. These contradictory prognostic findings could be a result of complex transcriptional or posttranscriptional responses in addition to the various genetic aberrations which contribute to the heterogeneous characteristics of RCCs [35]. It is postulated that the *VHL* independent activation of other signal transduction pathways such as the mammalian target of rapamycin (mTOR), nuclear factor kappa-light-chain-enhancer of activated B cells (NF-κB), signal transducer and activator of transcription 3 (STAT-3), or epidermal growth factor receptor (EGFR) pathways could be responsible for tumour progression and tumours activated by several different mechanisms could be more aggressive [42]. Moreover, ccRCC tumours caused by VHL syndrome are of lower grade, less likely to metastasize, and have better 10-year survival compared to sporadic *VHL* RCCs, which may harbour other predisposing mutations [21].

Nevertheless, the discovery of the *VHL* gene in familial and sporadic ccRCC has revolutionised treatment for advanced RCC. Targeted therapy aiming at suppressing angiogenesis through VEGF or PDGF mediated pathways has replaced immunotherapy such as interferon alpha (IFNα) and interleukin-2 (IL-2) as treatment for metastatic RCC. The current FDA approved targeted therapy drugs for RCC which are the tyrosine kinase inhibitors (sunitinib, sorafenib, pazopanib, and axitinib), monoclonal antibody to VEGF (bevacizumab), and the mTOR inhibitors (temsirolimus and everolimus) [45]. Targeted therapy has improved treatment outcome as the overall and cancer specific survival of metastatic RCC patients has improved in the targeted therapy era compared to the immunotherapy era [46, 47].

2.2. Chromosome 3 Translocations. A number of studies have reported hereditary ccRCC associated with translocation of chromosome 3, thus supporting the role of chromosome 3 in the pathogenesis of ccRCC. Cohen et al. (1979) first discovered a reciprocal translocation at (3;8)(p14.2;q24) in a family with hereditary ccRCC [48]. A possible gene of interest, *FHIT*, has been identified in that chromosome 3 region, which will be discussed in the next section. Since

then, other constitutional translocations in chromosome 3 regions have been reported. These translocations such as t(1;3)(q32;q13), t(2;3)(q33;q21), t(2;3)(q35;q21), t(3;6)(q12;q15), and t(3;8)(p13;q24) were found in familial ccRCC [49–54]. In some familial chromosome 3 translocations identified, t(3;4)(p13;p16), t(3;4)(q21;q13), t(3;6)(p13;q25), and t(3;15)(p11;q21), only one family member developed ccRCC [55–57]. The involvement of several TSG genes has been suggested, for example, t(1;3)(q32;q13) (*NORE1* and *LSAMP*), t(2;3)(q33;q21) (*DIRC1*), t(2;3)(q35;q21) (*DIRC2* and *DIRC3*), and t(3;8)(p14.2;q24) (*FHIT* and *TRC8*). However, these translocations result from different breakpoints and some translocations had no identifiable breakpoint associated genes [52, 53, 58]. Hence, a three-step model has been proposed for familial chromosome 3 translocation ccRCC. The first step is inherited translocation of chromosome 3, followed by the loss of the 3p segment, and finally somatic mutation of the remaining 3p allele, which may contain the VHL gene or other TSGs located at 3p [54, 59].

2.3. Fragile Histidine Triad (FHIT). Although *VHL* plays a significant role in our understanding of ccRCC, it is not the only genetic aberration in chromosome 3p region. In ccRCC with 3p deletion with and without *VHL* alterations, inactivation of TSGs at 3p12-p21 appears to play a role in tumourigenesis [33, 60]. Numerous studies have been carried out to identify potential TSGs along this region. One such gene is *FHIT* located in the 3p14.2 region. Chromosomal translocation at t(3;8)(p14.2;q24) was first described in hereditary RCC and a common region of loss in chromosome 3 was found in sporadic ccRCC [61–64]. *FHIT* gene has been identified at this locus in several other malignancies including lung, breast, cervical, gastric, and bladder cancers [65–69]. The *FHIT* gene encompasses the chromosomal fragile site FRA3B, a frequently observed breakpoint in many cancers including RCC [70, 71]. As a result of inactivation, FHIT protein expression is low or absent in most ccRCC tumours [72–74].

The specific function of the FHIT protein is still unclear, but studies have demonstrated the role of the *FHIT* gene in tumour suppression. For example, there was an increase in formation of spontaneous tumours and susceptibility to carcinogen-induced tumours in *FHIT* knockout mice compared to mice with functional *FHIT* [75, 76]. There is a significant correlation between low or absence of FHIT protein expression and low grade and early stage ccRCC tumours indicating that LOH of FHIT may play a role in early tumour development [73, 74, 77, 78]. Interestingly, Ramp et al. reported that higher FHIT protein expression is linked to poorer patient survival and is an independent prognostic marker in ccRCCs [73]. Although FHIT is lower in ccRCC compared to normal kidney, higher FHIT levels in higher grade and stage tumours do not support the tumour suppressor function of FHIT [72–74]. Ramp et al. suggested that reversible epigenetic inactivation such as gene hypermethylation or posttranslational events may reactivate FHIT as the tumour progresses [73, 77]. However, there has yet to be conclusive evidence for these mechanisms.

2.4. Ras Association Domain Family 1A (RASSF1A). Another TSG associated with ccRCC in 3p chromosome region is *RASSF1A* gene located at 3p21.3. RASS1A protein regulates microtubule formation, cell cycle control, and apoptosis [79]. Reintroduction of RASSF1A in lung and breast cancer cell lines inhibited cell cycle progression and proliferation [80]. *RASS1A* is inactivated by hypermethylation in the promoter region and this is frequently seen in ovarian, breast, and lung tumours, including ccRCC [81–83]. Peters et al. found significantly increased methylation in ccRCC tumours compared to normal tissues but also detected a subgroup of methylated sequences in the normal tissue [84]. The normal tissue was obtained from histologically benign region of the tumour bearing kidney, suggesting that hypermethylation of *RASSF1A* is involved in early tumour formation of RCC [84]. In ccRCC patients, hypermethylation of the *RASSF1A* promoter was significantly associated with advanced stage, higher grade, and unfavorable patient survival [85, 86]. Tezval et al. reported that most ccRCC tumours have low RASS1A protein expression but a subset of tumours with increased expression is associated with higher stage and grade [87]. This is somewhat contradictory to the tumour suppressor function of the protein. More studies on protein expression of RASSF1A in ccRCC tumour tissue are needed to understand its effect on patient prognosis. Although less frequently reported, *RASSF1A* inactivation is also found in approximately 44% of papillary RCC [88].

2.5. Chromatin Modification Genes. Recently, NGS or exome sequencing studies have discovered several novel genes involved in chromatin modification which are mutated in ccRCC [89–91]. The newly identified genes are polybromo-1 (*PBRM1*), AT-rich interactive domain-containing protein 1A (*ARID1A*), BRCA1 associated protein-1 (*BAP1*), SET domain-containing 2 (*SETD2*), and lysine- (K-) specific demethylase 5C (*KDM5C*) [89–93]. *PBRM1* mutations are found in up to 41% of ccRCC, making it the second most mutated gene after *VHL* [90]. *PBRM1*, *BAP1*, and *SETD2* are all located near the 3p21 region and, similar to *VHL*, are proposed to be inactivated through the Knudson two-hit model [94]. As loss or deletion of 3p chromosome region is common in ccRCC, inactivation of these genes is achieved by further mutations in the remaining allele [90].

The discovery of these frequently mutated genes along with advances in NGS technology has led to interest in intratumour heterogeneity analysis in ccRCC. This provides an insight into the various mutations that may take part in tumour initiation or progression and possibly aid in fine tuning targeted therapy in the future. Multiple regions from a single tumour region were subjected to sequencing and mutations were mapped onto a phylogenic tree to illustrate the evolution of mutational events. Early or ubiquitous mutations are located at the trunk while subsequent or intratumour subclonal mutations are located at the branches. A ubiquitous mutation is found in all regions of a tumour analysed, whereas subclonal mutations are only found in a subpopulation of tumour cells [94, 95].

VHL was mapped as a ubiquitous driver mutation in 64–100% of ccRCC tumours analysed by Gerlinger et al. and Sankin et al. [95, 96]. *BAP1*, *PBRM1*, *SETD2*, and *KDM5C* mutations were found in different subclones in the same tumour, indicating that these were later mutations [95, 96]. However, *PBRM1* was also a ubiquitous mutation in 20–30% of ccRCC tumours analysed [95, 96]. Sankin et al. reported an increased mutation frequency in intratumour multiregion analysis, compared to earlier large scale sequencing studies [96]. This was especially observed in nonubiquitous mutations, such as *SETD* and *KDM5C* [96]. They suggested that the actual mutation rate may be higher than reported in earlier studies, but this will have to be validated in a larger sample sized multiregion sequencing analysis. Although most studies have focused on mutations of these genes in sporadic ccRCC, germline *PBRM1* and *BAP1* mutations have been detected in familial ccRCC [97, 98]. Germline *BAP1* mutation also predisposes affected individuals to uveal melanoma, malignant pleural mesothelioma, and cutaneous melanoma [99].

These chromatin modification genes function as TSGs and have been implicated in other cancers, such as *ARID1A* and *SETD2* in breast cancer and *KDM5C* in prostate cancer [100–102]. Alterations of the chromatin modification proteins could lead to disruptions of transcriptional regulation and tumour formation [92]. For example, silencing of *PBRM1* in ccRCC cell lines increased proliferation and migration, supporting its role as a TSG [90]. In a RCC cell line with *BAP1* mutation, 769-P, cell proliferation was inhibited by the introduction of wild type *BAP1* [91].

The roles of these chromatin modification genes and their proteins products are not fully understood yet, but various studies have shown that the mutational status of these genes may possess prognostic influence on ccRCC. Low PBRM1 expression was reported to correlate with advanced stage, higher Fuhrman grade, and worse disease specific survival [103, 104]. In contrast, Hakimi et al. and Sato et al. found no relationship between disease-free or disease specific survival and *PBRM1* mutational status [105, 106]. BAP1 loss was associated with metastasis, advanced stage and Fuhrman grade, sarcomatoid differentiation, and worse overall and disease specific survival [91, 105, 107, 108]. Compared to tumours exclusively mutated for *PBRM1*, tumours with *BAP1* only mutation conferred adverse clinicopathological features and prognosis [109, 110]. Based on these findings, *BAP1* mutational status appears to be a strong prognostic indicator for ccRCC. Low ARID1A mRNA and BAF250a (protein product of *ARID1A*) levels also correlated with higher stage, grade, and worse prognosis while *SETD2* mutation was associated with worse disease specific survival [93, 105, 111].

2.6. Other Genetic Aberrations. Other genetic aberrations of interest, such as changes at chromosome regions 5q, 8p, 9p, and 14, may affect the prognosis of ccRCC. Copy number gains at 5q conferred a favourable prognosis whereas a loss had an adverse effect [112–114]. LOH in 8p, 9p, and 14q has been associated with higher grade, stage, unfavourable prognosis, and tumour recurrence [115–121]. Potential candidate genes include *CDK2NA* (cyclin-dependent kinase inhibitor 2A) at 9p21 and *HIF1A* at 14q23.2 [118, 119, 121]. *CDK2NA* encodes the p16 tumour suppressor protein which plays an important role in cell cycle regulation by preventing cells progressing from G1 phase to S phase [122].

Recent sequencing, transcriptome, and integrated data analyses have revealed frequently mutated signalling pathways in ccRCC such as the phosphoinositide 3-kinase PI3K-AKT-mTOR and p53 pathways [106, 123]. The PI3K-AKT-mTOR pathway, which regulates angiogenesis, cell cycle progression, and proliferation, is a target for mTOR inhibitors temsirolimus and everolimus. Together, genes involved in the pathway, consisting of *MTOR*, *PTEN*, *PIK3CA*, *AKT2*, and others, have alterations in 26–28% of ccRCC tumours [106, 123]. These findings provide concrete evidence on the genetic changes directly associated with the PI3K-AKT-mTOR pathway in ccRCC. Targeted therapy with mTOR inhibitors in RCC was based on the understanding that elevated HIF could induce the PI3K/AKT pathway and promote angiogenesis [124]. Alterations of the genes found in the p53 signalling pathway, which includes *TP53* and *CDK2NA*, could be detected in 40% of tumours [106]. The p53 pathway plays a role in apoptosis, inhibition of angiogenesis, and genomic stability. Knowledge in deregulated signalling pathways would help in providing patients with personalised targeted therapy and improving treatment outcome.

Differential Diagnosis

Clear Cell Tubulopapillary RCC. Clear cell tubulopapillary RCC is a recently identified RCC subtype comprising of cells with clear cytoplasm and papillary architecture. It is often reported in patients with end stage kidney disease but has been found in normal functioning kidneys and is typically low grade [125]. Although clear cell tubulopapillary RCC mimics ccRCC and pRCC histologically, it has a different genetic profile from both subtypes [126]. Clear cell tubulopapillary RCCs lack deletions of 3p typical of ccRCC or gains of chromosome 7 and loss of chromosome Y characteristic of pRCC [126–128]. In addition, clear cell tubulopapillary RCC lacks *VHL* mutation commonly found in the ccRCC subtype [129].

3. Papillary Renal Cell Carcinoma (pRCC)

Papillary RCC is the second most common subtype, making up approximately 10% of all RCCs. Papillary RCC is characterised by tumour cells arranged in tubulopapillary architecture. Delahunt and Eble have proposed the subclassification of pRCCs into two histological groups, type 1 and type 2 [130]. Type 1 tumours are characterised by small cells with scant cytoplasm and small nuclei while type 2 tumours have large cells with plentiful eosinophilic cytoplasm and large spherical nuclei. Type 2 tumours are generally more aggressive, with more advanced grade and stage than type 1 tumours [130, 131]. Compared to ccRCC, pRCCs have a better prognosis with a metastatic rate of 3.4–14.9% at presentation and 5-year cancer specific survival of 79.4–91% [12–14].

3.1. Chromosomes 7 and 17. Papillary RCCs frequently display gains of chromosomes 7 and 17 [132–134]. Trisomies 7 and 17 discovered in small papillary renal cell neoplasia indicate that these genetic alterations may be involved in initial tumour development [135]. Based on past studies, polysomy 7 is not a reliable predictor of survival, stage, grade, or proliferation rate of papillary renal tumours [132, 133, 136, 137]. Polysomy 7 in ccRCC however was correlated with higher stage and grade [133]. The prognostic value of polysomy 17 in pRCC is contradictory. Balint et al. found no significant association between chromosome 17 gains and tumour grade or size [132]. In contrast, Gunawan et al. and Klatte et al. significantly correlated chromosome 17 polysomy with lower stage, less lymph node, and distant metastases, as well as a favourable survival [137, 138].

3.2. MET Protooncogene. At present, only one gene on chromosome 7 has been positively identified and linked to pRCC. Hereditary pRCC (HPRC) associated with type 1 tumours is caused by the mutation of the *MET* protooncogene at 7q31. An activating missense mutation of the *MET* gene and duplication of chromosome 7 along with the mutated *MET* gene were postulated to increase the oncogenic effect of *MET* [139, 140]. *MET* mutation associated hereditary pRCC and sporadic pRCC are typically low grade, bilateral tumours with multiple lesions [8, 9, 141]. The protein product of the *MET* gene is c-met, a hepatocyte growth factor receptor (HGFR). Binding of the hepatocyte growth factor (HGF) or c-met to the MET receptor induces several biological responses which promote oncogenesis, including cell motility, cell differentiation, proliferation, angiogenesis, and invasion [142]. The role of c-met in pRCC has not been clearly elucidated but in hereditary pRCC it is suggested that germline mutations of the *MET* gene promote proliferation, tubulogenesis, and tumour initiation [143].

MET mutation is estimated to be present in 5–21.6% of sporadic pRCC [8, 108, 139, 141]. A recent study by Albiges et al. reported copy number gains of MET in 46% of type II pRCC and in 81% of type I pRCC [108]. The c-met protein is strongly expressed in 80–90% of pRCC, indicating a role of *MET* copy number gains in protein activation [108, 143, 144]. Interestingly, there is no significant difference between c-met expressions in type 1 and type 2 pRCC although tumours with MET mutations favour the type 1 histology [141, 143, 144]. Sweeney et al. found a significant correlation between c-met expression and higher tumour stage and a trend towards a favourable overall survival rate for patients with c-met negative tumours [143]. To date, no other studies have shown prognostic association of c-met protein or *MET* gene in pRCC. In contrast, c-met expression is lower in ccRCC but studies have shown significant correlation of positive c-met immunoreactivity with metastasis and higher grade and stage [144, 145]. A recent study by Gibney et al. reported a correlation of higher c-met expression with higher grade and stage and worse disease specific survival in RCCs [146]. This may not be specific to pRCCs as they analysed all RCC subtypes, including a majority of ccRCC [146]. Regardless of the prognostic significance, the c-met signalling pathway appears to be an attractive target for pRCC. Phase II clinical trials of c-met pathway inhibitors, volitinib and foretinib, are currently ongoing for advanced pRCC [147, 148].

3.3. Fumarate Hydratase (FH). Besides *MET* mutation associated HPRC, another form of hereditary pRCC is found in the autosomal dominant syndrome, hereditary leiomyomatosis, and renal cell carcinoma (HLRCC). Affected individuals are predisposed to develop cutaneous leiomyomas, uterine fibroids, and type 2 pRCC [149]. Renal tumours in HLRCC patients are characteristically solitary and unilateral with a propensity for nodal or distant metastasis [150, 151]. In rare cases, renal tumours are of collecting duct RCC histology [149, 152]. Germline mutation of the *FH* gene has been identified and mapped to chromosome 1q42-43 [152, 153]. Fumarate hydratase (FH) protein is an enzyme responsible for converting fumarate to malate in the Krebs cycle. As a consequence of missense, frameshift, insertion/deletion, nonsense, or complete deletions of the *FH* gene, enzymatic activity of FH is significantly decreased [154]. Loss of FH activity causes the accumulation of fumarate, which can act as a competitive inhibitor of HIF prolyl hydroxylase (HPH) [155]. HPH degrades hypoxia inducible factors (HIFs) in normoxia conditions; hence elevated levels of fumarate result in stabilization and accumulation of HIFs [155]. Elevated HIFs promote angiogenesis and tumour progression. Compared to *VHL* and *MET*, mutation of *FH* in sporadic RCC is very rare [156]. For example, according to the COSMIC (Catalogue of Somatic Mutations in Cancer) database, *FH* mutations were found in 3 out of 1383 renal tumours analysed [157].

3.4. Other Genetic Aberrations. Deletions are often found in chromosomes X and Y of pRCC tumours. The effects of these chromosomal losses in pRCC are not well documented in literature and no TSG has been identified yet. Only one study, by Jiang et al., has significantly linked losses of chromosome Xp with shorter patient survival [158]. Besides gains of chromosomes 7 and 17, gains of chromosomes 12, 16, and 20 and loss of chromosome Y have also been detected in renal papillary adenomas, suggesting that these chromosomal alterations may be involved in early neoplastic changes in pRCC [159, 160]. Multiregion sequencing analysis confirmed that gains in chromosomes 7, 12, 16, and 17 are ubiquitous early events in pRCC tumourigenesis [161]. *BAP1*, *SETD2*, *ARID2*, and the Nrf2 pathway genes (*KEAP1*, *NHE2L2*, and *CUL3*) were identified as pRCC driver mutations, often found in tumour subclones. ARID2 forms the subunit of the SWI/SNF chromatin-remodeling complex and is functionally related to ARID1A, while the NrF2 pathway protects cells against oxidative stress and regulates cell survival [161, 162]. However, less than 10% of pRCC harboured these mutations [161]. Most genetic changes were in the form of somatic copy number alterations, which were predominantly copy number gains, but the genes associated with these copy number alterations have yet to be identified [161].

Other chromosomal aberrations in pRCC are as listed in Table 1. Among these, loss of 9p may be a promising prognostic marker as Gunawan et al. and Klatte et al. associated the loss with higher stage, lymph node involvement, and increased risk of death from pRCC [137, 138]. Allelic

Table 1: (a) Chromosome and genetic aberrations in clear cell RCC. (b) Chromosome and genetic aberrations in papillary RCC. (c) Chromosome and genetic aberrations in chRCC, RO, and CDRCC.

(a)

Chromosome	Type of genetic alteration	Candidate gene	Incidence	Function of protein	Prognosis
3p25-26	LOH, hypermethylation, mutations	*VHL*	Found in 57–91% of tumours [30, 31, 37, 40, 163–165]	pVHL targets HIFa degradation; nonfunctioning pVHL does not degrade HIFa leading to angiogenesis	No clear association between *VHL* status and tumour grade and stage or survival of patients [31, 36–38, 40, 165]
3p14.2	LOH, translocation, hypermethylation	*FHIT* contains chromosome fragile site *FRA3B*	Aberrations in 69–90% of ccRCC [62, 64, 78, 166]; 51–90% of ccRCCs showed reduced or absent FHIT protein expression [72, 74, 77]	FHIT protein is involved in apoptosis and proliferation [167–170]	*FHIT* loss, an early event in RCC; correlation of inactivation with lower grade and stage as well as better survival [73, 74, 77, 78]
3p21.3	Hypermethylation	*RASSF1A*	Methylation in 23–91% ccRCC tumours [88, 171]	RASSF1A promotes cell cycle arrest, apoptosis, and microtubule stability [79]	Hypermethylation of the *RASSF1A* promoter is significantly associated with advanced stage, grade, and worse cancer specific survival [85, 86]; loss of RASS1A protein is found in most ccRCC; but tumours with RASSF1A immunopositivity associated with higher stage, grade, and worse survival [87]
3p21	Truncating and missense mutations	*PBRM1*	Mutations in 29–41% of ccRCC tumours [90, 92, 105, 109]	BAF180 subunit of the SWI/SNF (switch and sucrose nonfermentable) chromatin remodeling complex; SWI/SNF complex regulates cell differentiation, proliferation, replication, transcriptional regulation, and DNA repair [90, 172, 173]	Due to contradictory findings, relationship of *PBRM1* status and prognosis is still unclear [103–106]
1p36.11	Copy number loss	*ARID1A*	Copy number loss in 16% of patients with ccRCC [93]	BAF250a subunit of SWI/SNF complex	Low ARID1A mRNA and BAF250a immunostaining associated with higher stage, grade, and worse disease-free and disease specific survival [93, 111]
3p21.3	Truncating and missense mutations	*BAP1*	Inactivated in 6–15% of ccRCC [91, 92, 105, 109]	BAP1 is involved in cell cycle regulation [174]	*BAP1* is an indicator of worse prognosis [91, 105, 107–110]
3p21.31	Truncating and missense mutations	*SETD2*	Mutation in 8–16% of tumours [92, 105, 109]	SETD2 is a histone methyltransferase controlling transcriptional regulation [175]	*SETD2* mutation associated with worse disease specific survival [105]

(a) Continued.

Chromosome	Type of genetic alteration	Candidate gene	Incidence	Function of protein	Prognosis
Xp11.2	Truncating and missense mutations	*KDM5C*	Mutation in 4–8% of tumours [92, 109]	Histone demethylase, transcriptional regulation [176]	Tumours with mutations in *BAP1*, *SETD2*, or *KDM5C* are significantly associated with higher stage [92]
5q21.2~q21.3	Copy number loss or gain	NA	Copy number gain in 32–34% and loss in 52–56.2% of tumours [112, 113]	NA	Significant association of loss at 5q21.2~q21.3 with high grade tumours in patients with 3p loss [113]
5q22~q23	Copy number loss or gain	NA	Gains in 48–52.4% and loss in 42.9–46% of tumours [112, 113]	NA	Gain at 5q22.3~q23.2 associated with smaller, low grade tumours and better disease specific survival; loss at 5q22.3~q23.2 significantly related to larger, high grade tumours and poor disease specific survival [112, 113]
5q31–qter	Copy number gain	NA	Gain in of 56.8% ccRCCs [112]	NA	Gain of 5q31–qter had better overall survival compared with patients without gain of 5q [114]
8p	LOH	NA	LOH in 32-33% of RCC tissue specimen [115, 116, 177]	NA	LOH on chromosomes 8p and 9p, a significant predictor of recurrence [115]; LOH of 8p correlated with higher stage and grade [116]
9p	LOH	Possible candidate gene at 9p21 *CDK2NA/ARF* [118, 119]	LOH in 14–33% of RCC tissue specimen [115, 117, 119]	p16 is the protein product of *CDK2NA* which regulates cell cycle [118, 119]	Associated with high grade and stage, lymph node involvement, metastases, recurrence, and worse survival [115, 117–120]
14q	LOH	Possible *HIF1A* at 14q23.2 [121]	Loss in 38–55% of tumours [116, 121, 178, 179]	HIF1a is a transcription factor which regulates cellular response during hypoxia, for example, angiogenesis	Correlation of LOH at 14q with advanced stage, grade, larger tumour size, recurrence, and shorter cancer specific survival [116, 121, 178–180]
Chromosome 7	Polysomy	NA	Polysomy 7 in 9.5–56.2% ccRCC [133, 181]	NA	Polysomy 7 associated with higher tumour grade, stage, and higher proliferative rate [133]

NA indicates not available.

(b)

Chromosome	Type of genetic alteration	Candidate gene	Incidence	Function of protein	Prognosis
Chromosome 7	Polysomy	NA	Polysomy 7 in 50–100% pRCC [133, 181, 182]	NA	Polysomy 7 is not correlated with survival, clinical features, or proliferation rate of pRCC [132, 133, 136, 137]
7q31	Missense mutation, gene duplication	*MET*	*MET* mutation present in 5–21.6% of sporadic pRCC [8, 108, 139, 141]; copy number gains in 46% of type II pRCC and in 81% of type I pRCC [108]; strong c-met protein expression in 80–90% of sporadic pRCC [143, 144]	The c-met protein is involved in cell proliferation, motility, differentiation, invasion, and angiogenesis [142, 143]	One study showed association of increasing tumour stage with c-met expression and a trend of better overall survival in patients with no c-met expression in tumours [143]
Chromosome 17	Polysomy	NA	Gains in 14.3–95.5% of pRCC [132, 134, 137, 158, 183]	NA	Trisomy 17 associated with better prognosis (lower stage, less nodal involvement and metastases, longer survival) [137, 138]; Balint et al. showed no link with tumour size and grade [132]
Chromosome Y	Loss	NA	Affects 71–87% of tumours in men [137, 138, 158, 184]	NA	Loss of chromosome Y not linked to pathological variables and survival [137]
Chromosome X	Loss	NA	Loss involving Xp in 28% and Xq in 36% of pRCC tumours [158]	NA	Losses of chromosome Xp associated with short patient survival [158]
3p	loss	NA	Allelic changes in 14–37.5% of tumours [137, 185]	NA	Loss of 3p associated with higher stage and grade, lymph node involvement, distant metastasis, larger tumour size, and worse survival [137]
Gains of 1q, chromosomes 12, 16, and 20; losses of 1p, 4q, 5q, 6q, 8p, 9p, 11, 13q, 14q, and 18 [135, 137, 138, 158, 186]					Loss of 9p associated with higher stage, larger tumour size, metastasis, lymph node involvement, recurrence, and decreased survival [137, 138]; losses of 8p and chromosome 18 correlated with higher stage, metastasis, and worse recurrence free survival [138]

NA indicates not available.

(c)

Tumour type	Chromosome	Type of genetic alteration	Candidate gene	Incidence	Function of protein	Prognosis
chRCC	Losses at chromosomes 1 (73–90%), 2 (70–90%), 6 (62–96%), 10 (70–91%), 13 (51–86%), 17 (65–90%), and 21 (32–90%) [187–190]; *TP53* mutation in sporadic chRCC (24–32%) located at 17p13.1 [191–193]					No relation between chromosomal numerical changes and the Paner grading system [190]
RO	Loss or alterations of 1p (31–86%) [188, 194, 195], chromosomes Y (100% in males) [196] and 14 (15–50%) [188, 197]					NA
	11q13	Translocation	*CCND1*	*CCND1* translocation in 11–36% of ROs [198–200]	Cyclin D1 is involved in the regulation of cell cycle, G1-S phase, and cell proliferation	NA
CDRCC	Reported losses of chromosomes 1, 1p, 6, 8p, 9p, 14, 15, 16p, and 22 and gains in 13q in CDRCC tumours [201, 202]					NA

NA indicates not available.

Table 2: Hereditary RCCs and their related genetic aberrations.

Tumour type	Syndrome	Clinical manifestation	Chromosome	Candidate gene
ccRCC	Von Hippel-Lindau (VHL)	Retinal, cerebellar and spinal hemangioblastoma; pheochromocytoma; pancreatic, epididymal and renal cysts; hemangiomas of the adrenals, liver, and lungs; endolymphatic sac tumours; cystadenoma of the epididymis or broad ligament and ccRCC (40–75%) [19, 20]	3p25	*VHL*
	Constitutional chromosome 3 translocation	ccRCC	Various breakpoints in chromosome 3	Possible breakpoint associated genes: *NORE1*, *LSAMP*, *DIRC1*, *DIRC2*, *DIRC3*, *FHIT*, *TRC8* Possible known common gene lost from translocation: *VHL*
pRCC	Hereditary papillary RCC (HPRC)	pRCC	7q31	*MET*
	Hereditary leiomyomatosis and RCC (HLRCC)	Cutaneous leiomyomas, uterine fibroids, type II Renal tumours (14–18%) for example pRCC and CDRCC [149, 152, 154, 203]	1q42-43	*FH*
chRCC or RO	Birt-Hogg-Dubé (BHD)	Skin fibrofolliculomas, pulmonary cysts, spontaneous pneumothorax, and renal cancer (20–29%) (chRCC, RO, ccRCC and pRCC) [204–206]	17p11.2	*BHD*, *FLCN*

alteration of 3p, which is characteristic of ccRCC, is also found in pRCC, although the incidence is lower [137, 185]. Loss of 3p in pRCC was associated with worse prognosis such as higher T stage and grade, lymph node involvement, distant metastasis, larger tumour size, and worse survival [137].

Differential Diagnosis

(i) Type 1 and 2 pRCC. Besides histological differences, types 1 and 2 pRCC may have some distinguishable patterns of chromosome aberrations. Some studies showed no difference in polysomies 7 and 17 frequency in types 1 and 2 tumours [132, 135] but others reported higher frequency of chromosomes 7 and 17 gains in type 1 compared to type 2 [137, 138, 158, 184–186]. Additionally, type 2 tumours have been shown to contain more chromosomal irregularities than type 1 tumours [137, 138, 186]. For example, type 2 tumours have a higher frequency of chromosomes 3p, 8, and 18 losses and 1q, 2, and 8q gains [137, 138, 184, 186]. However, no specific chromosome marker that can distinguish the two pRCC types has been identified.

(ii) Metanephric Adenoma. Metanephric adenoma is a rare neoplasm of the kidney which has morphological similarities to pRCC. The tumours comprise of small basophilic cells arranged in a tubulopapillary pattern [207]. Most metanephric adenomas are benign with good prognosis but metastases have been reported in a few cases [208, 209]. Reports of chromosomes 7 and 17 gains and chromosome Y loss are conflicting in metanephric adenoma. Brown et al. found chromosomes 7 and 17 gains and sex chromosome loss in most of the 11 metanephric adenoma tumours analysed [210]. However, other more recent studies have reported no abnormalities in chromosomes 7, 17, X, or Y [207, 211, 212]. Brunelli et al. suggested that Brown et al. may have chosen a low threshold for chromosomal gains without normal tissue controls, resulting in the overestimation of chromosome gains [212]. Other genetic aberrations in metanephric adenoma are gains of chromosome 19 and deletions in chromosome 2 [211, 213–215].

Recently, an activating missense mutation in the *BRAF* gene was discovered, which could be specific to metanephric adenoma [215, 216]. The substitution of valine for glutamic acid in the *BRAF* gene results in the V600E variant protein, which has increased activation potential compared to the wild type BRAF [216]. It is interesting to note that the *BRAF* gene is located at 7q34, but no other RCC subtypes show *BRAF* mutation, except for one detection in a pRCC [216–218]. The BRAF protein regulates the MAPK/ERK kinase pathway, promoting cell proliferation and cell survival [219]. Due to the benign nature of metanephric adenoma, the constitutive activation of the MAPK/ERK kinase pathway may be inhibited by p16, which is overexpressed in metanephric adenomas [216]. The p16 tumour suppressor protein was suggested to be activated as a self-limiting mechanism to the MAPK/ERK kinase pathway [216].

(iii) Clear Cell Tubulopapillary RCC. As mentioned previously, clear cell tubulopapillary RCC lacks gains in chromosomes 7 and 17 and loss of chromosome Y frequently found in pRCC [126].

(iv) Mucinous Tubular and Spindle Cell Carcinoma (MTSCC). Mucinous tubular and spindle cell carcinoma (MTSCC) is a newly recognized RCC subtype in the World Health Organization (WHO) 2004 classification [220]. The prognosis for MTSC is generally favourable as tumours are usually of low pathological stage at diagnosis [221]. It shares some immunohistochemical and histological features with pRCC, particularly the type 1 pRCC variants [221]. FISH analysis found no gains of chromosomes 7 and 17 and loss or chromosome Y in ten MTSCC tumours [222]. However, separate analyses by other groups showed gains in chromosomes 7 and/or 17 in their MTSCC cases [223–226]. Hence, chromosomes 7 and 17 status may not be suitable for differentiating pRCC and MTSCC. The loss of chromosome Y has only been reported in one MTSCC [226]. Other genetic alterations reported in MTSCC include losses of chromosomes 1, 4, 6, 8, 9, 13, 14, 15, and 22 [227].

(v) Xp11.2 Translocation RCC. This subtype, like MTSCC, was a new addition in the WHO 2004 classification [220]. Xp11.2 translocation RCCs predominantly affect children and adolescents but are found in adults as well [228]. Clinically aggressive metastatic cases have been reported [228, 229]. Xp11.2 translocation RCC cells have mixed papillary or nested structure and eosinophilic cytoplasm which may be mistaken for pRCC. Xp11.2 translocation RCCs are characterised and identified by balanced translocations of the transcription factor E3 (*TFE3*) gene on chromosome Xp11.2, resulting in gene fusions of the *TFE3* gene [230, 231]. Depending on the breakpoint of the reciprocal gene, there are six known different *TFE3* gene fusion combinations [230]. The gene fusions lead to overexpression of TFE3 protein and immunoreactivity with TFE3 protein is a distinguishing feature of Xp11.2 translocation RCCs [232].

4. Chromophobe Renal Cell Carcinoma (chRCC)

Chromophobe RCC, arising from the intercalated cells of the renal collecting ducts, represents 5% of RCC cases. Histologically, chRCC can be grouped into the classic, eosinophilic, or mixed variants. Chromophobe RCC cells are large and polygonal with distinct cell borders and irregular, wrinkled nuclei. The classic variant has pale, finely granular cytoplasm while the eosinophilic variant has granular eosinophilic cytoplasm [201]. Clinical outcome is similar for the different variants [233]. Compared to other RCC subtypes, chRCC has a more positive clinical outcome as it is less likely to metastasize [233, 234]. Metastasis at presentation is approximately 2.5–2.8% and disease progression after surgical resection occurs in 4.1–16.3% of chRCC patients [233, 235].

4.1. Birt-Hogg-Dubé (BHD) Gene. Hereditary chRCC is found in individuals with Birt-Hogg-Dubé syndrome (BHD). BHD is an autosomal dominant disorder characterised by benign skin lesions (fibrofolliculomas, trichodiscomas, and acrochordons), renal tumours, pulmonary cysts, and spontaneous pneumothorax. Renal tumours of different histologies such as ccRCC, pRCC, chRCC, and oncocytoma have been reported in BHD sufferers with chRCC and oncocytomas being the predominant types [204]. Germline mutation of the BHD or folliculin (FLCN) gene was discovered and mapped to chromosome 17p11.2 in families with BHD syndrome [205, 236]. LOH, frameshift, or missense mutations inactivate the *BHD* gene, decreasing BHD mRNA levels and folliculin protein expression [237, 238]. The function of the folliculin protein has not been completely elucidated but studies have shown that folliculin plays a role in mTOR complex 1 (TORC1) regulation [239, 240]. Kidney specific BHD knockout mice developed polycystic kidneys with upregulation of the Akt-mTOR signalling pathway, providing a link between BHD loss and renal oncogenesis [239, 240]. Unlike the *VHL* gene in ccRCC, *BHD* mutation is rarely reported in sporadic renal tumours; hence the role of folliculin in sporadic RCC is unclear [241, 242]. However, Gad et al. reported *BHD* mutations in 10.9% of chRCC and 5.6% of oncocytomas from their case series of sporadic renal tumours [191].

4.2. Other Genetic Aberrations. Common genetic alterations found in sporadic chRCC are the LOH at chromosomes 1, 2, 6, 10, 13, 17, and 21 [187, 188, 243, 244]. There is no difference in chromosomal loss pattern between eosinophilic and classic variants of chRCC [189]. One frequently mutated candidate gene identified in sporadic chRCC is *TP53* at 17p13.1 [191–193]. The *TP53* TSG, which is commonly implicated in cancers, regulates cell cycle arrest, apoptosis, and cell differentiation, preventing impaired DNA from being passed on to the daughter cells [245]. Davis et al. identified mutations of PTEN in chRCC but an earlier study by Sükösd et al. found no *PTEN* mutation in chRCC [192, 246]. Currently, no other candidate genes have been confirmed yet. Information on the prognostic value of genetic alterations in chRCC is scarce, possibly because of the low metastasis rate and good prognosis in chRCC. Gains of chromosomes 1–4, 6–12, 14, 15, and 17 were associated with sarcomatoid transformation in chRCC but there was no relation between chromosome change and the Paner grading system [61, 190]. This grading system, proposed by Paner et al., provides superior prognostic value in chRCC, compared to the Fuhrman grading system commonly used for ccRCC and pRCC [247].

Differential Diagnosis

Renal Oncocytoma. Chromophobe RCC and RO pose a diagnostic challenge as both tumours have morphological overlaps. Correct diagnosis is important because RO is largely benign while chRCC is malignant. Losses of chromosomes 2, 6, 10, 13, 17, and 21, found in up to 93% of chRCCs, are not features of ROs and could be used to differentiate the two tumour types [243, 244, 248].

5. Renal Oncocytoma (RO)

Renal oncocytomas are benign neoplasms accounting for 3–7% of renal neoplasms. Originating from the collecting ducts, RO cells are arranged in a nested, tubular, or trabecular architecture with abundance of granular eosinophilic cytoplasm

and round uniform nuclei [4]. To date, there has only been one histologically confirmed case of metastatic RO [249].

5.1. Genetic Aberrations. Similar to chRCC, BHD syndrome predisposes affected individuals to develop RO, but BHD mutation is seldom found in sporadic cases [241]. Other genetic alterations characteristic of ROs are losses at chromosomes 1, 14, and Y, as well as chromosome rearrangement at 11q13 [194, 196, 197, 244, 250]. Rearrangement of cyclin D1 (*CCND1*) gene has been linked to the translocation at 11q13 [198, 250]. ROs with rearrangement at 11q13 have been reported along with overexpression of cyclin D1, the protein product of *CCDN1* gene [198, 250]. Cyclin D1 is involved in the regulation of cell cycle in the G1-S phase and is found to be overexpressed in a few tumours such as B-cell lymphoma, breast cancer, and squamous cell carcinoma [251]. Dysregulation of cyclin D1 may contribute to the overproliferation of cells leading to RO formation.

Differential Diagnosis

Chromophobe RCC. As illustrated previously, losses of chromosomes 2, 6, 10, 13, 17, and 21 in chRCC distinguishe RO from chRCC. Both RO and chRCC contain loss of chromosome 1. It was proposed that chromosome 1 loss may represent a common early event in the tumourigenesis of both RO and chRCC [197, 248]. Additional losses of chromosomes 2, 6, 10, 13, 17, and 21 in RO may lead to malignant transformation to chRCC [197, 248, 252].

6. Collecting Duct Renal Cell Carcinoma (CDRCC)

Collecting duct RCC is an uncommon histological subtype, accounting for 0.4–1.8% of all RCCs [253]. CDRCC cells have a tubulopapillary or hobnail structure, with eosinophilic cytoplasm and large nuclei. CDRCC is clinically aggressive with a higher metastatic rate and poorer prognosis compared to other RCC subtypes [253]. Patients are often diagnosed at an advanced stage, including 32–45% with distant metastasis and 42–44% with positive lymph nodes [253, 254].

6.1. Genetic Aberrations. A cytogenetics study found monosomies 1, 6, 14, 15, and 22 in three CDRCC tumours [202]. Another recent study in 29 CDRCC tumours reported genetic losses at 8p, 16p, 1p, and 9p and gains in 13q [201]. Loss of chromosome 3 is rarely reported in CDRCC whereas frequent loss of chromosome 1 is similarly seen in RO and chRCC, both originating from the renal collecting duct [255]. Hence, loss of chromosome 1 might be more characteristic of renal tumours from the collecting duct whereas chromosome 3p loss is more typical of renal tumours from the proximal tubule [256]. Steiner et al. detected a region of genetic loss at 1q32.1-32.2 in 69% of CDRCC but no TSG has been identified yet [256].

Due to the rarity of CDRCC, knowledge on genetic aberrations and the role they play in pathogenesis of the tumour is lacking. A better understanding of the contribution of genetic alterations in CDRCC would be interesting because of the aggressive behaviour of the disease.

Differential Diagnosis

(i) Upper Urinary Tract Urothelial Carcinoma. Upper urinary tract urothelial carcinoma (UUTUC) and CDRCC display some similarities in histology and immunoreactivity and hence may present some difficulties in diagnosis [257]. A cytogenetic comparison of UUTUC and CDRCC showed distinct genetic alterations in the two tumour types [201]. CDC showed frequent losses at 8p, 16p, 1p, and 9p and gains at 13q while UUTUC showed losses at 9q, 13q, and 8q and gains at 8p [201].

(ii) Renal Medullary Carcinoma. Renal medullary carcinoma (RMC) is a rare, highly aggressive form of kidney cancer with predominance in individuals with sickle cell trait. Renal medullary carcinoma and CDRCC are both aggressive with some similarities in morphology and immunoreactivity [258]. Swartz et al. analysed 9 RMC tumours for genetic aberrations but found only loss of chromosome 22 in one case [259]. The lack of genetic losses or gains was surprising given that RMCs are aggressive and are closely associated with sickle cell trait [259]. Gatalica et al. evaluated 3 patients with RMC for chromosomal abnormalities and compared their results with findings of other publications on RMC and CDRCC cytogenetics [260]. They concluded that no consistent chromosomal abnormalities were observed in RMCs or CDRCC [260]. However, limited studies due to the rarity of both tumour types may have contributed to these inconsistent findings.

(iii) Tubulocystic Renal Cell Carcinoma. Tubulocystic RCCs are characterised by multiple tubules and cysts with bubble-wrap appearance, eosinophilic cytoplasm, and presence of hobnail cells [261]. It was originally thought to originate from the collecting duct and was classified as low grade CDRCC due to its indolent clinical behaviour [262]. Recent analyses have suggested that tubulocystic RCC might be of proximal tubule origin from its immunostaining profile and ultrastructural features (Pax 2 positivity and presence of short microvilli with brush border structure) [261, 263]. Zhou et al. and Al-Hussain et al. reported either gains of chromosomes 7 or 17 and loss of chromosome Y in their case series of tubulocystic RCC tumours, indicating similarities to pRCC [263, 264]. The tumours that they analysed consisted of areas with coexisting pRCC or CDRCC morphologies [263, 264]. However, another case series by Amin et al. found none of these chromosomal anomalies typical of pRCC [261]. A possible reason for this discrepancy could be that the tumours analysed by Amin et al. were purely tubulocystic RCC without coexisting pRCC morphology. More studies are required for a clearer understanding of genetic changes in these tumours.

7. Conclusions

Each RCC subtype has a distinctive pattern of genetic aberrations, although there are some overlaps in chromosomal

and genetic changes. These genetic changes may play an important role in tumourigenesis and affect the progression or prognosis of the tumour. However, most genetic studies were concentrated on ccRCC and pRCC as they are two most common forms of RCC. More studies on other RCC subtypes are needed to identify the specific genetic changes which may be involved in tumourigenesis. Recent genetic studies have employed gene sequencing or gene expression profiling for discovery of novel gene mutations which could identify possible differentially expressed proteins in RCC subtypes. These proteins can be part of an immunoreactivity panel for diagnosis of RCC subtypes. Hence, detection of genetic or chromosomal changes could be a useful diagnostic or prognostic tool as adjunct to conventional immunohistochemistry and histology. Identification of frequently mutated genes and affected signalling pathways also allows for development of new therapeutic targets or personalised targeted therapy for better management of advanced RCC.

Conflict of Interests

The authors declare that there is no conflict of interests regarding the publication of this paper.

Acknowledgment

This review paper was supported by University Malaya Research Fund Assistance BK024-2013.

References

[1] M. Sun, R. Thuret, F. Abdollah et al., "Age-adjusted incidence, mortality, and survival rates of stage-specific renal cell carcinoma in North America: a trend analysis," *European Urology*, vol. 59, no. 1, pp. 135–141, 2011.

[2] N. Y. Yap, K. L. Ng, T. A. Ong et al., "Clinical prognostic factors and survival outcome in renal cell carcinoma patients—a Malaysian single centre perspective," *Asian Pacific Journal of Cancer Prevention*, vol. 14, no. 12, pp. 7497–7500, 2013.

[3] A. Znaor, J. Lortet-Tieulent, A. Jemal, and F. Bray, "International variations and trends in testicular cancer incidence and mortality," *European Urology*, vol. 65, no. 6, pp. 1095–1106, 2014.

[4] K. L. Ng, R. Rajandram, C. Morais et al., "Differentiation of oncocytoma from chromophobe renal cell carcinoma (RCC): can novel molecular biomarkers help solve an old problem?" *Journal of Clinical Pathology*, vol. 67, no. 2, pp. 97–104, 2014.

[5] D. Hanahan and R. A. Weinberg, "Hallmarks of cancer: the next generation," *Cell*, vol. 144, no. 5, pp. 646–674, 2011.

[6] B. Vogelstein and K. W. Kinzler, "Cancer genes and the pathways they control," *Nature Medicine*, vol. 10, no. 8, pp. 789–799, 2004.

[7] T. Sjöblom, "Systematic analyses of the cancer genome: lessons learned from sequencing most of the annotated human protein-coding genes," *Current Opinion in Oncology*, vol. 20, no. 1, pp. 66–71, 2008.

[8] A. Salvi, E. Marchina, A. Benetti, P. Grigolato, G. de Petro, and S. Barlati, "Germline and somatic c-met mutations in multifocal/bilateral and sporadic papillary renal carcinomas of selected patients," *International Journal of Oncology*, vol. 33, no. 2, pp. 271–276, 2008.

[9] S. Richard, R. Lidereau, and S. Giraud, "The growing family of hereditary renal cell carcinoma," *Nephrology Dialysis Transplantation*, vol. 19, no. 12, pp. 2954–2958, 2004.

[10] C. S. Ng, C. G. Wood, P. M. Silverman, N. M. Tannir, P. Tamboli, and C. M. Sandler, "Renal cell carcinoma: diagnosis, staging, and surveillance," *American Journal of Roentgenology*, vol. 191, no. 4, pp. 1220–1232, 2008.

[11] F. Algaba, H. Akaza, A. López-Beltrán et al., "Current pathology keys of renal cell carcinoma," *European Urology*, vol. 60, no. 4, pp. 634–643, 2011.

[12] B. C. Leibovich, C. M. Lohse, P. L. Crispen et al., "Histological subtype is an independent predictor of outcome for patients with renal cell carcinoma," *Journal of Urology*, vol. 183, no. 4, pp. 1309–1316, 2010.

[13] J.-J. Patard, E. Leray, N. Rioux-Leclercq et al., "Prognostic value of histologic subtypes in renal cell carcinoma: a multicenter experience," *Journal of Clinical Oncology*, vol. 23, no. 12, pp. 2763–2771, 2005.

[14] V. Ficarra, G. Martignoni, A. Galfano et al., "Prognostic role of the histologic subtypes of renal cell carcinoma after slide revision," *European Urology*, vol. 50, no. 4, pp. 786–794, 2006.

[15] K. Foster, P. A. Crossey, P. Cairns et al., "Molecular genetic investigation of sporadic renal cell carcinoma: analysis of allele loss on chromosomes 3p, 5q, 11p, 17 and 22," *British Journal of Cancer*, vol. 69, no. 2, pp. 230–234, 1994.

[16] J. C. Strefford, I. Stasevich, T. M. Lane, Y.-J. Lu, T. Oliver, and B. D. Young, "A combination of molecular cytogenetic analyses reveals complex genetic alterations in conventional renal cell carcinoma," *Cancer Genetics and Cytogenetics*, vol. 159, no. 1, pp. 1–9, 2005.

[17] M. I. Toma, M. Grosser, A. Herr et al., "Loss of heterozygosity and copy number abnormality in clear cell renal cell carcinoma discovered by high-density affymetrix 10K single nucleotide polymorphism mapping array," *Neoplasia*, vol. 10, no. 7, pp. 634–642, 2008.

[18] F. Latif, K. Tory, J. Gnarra et al., "Identification of the von Hippel-Lindau disease tumor suppressor gene," *Science*, vol. 260, no. 5112, pp. 1317–1320, 1993.

[19] S. Richard, B. Gardie, S. Couvé, and S. Gad, "Von Hippel-Lindau: how a rare disease illuminates cancer biology," *Seminars in Cancer Biology*, vol. 23, no. 1, pp. 26–37, 2013.

[20] C. A. Friedrich, "Von Hippel-Lindau syndrome. A pleomorphic condition," *Cancer*, vol. 86, no. 11, pp. 2478–2482, 1999.

[21] H. P. H. Neumann, B. U. Bender, D. P. Berger et al., "Prevalence, morphology and biology of renal cell carcinoma in von Hippel-Lindau disease compared to sporadic renal cell carcinoma," *Journal of Urology*, vol. 160, no. 4, pp. 1248–1254, 1998.

[22] M. Krieg, R. Haas, H. Brauch, T. Acker, I. Flamme, and K. H. Plate, "Up-regulation of hypoxia-inducible factors HIF-1α and HIF-2α under normoxic conditions in renal carcinoma cells by von Hippel-Lindau tumor suppressor gene loss of function," *Oncogene*, vol. 19, no. 48, pp. 5435–5443, 2000.

[23] P. H. Maxwell, M. S. Wlesener, G. W. Chang et al., "The tumour suppressor protein VHL targets hypoxia-inducible factors for oxygen-dependent proteolysis," *Nature*, vol. 399, no. 6733, pp. 271–275, 1999.

[24] M. E. Cockman, N. Masson, D. R. Mole et al., "Hypoxia inducible factor-alpha binding and ubiquitylation by the von Hippel-Lindau tumour suppressor protein," *The Journal of Biological Chemistry*, vol. 275, no. 33, pp. 25733–25741, 2000.

[25] J. Bellmunt, "Current treatment in advanced renal cell carcinoma (RCC): impact of targeted therapies in the management of RCC," *European Urology Supplements*, vol. 6, no. 7, pp. 484–491, 2007.

[26] P. Staller, J. Sulitkova, J. Lisztwan, H. Moch, E. J. Oakeley, and W. Krek, "Chemokine receptor CXCR4 downregulated by von Hippel-Lindau tumour suppressor pVHL," *Nature*, vol. 425, no. 6955, pp. 307–311, 2003.

[27] N. de Paulsen, A. Brychzy, M. C. Fournier et al., "Role of transforming growth factor-α in von Hippel-Lindau (VHL)$^{-/-}$ clear cell renal carcinoma cell proliferation: a possible mechanism coupling VHL tumor suppressor inactivation and tumorigenesis," *Proceedings of the National Academy of Sciences of the United States of America*, vol. 98, no. 4, pp. 1387–1392, 2001.

[28] W. Y. Kim and W. G. Kaelin, "Role of VHL gene mutation in human cancer," *Journal of Clinical Oncology*, vol. 22, no. 24, pp. 4991–5004, 2004.

[29] A. G. Knudson Jr., L. C. Strong, and D. E. Anderson, "Heredity and cancer in man," *Progress in Medical Genetics*, vol. 9, pp. 113–158, 1973.

[30] K. Kondo, M. Yao, M. Yoshida et al., "Comprehensive mutational analysis of the VHL gene in sporadic renal cell carcinoma: relationship to clinicopathological parameters," *Genes Chromosomes and Cancer*, vol. 34, no. 1, pp. 58–68, 2002.

[31] K. P. van Houwelingen, B. A. C. van Dijk, C. A. Hulsbergen-van de Kaa et al., "Prevalence of von Hippel-Lindau gene mutations in sporadic renal cell carcinoma: results from The Netherlands cohort study," *BMC Cancer*, vol. 5, article 57, 2005.

[32] C. Gallou, D. Joly, A. Méjean et al., "Mutations of the VHL gene in sporadic renal cell carcinoma: definition of a risk factor for VHL patients to develop an RCC," *Human Mutation*, vol. 13, no. 6, pp. 464–475, 1999.

[33] H. Moch, P. Schraml, L. Bubendorf et al., "Intratumoral heterogeneity of von Hippel-Lindau gene deletions in renal cell carcinoma detected by fluorescence in situ hybridization," *Cancer Research*, vol. 58, no. 11, pp. 2304–2309, 1998.

[34] S. C. Clifford, A. H. Prowse, N. A. Affara, C. H. C. M. Buys, and E. R. Maher, "Inactivation of the von Hippel-Lindau (VHL) tumour suppressor gene and allelic losses at chromosome arm 3p in primary renal cell carcinoma: evidence for a VHL-independent pathway in clear cell renal tumourigenesis," *Genes Chromosomes and Cancer*, vol. 22, no. 3, pp. 200–209, 1998.

[35] P. Schraml, K. Struckmann, F. Hatz et al., "VHL mutations and their correlation with tumour cell proliferation, microvessel density, and patient prognosis in clear cell renal cell carcinoma," *The Journal of Pathology*, vol. 196, no. 2, pp. 186–193, 2002.

[36] K. M. Smits, L. J. Schouten, B. A. C. van Dijk et al., "Genetic and epigenetic alterations in the von Hippel-Lindau gene: the influence on renal cancer prognosis," *Clinical Cancer Research*, vol. 14, no. 3, pp. 782–787, 2008.

[37] M. R. Alves, F. C. Carneiro, A. M. Lavorato-Rocha et al., "Mutational status of VHL gene and its clinical importance in renal clear cell carcinoma," *Virchows Archiv*, vol. 465, no. 3, pp. 321–330, 2014.

[38] M. M. Baldewijns, I. J. H. van Vlodrop, K. M. Smits et al., "Different angiogenic potential in low and high grade sporadic clear cell renal cell carcinoma is not related to alterations in the von Hippel-Lindau gene," *Cellular Oncology*, vol. 31, no. 5, pp. 371–382, 2009.

[39] H. Brauch, G. Weirich, J. Brieger et al., "VHL alterations in human clear cell renal cell carcinoma: association with advanced tumor stage and a novel hot spot mutation," *Cancer Research*, vol. 60, no. 7, pp. 1942–1948, 2000.

[40] A. C. Young, R. A. Craven, D. Cohen et al., "Analysis of VHL gene alterations and their relationship to clinical parameters in sporadic conventional renal cell carcinoma," *Clinical Cancer Research*, vol. 15, no. 24, pp. 7582–7592, 2009.

[41] A. S. Parker, J. C. Cheville, C. M. Lohse, T. Igel, B. C. Leibovich, and M. L. Blute, "Loss of expression of von Hippel-Lindau tumor suppressor protein associated with improved survival in patients with early-stage clear cell renal cell carcinoma," *Urology*, vol. 65, no. 6, pp. 1090–1095, 2005.

[42] J.-J. Patard, P. Fergelot, P. I. Karakiewicz et al., "Low CAIX expression and absence of VHL gene mutation are associated with tumor aggressiveness and poor survival of clear cell renal cell carcinoma," *International Journal of Cancer*, vol. 123, no. 2, pp. 395–400, 2008.

[43] M. Yao, M. Yoshida, T. Kishida et al., "VHL tumor suppressor gene alterations associated with good prognosis in sporadic clear-cell renal carcinoma," *Journal of the National Cancer Institute*, vol. 94, no. 20, pp. 1569–1575, 2002.

[44] J.-J. Patard, N. Rioux-Leclercq, D. Masson et al., "Absence of VHL gene alteration and high VEGF expression are associated with tumour aggressiveness and poor survival of renal-cell carcinoma," *British Journal of Cancer*, vol. 101, no. 8, pp. 1417–1424, 2009.

[45] M. N. Fishman, "Targeted therapy of kidney cancer: keeping the art around the algorithms," *Cancer Control*, vol. 20, no. 3, pp. 222–232, 2013.

[46] A. V. Soerensen, F. Donskov, G. G. Hermann et al., "Improved overall survival after implementation of targeted therapy for patients with metastatic renal cell carcinoma: Results from the Danish Renal Cancer Group (DARENCA) study-2," *European Journal of Cancer*, vol. 50, no. 3, pp. 553–562, 2014.

[47] R. A. Nelson, N. Vogelzang, and S. K. Pal, "A gap in disease-specific survival between younger and older adults with de novo metastatic renal cell carcinoma: results of a seer database analysis," *Clinical Genitourinary Cancer*, vol. 11, no. 3, pp. 303–310, 2013.

[48] A. J. Cohen, F. P. Li, S. Berg et al., "Hereditary renal-cell carcinoma associated with a chromosomal translocation," *The New England Journal of Medicine*, vol. 301, no. 11, pp. 592–595, 1979.

[49] D. Bodmer, M. Eleveld, M. Ligtenberg et al., "Cytogenetic and molecular analysis of early stage renal cell carcinomas in a family with a translocation (2;3)(q35;q21)," *Cancer Genetics and Cytogenetics*, vol. 134, no. 1, pp. 6–12, 2002.

[50] J. Chen, W.-O. Lui, M. D. Vos et al., "The t(1;3) breakpoint-spanning genes LSAMP and NORE1 are involved in clear cell renal cell carcinomas," *Cancer Cell*, vol. 4, no. 5, pp. 405–413, 2003.

[51] J. Podolski, T. Byrski, S. Zajaczek et al., "Characterization of a familial RCC-associated t(2;3)(q33;q21) chromosome translocation," *Journal of Human Genetics*, vol. 46, no. 12, pp. 685–693, 2001.

[52] B. Meléndez, S. Rodríguez-Perales, B. Martínez-Delgado et al., "Molecular study of a new family with hereditary renal cell carcinoma and a translocation t(3;8)(p13;q24.1)," *Human Genetics*, vol. 112, no. 2, pp. 178–185, 2003.

[53] M. J. Eleveld, D. Bodmer, G. Merkx et al., "Molecular analysis of a familial case of renal cell cancer and a t(3;6)(q12;q15)," *Genes Chromosomes and Cancer*, vol. 31, no. 1, pp. 23–32, 2001.

[54] A. C. M. Bonné, D. Bodmer, E. F. P. M. Shoenmakers, C. M. van Ravenswaaij, N. Hoogerbrugge, and A. G. van Kessel, "Chromosome 3 translocations and familial renal cell cancer," *Current Molecular Medicine*, vol. 4, no. 8, pp. 849–854, 2004.

[55] G. Kovacs, P. Brusa, and W. De Riese, "Tissue-specific expression of a constitutional 3;6 translocation: development of multiple bilateral renal-cell carcinomas," *International Journal of Cancer*, vol. 43, no. 3, pp. 422–427, 1989.

[56] R. P. Kuiper, L. Vreede, R. Venkatachalam et al., "The tumour suppressor gene FBXW7 is disrupted by a constitutional t(3; 4)(q21; q31) in a patient with renal cell cancer," *Cancer Genetics and Cytogenetics*, vol. 195, no. 2, pp. 105–111, 2009.

[57] A. G. van Kessel Geurts, H. Wijnhoven, D. Bodmer et al., "Renal cell cancer: chromosome 3 translocations as risk factors," *Journal of the National Cancer Institute*, vol. 91, no. 13, pp. 1159–1160, 1999.

[58] R. E. Foster, M. Abdulrahman, M. R. Morris et al., "Characterization of a 3;6 translocation associated with renal cell carcinoma," *Genes Chromosomes and Cancer*, vol. 46, no. 4, pp. 311–317, 2007.

[59] D. Bodmer, M. J. Eleveld, M. J. L. Ligtenberg et al., "An alternative route for multistep tumorigenesis in a novel case of hereditary renal cell cancer and a t(2;3)(q35;q21) chromosome translocation," *The American Journal of Human Genetics*, vol. 62, no. 6, pp. 1475–1483, 1998.

[60] A. Martinez, P. Fullwood, K. Kondo et al., "Role of chromosome 3p12-p21 tumour suppressor genes in clear cell renal cell carcinoma: analysis of VHL dependent and VHL independent pathways of tumorigenesis," *The Journal of Clinical Pathology—Molecular Pathology*, vol. 53, no. 3, pp. 137–144, 2000.

[61] F. P. Li, H.-J. H. Decker, B. Zbar et al., "Clinical and genetic studies of renal cell carcinomas in a family with a constitutional chromosome 3;8 translocation. Genetics of familial renal carcinoma," *Annals of Internal Medicine*, vol. 118, no. 2, pp. 106–111, 1993.

[62] T. Druck, K. Kastury, P. Hadaczek et al., "Loss of heterozygosity at the familial RCC t(3;8) locus in most clear cell renal carcinomas," *Cancer Research*, vol. 55, no. 22, pp. 5348–5353, 1995.

[63] F. Sükösd, N. Kuroda, T. Beothe, A. P. Kaur, and G. Kovacs, "Deletion of chromosome 3p14.2-p25 involving the VHL and FHIT genes in conventional renal cell carcinoma," *Cancer Research*, vol. 63, no. 2, pp. 455–457, 2003.

[64] R. B. Singh and P. S. Amare Kadam, "Investigation of tumor suppressor genes apart from *VHL* on 3p by deletion mapping in sporadic clear cell renal cell carcinoma (cRCC)," *Urologic Oncology*, vol. 31, no. 7, pp. 1333–1342, 2013.

[65] G. Toledo, J. J. Sola, M. D. Lozano, E. Soria, and J. Pardo, "Loss of FHIT protein expression is related to high proliferation, low apoptosis and worse prognosis in non-small-cell lung cancer," *Modern Pathology*, vol. 17, no. 4, pp. 440–448, 2004.

[66] A. Vecchione, C. Sevignani, E. Giarnieri et al., "Inactivation of the FHIT gene favors bladder cancer development," *Clinical Cancer Research*, vol. 10, no. 22, pp. 7607–7612, 2004.

[67] Q. Yang, M. Nakamura, Y. Nakamura et al., "Two-hit inactivation of FHIT by loss of heterozygosity and hypermethylation in breast cancer," *Clinical Cancer Research*, vol. 8, no. 9, pp. 2890–2893, 2002.

[68] C. Huiping, S. Kristjansdottir, J. T. Bergthorsson et al., "High frequency of LOH, MSI and abnormal expression of FHIT in gastric cancer," *European Journal of Cancer*, vol. 38, no. 5, pp. 728–735, 2002.

[69] D. Butler, C. Collins, M. Mabruk, C. B. Walsh, M. B. Leader, and E. W. Kay, "Deletion of the FHIT gene in neoplastic and invasive cervical lesions is related to high-risk HPV infection but is independent of histopathological features," *Journal of Pathology*, vol. 192, no. 4, pp. 502–510, 2000.

[70] V. Shridhar, L. Wang, R. Rosati et al., "Frequent breakpoints in the region surrounding FRA3B in sporadic renal cell carcinomas," *Oncogene*, vol. 14, no. 11, pp. 1269–1277, 1997.

[71] J. R. Karras, C. A. Paisie, and K. Huebner, "Replicative stress and the FHIT gene: roles in tumor suppression, genome stability and prevention of carcinogenesis," *Cancers*, vol. 6, no. 2, pp. 1208–1219, 2014.

[72] P. Hadaczek, A. L. Kovatich, J. Gronwald, J. Lubinski, K. Huebner, and P. A. Mccue, "Loss or reduction of Fhit expression in renal neoplasias: correlation with histogenic class," *Human Pathology*, vol. 30, no. 11, pp. 1276–1283, 1999.

[73] U. Ramp, E. Caliskan, T. Ebert et al., "FHIT expression in clear cell renal carcinomas: versatility of protein levels and correlation with survival," *Journal of Pathology*, vol. 196, no. 4, pp. 430–436, 2002.

[74] E. J. Eyzaguirre, M. Miettinen, B. A. Norris, and Z. Gatalica, "Different immunohistochemical patterns of Fhit protein expression in renal neoplasms," *Modern Pathology*, vol. 12, no. 10, pp. 979–983, 1999.

[75] N. Zanesi, V. Fidanza, L. Y. Fong et al., "The tumor spectrum in FHIT-deficient mice," *Proceedings of the National Academy of Sciences of the United States of America*, vol. 98, no. 18, pp. 10250–10255, 2001.

[76] T. Fujishita, Y. Doi, M. Sonoshita et al., "Development of spontaneous tumours and intestinal lesions in Fhit gene knockout mice," *British Journal of Cancer*, vol. 91, no. 8, pp. 1571–1574, 2004.

[77] P. Hadaczek, Z. Siprashvili, M. Markiewski et al., "Absence or reduction of FHIT expression in most clear cell renal carcinomas," *Cancer Research*, vol. 58, no. 14, pp. 2946–2951, 1998.

[78] M. Velickovic, B. Delahunt, and S. K. G. Grebe, "Loss of heterozygosity at 3p14.2 in clear cell renal cell carcinoma is an early event and is highly localized to the FHIT gene locus," *Cancer Research*, vol. 59, no. 6, pp. 1323–1326, 1999.

[79] H. Donninger, J. A. Clark, M. K. Monaghan, M. L. Schmidt, M. Vos, and G. J. Clark, "Cell cycle restriction is more important than apoptosis induction for RASSF1A protein tumor suppression," *The Journal of Biological Chemistry*, vol. 289, no. 45, pp. 31287–31295, 2014.

[80] L. Shivakumar, J. Minna, T. Sakamaki, R. Pestell, and M. A. White, "The RASSF1A tumor suppressor blocks cell cycle progression and inhibits cyclin D1 accumulation," *Molecular and Cellular Biology*, vol. 22, no. 12, pp. 4309–4318, 2002.

[81] J.-H. Yoon, R. Dammann, and G. P. Pfeifer, "Hypermethylation of the CpG island of the RASSF1A gene in ovarian and renal cell carcinomas," *International Journal of Cancer*, vol. 94, no. 2, pp. 212–217, 2001.

[82] W. Yeo, W. L. Wong, N. Wong, B. K. Law, G. M. Tse, and S. Zhong, "High frequency of promoter hypermethylation of RASSF1A in tumorous and non-tumourous tissue of breast cancer," *Pathology*, vol. 37, no. 2, pp. 125–130, 2005.

[83] N. Yanagawa, G. Tamura, H. Oizumi et al., "Promoter hypermethylation of RASSF1A and RUNX3 genes as an independent prognostic prediction marker in surgically resected non-small cell lung cancers," *Lung Cancer*, vol. 58, no. 1, pp. 131–138, 2007.

[84] I. Peters, K. Rehmet, N. Wilke et al., "RASSF1A promoter methylation and expression analysis in normal and neoplastic kidney indicates a role in early tumorigenesis," *Molecular Cancer*, vol. 6, article 49, 2007.

[85] Y. Kawai, S. Sakano, Y. Suehiro et al., "Methylation level of the RASSF1A promoter is an independent prognostic factor for clear-cell renal cell carcinoma," *Annals of Oncology*, vol. 21, no. 8, pp. 1612–1617, 2010.

[86] V. I. Loginov, D. S. Khodyrev, I. V. Pronina et al., "Methylation of promoter region of RASSF1A gene and frequencies of allelic imbalances in chromosome 3 critical regions are correlated with progression of clear cell renal cell carcinoma," *Molekuliarnaia Biologiia*, vol. 43, no. 3, pp. 429–438, 2009.

[87] H. Tezval, A. S. Merseburger, I. Matuschek, S. Machtens, M. A. Kuczyk, and J. Serth, "RASSF1A protein expression and correlation with clinicopathological parameters in renal cell carcinoma," *BMC Urology*, vol. 8, article 12, 2008.

[88] C. Morrissey, A. Martinez, M. Zatyka et al., "Epigenetic inactivation of the RASSF1A 3p21.3 tumor suppressor gene in both clear cell and papillary renal cell carcinoma," *Cancer Research*, vol. 61, no. 19, pp. 7277–7281, 2001.

[89] G. Duns, R. M. W. Hofstra, J. G. Sietzema et al., "Targeted exome sequencing in clear cell renal cell carcinoma tumors suggests aberrant chromatin regulation as a crucial step in ccRCC development," *Human Mutation*, vol. 33, no. 7, pp. 1059–1062, 2012.

[90] I. Varela, P. Tarpey, K. Raine et al., "Exome sequencing identifies frequent mutation of the SWI/SNF complex gene PBRM1 in renal carcinoma," *Nature*, vol. 469, no. 7331, pp. 539–542, 2011.

[91] S. Peña-Llopis, S. Vega-Rubín-De-Celis, A. Liao et al., "BAP1 loss defines a new class of renal cell carcinoma," *Nature Genetics*, vol. 44, no. 7, pp. 751–759, 2012.

[92] A. A. Hakimi, Y.-B. Chen, J. Wren et al., "Clinical and pathologic impact of select chromatin-modulating tumor suppressors in clear cell renal cell carcinoma," *European Urology*, vol. 63, no. 5, pp. 848–854, 2013.

[93] Z. Lichner, A. Scorilas, N. M. A. White et al., "The chromatin remodeling gene *ARID1A* is a new prognostic marker in clear cell renal cell carcinoma," *The American Journal of Pathology*, vol. 182, no. 4, pp. 1163–1170, 2013.

[94] L. Liao, J. R. Testa, and H. Yang, "The roles of chromatin-remodelers and epigenetic modifiers in kidney cancer," *Cancer Genetics*, 2015.

[95] M. Gerlinger, S. Horswell, J. Larkin et al., "Genomic architecture and evolution of clear cell renal cell carcinomas defined by multiregion sequencing," *Nature Genetics*, vol. 46, no. 3, pp. 225–233, 2014.

[96] A. Sankin, A. A. Hakimi, N. Mikkilineni et al., "The impact of genetic heterogeneity on biomarker development in kidney cancer assessed by multiregional sampling," *Cancer Medicine*, vol. 3, no. 6, pp. 1485–1492, 2014.

[97] P. R. Benusiglio, S. Couve, B. Gilbert-Dussardier et al., "A germline mutation in PBRM1 predisposes to renal cell carcinoma," *Journal of Medical Genetics*, vol. 52, no. 6, pp. 426–430, 2015.

[98] M. N. Farley, L. S. Schmidt, J. L. Mester et al., "A novel germline mutation in *BAP1* predisposes to familial clear-cell renal cell carcinoma," *Molecular Cancer Research*, vol. 11, no. 9, pp. 1061–1071, 2013.

[99] T. Popova, L. Hebert, V. Jacquemin et al., "Germline BAP1 mutations predispose to renal cell carcinomas," *American Journal of Human Genetics*, vol. 92, no. 6, pp. 974–980, 2013.

[100] J. Stein, M. Majores, M. Rohde et al., "KDM5C is overexpressed in prostate cancer and is a prognostic marker for prostate-specific antigen-relapse following radical prostatectomy," *The American Journal of Pathology*, vol. 184, no. 9, pp. 2430–2437, 2014.

[101] A. Mamo, L. Cavallone, S. Tuzmen et al., "An integrated genomic approach identifies ARID1A as a candidate tumor-suppressor gene in breast cancer," *Oncogene*, vol. 31, no. 16, pp. 2090–2100, 2012.

[102] W. Al Sarakbi, W. Sasi, W. G. Jiang, T. Roberts, R. F. Newbold, and K. Mokbel, "The mRNA expression of SETD2 in human breast cancer: correlation with clinico-pathological parameters," *BMC Cancer*, vol. 9, no. 1, article 290, 2009.

[103] R. Pawłowski, S. M. Mühl, T. Sulser, W. Krek, H. Moch, and P. Schraml, "Loss of PBRM1 expression is associated with renal cell carcinoma progression," *International Journal of Cancer*, vol. 132, no. 2, pp. E11–E17, 2013.

[104] W. H. da Costa, M. Rezende, F. C. Carneiro et al., "Polybromo-1 (PBRM1), a SWI/SNF complex subunit is a prognostic marker in clear cell renal cell carcinoma," *BJU International*, vol. 113, no. 5b, pp. E157–E163, 2014.

[105] A. A. Hakimi, I. Ostrovnaya, B. Reva et al., "Adverse outcomes in clear cell renal cell carcinoma with mutations of 3p21 epigenetic regulators BAP1 and SETD2: A report by MSKCC and the KIRC TCGA research network," *Clinical Cancer Research*, vol. 19, no. 12, pp. 3259–3267, 2013.

[106] Y. Sato, T. Yoshizato, Y. Shiraishi et al., "Integrated molecular analysis of clear-cell renal cell carcinoma," *Nature Genetics*, vol. 45, no. 8, pp. 860–867, 2013.

[107] P. Kapur, A. Christie, J. D. Raman et al., "BAP1 immunohistochemistry predicts outcomes in a multi-institutional cohort with clear cell renal cell carcinoma," *Journal of Urology*, vol. 191, no. 3, pp. 603–610, 2014.

[108] L. Albiges, J. Guegan, A. Le Formal et al., "MET is a potential target across all papillary renal cell carcinomas: result from a large molecular study of pRCC with CGH array and matching gene expression array," *Clinical Cancer Research*, vol. 20, no. 13, pp. 3411–3421, 2014.

[109] L. Gossage, M. Murtaza, A. F. Slatter et al., "Clinical and pathological impact of VHL, PBRM1, BAP1, SETD2, KDM6A, and JARID1c in clear cell renal cell carcinoma," *Genes Chromosomes and Cancer*, vol. 53, no. 1, pp. 38–51, 2014.

[110] P. Kapur, S. Peña-Llopis, A. Christie et al., "Effects on survival of BAP1 and PBRM1 mutations in sporadic clear-cell renal-cell carcinoma: a retrospective analysis with independent validation," *The Lancet Oncology*, vol. 14, no. 2, pp. 159–167, 2013.

[111] J. H. Park, C. Lee, J. H. Suh, J. Y. Chae, H. W. Kim, and K. C. Moon, "Decreased ARID1A expression correlates with poor prognosis of clear cell renal cell carcinoma," *Human Pathology*, vol. 46, no. 3, pp. 454–460, 2015.

[112] K. Nagao, S. Yoshihiro, H. Matsuyama, S. Yamaguchi, K. Oba, and K. Naito, "Clinical significance of allelic loss of chromosome region 5q22.3 approximately q23.2 in nonpapillary renal cell carcinoma," *Cancer Genetics and Cytogenetics*, vol. 136, no. 1, pp. 23–30, 2002.

[113] K. Nagao, S. Yamaguchi, H. Matsuyama et al., "Allelic loss of 3p25 associated with alterations of 5q22.3~q23.2 may affect the prognosis of conventional renal cell carcinoma," *Cancer Genetics and Cytogenetics*, vol. 160, no. 1, pp. 43–48, 2005.

[114] B. Gunawan, W. Huber, M. Holtrup et al., "Prognostic impacts of cytogenetic findings in clear cell renal cell carcinoma: gain of

5q31-qter predicts a distinct clinical phenotype with favorable prognosis," *Cancer Research*, vol. 61, no. 21, pp. 7731–7738, 2001.

[115] J. C. Presti Jr., M. Wilhelm, V. Reuter, P. Russo, R. Motzer, and F. Waldman, "Allelic loss on chromosomes 8 and 9 correlates with clinical outcome in locally advanced clear cell carcinoma of the kidney," *The Journal of Urology*, vol. 167, no. 3, pp. 1464–1468, 2002.

[116] D. Schullerus, J. Herbers, J. Chudek, H. Kanamaru, and G. Kovacs, "Loss of heterozygosity at chromosomes 8p, 9p, and 14q is associated with stage and grade of non-papillary renal cell carcinomas," *Journal of Pathology*, vol. 183, no. 2, pp. 151–155, 1997.

[117] J. la Rochelle, T. Klatte, A. Dastane et al., "Chromosome 9p deletions identify an aggressive phenotype of clear cell renal cell carcinoma," *Cancer*, vol. 116, no. 20, pp. 4696–4702, 2010.

[118] B. Grady, R. Goharderakhshan, J. Chang et al., "Frequently deleted loci on chromosome 9 may harbor several tumor suppressor genes in human renal cell carcinoma," *Journal of Urology*, vol. 166, no. 3, pp. 1088–1092, 2001.

[119] P. Schraml, K. Struckmann, R. Bednar et al., "CDKN2A mutation analysis, protein expression, and deletion mapping of chromosome 9p conventional clear-cell renal carcinomas: evidence for a second tumor suppressor gene proximal to CDKN2A," *American Journal of Pathology*, vol. 158, no. 2, pp. 593–601, 2001.

[120] D. de Oliveira, M. F. Dall'Oglio, S. T. Reis et al., "Chromosome 9p deletions are an independent predictor of tumor progression following nephrectomy in patients with localized clear cell renal cell carcinoma," *Urologic Oncology*, vol. 32, no. 5, pp. 601–606, 2014.

[121] F. A. Monzon, K. Alvarez, L. Peterson et al., "Chromosome 14q loss defines a molecular subtype of clear-cell renal cell carcinoma associated with poor prognosis," *Modern Pathology*, vol. 24, no. 11, pp. 1470–1479, 2011.

[122] W. H. Liggett Jr. and D. Sidransky, "Role of the p16 tumour suppressor gene in cancer," *Journal of Clinical Oncology*, vol. 16, no. 3, pp. 1197–1206, 1998.

[123] Cancer Genome Atlas Research Network, "Comprehensive molecular characterization of clear cell renal cell carcinoma," *Nature*, vol. 499, no. 7456, pp. 43–49, 2013.

[124] H. Guo, P. German, S. Bai et al., "The PI3K/AKT pathway and renal cell carcinoma," *Journal of Genetics and Genomics*, 2015.

[125] R. Bhatnagar and B. A. Alexiev, "Renal-cell carcinomas in end-stage kidneys: a clinicopathological study with emphasis on clear-cell papillary renal-cell carcinoma and acquired cystic kidney disease-associated carcinoma," *International Journal of Surgical Pathology*, vol. 20, no. 1, pp. 19–28, 2012.

[126] S. Gobbo, J. N. Eble, D. J. Grignon et al., "Clear cell papillary renal cell carcinoma: a distinct histopathologic and molecular genetic entity," *American Journal of Surgical Pathology*, vol. 32, no. 8, pp. 1239–1245, 2008.

[127] J. Adam, J. Couturier, V. Molinié, A. Vieillefond, and M. Sibony, "Clear-cell papillary renal cell carcinoma: 24 cases of a distinct low-grade renal tumour and a comparative genomic hybridization array study of seven cases," *Histopathology*, vol. 58, no. 7, pp. 1064–1071, 2011.

[128] H. Aydin, L. Chen, L. Cheng et al., "Clear cell tubulopapillary renal cell carcinoma: a study of 36 distinctive low-grade epithelial tumors of the kidney," *American Journal of Surgical Pathology*, vol. 34, no. 11, pp. 1608–1621, 2010.

[129] S. M. Rohan, Y. Xiao, Y. Liang et al., "Clear-cell papillary renal cell carcinoma: molecular and immunohistochemical analysis with emphasis on the von Hippel-Lindau gene and hypoxia-inducible factor pathway-related proteins," *Modern Pathology*, vol. 24, no. 9, pp. 1207–1220, 2011.

[130] B. Delahunt and J. N. Eble, "Papillary renal cell carcinoma: a clinicopathologic and immunohistochemical study of 105 tumors," *Modern Pathology*, vol. 10, no. 6, pp. 537–544, 1997.

[131] G. Pignot, C. Elie, S. Conquy et al., "Survival analysis of 130 patients with papillary renal cell carcinoma: prognostic utility of type 1 and type 2 subclassification," *Urology*, vol. 69, no. 2, pp. 230–235, 2007.

[132] I. Balint, A. Szponar, A. Jauch, and G. Kovacs, "Trisomy 7 and 17 mark papillary renal cell tumours irrespectively of variation of the phenotype," *Journal of Clinical Pathology*, vol. 62, no. 10, pp. 892–895, 2009.

[133] P. S. Amare, C. Varghese, S. H. Bharde et al., "Proliferating cell nuclear antigen and epidermal growth factor receptor (EGFr) status in renal cell carcinoma patients with polysomy of chromosome 7," *Cancer Genetics and Cytogenetics*, vol. 125, no. 2, pp. 139–146, 2001.

[134] C. L. Corless, H. Aburatani, J. A. Fletcher, D. E. Housman, M. B. Amin, and D. S. Weinberg, "Papillary renal cell carcinoma: quantitation of chromosomes 7 and 17 by FISH, analysis of chromosome 3p for LOH, and DNA ploidy," *Diagnostic Molecular Pathology*, vol. 5, no. 1, pp. 53–64, 1996.

[135] M. Brunelli, J. N. Eble, S. Zhang, G. Martignoni, and L. Cheng, "Gains of chromosomes 7, 17, 12, 16, and 20 and loss of Y occur early in the evolution of papillary renal cell neoplasia: a fluorescent in situ hybridization study," *Modern Pathology*, vol. 16, no. 10, pp. 1053–1059, 2003.

[136] J. Pailoor, R. Rajandram, N. Y. Yap, K. L. Ng, Z. Wang, and K. R. Iyengar, "Chromosome 7 aneuploidy in clear cell and papillary renal cell carcinoma: detection using silver in situ hybridization technique," *Indian Journal of Pathology and Microbiology*, vol. 56, no. 2, pp. 98–102, 2013.

[137] T. Klatte, A. J. Pantuck, J. W. Said et al., "Cytogenetic and molecular tumor profiling for type 1 and type 2 papillary renal cell carcinoma," *Clinical Cancer Research*, vol. 15, no. 4, pp. 1162–1169, 2009.

[138] B. Gunawan, A. Von Heydebreck, T. Fritsch et al., "Cytogenetic and morphologic typing of 58 papillary renal cell carcinomas: evidence for a cytogenetic evolution of type 2 from type 1 tumors," *Cancer Research*, vol. 63, no. 19, pp. 6200–6205, 2003.

[139] J. Fischer, G. Palmedo, R. Von Knobloch et al., "Duplication and overexpression of the mutant allele of the MET proto-oncogene in multiple hereditary papillary renal cell tumours," *Oncogene*, vol. 17, no. 6, pp. 733–739, 1998.

[140] Z. Zhuang, W.-S. Park, S. Pack et al., "Trisomy 7-harbouring non-random duplication of the mutant MET allele in hereditary papillary renal carcinomas," *Nature Genetics*, vol. 20, no. 1, pp. 66–69, 1998.

[141] I. A. Lubensky, L. Schmidt, Z. Zhuang et al., "Hereditary and sporadic papillary renal carcinomas with c-met mutations share a distinct morphological phenotype," *American Journal of Pathology*, vol. 155, no. 2, pp. 517–526, 1999.

[142] S. L. Organ and M. S. Tsao, "An overview of the c-MET signaling pathway," *Therapeutic Advances in Medical Oncology*, vol. 3, no. 1, supplement, pp. S7–S19, 2011.

[143] P. Sweeney, A. K. El-Naggar, S.-H. Lin, and L. L. Pisters, "Biological significance of c-met over expression in papillary renal cell carcinoma," *Journal of Urology*, vol. 168, no. 1, pp. 51–55, 2002.

[144] S. C. Jong, M. K. Kim, W. S. Jin et al., "MET expression in sporadic renal cell carcinomas," *Journal of Korean Medical Science*, vol. 21, no. 4, pp. 672–677, 2006.

[145] Y. Miyata, H. Kanetake, and S. Kanda, "Presence of phosphorylated hepatocyte growth factor receptor/c-Met is associated with tumor progression and survival in patients with conventional renal cell carcinoma," *Clinical Cancer Research*, vol. 12, no. 16, pp. 4876–4881, 2006.

[146] G. T. Gibney, S. A. Aziz, R. L. Camp et al., "c-Met is a prognostic marker and potential therapeutic target in clear cell renal cell carcinoma," *Annals of Oncology*, vol. 24, no. 2, pp. 343–349, 2013.

[147] T. K. Choueiri, U. Vaishampayan, J. E. Rosenberg et al., "Phase II and biomarker study of the dual MET/VEGFR2 inhibitor foretinib in patients with papillary renal cell carcinoma," *Journal of Clinical Oncology*, vol. 31, no. 2, pp. 181–186, 2013.

[148] Y.-W. Zhang, "Promise and challenges on the horizon of MET-targeted cancer therapeutics," *World Journal of Biological Chemistry*, vol. 6, no. 2, pp. 16–27, 2015.

[149] M.-H. Wei, O. Toure, G. M. Glenn et al., "Novel mutations in FH and expansion of the spectrum of phenotypes expressed in families with hereditary leiomyomatosis and renal cell cancer," *Journal of Medical Genetics*, vol. 43, no. 1, pp. 18–27, 2006.

[150] R. L. Grubb III, M. E. Franks, J. Toro et al., "Hereditary leiomyomatosis and renal cell cancer: a syndrome associated with an aggressive form of inherited renal cancer," *Journal of Urology*, vol. 177, no. 6, pp. 2074–2080, 2007.

[151] M. J. Merino, C. Torres-Cabala, P. Pinto, and W. Marston Linehan, "The morphologic spectrum of kidney tumors in hereditary leiomyomatosis and renal cell carcinoma (HLRCC) syndrome," *The American Journal of Surgical Pathology*, vol. 31, no. 10, pp. 1578–1585, 2007.

[152] J. R. Toro, M. L. Nickerson, M.-H. Wei et al., "Mutations in the fumarate hydratase gene cause hereditary leiomyomatosis and renal cell cancer in families in North America," *American Journal of Human Genetics*, vol. 73, no. 1, pp. 95–106, 2003.

[153] D. L. Smit, A. R. Mensenkamp, S. Badeloe et al., "Hereditary leiomyomatosis and renal cell cancer in families referred for fumarate hydratase germline mutation analysis," *Clinical Genetics*, vol. 79, no. 1, pp. 49–59, 2011.

[154] B. Gardie, A. Remenieras, D. Kattygnarath et al., "Novel FH mutations in families with hereditary leiomyomatosis and renal cell cancer (HLRCC) and patients with isolated type 2 papillary renal cell carcinoma," *Journal of Medical Genetics*, vol. 48, no. 4, pp. 226–234, 2011.

[155] J. S. Isaacs, Y. J. Jung, D. R. Mole et al., "HIF overexpression correlates with biallelic loss of fumarate hydratase in renal cancer: novel role of fumarate in regulation of HIF stability," *Cancer Cell*, vol. 8, no. 2, pp. 143–153, 2005.

[156] M. Kiuru, R. Lehtonen, J. Arola et al., "Few FH mutations in sporadic counterparts of tumor types observed in hereditary leiomyomatosis and renal cell cancer families," *Cancer Research*, vol. 62, no. 16, pp. 4554–4557, 2002.

[157] COSMIC Catalogue of somatic mutations in cancer, 2015, http://cancer.sanger.ac.uk/wgs/browse/tissue.

[158] F. Jiang, J. Richter, P. Schraml et al., "Chromosomal imbalances in papillary renal cell carcinoma: genetic differences between histological subtypes," *The American Journal of Pathology*, vol. 153, no. 5, pp. 1467–1473, 1998.

[159] M. Brunelli, S. Gobbo, P. Cossu-Rocca et al., "Chromosomal gains in the sarcomatoid transformation of chromophobe renal cell carcinoma," *Modern Pathology*, vol. 20, no. 3, pp. 303–309, 2007.

[160] G. Kovacs, L. Fuzesi, A. Emanuel, and H.-F. Kung, "Cytogenetics of papillary renal cell tumors," *Genes Chromosomes and Cancer*, vol. 3, no. 4, pp. 249–255, 1991.

[161] M. Kovac, C. Navas, S. Horswell et al., "Recurrent chromosomal gains and heterogeneous driver mutations characterise papillary renal cancer evolution," *Nature Communications*, vol. 6, article 6336, 2015.

[162] M. C. Jaramillo and D. D. Zhang, "The emerging role of the Nrf2-Keap1 signaling pathway in cancer," *Genes & Development*, vol. 27, no. 20, pp. 2179–2191, 2013.

[163] L. E. Moore, M. L. Nickerson, P. Brennan et al., "Von Hippel-Lindau (VHL) inactivation in sporadic clear cell renal cancer: associations with germline VHL polymorphisms and etiologic risk factors," *PLoS Genetics*, vol. 7, no. 10, Article ID e1002312, 2011.

[164] M. L. Nickerson, E. Jaeger, Y. Shi et al., "Improved identification of von Hippel-Lindau gene alterations in clear cell renal tumors," *Clinical Cancer Research*, vol. 14, no. 15, pp. 4726–4734, 2008.

[165] R. E. Banks, P. Tirukonda, C. Taylor et al., "Genetic and epigenetic analysis of von Hippel-Lindau (VHL) gene alterations and relationship with clinical variables in sporadic renal cancer," *Cancer Research*, vol. 66, no. 4, pp. 2000–2011, 2006.

[166] S. Kvasha, V. Gordiyuk, A. Kondratov et al., "Hypermethylation of the 5′CpG island of the FHIT gene in clear cell renal carcinomas," *Cancer Letters*, vol. 265, no. 2, pp. 250–257, 2008.

[167] W.-G. Deng, M. Nishizaki, B. Fang, J. A. Roth, and L. Ji, "Induction of apoptosis by tumor suppressor FHIT via death receptor signaling pathway in human lung cancer cells," *Biochemical and Biophysical Research Communications*, vol. 355, no. 4, pp. 993–999, 2007.

[168] J. C. Saldivar, H. Shibata, and K. Huebner, "Pathology and biology associated with the fragile FHIT gene and gene product," *Journal of Cellular Biochemistry*, vol. 109, no. 5, pp. 858–865, 2010.

[169] C. Sevignani, G. A. Calin, R. Cesari et al., "Restoration of fragile histidine triad (FHIT) expression induces apoptosis and suppresses tumorigenicity in breast cancer cell lines," *Cancer Research*, vol. 63, no. 6, pp. 1183–1187, 2003.

[170] L. Roz, M. Gramegna, H. Ishii, C. M. Croce, and G. Sozzi, "Restoration of fragile histidine triad (FHIT) expression induces apoptosis and suppresses tumorigenicity in lung and cervical cancer cell lines," *Proceedings of the National Academy of Sciences of the United States of America*, vol. 99, no. 6, pp. 3615–3620, 2002.

[171] K. Dreijerink, E. Braga, I. Kuzmin et al., "The candidate tumor suppressor gene, RASSF1A, from human chromosome 3p21.3 is involved in kidney tumorigenesis," *Proceedings of the National Academy of Sciences of the United States of America*, vol. 98, no. 13, pp. 7504–7509, 2001.

[172] C. Simone, "SWI/SNF: the crossroads where extracellular signaling pathways meet chromatin," *Journal of Cellular Physiology*, vol. 207, no. 2, pp. 309–314, 2006.

[173] J.-H. Park, E.-J. Park, S.-K. Hur, S. Kim, and J. Kwon, "Mammalian SWI/SNF chromatin remodeling complexes are required to prevent apoptosis after DNA damage," *DNA Repair*, vol. 8, no. 1, pp. 29–39, 2009.

[174] Z. M. Eletr and K. D. Wilkinson, "An emerging model for BAP1's role in regulating cell cycle progression," *Cell Biochemistry and Biophysics*, vol. 60, no. 1-2, pp. 3–11, 2011.

[175] G. Duns, E. D. van Berg, I. van Duivenbode et al., "Histone methyltransferase gene SETD2 is a novel tumor suppressor gene

in clear cell renal cell carcinoma," *Cancer Research*, vol. 70, no. 11, pp. 4287–4291, 2010.

[176] X. Niu, T. Zhang, L. Liao et al., "The von Hippel-Lindau tumor suppressor protein regulates gene expression and tumor growth through histone demethylase JARID1C," *Oncogene*, vol. 31, no. 6, pp. 776–786, 2012.

[177] D. Schullerus, R. von Knobloch, J. Chudek, J. Herbers, and G. Kovacs, "Microsatellite analysis reveals deletion of a large region at chromosome 8p in conventional renal cell carcinoma," *International Journal of Cancer*, vol. 80, no. 1, pp. 22–24, 1999.

[178] K. Mitsumori, J. M. Kittleson, N. Itoh et al., "Chromosome 14q LOH in localized clear cell renal cell carcinoma," *Journal of Pathology*, vol. 198, no. 1, pp. 110–114, 2002.

[179] A. Alimov, B. Sundelin, N. Wang, C. Larsson, and U. Bergerheim, "Loss of 14q31-q32.2 in renal cell carcinoma is associated with high malignancy grade and poor survival," *International Journal of Oncology*, vol. 25, no. 1, pp. 179–185, 2004.

[180] H. Kaku, S. Ito, S. Ebara et al., "Positive correlation between allelic loss at chromosome 14q24-31 and poor prognosis of patients with renal cell carcinoma," *Urology*, vol. 64, no. 1, pp. 176–181, 2004.

[181] J. An, J. Choi, B. K. Shin, A. Kim, H. K. Kim, and I. Kim, "Chromogenic in situ hybridization detection of chromosome 7 and 17 abnormalities in renal cell carcinomas and comparison to flow cytometric DNA ploidy patterns," *Basic and Applied Pathology*, vol. 1, no. 2, pp. 66–71, 2008.

[182] D. J. Lager, B. J. Huston, T. G. Timmerman, and S. M. Bonsib, "Papillary renal tumors: morphologic, cytochemical, and genotypic features," *Cancer*, vol. 76, no. 4, pp. 669–673, 1995.

[183] M. D. Hughson, K. Dickman, S. A. Bigler, A. M. Meloni, and A. A. Sandberg, "Clear-cell and papillary carcinoma of the kidney: an analysis of chromosome 3, 7, and 17 abnormalities by microsatellite amplification, cytogenetics, and fluorescence in situ hybridization," *Cancer Genetics and Cytogenetics*, vol. 106, no. 2, pp. 93–104, 1998.

[184] W. Yu, W. Zhang, Y. Jiang et al., "Clinicopathological, genetic, ultrastructural characterizations and prognostic factors of papillary renal cell carcinoma: new diagnostic and prognostic information," *Acta Histochemica*, vol. 115, no. 5, pp. 452–459, 2013.

[185] M. E. Sanders, R. Mick, J. E. Tomaszewski, and F. G. Barr, "Unique patterns of allelic imbalance distinguish type 1 from type 2 sporadic papillary renal cell carcinoma," *The American Journal of Pathology*, vol. 161, no. 3, pp. 997–1005, 2002.

[186] X. J. Yang, M. H. Tan, H. L. Kim et al., "A molecular classification of papillary renal cell carcinoma," *Cancer Research*, vol. 65, no. 13, pp. 5628–5637, 2005.

[187] R. F. Schwerdtle, S. Storkel, C. Neuhaus et al., "Allelic losses at chromosomes 1p, 2p, 6p, 10p, 13q, 17p, and 21q significantly correlate with the chromophobe subtype of renal cell carcinoma," *Cancer Research*, vol. 56, no. 13, pp. 2927–2930, 1996.

[188] A. Nagy, I. Buzogany, and G. Kovacs, "Microsatellite allelotyping differentiates chromophobe renal cell carcinomas from renal oncocytomas and identifies new genetic changes," *Histopathology*, vol. 44, no. 6, pp. 542–546, 2004.

[189] M. Brunelli, J. N. Eble, S. Zhang, G. Martignoni, B. Delahunt, and L. Cheng, "Eosinophilic and classic chromophobe renal cell carcinomas have similar frequent losses of multiple chromosomes from among chromosomes 1, 2, 6, 10, and 17, and this pattern of genetic abnormality is not present in renal oncocytoma," *Modern Pathology*, vol. 18, no. 2, pp. 161–169, 2005.

[190] M. Sperga, P. Martinek, T. Vanecek et al., "Chromophobe renal cell carcinoma—chromosomal aberration variability and its relation to Paner grading system: an array CGH and FISH analysis of 37 cases," *Virchows Archiv*, vol. 463, no. 4, pp. 563–573, 2013.

[191] S. Gad, S. H. Lefèvre, S. K. Khoo et al., "Mutations in BHD and TP53 genes, but not in HNF1beta gene, in a large series of sporadic chromophobe renal cell carcinoma," *British Journal of Cancer*, vol. 96, no. 2, pp. 336–340, 2007.

[192] C. Davis, C. J. Ricketts, M. Wang et al., "The somatic genomic landscape of chromophobe renal cell carcinoma," *Cancer Cell*, vol. 26, no. 3, pp. 319–330, 2014.

[193] H. Contractor, M. Zariwala, P. Bugert, J. Zeisler, and G. Kovacs, "Mutation of the p53 tumour suppressor gene occurs preferentially in the chromophobe type of renal cell tumour," *Journal of Pathology*, vol. 181, no. 2, pp. 136–139, 1997.

[194] M. M. Picken, B. Chyna, R. C. Flanigan, and J. M. Lee, "Analysis of chromosome 1p abnormalities in renal oncocytomas by loss of heterozygosity studies: correlation with conventional cytogenetics and fluorescence in situ hybridization," *American Journal of Clinical Pathology*, vol. 129, no. 3, pp. 377–382, 2008.

[195] V. Lindgren, G. P. Paner, A. Omeroglu et al., "Cytogenetic analysis of a series of 13 renal oncocytomas," *Journal of Urology*, vol. 171, no. 2, pp. 602–604, 2004.

[196] J. A. Brown, S. Takahashi, A. Alcaraz et al., "Fluorescence in situ hybridization analysis of renal oncocytoma reveals frequent loss of chromosomes Y and 1," *Journal of Urology*, vol. 156, no. 1, pp. 31–35, 1996.

[197] L. Füzesi, D. Frank, C. Nguyen, R.-H. Ringert, H. Bartels, and B. Gunawan, "Losses of 1p and chromosome 14 in renal oncocytomas," *Cancer Genetics and Cytogenetics*, vol. 160, no. 2, pp. 120–125, 2005.

[198] W. R. Sukov, R. P. Ketterling, D. J. Lager et al., "*CCND1* rearrangements and cyclin D1 overexpression in renal oncocytomas: frequency, clinicopathologic features, and utility in differentiation from chromophobe renal cell carcinoma," *Human Pathology*, vol. 40, no. 9, pp. 1296–1303, 2009.

[199] E. Van Den Berg, T. Dijkhuizen, S. Störkel et al., "Chromosomal changes in renal oncocytomas: evidence that t(5;11)(q35;q13) may characterize a second subgroup of oncocytomas," *Cancer Genetics and Cytogenetics*, vol. 79, no. 2, pp. 164–168, 1995.

[200] L. Fuzesi, B. Gunawan, S. Braun et al., "Cytogenetic analysis of 11 renal oncocytomas: further evidence of structural rearrangements of 11q13 as a characteristic chromosomal anomaly," *Cancer Genetics and Cytogenetics*, vol. 107, no. 1, pp. 1–6, 1998.

[201] F. Becker, K. Junker, M. Parr et al., "Collecting duct carcinomas represent a unique tumour entity based on genetic alterations," *PLoS ONE*, vol. 8, no. 10, Article ID e78137, 2013.

[202] L. Fuzesi, M. Cober, and C. Mittermayer, "Collecting duct carcinoma: cytogenetic characterization," *Histopathology*, vol. 21, no. 2, pp. 155–160, 1992.

[203] L. S. Schmidt and W. M. Linehan, "Hereditary leiomyomatosis and renal cell carcinoma," *International Journal of Nephrology and Renovascular Disease*, vol. 7, pp. 253–260, 2014.

[204] C. P. Pavlovich, R. L. Grubb III, K. Hurley et al., "Evaluation and management of renal tumors in the Birt-Hogg-Dubé syndrome," *The Journal of Urology*, vol. 173, no. 5, pp. 1482–1486, 2005.

[205] L. S. Schmidt, M. L. Nickerson, M. B. Warren et al., "Germline BHD-mutation spectrum and phenotype analysis of a large

cohort of families with Birt-Hogg-Dubé syndrome," *The American Journal of Human Genetics*, vol. 76, no. 6, pp. 1023–1033, 2005.

[206] C. P. Pavlovich, M. M. Walther, R. A. Eyler et al., "Renal tumors in the Birt-Hogg-Dubé syndrome," *The American Journal of Surgical Pathology*, vol. 26, no. 12, pp. 1542–1552, 2002.

[207] A. Szponar, M. V. Yusenko, and G. Kovacs, "High-resolution array CGH of metanephric adenomas: lack of DNA copy number changes," *Histopathology*, vol. 56, no. 2, pp. 212–216, 2010.

[208] R. Drut, R. M. Drut, and C. Ortolani, "Metastatic metanephric adenoma with foci of papillary carcinoma in a child: a combined histologic, immunohistochemical, and FISH study," *International Journal of Surgical Pathology*, vol. 9, no. 3, pp. 241–247, 2001.

[209] A. A. Renshaw, D. R. Freyer, and Y. A. Hammers, "Metastatic metanephric adenoma in a child," *American Journal of Surgical Pathology*, vol. 24, no. 4, pp. 570–574, 2000.

[210] J. A. Brown, K. L. Anderl, T. J. Borell, J. Qian, D. G. Bostwick, and R. B. Jenkins, "Simultaneous chromosome 7 and 17 gain and sex chromosome loss provide evidence that renal metanephric adenoma is related to papillary renal cell carcinoma," *Journal of Urology*, vol. 158, no. 2, pp. 370–374, 1997.

[211] C.-C. Pan and J. I. Epstein, "Detection of chromosome copy number alterations in metanephric adenomas by array comparative genomic hybridization," *Modern Pathology*, vol. 23, no. 12, pp. 1634–1640, 2010.

[212] M. Brunelli, J. N. Eble, S. Zhang, G. Martignoni, and L. Cheng, "Metanephric adenoma lacks the gains of chromosomes 7 and 17 and loss of Y that are typical of papillary renal cell carcinoma and papillary adenoma," *Modern Pathology*, vol. 16, no. 10, pp. 1060–1063, 2003.

[213] M. Stumm, A. Koch, P. F. Wieacker et al., "Partial monosomy 2p as the single chromosomal anomaly in a case of renal metanephric adenoma," *Cancer Genetics and Cytogenetics*, vol. 115, no. 1, pp. 82–85, 1999.

[214] T. Pesti, F. Sükösd, E. C. Jones, and G. Kovacs, "Mapping a tumor suppressor gene to chromosome 2p13 in metanephric adenoma by microsatellite allelotyping," *Human Pathology*, vol. 32, no. 1, pp. 101–104, 2001.

[215] B. Dadone, D. Ambrosetti, X. Carpentier et al., "A renal metanephric adenoma showing both a 2p16-24 deletion and BRAF V600E mutation: a synergistic role for a tumor suppressor gene on chromosome 2p and BRAF activation?" *Cancer Genetics*, vol. 206, no. 9-10, pp. 347–352, 2013.

[216] T. K. Choueiri, J. Cheville, E. Palescandolo et al., "*BRAF* mutations in metanephric adenoma of the kidney," *European Urology*, vol. 62, no. 5, pp. 917–922, 2012.

[217] S. Gattenlöhner, B. Etschmann, H. Riedmiller, and H.-K. Müller-Hermelink, "Lack of KRAS and BRAF mutation in renal cell carcinoma," *European Urology*, vol. 55, no. 6, pp. 1490–1491, 2009.

[218] A. Nagy, I. Balint, and G. Kovacs, "Frequent allelic changes at chromosome 7q34 but lack of mutation of the BRAF in papillary renal cell tumors," *International Journal of Cancer*, vol. 106, no. 6, pp. 980–981, 2003.

[219] E. W. Joseph, C. A. Pratilas, P. I. Poulikakos et al., "The RAF inhibitor PLX4032 inhibits ERK signaling and tumor cell proliferation in a V600E BRAF-selective manner," *Proceedings of the National Academy of Sciences of the United States of America*, vol. 107, no. 33, pp. 14903–14908, 2010.

[220] J. N. Eble, *Pathology and Genetics of Tumours of the Urinary System and Male Genital Organs*, IARC, 2004.

[221] S. S. Shen, J. Y. Ro, P. Tamboli et al., "Mucinous tubular and spindle cell carcinoma of kidney is probably a variant of papillary renal cell carcinoma with spindle cell features," *Annals of Diagnostic Pathology*, vol. 11, no. 1, pp. 13–21, 2007.

[222] P. Cossu-Rocca, J. N. Eble, B. Delahunt et al., "Renal mucinous tubular and spindle carcinoma lacks the gains of chromosomes 7 and 17 and losses of chromosome Y that are prevalent in papillary renal cell carcinoma," *Modern Pathology*, vol. 19, no. 4, pp. 488–493, 2006.

[223] N. Kuroda, T. Naroda, M. Tamura et al., "High-grade mucinous tubular and spindle cell carcinoma: comparative genomic hybridization study," *Annals of Diagnostic Pathology*, vol. 15, no. 6, pp. 472–475, 2011.

[224] P. Brandal, A. K. Lie, A. Bassarova et al., "Genomic aberrations in mucinous tubular and spindle cell renal cell carcinomas," *Modern Pathology*, vol. 19, no. 2, pp. 186–194, 2006.

[225] K. Okoń, A. Klimkowska, A. Pawelec, Z. Dobrowolski, Z. Kohla, and J. Stachura, "Immunophenotype and cytogenetics of mucinous tubular and spindle cell carcinoma of the kidney," *Polish Journal of Pathology*, vol. 58, no. 4, pp. 227–233, 2007.

[226] Y. Zhang, X. Yong, Q. Wu et al., "Mucinous tubular and spindle cell carcinoma and solid variant papillary renal cell carcinoma: a clinicopathologic comparative analysis of four cases with similar molecular genetics datum," *Diagnostic Pathology*, vol. 9, no. 1, article 194, 2014.

[227] C. Rakozy, G. E. Schmahl, S. Bogner, and S. Störkel, "Low-grade tubular-mucinous renal neoplasms: morphologic, immunohistochemical, and genetic features," *Modern Pathology*, vol. 15, no. 11, pp. 1162–1171, 2002.

[228] P. Argani, S. Olgac, S. K. Tickoo et al., "Xp11 Translocation renal cell carcinoma in adults: expanded clinical, pathologic, and genetic spectrum," *American Journal of Surgical Pathology*, vol. 31, no. 8, pp. 1149–1160, 2007.

[229] Y. Komai, M. Fujiwara, Y. Fujii et al., "Adult Xp11 translocation renal cell carcinoma diagnosed by cytogenetics and immunohistochemistry," *Clinical Cancer Research*, vol. 15, no. 4, pp. 1170–1176, 2009.

[230] H. B. Armah and A. V. Parwani, "Xp11.2 translocation renal cell carcinoma," *Archives of Pathology and Laboratory Medicine*, vol. 134, no. 1, pp. 124–129, 2010.

[231] P. Ahluwalia, B. Nair, and G. Kumar, "Renal cell carcinoma associated with Xp11.2 translocation/TFE3 gene fusion: a rare case report with review of the literature," *Case Reports in Urology*, vol. 2013, Article ID 810590, 4 pages, 2013.

[232] P. Argani, P. Lal, B. Hutchinson, M. Y. Lui, V. E. Reuter, and M. Ladanyi, "Aberrant nuclear immunoreactivity for TFE3 in neoplasms with TFE3 gene fusions: a sensitive and specific immunohistochemical assay," *The American Journal of Surgical Pathology*, vol. 27, no. 6, pp. 750–761, 2003.

[233] C. G. Przybycin, A. M. Cronin, F. Darvishian et al., "Chromophobe renal cell carcinoma: a clinicopathologic study of 203 tumors in 200 patients with primary resection at a single institution," *The American Journal of Surgical Pathology*, vol. 35, no. 7, pp. 962–970, 2011.

[234] S. D. W. Beck, M. I. Patel, M. E. Snyder et al., "Effect of papillary and chromophobe cell type on disease-free survival after nephrectomy for renal cell carcinoma," *Annals of Surgical Oncology*, vol. 11, no. 1, pp. 71–77, 2004.

[235] M. B. Amin, G. P. Paner, I. Alvarado-Cabrero et al., "Chromophobe renal cell carcinoma: Histomorphologic characteristics

and evaluation of conventional pathologic prognostic parameters in 145 cases," *American Journal of Surgical Pathology*, vol. 32, no. 12, pp. 1822–1834, 2008.

[236] M. L. Nickerson, M. B. Warren, J. R. Toro et al., "Mutations in a novel gene lead to kidney tumors, lung wall defects, and benign tumors of the hair follicle in patients with the Birt-Hogg-Dubé syndrome," *Cancer Cell*, vol. 2, no. 2, pp. 157–164, 2002.

[237] M. B. Warren, C. A. Torres-Cabala, M. L. Turner et al., "Expression of Birt-Hogg-Dube gene mRNA in normal and neoplastic human tissues," *Modern Pathology*, vol. 17, no. 8, pp. 998–1011, 2004.

[238] C. D. Vocke, Y. Yang, C. P. Pavlovich et al., "High frequency of somatic frameshift BHD gene mutations in Birt-Hogg-Dubé-associated renal tumors," *Journal of the National Cancer Institute*, vol. 97, no. 12, pp. 931–935, 2005.

[239] J. Chen, K. Futami, D. Petillo et al., "Deficiency of FLCN in mouse kidney led to development of polycystic kidneys and renal neoplasia," *PLoS ONE*, vol. 3, no. 10, Article ID e3581, 2008.

[240] M. Baba, M. Furihata, S.-B. Hong et al., "Kidney-targeted Birt-Hogg-Dubé gene inactivation in a mouse model: Erk1/2 and Akt-mTOR activation, cell hyperproliferation, and polycystic kidneys," *Journal of the National Cancer Institute*, vol. 100, no. 2, pp. 140–154, 2008.

[241] A. Nagy, D. Zoubakov, Z. Stupar, and G. Kovacs, "Lack of mutation of the folliculin gene in sporadic chromophobe renal cell carcinoma and renal oncocytoma," *International Journal of Cancer*, vol. 109, no. 3, pp. 472–475, 2004.

[242] T. Murakami, F. Sano, Y. Huang et al., "Identification and characterization of Birt-Hogg-Dubé associated renal carcinoma," *Journal of Pathology*, vol. 211, no. 5, pp. 524–531, 2007.

[243] M. Brunelli, B. Delahunt, S. Gobbo et al., "Diagnostic usefulness of fluorescent cytogenetics in differentiating chromophobe renal cell carcinoma from renal oncocytoma: a validation study combining metaphase and interphase analyses," *American Journal of Clinical Pathology*, vol. 133, no. 1, pp. 116–126, 2010.

[244] M. V. Yusenko, R. P. Kuiper, T. Boethe et al., "High-resolution DNA copy number and gene expression analyses distinguish chromophobe renal cell carcinomas and renal oncocytomas," *BMC Cancer*, vol. 9, article 152, 2009.

[245] D. P. Liu, H. Song, and Y. Xu, "A common gain of function of p53 cancer mutants in inducing genetic instability," *Oncogene*, vol. 29, no. 7, pp. 949–956, 2010.

[246] F. Sükösd, B. Digon, J. Fischer, T. Pietsch, and G. Kovacs, "Allelic loss at 10q23.3 but lack of mutation of *PTEN/MMAC1* in chromophobe renal cell carcinoma," *Cancer Genetics and Cytogenetics*, vol. 128, no. 2, pp. 161–163, 2001.

[247] G. P. Paner, M. B. Amin, I. Alvarado-Cabrero et al., "A novel tumor grading scheme for chromophobe renal cell carcinoma: prognostic utility and comparison with fuhrman nuclear grade," *The American Journal of Surgical Pathology*, vol. 34, no. 9, pp. 1233–1240, 2010.

[248] M. H. Tan, C. F. Wong, H. L. Tan et al., "Genomic expression and single-nucleotide polymorphism profiling discriminates chromophobe renal cell carcinoma and oncocytoma," *BMC Cancer*, vol. 10, article 196, 2010.

[249] J. D. Oxley, J. Sullivan, A. Mitchelmore, and D. A. Gillatt, "Metastatic renal oncocytoma," *Journal of Clinical Pathology*, vol. 60, no. 6, pp. 720–722, 2007.

[250] J. S. Jhang, G. Narayan, V. V. V. S. Murty, and M. M. Mansukhani, "Renal oncocytomas with 11q13 rearrangements: cytogenetic, molecular, and immunohistochemical analysis of cyclin D1," *Cancer Genetics and Cytogenetics*, vol. 149, no. 2, pp. 114–119, 2004.

[251] S. Zanssen, B. Gunawan, L. Fuzesi, D. Warburton, and E. A. Schon, "Renal oncocytomas with rearrangements involving 11q13 contain breakpoints near *CCND1*," *Cancer Genetics and Cytogenetics*, vol. 149, no. 2, pp. 120–124, 2004.

[252] T. Dijkhuizen, E. van den Berg, S. Storkel et al., "Renal oncocytoma with t(5;12;11), der(1)1;8) and add(19): 'true' oncocytoma or chromophobe adenoma?" *International Journal of Cancer*, vol. 73, no. 4, pp. 521–524, 1997.

[253] N. Tokuda, S. Naito, O. Matsuzaki, Y. Nagashima, S. Ozono, and T. Igarashi, "Collecting duct (Bellini duct) renal cell carcinoma: a nationwide survey in Japan," *The Journal of Urology*, vol. 176, no. 1, pp. 40–43, 2006.

[254] M. May, V. Ficarra, S. F. Shariat et al., "Impact of clinical and histopathological parameters on disease specific survival in patients with collecting duct renal cell carcinoma: development of a disease specific risk model," *Journal of Urology*, vol. 190, no. 2, pp. 458–463, 2013.

[255] M. Schoenberg, P. Cairns, J. D. Brooks et al., "Frequent loss of chromosome arms 8p and 13q in collecting duct carcinoma (CDC) of the kidney," *Genes Chromosomes and Cancer*, vol. 12, no. 1, pp. 76–80, 1995.

[256] G. Steiner, P. Cairns, T. J. Polascik et al., "High-density mapping of chromosomal arm 1q in renal collecting duct carcinoma: region of minimal deletion at 1q32.1-32.2," *Cancer Research*, vol. 56, no. 21, pp. 5044–5046, 1996.

[257] A. Orsola, I. Trias, C. X. Raventós, I. Español, L. Cecchini, and I. Orsola, "Renal collecting (Bellini) duct carcinoma displays similar characteristics to upper tract urothelial cell carcinoma," *Urology*, vol. 65, no. 1, pp. 49–54, 2005.

[258] R. Gupta, A. Billis, R. B. Shah et al., "Carcinoma of the collecting ducts of bellini and renal medullary carcinoma: clinicopathologic analysis of 52 cases of rare aggressive subtypes of renal cell carcinoma with a focus on their interrelationship," *American Journal of Surgical Pathology*, vol. 36, no. 9, pp. 1265–1278, 2012.

[259] M. A. Swartz, J. Karth, D. T. Schneider, R. Rodriguez, J. B. Beckwith, and E. J. Perlman, "Renal medullary carcinoma: clinical, pathologic, immunohistochemical, and genetic analysis with pathogenetic implications," *Urology*, vol. 60, no. 6, pp. 1083–1089, 2002.

[260] Z. Gatalica, S. L. Lilleberg, F. A. Monzon et al., "Renal medullary carcinomas: histopathologic phenotype associated with diverse genotypes," *Human Pathology*, vol. 42, no. 12, pp. 1979–1988, 2011.

[261] M. B. Amin, G. T. MacLennan, R. Gupta et al., "Tubulocystic carcinoma of the kidney: clinicopathologic analysis of 31 cases of a distinctive rare subtype of renal cell carcinoma," *The American Journal of Surgical Pathology*, vol. 33, no. 3, pp. 384–392, 2009.

[262] G. T. Maclennan, G. M. Farrow, and D. G. Bostwick, "Low-grade collecting duct carcinoma of the kidney: report of 13 cases of low-grade mucinous tubulocystic renal carcinoma of possible collecting duct origin," *Urology*, vol. 50, no. 5, pp. 679–684, 1997.

[263] M. Zhou, X. J. Yang, J. I. Lopez et al., "Renal tubulocystic carcinoma is closely related to papillary renal cell carcinoma:

implications for pathologic classification," *American Journal of Surgical Pathology*, vol. 33, no. 12, pp. 1840–1849, 2009.

[264] T. O. Al-Hussain, L. Cheng, S. Zhang, and J. I. Epstein, "Tubulocystic carcinoma of the kidney with poorly differentiated foci: a series of 3 cases with fluorescence in situ hybridization analysis," *Human Pathology*, vol. 44, no. 7, pp. 1406–1411, 2013.

Hindawi Publishing Corporation
BioMed Research International
Volume 2014, Article ID 629496, 7 pages
http://dx.doi.org/10.1155/2014/629496

Research Article

Epithelial-Mesenchymal Transition and Somatic Alteration in Colorectal Cancer with and without Peritoneal Carcinomatosis

Y. A. Shelygin, N. I. Pospekhova, V. P. Shubin, V. N. Kashnikov, S. A. Frolov, O. I. Sushkov, S. I. Achkasov, and A. S. Tsukanov

State Scientific Centre of Coloproctology, 2 Salyam Adil Street, Moscow 123423, Russia

Correspondence should be addressed to Y. A. Shelygin; colgenlab@mail.ru

Received 24 April 2014; Accepted 5 July 2014; Published 3 August 2014

Academic Editor: Konstantinos Arnaoutakis

Colorectal cancer is highly metastatic even when the tumors are small. To disseminate, cells use a complex and multistage process known as the epithelial-mesenchymal transition, in which epithelial phenotype is transformed into mesenchymal phenotype. The objective of this study is to describe the epithelial-mesenchymal transition in terms of gene expression profile and somatic alterations in samples of colorectal cancer with or without peritoneal carcinomatosis. We analyzed samples taken from 38 patients with colorectal cancer (stages II-IV) and samples from 20 patients with colorectal cancer complicated by peritoneal carcinomatosis. The expression of *ZEB1, ZEB2, CDH1, VIM*, and *SNAI1* was analyzed by real-time PCR. *KRAS/BRAF* mutations were mapped using sequencing. Microsatellite instability was evaluated by fragment analysis. Epithelial-mesenchymal transition was detected in 6 out of 38 samples of colorectal cancer (stages II-IV), 7 out of 20 tumors from patients with peritoneal carcinomatosis, and 19 out of 20 samples taken from carcinomatous nodules. Tumors of the mesenchymal subtype displayed high frequency of somatic mutations, microsatellite stability, and low degree of differentiation. The identification of epithelial-mesenchymal transition may be used as a marker of high metastatic potential, which is particularly relevant at early stages of tumor growth.

1. Introduction

Adenocarcinomas originating in intestinal epithelium make up an overwhelming majority of malignant tumors of the colon. As the tumor grows, its cells infiltrate the surrounding stroma, penetrate blood and lymphatic vessels, and are passively carried to remote organs, where they form metastases. Such spreading of the primary tumor, or metastasis, is the leading cause of death from colorectal cancer (CRC). In 2002 the French oncologist Thiery formulated a hypothesis explaining how metastasis occurs [1]. To disseminate, tumor cells use a complex and multistage process, in which epithelial phenotype is transformed into mesenchymal phenotype. This process is now known as the epithelial-mesenchymal transition (EMT). The sequence of events characteristic of the EMT is crucial to the formation and differentiation of body organs during embryonal development. As a pathological process, EMT triggers tumor progression; its cells acquire migrating potential and may invade the surrounding stroma and enter circulating blood [1–3]. The expression of a considerable number of genes is altered during EMT; some transcription factors (*SNAI1/2, TWIST, ZEB1/2,* and so on) and mesenchymal markers are overexpressed, while the expression of epithelial phenotype markers is suppressed.

The objective of this study is to describe the epithelial-mesenchymal transition in terms of gene expression profile and somatic changes, molecular as well as genetic, in samples of colorectal cancer of various stages, with or without peritoneal carcinomatosis (PC).

2. Materials and Methods

2.1. Patients. This study was performed in samples of tumors, carcinomatous nodules, and healthy mucous membranes (in total 136 samples), which were obtained from the colon of 58 patients undergoing surgery for colorectal cancer at the State Research Center of Coloproctology between November 2012 and February 2014. In 38 cases we collected a sample from both the tumor and the normal mucosa, and in 20 cases three samples were taken from the tumor, carcinomatous nodulus,

Table 1: The clinical characteristics of patients.

Characteristics	CRC without PC ($n = 38$)	CRC with PC ($n = 20$)
Mean age (min–max)	62.1 (32–81)	63.7 (26–84)
Male/female	13/25	11/9
Tumor localization:		
Rectum	4	1
Left side	21	8
Right side	13	11
Stage:		
I (T1-2N0M0)	2	
II (T3-4N0M0)	17	
III (TanyN1-2M0)	16	
IV (TanyNanyM1)	3	20

and normal mucosa. The clinical characteristics of all patients are listed in Table 1.

2.2. DNA and RNA Extraction. DNA was extracted from the tumors using a PROBE-GS-GENETICA kit (DNA Technology, Russia) according to the procedure described by the manufacturer. Tissue samples were placed in lysis buffer immediately after collection, and total RNA was extracted by PureLink RNA Mini Kit (Ambion, USA) following the procedure specified by the manufacturer. The quality of RNA extraction was verified by electrophoresis in 1.8% agarose gel. The product was stained with ethidium bromide and analyzed using Gel Doc XR+ imaging system (BioRad, USA) in ultraviolet light. The concentration of extracted RNA was measured with a P300 spectrophotometer (IMPLEN).

2.3. Detection of Mutations. Somatic mutations in the *KRAS* (exon 2, codons 12/13) and *BRAF* (codon 15, V600E) genes were detected by polymerase chain reaction and a Tertsik amplifier (DNA Technology, Russia), and both complementary chains were sequenced with ABI PRISM 3500 (8 capillaries; Applied Biosystems, USA).

2.4. Microsatellite Instability. Microsatellite instability was evaluated in tumor samples using fragment analysis for five markers (NR21, NR24, NR27, BAT25, and BAT26) with ABI PRISM 3500 (8 capillaries; Applied Biosystems, USA).

2.5. Reverse Transcription. Reverse transcription was performed with ImProm-II Reverse Transcriptase kit (Promega) in accordance with the procedure described by the manufacturer. Once the reaction was complete, we measured the concentration of cDNA with a P300 spectrophotometer (IMPLEN).

2.6. Real-Time PCR. To evaluate gene expression, we used StepOnePlus (Applied Biosystems, USA). PCR was performed with 20 μL of solution consisting of: 100–200 ng of DNA, 10 pM of gene-specific primers, 2 mM dNTP, 0.5 U Taq DNA polymerase (Sib Enzyme, Russia), PCR buffer, and Eva Green dye. Ct values for each gene were normalized by Ct values for control genes. Two control genes were analyzed: *GAPDH* and *TFRC*. The change in gene expression was calculated using ΔΔCt method (estimated as lg).

2.7. Statistical Analysis. Statistical analysis was performed in standard Statistica software (version 10.0, Statsoft Inc., USA) using χ^2 and Fisher's exact test for four-cell tables.

3. Results

Gene expression was analyzed using real-time PCR in tumor samples obtained from patients ($n = 58$) with CRC of different types defined by TNM classification, morphological characteristics, and presence or absence of peritoneal carcinomatosis (PC). The epithelial-mesenchymal transition (EMT) program was analyzed with regard to the expression of five genes (*ZEB1, ZEB2, CDH1, VIM,* and *SNAI1*), which were selected based on previous studies and are known to be associated with progressive EMT. Once this process is under way in a tumor, it is typical to find a coordinated alteration in the expression of all these genes: the expression of *ZEB1, ZEB2, VIM,* and *SNAI1* is upregulated, while the expression of *CDH1* is downregulated.

3.1. EMT and Somatic Mutations in the KRAS and BRAF Genes and MSI Status in Stage II-IV Colorectal Cancer. EMT process was detected in 6 out of 38 (15.8%) samples of CRC. The gene expression signature in samples with and without EMT is shown in Figure 1.

The frequency and characteristics of some molecular and genetic alterations typical for CRC, such as mutations in *KRAS* and *BRAF* genes and MSI status, are presented in Table 2.

Mutations in the *KRAS* gene were detected in 39.5% of tumors. V600E mutation was discovered in the *BRAF* gene of one patient. The majority of tumors were microsatellite stable—MSS (84.2%). A high level of microsatellite instability (MSI-H) was detected in 5 samples.

3.2. EMT and Somatic Mutations in the KRAS and BRAF Genes and MSI Status in Colorectal Cancer with Peritoneal Carcinomatosis. We analyzed paired samples from the tumors/carcinomatous nodules of 20 patients with CRC and peritoneal carcinomatosis. EMT was detected in 7 out of 20 samples of the primary tumor (35%). However, the frequency of EMT reached 95% in carcinomatous nodules (19 out of 20). The gene expression signature in samples of primary tumors and carcinomatous nodules is shown in Figure 1.

The frequency and characteristics of somatic mutations in the *KRAS* and *BRAF* genes and MSI status are presented in Table 2.

Mutations in the *KRAS* gene were detected in 55% of all tumors. V600E-*BRAF* mutation was found in 3 samples. In two cases we discovered discordance between the primary tumor and the carcinomatous nodulus in terms of their mutational status: a mutation detected in the tumor was absent in

Table 2: The *KRAS*- and *BRAF*-mutation frequency and MSI status in CRC without and with PC.

	CRC without PC, $n = 38$	%	CRC with PC, $n = 20$	%	P
KRAS-mut	15	39.5	11	55	0.197
BRAF V600E	1	2.6	3	15	0.114
KRAS-mut + *BRAF* V600E	16	42.1	14	70	**0.04**
KRAS + *BRAF* wt	22	57.9	6	30	**0.04**
MSI-H	5	13.2	0	0	0.11
MSI-L	1	2.6	2	10	0.23
MSS	32	84.2	18	90	0.43

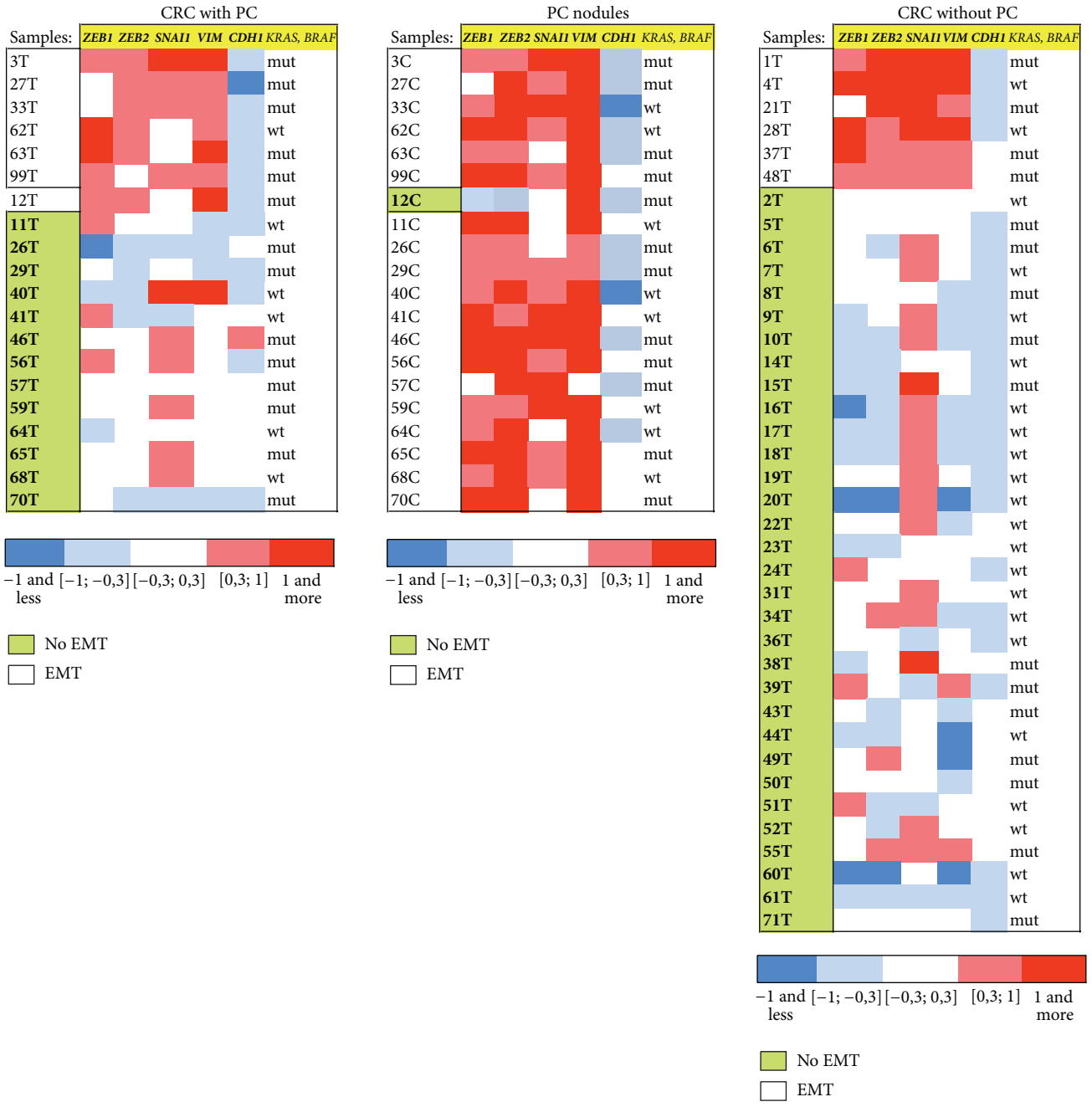

Figure 1: The gene expression signature in CRC without/with PC and carcinomatous nodules.

Table 3: The data of tumor grade.

Grade	CRC without PC, $n = 38$ (%)	CRC with PC, $n = 20$ (%)	P
G1	0	0	
G2	24 (63.2)	6 (30)	**0.006**
G3	11 (28.9)	14 (70)	**0.006**
Unknown	3	0	

the sample taken from the carcinomatous nodulus. However, the gene expression profile in carcinomatous nodules corresponded to the mesenchymal subtype. The overall frequency of mutations in both genes in CRC with PC was 70%, compared to 39% in CRC without carcinomatosis; this difference was statistically significant ($P = 0.04$). Eighteen samples taken from tumors were microsatellite stable (90%). High level of microsatellite instability was not detected in any of the analyzed samples.

3.3. Pathomorphological Characteristics of the Tumors. The frequency of highly, moderately, and poorly differentiated tumors among study samples is presented in Table 3. CRC with carcinomatosis was typically poorly differentiated compared to CRC without carcinomatosis ($P = 0.006$).

3.4. A Comparison of EMT-Negative and EMT-Positive Tumors. EMT was detected in 13 out of the total of 58 tumor samples (22.4%) and in 19 out of 20 carcinomatous nodules (95%). The mean expression levels of *ZEB1, ZEB2, VIM, SNAI1, and CDH1* genes in samples with and without EMT and carcinomatous nodules are shown in Figure 2. The difference of expression levels of all genes between EMT-negative tumors/EMT-positive tumors and EMT-negative tumors/carcinomatous nodules was statistically significant.

The frequencies of somatic mutations in the *KRAS* and *BRAF* genes and MSI status in EMT-negative and EMT-positive tumors are presented in Table 4.

The *BRAF*-mutation frequency in EMT-negative CRC was 2.2%, compared to 23.1% in EMT-positive CRC; this difference was statistically significant ($P = 0.03$). The overall frequency of mutations in both genes in EMT-negative CRC was 44.4%, compared to 76.9% in EMT-positive CRC; this difference was statistically significant ($P = 0.039$).

The number of moderately and poorly differentiated tumors is shown in Table 5. EMT-positive tumors were usually poorly differentiated compared to EMT-negative tumors ($P = 0.001$).

4. Discussion

The current view is that EMT, which transforms immobile epithelial cells into mobile and invasive cells, plays a central role in enhancing the metastatic potential of various cancers, including CRC. This multistage process is accompanied by structural and morphological alterations in tumor cells, whose morphology is transformed as a result [1–3].

In recent studies CRC was subdivided into various molecular subtypes depending on gene transcription profiles, somatic mutations, MSI status, and gene methylation status. In the genetic classification of CRC developed by Roepman et al. [4] this cancer is divided into three subtypes: A-subtype, B-subtype, and C-subtype. The molecular and genetic criteria employed in this classification include epithelial-mesenchymal transition, defect in the DNA mismatch-repair system manifested as a high degree of microsatellite instability, and proliferation activity of tumor cells. Marisa et al. distinguish among seven subtypes of CRC [5]. Another study by Zhu et al. describes three different subtypes [6]. However, in all these studies one of CRC subtypes is colorectal cancer associated with triggering the EMT program.

In our study EMT was detected in samples of colorectal cancer based on coordinated changes in the expression of the following genes: *ZEB1*, *ZEB2*, *SNAI1*, *CDH1*, and *VIM*. The expression of these genes was studied because IHC analysis was not possible to carry out technically. The protein products of *ZEB1*, *ZEB2*, and *SNAIL1* are transcription factors which, along with some other factors, play a key role in triggering the EMT [7–9]. Proteins E-cadherin (encoded by the *CDH1* gene) and vimentin (encoded by *VIM*) are cellular markers of epithelial and mesenchymal tissues, respectively. The coordinated upregulation or, not uncommonly, overexpression of *ZEB1*, *ZEB2*, *SNAI1*, and *VIM* and the downregulation of *CDH1* indicated that EMT was under way, making the tumor cells assume a mesenchymal phenotype. Notably, overexpression of *SNAI1* and downregulation of *CDH1* were often observed in other samples, which we classified them as EMT-negative. This phenotype apparently reflects an ongoing transition and can be seen as an intermediate type between the epithelial and the mesenchymal subtypes of tumors [10]. Only 13 out of 58 (22.4%) primary tumors were judged to be EMT-positive, including 6 out of 38 cases of stage II-IV CRC and 7 out of 20 cases of CRC with peritoneal carcinomatosis. In many studies, such as that by Roepman et al. [4] mentioned above, the mesenchymal subtype of CRC is described as a tumor with intrinsically poor prognosis and resistant to adjuvant chemotherapy. In our sample, a considerable proportion of patients ($n = 20$) had CRC with peritoneal carcinomatosis. Cells from the primary tumor that have migrated into the peritoneum are the likely source of carcinomatous nodules. It is these cells, which assume a mesenchymal phenotype with overexpression of vimentin and suppressed expression of *CDH1*, leading to disrupted regulation of cellular adhesion, that may have been the source of metastases. All but one sample from peritoneal nodules (95%) were of the mesenchymal phenotype. In one case EMT was detected only in the tumor. EMT concordance was observed only in 6 cases, where the expression profile was nearly identical in the primary tumor and the peritoneal nodulus. Possibly, the cells of the primary tumor may lose their mesenchymal phenotype over time (a reverse epithelial-mesenchymal transition) [11], or else the tumor may be highly heterogeneous [12]. The fact that the EMT was detected in an overwhelming majority of carcinomatous tumors in this study thus proves that CRC of the mesenchymal subtype is aggressive and confers a poor prognosis. As for stage II-III tumors, the EMT was detected

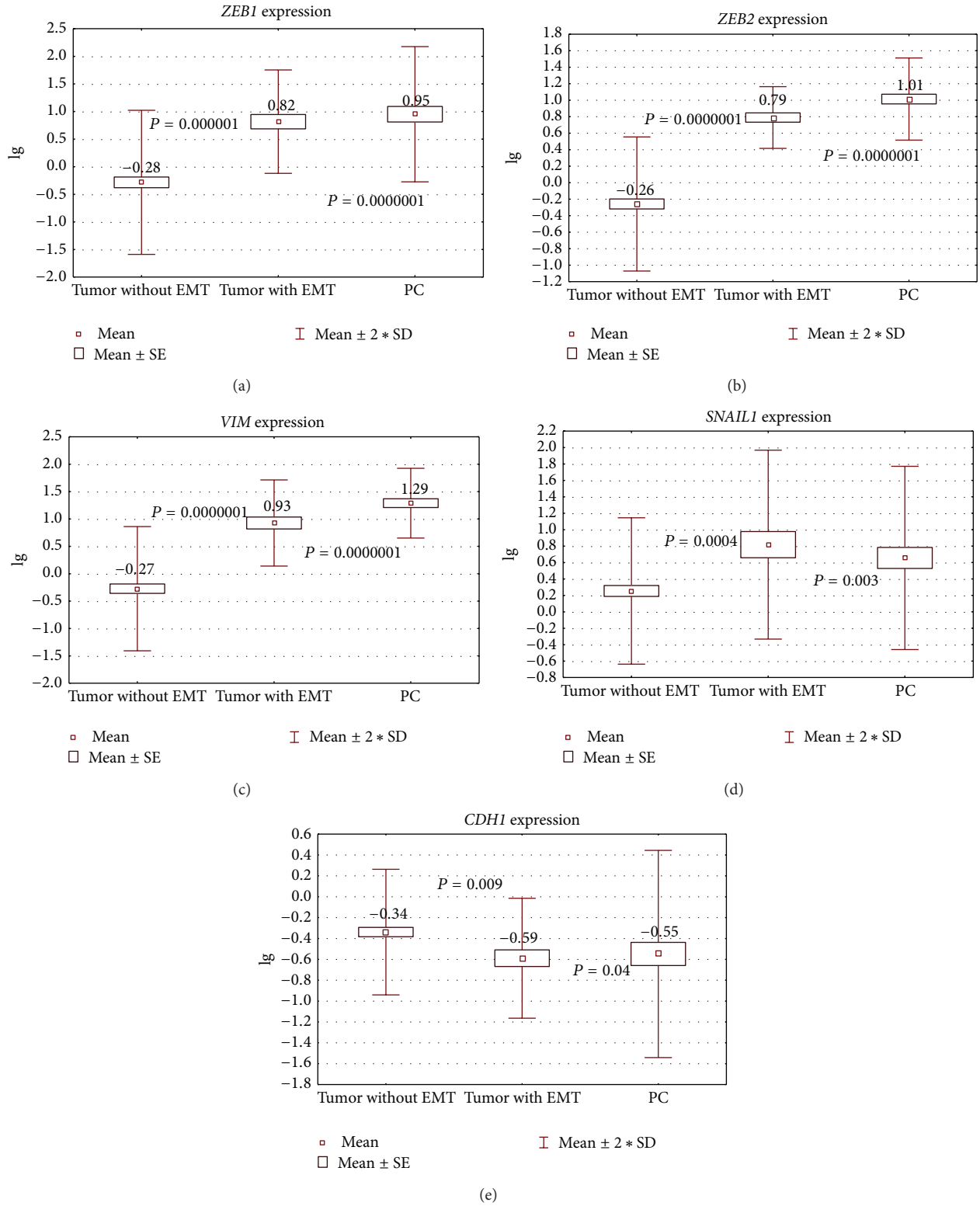

Figure 2: The expression levels of genes in samples with/without EMT and carcinomatous nodules.

Table 4: The *KRAS*- and *BRAF*-mutation frequency and MSI status in EMT-negative and EMT-positive tumors.

	EMT-negative CRC, $n = 45$ (%)	EMT-positive CRC, $n = 13$ (%)	P
KRAS-mut	19 (42.2)	7 (53.8%)	0.33
BRAF V600E	1 (2.2)	3 (23.1)	**0.03**
KRAS-mut + *BRAF* V600E	20 (44.4)	10 (76.9)	**0.039**
KRAS + *BRAF* wt	25 (55.6)	3 (23.1)	**0.039**
MSI-H	5	0	0.27
MSI-L	2	1	0.54
MSS	38	12	0.42

Table 5: The data of EMT-negative/EMT-positive tumors grade.

Grade	EMT-negative CRC, $n = 45$ (%)	EMT-positive CRC, $n = 13$ (%)	P
G1	0	0	
G2	28 (62.2)	2 (15.4)	**0.001**
G3	14 (31.1)	11 (84.6)	**0.001**
Unknown	3	0	

in 5 out of 35 samples (14.3%). This value is very close to that reported by Roeman et al. [4], who classified 16% of tumors as C-subtype (mesenchymal tumors).

The frequency of somatic mutations in the *KRAS* and *BRAF* genes varies in tumors of these two subtypes; but it is significantly higher in mesenchymal tumors, and 3 out of 4 *BRAF*-V600E mutations were discovered in these tumors. According to Roepman et al. [4], CRC of the mesenchymal subtype abounds in mutations in these genes, especially in *BRAF*. Activating mutations in this gene are interpreted as a poor prognostic factor in CRC patients [13]. The association between these mutations and the mesenchymal phenotype was demonstrated by Makrodouli et al. [14]. The data they collected using cell lines of colon adenocarcinoma shows that *BRAF*-V600E induces migration and enhances the invasive potential of these cells. One of the mutations found in *KRAS* (G12V) also promotes cellular migration and invasion [14]. It is worth pointing out that we detected G12V among *KRAS* mutations on four occasions, of which three were in EMT-positive samples. All tumors with a high degree of microsatellite instability (MSI-H) were of the epithelial subtype, which is in line with the traditional interpretation of microsatellite instability in a tumor as a good prognostic factor.

To summarize, our study of the profile of gene expression identified the tumors undergoing the process of epithelial-mesenchymal transition. Classifying cancer cases based on EMT may help to detect the malignant mesenchymal subtype, which is associated with poorly differentiated and highly metastatic tumors. The association between EMT and peritoneal carcinomatosis indicates that EMT-positive tumors have high metastatic potential, which is particularly important at early stages of tumor growth.

Conflict of Interests

The authors declare that there is no conflict of interests regarding the publication of this paper.

References

[1] J. P. Thiery, "Epithelial-mesenchymal transitions in tumour progression," *Nature Reviews Cancer*, vol. 2, no. 6, pp. 442–454, 2002.

[2] J. Yang and R. A. Weinberg, "Epithelial- mesenchymal transition: at the crossroads of development and tumor metastasis," *Developmental Cell*, vol. 14, no. 6, pp. 818–829, 2008.

[3] J. P. Thiery, H. Acloque, R. Y. J. Huang, and M. A. Nieto, "Epithelial-mesenchymal transitions in development and disease," *Cell*, vol. 139, no. 5, pp. 871–890, 2009.

[4] P. Roepman, A. Schlicker, J. Tabernero et al., "Colorectal cancer intrinsic subtypes predict chemotherapy benefit, deficient mismatch repair and epithelial-to-mesenchymal transition," *International Journal of Cancer*, vol. 134, no. 3, pp. 552–562, 2013.

[5] L. Marisa, A. de Reynies, A. Duval et al., "Gene expression classification of colon cancer into molecular subtypes: characterization, validation, and prognostic value," *PLOS Medicine*, vol. 10, no. 5, Article ID e1001453, 2013.

[6] J. Zhu, J. Wang, Z. Shi et al., "Deciphering genomic alterations in colorectal cancer through transcriptional subtype-based network analysis," *PLoS One*, vol. 8, no. 11, Article ID e79282, 2013.

[7] H. Peinado, D. Olmeda, and A. Cano, "Snail, ZEB and bHLH factors in tumour progression: an alliance against the epithelial phenotype?" *Nature Reviews Cancer*, vol. 7, no. 6, pp. 415–428, 2007.

[8] T. Joyce, D. Cantarella, C. Isella, E. Medico, and A. Pintzas, "A molecular signature for Epithelial to Mesenchymal transition in a human colon cancer cell system is revealed by large-scale microarray analysis," *Clinical and Experimental Metastasis*, vol. 26, no. 6, pp. 569–587, 2009.

[9] J. Lim and J. P. Thiery, "Epithelial-mesenchymal transitions: insights from development," *Development*, vol. 139, no. 19, pp. 3471–3486, 2012.

[10] R. Y.-J. Huang, M. K. Wong, T. Z. Tan et al., "An EMT spectrum defines an anoikis-resistant and spheroidogenic intermediate mesenchymal state that is sensitive to e-cadherin restoration by a src-kinase inhibitor, saracatinib (AZD0530)," *Cell Death and Disease*, vol. 4, article e915, 2013.

[11] F. Sipos and O. Galamb, "Epithelial-to-mesenchymal and mesenchymal-to-epithelial transitions in the colon," *World Journal of Gastroenterology*, vol. 18, no. 7, pp. 601–608, 2012.

[12] C. Meacham and S. Morrison, "Tumour heterogeneity and cancer cell plasticity," *Nature*, vol. 501, pp. 328–337, 2013.

[13] J. Souglakos, J. Philips, R. Wang et al., "Prognostic and predictive value of common mutations for treatment response and survival in patients with metastatic colorectal cancer," *British Journal of Cancer*, vol. 101, no. 3, pp. 465–472, 2009.

[14] E. Makrodouli, E. Oikonomou, M. Koc et al., "BRAF and RAS oncogenes regulate Rho GTPase pathways to mediate migration and invasion properties in human colon cancer cells: a comparative study," *Molecular Cancer*, vol. 10, article 118, 2011.